

NCHRP

Web-Only Document 179:

Procedures for Verification and Validation of Computer Simulations Used for Roadside Safety Applications

**Malcolm H. Ray
Mario Mongiardini
Worcester Polytechnic Institute
Worcester, MA**

**Chuck A. Plaxico
Battelle Memorial Institute
Columbus, OH**

**Marco Anghileri
Politecnico di Milano
Milan, Italy**

Contractor's Final Report for NCHRP Project 22-24
Submitted March 2010

National Cooperative Highway Research Program

TRANSPORTATION RESEARCH BOARD
OF THE NATIONAL ACADEMIES

ACKNOWLEDGMENT

This work was sponsored by the American Association of State Highway and Transportation Officials (AASHTO), in cooperation with the Federal Highway Administration, and was conducted in the National Cooperative Highway Research Program (NCHRP), which is administered by the Transportation Research Board (TRB) of the National Academies.

COPYRIGHT INFORMATION

Authors herein are responsible for the authenticity of their materials and for obtaining written permissions from publishers or persons who own the copyright to any previously published or copyrighted material used herein.

Cooperative Research Programs (CRP) grants permission to reproduce material in this publication for classroom and not-for-profit purposes. Permission is given with the understanding that none of the material will be used to imply TRB, AASHTO, FAA, FHWA, FMCSA, FTA, Transit Development Corporation, or AOC endorsement of a particular product, method, or practice. It is expected that those reproducing the material in this document for educational and not-for-profit uses will give appropriate acknowledgment of the source of any reprinted or reproduced material. For other uses of the material, request permission from CRP.

DISCLAIMER

The opinions and conclusions expressed or implied in this report are those of the researchers who performed the research. They are not necessarily those of the Transportation Research Board, the National Research Council, or the program sponsors.

The information contained in this document was taken directly from the submission of the author(s). This material has not been edited by TRB.

THE NATIONAL ACADEMIES

Advisers to the Nation on Science, Engineering, and Medicine

The **National Academy of Sciences** is a private, nonprofit, self-perpetuating society of distinguished scholars engaged in scientific and engineering research, dedicated to the furtherance of science and technology and to their use for the general welfare. On the authority of the charter granted to it by the Congress in 1863, the Academy has a mandate that requires it to advise the federal government on scientific and technical matters. Dr. Ralph J. Cicerone is president of the National Academy of Sciences.

The **National Academy of Engineering** was established in 1964, under the charter of the National Academy of Sciences, as a parallel organization of outstanding engineers. It is autonomous in its administration and in the selection of its members, sharing with the National Academy of Sciences the responsibility for advising the federal government. The National Academy of Engineering also sponsors engineering programs aimed at meeting national needs, encourages education and research, and recognizes the superior achievements of engineers. Dr. Charles M. Vest is president of the National Academy of Engineering.

The **Institute of Medicine** was established in 1970 by the National Academy of Sciences to secure the services of eminent members of appropriate professions in the examination of policy matters pertaining to the health of the public. The Institute acts under the responsibility given to the National Academy of Sciences by its congressional charter to be an adviser to the federal government and, on its own initiative, to identify issues of medical care, research, and education. Dr. Harvey V. Fineberg is president of the Institute of Medicine.

The **National Research Council** was organized by the National Academy of Sciences in 1916 to associate the broad community of science and technology with the Academy's purposes of furthering knowledge and advising the federal government. Functioning in accordance with general policies determined by the Academy, the Council has become the principal operating agency of both the National Academy of Sciences and the National Academy of Engineering in providing services to the government, the public, and the scientific and engineering communities. The Council is administered jointly by both Academies and the Institute of Medicine. Dr. Ralph J. Cicerone and Dr. Charles M. Vest are chair and vice chair, respectively, of the National Research Council.

The **Transportation Research Board** is one of six major divisions of the National Research Council. The mission of the Transportation Research Board is to provide leadership in transportation innovation and progress through research and information exchange, conducted within a setting that is objective, interdisciplinary, and multimodal. The Board's varied activities annually engage about 7,000 engineers, scientists, and other transportation researchers and practitioners from the public and private sectors and academia, all of whom contribute their expertise in the public interest. The program is supported by state transportation departments, federal agencies including the component administrations of the U.S. Department of Transportation, and other organizations and individuals interested in the development of transportation. www.TRB.org

www.national-academies.org

Table of Contents

CHAPTER 1 INTRODUCTION	1
The Finite Element Method	1
Finite Element Method In Roadside Safety	3
Other Areas of Computational Mechanics	5
Summary	6
CHAPTER 2 LITERATURE REVIEW	9
Definitions	9
Introduction.....	9
Verification	10
Validation.....	13
Calibration.....	14
Validation Process	15
Metrics	19
Comparison of Metrics and Repeatability of Full-Scale Crash Tests	46
Hierarchical Modeling	54
Validation in the Roadside Safety Literature	61
Materials and Components	61
Vehicle Models	73
Roadside Hardware Models	81
Verification	94
Process	94
Calculation Verification.....	96
Calculation Verification Process.....	96
Model Assurance Verification	97
CHAPTER 3 SURVEY OF MODELING BEST PRACTICES	105
Introduction	105
Verification	105
Definition	105
Geometry Generation.....	105
Mesh Sensitivity and Quality Determination.....	107
Contact Stability Issues.....	107
Energy Balance and Comparisons	108
Time Step Issues Regarding Element Size, Mesh Density and Mass Scaling.....	108
Validation	108
CHAPTER 4 PROCEDURES	111
Introduction	111

Definitions.....	112
Verification	112
Validation.....	112
Calibration.....	113
Procedures	113
Introduction.....	113
Identify the Baseline Experiment.....	115
Build the Model	116
Compare the Baseline Test to the Computer Simulation.....	119
Predict the Performance of the Incremental Improvement.....	122
Provide Documentation to Decision Makers	123
Implementation	124
CHAPTER 5 COMPARING TIME HISTORIES.....	126
Introduction.....	126
RSVVP	127
Preprocessing	127
Metrics	131
Application to Simple Analytical Curves.....	135
Definition of Test Functions	135
MPC Metric Results.....	137
Single Value Metric Results	139
ANOVA Metric Results.....	140
Application to Repeated Crash Tests.....	141
Repeated Crash Tests	141
Acceptance Criteria.....	144
Results Using Velocity Time Histories.....	147
Acceptance Criteria.....	150
Independent Acceptance Criteria Assessment	150
Conclusions.....	152
CHAPTER 6 BENCHMARK CASES	154
Introduction.....	154
Test Case 1: Pickup Truck Striking a Guardrail	154
Introduction.....	154
PIRT for the G4(1S).....	156
PIRT for the C2500R Vehicle Model	157
Validation of the G4(1S) Guardrail Model.....	159
Test Case 2: Pickup Truck Striking a Guardrail with a Curb.....	178
Introduction.....	178
PIRT for the Curb and Vehicle Models	178
Validation of the G4(1S) Guardrail with Curb Model.....	179

Test Case 3: Geo Metro Striking a Rigid Barrier	195
Introduction.....	195
PIRT for the Geo Metro Vehicle Model.....	196
PIRT for the Concrete Barrier.....	197
Validation of the Geo Metro Model.....	197
Test Case 4: Tractor and Semitrailer FE Model.....	217
Introduction.....	217
PIRT for the Tractor-Semitrailer Model.....	217
PIRT for the Median Barrier Model	222
Validation of the Tractor-Semitrailer Finite Element Model	222
 CHAPTER 7 CONCLUSIONS.....	 240
 REFERENCES.....	 241
 APPENDIX A RSVVP USER’S MANUAL	 A-1
 APPENDIX B RSVVP PROGRAMMER’S MANUAL.....	 B-1
 APPENDIX C BENCHMARK CASE EXAMPLE FORMS	 C-1
 APPENDIX D SURVEY OF PRACTITIONERS	 D-1
 APPENDIX E VALIDATION/VERIFICATION REPORT FORMS	 E-1

LIST OF FIGURES

Figure 1. Schematic representation of the verification processes. (16)	10
Figure 2. Schematic representation of the validation. (16).....	13
Figure 3. Typical validation and verification activities (17).....	20
Figure 4. Comparison between experimental and analytical time history results. (13).....	21
Figure 5. Russell metrics for 30 accelerometers in a ship blast model validation. (34)	36
Figure 6. Russell combined metric plotted versus the longitudinal position of the sensor in a ship blast validation activity. (34)	37
Figure 7. Effect of soil and wood material parameter variation on the performance of the MELT guardrail terminal. (40)	45
Figure 8. Response corridors for the femur force of a 50 th percentile male in a frontal impact for 15 physical tests and one LSDYNA simulation. (41)	48
Figure 9. SID ATD response corridors for the lower rib acceleration (LURY) compared to the response of two finite element models. (42).....	48
Figure 10. Comparison of measured velocity wave form with three simulation results (32).....	53
Figure 11. Hierarchy of a typical roadside hardware finite element model.....	55
Figure 12. Three-dimensional rendering of the leaf-spring suspension for a Freightliner FLD 120 tractor.....	56
Figure 13. Finite element model of the leaf-spring suspension for a Freightliner FLD 120 tractor....	56
Figure 14. Laboratory test of a Freightliner FLD120 Tractor front suspension leaf spring	57
Figure 15. Force-displacement response of the test and simulation of a Freightliner FLD120 Tractor front suspension leaf spring.....	57
Figure 16. Test setup for the tire de-beading test.....	58
Figure 17. Comparison of the force-deflection response of a pickup truck tire subjected to a quasi-static horizontal de-beading load.	59
Figure 18. Steel hub and fixture used in the compression test.....	59
Figure 19. Comparison between the test and the simulation of the deformed shape at different loads (45).....	60
Figure 20. Sequential views from a full-scale test and simulation showing tire response during impact with a curb.....	60
Figure 21. Finite element model of a W-beam (right) and time history comparison of the simulation and experiment (left). (48)	62
Figure 22. Behavior of LSDYNA material 147 for guardrail post rotation. (60).....	65
Figure 23. Damage to an under-reinforced concrete beam showing two crack rebar failure, (top) test specimen and (bottom) simulation. (58).....	65
Figure 24. Qualitative comparison of damage in a quasi-static pull-test of a wood guardrail post (left) experiment and (right) simulation. (59)	66
Figure 25. Comparison of the force-deflection response for (i) the mean experimental	

response, (ii) an envelope of the observed experimental responses and (iii) an LSDYNA simulation. (59).....	67
Figure 26. Summary of materials used in the SUT model. (63).....	68
Figure 27. Qualitative comparison of NCAP results for a C2500 pickup truck for (a) a simulation without strain-rate effects, (b) a simulation with strain-rate effects and (c) an NCAP experiment. (66).....	69
Figure 28. Longitudinal acceleration-time comparison (66).	70
Figure 29. Qualitative comparison of barrier deformation. (69)	71
Figure 30. Comparisons between three rigid pole crash tests and a simulation of a 32 km/hr centerline impact between an 820C vehicle and a rigid pole. (75).....	75
Figure 31. Comparison of the original and modified models of the Geo Metro in a 100 km/hr 20 degree impact with deformable guardrail. (78).....	76
Figure 32. Comparison of crash test (left) and simulation (right) results showing successive crush (deformation) of the honeycomb nose material at 45 msec. (49).....	77
Figure 33. Deformation (top) and time history (below) comparisons of a side impact deformable barrier. (79).....	77
Figure 34. Qualitative comparison of deformations in a C2500 crash test into a rigid wall (left)	78
and the corresponding simulation (right). (81)	78
Figure 35. Time history comparison of a C-2500 pickup truck striking a median barrier. (81).....	79
Figure 36. Comparison of crash test (right) versus finite element (left) results. (63).....	80
Figure 37. Photograph (left) and corresponding finite element model (right) of the pre- collision with a sign post.	82
Figure 38. Vehicle deformation comparison after sign post impact crash test (left) and finite element simulation (right). (88)	82
Figure 39. Qualitative comparison of pickup truck impact with an F-shape portable concrete barrier. (106).....	89
Figure 40. Comparison between a simulation and test of the displacement of a guardrail splice in tension (129).	102
Figure 41. Roadside safety validation and incremental design process.....	114
Figure 42. Hierarchy of a typical roadside hardware finite element model.....	116
Figure 43. Shift between a test and simulation time history.....	132
Figure 44. Analytical wave forms created for a (a) the magnitude test or (b) the phase test	137
Figure 45. Full-scale crash test setup for the repeated ROBUST crash tests (43).....	142
Figure 46. 90 th percentile envelope and acceleration time histories for (a) set #1, (b) set #2 and (c) sets #1 and #2 combined.....	143
Figure 47. Cumulative density function of the residual accelerations for (a) Set #1, (b) Set #2 and (c) the combination of Sets #1 and #2.....	148
Figure 48. 90 th percentile envelope and velocity time histories for Set#1.....	149
Figure 49. Cumulative density functions of the residual velocities for Set #1.....	150
Figure 50. Modified G4(1S) guardrail with routed wood blockouts.	156

Figure 51. Finite element model of the G4(1S).	156
Figure 52. Example of a Validation Sheet from a roadside hardware PIRT.	159
Figure 53. Sequential views of TTI Test 405421-1 and the finite element simulation from a downstream perspective.	162
Figure 54. Plot of global energy-time histories for test case 1.	163
Figure 55. RSVVP preprocessing input and results for the x-channel data for test case 1	164
Figure 56. RSVVP metrics evaluation selection for test case 1	165
Figure 57. X-channel (a) acceleration-time history data used to compute metrics and (b) integration of acceleration-time history data, test case 1	167
Figure 58. Y-Channel (a) acceleration-time history data used to compute metrics and (b) integration of acceleration-time history data, test case 1	167
Figure 59. Z-Channel (a) acceleration-time history data used to compute metrics and (b) integration of acceleration-time history data, test case 1	168
Figure 60. Roll-Channel (a) angular rate-time history data used to compute metrics and (b) integration of angular rate-time history data, test case 1.....	168
Figure 61. Pitch-Channel (a) angular rate-time history data used to compute metrics and (b) integration of angular rate-time history data, test case 1.....	169
Figure 62. Yaw-Channel (a) angular rate-time history data used to compute metrics and (b) integration of angular rate-time history data, test case 1.....	169
Figure 63. Comparison of multi-channel weight values computed using the Area II and the Inertia methods, test case 1	173
Figure 64. Finite element model for the analysis of the G4(1S) and AASHTO B curb.....	179
Figure 65. Sequential views from E-TECH test 52-2556-001 and simulation from a downstream perspective.for Case 2	181
Figure 66. Sequential views from E-TECH test 52-2556-001 and simulation from an overhead perspective for Case 2.	183
Figure 67. X-channel (a) acceleration-time history data used to compute metrics and (b) integration of acceleration-time history data, test case 2	188
Figure 68. Y-Channel (a) acceleration-time history data used to compute metrics and (b) integration of acceleration-time history data, test case 2	188
Figure 69. Z-Channel (a) acceleration-time history data used to compute metrics and (b) integration of acceleration-time history data, test case 2	189
Figure 70. Roll-Channel (a) angular rate-time history data used to compute metrics and (b) integration of angular rate-time history data, test case 2.....	189
Figure 71. Pitch-Channel (a) angular rate-time history data used to compute metrics and (b) integration of angular rate-time history data, test case 2.....	190
Figure 72. Yaw-Channel (a) angular rate-time history data used to compute metrics and (b) integration of angular rate-time history data, test case 2.....	190
Figure 73. Comparison of multi-channel weight values computed using the Area II and the Inertial methods.....	192

Figure 74. Temporary vertical concrete barrier used in Case 3.....	196
Figure 75. Vehicle used in (a) Test 1 and (b) Test 2.....	197
Figure 76. Finite element model of the concrete barrier.....	199
Figure 77. Sequential views of experimental tests and the finite element simulation for Case 3.	201
Figure 78. Plot of normalized global energy time histories for Case 3.	203
Figure 79. Original and preprocessed acceleration curves for Case 3 with Test 1.....	205
Figure 80. Original and preprocessed yaw rate curves for Case 3 with Test 1.....	205
Figure 81. Original and preprocessed acceleration curves for Case with Test 2.....	206
Figure 82. Original and preprocessed rotational rate curves for Case with Test 2.....	207
Figure 83. Comparison of the integral functions for each of the acceleration channels for Case 3 ..	210
Figure 84. Comparison of the integral functions for each of the rotational rate channels for Case 3.	211
Figure 85. X-acceleration: time of max longitudinal ORA considering the intervals	216
Figure 86. NCAC/Battelle tractor-semitrailer model.....	217
Figure 87. Laboratory Test of a 1992 Freightliner FLD120 Leaf-spring Suspension, Case 4	219
Figure 88. Digitized three dimensional geometry of the 1992 Freightliner FLD 120 suspension, Case 4.	219
Figure 89. Exploded view of leaf-spring thin shell model, Case 4.....	220
Figure 90. Finite element model for validating leaf-spring stiffness response, Case 4.	220
Figure 91. Force-displacement Response of Leaf Spring from Test and FEA.....	221
Figure 92. Comparison of FE vehicle model dimensions to those of the test vehicle for Case 4.	224
Figure 93. Summary of Phenomenological Events that Occurred during Full-scale Test and FE Model Simulation in Case 4.	225
Figure 94. EDR locations and nomenclature used in test reports for Case 4.....	228
Figure 95. X-channel (a) acceleration-time history data used to compute metrics and (b) 50-millisecond average acceleration -time history data for Case 4	230
Figure 96. Y-channel (a) acceleration-time history data used to compute metrics and (b) 50-millisecond average acceleration -time history data for Case 4	230
Figure 97. Z-channel (a) acceleration-time history data used to compute metrics and (b) 50-millisecond average acceleration -time history data for Case 4	231
Figure 98. Roll angle-time history plot for Case 4	234

LIST OF TABLES

Table 1. Report 350 evaluation criteria for test 3-31 on the Plastic Safety System CrashGard Sand Barrel System – test (left) and simulation (right). (26).....	24
Table 2. EN 1317 evaluation criteria for test 3-31 on the Plastic Safety System CrashGard Sand Barrel System – test (left) and simulation (right). (26).....	26
Table 3. Results of a ROBUST round robin crash test activity involving a 900-kg car striking a vertical concrete wall. (43)	50
Table 4. Comparison of the six tests for the Ford Festiva rigid pole test (35).....	51
Table 5. Metric components for the three simulation curve of Figure 10 (32).....	53
Table 6. Qualitative comparison of simulation results to full-scale test results (75).....	74
Table 7. EN 1317 domain-specific metric comparisons of a simulation and crash test of a small car striking a concrete wall at 20 degrees and 100 km/hr. (78)	76
Table 8. NARD time-domain metrics comparing a 100 km/hr, 25 degrees impact between a pickup truck and the weak-post w-beam guardrail. (95)	83
Table 9. Domain-specific TRAP metrics for TTI test 471470-26 and LSDYNA simulations of two strong-post w-beam guardrails. (11).....	87
Table 10. NARD and ANOVA metrics for TTI test 471470-26 and LSDYNA simulations of two strong-post w-beam guardrails. (11).....	88
Table 11. Summary of methods used to validate models in roadside safety publications.....	95
Table 12. Average shell element dimensions used in simulation studies	107
Table 13. Average solid element dimensions used in simulation studies.....	107
Table 14. Definition of MPC metrics	134
Table 15. Definition of single-value metrics	135
Table 16. Comparison metrics for the analytical curves for (1) the magnitude test and (2) the phase test.	139
Table 17. Comparison metrics for Set #1, Set #2 and the combination of both sets	146
Table 18. Values of the comparison metrics using velocity time histories for Set #1.....	149
Table 19. Comparison metrics for four essentially identical crash tests of a strong-post w-beam guardrail with different blockouts.....	152
Table 20. Phenomena Importance Ranking Table (PIRT) for the G4(1S).	158
Table 21. Partial PIRT for the NCAC C2500R pickup truck. (83)	160
Table 22. Analysis solution verification table for test case 1.	163
Table 23. Roadside safety validation metrics rating table for test case 1– (single channel).	166
Table 24. Roadside safety validation metrics rating table for test case 1–(multi-channel,Area II)...	171
Table 25. Roadside safety validation metrics rating table for test case 1– (multi-channel, Inertial).172	172
Table 26. Evaluation criteria test applicability table for test case 1.	174
Table 27. Structural adequacy phenomena for test case 1.....	175
Table 28. Occupant risk phenomena for test case 1.....	176
Table 29. Vehicle trajectory phenomena for test case 1.	177
Table 30. Summary of the test and simulation impact conditions for Case 2.	180

Table 31. Summary of Global Energy Checks for Case 2.....	180
Table 32. Roadside safety validation metrics rating table for Case 2– (single channel option).....	185
Table 33. Roadside safety validation metrics rating table for Case 2 – (multi-channel, Area II).	187
Table 34. Roadside safety validation metrics rating table for Case 2 – (multi-channel, Inertial). ...	191
Table 35. Structural Adequacy Phenomena for Case 2.	192
Table 36. Occupant Risk Phenomena for Case 2.....	193
Table 37. Vehicle Trajectory Phenomena for Case 2.	195
Table 38. Partial PIRT for the Geo-Metro model. (43)	129
Table 39. Vehicle type and impact conditions for the two tests in Case 3.	200
Table 40. Analysis Solution Verification Table for Case 3.....	202
Table 41. Roadside safety validation metrics rating table for Case 3 (single channel option).....	209
Table 42. Roadside safety validation metrics rating table for the Case 3 (multi-channel option).....	212
Table 43. Structural Adequacy Phenomena for Case 3 with Test 1.	214
Table 44. Occupant Risk Phenomena for the Case 3 with Test 1.....	215
Table 45. Vehicle Trajectory Phenomena for the Case 3 with Test 1.	216
Table 46. Phenomenon Importance Ranking Table for Tractor-Semitrailer Model (Case 4).	218
Table 47. Metric Evaluation Table for Leaf Spring Response (Case 3 Vehicle PIRT).....	221
Table 48. Summary of the test and simulation impact conditions for Case 4.	222
Table 49. Summary of Global Energy Checks for Case 4.....	227
Table 50. Roadside safety validation metrics rating table for Case 4 – (single channel option).....	229
Table 51. Roadside safety validation metrics rating table for the Case 4 – (multi-channel option)..	232
Table 52. Evaluation Criteria Test Applicability Table for Case 4.	233
Table 53. Structural Adequacy Phenomena for Case 4.	235
Table 54. Occupant Risk Phenomena for Case 4.....	236
Table 55. Comparison of Phenomenological Events for Case 4.	237

CHAPTER 1 INTRODUCTION

THE FINITE ELEMENT METHOD

Obtaining accurate and reliable finite element simulations requires careful attention to detail and careful verification of material properties, energy management, numerical stability and a number of other important computational characteristics. Confidence in the results of computations depends on careful verification and validation. The purpose of this research is to develop potential verification and validation procedures, quantifiable evaluation metrics and acceptance criteria for roadside safety research that maximize the accuracy and utility of using finite element simulations in much the same way NCHRP Report 350 and MASH ensure the accuracy and utility of full-scale crash tests. Developing procedures and evaluation metrics allows for results to be quickly checked and compared with other simulations.

Before examining the details of verification and validation, it is useful to first review the development of the finite element method in general and, in particular, its application to roadside safety. The foundations for the finite element method were laid in the 1940s but it was the development of the digital computer in the 1950s that transformed a collection of obscure numerical methods into a powerful engineering design tool. Finite element methods and computers evolved together in a symbiotic relationship that began in earnest in the middle 1950s with pioneering work by engineers working for Boeing.(1) In a very real sense, applications and the needs of practicing designers have always been the fuel that ignited innovation in structural finite element software development. As is often the case, there were similar independent advances in Europe as, for example, by Argyris.(2) Many researchers followed the lead of these early analysts and the general finite element literature is now, of course, vast and highly differentiated.

The Boeing group included Ray Clough, a civil engineering professor from the University of California at Berkeley, who brought the innovations and ideas from Boeing back to Berkeley. Berkeley became a center of research and a training ground for many researchers and academics who would make important contributions to finite element analysis.(3) Researchers such as Clough and Wilson mentored, trained and worked with a generation of researchers who took the finite element method with them as they took up teaching and research posts throughout the world. Belytschko points out that in addition to their ground breaking work in finite element analysis, the willingness of researchers like Clough and Wilson to freely and widely distribute their early finite element codes played an important role in bringing the method to a wider audience.(4) These first applications generally involved linear static solutions and it took nearly a decade before researchers began exploring solutions to nonlinear problems.(5) The names of the researchers and the codes they developed during this period are still familiar today: Marcal developed the program MARC, Swanson developed ANSYS, Hibbitt developed ABAQUS and Bathe developed ADINA.

While the codes and researchers mentioned above were exploring nonlinear materials and geometric nonlinearities, they were primarily concerned with static or steady-state dynamic solutions. None of these codes, at least at the time, used explicit time integration methods in their solution procedures and none really addressed the general contact and impact problems needed to model vehicle crashes.

Interestingly, some insightful engineers recognized the potential for using finite element method to simulate vehicle impacts early in the 1970s. , Belytschko describes some of the very early explicit impact codes such as SAMSON and WRECKER and notes the great deal of work sponsored by the US Department of Transportation.(4) In particular, the USDOT was interested in design tools for automobiles and roadside barriers and was funding finite element development work.

An often overlooked researcher from Berkeley who developed a very early explicit two-dimensional code for solving roadside barrier problems was Powell who developed the program BARRIER in 1971.(6) Powell's program was relatively simple, using simple discreet elements such as springs, dash-pots, beams and truss elements to model components of guardrails and vehicles. The results proved so useful that the final version of the program, BARRIER VII, is still sometimes used in the roadside safety design community for quick calculations of barrier deformations.(6)

Giavotto developed similar mixed-method codes called VEDYAC and later MUSIAC for evaluating roadside hardware designs.(7) The specialty codes GUARD and NARD were also developed during this time period but never really gained the confidence of roadside safety researchers. Significantly, however, NARD included a validation manual, which appears to be the first attempt of the roadside safety community to incorporate validation and verification techniques into computer-aided roadside design. These are probably just a few of what might be called specialty codes that were developed in the 1970s under DOT sponsorship to solve specific automotive and highway safety design problems. In the mid-1970s, the DOT stopped funding numerical methods and shifted more resources into full-scale testing both in the area of vehicle design (i.e., the National Highway Traffic Safety Administration (NHTSA)) and in barrier design (i.e., the Federal Highway Administration (FHWA)). It would be some twenty years before DOT came back to the use of finite element codes.

The first true general-purpose impact finite element code was developed by Hallquist at Lawrence Livermore National Laboratories (LLNL) starting roughly in 1976.(8) The era of computational impact mechanics is, then, just over 30 years old and practical industrial solutions have only been widespread for little more than a decade. Given the importance and ubiquity of finite element calculations in the design of complex structures such as automobiles, aircraft, and occupant safety systems, it is sometimes difficult to remember that all these methods and tools have reached the commercial market place in a very short period. The combination of rapidly improving numerical methods coupled with an equally dramatic

increase in inexpensive computational power brought impact finite element codes out of the government research laboratories and into engineering design studios for a once unimaginable range of applications.

Hallquist named his code DYNA3D, an acronym indicating nonlinear dynamic analysis of solids in three dimensions. DYNA3D resulted from the convergence of three ideas that Hallquist combined uniquely:

- The use of explicit central difference time integration,
- The use of under-integrated elements, and
- The calculation of contact forces.

Much of the FE methods research at the time involved developing more sophisticated elements and integration schemes. DYNA3D adopted nearly the opposite approach – very fine spacial discretization and small time steps with a relatively straight-forward integration scheme. DYNA3D demonstrated that it would be possible to develop a general purpose three dimensional continuum mechanics contact-impact code using this approach. As Wilson freely distributed SAP a decade earlier, LLNL made DYNA3D available, with some security restrictions, to academics and engineers who in turn added features and improvements. The result was a code that was increasingly seen as a viable general-purpose code for dynamic impact and contact problems. All subsequent crashworthiness codes derive either directly or indirectly from the early LLNL codes.

FINITE ELEMENT METHOD IN ROADSIDE SAFETY

As discussed above, finite element computer simulations have been used in roadside safety research and design from a surprisingly early date. Programs like Barrier VII, NARD and Guard were used to gain insight into roadside hardware crashes at a time when finite element analysis in general was in its early development.⁽⁹⁾ These early tools, however, had significant limitations and could really only be used to perform simple parametric evaluations that would later be more extensively explored using full-scale crash tests. In the early 1990s, the FHWA sponsored several projects to examine finite element simulation in roadside safety. A consensus eventually developed to focus on the use of DYNA3D and its commercial counterpart LSDYNA. By the early 1990s, LSDYNA had become an important design and evaluation tool in the automotive and aerospace industries for evaluating crash scenarios. Its importance is shown by the fact that each Transportation Research Board (TRB) Annual Meeting in the past several years has had one full session devoted to papers involving LSDYNA simulations in roadside safety. Numerous papers are also being published in a variety of journals. LSDYNA has become a “main stream” tool in roadside safety design in a relatively short period of time.

Verification and validation have been a component of these developments from the very start. The NARD program contained a Validation Manual with a variety of validation metrics which will be discussed later. The first roadside safety researcher to seriously address the issue

of finite element verification and repeatability of full-scale crash tests was Ray, who in 1996 published a paper comparing six identical full-scale crash tests and an LSDYNA finite element simulation of the same impact scenario. Unsurprisingly, Ray discovered that the acceleration, velocity and displacement time histories obtained from crash tests were not identical but were subject to random experimental variations. Ray performed a DYNA3D simulation of the same impact scenario and the results generally remained inside the 90th percentile corridor until after the peak response. Considering the period during which this work was performed and the simplicity of the vehicle model, the results were very encouraging.

There was an attempt by the FHWA to encourage users of LSDYNA simulation in roadside safety to calculate and report a variety of validation and verification metrics but the community resisted attempts to standardize procedures at the time. Instead, each research group developed its own *ad hoc* qualitative methods of assessing validity.

At about this time, the FHWA established its “Center of Excellence” program to encourage roadside safety researchers to incorporate finite element analysis into roadside hardware design and testing. This effort used a small amount of funding to encourage the Centers to piggy-back finite element simulation efforts onto existing roadside hardware development projects. From that perspective, the program was quite successful; today, it is very common to see finite element simulations being used as an integral part of the roadside safety research and development process. In fact, roadside hardware development efforts that do not include finite element simulations are the exception rather than the rule.

Early efforts using LSDYNA focused on replicating the results of crash tests that had already been performed but it was not long before simulation was used to predict the likely outcome of crash tests. Perhaps the first use of LSDYNA to explore roadside hardware performance and obtain an FHWA acceptance letter based only on LSDYNA analyses was performed by Plaxico and Ray for the Iowa DOT.(10) Iowa had used a much larger wood post than was typical and sought to obtain FHWA approval of its design. Instead of sponsoring crash tests, Iowa DOT asked Plaxico and Ray to evaluate the safety performance of the G4(2W) and the G4(1W) using finite element analysis. Since there were several crash tests available for the G4(2W), the research team first simulated those crash tests to verify that the finite element models produced accurate and reliable results. After this was established, the performance of the similar G4(1W) was explored with an LSDYNA model that was constructed in a similar way and used many of the same components (e.g., same vehicle model, same material models, and similar mesh densities). The simulation results for the never-tested G4(1W) showed that it was very likely to perform well in a Test 3-11 crash test. The results were forwarded to the FHWA which was confident enough in the results to issue an acceptance letter (FHWA). We believe that this was the first instance of an FHWA approval letter being written solely based on the results of finite element simulation.

This process has accelerated such that there are now numerous examples of LSDYNA

analyses being used in the roadside safety design process. Many of these projects will be described later in the literature review section.

Many researchers in Europe were also using finite element analyses to design roadside hardware and some of the EU countries even recommended accepting designs based only on finite element results. Beginning in 1998, the European Union sponsored the “Road barrier upgrade of standards” (i.e., the ROBUST Project) to improve the scientific and technical knowledge that form the basis of the EN1317 European crash test standards.(11, 43) One of the primary goals of the project is to “improve the accuracy and ease of use of computational mechanics as a complement to full-scale tests.” ROBUST Working Group Six in particular is charged with exploring computational mechanics (i.e., computer simulation programs) in aiding the design, evaluation and approval process. Verification and validation of finite element models is a major portion of the work of the ROBUST consortium. To-date the group has tackled several very important issues relating both to the repeatability of full-scale crash tests and the validation of finite element models.

The ROBUST project has produced a number of interesting studies relevant to this research including the following:

- A verification study of a modified Geo Metro finite element model developed by Anghileri striking a Norwegian standard guardrail,
- A verification study to assess further revisions of the Geo Metro model including a finite element dummy and two seats,
- A verification study to assess further revision of the Geo Metro model to include steering and suspension effects and
- A study on how to best record vehicle acceleration data in finite element simulations so that they can be compared directly to full-scale tests.

Generally, the ROBUST validation procedures involve careful documentation of changes from one version of a model to the next and comparison of crash test measures like the ASI, THIV and ORA. An example of typical ROBUST procedures is included in the validation report for the Geo Metro model.(12) One of the interesting features of the ROBUST reports is that a standard method of reporting is evolving such that finding and comparing information is much easier.

OTHER AREAS OF COMPUTATIONAL MECHANICS

The integration of computer aided engineering techniques into roadside safety design has been paralleled in many other fields including aerospace, medicine and vehicle design. The automotive industry in particular has been a leader in integrating computer aided engineering into the routine design process. Automotive companies are generally under great pressure to

develop and test new product lines quickly and efficiently. Codes like LSDYNA have become increasingly sophisticated in large part due to the needs of automotive manufacturers and their suppliers to perform rapid proto-typing of new designs. Computer simulation methods have become so main-stream in recent years, however, that the need for verification and validation procedures has shifted to the public sector as well. Today, several governmental bodies have developed validation and verification procedures in order to evaluate designs from the engineering community. For example, today the Federal Aviation Administration (FAA) allows aircraft seats to be designed and approved for use based solely on finite element analysis.⁽¹³⁾ There is also a computation technique approved by the FAA to simulate bird strike impacts with engine turbines. Similarly, the Federal Food and Drug Administration FDA is developing validation procedures for use in evaluating human structural implants (e.g., artificial joints). In-vivo testing of new joint designs is not possible so using computational methods is one of the few ways to evaluate new biomedical devices prior to the start of human trials. The European Standard for rail car crashworthiness also allows for the use of computer simulations in the approval process of new rail-car vehicles.⁽¹⁴⁾ The National Aeronautics and Space Administration (NASA), the Department of Defense (DoD) and many of the national laboratories have developed high-level managerial procedures for validating computer models. These approval procedures will be discussed at greater length in the Literature Review section of this report but they are mentioned here to illustrate that the use of computer simulation methods have become widely used throughout the engineering design community and are being used in the approval and acceptance process by several governmental organizations.

SUMMARY

There is a long history of using finite element methods to design and evaluate mechanical devices in general and roadside safety hardware in particular. While computer simulations have become widespread the issue of verification and validation has only recently begun to be addressed. The objective of this research is to develop guidelines for verification and validation of detailed finite element analyses for crash simulations of roadside safety features. The focus of these guidelines is establishing accuracy, credibility, and confidence in the results of crash test simulations intended (i) to support policy decisions and (ii) to be used for approval of design modifications to roadside safety devices that were originally approved through full-scale crash testing.

The following chapters in this report include an in-depth review of the literature, a “best practices” guide to modeling roadside safety hardware, the research team’s recommended procedures for verifying and validating finite element models used in roadside safety applications, and an assessment of the procedures with the perspective of using the guidelines. The literature review chapter provides a review of the methods that have been used in verification and validation efforts – both in the roadside safety area as well as computational mechanics in general. Gaps in the literature were identified, which were later addressed in the

development of the research team's recommended procedures for verification and validation. Chapter 3 identifies model building best practices in easily retrieved form so that both new and experienced users can develop models that are highly likely to run without errors. The best practices information was garnered from a survey of practitioners that was conducted to determine modeling techniques and the range of acceptable variation when performing typical roadside safety simulations. Chapter 4 presents recommendations for verifying solutions and validating computer simulations in roadside safety, and Chapter 5 presents several example cases to demonstrate the process of applying the procedures.

CHAPTER 2 LITERATURE REVIEW

DEFINITIONS

Introduction

The purpose of this research was to develop verification and validation procedures for using computer simulations in developing incremental improvements to roadside safety hardware. Defining what is meant by the terms “validation” and “verification” was an important first step. The issue of verifying and validating mathematical and computational models has been of interest in many disciplines in recent years; roadside safety simulations are just one of many applications in the general area of computational mechanics. The Department of Defense (DoD) and the American Institute of Aeronautics and Astronautics (AIAA) define validation and verification as follows:(15, 16)

Verification: The process of determining that a model implementation represents the developer’s conceptual description of the model and the solution to the model.

Validation: The process of determining the degree to which a model is an accurate representation of the real world from the perspective of its intended use.

In 2006 the American Society of Mechanical Engineers (ASME) published its “Guide for verification and validation in computational solid mechanics,” ASME V&V 10-2006.(17) This guide is the result of a 10-year effort by the PTC-60 committee to standardize definitions and establish the basic process for validation and verification activities. The ASME guide governs the terminology and processes used throughout the remainder of this report. The guide does not provide specific validation and verification procedures but rather establishes a philosophical backdrop that can be used to create appropriate procedures in particular domains such as roadside safety. Since the needs of each technical area in computational mechanics are different, it is not possible to have a single validation and verification procedure, but the ASME guide provides an essential basis for creating domain-specific procedures.

ASME V&V 10-2006 defines validation, verification and calibration as follows:

Verification: The process of determining that a computational model accurately represents the underlying mathematical model and its solution.

Validation: The process of determining the degree to which a model is an accurate representation of the real world from the perspective of the intended uses of the model.

Calibration: The process of adjusting physical modeling parameters in the computational model to improve agreement with experimental data.

The ASME definitions are essentially the same as the AIAA/DoD definitions. Since the ASME definitions and philosophy represent a broad consensus of engineers and analysts, it makes sense for the roadside safety community to build upon these existing definitions.

Figure 1 shows a schematic representation of the verification processes from the AIAA Guide. Verification, according to this definition, involves comparing the computerized discrete numerical solution (e.g., typically but not exclusively LSDYNA in roadside safety) to known mathematical solutions. Verification is concerned with how well the discrete numerical approximation (e.g., the LSDYNA simulation) agrees with the known mathematical solution (i.e., differential equation solution). Verification does not address the relationship between the computer simulation and the real world or experiments. Validation, on the other hand, is concerned exclusively with comparing the discrete numerical solutions to real-world physical experiments. The following sections will discuss the implications of these definitions with respect to roadside safety simulations.

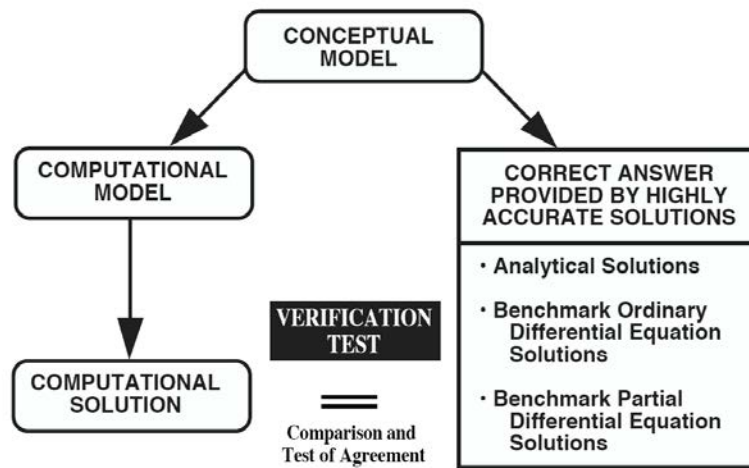


Figure 1. Schematic representation of the verification processes. (16)

Verification

Computational modeling is a way of representing physical phenomena using mathematical techniques. Verification is concerned with how well the discrete numerical approximation (e.g., typically but not exclusively LS-DYNA in roadside safety) agrees with the known mathematical solution (i.e., differential equation solution). For example, the following equation represents a mathematical theory about how waves propagate through solids:(18, 19)

$$\frac{\partial^2 u}{\partial t^2} = \sqrt{\frac{E}{\rho}} \frac{\partial^2 u}{\partial x^2}$$

The mathematical theory may or may not be correct with respect to its ability to predict physical experiments, but the solution is known and mathematically unambiguous. A researcher or code developer might develop a discrete numerical approximation (i.e., a computer simulation) of a wave propagating along a long rod, for example. Verification would be the process of comparing the solutions of the computational numerical experiment with the solution of the partial differential equation shown above. If the numerical computations replicate the known analytical solution, the computational model is considered “verified.” In verification, the issue is not comparison to physical experiments but rather a comparison to the underlying physics. Verification is about comparing numerical approximations to the known solutions such as the solution of a differential equation. As such, verification could be defined as:

The process of ensuring that the computational model provides results consistent with the developer’s conceptual description of the model and the underlying assumptions that form the basis of the mathematical model (i.e., the model responds as the developer intends) and that computed results adhere to basic physical laws, such as conservation of energy and momentum.

With respect to this research project, the definition of verification presents some problems. Aside from known solutions from basic mechanics (e.g., the impact of long rods or impulsively loaded beams) there are no known analytical solutions in the realm of roadside safety. Stated another way, in roadside safety we do not have simple benchmark problems with known differential equation solutions against which we can test analysis codes. While some basic cases of simple impacts could be verified, a researcher developing a model of a particular roadside hardware system or component generally has no “known” solution to work from. In fact, the lack of a “known” solution is the whole point of using a computer approximation.

Code developers like LSTC perform software verification to ensure that the computer programs produce solutions consistent with the algorithms used to develop them. ASME V&V 10-2006 refers to this as code verification. Code developers and users also often perform simple verification experiments to demonstrate that a particular code such as LSDYNA produces solutions to simple mechanics problems with known solutions. One graduate course at Worcester Polytechnic Institute, for example, is largely concerned with students verifying for themselves that LSDYNA produces the correct results for a number of simple mechanics problems:

- One dimensional wave propagation problems are verified by comparing to particular solutions of the wave equation.
- Elastic-plastic material behavior is verified by performing simulations of a rigid hammer axially striking a solid rod and comparing the results to Taylor’s momentum approach.
- Wave propagation and failure properties are verified by performing simulations of the Landon-Quinney experiment with concrete rods and verifying the results with one-dimensional wave theory predictions.

- Simulations of impulsively loaded beams in three and four-point bending are verified using Jones's upper and lower bound collapse theorems.

Comparisons between simulations of these types of events and the known analytical solutions verify that LSDYNA produces results consistent with the physics of the known mathematical models. A general purpose, widely used computer program like LSDYNA can, therefore, be considered "verified" for general nonlinear dynamic contact/impact problems and this level of verification is generally the responsibility of the developer. In addition, since the source code is not generally available, it is nearly impossible for someone other than the code developer to verify the code. This report will not address the issue of code verification.

In the context of roadside safety research, what is meant by the term "verification?" There are two approaches: (i) roadside safety benchmark cases and (ii) model assurance verification. Benchmark verification is based on "calculation verification," which is defined as "the process of determining the solution accuracy of a particular calculation."(17) There is a need for some standardized roadside safety benchmark cases that can be used to verify new versions of code (e.g., are the results the same after updating from LSDYNA 960 to 970) and to verify solutions between platforms (e.g., are the results the same on a 10-cpu Linux cluster as a dual-cpu workstation?). This type of activity would be defined as calculation verification since prior solutions on previous hardware/software platforms are available and the results of new calculations on new computational platforms could be verified. The issue when running a standardized benchmark is not the correctness of the solution with respect to physical crash tests, but whether the new numerical solution arrangement (i.e., a new version of the code, a different computational platform, or both) produces the same results as the previous arrangement using the same unmodified model. Most analysts do this type of verification informally by re-running an old model that they have confidence in on a new hardware/software platform. The advantage of developing standardized benchmarks is that the roadside safety computational mechanics community would be able to more effectively share information and would be able to develop more relevant benchmark cases. Model assurance verification involves developing procedures and metrics for a particular model of a vehicle, barrier, occupant or other component of a roadside hardware simulation to ensure that results adhere to basic physical laws, such as conservation of energy and momentum, and to maximize the likelihood that there will be no numerical or computational problems in the model.

Model assurance verification seeks to confirm that models obey basic physical laws. The total energy and momentum balances should be checked to ensure that they do not change beyond reasonable amounts (e.g., five percent of the initial kinetic energy and initial momentum). Likewise, computational items like hourglass energy and mass added should be checked to ensure that these items stay below some agreed upon value. Accelerations of the center of gravity are often saved for use in post-processing and steps must be taken to verify that the data has been collected at an appropriate rate to avoid aliasing. A simple check for

aliasing of acceleration data from a finite element analysis is to integrate the acceleration-time history (e.g., collected at a nodal point) and check that the result is consistent with the velocity-time history collected from the same location (a good discussion of aliasing can be found at http://www.dagarta.com/dw_Ohaa.htm).

These types of verification exercises ensure that the model results conform to the basic laws of physics. If any of these types of checks fail (i.e., the total energy grows beyond the allowed value or the hourglass energy becomes large) it is an indication that there is some type of computational problem that should be identified and corrected before the model is used for either validation or prediction.

Validation

Validation is conceptually much easier to define since it involves any comparison between a numerical simulation and a physical experiment. Validation procedures can be used to compare numerical results to component-level tests, sub-assembly tests, material characterization experiments or full-scale crash tests. The ASME V&V 10-2006 definition of validation, illustrated in Figure 2, is “the process of determining the degree to which a model is an accurate representation of the real world from the perspective of the intended uses of the model.”(17)

Validation, as defined above, involves a comparison of the simulation and experiment to determine “the degree to which a model is an accurate representation of the real world from the perspective of the intended uses of the model”.(17)

A finite element simulation whose intended use is, for

example, to design the crashworthiness of a vehicle may differ from a model intended to examine the NCHRP Report 350 evaluation parameters. In the former, for example, the deformations of parts of the vehicle would be highly relevant even if they do not affect the kinematics of the vehicle, whereas in the latter, such deformations would probably have little effect on parameters like occupant risk or ride-down accelerations.

Similarly, the choice of validation metrics is tied to the intended use. If the purpose of a finite element model of a cantilever beam is to predict the tip deflection of the beam under

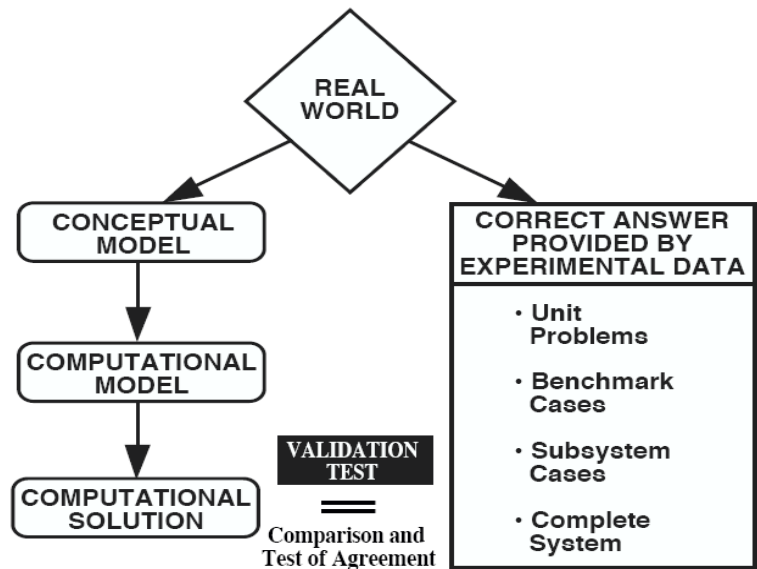


Figure 2. Schematic representation of the validation. (16)

some loading, the metric that should be used in validating the model is the tip deflection. The validation metrics are indicative of the intended use of the model and the expertise needed to evaluate the model.

In general, the purpose of performing a finite element simulation in roadside safety is to assess the safety performance of a roadside hardware device by simulating the equivalent of a full-scale crash test. Full-scale crash tests are evaluated using the criteria provided in NCHRP Report 350 in the US or EN 1317 in Europe so ultimately, a simulation should be judged successful if the computer simulation results in good predictive values of the Report 350/EN 1317 evaluation criteria (e.g., occupant ride down accelerations, occupant impact velocities, THIV, and ASI). The objective of this project is “to develop guidelines for verification and validation of detailed finite element analysis for crash simulations of roadside safety features. The focus of these guidelines will be on establishing accuracy, credibility, and confidence in the results of crash test simulations intended (i) to support policy decisions and (ii) to be used for approval of design modifications to roadside safety devices that were originally approved with full-scale crash testing.” This statement clearly indicates that the use of computation models being validated is intended to support policy decisions and approval of design modifications so the crash test evaluation metrics will of necessity be used in the validation process. We propose, therefore, the following purpose for computer simulations in roadside safety:

The purpose of performing roadside safety computer simulations is to assess the response of the vehicle, barrier and occupant in a collision such that (i) the NCHRP Report 350 evaluation parameters can be predicted and (ii) the structural performance of the barrier can be assessed.

Combining the ASME V&V 1-2006 definition of validation with the purpose of performing roadside safety simulations yields a definition of validation as it relates to simulations of roadside devices. Validation in the area of roadside safety is:

The process of determining the degree to which a roadside safety computer model is an accurate representation of the real world crash tests from the perspective of accurately replicating (i) the NCHRP Report 350 or EN 1317 crash test evaluation parameters, (ii) the structural performance of the barrier and (iii) the response of the vehicle.

Calibration

Calibration is often confused with verification and validation. Verification and validation involve comparisons with physical experiments or solutions that are independent of the model development, whereas calibration is the use of physical experiments, the literature and analytical solutions to estimate the values of the parameters needed to develop the model. For example, if a material model is needed in a particular finite element simulation, the analyst may perform some physical tension tests in the laboratory to obtain the stress-strain response of the model. These physical test results can then be used to estimate the values of the parameters needed for the computational material model. Such a material model has been “calibrated” by

the physical tests and so the same physical tests cannot be used to “validate” the material model. Physical experiments, therefore, can be used either to estimate the values of the parameters and thereby calibrate a model, or to validate a model, but not both.

VALIDATION PROCESS

As defined earlier, validation in the context of roadside safety computer simulations is:

The process of determining the degree to which a roadside safety computer model is an accurate representation of the real world crash tests from the perspective of accurately replicating (i) the Report 350 or EN 1317 crash test evaluation parameters, (ii) the structural performance of the barrier and (iii) the response of the vehicle.

Validation always involves comparing a computer simulation or numerical experiment to a physical experiment of some type. The question at the root of the validation exercise is whether the simulation replicates the physical experiment and whether it can be used to explore and predict the response of new or modified roadside hardware in the real-world.

Validation activities can be performed not only for full-scale crash tests but for material models, sub-assembly models and component models. Ideally, each portion of a large complex model should be validated separately if it is possible to perform a meaningful physical test. The following sections discuss various aspects of validation including validation metrics and procedures; validation of materials, components and subassemblies; and the repeatability and validation of full-scale tests.

Significant activity in recent years has aimed at formalizing verification and validation processes in computational solid mechanics. As mentioned earlier the AIAA guide was developed almost a decade ago and the ASME guide was published just last year.(15, 16) This project is concerned mainly with developing procedures that can be used as part of the evaluation and acceptance process. Designers have been using computer simulations to develop roadside hardware for a decade now but acceptance decisions are still generally made based on crash tests. A computer simulation used in the design process is useful since it helps to minimize the number of development crash tests needed and provides insight into how a device functions. Using computer simulations in the acceptance process, however, requires more formality and uniformity since the person evaluating the model did not participate in the model or hardware development.

The full-scale crash test procedures illustrate the process. Crash test procedures in roadside safety have existed for nearly 40 years. The roadside safety community has learned to trust the results of crash tests if they are performed according to the accepted guidelines of NCHRP Report 350.(20) A similar procedure is necessary for the use of computer simulations – the roadside safety community needs to develop procedures for validating and verifying computational results to enable them to be trusted by those making acceptance decisions. Report 350 enables a hardware developer to state that the testing was performed in accordance

with the recommendations of NCHRP Report 350 and to determine that the proper crash performance information is being submitted to those making acceptance decisions. These validation and verification procedures can likewise become an analogous process for the computational results.

The basic approach of developing a quality control procedure for gaining confidence in the validity of the results has been used in other areas for both crash/dynamic testing and computational modeling. For example, FAA Advisory Circular 20-146 presents a procedure whereby computer simulation results can be used to qualify aircraft and rotorcraft seats.(13) The basic process recommended by the FAA circular is:

- Develop a model of an already tested and approved seat configuration for which dynamic test results are available. This is referred to as the baseline seat model.
- Validate the results of the computer simulation of the baseline seat model against the already-existing dynamic tests.
- Modify the baseline seat model to replicate any desired changes in the structure or positioning of the seat and its occupant and perform the simulations of the new configuration.
- Evaluate the results of the new seat configuration using the same requirements for the dynamic tests. If the results of the simulation indicate passing performance using the seat test metrics, the seat can be approved for use.

Circular 20-146 allows the use of LSDYNA, MADYMO and MCS/DYTRAN as acceptable analysis codes. It states that models must be validated against dynamic tests and that the tests used for the validation must be as similar as possible to the extrapolated design. For example, results from a three-legged seat cannot be used to validate a model which will then be used to examine a four-legged seat design. Since the seats are tested with anthropometric dummies, the computational models also include models of the dummy. The test evaluation criteria involve the responses of the anthropometric dummy in terms of the head injury criteria (HIC), lumbar spine loading and femur force. Time histories from the computational model are used to calculate these same response parameters and specific deterministic acceptance values are provided. For example, a HIC greater than 700 is considered a failure in the tests. When validating the model, the numerically-obtained HIC must be within +/- 50 units of the experimentally measured value. Similarly, the maximum lumbar spine compression is measured in the test and estimated in the computational solution. The maximum limit is 1500 lbs and the computational value must agree within 10 percent of the experimental value. The femur load should also agree with the physical test within 10 percent. The FAA Circular does allow some flexibility stating that some values are not as critical in some situations so while good HIC validation is always required, validation of the lumbar spine might not be as critical. This procedure is a deterministic evaluation in the sense that it does not address uncertainty

about either the physical test or the numerical calculation—the evaluation parameters are calculated and required to be within an appropriate range compared to the physical test.

The results of the validation process must be documented in a report, analogous to a test report. The report documents the results, comparisons with the physical tests, the software/hardware used and the sources of material and geometric data. The analyst must address some particular issues like the energy balance and hourglass modes and the Circular specifies that the analysis results be filtered using SAE J211 Class 1000, the same filter specifications used in the dynamic tests.

Engine inlets of turbofan planes must be verified with bird strike impacts. These impacts are usually performed experimentally with birds of 2 pounds launched at speed around 150 m/s (depending on the airplane) against the structure. Pass fail criterion is the capability of the structure to avoid the penetration, during shots at critical impact points, of the bird after the main bulkhead. These tests are performed on high technological structures made of titanium, steel, aluminum alloy, carbon fibers, Kevlar fibers, honeycomb and special acoustic panels. The result is that the certification shots require a strong effort for the industries that must build several of these structures. In the last years a new procedure has been accepted where the producer can provide a FEM simulation before the first certification shot and, if the comparison between the simulation and the test is accepted, the following shots can be performed numerically. The comparison is usually based on the deformations and failures found in the structures. Lately also the amount of bird penetrating the structure is used as indicator.

The same approach has been used for helicopter fuel tank approval where simulations of impact tests have been used to certify the AB139 Agusta Westland helicopter.⁽²¹⁾ The design of helicopters for crashworthiness is based on US military specification MIL-STD-1290A. One component of helicopter crashworthiness is the design of the fuel tanks. The fuel tanks must not rupture in a crash so a standard impact condition is specified for the approval of fuselage and tank designs. Invernizzi describes a recent example where an LSDYNA model of a cross-section of the helicopter including the fuel tanks was developed. Vertical drop impacts were performed at the drop-test facility at the Politecnico di Milano of the same AB139 Agusta-Westland design. The deformed shapes and location of tank-seam failures were compared between the test and the simulation to validate the computation model. The validated model can then be used to develop improved designs and the approval of the design can be based on the computation model without the necessity of performing another full-scale drop test.

Finite element simulation programs like LSDYNA have been used to design and evaluate rolling stock for several years. While crash tests with full-scale trains are occasionally performed such tests are obviously very expensive and the number needs to be minimized when developing new designs. The draft European Standard prEN 15227 is aimed at the approval and self-certification of rail car crashworthiness.⁽¹⁴⁾ prEN 15227 identifies four basic impact scenarios and allows the design to be evaluated using computer simulations which are then

validated against at least one full-scale test. The standard encourages building models of the major subassemblies and then calibrating the models with the results of experiments on the assemblies. Once the assemblies are calibrated, the full model of the rail car is developed and subjected to the four reference crash scenarios. Generally, the objective in designing rail cars is to absorb energy in particular areas of the rail car and to provide “survival space” for occupants. prEN 15227 states that if the total energy absorbed and the total stroke of the computational model is within 10 percent of the validation test, then the result is acceptable. A plot of the total force versus time curve is also required and the norm states that high frequency spikes shorter than 5 msec in the numerical calculation can be ignored. This rail car approval process allows designers to create designs using computer models and then validate the results based on comparison with a physical test corresponding to the worst-case crash scenario. If the model adequately predicts the results for this one physical test, then the model results for all other crash scenarios are considered valid and may be used as the basis of approval.

Kokkins et al also developed a technique to simulate the dynamic, nonlinear structural behavior of moving rail vehicles during a collision.(22) Kokkins considered the interdependence of the many vehicles connected in a typical train. He accomplished this by the innovation of combining the dynamic modeling of the overall model with embedded detailed models of the lead locomotive, other railcars in the overall model and the objects with which it collides, including standing car and ISO-type shipping containers. LSDYNA was used to simulate the three-dimensional effects of non-linear, elastoplastic material behavior in addition to the effects of large deflections, buckling, energy absorption, and fracture. It was possible to generate and visualize the collision process and view the most significant locomotive structural deformations, movements, and decelerations. These insights into the structural performance and interactions of the various areas of the locomotive, including the cab and interior areas, relate directly to crew survivability in collisions. Several types of locomotive design improvements were also assessed with this method. Validation studies using a historical accident were also performed.

Dynamic finite element methods are also being used in the medical device industry to design implants such as heart valves, pacing lead coils, and artificial joints.(23,24) Analysis is particularly important for medical devices since performing experiments in living human beings under typical *in vivo* conditions is not only expensive and extremely risky but is also of questionable morality. Before such experiments can be performed, the developer must have a high degree of confidence in the design.

Another interesting example is the evaluation of ship hull designs. Full-scale testing of ships is extremely complex and extremely expensive, and by the time the first hull is built, it is difficult to make any large changes in the structure. The U.S. Navy (USN) has been investigating the use of LSDYNA to design ships for blast loadings but before the process could be used widely the USN decided to validate LSDYNA models using several prior full-scale shock experiments. (25) Five full-scale ship shock trials have been performed over the

past 20 years involving the AEGIS class ships. Each shock trial involves detonating an underwater blast and measuring the response of the ship structure at a large number of locations on the ship. Didoszak *et al* describes a validation of an LSDYNA model of an AGEIS guided missile destroyer (DDG 81) compared to a full-scale shock trial. The results were compared quantitatively using the Russell Comprehensive metric described in a later section. The results of the comparison were generally good and the USN decided that the use of LSDYNA models was appropriate for the evaluation of ship hull designs in blast loadings.

The validation procedures discussed above all conform to the recommended validation and verification process described by ASME V&V 10-2006 and illustrated in Figure 3. The first step in each procedure is determining the physical responses of interest and formulating a conceptual model. At this point, the process breaks into two separate paths, one involving computational modeling and the other involving physical experiments. In the computational modeling branch, the mathematical model is developed, calibrated and verified and then used to produce numerical simulations of the “reality of interest.” On the experimental branch, experiments are performed that provide useful tests of the phenomena being investigated. The two branches come back together in the validation stage where the results of the simulations are compared with the results of the experiments. If the results agree, the model is validated and can then be used to investigate other scenarios.

Metrics

Introduction

Visually comparing time histories from computational and experimental results to assess the degree of similarity is the most common way of qualitatively validating a model. For example, Figure 4 shows two time histories. An evaluator might look at the results and consider the two curves substantially similar since they “look” similar—since this way of comparing computational and experimental results on the same graph is no more than a subjective comparison, it is qualitative rather than quantitative validation.

Qualitative comparison between experimental and numerical results cannot provide several important features such as: quantification of numerical difference between the experiment and calculation, quantification of computational uncertainties (e.g., model sensitivity to the change of some parameters or poorly defined boundary conditions) and an estimate of the experimental and calculation uncertainty. If comparisons are only qualitative, one reviewer’s “good” correlation may become another’s “poor” correlation, and since the evaluation is qualitative, the inconsistency cannot be resolved. Approval decisions need to be based as much as possible on quantitative criteria that are unambiguous and mathematically precise.

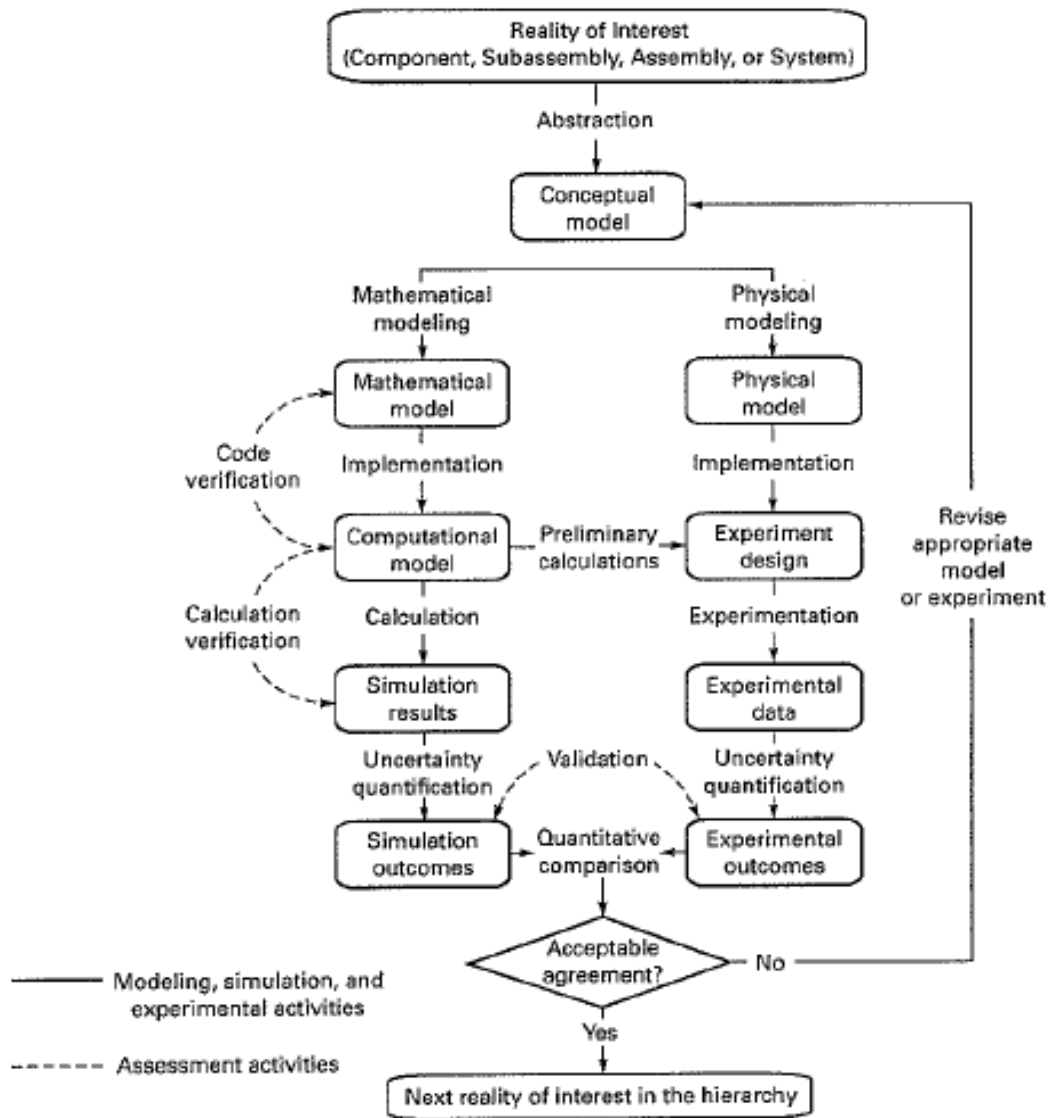


Figure 3. Typical validation and verification activities.(17)

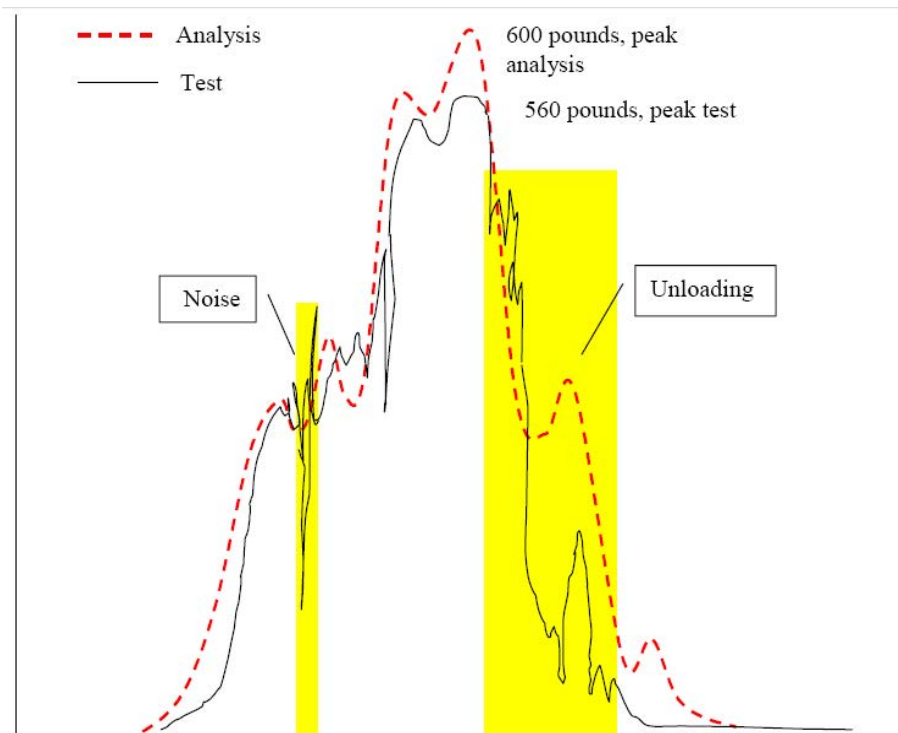


Figure 4. Comparison between experimental and analytical time history results.(13)

A validation metric is a “mathematical measure that quantifies the level of agreement between simulation outcomes and experimental outcomes.”(17) A variety of validation metrics can be found in literature but essentially they can be grouped into two main categories: (i) deterministic metrics and (ii) stochastic metrics. Deterministic metrics do not specifically address the probabilistic variation of either experiments or calculation—they are deterministic because given the same input the calculation results in the same result every time. Such metrics simply are characteristics that can be determined by examining the experiments and calculations. Stochastic metrics involve computing the likely variation in both the simulation and the experiment due to parameter variations.

There are two types of deterministic metrics: domain-specific metrics and shape comparison metrics. As discussed earlier, the intended use of the model helps to identify the domain-specific metrics. For the example of designing a railroad car, prEU 15227 requires comparing the energy absorption of the rail car for both the experiment and simulation.(14) In this case, the total energy absorption is a domain-specific metric that is relevant to rail car design but may not be relevant to some other type of design. Similarly, designing an aircraft seat involves comparing the Head Injury Criteria (HIC) number from the simulation to the HIC observed in an experiment.(13) The HIC in this case is a domain-specific metric that is only relevant to design situations in which dummy head impact is a part of the design criteria. One

step in choosing validation metrics, therefore, is to choose the parameters that are necessary when judging the performance of an experiment. Domain specific metrics are generally the same as the dynamic or crash test evaluation metrics in a particular design field. Just as aircraft seat and rail car designers use the metrics common in their respective crash test programs, roadside safety designers should use domain-specific metrics found in crash test guidelines like Report 350 and EN 1317.

The other type of deterministic metric involves comparisons of shape. In dynamic domains such as roadside safety design, aircraft crashworthy seat design, ship blast-worthiness or vehicle crashworthiness analysis, the shapes being compared are generally based on time history data (i.e., acceleration, velocity and displacement at a specific sensor location). Shape metrics found in the literature include the following:

1. Frequency domain metrics
2. Relative absolute difference of Moments of the two signals
3. Root Mean Square (RMS) log measure of the difference between two signals
4. Correlation Coefficient
5. Geer MPC Metrics
6. Knowles and Gear MPC metrics
7. Russell Metrics
8. ANOVA Metrics
9. Velocity of the Residual Errors

Once a particular deterministic metric is chosen, a procedure for deciding if the comparison is acceptable is necessary. There are two basic approaches to the developing an acceptance criteria: *ad-hoc* and probabilistic. *Ad hoc* acceptance criteria bases acceptance on community experience or engineering judgment. For example, the HIC value in an experiment might be found to be 352 and the corresponding simulation might result in a HIC of 398. The two values are similar but not identical. An *ad hoc* acceptance approach simply sets a criterion for the range of acceptable measurements without any real basis in the probabilistic variation of the parameters. Based on experience in the specific domain, for example, the FAA considers a HIC comparison that is within +/- 50 HIC units as sufficiently close. Based on the FAA criteria, therefore, the results of the simulation and experiment in this example would be sufficient. *Ad hoc* criteria are generally based on the experience of the community and the degree of closeness that the community feels it can achieve.

A better approach is to base the acceptance on the probabilistic variation of the experiments. For example, if 10 experiments are performed and the mean HIC is found to be 385 with a standard deviation of 11 HIC units, the analyst can estimate that the 90th percentile confidence limit for the HIC experiments is $385 \pm 1.65 \cdot 11 = 18$ HIC units. Stated another way, if 100 tests were performed, 90 of those should be in the range of 334 to 370 HIC units. In this case the simulation estimate of 398 is outside the 90th percentile confidence range so the conclusion would be that the simulation is not sufficiently close to the experiment. If the

simulation were as good as another experiment, the simulation result would have fallen in the specified range. This approach is better than the deterministic approach since it incorporates the uncertainty in physical experiments but it does require some *prior* knowledge about the level of uncertainty typical in experiments which may be difficult to obtain. These methods generally involve some type of classical hypothesis testing such as a t or z test or the Kamalgorov-Smirnov test. The subject of repeatability of crash tests is more completely discussed later in this chapter.

A validation metric, therefore, potentially has two parts: the deterministic metric and an acceptance criterion. The acceptance criteria may be either a deterministic *ad hoc* value or a probabilistically determined range. Domain-specific metrics should be chosen that correspond to the testing typically performed in a particular solid mechanics area to facilitate comparisons between physical tests and computational simulations.

Domain-Specific Deterministic Metrics in Roadside Safety

In the case of roadside safety, tests are performed and evaluated according to Report 350 in the US or EN 1317 in Europe. Both these crash testing guidelines include specific metrics like the occupant impact velocity, the occupant ridedown acceleration, THIV, ASI and exit conditions. Each of these metrics is calculated based on time history data collected in a crash test. Since the purpose of performing computer simulations is generally to design roadside hardware such that the Report 350 or EN 1317 test response can be predicted, it makes sense to include these test-based evaluation parameters in any discussion of validation.

Table 1, for example, shows a comparison between the Report 350 evaluation table and the results of an LSDYNA simulation for the Plastic Safety System CrashGard Sand Barrel System.(26) A model of the system was developed and then simulations of baseline full-scale crash tests were performed. The domain-specific results from the simulation are compared to the full-scale crash test results for test 3-31 in Table 1. The Report 350 evaluation table contains 14 specific evaluation metrics, eight of which apply to test 3-31. Of the eight evaluation criteria, six are pass/fail qualitative assessments (i.e., criteria C, D, F,G, K and L) based on the global performance of the system. The two remaining criteria (i.e., H and I) are calculated quantities based on the time histories.

As shown in Table 1, the qualitative criteria like “acceptable test article performance” (i.e., criterion C) and the detached fragment criterion (i.e., criterion D) can be used to compare results of crash tests and simulations. It is best if these criteria are unambiguous but the simulation results can be judged in the same way as the experimental results. Also shown in Table 1 are the deterministic domain-specific metrics occupant impact velocity (OIV) and occupant ride down acceleration (ORA) (i.e., criteria H and I). In these cases, the longitudinal OIV value is 20 percent greater than the experimental value so if 20 percent were the allowable acceptance criteria, this domain-specific metric would be acceptable. If the acceptance criteria were 10 percent, however, the longitudinal value would be judged not acceptable. This has

certain diagnostic value since a higher simulation value indicates the model may be too stiff so the analyst can investigate possible reasons. The ORA (i.e., criteria I) values in the longitudinal and lateral directions are both less than five percent so the simulation would be judged

Table 1. Report 350 evaluation criteria for test 3-31 on the Plastic Safety System CrashGard Sand Barrel System – test (left) and simulation (right).(26)

Evaluation Factors	Evaluation Criteria	Crash Test	FE	Difference %										
Structural Adequacy	A. Test article should contain and redirect the vehicle; the vehicle should not penetrate, underride, or override the installation although controlled lateral deflection of the test article is acceptable.	NA	NA	-										
	B. The test article should readily activate in a predictable manner by breaking away, fracturing or yielding.	NA	NA	-										
	C. Acceptable test article performance may be by redirection, controlled penetration or controlled stopping of the vehicle.	Passed	Passed	-										
Occupant Risk	D. Detached elements, fragments or other debris from the test article should not penetrate or show potential for penetrating the occupant compartment, or present an undue hazard to other traffic, pedestrians or personnel in a work zone.	Passed	Passed	-										
	E. Detached elements, fragments or other debris from the test article, or vehicular damage should not block the driver’s vision or otherwise cause the driver to lose control of the vehicle.	NA	NA	-										
	F. The vehicle should remain upright during and after the collision although moderate roll, pitching and yawing are acceptable.	Passed	Passed	-										
	G. It is preferable, although not essential, that the vehicle remain upright during and after collision.	Passed	Passed	-										
	H. Occupant impact velocities should satisfy the following:													
	<table border="1"> <thead> <tr> <th colspan="3">Occupant Impact Velocity Limits (ft/s)</th> </tr> <tr> <th>Component</th> <th>Preferred</th> <th>Maximum</th> </tr> </thead> <tbody> <tr> <td>Longitudinal and Lateral</td> <td>30</td> <td>40</td> </tr> </tbody> </table>		Occupant Impact Velocity Limits (ft/s)			Component	Preferred	Maximum	Longitudinal and Lateral	30	40	24.27 ft/s	29.2 ft/s	20
	Occupant Impact Velocity Limits (ft/s)													
	Component	Preferred	Maximum											
	Longitudinal and Lateral	30	40											
			0 ft/s	0 ft/s	NA									
<table border="1"> <tbody> <tr> <td>Longitudinal</td> <td>10</td> <td>15</td> </tr> </tbody> </table>		Longitudinal	10	15	NA	NA	-							
Longitudinal	10	15												
I. Occupant ridedown accelerations should satisfy the following:														
<table border="1"> <thead> <tr> <th colspan="3">Occupant Ridedown Acceleration Limits (g’s)</th> </tr> <tr> <th>Component</th> <th>Preferred</th> <th>Maximum</th> </tr> </thead> <tbody> <tr> <td>Longitudinal and Lateral</td> <td>15</td> <td>20</td> </tr> </tbody> </table>		Occupant Ridedown Acceleration Limits (g’s)			Component	Preferred	Maximum	Longitudinal and Lateral	15	20	10.9 g’s 1.8 g’s	11.4 g’s 1.6 g’s	4.5 11	
Occupant Ridedown Acceleration Limits (g’s)														
Component	Preferred	Maximum												
Longitudinal and Lateral	15	20												
J. (Optional) Hybrid III dummy responses.		NA	NA	-										
Vehicle Trajectory	K. After collision it is preferable that the vehicle’s trajectory not intrude into adjacent traffic lanes.	Passed	Passed	-										
	L. The occupant impact velocity in the longitudinal direction should not exceed 40 ft/sec and the occupant ridedown acceleration in the longitudinal direction should not exceed 20 G’s.	Passed	Passed	-										

	M. The exit angle from the test article preferable should be less than 60 percent of test impact angle, measured at the time of vehicle loss of contact with test device.	NA	NA	-
	N Vehicle trajectory behind the test article is acceptable.	NA	NA	-

acceptable by this domain-specific metric if the acceptance criteria were either 10 or 20 percent. The point of Table 1 is to show that the same experimental evaluation metrics can be used as deterministic domain-specific metrics when comparing full-scale crash test experiments to simulations.

The EN 1317 values like THIV, PHD and ASI could likewise be used as deterministic domain-specific validation metrics as shown in Table 2 for the same CrashGard Sand Barrel System shown in Table 1.(26) Another interesting feature of the metrics in Table 2 is the use of time as an evaluation criterion. Not only can the value of the metric (i.e., the THIV or PHD) be used but the time of arrival of that metric can likewise be used to assess the validity of the simulation.

Table 2. EN 1317 evaluation criteria for test 3-31 on the Plastic Safety System CrashGard Sand Barrel System – test (right) and simulation (left).(26)

FEA Results vs Test TRC 061111 (T3-41)		
	FEA (430 ms of event)	Test (430 ms of event)
Impact Velocity (m/s)		
x-direction	7.4	8.9
y-direction	0.0	0.4
THIV (km/hr):	26.6	32.1
THIV (m/s):	7.4	8.94
Ridedown Accelerations (g's)		
x-direction	-11.4	-10.9
y-direction	-1.8	-1.6
PHD (g's):	11.4	11.5
ASI:	0.66	0.68
Max. 50msec Moving Avg. Accelerations (g's)		
x-direction	-7.7	7.7
y-direction	-0.8	-0.9
z-direction	1.6	-2.8

Deterministic Shape Metrics with ad-hoc acceptance criteria

The following section presents the details of all the common shape-comparison metrics found in the literature review. The basic method for calculating the metric is presented along with a reference to its original derivation. If the metric has been used in a design and evaluation project the paper or report is cited. In all the following sections, the terms m_i and c_i refer to the measured and computed quantities respectively. The “i” subscript indicates the measurement at a specific instant in time.

When comparing two or more time histories, the simplest technique is the point-to-point comparison in which the magnitude of the curve (e.g., the acceleration) at a particular point in time in the experiment is compared to the magnitude of the simulation curve at the corresponding time. Point-to-point comparisons are performed in the time domain. When the comparison involves a time varying quantity, it is possible that there may be a time shift between the two curves.

When comparing two time histories, the magnitude and the phase should be considered simultaneously.

Frequency Domain

The NARD Validation Manual provides three validation metrics in the frequency domain for the comparison of transformed signals of the measured curve, $M(\omega)$, and the transformed signal of the computed curve, $C(\omega)$:(27)

- The relative absolute difference of amplitude of two signals,
- The point-wise absolute difference of amplitudes of two signals and
- The root-mean-squared (RMS) log spectral difference between two signals.

The time domain signal is transformed into its corresponding frequency domain signal using a Fourier transformation. Any time domain signal can be expressed in the form:

$$f(t) = \sum_{-\infty}^{\infty} A_n \cos(n\omega t) + B_n \sin(n\omega t)$$

If A_m and B_m are coefficients of M_t and A_c and B_c are coefficients of C , the point-wise absolute differences are defined as:

$$\Delta_A = |A_m - A_c| \quad ; \quad \Delta_B = |B_m - B_c|$$

The relative absolute difference is defined as:

$$\Delta AB_{rel} = \left| \sqrt{A_m^2 + B_m^2} - \sqrt{A_c^2 + B_c^2} \right|$$

For both the point-wise absolute differences and the relative absolute difference, the measured and computed curve are considered by the NARD Validation Manual to be close to one another if the difference is less than 20 percent.

The RMS log spectral distance measures the distance between the smooth power spectra of the measured and computed signals. In order to define the smooth power spectrum, it is first necessary to define the auto covariance functions associated with the measured and computed signals:

$$\left\{ \begin{array}{l} C_m(\tau) = \lim_{T \rightarrow \infty} \frac{1}{T} \int_{-T/2}^{T/2} m(t)m(t+\tau)dt \\ C_c(\tau) = \lim_{T \rightarrow \infty} \frac{1}{T} \int_{-T/2}^{T/2} c(t)c(t+\tau)dt \end{array} \right.$$

The smooth power spectrum of the measured and calculated functions is defined as:

$$\left\{ \begin{array}{l} \Gamma_m(\omega) = \int_{-\infty}^{\infty} w(\omega)C_m(\tau)e^{-i\omega\tau} d\tau \\ \Gamma_c(\omega) = \int_{-\infty}^{\infty} w(\omega)C_c(\tau)e^{-i\omega\tau} d\tau \end{array} \right.$$

where $w(\omega)$ is the spectral window.

Eventually, the RMS log spectral distance in units of decibels (db) is given by:

$$D = \frac{1}{2\pi} \int_{-\pi}^{\pi} \left| \ln(\Gamma_m(\omega)/\Gamma_c(\omega)) \right|^2 d\omega$$

The smaller the RMS log spectral distance between the signals is, the closer the signals are. A distance of 20 db or less indicates that the difference between the signals is not more than 20 percent. Both the RMS log spectral distance and the relative absolute RMS are deterministic metrics with an *ad hoc* acceptance criterion of 20 percent.

In the Roadside Safety literature no application of the NARD frequency analysis metrics was found. In fact, no example of the use of frequency domain metrics was found in any of the solid mechanics literature. This may be due to the difficulties which arise when trying to apply these particular metrics to the very short time histories of a crash event.

Time Domain

Comparisons based on time-domain point-to-point measures are far more common in a variety of solid mechanics domains.

Relative Absolute difference of Moments of the two signals

One of the simplest ways to compare two signals is to compare the moments of the shapes as proposed by the NARD Validation manual.(27) The relative absolute difference of the moments is based on the comparison of the moments of the area under the time history curve. Moments are mathematical characteristics of a shape (e.g., moments of inertia) and can be defined by the following general expression:

$$M_{j,m} = \sum_{i=1}^n t_i^j m_i \cdot \Delta t$$

$$M_{j,c} = \sum_{i=1}^n t_i^j c_i \cdot \Delta t$$

The lower order moments have some physical meaning. For example, the zero order moment ($j = 0$) when divided by the number of samples is the average acceleration. The 1st order moment ($j = 1$) divided by the 0th order moment locates the time at the centroid of the time history. Moments of order greater than one have little physical meaning when comparing time histories and are simply mathematical characteristics of the shapes. The more moments (i.e., shape characteristics) that two shapes have in common the more likely, in a general sense, they are to represent the same shape. If enough characteristics of the measured acceleration history shape match the characteristics of the calculated acceleration history the shapes should be similar. The ratio R between the difference of the n^{th} moment of a measured (m_i) and a calculated (c_i) signal and the n^{th} moment of the calculated signal is given by:

$$R = \frac{\left| \sum_{i=1}^n t_i^n m_i - \sum_{i=1}^n t_i^n c_i \right|}{\sum_{i=1}^n t_i^n c_i}$$

The NARD validation procedure recommends that the 0th through 5th relative differences of the moments defined by equation (8) be calculated. The NARD Validation Manual arbitrarily considers the measured and calculated moments to be similar if the absolute difference between the respective moments of order n $M_n(m_i)$ and $M_n(c_i)$ is less than 0.2. All the relative moment metrics are, therefore, deterministic shape metrics with an *ad hoc* acceptance criterion of 20 percent.

Interestingly, the NARD validation procedure makes the comparison with respect to the calculated value rather than the experimental value. It is more appropriate to make the comparison with the experimental value since, from a validation point of view; the experimental value is the “true” response.

Root Mean Square (RMS) log measure of the difference between two signals

The mean value of a signal is simply the algebraic sum of the values divided by the number of values.(27) Similarly, the mean squared is the algebraic sum of the square of the values divided by the number of values. If the square root of the mean squared is taken, the root mean square (RMS) of the measured and computed signals are obtained as shown below:

$$RMS_m = \sqrt{\frac{1}{n} \sum_{i=1}^N m_i^2}$$

$$RMS_c = \sqrt{\frac{1}{n} \sum_{i=1}^N c_i^2}$$

The RMS is the average value of the signal without respect to its sign. The RMS of two signals can be compared by taking the difference of the two RMS and dividing by the average of the two RMS as follows:

$$\Delta RMS^r = \sqrt{\frac{\sum_{i=1}^N m_i^2 - \sum_{i=1}^N c_i^2}{\left(\sum_{i=1}^N m_i^2 + \sum_{i=1}^N c_i^2\right)/2}}$$

As with the relative moments, the choice of denominator is ambiguous. For moments, the difference is calculated with respect to the calculated signal whereas for the relative RMS, the difference is calculated with respect to the average. Again, since these are validation metrics, the “true” experimental solution should be the reference value in the denominator.

Like the relative moments, the RMS is simply a characteristic of a particular shape. In the case of an acceleration time history, it is the average value of the accelerations without respect to the sign.

The logarithmic form of the RMS difference can also be considered, as suggested by the NARD Validation Manual:

$$\Delta RMS_{\log}^r = \sqrt{\frac{2 \sum_{i=1}^N 10 \log(m_i^2 / c_i^2)^2}{\sum_{i=1}^N \left(10 \log(m_i^2)^2 + 10 \log(c_i^2)^2\right)}}$$

Both the relative RMS and the logarithmic relative RMS are deterministic shape metrics with an *ad hoc* acceptance criteria of 20 percent.

Correlation Coefficient

The correlation coefficient, proposed in the NARD Validation Manual, measures the correlation between two signals.(27) Correlation in this context does not mean that the signals are identical but only that one can be linearly transformed into the other. The correlation coefficient is, therefore, a measure of the relative phasing of the two signals. The correlation coefficient of two signals is given in the NARD Validation Manual as:

$$\rho = \frac{\sum_{i=1}^N c_i m_i}{\sqrt{\sum_{i=1}^N c_i^2} \sqrt{\sum_{i=1}^N m_i^2}}$$

The closer the correlation ratio is to unity, the more the calculated and measured signals can be linearly transformed into each other. Several applications of the NARD validation metrics were found in literature for roadside safety finite element simulations. For example Ray, in an unpublished paper quantitatively evaluated four finite element models using the NARD metrics in the time domain among others.(28) The results of Ray's analysis will be described in a later section. In 2000, Tabiei and Wu used the RMS log measure of difference and correlation coefficient to quantitatively validate the results obtained from a finite element model of a strong-post W beam guardrail system and a pick-up truck.(29) In 2005, Atahan and Cansiz used the relative absolute difference of moments between two signals to quantitatively evaluate the accuracy of the results from a baseline simulation of a full-scale test of a guardrail to bridge rail transition with a pick-up truck.(30) The correlation coefficient is, therefore, a deterministic shape metric with an *ad hoc* acceptance criterion.

Geers MPC Metrics

Geer developed a three part metric that includes quantitative assessments of the magnitude and phase which are then combined into a single value that represent the whole comparison.(31) First, the magnitude and phase components of the metric are calculated. The two components (i.e., M and P) are then combined into a single metric (C) that represents the combined effect of both magnitude and phase. All the Geers metrics are arranged such that the values range from zero to unity with values closer to zero representing a higher level of agreement. The Geers MPC metrics are defined by the following summations:

$$M_G = \sqrt{\left[\frac{\sum_{i=1}^N c_i^2}{\sum_{i=1}^N m_i^2} \right]} - 1$$

$$P_G = 1 - \left[\frac{\sum_{i=1}^N m_i c_i}{\sqrt{\sum_{i=1}^N m_i^2 \sum_{i=1}^N c_i^2}} \right]$$

$$C_G = \sqrt{M_G^2 + P_G^2}$$

Geers showed that the phase component is insensitive to magnitude differences but is sensitive to differences in phasing or timing between the two time histories. Similarly, the magnitude component is sensitive to differences in magnitude but relatively insensitive to differences in phase. These characteristics give the Geers metrics good diagnostic value since they identify the aspects of the curves that do not agree. For example, if the phase metric is acceptable but the magnitude metric is not, the analyst can examine the stiffness and strength of the model to make sure it is correct. As a note, the Geers magnitude metric can be simply seen as the one subtracted from the ratio between the measured and calculated root RMS signals defined in the NARD validation metrics, while the Geers phase metric is one minus the square root of the correlation coefficient.

Once the magnitude component and the phase component have been calculated, the combined metric C is calculated by combining the two component metrics into a single value. All the components of the Geer metrics range between zero and unity with values of zero corresponding to exact agreement between the curves. The components can be thought of as coordinates of a circle where the M and P values define the coordinates of a point on the circle and C defines the radius.

Sprague and Geers later modified the phase component of the MPC metrics in order to better scale the magnitude and phase components. They found that the original formulation of the phase component did not scale similar to the magnitude component. (32) A magnitude component of 10 percent, for example, did not reflect the same degree of comparability as a phase component of 10 percent. Sprague and Geers modified the original MPC metrics to include a trigonometric term that helped the two components scale more similarly. Sprague and Geers used a phase formulation based on Russell, a metric discussed later in this section. The Sprague and Geers is structured in the same way as the original version with magnitude, phase and combined metrics. Only the phase component is different. The three components of the Sprague and Geers metric are given by the following equations:

$$M_{SG} = \sqrt{\frac{\sum_{i=1}^N c_i^2}{\sum_{i=1}^N m_i^2}} - 1$$

$$P_{SG} = \frac{1}{\pi} \cos^{-1} \left[\frac{\sum_{i=1}^N m_i c_i}{\sqrt{\sum_{i=1}^N m_i^2 \sum_{i=1}^N c_i^2}} \right]$$

$$C_{SG} = \sqrt{M_{SG}^2 + P_{SG}^2}$$

Knowles and Gear MPC metrics

The most recent variation of an MPC-type metric is the Knowles and Gear metric.¹(32) Like Geers's original metrics and the Sprague and Geers metrics, the Knowles and Gear metrics are composed of three parts: a magnitude component, a phase component and a combination parameter. As in the other versions of these metrics, the values range between zero and unity with zero representing exact agreement between the curves. Knowles and Gear recognized that if two shapes were arbitrarily shifted from each other the phase component may erroneously indicate poor phase correlation that was simply due to not synchronizing the two signals. For example, if the time of impact was not precisely defined in the experimental curve, some of the phase error might actually be due to the poor identification of the impact point. Before a good comparison of the phasing can be performed, the two signals must be synchronized so they start at the same point.

Synchronizing the signals was accomplished by defining the time of arrival (TOA). The TOA of a time history is the time at which the time history attains some percentage of the maximum wave form value. Typically, for time histories with relatively fast rise times, a range of 5 – 10% is recommended, but this range may be changed in case of slower rise times. Defining TOA_c and TOA_m as the times of arrival of the simulation and measured time histories respectively, then the TOA metric is defined as:

$$M_{TOA} = \frac{|TOA_c - TOA_m|}{TOA_m}$$

The magnitude component M_{KG} of the Knowles and Gear metric is defined as a weighted sum-of-squared differences between the simulated and measured time histories. Considering a discrete time history characterized by N time samples, M_{KG} is defined as:

$$M_{KG} = \sqrt{\sum_{i=1}^N Q_i (\tilde{c}_i - m_i)^2 / QS}$$

where, m_i is the measured time history at the i^{th} sample and $\tilde{c}(t) = c(t - \tau)$ is the time-of-arrival shifted simulation history (i.e., if TOA_c and TOA_m are the times of arrival of the simulation and measured time histories and $TOA_c > TOA_m$, then $\tau = TOA_c - TOA_m$). Shifting the simulation time history using the function $\tilde{c}(t)$ instead of $c(t)$ allows the metric to focus only on the magnitude comparison between the curves without complications arising from the asynchronous signals. Q_i and QS represent respectively the weighting and normalization factors.

¹ Note that Geers and Gear are two different people.

The weighting factor is designed to scale the sum-of-squares differences to the maximum value of the measurement to the maximum value of the measurement:

$$Q_i = \left(\frac{|m_i|}{m_{\max}} \right)^p (t_{i+1} - t_{i-1})$$

where, a unit value of p is recommended to place more weight on the large values of $m(t)$.

In order to avoid creating a gap between time histories characterized by a large magnitude and those characterized by a smaller one, the magnitude has to be normalized. In this metric, the normalization factor QS is chosen to define a value of unity when the magnitude of the time histories differs by 100 percent:

$$QS = \sum_{i=1}^N \left(\frac{|m_i|}{m_{\max}} \right)^p m_i^2 (t_{i+1} - t_{i-1})$$

If a uniform time sampling is chosen, the magnitude component simplifies to the following form:

$$M_{KG} = \sqrt{\frac{\sum_{i=1}^N \left(\frac{|m_i|}{m_{\max}} \right)^p (\tilde{c}_i - m_i)^2}{\sum_{i=1}^N \left(\frac{|m_i|}{m_{\max}} \right)^p (m_i)^2}}$$

In an analogous case as for the Gears metrics, once the magnitude component and the phase component have been evaluated, the Knowles and Gear combination metric is evaluated by combining the two component metrics by mean of a weighted average:

$$C_{KG} = \sqrt{\frac{10M_{KG}^2 + 2M_{TOA}^2}{12}}$$

In the Knowles and Gear combined metric, the magnitude and phase factors are weighted such that the phase value does not dominate the combined metric. The main limitation of the Knowles and Gear metric is that it cannot differentiate between an under or over prediction because it is based on the sum of the square differences between the measured and the simulation curve. The C_{KG} metric represents the comparison of a single response quantity like the acceleration time history of the vehicle center of mass. The Knowles and Gear metric can be also applied in a more general case when different system response quantities are considered at the same time.

Russell Metrics

Another metric based on the concept of magnitude and phase differences between two curves was developed by Russell in 1997. (33) Russell defined the relative magnitude error between the measured and computed curve as:

$$m = \frac{\sum_{i=1}^N m_i^2 - \sum_{i=1}^N c_i^2}{\sqrt{\sum_{i=1}^N m_i^2 \cdot \sum_{i=1}^N c_i^2}}$$

The phase correlation between the measured and computed curve is:

$$p = \frac{\sum_{i=1}^N m_i \cdot c_i}{\sqrt{\sum_{i=1}^N m_i^2 \cdot \sum_{i=1}^N c_i^2}}$$

Hence Russell derived the magnitude and phase error respectively from the corresponding relative magnitude error and phase correlation. The resulting form for the magnitude error is:

$$M_R = \sin(m) \log_{10}(1 + |m|)$$

The phase error is computed as:

$$P_R = \frac{\cos^{-1}(p)}{\pi}$$

The comprehensive error of the Russell's metric is defined as:

$$C_R = \sqrt{\frac{\pi}{4} (M_R^2 + P_R^2)}$$

Shin and Schneider used the Russell metrics to evaluate the blast-worthiness of a naval ship.(34) An experiment using the DDG51 class vessel USS *Winston Churchill* was replicated with an LSDYNA model. As illustrated in Figure 5, the ship was instrumented with 30 accelerometers at various locations to measure the local accelerations in the ship hull when the vessel was in the vicinity of a blast.

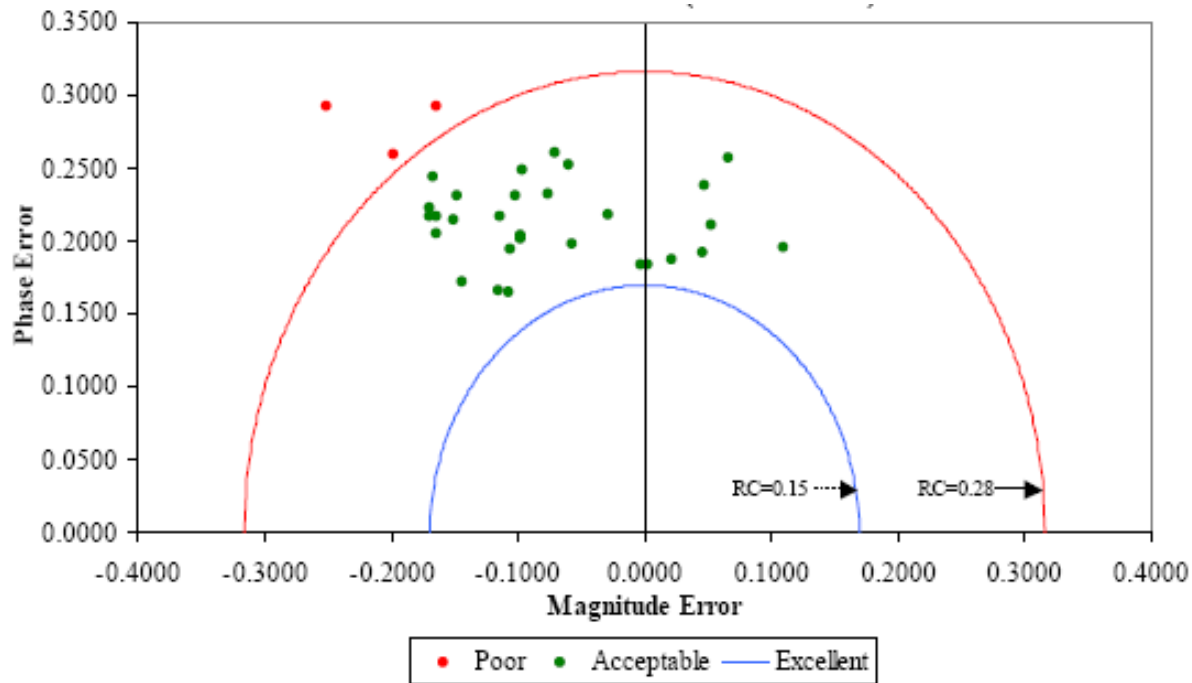


Figure 5. Russell metrics for 30 accelerometers in a ship blast model validation.(34)

The magnitude and phase components of the Russell metrics were computed and then the results for all the sensors were plotted as shown in Figure 5. The two component metrics can be considered coordinates of a point with the magnitude component plotted on the x axis and the phase component on the y axis. The radial distance to the origin represents the combined metric. The RC (Russell Combined) values shown in Figure 5 represent the values of the combined metric for two different acceptance levels. If the combined metric is less than 0.15 (i.e., 15 percent) the comparison is excellent. If the combined metric is between 0.15 and 0.28, the comparison is acceptable whereas if the combined metric is greater than 0.28, the comparison is unacceptable. Figure 5 shows not only of the use of the Russell metrics but the combination of sensor data from a number of different sensors on the same plot to assess the overall utility of a model. For example, the three data points outside the acceptable range in Figure 5 might not invalidate the whole model, but they call the analyst's attention to regions in which the experiment and calculation did not agree.

Shin and Schneider also plotted the Russell combined metric against the longitudinal position of the sensor as shown in Figure 6.(34) This figure clearly shows that the results of the comparison degraded at sensors located at the extreme ends of the vessel. This plot helps the analyst and the experimenter to identify problems with the model or with the location and mounting of sensors that can be used to improve both subsequent experiments and model development.

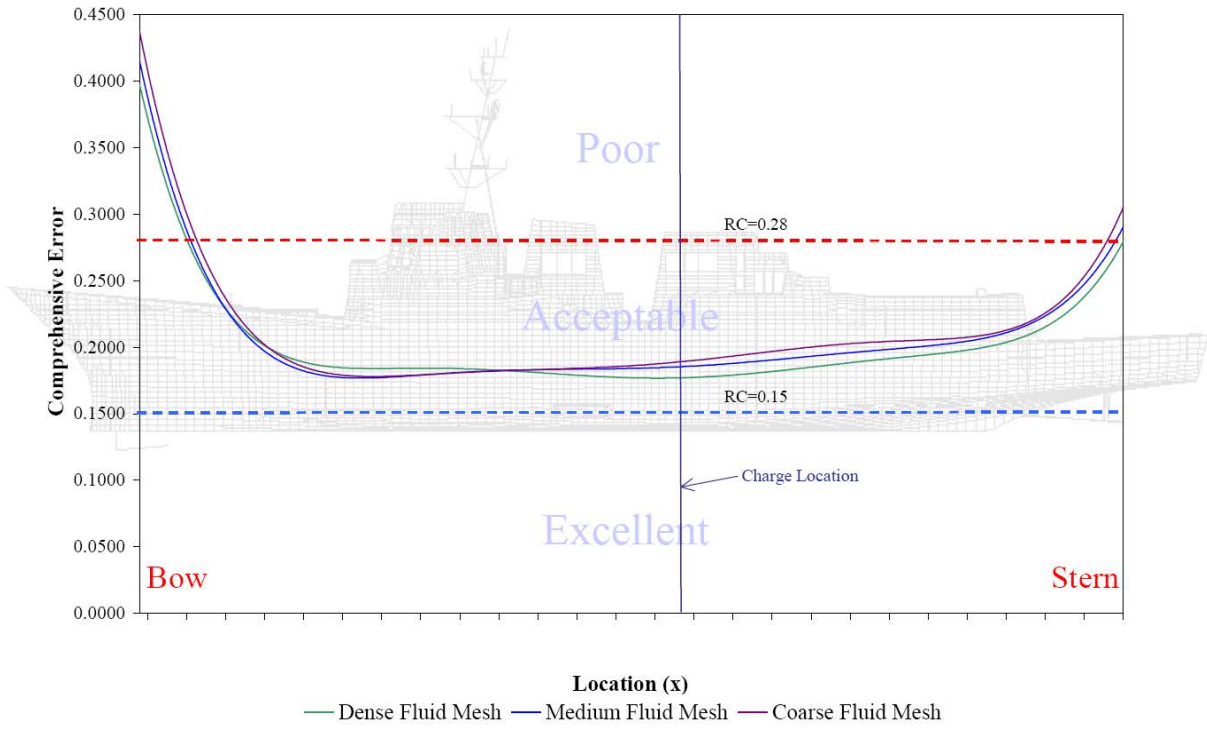


Figure 6. Russell combined metric plotted versus the longitudinal position of the sensor in a ship blast validation activity.(34)

ANOVA Metrics

Analysis of variance (ANOVA) is a standard statistical technique that is commonly used in the analysis of statistical data and for building regression models. Ray suggested a series of simple statistical tests based on an analysis of the variance of the residuals (i.e., differences) between repeated crash test acceleration histories.(35) If two time histories are assumed to represent the same event, the differences between them (i.e., the residuals) should be attributable only to random experimental error. Hence, if the residuals are truly random, then they should be normally distributed around a mean error of zero (i.e., typical bell-shaped Gaussian distribution). If the mean error is not zero and the error distribution does not conform to random experimental error, then it can be reasonably concluded that there is some underlying systematic error (i.e., there is some physical reason that the curves are different).The assumption that residuals are normally distributed about a mean of zero can be examined by means of a paired t-tail test performed with the mean and standard deviation:

$$T = \frac{\bar{e}}{\sigma/\sqrt{n}}$$

where \bar{e} is the average residual between the two curves, σ is the standard deviation of the residuals and n is the number of paired samples. For convenience in comparing different types of impacts, the average residual \bar{e} and the standard deviation of residuals σ may be divided by the maximum observed experimental value (e.g., the peak measured acceleration) to obtain the relative average residual error, \bar{e}^r , and the relative standard deviation of the residual errors, σ^r .

The terms \bar{e}^r and σ^r are calculated as follows:

$$\bar{e}^r = \frac{\sum_{i=1}^n (m_i - c_i)}{m_{\max}} \cdot \frac{1}{n}$$
$$\sigma^r = \sqrt{\frac{1}{n} \sum_{i=1}^n (m_i - c_i - \bar{e}^r)^2}$$

When two time histories represent the same physical event, both time histories should be identical such that \bar{e} and σ are zero, but this is almost never the case in practical situations since experimental error causes small variations between tested responses. The conventional T statistic provides an effective method for testing the assumption that the observed \bar{e} is close enough to zero to represent only experimental error. In fact, the t -test indicates if the differences

between the two responses can be reasonably attributed to normal experimental error without having a series of repeated tests. One of the biggest advantages of the t -test is that it requires only two curves: a test curve and a simulation curve.

In order to correctly evaluate the residuals, it is important that the two time histories are correctly paired. In case there is a random offset between the two time histories, the most probable starting point can be obtained using the method of the least squares, analogous to the standard use of least squares in surveying to balance a traverse so that it closes. Although synchronizing the two signals was discussed in the previous section regarding the Knowles and Gear metrics, the method of least squares is a better approach because it is not based on an arbitrary point in the curve as Knowles and Gear assumed for the TOA metric but is based on minimizing the error between the curves for the whole event. With the method of least squares, the residual area is calculated and the curves are shifted in time with respect to each other until the error (i.e., the area of the residuals) is at a minimum. This point is the statistically most likely point of synchronization. Ray implemented the least squares method to find the most likely synchronization point in his computer program CTRP.(35)

The analysis of residuals should be performed only on measured time histories and not on time histories mathematically derived from primary measurements (e.g., velocity obtained from the integration of the acceleration). In fact, certain numerical operations such as integration cause an accumulation of the residuals that are supposed to be independent from one instant to another. While Ray discusses this explicitly, this is really the case for all the metrics discussed in this section in which sensor data is used to compare curves. Comparisons (and therefore validations) should always be made using the original data from the sensor (e.g., accelerations from an accelerometer, rotation rates from a rate transducer or displacements from a string-pot displacement transducer).

Ray proposed the following acceptance criteria based on an examination of repeated crash tests of rigid poles:

- The average relative residual (i.e., \bar{e}^r) should be less than 5 percent,
- The standard deviation of the residuals (i.e., σ^r) should be less than 20 percent and the t -statistic should be calculated between the test and simulation curve. The absolute value of the calculated t statistic should be less than the critical t -statistic for a two-tailed t -test at the 5-percent level, $t_{0.005,\infty}$ (90th percentile).

Once the mean and variance of the residual distribution are known, they can be used to plot an envelope around the average response (i.e., the admissible error corridor). In order to be considered the same events, the curve obtained from the simulation should be always inside the above defined corridor. Ray developed the computer program CTRP (mentioned above) that calculated these metrics along with the original Geer metrics and NARD validation metrics.

The analysis of variance method involves three deterministic metrics with acceptance criteria that are based on the probabilistic distribution of expected variation between crash tests.

Apart from the work in which Ray proposed the ANOVA metrics, the above described analysis of variance method has been applied as a validation procedure by some other authors in the roadside safety literature.(35) In 1998, Sean and Wekezer applied this metric to compare the results from a finite element simulation and a full crash of a pick-up truck against a G2 guardrail. In 2005, Atahan and Cansiz applied the analysis of variance metrics to compare a baseline finite element model of a full-scale test of a guardrail to bridge rail transition with a pick-up truck.(30) Ray also used this method in several projects that will be mentioned later in our discussion of the repeatability of full-scale tests.

Larsson, Petterson and Svensson used Ray’s method to develop a JAVA program called “Curve Analyzer v1.0.”(130) CurveAnalyzer inputs the accelerations from two curves. The user can perform several adjustments like shifting the baseline, shifting the times (presumably to achieve better synchronization), changing units (e.g., from msec to secs or G’s to m/s²), etc. Once the analyst is satisfied with the two curves, the mean and maximum residuals, standard deviation of the residuals, and correlation coefficient are computed in the “analysis” phase of the program. Finally, the “results” phase of the program presents the values obtained and indicates if the curves have passed the criteria. For example, the T test must be satisfied at the 95 percentile confidence level, the correlation coefficient must be greater than 0.8, the mean residual must be less than 20 percent, etc. CurveAnalyzer uses essentially the same acceptance criteria proposed by Ray with the exception that the mean residual must be less than 20 percent rather than 5 percent. The CurveAnalyzer program has been used to some degree by members of the ROBUST team in comparing curves although documentation of results has not been found. One other interesting feature of the program is that it allows the user to restrict the area of analysis to a particular window in time. This way the analyst can look at the whole impact event or some portion of the event. This is often a useful way of finding out where in time problems in a comparison might occur.

Oberkampf et al. developed a metric they called the “simple validation metric, VM.” (16). They define this metric as:

$$VM = 1 - \frac{1}{N} \sum_{i=1}^N \tanh \left| \frac{c_i - m_i}{m_i} \right|$$

The term $\frac{c_i - m_i}{m_i}$ is the point-by-point residual error between the computational and measured curve. The error is normalized by the value of the experimental measurement. The tanh function is used to map the result into the zero to unit space. The summation is the sum of all the residual errors between the measured and computed result so dividing by N yields the

average residual error. After using this metric it became apparent that the tanh function did not add much value so it was dropped.

Oberkampf and Barone continued the development of this type of validation metric based on the same concept of statistical confidence intervals used earlier by Ray. (36) They developed two specific metrics: one requiring interpolation of experimental data and another requiring regression (i.e., curve fitting) of experimental data. Although they developed it independently, Oberkampf and Barone's method, as will be shown shortly, is identical to the method proposed by Ray and discussed in the previous paragraphs. (35)

As Oberkampf and Barone were interested in an error measure between a deterministic computational result and the mean of the population of experimental measurements, their key issue was the statistical nature of the sample mean of the measured response of the system. In other words, they were particularly concerned with a statistical estimate of a confidence interval for the true mean of the residuals.

They first defined and constructed a statistical confidence interval for the population mean using sampled quantities for the mean and standard deviation:

$$\mu \sim \left(\bar{y} - z_{\alpha/2} \cdot \frac{s}{\sqrt{n}}, \bar{y} + z_{\alpha/2} \cdot \frac{s}{\sqrt{n}} \right)$$

where \bar{y} and s are respectively the sample mean and standard deviation based on n observations and $z_{\alpha/2}$ is the value of the random variable z (i.e., standardized random variable) for which the integral of Z from $z_{\alpha/2}$ to $+\infty$ is equal to α . From standard statistics, the level of confidence that μ is in the interval given by the above equation is $100 \cdot (1/\alpha)$ percent.

As the number of observations in an experiment is usually limited, they used a t distribution instead of a normal distribution resulting in the following test:

$$\mu \sim \left(\bar{y} - t_{\alpha/2,v} \cdot \frac{s}{\sqrt{n}}, \bar{y} + t_{\alpha/2,v} \cdot \frac{s}{\sqrt{n}} \right)$$

where $t_{\alpha/2,v}$ is the $1-\alpha/2$ quintile of the t distribution for $v = n - 1$:degrees of freedom.

The validation metric developed by Oberkampf and Barone was initially applied to the case of a scalar value and then extended to the case of a vector of values (e.g., functions of time or space).(36)

The main idea of the Oberkampf and Barone metric was to estimate an error of the computational result based on the difference \tilde{E} between the numerical solution, y_c , and the *estimated* mean of the population of the experimental results, \bar{y}_m .

$$\tilde{E} = y_c - \bar{y}_m$$

The second step to build their metric was to compute an interval containing the true error at a specified level of confidence. In order to achieve this target, the confidence interval expression was rewritten as an inequality relation using the above mentioned notation:

$$\bar{y}_m - t_{\alpha/2,v} \cdot \frac{s}{\sqrt{n}} < \mu < \bar{y}_m + t_{\alpha/2,v} \cdot \frac{s}{\sqrt{n}}$$

where μ is the true mean and s is the sample standard deviation given by:

$$s = \sqrt{\frac{1}{n-1} \sum_{i=1}^n (y_m^i - \bar{y}_m)^2}$$

Multiplying by -1 and adding y_c to each term, it becomes:

$$y_c - \bar{y}_m + t_{\alpha/2,v} \cdot \frac{s}{\sqrt{n}} > y_c - \mu > y_c - \bar{y}_m - t_{\alpha/2,v} \cdot \frac{s}{\sqrt{n}}$$

Defining the true error as:

$$E = y_c - \mu$$

where the inequality relation can be further rewritten as:

$$\tilde{E} + t_{\alpha/2,v} \cdot \frac{s}{\sqrt{n}} > E > \tilde{E} - t_{\alpha/2,v} \cdot \frac{s}{\sqrt{n}}$$

The inequality above represents an interval containing the true error with a level of confidence of $100(1-\alpha)\%$. Using a traditional level of confidence of 90%, the metric becomes:

$$\tilde{E} + t_{0.05,v} \cdot \frac{s}{\sqrt{n}} > E > \tilde{E} - t_{0.05,v} \cdot \frac{s}{\sqrt{n}}$$

Considering now the case for which the measured and the computed values are functions of an input variable x (e.g., acceleration vs. time), the following assumptions are necessary:

- The mean value of both the computed and measured results is obtained using a sufficient number of values over the range of the input variables.
- The input variables from the computation are measured much more accurately than the measured experimental values.
- Two or more experimental replications have been obtained and each replication has multiple measurements of the variable of interest over the range of the input values.
- The measurement uncertainty is given by a normal distribution.
- There is no correlation or dependence between one experimental replication and another.

With the previous assumptions, the metric can be easily rewritten as:

$$\tilde{E}(x) + t_{0.05,v} \cdot \frac{s(x)}{\sqrt{n}} > E > \tilde{E}(x) - t_{0.05,v} \cdot \frac{s(x)}{\sqrt{n}}$$

where the standard deviation $s(x)$ is defined as:

$$s = \sqrt{\frac{1}{n-1} \sum_{i=1}^n (y_m^i(x) - \bar{y}_m(x))^2}$$

Examination of the metrics developed by Oberkampf et al (16), Oberkampf and Barone (36) and Ray (35) show that they are, in fact, nearly identical. Barone and Oberkampf's term \bar{y}_m is almost identical to Ray's \bar{e}^r . The difference is that Ray sums all the residuals and then divides by the peak measured response whereas Oberkampf normalizes the response by the measured value at each point. Both represent the mean value of the residuals between the computed and experimental curve. Likewise, Barone and Oberkampf's s is identical to Ray's σ^r ; both represent the standard deviation of the residuals. Barone and Oberkampf and Ray then use the same standard statistical test, the t-test, to test the hypothesis that the experimental and computational curves are the same within the expected variation of the residuals.

Velocity of the Residual Errors

Ray and Hiranmayee developed a metric based on calculating the area between two curves. This method examines the point-to-point differences between specific points on the

simulation and experimental curve. The difference between the values at a specific time is referred to as the residual or error. If two curves are identical, there would be no area between the curves and the residuals would be zero. This method arose from using the method of least squares to find the best pairing or synchronization point for two signals. The minimum value of the area between the two curves defines the most likely point of synchronization. The area between two curves is given by Ray and Hiranmayee as:(28)

$$V_e = \sqrt{\sum_{i=1}^n (m_i - c_i)^2} \cdot \Delta t$$

In the case of signals representing the acceleration time history of a simulation and full-scale test (i.e., c_i and m_i , respectively), the area under the acceleration time history curve has units of velocity, so the area between the acceleration curves will also have units of velocity. In order to obtain a non-dimensional measure of the amount of the residual error between the two time histories, the area of the residuals can be divided by the initial impact velocity, V_0 , which should be the same in both test and simulation:

$$V_e^r = \frac{\sqrt{\sum_{i=1}^n (m_i - c_i)^2} \cdot \Delta t}{V_0}$$

Smaller values of V_e^r indicate smaller residual errors between the physical test and the simulated event with a value of zero indicating identical point-to-point responses.

Stochastic Methods

In the previous section describing ANOVA techniques and metrics, there was an implicit assumption that the computational results were deterministic (i.e., the same result occurs given the same input) but the experimental results were probabilistic (i.e., substantially identical experiments can result in a range of outputs due to random experimental error). Oberkampf and Barone (36); Oberkampf et al (16); and Ray (35) all developed metrics that examined the computational results to see if they fall within the expected probabilistic range of experimental results.

Computational results, however, need not be deterministic. Every computed result is based on input data like material properties, geometry and initial conditions. If these input parameters are varied, the results of the computation will likewise vary. For example, an analyst may use the yield stress reported in an engineering handbook to develop a computational model. Although the real physical material exhibits random variation in its properties, the analyst usually just assumes the mean value of the parameter (i.e., the handbook value). Stochastic methods, on the other hand, treat the input to the finite element model as parameters that can experience random variation. If mean values are used to perform the simulation, as is usually the case, the result is a deterministic mean response. If the input variables are allowed to

vary randomly as they do in the physical world, the simulation response would vary as well. The idea of stochastic variation of parameters is a key component of computational optimization. If three computations were performed at, say, the minimum, mean and maximum yield stress, the response of the simulation would likewise vary. If the variation of the computation is compared with the expected variation in the experiments a stochastic comparison technique is being used.

The brute-force way of performing a Bayesian or stochastic analysis is to first characterize the probabilistic distributions of all the variables in the model (i.e., Young's moduli, yield strains, rate affects, densities, etc.). Next, specific parameter values can be randomly selected using a Monte Carlo technique and then a trial simulation is performed and the response of interest is generated (e.g., acceleration time history). The process is repeated with another set of randomly selected variations and the simulation is performed again. This process continues until the analyst has adequately characterized the response. The result will be a variety of acceleration time histories that are similar but vary in random ways much as experiments do. Obviously, this method requires a great deal of computer run time and a great deal of analyst intervention so it is not very practical except for small problems.

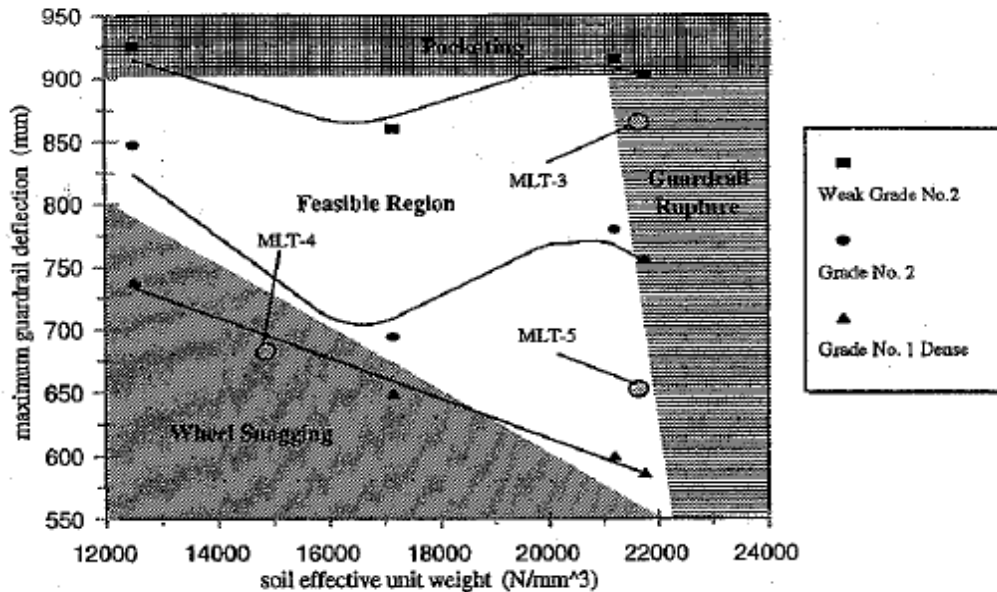


Figure 7. Effect of soil and wood material parameter variation on the performance of the MELT guardrail terminal.(40)

Techniques for estimating the response under Bayesian parameters variations have been developed in the field of structural optimization that can reduce the computational demand somewhat. Several authors have proposed techniques and processes for performing such analyses for crashworthiness problems but there are relatively few examples of practical

applications and none dealing with large models as would be typical of roadside safety applications.(37,38). Faravelli used this technique to perform a stochastic analysis of the front frame of a vehicle.(39) In her case she only varied the angles on the frame horn to observe the change in responses. In fact, Patzner did something like this when he examined the response variation due to changes in soil parameters and timber materials properties for guardrail posts.(40) He varied the soil and wood properties in a model of the MELT guardrail terminal and computed the range of responses. The result, summarized in Figure 7, shows a plot of the soil density versus the maximum guardrail deflection at the rail height. He found that certain vehicle responses were associated with different combinations of the soil and wood material properties. If, for example, Grade 1 dense wood post were used in a poorly compacted soil (i.e., low density), the vehicle tended to snag on the guardrail post. If weak Grade 2 wood posts were used in over consolidated soils (i.e., high density), the chance of guardrail rupture was maximized. In Patzner's case only a half dozen or so material parameters were being varied but the run time to produce the plot in Figure 7 was significant.

While stochastic methods provide very interesting and useful information about the range of results of a computation, they are probably not practical for large models at this time. The amount of work and run-time required to vary even a few parameters would be prohibitive and most analysts would likely refuse to perform such analyses. Stochastic variation is mathematically very similar to optimization and many software vendors are developing improved tools for optimization such as LSDYNAOP that may hold promise in the future. For now, however, stochastic methods do not appear to be practical for roadside safety validation and verification efforts.

COMPARISON OF METRICS AND CRASH TEST REPEATABILITY

In addition to the papers described in the previous sections proposing and defining validation metrics, there have been a few papers that compare several validation metrics. Papers and presentations by Schwer, Moorecroft and Ray have each examined the utility and fidelity of several metrics and a summary of these papers will be presented in this section.

At the heart of all discussions of validation and verification metrics is the issue of repeatability. Several authors have examined different validation metrics by calculating the metrics for multiple experiments and comparing the results. Such an exercise provides insight into appropriate acceptance criteria and the expected range of values that should be expected.

Any series of physical tests of a mechanical system will produce some variation in response. No two experiments or crash tests are ever identical so when comparing a numerical solution to a physical test the requirement should be that the numerical experiment (i.e., the computer simulation) cannot be distinguished from the responses of the physical experiments. If the computed response cannot be distinguished from an array of "identical" physical responses, then the computed response is as good as another physical test. Such a computer simulation would be validated by the comparison to the physical test responses. This technique

is widely used in biomechanics where a series of physical tests are used to develop corridors for the typical human response and as long as a computational model remains within the corridor it is considered to be a good predictor of the physical system. For example, Ray and Silvestri developed an LSDYNA model of the lower extremities of a 50th percentile male for use in frontal crash simulations.(41) The model was validated for three different failure conditions: fractures of the femoral head, fractures of the femoral condyles and fractures of the pelvis. The response corridors for the femoral head simulations are shown in Figure 8. The outer lines represent the range in response for 15 physical tests, the center line represents the averaged response from the physical tests and the thicker line represents a finite element simulation response. As shown in Figure 8, the computer simulation response is at the lower end of the physical response corridors but since it lies within the corridors it is a valid response. While ideally it might be better for the simulation response to follow the mean response, there would be no way to distinguish a simulation response at the bottom end of the corridor from a test response at the bottom end of the corridor.

Figure 9 shows another example of the use of response corridors in biomechanics. Ray, Hiranmayee and Kirkpatrick developed an LSDYNA model of the US SID side impact anthropometric test device (ATD).(42) The purpose of using an ATD in a crash test is to estimate the likely response of a human in a similar crash environment. Ray et al developed a model of the ATD used in side impact crash tests and then compared the response of the ATD model to the response corridors published by NHTSA for calibrating the physical ATD. These response corridors are based on many repeated physical tests. The SID ATD model was validated against two calibration tests scenarios: one with the impact on the pelvis and the other at the mid-thorax. Two versions of the computation model are shown: an original version and a version improved by Ray, Hiranmayee and Kirkpatrick. As shown in Figure 9, the improved SID ATD model resulted in better though not perfect agreement with the test corridors. The response was within the test corridors through the end of the first and most important peak and the computation response agreed with the NHTSA ATD acceptance criteria. Response corridors are very useful but they require repeated physical test data that is most often not available in roadside safety.

Unfortunately there is little information about the repeatability of full-scale crash tests in roadside safety since repeated tests are seldom performed so constructing response corridors based on physical tests is not in general possible. There have been a few exceptions, however, that are relevant to establishing verification and validation procedures.

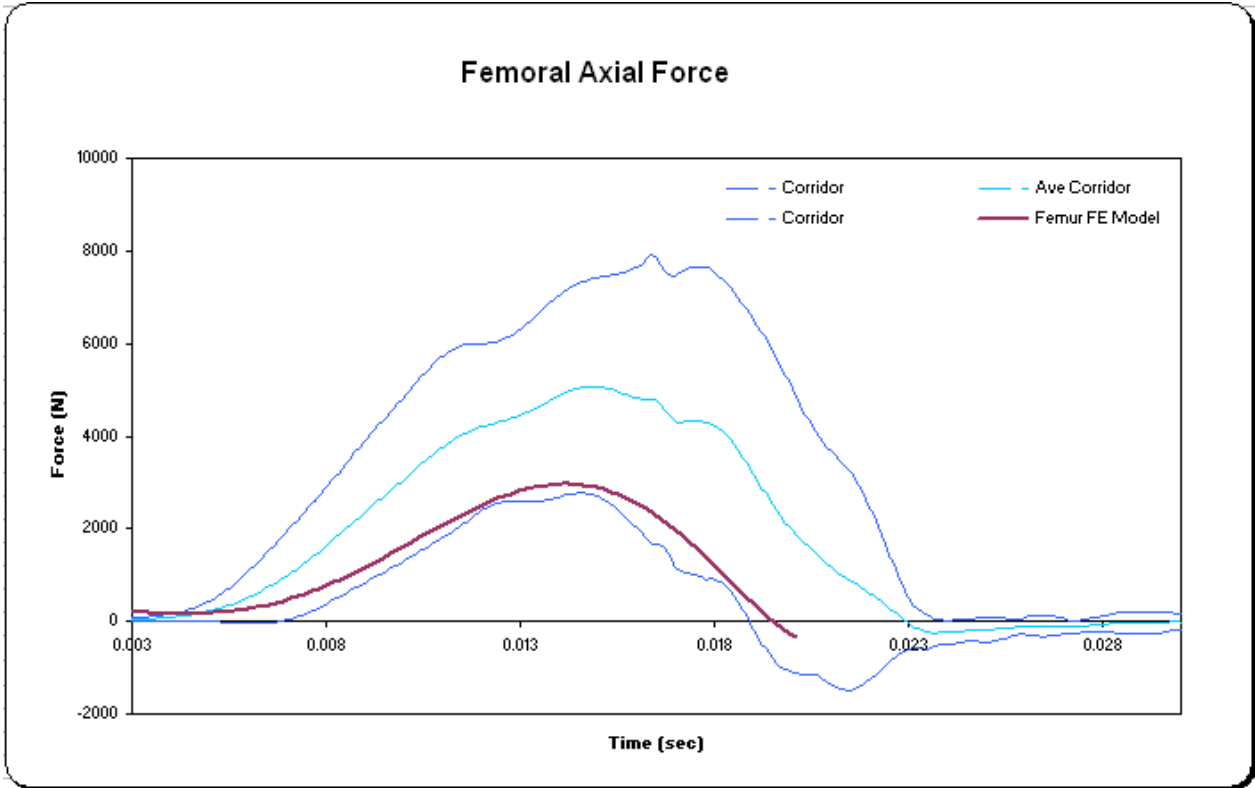


Figure 8. Response corridors for the femur force of a 50th percentile male in a frontal impact for 15 physical tests and one LSDYNA simulation.(41)

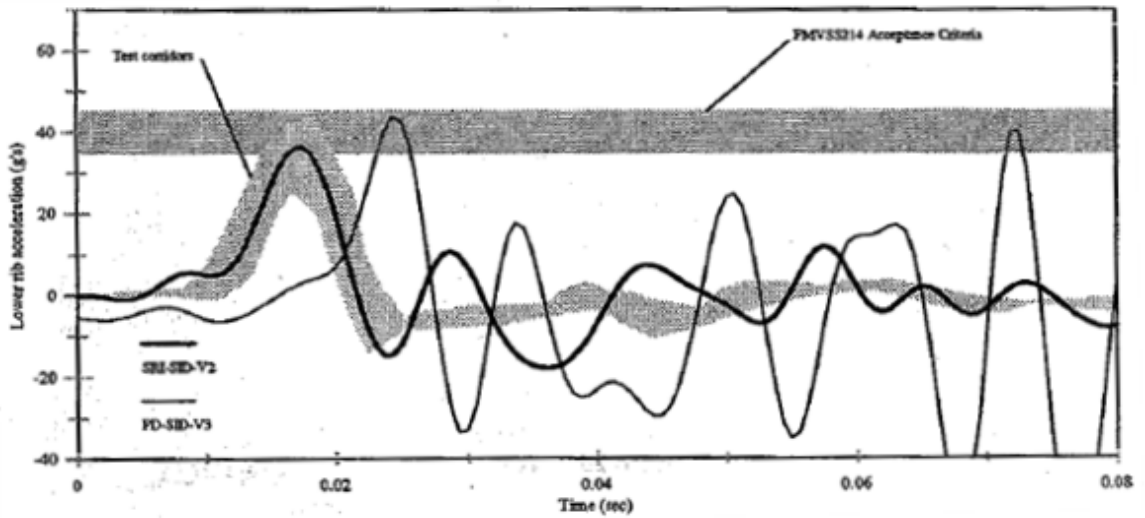


Figure 9. SID ATD response corridors for the lower rib acceleration (LURY) compared to the response of two finite element models.(42)

Recently, an activity was performed as a part of the ROBUST project in Europe where a series of full-scale tests were repeated to study the sources of experimental error and repeatability in roadside safety tests.(43) The same rigid barrier (e.g., a 0.8-m tall vertical flat wall) was tested with a 900-kg passenger car at 100 km/h and a 20° angle. The following two variations were considered:

- The same rigid barrier with the same model new car to underline the influence of the test house procedures and tolerances.
- The same rigid barrier with the vehicles normally used inside the test houses (note: EN1317 does not require the use of exactly the same vehicle) to investigate influences arising from different vehicle models.

Each of the five test agencies calculated the ASI, THIV and PHD for both their own crash test experiment as well as others performed at the other agencies. The results are shown in Table 3. Results on the main diagonal represent each test agency's evaluation of its own test whereas the off-diagonal terms represent evaluations of other agency's tests. The purpose of this part of the activity was to assess how consistent the software in each test agency was with the others.

The statistics of the data are shown at the lower left of Table 3. Based on Table 3, the range in, for example, the THIV (similar to the Report 350 OIV) was between 31 and 34 m/sec with a mean value of 32.6 m/s. This might suggest that THIV values are only accurate to the +/- 1.6 m/sec. Likewise, the mean PHD (similar to the Report 350 ORA) was found to be 14.1 g's and it varied from a minimum of 10.78 g's to a maximum of 18.27 g's. If used as a quantitative metric, the PHD acceptance criteria might be +/- 4.2 g's. A computation that resulted in a THIV that was within 1.6 m/sec of the experimentally measured THIV and a PHD that was within 4.2 g's of the experimentally measured PHD would be considered as good as another test and thereby validated.

After this initial phase a second round of tests was performed four times using the same test on a deformable barrier (always with a 900 kg vehicle at 100 km/h 20°) to investigate the influence of soil. The recommendations developed are now being incorporated into the next revision of EN1317. After reviewing the data from this first phase recommendations were made to reduce scatter starting from the procedures to install and acquire signal and ending with the software used for the severity indices evaluation. These recommendations have been finally used in a third series of tests to verify them. A total of 12 tests on the same barrier have been performed. This ROBUST project activity shows how repeated tests can be used to establish acceptance criteria for domain-specific parameters based on the probabilistic variation of repeated crash tests.

Table 3. Results of a ROBUST round robin crash test activity involving a 900-kg car striking a vertical concrete wall.(43)

		Test Laboratory Performing the Test														
		A			B			C			D			E		
		asi	thiv	phd	Asi	thiv	phd	asi	thiv	phd	asi	thiv	phd	asi	thiv	phd
E v a l u a t e d b y	A	asi	1.83			1.84			1.91			1.87				
		thiv		32.40			31.40			32.80			33.80			
		phd			17.70			11.90			11.00			18.27		
	B	asi	1.79			1.85			1.88			1.85				
		thiv		31.44			32.57			33.29			32.63			
		phd			17.22			12.26			10.78			15.00		
	C	asi	1.81			1.84			1.91							
		thiv		32.78			32.40			34.20						
		phd			17.74			11.95			11.40					
	D	asi	1.87			1.85			1.86			1.84				
		thiv		33.67			32.42			32.82			32.40			
		phd			18.27			13.72			10.94			15.24		
	E	asi												2.17		
		thiv													31.05	
		phd														12.93
Summary		asi	thiv	phd												
Mean		1.87	32.6	14.1												
Stnd Dev.		0.085	0.859	2.888												
Min		1.79	31.05	10.78												
Max.		2.17	34.2	18.27												

Brown performed six essentially identical tests of Ford Festivas striking an instrumented rigid pole which Ray then used to explore the issue of full-scale crash test repeatability.(44) Each of the six tests involved the same vehicle type, the same nominal impact conditions and the same struck object. They were performed at the same laboratory and the same data reduction techniques were used to process the test data. While the “inputs” were as identical as practically possible, there was still some variation in the response for this series of tests.

In an unpublished paper, Ray calculated a variety of metrics including the time-domain NARD Validation Manual metrics, Geer’s original MPC metrics and the analysis of the variance metrics for the six identical tests performed by Brown.(44) The results are shown in Table 4.

Table 4. Comparison of the six tests for the Ford Festiva rigid pole test.(35)

Parameters	91F049	92F032	92F033	94F001	94F002	94FO11
<i>Analysis of residuals</i>						
\bar{e}^r	3.53 %	3.32 %	3.73 %	4.32 %	3.98 %	4.42 %
σ_e^r	16.91 %	18.53 %	16.59 %	17.81 %	14.43 %	16.92 %
T_p	3.24	2.79	3.50	3.75	4.28	4.05
$p(T_p) >$	0.0012	0.0052	0.0022	0.0004	0.0002	0.0002
V_e^r	5.08 %	5.06 %	4.92 %	5.13 %	4.61 %	4.82 %
<i>NARD Validation</i>						
ΔM_n^r	12 %	11 %	13%	14%	14%	14%
ΔM_1^r	3%	5%	0%	3%	1%	4%
ΔM_2^r	20%	17%	6%	5%	13%	7%
ΔM_3^r	65 %	40%	16%	21 %	48%	36%
ΔM_4^r	422%	116%	50%	77%	277 %	206%
ΔM_5^r	284%	3820%	284%	1330%	302%	327%
$\Delta RMS_{1...5}^r$	72%	74%	79%	75%	72%	73%
ρ	0.92	0.92	0.92	0.92	0.94	0.90
ΔAB_{rot}	0.29	0.32	0.32	0.35	0.26	0.31
D	0.0032	0.0088	0.0067	0.0079	0.0046	0.0098
<i>Geer’s MPC</i>						
M	-1 %	6%	8%	5%	0%	1%
P	4%	4%	4%	4%	3%	4%
C	4%	7%	9%	6%	3%	4%

Table 4 shows the typical range of a variety of metrics for the six identical frontal rigid pole tests. The analysis of variance technique resulted in mean residuals errors, \bar{e}^r , between 3.32 and 4.32 percent with standard deviations, σ_e^r , of between 14 and 18 percent. The t-scores ranged between 2.79 and 4.28 which in turn represent the possibility of not being the same

event less than 0.52 percent at the 90th percentile. Ray suggested the following acceptance criteria based on these results:

- The average relative residual (i.e., \bar{e}^r) should be less than 5 percent,
- The standard deviation of the residuals (i.e., σ^r) should be less than 20 percent and
- The t-statistic should be calculated between the test and simulation curve. The absolute value of the calculated t statistic should be less than the critical t -statistic for a two-tailed t -test at the 5-percent level, $t_{0.005,\infty}$ (90th percentile).

Referring again to Table 4, the zero through second relative moments all were less than 20 percent indicating that the value recommended for acceptance in the NARD Validation Manual was a good choice. The higher order moments (i.e., 3rd through 5th), however, varied widely and seem to have little diagnostic value since they are not able to detect that these six tests are identical. The correlation coefficient was generally over 0.9 for all the tests and the $\Delta RMS'_{\log}$ values were generally about 72 percent indicating that these metrics correctly detected the similarity of the curves.

Ray used Geers' original MPC metrics as shown in Table 4. In all six crash tests, the magnitude, phase and combined metrics were less than 10 percent. This indicated that the MPC metrics did a good job detecting that these six curves represent the same event and an acceptance value of 10 percent would be a reasonable assumption in using these metrics in roadside safety.

One of the drawbacks of Ray's work was that these six tests involved one of the simplest, most repeatable types of tests in roadside safety. The vehicle was striking the rigid pole head-on, the vehicles were all of the same make and model and were from similar model years, and the struck object was a rigid pole so most of the variability was isolated in the vehicle. The variations in the impact velocity and offset distance were also factors. The frontal crush characteristics of these vehicles are quite sensitive to variations in the offset distance between the centerlines of the vehicle and the pole. Crash tests involving, for example, flexible barriers, a range of vehicles and multiple crash test laboratories would likely exhibit much more scatter.

Schwer has also examined the utility of the Sprague and Geers and Knowles and Gear metrics in a recent paper.(32) He calculated the Sprague and Geers and the Knowles and Gear metrics and compared the experimental and numerical velocity wave form in a geological medium due to the application of energy from a nearby source. Figure 10 shows the three simulation curves and the experimental curve and Table 5 shows the calculated values of the Sprague and Geers and Knowles and Gear metrics.

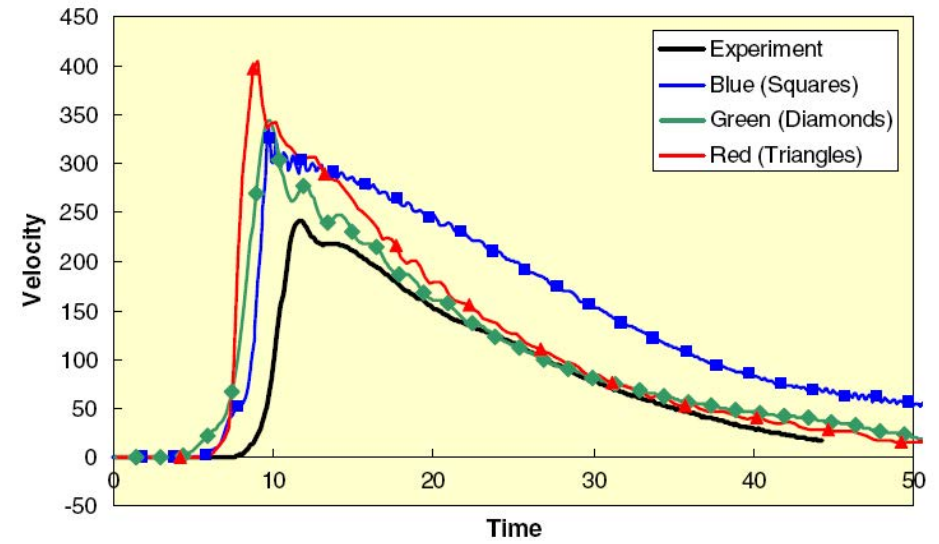


Figure 10. Comparison of measured velocity wave form with three simulation results.(32)

Table 5. Metric components for the three simulation curves of Figure 10.(32)

	Sprague and Geers			Knowles and Gear		
	<i>M</i>	<i>P</i>	<i>C</i>	<i>M</i>	<i>P</i>	<i>C</i>
Blue (Squares)	0.60	0.08	0.61	0.54	0.17	0.50
Green (Diamonds)	0.26	0.13	0.29	0.27	0.23	0.26
Red (Triangles)	0.45	0.15	0.47	0.48	0.21	0.45

Qualitatively, the green and diamond curve is the best comparison with the experiment (i.e., the solid black line). As shown in Table 5, both methods correctly identify the green or diamond curve as having the best magnitude agreement of all three curves. Both methods also indicate that the blue and square curve has the best phase agreement. Further, both methods indicate the green and diamond curve is the best overall fit.

An important feature of all three of the Geers family of metrics is that they are all “non-symmetric” since they produce different values when the measurement and calculated response are interchanged. This is because the measured value is always considered the true value in these metrics and the variation is always made in comparison to the experimentally observed values. All the Geers metrics are deterministic shape metrics and they have been used with a variety of *ad hoc* acceptance criteria, typically in the 10 to 20 percent range.

Of the metrics examined by both Ray and Schwer, all the MPC metrics (i.e., the original Geers, Sprague-Geers and Knowles-Gear), the analysis of variance (i.e., the metrics by Ray and those by Barone and Oberkampf), the zero through second order relative moments, the correlation coefficient and the relative RMS all show promise as validation metrics. The lower order moments, relative RMS and correlation coefficient can all be shown to be closely related to one of the other metrics, however, so the best candidates for future use appear to be some version of the MPC metrics or the analysis of variance metrics.

HIERARCHICAL MODELING

A complex finite element model is a hierarchy of parts, sub-assemblies and assemblies as shown in Figure 11. This figure represents a small car impact with the so-called European “super rail.” The super rail is composed of an unusually large number of parts for a longitudinal barrier. At the top level is the whole model comprising all the parts of the vehicle and barrier, boundary conditions, initial conditions, etc. The vehicle and the barrier constitute the two main assemblies of the complete model. Often, these major assemblies are separately developed and combined for a specific simulation. For example, the small car vehicle model has been used in numerous other simulations and the model of the super rail barrier would be used in impact simulations with other vehicles. Each assembly is composed of a variety of subassemblies. In the case of Figure 11, the barrier is composed of a top-rail subassembly, a mid-rail subassembly, a post subassembly and a rub-rail subassembly. Each of these can be further reduced to a series of parts. For example, the mid-rail subassembly is composed of the guardrail component, a spacer, a blockout and a back up rail. Each of these parts is composed of some geometry and material properties. The part level is the lowest level in the typical model. In addition to these components, important features like contact interfaces, connections, boundary conditions and initial conditions must be specified. Calibration, verification and validation can be performed on each of these different levels of the model hierarchy.

As an example of hierarchical modeling, researchers at Battelle Memorial Institute are currently working on a project for the National Transportation Research Center (NTRCI) involving the development of a tractor-trailer finite element model for use in roadside safety research. This model was developed for the purpose of simulating tractor-trailer crash events with particular emphasis on those crash events involving roadside safety hardware (e.g., bridge rails, median barriers, etc.). As part of that study, certain components of the model have been developed and their response validated through comparison with laboratory tests, including the leaf spring in the front suspension assembly.

In the process of developing a model, consideration must be given to both computational efficiency and accuracy of the model results. As computational efficiency improves, the accuracy in results tend to degrade, thus one must strive to develop a model that produces as much accuracy as possible with a computational cost that can be afforded. For any given component in a model, the increase in the number of degrees of freedom resulting from a

higher fidelity in geometric representation or higher order element formulation, will not likely affect the overall analysis time of a simulation. But, the model developer must consider the affects of element size on the time step required for the analysis. For example, if a component is modeled with element dimensions or properties that require a time step smaller than that of the current model, the analysis time for the full model could be increased significantly.

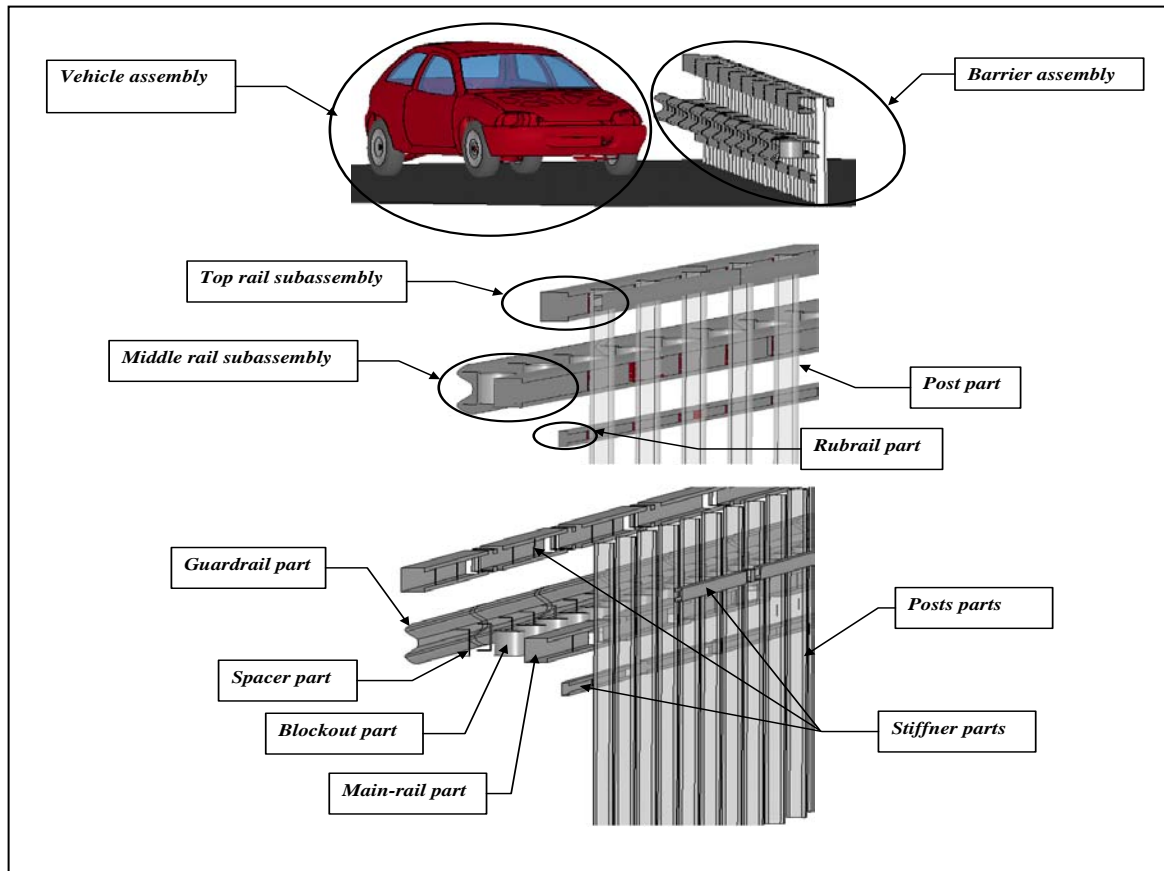


Figure 11. Hierarchy of a typical roadside hardware finite element model.

For example, a leaf-spring assembly was digitized to develop a three-dimensional geometric model and a finite element model was developed based on two different mesh sizes: (i) an element size of 20 mm by 20 mm and (ii) an element size 10 mm by 10 mm. A rendering of the geometric model is shown in Figure 12.

The finite element model of the component is shown in Figure 13 where the element size is 20 mm by 20 mm). The model consists of 1380 elements (i.e., 6,900 DOF) and the critical time step for the model is $1.4(10)^{-6}$ seconds which is consistent with the critical time step of the overall vehicle model.

The response of the model subjected to a compressive load was compared to the results from a test conducted on the physical component to assess the accuracy of the model. A photograph of the test is shown in Figure 14 showing the deformed geometry of the leaf spring under a load of 6,000 lbs.

Figure 15 shows the results of the finite element analyses for each of the two cases compared to the results from the laboratory test. Also included on the graph is the force-displacement characterization of a generic tractor suspension used by other Battelle staff in vehicle dynamics simulations.



Figure 12. Three-dimensional rendering of the leaf-spring suspension for a Freightliner FLD 120 tractor

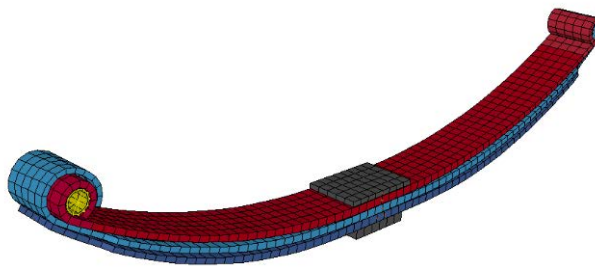


Figure 13. Finite element model of the leaf-spring suspension for a Freightliner FLD 120 tractor.



Figure 14. Laboratory test of a Freightliner FLD120 Tractor front suspension leaf spring

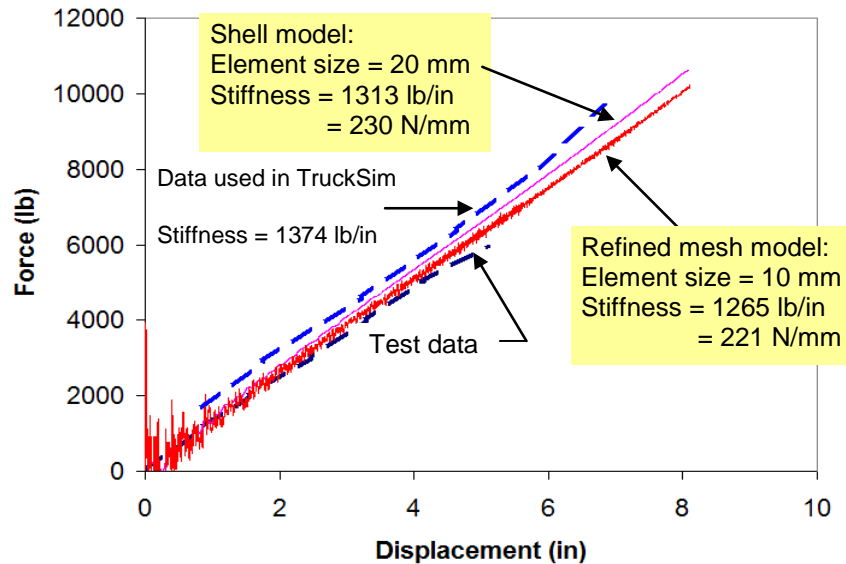


Figure 15. Force-displacement response of the test and simulation of a Freightliner FLD120 Tractor front suspension leaf spring

As can be ascertained from the results, the simulation results improve as the finite element mesh is refined; however, the economy of the solution is greatly reduced for the refined mesh model where the critical time step is approximately $1.0E-6$. Based on a qualitative evaluation of the data, both finite element models were considered to produce acceptable results and were thus both considered “valid” for use in the tractor model.

In a study by Orengo et al, a finite element model of a pickup truck tire was developed and was validated by comparing the response of the tire model subjected to various load cases with

experimental data measured in the laboratory.(45) The model was further validated by comparison of simulation results with full-scale, non-tracking impacts of a pickup into various types of curbs.

Although the tire model was not a detailed representation of all the components and structures in a tire, the critical parts of the structure that affect the overall tire mechanics were incorporated into the model, such as bead coils, radial fibers, rubber sidewall, under belt radial fibers, steel belt and tire tread.

Two laboratory tests were conducted to assess the fidelity of the tire model. The first test was conducted to measure the force vs. displacement required to break the air-seal and deflate the tire (details of the load applicator and boundary conditions were not described, but are shown in Figure 16).



Figure 16. Test setup for the tire de-beading test.

Figure 17 shows the results computed in the finite element analysis and the results measured in the laboratory tests. A quantitative, statistical validation of the results was not conducted, but based on a qualitative evaluation of the model's results compared to the test, the model was considered acceptable (taking into consideration the repeatability of tests, possible error in assumptions made in modeling boundary conditions and the specific application of the model).

Compression Test

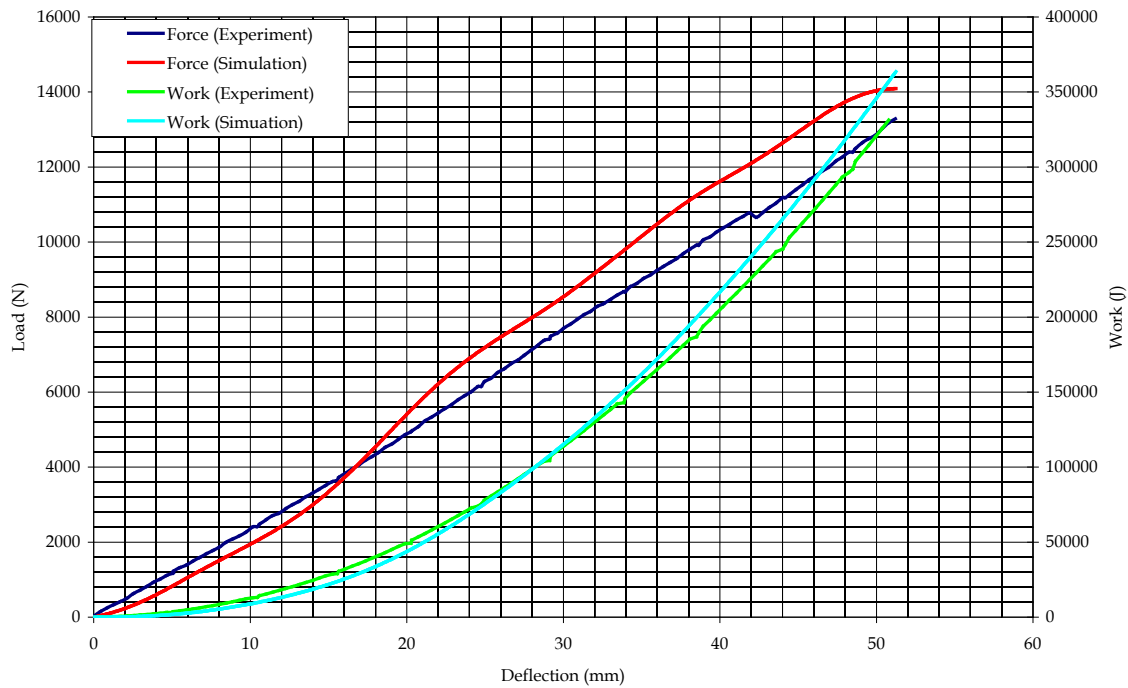


Figure 17. Comparison of the force-deflection response of a pickup truck tire subjected to a quasi-static horizontal de-beading load.

The second test was intended to measure the global stiffness of the inflated tire with a vertical load applied to the rim. The test was performed using a hydraulic uniaxial test machine (Instron 8803) as shown in Figure 18. The tire-rim assembly was loaded by a displacement time-history applied to the rim with the tread surface of the tire pressing against a flat steel plate. The tire-wheel assembly was loaded up to 13.345 kN, approximately twice that of the static load of the truck.



Figure 18. Steel hub and fixture used in the compression test.

Again, a quantitative validation of the model was not conducted but the model was considered to be valid based on a qualitative comparison of the tire responses like those shown in Figure 19. The tire model was implemented into the WPI version of the National Crash Analysis Center (NCAC) Chevrolet C2500 pickup model. The modified vehicle model was used in the analyses of non-tracking impacts into various roadside curbs to study the curb-tire interaction and vehicle stability.

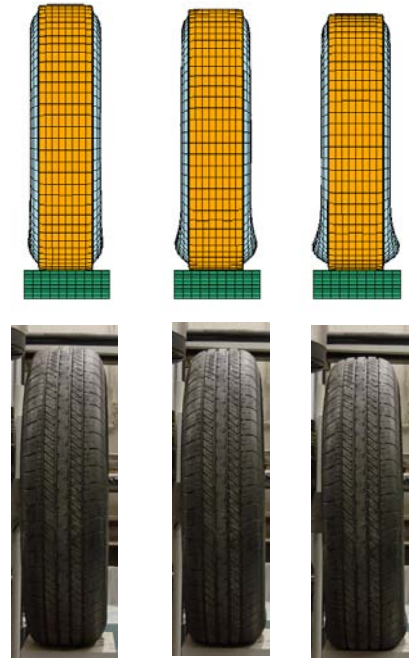


Figure 19. Comparison between the test and the simulation of the deformed shape at different loads (45)

Figure 20 shows the behavior of the tire model in the finite element analysis simulation of the truck model impacting a four-inch sloped curve compared to the results of the full-scale test. The tire model accurately captures critical events during the impact with the curb, including tire deflation and the behavior of the deflated tire as it interacts with the curb and the ground surface. The behavior of the tire model was considered acceptably valid for the given application.

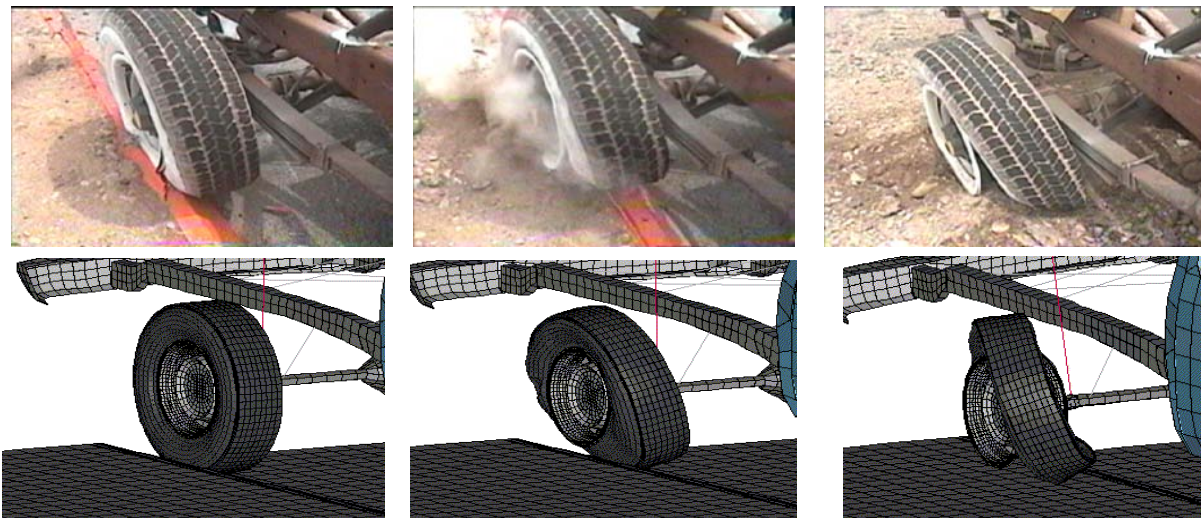


Figure 20. Sequential views from a full-scale test and simulation showing tire response during impact with a curb.(45)

It should be noted that this model adequately simulates the behavior of the tire in the applications that it was developed for; namely, the large-scale, overall response of the vehicle during impact with other structures such as roadside hardware, where the tires are only one aspect of many intricate parts that must be modeled. This same model may not be appropriate for investigating stresses and deformations in order to evaluate the performance of commercial tires, where one must take into account ply orientation, ply overlapping and mechanical properties of different layers of the composite structure of the tire.

VALIDATION IN THE ROADSIDE SAFETY LITERATURE

This section summarizes most of the finite element simulation work that has been done in roadside safety since the mid-1990's with respect to validating models. There has been a rapid expansion in activities over the past decade in using software tools like LSDYNA in roadside safety. Validation has been an issue nearly from the beginning of the roadside safety community's efforts to use modern general purpose contact-impact codes. Papers and reports are described in this section to show how the authors treated validation issues.

Materials and Components

Material models are the foundation of any finite element simulation. A typical model of a vehicle striking a barrier may easily have 100 or more material models using a variety of constitutive models and a variety of parameters.

Wright and Ray performed a series of experiments to determine input parameters for LSDYNA to replicate the behavior of AASHTO M-180, the steel commonly used in guardrails. (46) First, material properties of standard AASHTO M-180 guardrail steel, such as yield stress and the plastic stress-strain curve, were obtained from coupon test experiments. These quantities were then incorporated into material number 24 (*MAT_PIESEWISE_LINEAR_PLASTICITY) in LSDYNA. The simulation results compared favorably with the physical test results. At that time, Wright and Ray incorrectly called this activity a validation exercise whereas according to today's ASME V&V definitions it would more properly be a calibration exercise since the physical tests were used to estimate the parameter values.

Gentry and Bank investigated the experimental and simulated response of steel W-beam guardrail components to pendulum impact loadings for velocities of 20 km/h, 30 km/h, and 35 km/h.(47) The guardrails were supported by four posts and were cable-anchored at each end to ensure that the full tension capacity of the rail could be developed. Experiments carried out with a 912-kg impact pendulum were compared with LSDYNA finite-element simulations of the impact events. Acceleration, velocity, and displacement time histories were compared for the pendulum impact test and the LSDYNA simulations. Comparisons of the experimental and simulation acceleration records were made using the NARD time-domain statistics. The comparative statistics showed that the simulations were in good agreement with the

experiments. Results show that the guardrail was close to its tension yield point when impacted at an initial velocity of 35 km/h.

Tabiei investigated the potential of using fiber reinforced composite materials for applications in highway structures.(48) The feasibility and application of composite materials were analyzed through a series of impact tests on laboratory specimens and numerical simulations were performed to replicate the results. First, the impact characteristics and failure modes of pultruded box-beams under impact loads were explored and the loading rate sensitivity of pultruded box-beams with different resin systems was investigated using physical tests. In order to compare the results for the composite guardrails to conventional steel guardrails, a series of pendulum experiments were performed at the FHWA Federal Outdoor Impact Laboratory (FOIL). Next, numerical simulations of a series of impact tests of steel guard rails replicating the experiments were performed. As shown in Figure 21, a finite element model of the pendulum fixture of the FOIL was developed to (i) determine the feasibility of simulating full-scale impact tests of guardrails made of isotropic and anisotropic materials and (ii) to identify the critical parameters governing a successful simulation of a test fixture pendulum impact. Qualitative comparisons such as the deformed shape of the barrier and acceleration, velocity and deformation time histories were used to qualitatively validate the numerical model.

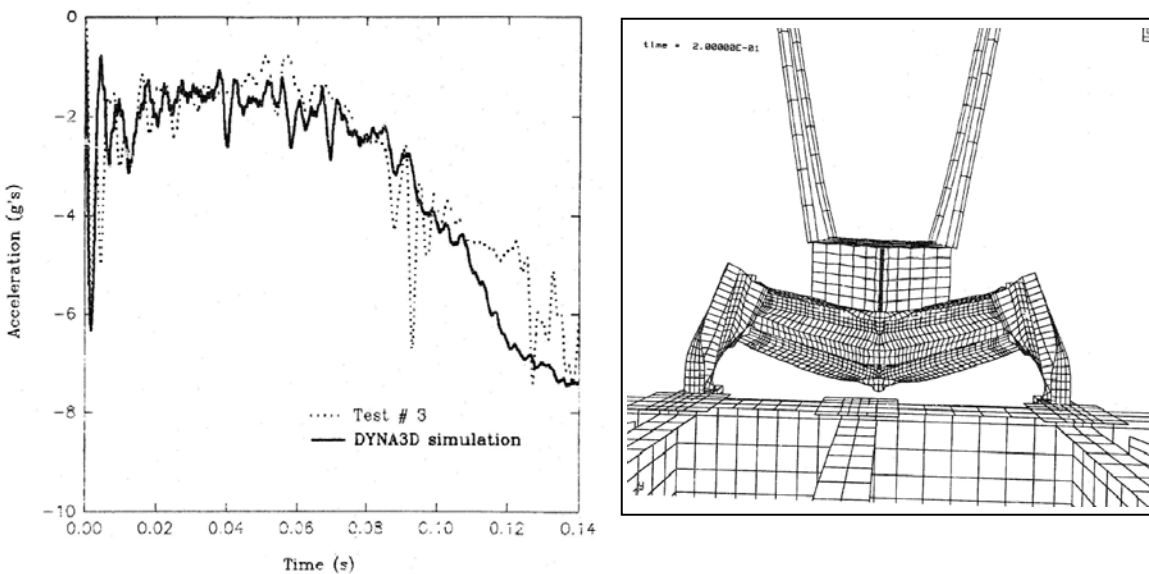


Figure 21. Finite element model of a W-beam (right) and time history comparison of the simulation and experiment (left).(48)

Eskandarian et al describes the development of a finite element model of the FOIL bogie vehicle and in particular its honeycomb impact nose.(49) The effort consisted mainly of correlating the honeycomb response in the simulations and experiments such that the model produced realistic results. Honeycomb material parameters were developed for DYNA3D and

force-deflection data from compression test experiments were used to calibrate the honeycomb material model. After successfully calibrating the honeycomb material model, a model of the bogie with a crushable nose containing the calibrated honeycomb material parameters was constructed. Simulations of the bogie model were then compared to full-scale crash test experiments with the FOIL bogie vehicle. Acceleration, velocity and displacement time histories as well as sequential pictures of the crush of the honeycomb nose data obtained from bogie crash testing compared favorably with those of the simulation. These comparisons were used to qualitatively validate the honeycomb material model and bogie model.

Numerical and experimental data were used to validate an aluminum material model as presented in paper by Langseth et al.(50) A material model for LSDYNA was validated against static and dynamic tests on aluminum tubes. An LSDYNA model of the tubes was developed and subjected to the same impact scenarios. Good predictions of the response of the tubes were found by using isotropic elasticity, the von Mises yield criterion, the associated flow rule and non-linear isotropic strain hardening. The plastic material parameters such as the initial yield stress and the strain hardening were determined from uniaxial tensile tests.

Borvik tested notched specimens of the structural steel Weldox 460 E at high strain rates in a series of Split Hopkinson Tension Bar tests.(51) The aim was to study the combined effects of strain rate and stress triaxiality on the strength and ductility of the material. The force and elongation of the specimens were measured continuously by strain gauges on the half-bars while the true fracture strain was calculated based on measurements of the fracture area. Optical recordings of the notch deformation were obtained using a digital high-speed camera system. Using the digital images, it was possible to estimate the true strain versus time at the minimum cross-section in the specimen. The ductility of the material was found to depend considerably on the stress triaxiality. Non-linear finite element analyses of the notched tensile specimens at high strain rates were then carried out using LSDYNA. A computational material model including viscoplasticity and ductile damage was implemented in LSDYNA and determined for Weldox 460 E steel.

Du Bois et al discussed modeling laminated safety glass for vehicle windshield applications.(52) The paper compared stress-strain data obtained from different material models to experimental data to validate a numerical model of laminated safety glass. As a continuation, Timmel et al discusses the validation of two different laminated glass models.(53) Force-displacement data obtained from four-point bending tests as well as acceleration time histories obtained from the impact tests were used to illustrate the success of numerical simulations in representing actual behavior of laminated glass. In 2004, Du Bois et al presented a comparative review of material models for polymers subjected to impact loading.(54) Material laws which allow for fast generating of input data based on uniaxial static and dynamic tensile tests at different strain rates was presented. For thermoplastics, an overview of suitable material laws was given and techniques for characterizing approximately polymer behavior using the metal plasticity models in LSDYNA were shown. The numerical results

were qualitatively validated using visual comparisons of acceleration time histories. In 2005, Sun et al presented another study on modeling the failure behavior of laminated glass windscreens.(55) A special element structure with three layers (shell/volume/shell) was used to model the laminated glass windscreen. A fracture criterion for brittle fracture based on the maximum principal stress was applied to model the fracture behavior of glass. The critical fracture stress of glass was determined by curve fitting the failure force measured from static bending tests on laminated glass windscreens. Qualitative comparisons showing the fracture patterns for different load cases were used to validate the numerical models.

Atahan and Ross developed an LSDYNA model to evaluate the crashworthiness of a guardrail system with posts made of recycled materials.(56) Material properties for the recycled materials were obtained from laboratory experiments used to calibrate the accuracy of the LSDYNA material models. Results of a full-scale crash test were used to validate the accuracy of the finite element models used in the simulation study. Qualitative comparisons of deformations and velocity-time history were used to assess the validity of the models.

In the mid-1990's the FHWA sponsored three projects to develop LSDYNA material models that were better suited for use in roadside safety research. Models for soil, wood and concrete were developed that addressed the special needs of roadside safety analysts. (57)(58)(59) The objective of the first of these projects was to develop a soil model that could be used to provide support for components like guardrail posts. Lewis first examined the material models available in LSDYNA and found that all the soil models were designed for confined soils. This meant that for cases like a guardrail post mounted in soil where the upper surface was unconfined the material model was unstable.(57) Instead of modifying an existing model, Lewis developed a new model that would be stable under low or no-confinement pressures. Unfortunately, there was very little validation. Only one experiment was used for comparison and the experimental results were questionable so the model was never validated.

Fortunately, Reid et al was able to evaluate the new soil material model as reported in 2004.(60) The behavior of the newly developed soil model during post rotation is shown in Figure 22. The model uses 18 parameters to represent the soil material. The focus of the project was (i) estimating the appropriate parameter values through testing or analytical means, (ii) providing an engineering understanding of the parameters and (iii) providing bounds for the effects of varying the parameters. Qualitative comparisons, such as force-deflection and energy-deflection plots as well as sequential pictures obtained from experiments were used to calibrate the soil material model (i.e., LSDYNA material 147). In 2007, Tong and Tuan also developed and validated a soil model; their work used a viscoplastic cap model for simulating high strain rate behavior of soils.(61) An associative viscous flow rule was used to represent time-dependent soil behaviors. The viscoplastic cap model was qualitatively validated against experimental data from static and dynamic soil tests. Stress-strain and the wave propagation speed in soil with depth of burial were considered in the validation process. The model was also compared with soil behaviors under creep and stress relaxation with good agreement. The

qualitatively validated model was subsequently integrated into LSDYNA for finite-element simulations of high strain rate behaviors of sandy and clay soils in explosive tests (i.e., LSDYNA material 8, MAT_HIGH_EXPLOSIVE_BURN).

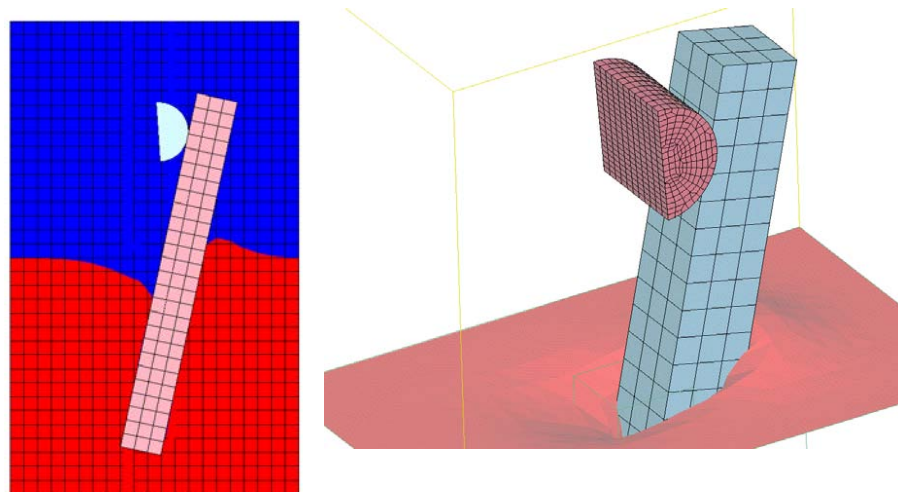


Figure 22. Behavior of LSDYNA material 147 for guardrail post rotation. (60)



Figure 23. Damage to an under-reinforced concrete beam showing two crack rebar failure, (top) test specimen and (bottom) simulation.(58)

Murray developed a concrete material model (i.e., LSDYNA material 159) for use in LSDYNA in the second FHWA-sponsored project to develop roadside safety materials.(58) The model was developed from basic principles and the parameters chosen where those based on conventional concrete specifications. Once the model was developed, its accuracy was evaluated using dynamic impact experiments with 47 reinforced concrete beams representing over / under reinforced beams and plain concrete beams performed in WPI's impact laboratory (see Figure 23). Comparisons between the location and number of cracks were tabulated and the results assessed quantitatively. Further bogie and pendulum impact experiments were

performed at the MwRSF at the University of Nebraska. Qualitative comparisons of damage modes were performed and acceleration time histories were qualitatively compared to validate the model as well as quantitative comparisons of the maximum load. Once the model had been developed and validated, the model results were verified by comparing the developer's solutions (i.e., the known solution) to a user's solution of the same problem. In a follow up study in 2007, Murray developed an elasto-plastic damage model with rate effects for concrete and implemented it into LSDYNA.(62) This report includes the theory of the concrete material model, description of the required input format as well as example problems for use as a learning tool. A default material property input option was provided for normal strength concrete. The model was developed for roadside safety applications, such as concrete bridge rails and portable barriers impacted by vehicles, but it should also be applicable to other dynamic applications.



Figure 24. Qualitative comparison of damage in a quasi-static pull-test of a wood guardrail post (left) experiment and (right) simulation.(59)

In the third FHWA sponsored project, Murray et al developed a new material model to describe the constitutive behavior of wood, especially in roadside safety applications.(59) The result of her work was a new material model in LSDYNA (i.e., material 143). Like the concrete model in material 159, Murray provided input in terms of simple conventional engineering descriptions as well as more comprehensive constitutive parameters. In particular she provided default values for common roadside safety guardrail post materials like southern yellow pine and Douglas fir. The initial versions of the model were developed with test data on “clear” wood samples provided by the Forrest Products Laboratory. A variety of single-element simulations were performed to assess the stability and numerical performance of the model. Next, a series of quasi-static pull-tests of typical guardrail posts of several grades were

performed by MwRSF at UNL. Each grade post was tested approximately 10 times so a statistical envelope of typical responses was constructed for the force-deflection response of each grade. Simulations were then performed to see if the simulated force-deflection response remained within the experimental response curve envelopes. The results were generally good although the simulated response seldom remained completely inside the experimental response corridors. Impact experiments with full size posts were also performed and the time history results were compared to the simulations. Murray also verified the model on several different computer platforms to ensure the material model was not sensitive to numerical issues associated with a particular platform or setup. The resulting wood material model was a significant improvement over other options available in LSDYNA for modeling wood in roadside safety simulations. A comparison of an experiment and simulation for one of the quasi-static experiments used in validating the wood post model is shown in Figure 24. Figure 25 shows an example of the experimental force-deflection response corridors and the simulation response used in the validation process.

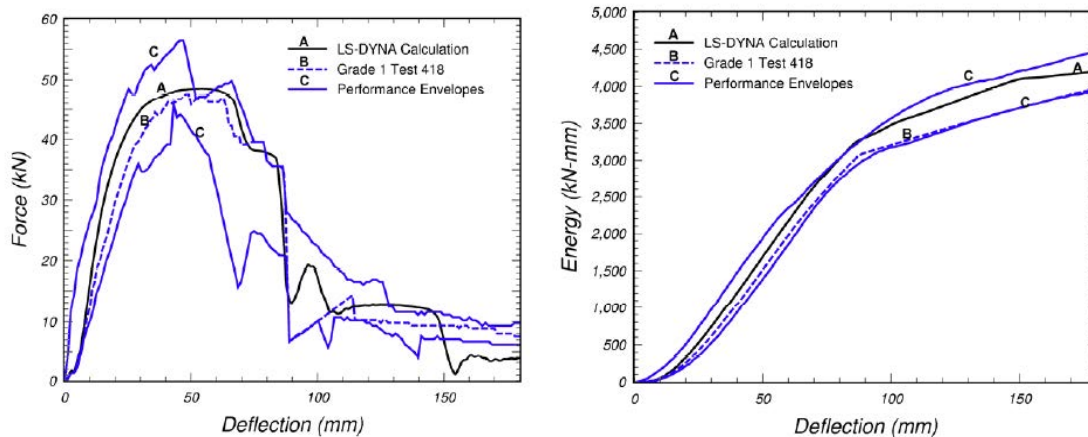


Figure 25. Comparison of the force-deflection response for (i) the mean experimental response, (ii) an envelope of the observed experimental responses and (iii) an LSDYNA simulation.(59)

Miele et al evaluated the single unit truck (SUT) finite element model initially developed by the National Crash Analysis Center (NCAC) at George Washington University. The model was evaluated to assess its ability to accurately simulate its interaction with roadside safety hardware and to identify areas of possible improvements.(63) Miele was particularly interested in the failure of suspension components. While this model is discussed further in a later section, Miele also examined the material models used in the SUT model. Stress-strain data obtained from experiments were used to calibrate the material models. A summary of the material information used in the SUT model is shown in Figure 26.

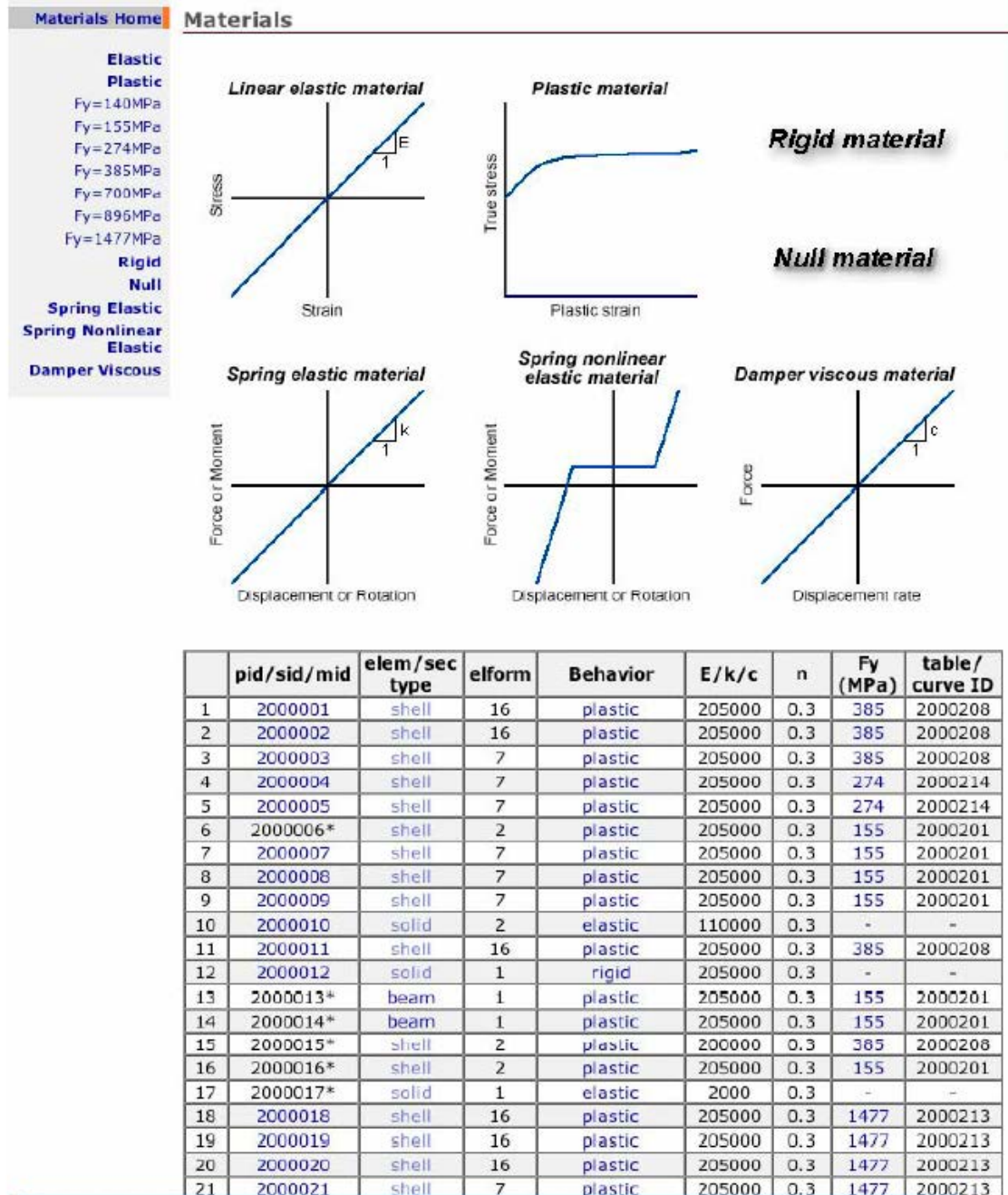


Figure 26. Summary of materials used in the SUT model.(63)

Haufe et al developed a semi-analytical process for calibration, verification and validation of automotive polymer materials.(64) He describes identifying the characteristics of the polymer, verifying the constitutive models with known solutions, calibrating the verified constitutive models with simple laboratory tensile “dog-bone” tests and finally validating simulations with experiments representing realistic automotive parts. Comparisons are made using qualitative assessments of the force-deformation curves obtained from the experiments and simulations.

Wood et al studied the stochastic variation of automotive steels to establish material properties in standard quasi-static tensile tests.(65) Stochastic variation is when the material parameters vary randomly about a mean value. These random variations can affect the results of the test and, hence, the material properties. Eleven specimens were cut from the same coil of steel and subjected to tensile tests. The stress-strain response was experimentally determined and the variation among the 11 specimens was used to probabilistically characterize the material. Simulation model inputs were then determined by randomly assigning material properties using the probability distributions determined in the tests. This work is an interesting example of stochastic calibration of a material model Dietemberger et al examined the affect of using different LSDYNA material models to incorporate strain-rate into vehicle crash simulations.(66) The authors identified three types of automotive steels present in the C2500 Chevrolet pickup truck and collected rate sensitivity data from the literature. They used the NCAC version of the C2500 pickup truck model in their investigation of strain-rate sensitivity. They then used five different LSDYNA constitutive models to determine the influence of strain-rates on the overall behavior of the vehicle. LSDYNA simulations were performed with each of the different material models using the C2500 pickup truck model and the NCAP crash configuration. Qualitative comparisons of the deformation such as that shown in Figure 27 were made as well as qualitative comparisons of the longitudinal acceleration time history as shown in Figure 28. The authors found that the effect of strain-rate on the NCAP result was relatively small and constituted a second order effect, probably because the deformations while large are highly localized and affect only a select number of materials.

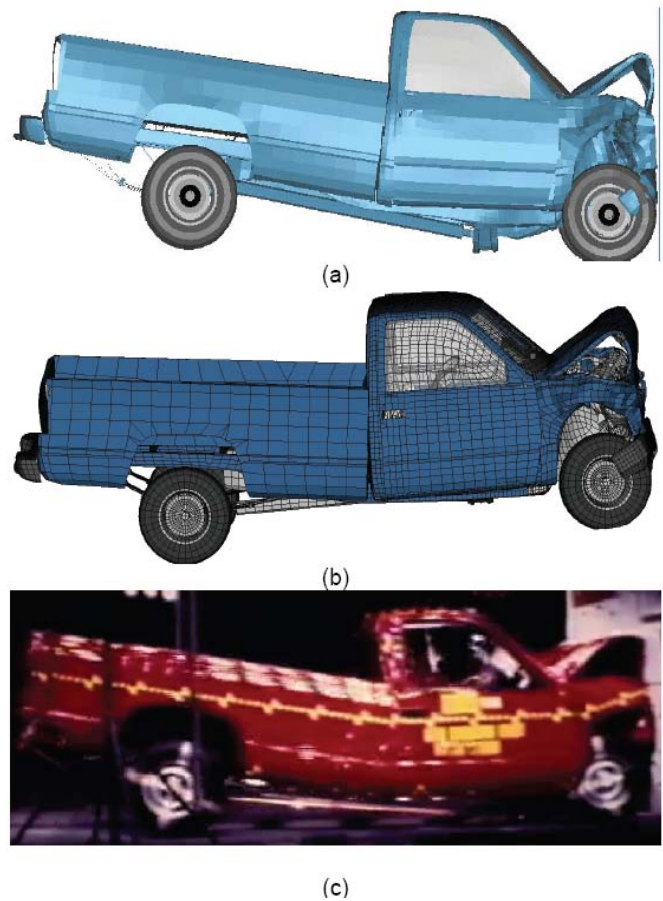


Figure 27. Qualitative comparison of NCAP results for a C2500 pickup truck for (a) a simulation without strain-rate effects, (b) a simulation with strain-rate effects and (c) an NCAP experiment. (66)

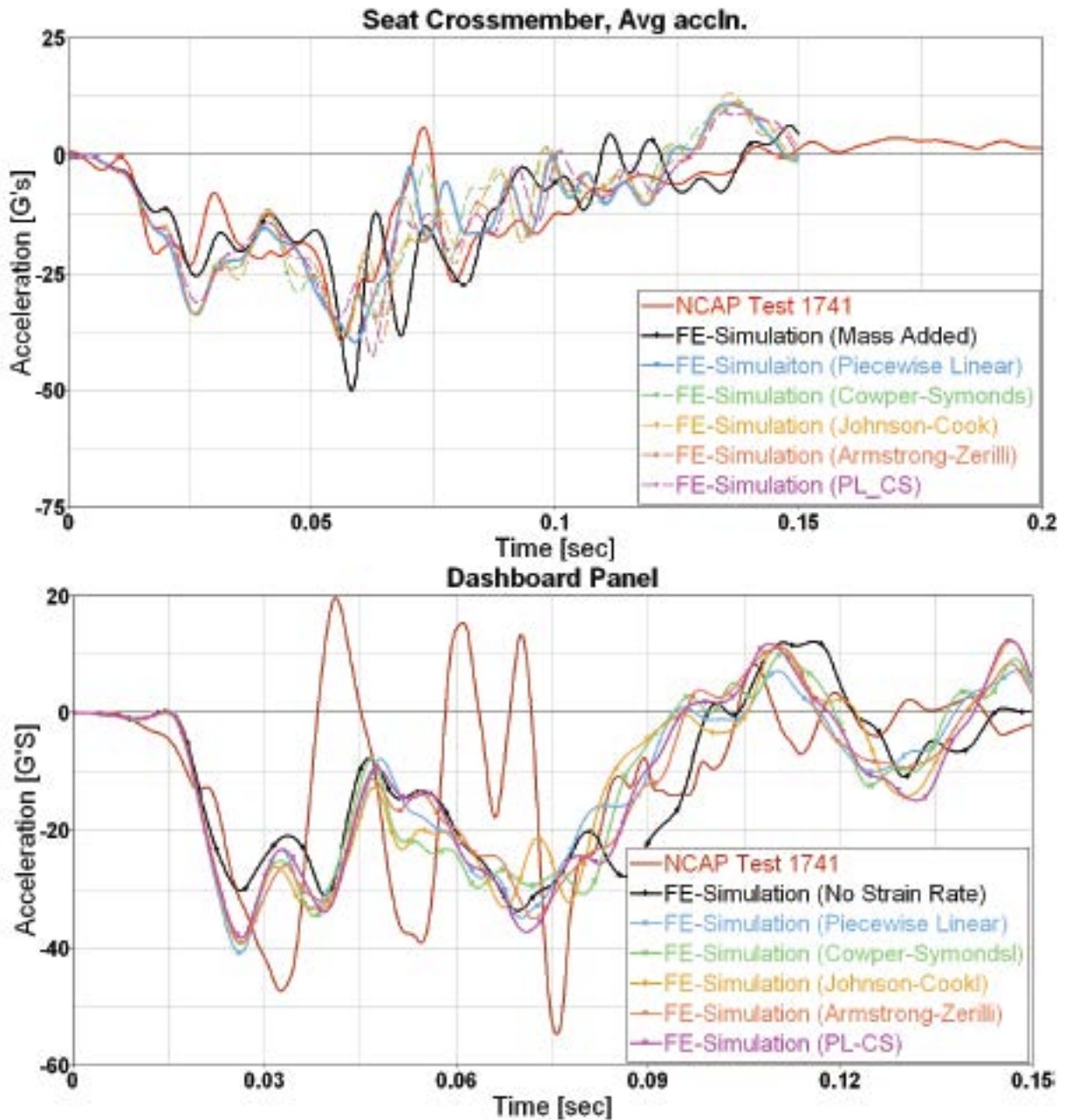


Figure 28. Longitudinal acceleration-time comparison.(66)

Gerhard et al discussed the validation process of energy absorbing foam for automotive applications. (67) Numerical models of the foam material were developed and high speed drop tower tests were used to define the basic material model parameters. Sled tests with a rigid impactor shape based upon the Side Impact Dummy II's (SID II) dummy pelvis and head impact tests with a Free Motion Head (FMH) form according to Federal Motor Vehicle Safety Standard (FMVSS) 201-U were used to validate the models and assess their accuracy with respect to various complexities of foam sample geometry. Load-displacement curves and acceleration-time histories were used in the qualitative validation process for the foam material model.

Blankenhorn et al discussed the validation of a numerical model for a carillon bell.(68) The results of experimental and numerical investigations were used to estimate the quality of the numerical model. For this purpose, the Eigen frequencies of the experimental and numerical models are compared and the orthogonality of the Eigen modes is evaluated via a modal assurance criterion.

Walker et al developed new LSDYNA models of experimental crash barriers used in automotive testing.(69) Most of these barriers use honeycomb and glue materials. As shown in Figure 29, experimental and numerical simulation studies were performed to qualitatively validate the accuracy of the developed new crash barrier model as well as the individual material models. In addition to deformations, acceleration, velocity and force time histories, energy balance comparisons were used in the validation process.

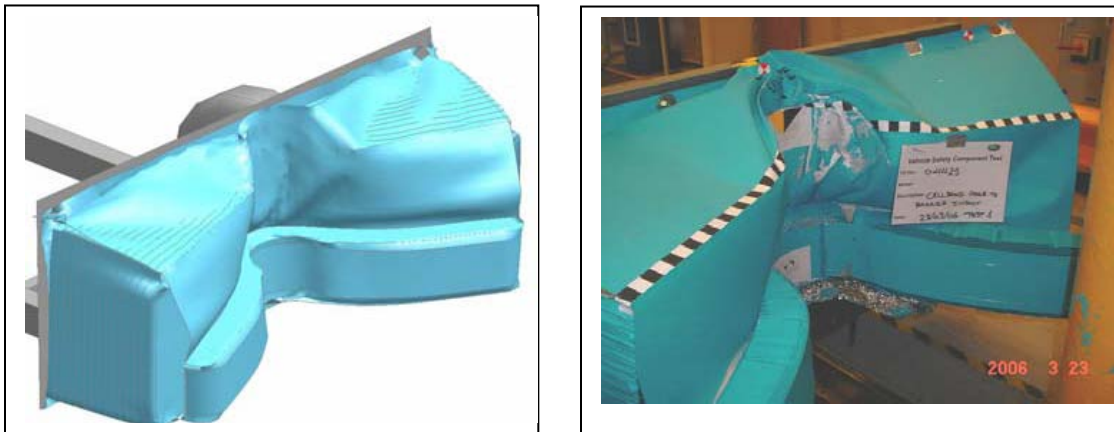


Figure 29. Qualitative comparison of barrier deformation.(69)

Wood et al investigated three-point bending and constant velocity boundary condition performance of thin-wall open channel and steel beams.(70) Experimental data was used to qualitatively validate the numerical simulations using stress-strain plots. Force and energy comparisons were also used to emphasize the accuracy of the steel material model.

Sheikh et al describes the development of an energy absorbing guardrail end terminal developed for use with the European box beam guardrail system.(71) The overall design effort used finite element simulations, component tests using a bogie vehicle and an impact pendulum. The component models were calibrated using the component experiments and the whole model was qualitatively validated with full scale vehicle crash testing. The design process involved addressing several individual component performance issues. Of these were the design of an extruder head, splice connections for attaching adjacent rail segments, the post to rail attachment connection and anchorage of the rail.

Shoukry et al examined the response of dowel jointed concrete pavements to the combined effect of nonlinear thermal gradient and moving axle loads using three-dimensional

finite-element (3D FE) modeling.(72) The 3D FE-computed responses to moving axle loads were field validated versus measured concrete slab response to a fully loaded moving dump truck. Moment vs. temperature gradient and stress vs. distance data obtained from the field measurements were used to validate the accuracy of the finite element models. The 3D FE-predicted slab curling due to the nonlinear thermal gradient through the slab thickness was validated versus: (i) corner-dowel bar bending as measured using instrumented dowels embedded in an instrumented rigid pavement section in West Virginia; and (ii) Westergaard's closed-form solution. The effects of slab thickness, slab length, axle loading position, and axle type on slab stresses are examined. It is shown that while a negative temperature gradient reduces the intensity of traffic-induced stresses, positive temperature gradient increases it several fold. Formulas were developed for the computation of the peak principal stresses due to the combined effect of tandem axle load and nonlinear thermal gradient.

Horstemeyer et al presented a comprehensive experimental material characterization and full-scale testing of structural connections of paratransit buses.(73) Structure-property relations were quantified for the constitutive material models used for finite element simulation-based crashworthiness research of paratransit buses. Static coupon tests along with a dynamic wall panel test with an impact hammer provided validation data for the finite element simulations. In addition to FE model calibration, the connection testing allowed for thorough qualitative assessment of connection design, which resulted in improved crashworthy connection details.

The material models discussed above illustrate several important points with respect to validation. First, a general process has evolved where simple laboratory experiments like tensile coupon tests, compressive cylinder tests and beam bending tests are used to estimate material parameters and thereby calibrate a material model. Simulations are then performed with the calibrated material models and then compared to the component-level tests to provide validation. The two projects by Murray are good examples of this process.(58)(59) This is a good way to develop and validate material models. Second, most analysts and developers have used qualitative comparisons of time histories and force-deflection data to validate their models. Shape-comparison metrics like those discussed earlier should be used in the future to eliminate the subjectivity of the comparisons. Most material model developers have used quantitative comparisons for domain-specific parameters like the total deflection, location of cracks and deformed shapes. The third point, more apparent in the following sections, is that often the calibration or validation of materials is not documented at all, leaving reviewers uncertain about the quality of the underlying materials models.

Material models, as shown in this section, are most often validated by first using simple laboratory tests to perform calibration studies to estimate the parameter values needed for a constitutive model in LSDYNA. Next, a component or subassembly simulation is performed and compared to a laboratory experiment. The component or subassembly simulation is then

compared to the experimental result using some appropriate domain-specific metric like the maximum deflection or the location of failure points.

Vehicle Models

In the discussion of validation and verification in roadside safety, vehicle models deserve some special consideration. One of the reasons finite element analysis has become so widespread in computational roadside safety is that researchers are able to re-use a standard set of vehicle models and thereby avoid the cost and time required to create such models. Since full-scale crash testing is based on the guidelines in Report 350 or its new update, researchers are generally only interested in models of one of the six standard crash test vehicles. Of these six, two (i.e., the 820C and 2000P vehicles in Report 350) represent by far the most used vehicles. Since the same vehicle models are used over and over again in a variety of different roadside safety application projects, it is particularly important that vehicle models be reliable, well documented and validated.

One of the first vehicle models for use in roadside safety applications with general purpose contact-impact codes like LSDYNA was developed for the FHWA by EASi Engineering and is documented in a 1995 report.⁽⁷⁴⁾ Mendis et al developed a model for DYNA-3D using a reverse engineering process where they obtained and then disassembled two 1983 Honda Civics. Individual components were cut apart or separated from the vehicle and the geometry was digitized and imported into the pre-processor INGRID. The model was then created from this digitized geometry data. The resulting model was very crude by today's standards with 63 parts and a total of about 13,000 elements. Only the front of the vehicle was represented in geometric detail so this model was only useful for frontal impacts with roadside objects like signs and luminaire supports. The final model was compared to the results of a full-scale crash test performed at the FOIL. Qualitative comparisons of the longitudinal acceleration time histories and final deformed shapes of vehicle components were made in an attempt to validate the model. While the overall shape response was apparent in the acceleration time history, the qualitative comparison was not particularly good at least by today's standards.

At about the same time, Cofie developed a very simple model of a small 820C vehicle for roadside hardware simulations.⁽⁷⁵⁾ Cofie was not particularly concerned with a faithful geometric representation but was more concerned with replicating the inertial properties and overall shape of the vehicle. His assumption was that roadside hardware responded primarily to inertial affects and the detailed structural response of the vehicle itself would be a secondary affect. The resulting model was given the general properties of an early 1990's Ford Festiva. Simulations were performed with the vehicle striking a rigid pole at the center and the quarter point of the bumper. A number of crash tests were available from the FOIL that used the same impact conditions. As shown in Table 6, Cofie compared the results of the simulation to the experiments based on qualitative comparisons of the longitudinal acceleration time histories and the energy time histories and found that in general that the results were fairly good

especially up to the peak loading. Cofie also made quantitative comparisons between the experiments and the changes in velocity, kinetic energy and impulse. Examples of his quantitative comparisons are shown in Figure 30 along with an energy time history. The velocity, energy, work and impulse values up to the peak value were all less than five percent, usually much smaller as shown in Figure 30. The comparisons at the end of the event (i.e., 100 msec) were all less than 25 percent. Given the early date of this work and the primitive nature of the model, these results were quite encouraging. One of the notable aspects of Cofie's validation efforts is that he compared his finite element results to the average acceleration response of all the experiments in recognition that there would be some experimental variation. Another notable feature of Cofie's work is that he demonstrated that most of the response was due to the large-scale inertial characteristics of the vehicle even in this rigid pole impact.

Table 6. Qualitative comparison of simulation results to full-scale test results.(75)

	longitudinal change in velocity (m/s)	longitudinal change in kinetic energy (kJ)	longitudinal work done (kJ)	longitudinal impulse transferred (kN s)
time = 70 ms				
Simulation	8.9	32.65	32.50	6.33
Test 91F049	9.0	32.65	33.10	6.53
Test 92F032	8.9	32.65	32.36	6.45
Test 92F033	8.9	32.65	32.36	7.0
Percentage difference	0.4 %	0.0 %	0.4 %	5.0 %
time = 100 ms				
Simulation	9.6	32.65	32.50	8.07
Test 91F049	12.5	27.40	30.0	10.17
Test 92F032	12.3	27.70	30.0	9.97
Test 92F033	12.3	27.70	29.0	9.99
Percentage difference	22.4 %	18.3 %	9.5 %	19.7 %

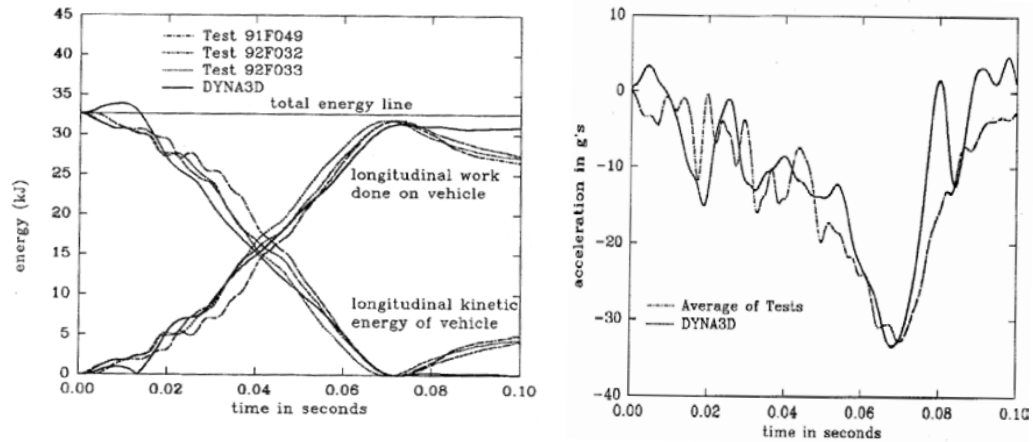


Figure 30. Comparisons between three rigid pole crash tests and a simulation of a 32 km/hr centerline impact between an 820C vehicle and a rigid pole.(75)

Thacker describes a reverse engineering project to develop a general purpose LSDYNA model of a 1997 Honda Accord.(76) Like the Easi Honda Civic, the model was developed using a reverse engineering process. The model was intended for use in compatibility impact studies for NHTSA. Unlike the Easi Honda, however, the objective in developing the Accord model was to develop a single model that could be used in a variety of different crash situations (i.e., full-frontal NCAP tests, off-set frontal tests, side impact tests and oblique vehicle-to-vehicle tests). The results were compared to crash tests using qualitative comparisons of the acceleration time histories.

In 2001, the NCAC made available a 193,000 element model of a Geo Metro on its website (no papers or reports have been found describing the development of this model). Because the Geo Metro is very similar to the types of small cars often found in Europe, the ROBUST group decided to evaluate the model for use in roadside safety simulations of European barriers. Mongiardini reviewed the original version of the Geo Metro and determined that it would be a good platform for roadside safety work but a functioning suspension and steering system needed to be added.(77) These features were added to the model and the improvements appeared to make the kinematic response of the vehicle much more realistic. The change in the vehicle behavior of the two models is illustrated in Figure 31. Sango continued the work and used the Geo Metro model in simulations with several common European barrier systems and compared the results of the original model with the improved model with suspension and steering systems.(12)(78) Finally, Sango and Haukass compared the results of the Geo Metro simulations in EN 1317 TB11 impacts with a vertical concrete wall, the EU2 guardrail and the Norwegian Standard Vehicle Parapet Type 1b-80 to full-scale crash tests.(78) For each of the three barriers, the researchers compared the EN 1317 domain-specific metrics THIV, ASI and PHD for the computer simulations and the experiments. An example from the concrete wall case is shown in Table 7. For all the quantitative comparisons, the simulation

was always within 1.2 percent of the experimentally observed value. Unfortunately, qualitative and quantitative comparisons of the time history data were not included in the report.

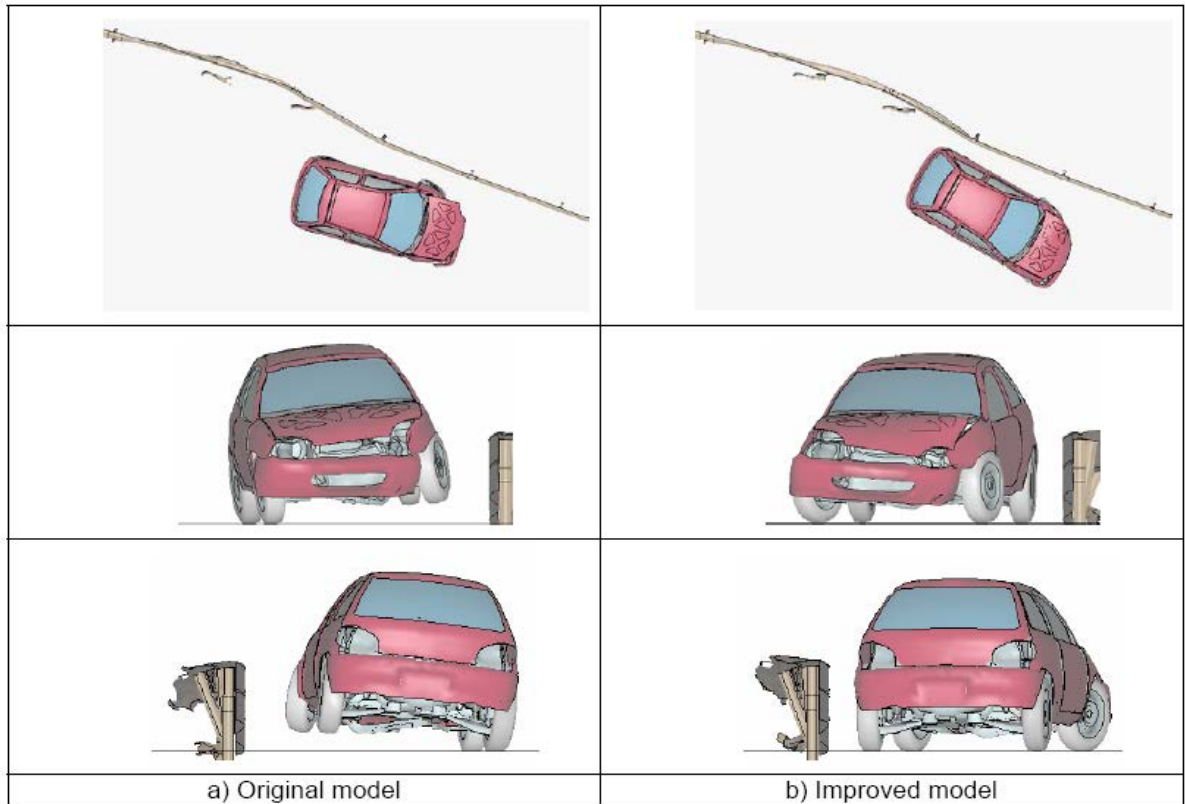


Figure 31. Comparison of the original and modified models of the Geo Metro in a 100 km/hr 20 degree impact with deformable guardrail.(78)

Table 7. EN 1317 domain-specific metric comparisons of a simulation and crash test of a small car striking a concrete wall at 20 degrees and 100 km/hr.(78)

ASI		
<i>Full-scale-test</i>	<i>Computer simulation</i>	<i>Ratio</i>
1.86	1.69	0.91
THIV		
<i>Full-scale-test [km/h]</i>	<i>Computer simulation [km/h]</i>	<i>Ratio</i>
32.9	34.7	1.05
PHD		
<i>Full-scale-test</i>	<i>Computer simulation</i>	<i>Ratio</i>
14.1	6.8	0.48

Eskandarian et al developed and validated a finite element model of the bogie vehicle. (49) The performance of the model and, in particular, the honeycomb material used in the nose of the bogie vehicle was assessed in impacts with an instrumented rigid pole. The deformed shape of the bogie nose (i.e., see Figure 32) and the corresponding time history comparisons were used to validate the finite element model.

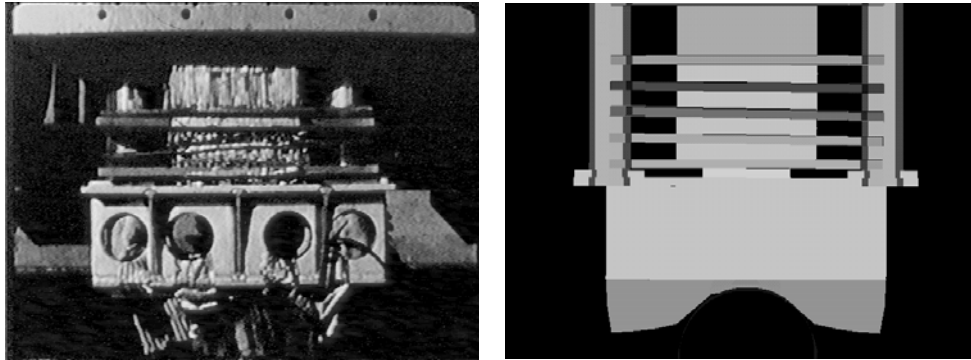


Figure 32. Comparison of crash test (left) and simulation (right) results showing successive crush (deformation) of the honeycomb nose material at 45 msec.(49)

Zaouk and Marzougui developed a model representing the US deformable barrier for use in side impact simulations.(79) Special emphasis was given to the adhesives and honeycomb materials and the way they were modeled in LSDYNA. As shown in Figure 33, qualitative comparisons, such as deformed shapes and time histories were made between the finite element simulation and full-scale test to validate the models.

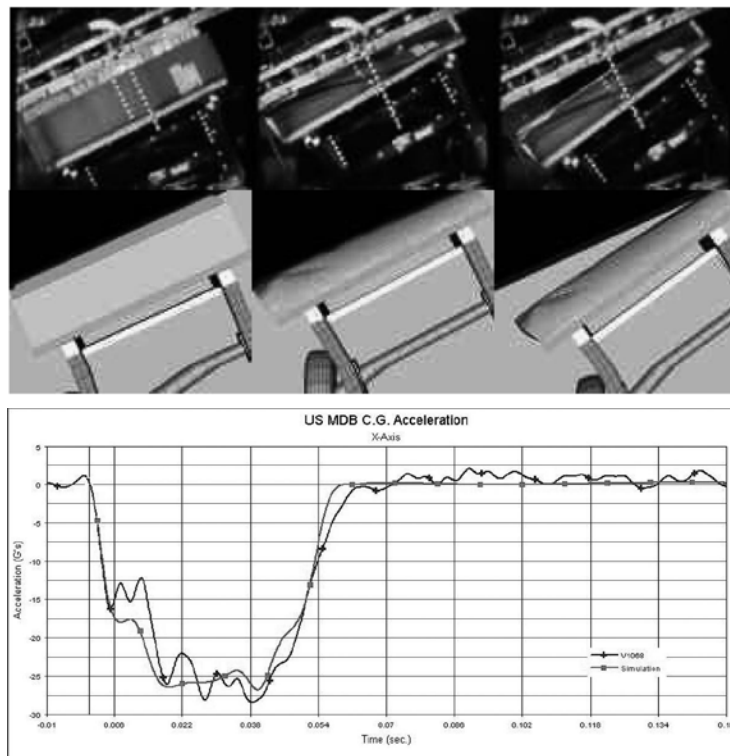


Figure 33. Deformation (top) and time history (below) comparisons of a side impact deformable barrier.(79)

Zaouk et al described the development of a detailed multi-purpose finite element model of a 1994 Chevrolet C-1500 pick-up truck.(80) This was the first model of its kind developed specifically to address general vehicle safety issues, including front and side performance, as well as roadside hardware design. The idea behind the vehicle model was to provide roadside safety and highway safety researchers with a common model they could use to explore safety issues. This paper described the results of a non-linear finite element computer simulation using this model for frontal full barrier and median highway barrier impacts. Full scale vehicle crash tests conducted by NHTSA and FHWA were used to validate the model. Two tests were compared, a frontal impact with a full rigid wall and a corner impact to a 42-inch vertical concrete median barrier. The comparisons between tests and simulations in terms of overall impact deformation, component failure modes, velocity and acceleration at various locations in the vehicle were presented.

Later, Zaouk presented the results of the development of a reduced element “bullet” model of the same C1500 vehicle more specifically modeled for roadside safety applications. (81) Full scale vehicle crash tests conducted by NHTSA and FHWA were used to evaluate the performance of the model. Two tests were used for comparison purposes: a frontal impact with a full rigid wall and a corner impact to a 42-inch vertical concrete median barrier. Mostly qualitative comparisons, such as deformation, component failure modes, velocity and acceleration at various locations in the vehicle for both the detailed and reduced models were made between physical tests and simulations in terms of overall impact. Further research was recommended to fully validate both vehicle models.

Similarly, another study concentrated on the development and validation of a C-2500 pickup truck model for roadside hardware evaluation.(82) The C-1500 pickup truck model discussed by Zaouk was modified such that it represented the 2000P crash test vehicle recommended in Report 350 (i.e., the Chevrolet C2500). Model validation was done through a series of qualitative comparisons including pictures and time histories (see Figure 34 and Figure 35).

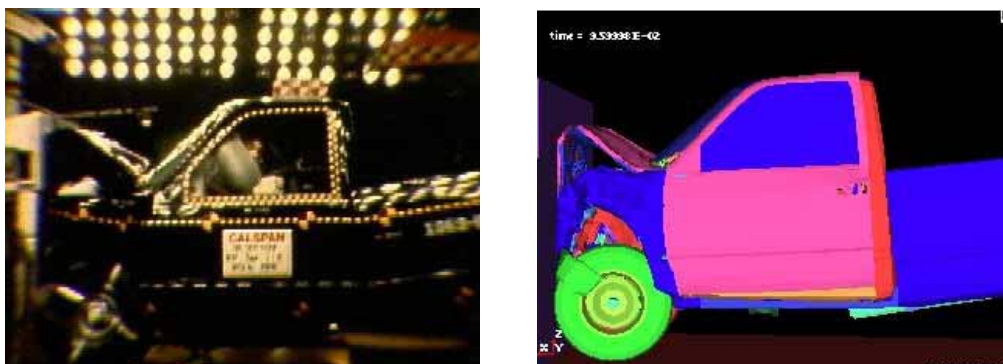


Figure 34. Qualitative comparison of deformations in a C2500 crash test into a rigid wall (left) and the corresponding simulation (right).(81)

In 1998, Zaouk et al discussed the development process of a detailed Chevrolet C-1500 pickup truck model for multiple impact applications. Several crash conditions were used to make the model as accurate as possible. Full-scale crash tests were used to validate the model using qualitative comparisons such as sequential pictures and time histories.(81)

Tiso et al performed an extensive program to develop functioning suspension and steering capabilities for the widely used NCAC C2500 pickup truck model in 2002.(83) In many roadside hardware impacts, the effect of the suspension on the impact performance of the barrier is considerable so having vehicle models with functioning suspension models was becoming very important. The major components of the suspension were examined using curb traversal tests and the results were compared to the original model. A number of sub-assembly laboratory tests such as shock absorber extension/compression tests and leaf-spring deflection tests were used to validate components of the model. Improvements to the leaf springs, shock absorbers, coil springs and steering linkages were made and then compared to the curb-traversal tests again. The results of the model improvements were qualitatively compared to the experiments and quantitative assessments of domain-specific values like maximum displacements were performed.

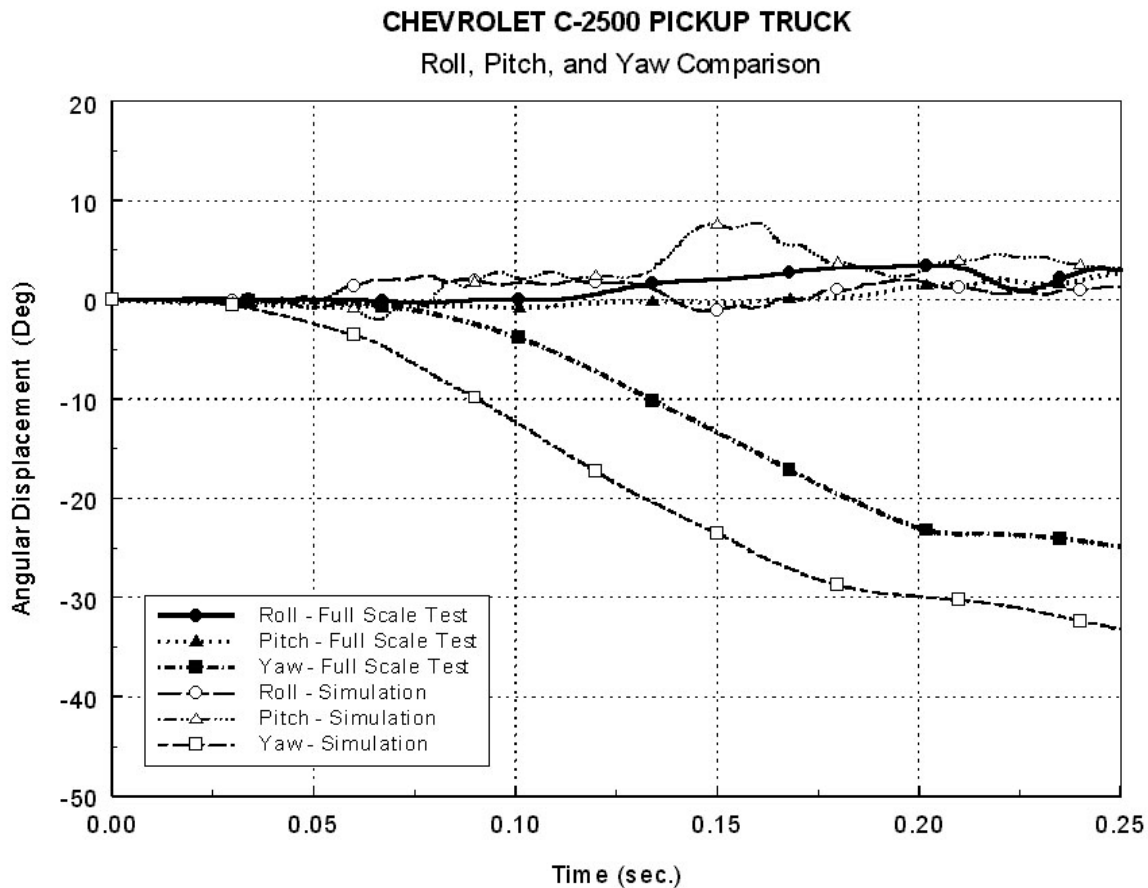


Figure 35. Time history comparison of a C-2500 pickup truck striking a median barrier.(81)

Orengo continued this work by adding a tire model to the C2500 that would experience de-beading failures when the vehicle interacted with curbs and edge drop offs.(46) The tire model was validated first using in-laboratory assembly tests and then validated by full-scale non-tracking curb impact tests where the tires failed by debanding. This work was described in the last section as a good example of component modeling in the hierarchical modeling section.

Marzougui et al also discussed the development of a detailed rear suspension model for the C2500 pickup truck model in a 2004 paper.(84) Pendulum tests were conducted at the Federal Highway Administration’s Federal Outdoor Impact Laboratory (FHWA’s FOIL). The pendulum test data was used in the validation of the suspension model. Simulations were conducted and the results were quantitatively compared to the pendulum tests in terms of deformation, displacement and acceleration at various locations.

Miele et al conducted an evaluation of the single unit truck (SUT) finite element model initially developed by the NCAC to assess its ability to accurately simulate its interaction with roadside safety hardware and to identify areas of possible improvements.(63) The SUT model is intended to be a so-called “bullet” model (i.e., a vehicle model with a reduced number of elements) for computational evaluation of roadside safety hardware. A very detailed model description is available at on-line [http:// thyme.ornl.gov/FHWA/F800WebPage/simulations/simulation1.html](http://thyme.ornl.gov/FHWA/F800WebPage/simulations/simulation1.html). The researchers were particularly concerned with modeling and replicating suspension system failures that are typical in SUT re-directional crash tests. The improved model was compared to results of a full-scale crash test performed at Texas Transportation Institute. Comparisons with the crash test included quantitative domain-specific parameters like the OIV, ORA, THIV, ASI, PHD, 50 msec average and maximum roll, pitch and yaw angles. Qualitative comparisons of the rotations in the experiment and simulation were also presented. A comparison of photographs from the crash test and corresponding simulation are shown in Figure 36. One of the notable aspects of this project was the excellent documentation provided on-line to users. Vehicle model developers should be encouraged to provide this level of detail for vehicle models that will be used repeatedly as “bullet” vehicles in roadside safety research.

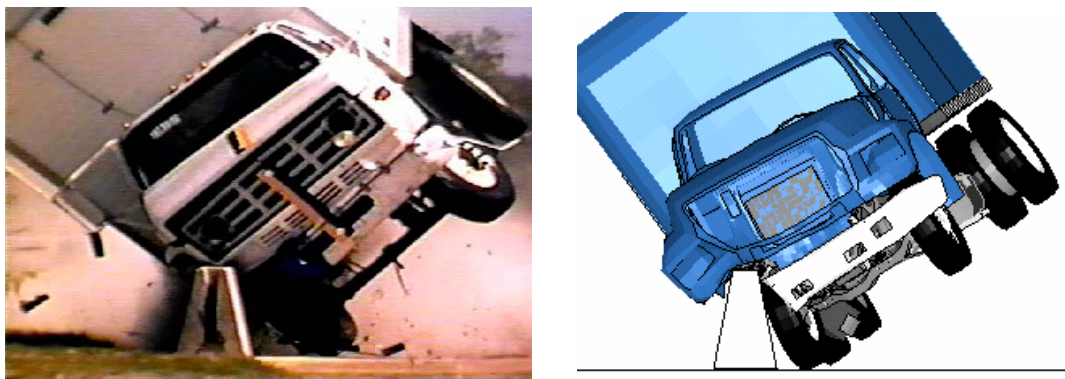


Figure 36. Comparison of crash test (left) versus finite element (right) results. (63)

Mohan et al also evaluated the Ford F800 Single Unit Truck (SUT) model.(85) The characteristics of the SUT model were investigated and several modifications were incorporated into the model to facilitate using it in roadside safety hardware development projects. A full-scale crash test of the Ford F800 SUT impacting an F-shape Portable Concrete Barrier (PCB) was conducted at FHWA's FOIL and used as a validation baseline test. Qualitative comparisons such as sequential pictures of the impact and acceleration time histories were used to assess the model.

Pernetti and Scalera developed a multipurpose finite element model of an articulated truck.(86) The model was intended to address two particular impact scenarios, the first against a concrete wall and the second against a steel bridge railing. The results obtained demonstrated that the model was accurate and the articulated truck model is suitable for a wide range of impact conditions.

As shown in these descriptions of previous work on vehicle modeling, vehicle models for use in roadside safety improvements have generally been the product of continuous improvement sometimes over as much as a decade. When a vehicle model is first developed, it is often validated with tests in the NHTSA literature like the NCAP tests. As the model is used for a wider variety of situations in roadside safety improvements are added to address particular concerns and these improvements remain in the model making it increasingly more general and more reliable as each new revision is developed. One of the draw backs of the way vehicle modeling has evolved in roadside safety is that there is very poor version control and documentation of the models. The models tend to be modified by each research organization and often the models diverge into several variations that are separately improved and modified. This results in a duplication of effort as well as confusion over what level of validation any particular model has achieved. Ideally, it would be useful to collaborate more effectively on model improvements and share these results with other researchers.

Roadside Hardware Models

Probably the first paper to address the use of nonlinear dynamic finite element analysis in roadside safety was a paper by Wekezer in 1993.(87) Wekezer examined an impact simulation of a compact car with a light pole. The paper illustrated that models with even relatively small numbers of degrees of freedom in DYNA3D can predict the kinematics of highway vehicles in impacts. Wekezer's study was a preliminary feasibility study to develop the next generation of roadside safety computer software for vehicle impact simulation and analysis.

In 1994, Ray examined the impact of a 820-kg small car striking a 5.5 kg/m flange-channel sign post at nine meters per second.(88) As shown in Figure 37, the 13,000-element vehicle model developed by EASi Engineering was used to examine the collision sequence in much greater detail than is possible with a full-scale crash test.(74) The state of stress of any vehicle or barrier component can be examined in detail to determine the actual failure

mechanisms involved in the collision. Qualitative comparisons of the deformed vehicle shape and acceleration-time histories were used to assess the accuracy of the model. As shown in Figure 38, the model successfully captured the basic phenomenon involved in the impact.

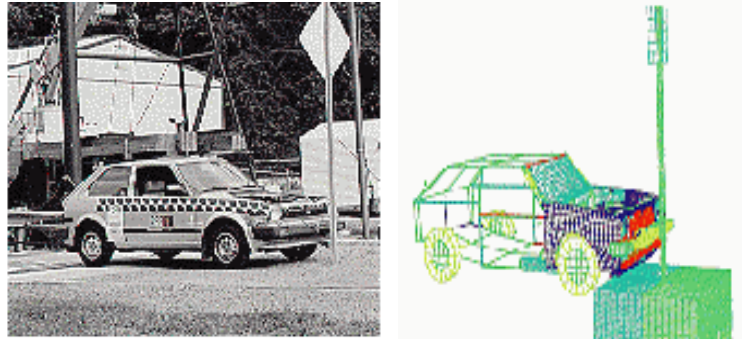


Figure 37. Photograph (left) and corresponding finite element model (right) of the pre-collision with a sign post.(88)

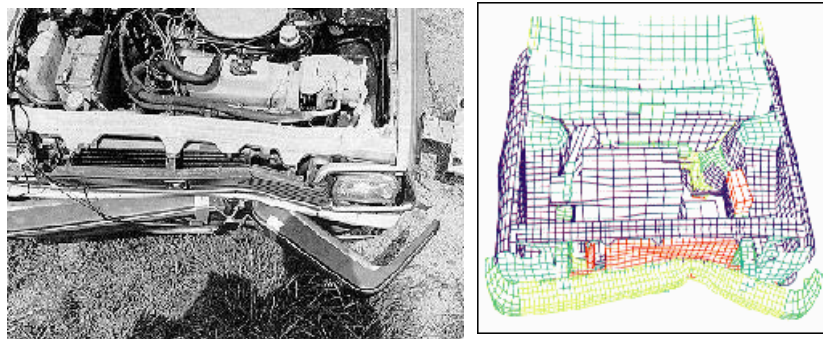


Figure 38. Vehicle deformation comparison after sign post impact crash test (left) and finite element simulation (right).(88)

In 1997 the FHWA sponsored the publication of a collection of seven papers by their Centers of Excellence regarding using LSDYNA and DYNA-3D in roadside safety research. (81) The report contained papers regarding:

- The development of a C1500 pickup truck model for use in roadside hardware simulations,(81)
- The development of a model of the MELT guardrail terminal,(89)
- The development of a model of a transformer base,(90)
- The development of a thrie-beam guardrail model,(91)
- The development of models for the Nebraska turned-down terminal, the dual-support breakaway sign, the buffalo guardrail and a breakaway mailbox and(92)
- The development of a slip-base luminaire support.(93)

These papers are discussed in the following paragraphs.

Another paper that appeared in the mentioned FHWA sponsored publication addressed the development and validation of a weak post W-beam G2 guardrail.(94) Modeling details, such as post-soil interaction, W-beam end anchorage, post-to-W-beam connection were explained. Results of a full-scale crash test were qualitatively compared to the simulation results.

Martin and Wekezer continued work on the development of a finite element model of the G2 weak post w-beam guardrail.(95) The NCAC model of the 1994 Chevrolet pickup truck was used to simulate an impact with the barrier at 100 km/hr and 25 degrees. Data obtained from a full-scale crash test were used to validate the weak post w-beam guardrail model. Acceleration time histories obtained from the crash test and simulation study were used to make both qualitative and quantitative comparisons. The NARD validation metrics, the ANOVA metrics proposed by Ray and Wekezer’s protocol validation method were also used to compare the simulated and experimental responses. The results for the NARD metrics are shown in Table 8.

Table 8. NARD time-domain metrics comparing a 100 km/hr, 25 degrees impact between a pickup truck and the weak-post w-beam guardrail.(95)

Relative Moment Difference
Moment 0 = 0.432 Relative moment difference = 0.27
Moment 1 = 0.078 Relative moment difference = 0.24
Moment 2 = 0.018 Relative moment difference = 0.22
Moment 3 = 0.005 Relative moment difference = 0.21
Moment 4 = 0.002 Relative moment difference = 0.20
Moment 5 = 0.001 Relative moment difference = 0.20
Root Mean Square (RMS) Log Measures
RMS Log Difference (R3) 8.4
RMS Log Average (R4) 6.6
RMS Log Form of Signal #1 (R1) 6.9
RMS Log Form of Signal #2 (R2) 6.3
RMS Log Ratio (R3/R4) 1.3
Correlation Measure
Energy Measure of Correlation 0.49

Ray and Plaxico continued the work on weak-post w-beam guardrails when crash tests of the standard weak-post w-beam guardrail involving the 2000-kg pickup truck resulted in a series of unacceptable test results including over-riding and penetrating the guardrail.(96)

Design modifications to the weak-post w-beam guardrail were explored using finite element simulations and full-scale crash tests. Qualitative and quantitative comparisons were made between the crash test results and simulation results to validate the accuracy of the finite element model. An improved version of the weak post w-beam guardrail system was developed and tested and found to satisfy the requirements of Report 350 for test level three.

A finite element model of the slipbase luminaire support research was also included in the same FHWA sponsored publications.(97) A detailed finite element simulation study was performed to evaluate the important characteristics of the slipbase design. Cofie's small car model was used to impact the support and the results of the simulation study were compared to those obtained from full-scale crash tests to validate the models.(75) Pictures and time histories were used in the qualitative assessment process.

A paper by Eskandarian et al describes a model of a slip-base sign support system and its crash performance with vehicles using DYNA3D.(97) The geometric features, as well as several physical phenomena of components of the slip-base mechanism, e.g., sliding friction, clamping forces, bolt-plate interactions, and plate rupture, are modeled and verified in simulation. The FE modeling methods for the required features are described in detail. A validated model of Bogie and its honeycomb material is used as the impacting vehicle. FE crash simulations of Bogie with flexible honeycomb nose impacting the slip-base sign support are validated using the corresponding instrumented crash tests. The simulation model reveals the correct behavior of the breakaway system response upon impact. The slipping mechanism and Bogie acceleration and velocity responses are accurate as compared with actual crash test results. The FE approach and this validated model can be exercised in numerous crash scenarios for design optimization of other variations of slip-base systems in size, orientation, etc., or for performance evaluation of impacts with various vehicles. In a similar study, finite element simulation and its application to crashworthiness evaluation and safety analysis of roadside hardware appurtenances is presented.(98) Three specific case studies are discussed to demonstrate the effectiveness of these methods in modeling and simulating roadside hardware objects. The first case study involved finite element modeling and analysis of various slipbase sign support systems. Models were validated against full-scale crash test results. Only qualitative comparisons, such as acceleration, velocity and displacement vs. time graphs were compared. In the second case, the safety performance of a portable concrete barrier (PCB) during high-speed impact was investigated and design modifications were analyzed to improve their performance. The third case study utilized finite element analysis to predict the safety of a U-post sign support system. The effect of its height on intrusions into the occupant compartment was analyzed.

Reid et al analyzed the turned-down guardrail terminal using LSDYNA and full-scale crash tests. (99) Finite element simulations were performed on the existing turned-down approach terminal section as well as on various retrofit options to understand the crash performance of end terminals and evaluate the performance of design alternatives. Modified

designs were subjected to one high-speed and six low-speed full-scale crash tests with an 820 kg vehicle. Deformations and crash test pictures were used to validate the accuracy of the finite element models.

In another study, Paulsen and Reid modeled a dual support breakaway sign system using LSDYNA.(100) Component models were first constructed on critical parts of the breakaway sign system. The component models were compared with physical component tests to aid in the development process, as well as to validate the component simulation results. The components were then assembled into a complete system model. Very few changes were made in the complete sign model, because problems were worked out in component modeling phase. Qualitative comparisons were made between the simulation results and two full-scale vehicle crash tests were used to validate the model.

Ray and Patzner describe the development of an LSDYNA model of a MELT guardrail terminal to learn more about the performance of this type of guardrail terminal.(101) Results of the analysis are discussed and compared to data from a full-scale crash test involving a small passenger car. Qualitative comparisons of the acceleration and velocity time histories were made and quantitative comparisons of the occupant risk criteria and a statistical method were used to illustrate the validity of the models. The quantitative comparison was performed using the Test Report Analysis Program (TRAP), which automatically evaluates the occupant risk criteria defined in NCHRP Report 350 using the acceleration curves obtained from the simulation data. TRAP was developed by Texas Transportation Institute (TTI) primarily for analyzing crash test data, but it can also be used for analyzing the data from crash test simulations. (149)

In a similar study, Plaxico provided a description of the development of a model of a breakaway timber post and soil system used in the breakaway cable terminal (BCT) and the modified eccentric loader terminal (MELT).(102) The model is described and simulation results are qualitatively compared with data from physical tests of BCT/MELT posts.

A guardrail system capable of capturing and redirecting a larger range of vehicle types and sizes was developed.(103) The new guardrail system, called the Buffalo Rail, was designed with a new w-beam cross-sectional shape with an effective depth of 311 mm compared to 194 mm for the W-beam, a rail thickness of 13 gauge, and a post spacing of 2500 mm. Finite element analyses were performed to evaluate the impact performance of the new barrier. The LSDYNA simulations predicted that the safety performance of the Buffalo Rail would be acceptable for the Report 350 test 3-11 pickup truck. Qualitative and quantitative comparisons were made to validate the finite element model of the Buffalo Rail.

LSDYNA was used to develop a model of the sequential kinking process for energy dissipation used in a new guardrail terminal concept.(104) The sequential kinking process involves using a deflector plate to force a steel beam guardrail element to be bent around a rigid

beam until it forms a plastic hinge. Qualitative comparisons between the full-scale tests and finite element results were used to validate the model. Full-scale crash tests showed that predictions of the energy dissipation for the sequential kinking impact head were only seven percent below values obtained from dynamic impact tests.

Reid and Bielenberg designed and successfully crash tested a bullnose median barrier head-on at 100 km/h with a 2000-kg pickup truck.(105) After a failed pickup truck test, LSDYNA was used to simulate the failed system in order to determine the cause of the failure and evaluate solutions to the problem. Subsequent testing substantiated the LSDYNA predictions and qualitative comparisons used to validate the models used in the simulation study. To keep up with the design project deadlines, some features of the simulation model were simplified. For other features, however, great attention to detail was required to make a useful model. Specifically, a considerable amount of effort went into defining the material failure criteria and appropriate mesh density for the guardrail, rolling tires for the truck model, and application of the relatively new cable element in LSDYNA.

Tabiei and Wu developed a simulation of a truck impacting a strong-post w-beam guardrail system, the most common system in the USA.(29) Detailed methods for developing the simulation were presented and three major issues were identified: The rail to blockout bolt connection, dynamic soil-post interaction and the effect of the end anchorage of the guardrail. Soil-post interaction was modeled using both Lagrangian and Eulerian meshes and the results using the two methods were presented. Sequential pictures and acceleration time histories were used to make qualitative comparisons. The NARD metrics were used to make quantitative comparisons between physical crash test results and simulation results.

Plaxico and Ray evaluated the crashworthiness of two similar strong post guardrails (i.e., the G4(2W) and the G4(1W)) using LSDYNA. (10) A model of the G4(2W) guardrail was first developed and validated with the results of a full-scale crash test from the literature. As shown in Table 9 and Table 10, quantitative comparisons of the two impacts were performed using TRAP domain-specific metrics, the NARD time-domain metrics, the ANOVA metrics and Geer's MPC metrics. Moreover, qualitative comparisons, such as acceleration, velocity and yaw angle time histories were used to validate the G4(2W) model. After the G4(2W) model had been validated, a model of the G4(1W) guardrail system was developed based on the validated G4(2W) which uses larger 8x8 inch posts. The results from the simulations of the two guardrail models were compared with respect to deflection, vehicle redirection and occupant risk factors. The results of the analysis indicated that the G4(1W) and G4(2W) perform similarly in collisions and they both satisfy the requirements of Report 350 for the test 3-11 conditions.

Table 9. Domain-specific TRAP metrics for TTI test 471470-26 and LSDYNA simulations of two strong-post w-beam guardrails.(11)

Occupant Risk Factors		Test 471470-26	G4(2W) F.E.A.	G4(1W) F.E.A.
Occupant Impact Velocity	at time (seconds)	0.1500	0.1447	0.1313
	x-direction (m/s)	5.7	5.9	5.1
	y-direction (m/s)	-5.7	-5.8	-6.4
THIV (km/hr)		25.8 (at 0.1453 seconds)	31.9 (at 0.1507 seconds)	29.4 (at 0.1313 sec)
Ridedown Acceleration	x-direction (g's)	-10.1 (0.1903 - 0.2003 seconds)	-10.7 (0.1957 - 0.2057 seconds)	-15.2 (0.1370 - 0.1470 sec)
	y-direction (g's)	8.9 (0.1990 - 0.2090 seconds)	10.8 (0.1730 - 0.1830 seconds)	14.1 (0.1310 - 0.1410 sec)
PHD (g's)		11.4 (0.2430 - 0.2530 seconds)	12.4 (0.1730 - 0.1830 seconds)	19.2 (0.1357 - 0.1457 sec)
ASI		0.95 (0.2160 - 0.2660 seconds)	0.94 (0.0967 - 0.1467 seconds)	1.30 (0.1007 - 0.1507 sec)
Maximum 50 ms moving avg acceleration	x-direction	-6.0 (0.1277 - 0.1777 seconds)	-7.4 (0.0950 - 0.1450 seconds)	-9.2 (0.1057 - 0.1557 sec)
	y-direction	6.5 (0.1010 - 0.1510 seconds)	6.0 (0.0957 - 0.1457 seconds)	9.3 (0.1497 - 0.1997 sec)

Table 10. NARD and ANOVA metrics for TTI test 471470-26 and LSDYNA simulations of two strong-post w-beam guardrails.(11)

Comparison Parameters		x-g's	y-g's	z-g's
Comparison over 0.300 seconds of impact				
$\frac{M_n(\text{test}) - M_n(\text{simulation})}{M_n(\text{test})}$ n th Relative Absolute Difference of moments = (should be <0.2)	0 th moment difference	0.02	0.03	1.11
	1 st moment difference	0.04	0.02	2.73
	2 nd moment difference	0.01	0.02	1.20
	3 rd moment difference	0.02	0.01	0.05
	4 th moment difference	0.07	0.01	0.21
	5 th moment difference	0.11	0.02	0.32
Correlation Factor		0.68	0.75	0.52
T-statistic (should be < 2.58)		0.23	0.52	2.56
Geer's Parameters (should be < 0.2)	Magnitude	0.01	0.17	-0.16
	Phase	0.17	0.13	0.28
	Correlation	0.17	0.22	0.32
Comparison over 0.600 seconds of impact				
$\frac{M_n(\text{test}) - M_n(\text{simulation})}{M_n(\text{test})}$ n th Relative Absolute Difference of moments = (should be < 0.2)	0 th moment difference	0.14	0.17	1.92
	1 st moment difference	0.19	0.29	1.89
	2 nd moment difference	0.18	0.36	1.95
	3 rd moment difference	0.15	0.39	2.00
	4 th moment difference	0.16	0.37	2.04
	5 th moment difference	0.23	0.29	2.06
Correlation Factor		0.48	0.59	0.10
T-statistic (should be < 2.58)		1.71	3.28	4.66
Geer's Parameters (should be < 0.2)	Magnitude	0.04	0.05	-0.55
	Phase	0.30	0.23	0.68
	Correlation	0.31	0.24	0.88

Marzougui et al discuss the effect of w-beam guardrail height on the crash test performance of the G4(1S) strong-post w-beam guardrail.(106) First, a detailed model of the G4(1S) guardrail was created. The model incorporated the details of the rail, connections, the post, the blockout, and the soil in which the post was embedded. To validate the model of the W-beam guardrail system, a model of the setup of this W-beam system in previous full-scale crash tests was created. Simulations were performed using this model and the results were compared to the full-scale crash test data. Qualitative and quantitative comparisons showed that the model was an accurate representation of the actual system. In the second step of the study,

the validated model served as the basis for four additional models of the G4(1S) guardrail to reflect varying rail heights. In two of the four models, the rails were raised 40 and 75 mm (1.5 and 3 inches). In the other two models, the rails were lowered 40 and 75 mm. Simulations with these four new models were carried out and compared to the first simulation to evaluate the effect of rail height on safety performance. The simulation results indicated that the effectiveness of the barrier to redirect a vehicle is compromised when the rail height is lower than recommended. The third step of the study consisted of performing full-scale crash tests with the guardrail at standard height and 60 mm (2.5 inches) lower. The data from the crash tests validated the simulation results.

Marzougui et al used LSDYNA simulations to evaluate the safety of portable concrete barriers (PCB).(107) A methodology for creating accurate models of PCBs was first developed. This was achieved by developing a model of an F-shape PCB design and using full-scale crash test data to validate the model. Qualitative comparisons were made to validate the model (see Figure 39). Once the model had been qualitatively validated, models of two modified PCB designs were created and their safety performance was evaluated. Based on the simulation results, a third design was developed and its performance was analyzed as well. The safety performances of the three designs were compared.

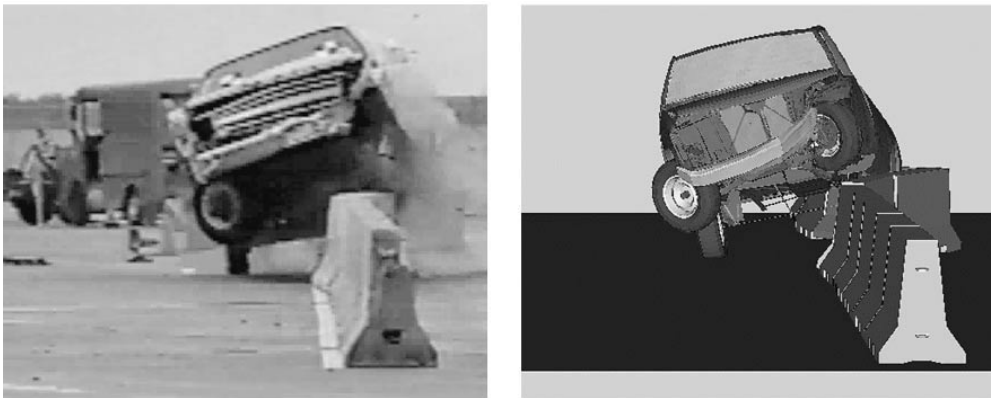


Figure 39. Qualitative comparison of pickup truck impact with an F-shape portable concrete barrier.(106)

A new bullnose guardrail system for the treatment of median hazards was developed and successfully crash tested according to the safety criteria in Report 350 by Bielenberg et al. (108) The new system consists of a nose section and a special cable structure. The first five sections of guardrail had horizontal slots cut in the valleys of the rail to improve vehicle capture and reduce the formation of large kinks that could pose a threat to a vehicle as the system deformed to absorb an impact. The research study included computer simulation modeling using LSDYNA and full-scale vehicle testing. Qualitative comparisons between the simulation and crash test results were used to validate the finite element models.

Marzougui et al used LSDYNA to analyze the safety performance of roadside sign support systems.(109) Specifically, they investigated the effect of sign height on the amount of intrusion into the occupant compartment. Models of 5ft (1.5m) and 7ft (2.1m) height signs were created and impacted with a set of vehicle models at different impact speeds. Five vehicle models were used in the study: the Chevrolet C2500 pickup, Geo Metro, Ford Taurus, Plymouth Neon, and Dodge Caravan. Three impact speeds were analyzed: 20, 40, and 60 mph (32, 64, and 96km/h). A total of 18 simulations were performed and the results were compared to evaluate intrusion of the signs into the occupant compartment. The simulation results were verified qualitatively by using full-scale test results obtained from the worst-case scenario test, a Geo Metro into a U-post at 60 mph.

Engstrand et al discussed simulation of vehicle models used in roadside safety research. (110) According to a recent European regulation, the passive safety of all new roadside barriers must be verified in impact tests with real vehicles. The test matrix includes a small car but, depending on the road containment level, also a medium-size car, a bus, a medium weight truck or a heavy truck. Obviously, it is important and efficient to first assure the passive safety of the barrier using simulations before the actual tests are conducted. In a simulation of the vehicle crash on a roadside barrier, the quality of the vehicle model is as important as the barrier model. In this study, qualitative comparisons between the simulations and full-scale tests were used to validate the accuracy of the vehicle models developed.

After a failed crash test on a strong-post guardrail system, Atahan used LSDYNA to simulate the system and determine the potential problems with the design.(111) The accuracy of the finite element models used in the simulation study was evaluated by comparing the results against those obtained from the full scale crash test. Qualitative comparisons, such as sequential pictures, article deformations and vehicle velocity time graphs were made. After validating the model, a second simulation was performed on an improved version of the system. Simulation results indicated that the improved system would perform much better than the original design.

Reid et al discusses the development of a new barrier system to improve the safety of drivers participating in automobile racing events.(112) Several barrier prototypes were investigated and evaluated using static and dynamic component testing, computer simulation modeling with LSDYNA and 20 full-scale vehicle crash tests. The full-scale crash testing program included bogie vehicles, small cars, and a full-size sedan, as well as Indy-style open-wheeled race cars and NASCAR race cars. LSDYNA models were validated using qualitative comparisons with full-scale test results.

Bielenberg discussed the development of barriers for race venues. He describes a barrier with foam blocks placed between an outer steel tube structure and the existing race track concrete wall.(113) Polystyrene insulation foams were shown to have good energy absorbing capabilities and were used as a primary means of energy absorption in the barrier. Simulations

of the dynamic tests with LSDYNA used the *MAT_CRUSHABLE_FOAM material model. After successfully modeling the bogie tests, the component model of the foam was placed in the full-scale model of the SAFER barrier. Later in the research program, the cubic shape foam blocks were replaced with a trapezoidal shape. These trapezoidal shapes were also tested and then, successfully simulated. Sequential pictures and time history data was used to validate the finite element models.

Ray et al described the design and analysis of an extruded aluminum truss-work bridge railing for Report 350 test levels three and four conditions.(114) In this case there were no crash tests available to assess the performance of the model so LSDYNA was used to determine if the bridge railing would be likely to result in successful crash tests. The LSDYNA simulations indicated that the truss-core panels would be strong enough in an impact and a subsequent AASHTO LRFD analysis supported the LSDYNA results. The design documented in this report was found to be of comparable strength to other F-shaped bridge railings so that successful crash test results are highly likely. The FHWA issued an acceptance letter for this new type of bridge railing based only on the computational analysis.

Whitworth et al evaluated the crashworthiness of a modified w-beam guardrail design. (115) A model of the guardrail was developed and the crash response simulated for an impact by a pickup truck traveling at 100 km/hr. A model of a Chevrolet C2500 pickup truck was combined with the guardrail model to simulate the crash test. The model evaluation focused on comparison of actual crash test data with the simulation results in terms of roll and yaw angle measurements. Simulation results were found to be in good agreement with the crash test data. Additionally, simulations were also performed to evaluate the effect of certain guardrail design parameters, such as rail mounting height and routed/non-routed blockouts, on the crashworthiness and safety performance of the system.

Mohan et al developed a detailed finite element model of a three-strand cable barrier. (116) The accuracy of the model was validated against a previously conducted full-scale crash test. The full-scale crash test and simulation were set up for an impact of the cable barrier with a 2000 kg pickup truck at an angle of 25 deg and an initial velocity of 100 km/hr. Details for simulating the dynamic interactions of the soil and post, post and hook bolts, cable and hook bolts and cable to truck were presented in the paper. Qualitative comparisons between the simulations and full-scale crash test were presented.

Atahan and Cansiz studied a vertical flared back concrete bridge rail-to-guardrail transition to evaluate its compliance with Report 350 test level three requirements.(30) In a crash test, the system failed to meet the Report 350 requirements because the vehicle rolled over. To gain insight about the crash test phenomena, a simulation study was performed. The accuracy of the simulation was verified using qualitative and quantitative comparisons, such as sequential crash test pictures and TRAP, NARD, ANOVA and Geer's metrics, respectively. Based on examination of the crash test and simulation, the w-beam height of 685 mm was

determined to be the main cause for vehicle rollover. The transition model was modified to have an 810 mm top rail height. A subsequent simulation resulted in a prediction that the improved model would contain and redirect the vehicle in a stable manner without rollover. No wheel snagging was observed due to increased rail height. The performance of the improved transition design was so good that consideration was given to testing it at the next level, test level four.

Finite element computer simulations coupled with experimental testing were used to investigate the safety of mailbox supports and establish some guidelines on their use and installation.(117) First, a model of the mailbox support was developed and validated against pendulum crash tests. Second, a parametric finite element analysis was performed with various mailbox sizes, heights, mounting configurations and post sizes in order to evaluate the mailbox support crashworthiness performance. Third, the simulation results were qualitatively validated using the most critical case. A full scale crash test was performed using the critical impact scenario and compared with the corresponding simulation.

Sheik et al discussed the development of the energy absorbing end terminal, HEART.(118) The HEART terminal was developed using LSDYNA modeling The paper presents the simulation approach adopted for the development of the HEART including the construction details, qualitative comparisons for the model validation and the description and results of crash tests performed so far to evaluate its performance.

LSDYNA was used to analyze and improve the crash test behavior of the New York Department of Transportation Portable Concrete Barrier (NYPCB).(119) A full-scale crash test demonstrated that the current NYPCB design was unable to meet Report 350 standards. An inspection after the test revealed that the welding at the metal connectors forming the joint between the barrier segments was not properly fabricated. An LSDYNA model of the crash-tested barrier was developed with a special fillet weld with failure model and subjected to the same impact conditions as the failed crash test. Qualitative comparisons were made between the test and simulation such as force-deformation plots, roll angle time histories and sequential pictures of the crash event. Quantitative domain-specific comparisons using the TRAP metrics were also made. The results showed that the baseline model simulation replicated the failure in the crash test. After validating the model, an improved NYPCB model was developed by using proper welding details and subjected to full-scale impact simulation conditions to determine whether this design would satisfy the crash testing requirements. The results of the simulation were encouraging and it was predicted that the barrier would successfully contain and redirect the impacting vehicle in a stable manner. Subsequent full-scale crash testing on the NYPCB with proper welding details passed the NCHRP Report 350 requirements and substantiated the LSDYNA predictions.

Concrete barriers have often been considered too stiff for small vehicles in European regulations.(120) As a result, there has been very little change in the design of concrete barriers

in Italy over the past 20 years. Bonin re-examined the use of concrete barriers for the European EN 1317 regulations and, in particular, used lightweight concrete and shorter section length than commonly used in Italy. A lighter concrete portable barrier would likely deform more in the lateral direction leading to more energy dissipation and decreased occupant risk values. Bonin examined these new alternatives using LSDYNA models. First the model was validated by comparing the results of the simulation to prior crash tests using the existing Italian concrete barrier design and the predictions of the LSDYNA model. Next, alternative designs were examined that used lighter-weight concrete and shorter segment lengths. The performance of both the ODOT GR-2.2 guardrail and the ODOT GR-3.4 transition system in Report 350 test level three conditions was investigated by Plaxico.(121) Modifications that would improve the crashworthiness of these transitions were proposed. LSDYNA was used to simulate Report 350 tests 3-10 and 3-11 for the improved transitions. The analyses indicated that the original ODOT GR-2.2 guardrail would successfully meet all Report 350 test level three criteria but the analyses also indicated that the performance of the system could be significantly improved with simple modifications to the guardrail.

Plaxico developed a model of a 50-inch high portable concrete barrier which is tall enough to serve as its own glare-shield.(122) Finite element analysis was used to investigate various barrier shapes and connection schemes to identify a successful crashworthy design that would meet requirements of Report 350 for test level three. A full-scale crash test was performed of the barrier after it was developed using LSDYNA at the Transportation Research Center in East Liberty, Ohio. The results of the crash test were used to validate the simulation results using qualitative comparisons of the time histories and sequential pictures as well as quantitative comparisons of the TRAP domain-specific metrics

Anghileri considered the crash test scenario of a small passenger car with a total mass of 900 kg striking a rigid concrete barrier at 100 km/hr and 20 degrees.(123) The impact conditions represent the EN 1317 TB11 impact conditions. An accelerometer sensor was included in the vehicle model in order to collect the acceleration and velocity-time histories of the vehicle and to consequently assess the occupant risk factors during the impact simulation. LSDYNA card *ELEMENT_SEATBELT_ACCELEROMETER was used for this purpose. The results of the impact simulation were used to evaluate the influence of the output frequency on the computation of the acceleration-time histories and occupant risk factors. The same impact scenario and finite element model were used to evaluate the effect of the location of the accelerometer sensor. Anghileri's work was used to explain some of the variation in crash test results that were observed in the ROBUST round-robin crash test series where the same test was performed by five different crash test laboratories.

Finite element simulations, vehicle dynamics simulations and full-scale crash tests were used to study the effect of sloped terrain on the safety performance of cable median barriers. (124) A detailed finite element model of a three-strand cable barrier was developed and validated against a previously conducted full-scale crash test. The full-scale crash test and

simulation were setup for an impact of the cable barrier according to Report 350 TL3 conditions. Then the computer simulations were performed to assess the barrier performance under different impact scenarios and terrain profiles. Vehicle dynamics analyses were also conducted to compute the vehicle trajectory and dynamics as it crossed the sloped terrain and struck the cable median barrier. After completing the computer simulations, full-scale crash tests were performed to validate the results.

A summary of the methods used to validate vehicle and barrier models in roadside safety research is shown in Table 11. As shown in the previous section on vehicle and barrier modeling, the most common methods for validating simulations are qualitative comparisons of time histories and sequential photographs and the comparison of domain-specific metrics from TRAP. There have been a few instances of using shape-comparison metrics but these have been relatively few.

VERIFICATION

Process

Two types of verification are discussed in this section. The first might be referred to as calculation verification where solutions to standardized benchmark problems provide verification that new versions of software, new computing machinery or new software provide the same answers as previously accepted solutions.

The other type of verification activity might be referred to as model assurance verification, where the model and its results are critiqued based on basic laws of physics and sound engineering practice; Qualitatively, do the results make sense based on basic laws of physics? In this type of activity, there is no known solution but modeling techniques and procedures can be used to maximize the likelihood of producing a numerically stable solution that adheres to fundamental physical laws. The following sections will describe each type of verification activity based on a review of the literature.

Table 11. Summary of methods used to validate models in roadside safety publications.

Publication	VALIDATION METHOD					
	QUALITATIVE		QUANTITATIVE			
	Time	Deformation	Geer's	NARD	TRAP	Hypothesis
Ray, 1994	√	√				
Zaouk et al 1996	√	√				
Marzougui et al 1996	√	√				
Hendricks and Wekezer (1996)	√	√				
Abu-Odeh et al.1997	√	√				
Reid et al 1996		√				
Paulsen and Reid, 1996	√	√				
Eskandarian et al 1997	√	√				
Ray and Patzner, 1997	√	√			√	√
Reid et al 1997	√	√			√	
Zaouk et al 1997	√	√				
Gentry and Bank, 1998	√	√		√		
Plaxico et al 1998	√	√				
Zaouk et al 1998	√	√				
Martin and Wekezer, 1998		√		√		√
Reid and Sicking, 1998	√	√				
Reid and Bielenberg, 1999	√	√				
Tabiei and Wu 2000		√		√		
Plaxico and Ray 2000	√	√	√	√	√	√
Marzougui et al 2000a		√				
Marzougui et al 2000b		√				
Eskandarian et al 2000	√	√		√		
Bielenberg et al 2001		√				
Ray et al 2001		√			√	
Marzougui et al 2001	√	√				
Zaouk and Marzougui 2001	√	√				
Engstrand et al 2001	√	√				
Kokkins et al 2001		√				
Atahan 2002	√	√				
Orengo et al 2003	√	√				
Reid et al 2003	√	√				
Marzougui et al 2004	√	√				
Ray et al 2004		√			√	
Whitworth et al 2004	√	√				
Atahan and Ross, Jr 2004		√				
Bielenberg, 2004	√	√				
Mohan et al 2005	√	√				
Atahan and Cansiz 2005	√	√	√	√	√	√
Miele et al 2005	√	√			√	
Tahan et al 2005	√	√				
Sheikh et al 2005	√	√				
Atahan 2006	√	√			√	
Bonin et al 2006		√				
Bhargava et al (2006)		√				
Plaxico et al 2006a		√				
Plaxico et al 2006b	√	√			√	
Anghileri 2006	√	√			√	
Pernetti and Scalera 2007	√	√				
Mohan et al 2007a	√	√				
Marzougui et al 2007a	√	√				
Marzougui et al 2007b	√	√			√	

Calculation Verification

As discussed earlier, software or platform verification involves running computer models that have provided solutions previously with a particular software and computational platform on new versions of the software or different computation platforms or setups. For example, Ray made available Cofie's simple model of an 820C passenger vehicle striking a rigid pole as a performance benchmark case for LSDYNA in about 1997 and placed the model on the internet.⁽⁷⁵⁾ Users from around the world used that benchmark model to benchmark the performance (i.e., the run-time speed) on new computers and new computer set-ups as they came onto the market.⁽¹²⁵⁾ The frontal NCAP models of the NCAC Taurus and Neon have also been used as run-time benchmarks.⁽¹²⁶⁾

While these models were only used to compare run-time speeds, their use as benchmarks does illustrate the utility and importance of providing "known" solutions to test new software and computation platforms. It is likely that most serious roadside safety simulation researchers have their own informal benchmark cases that they run to verify that new versions of the software provide similar results to prior versions. Unfortunately, such activity is rarely documented in the literature and there is no standardization from one research group to another.

Recently, during the Robust project in Europe, simulations with nominally identical models of the round-robin tests (i.e., 900-kg vehicle, impact angle of 20° and initial velocity of 100 km/h against a rigid barrier) were independently run by different organizations to verify consistency of results and procedures. This activity demonstrated that a common procedure to extract and elaborate signals was needed. After such a procedure was developed, the scatter, related to severity indices, obtained between the organizations was very low and much lower than was achieved in the experimental round robin tests.

Calculation Verification Process

Verification activities should use the same general process as used in validation with the exception that a known computational solution is used instead of an experimental solution. The same types of metrics used for validation can and should also be used for calculation verification. Since the purpose of the simulations is the same (i.e., roadside safety research) the same domain-specific validation metrics can be used to verify solutions. Likewise, the same shape comparison metrics can and should be used to compare known computational solutions to new computational solutions. This approach has the advantage of simplifying the validation and verification process since the same tools, techniques and procedures can be used in both areas.

Model Assurance Verification

Model assurance verification should begin at the individual component level. Components in this context can be parts of the vehicle or barrier models (i.e., splices, connections, suspension parts, etc.) and can include both time history comparisons and phenomenological comparisons. Various checks should be made prior to analysis regarding mesh quality, structural idealization of components and connections, and material characterization. The analyst should also make various verification checks during analysis regarding energy balance, mesh distortion, contact stability, initial penetrations between components, etc., to ensure that the results are indicative of a well-behaved and stable model. The performance of the individual components of the model should also be assessed to ensure that they provide realistic behavior throughout the analysis.

Basic Assessment of the Finite Element Mesh

The verification procedures for the finite element mesh may specify metrics for element distortion, element aspect ratio, element warping, element surface normal direction, element Jacobians, connectivity problems, etc. Most finite element pre-processors are capable of performing basic quality checks of the finite element mesh and some also include tools to automatically optimize selected elements of a mesh based on a set of given parameters; this is a considerable advantage when working with a mesh on complex geometries.

Assessment of Finite Element Model Mesh Discretization

It is good practice to conduct a mesh sensitivity study, where the goal is to achieve a desired degree of accuracy with the model with minimal computational effort. In general the mesh should be refined in areas of higher strain. In a linear elastic stress analysis problem deformations are typically small and an experienced analyst can easily identify potential areas with stress risers and tailor the mesh accordingly by refining it in those regions. In many cases, however, it is difficult to determine a priori where areas of high strains may occur. In a crash analysis problem, for example, deformations can be very large and deformation patterns are not easily determined prior to the analysis. A coarse mesh on such a model will result in a stiffer response than that of a more refined mesh; therefore, refining the mesh in specific areas will effectively introduce “weak points” in the mesh. In fact, selective mesh refinement may inadvertently bias the deformation pattern to correspond to the regions of higher mesh density, especially if the structural member is subject to buckling loads.

There are several strategies available for quantifying the error in mesh discretization to help guide model revision. These errors are often calculated based on differences in the element-by-element stress field and the averaged or smoothed stress field.(127) If the results of an analysis show steep gradients in certain elements, the error indicators will show larger errors in those areas than in regions where the gradients are less, and the mesh should be revised accordingly. These strategies are much less successful for transient loading due to the fact that inertia effects and time integration schemes introduce additional complexity and approximations.

For under-integrated elements, which are commonly used in crash analysis, there are no reliable error estimation techniques available based on stress gradients. A more qualitative assessment of mesh convergence can be achieved by refining the mesh and comparing results or by judging the smoothness of the deformed mesh. A finite element mesh developed for a component that is expected to experience large deformations should be able to accurately capture the deformed geometry. If the mesh density is refined enough to allow for a smooth representation of the deformed mesh then the mesh is acceptably convergent.(128)

A metric could be developed based on maximum allowable angle between adjacent elements in either the undeformed or deformed mesh; however, such calculations for an entire model would be impractical. An alternative would be to simply provide a qualitative assessment of the mesh quality based on the analyst's perception of the deformed mesh (e.g., is the deformed mesh free of apparent geometric inaccuracies and does the mesh adequately capture deformed geometry?)

Energy Balance

When under-integrated elements are used, there may exist one or more deformation modes that result in zero strain at all the Gauss points in an element (i.e., hourglassing). Since the element perceives no strain during these deformation modes, the deformations will occur with no resistance from the element and will lead to erroneous results and often numerical instability. Most element types used in crash analysis are based on selective reduced integration or single point integration and will have deformation patterns that may result in zero-energy modes (i.e., hourglass modes).

Finite elements codes that use under-integrated element formulations include options for controlling zero-energy modes. The classical method of controlling zero-energy modes is to apply forces at the nodes of an element to resist those deformations that lead to zero strains at the integration points. The magnitude of these forces is calculated by the code as a function of element dimensions, material properties and a user defined penalty factor (i.e., scale factor).

These hourglass forces correspond to non-physical forces that tend to reduce the kinetic energy in a crash analysis. Since the hourglass forces cannot exactly compensate for the missing stiffness of the elements, the energy resulting from these forces should be low compared to the internal energy of the element to ensure reasonable accuracy of the solution, say:

$$\frac{h_e}{i_e} \leq \lambda \approx 0.1$$

where h_e is hourglass energy and i_e is internal energy.(128)

Finite element programs generally provide energy calculations for the complete model and for individual part IDs in the model. They can also provide energy calculations on

individual elements, but to do so for the entire model would be impractical due to resulting file size. A metric may be developed that defines an acceptable limit of hourglass energy based on the amount of internal energy computed for the overall model and for each individual part. This, however, is not necessarily a fool-proof means of quantifying that hourglass energy is below acceptable limits. For example, a guardrail model may be developed with the entire length of w-beam rail elements identified in a single part ID. Only a small percentage of the overall length of rail will experience significant deformation in a crash, so comparing the amount of hourglass energy to the amount of internal energy experienced by the entire rail would likely result in a small value for λ even if hourglass forces were very high in the impact region. Nonetheless, providing a metric would, at a minimum, require documentation of the hourglass energy in the model.

In addition, the total energy in the model should be checked to ensure that total energy remains essentially constant. Checking the total energy, kinetic energy and momentum of a simulation is quite straightforward in LSDYNA so the maximum change in energy over the simulation run can be reported. Ideally, there should be no change in total energy but as a practical matter, total energy sometimes varies due to a variety of computation affects including hourglass energy, as discussed above, as well as contact and frictional forces. If the change in energy and momentum as a percent of the initial energy and momentum is below some threshold value (e.g., say 5 or 10 percent) then the non-physical errors in the simulation are probably adequately small. If, on the other hand, either the energy or momentum grow above this threshold, there is likely a numerical problem in the simulation that should be identified and corrected before the simulation is used for either validation or predictive purposes.

Mass Scaling

Another important issue that can affect reliability of model results is mass scaling. Mass scaling is often utilized to improve numerical stability of an analysis or to maintain acceptable analysis time when employing the explicit time integration method to transient problems. The explicit time integration method is the most suitable and the most used by analyst for crash analysis problems. The primary drawback of the explicit time integration method is that the stability of the solution is dependent upon the time-step used in the analysis. The critical time-step, Δt , is defined as:

$$\Delta t = \frac{2}{\omega_{\max}}$$

where ω_{\max} is the highest frequency in the structure. Determining the highest frequency in a structure, however, is a considerable effort in its own right. Most finite element software codes use a more simple method of determining a suitable time-step based on the Courant, Friedrichs and Lewy (CFL) condition, which calculates an upper bound on the frequency of the structural

model based on the shortest time it takes a stress wave to traverse each individual element in the model. The time-step in LS_DYNA, for example, is taken as:

$$\Delta t = \alpha \frac{l_e}{c_e}$$

where l_e is the characteristic length of an element, c_e is the element wave speed and α is a reduction factor that accounts for destabilizing effects due to nonlinearities. Thus the critical time-step can be determined by knowing the size and properties of each element and is computed internally by the finite element program prior to the start of the analysis.

For a finite element analysis of a crash event to be computationally efficient, a practical time-step for the analysis must be maintained (e.g., typically on the order of one- to three-microseconds for crash analysis problems- based on a combination of model size and current computation speed of computer hardware). For the analyst, this means that care should be taken when building the finite element mesh to ensure that small elements are not created that will result in an unreasonably small time-step for the analysis.

Some geometries, however, cannot be meshed without using very small elements in certain areas, such as bolts, bolt holes and geometrical stiffeners in sheet metal. In these cases, the analyst must make presumptions regarding the expected physical response of this part and balance computation time with acceptable accuracy of the model. When the geometry and stiffness are of primary importance, it may be acceptable to increase the mass of these elements (i.e., lower the wave speed) in order to maintain a reasonable time step for the solution, but mass increase should be documented and justified by the analyst. This technique, called mass scaling, is very useful for maintaining run-time efficiency and maintaining stability of an analysis and if used carefully will not affect the results. On the other hand, if used indiscriminately, mass scaling can create incorrect results since mass is being artificially added.

From the Survey of Practitioners, shown in Appendix D, it was shown that nearly all analysts use mass scaling to some degree. A metric could be established that limits the amount of mass added in the analysis that is based on:

- 1) *Percentage of the total mass of the model* – Typically, the amount of mass added should be small in comparison to the overall mass of the model.
- 2) *Percentage of the “moving” mass of the model* – Too much mass added to moving parts will result in a non-physical increase in the initial kinetic energy of the system.
- 3) *Percentage of mass added to individual elements of the model* – Abrupt density changes in a mesh due to mass added to individual elements will influence transmission and reflection of stress waves through the system.

Any model that exceeds the specified limit should be reported and justification provided.

Assessment of Structural Idealization

Due to the immense computational requirements of analyzing a system in complete geometric and material detail, certain components of a system are often idealized in an attempt to balance analysis time with acceptable accuracy of the results. For example, structural members may be idealized as one-dimensional rods or beams, two-dimensional plates or shells or three-dimensional solid elements. Bolted connections and other fasteners are often modeled using kinematic idealizations (e.g., such as using a constrained joint approach), discrete elements (e.g., such as nonlinear springs) or simple multi-point constraints. Understanding the response and limitations of each of these modeling methodologies are very important in assessing their applicability to the given model.

As discussed earlier, to maintain computational efficiency in the analysis, a practical time-step must be maintained. If the various connections in a system, such as bolts, rivets and welds, are modeled in geometric detail, a very refined mesh in those local areas would be required in order to obtain the correct geometry of those components and to accurately compute the high stress and strain concentrations in the local vicinity of the connections. It is common practice to model these connections using more simplistic modeling techniques such as spotwelds-with-failure or non-linear springs. Whatever method an analyst uses to model a particular component of a model, it should be verified that the model produces results consistent with its expected behavior.

In a dissertation by Plaxico, the model of a strong post guardrail system was developed and the process of applying mathematical modeling techniques based on an understanding of the physical problem and correlation to physical tests was illustrated.⁽¹²⁹⁾ For example, Plaxico's study showed that using a relatively fine mesh around the bolted connection of the w-beam splice in the model required a time-step on the order of 0.1 microseconds which was not practical for the analysis of the full-scale impact event which lasts 0.6 to 1.2 seconds (e.g., the analysis would require 6,000,000 to 12,500,000 time-steps to complete the simulation). Thus, more simplistic modeling techniques were investigated to simulate the bolted connections such as nodal rigid body spot-welds, non-linear springs and modeling the connection in geometric detail with a relatively coarse mesh. Nodal rigid bodies were not able to simulate the relative movement of the two w-beam sections in the splice, since they are rigid connections and were, therefore, not recommended. It was determined in the study that when the splice is subjected to uniaxial loading an appropriate method of connecting the w-beams together is to use non-linear springs with a force-displacement relationship defined such that the correct axial displacement of the splice is obtained for a given tensile load in the w-beam. This is especially important in the upstream and downstream regions of the guardrail model away from the impact zone, where the rail is in "pure" tension. In the impact zone where the loading on the splice is more complicated an explicit geometric model of the bolted connection may be required. Figure 40 shows the results of a finite element simulation compared to a physical test of a splice

connection subjected to a pure tensile load. A qualitative assessment of the two curves indicates the fidelity of the nonlinear springs to simulate the splice connection behavior.

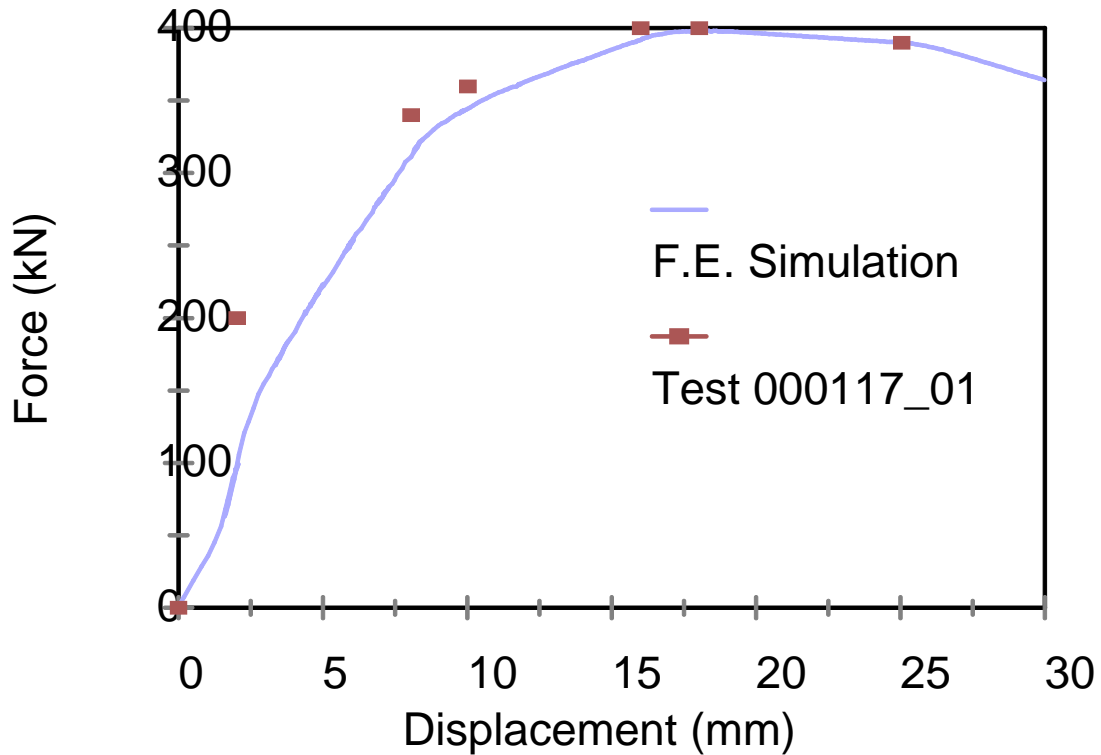


Figure 40. Comparison between a simulation and test of the displacement of a guardrail splice in tension.(129)

The forgoing example discussed the process used by members of the research team to qualitatively verify and validate the accuracy of an idealized modeling technique to simulate a bolted connection. Other components of the model, including those modeled in geometric detail, should be verified in like manner, to ensure that proper element type, element discretization and material characterization used in the model are appropriate for the given problem.

Assessment of Material Characterization of Individual Components

Material properties in particular can significantly affect results, and unfortunately, some materials common to roadside safety barrier systems have widely varying mechanical properties (e.g., soil and wood) and may be sensitive to load rate and environmental conditions

(e.g., temperature, moisture, ultraviolet exposure and aging). Achieving accurate correlation between numerical simulation and physical tests requires accurate material properties to be used in the analysis.

Metals, such as steel and aluminum, are relatively easy to characterize using standard material models available in most commercial finite element codes. LSDYNA, for example, has several material models appropriate for simulating the behavior (including thermal and strain-rate effects) of metals. Obtaining the input properties from design handbooks, however, may be misleading. For instance, the yield point of a material obtained from design handbooks usually provides a minimum value, which may be significantly less than the actual yield stress of the material. Although this value may be acceptable for design based on linear elastic stress analysis it may not be appropriate in the design of crashworthy structures where energy management through plastic deformation is the governing response.

Obtaining material properties by conducting laboratory tests on samples taken directly from the part in question is by far the most desirable method, but test setup and conduct may be challenging due to limitations in testing equipment, in particular, regarding characterization of rate effects in materials. Wright and Ray, for example, developed material properties for AASHTO M-180 guardrail steel by cutting coupons of actual guardrail material, performing standard ASTM tensile tests to obtain material properties and then using those properties in several LS-DYNA constitutive models.(46)

It is not considered practical to develop a metric for verifying methods used for generating material properties or for application of material constitutive laws to components of a model. Finite element models are developed for a wide range of structural systems and the types of materials that may be used in those designs are limitless. It is suggested, however, that analysts provide documentation of all material properties used in a model and a reference to where those properties were obtained. Over time this should result in a literature documenting validated material models for roadside hardware use. An analyst need not perform a validation of every material every time they perform a new simulation as long as the material properties used can be attributed to a source in the literature where the material properties were validated.

Model Assurance Verification Process

The metrics for verification should include parameters that analysts generally examine to assess energy balance, numerical stability and quality of the model. Such metrics may include common sources of uncertainty in models such as geometry detail, spatial discretization, element quality, element type, boundary conditions, loading conditions, appropriateness of material constitutive laws, material properties, structural idealization of the mechanics problem, and conservation of mass and energy during calculations. A datasheet could be developed for the analyst to use for documenting such verification metrics.

CHAPTER 3 SURVEY OF MODELING BEST PRACTICES

INTRODUCTION

Identifying model building best practices provides a means for the roadside safety computational mechanics community to capture its best practices in easily retrieved form so that both new and experienced users can develop models that are highly likely to run without errors. Unfortunately, most papers and reports that present the results of finite element simulations rarely reveal all the details of the simulations so there is relatively little to be found in the literature with specific recommendations for, say, minimum time steps or the maximum change in total energy. Likewise, most papers and reports on verification and validation do not address this subject because it is highly specific to the application. For example, parameter variations that may be perfectly acceptable in roadside safety may have little relevance to computational fluid dynamics problems.

Since there is little in the literature to help define reasonable parameter variations, a survey of practitioners in the art of roadside safety computer simulations was conducted. The original survey form and the tabulated responses are included in Appendix D. The survey asked practitioners what types of techniques they use and what range of variation they considered acceptable when performing typical roadside safety simulations. The results of the survey will be discussed for each parameter in the following sections; more information about the survey can be found in Appendix D.

Several other solid mechanics communities appear to be in the process of developing best practices guides although none appear to be very far along at this point. ASME PTC-10, for example, is planning a series of documents that expand on the general framework of the ASME V&V guide. These documents will constitute a series of best practices guides on a variety of topics including model building, incorporating uncertainty, calculating metrics, etc. The aircraft seat committee of SAE is also in the process of developing a best practices guide to complement the FAA Circular Advisory. This guide will describe typical model procedures like minimum time steps, the use of mass scaling, element dimensions and type among other model building details.

VERIFICATION

Definition

Fifty seven percent of practitioners agreed with the definition of verification given in the survey.

Geometry Generation

Survey responses show that geometries for roadside hardware models are generated from drawings and based on previously developed successful models. The vehicle models, on the

other hand, are mostly obtained from NCAC library at George Washington University. Other public domain sources are sometimes used to obtain vehicle models. Purchasing proprietary models as well as obtaining models from the automotive industry was not common among the surveyed practitioners. One out of three practitioners that participated in the survey sometimes chooses to build their own vehicle model. The single unit truck, reduced C2500 pickup truck and detailed and reduced Geo Metro were selected as the most frequently used models from the NCAC. All four of these vehicle models, however, were often used after modifications by practitioners. The remainder of the vehicles available at the NCAC vehicle library seems to be rarely used by survey respondents. Practitioners were also asked whether they were using any updated vehicle models. Based on the responses, the updated version of Geo Metro model by Politecnico di Milano was most frequently used followed by the F800 single unit truck and the C2500 pickup truck model.

Practitioners agree that articulated suspensions, rolling tires and coarser meshes are highly desirable model features at least in the area of roadside safety. Detailed geometry, failing tires and vehicle component failure are considered as medium important modeling features, unless a particular crash scenario requires a more detailed model. Also, responses from practitioners varied when they were asked about whether they used detailed or kinematic equivalent systems to model complex articulated systems, such as suspensions and steering systems. 32 percent of the surveyed responded that they mostly used detailed modeling, whereas 40 percent of the surveyed said that they mostly used kinematic equivalent systems.

Most practitioners used approximation when modeling bolts (62%), rivets (93%), welds (87%), soil (62%) and road surface (90%). Some practitioners, on the other hand, choose to use detailed bolt and soil models, probably in response to specific project needs. 58 percent of practitioners agreed that material properties of models are mostly obtained from laboratory experiments. Sometimes they obtain material properties from material specifications and other successful finite element simulation studies. According to the survey, material failure is frequently determined from maximum effective plastic strain followed by element erosion (i.e., 88 percent and 73 percent, respectively). Some of the practitioners choose not to specify any failure in their models. Failure parameters in models are mostly obtained from experimental data and previously used successful models. Results show that 61 percent of practitioners use strain rate sensitive material models.

Welded connections are sometimes modeled as merged nodes or as tied contacts (i.e., 47 percent), however, welds are most often (i.e., 52 percent) modeled as spot welds with failure. Modeling welds with tied contacts with failure is not very common. Bolted connections, as opposed to welded connections, are never represented with tied contact or tied contact with failure. Springs are sometimes or rarely used to model bolted connections (i.e., 37 percent). According to survey results, bolted connections are mostly modeled with spot welds with failure and sometimes with merged nodes if failure is not expected. On the other hand, a significant

number of practitioners (i.e., 38 percent) choose not to use merged nodes to represent bolted connections.

Finally, when practitioners were asked about how they model post-soil interaction, the survey determined that the majority (i.e., 52 and 48 percent) never used Eulerian solid meshing and fixed nodes, respectively. Some practitioners favored the use of nonlinear springs (i.e., 37 percent) to model soils. 31 percent of the participants typically use explicit geometric models of the post and soil continuum and an equal percentage who never use them.

Mesh Sensitivity and Quality Determination

Practitioners were asked about the largest shell element dimensions they use in modeling steel components. The average smallest element dimension when used in a contact region was 23 mm. Outside of the contact region but expected to deform significantly it was 44 mm. Outside of the contact region and where no deformation was expected, it was 93 mm. When the question asked was about the largest solid element dimension to be used in modeling a wood post, the average solid element dimension resulted was 21 mm in case the post was expected to fracture, 33 mm in case the post was expected not to fracture but displace in the soil and 56 mm for posts which did not experience any deformation. These results are shown in Table 1 and Table 2.

Table 1. Average shell element dimensions used in simulation studies

	Contact Region	Not in contact region but expected significant deformation	Not in contact nor deformation region
Shell Element (mm)	23	44	93

Table 2. Average solid element dimensions used in simulation studies

	Fracture Region	Not expected to fracture but displace in the soil	Not expected to deform nor displace significantly
Solid Element (mm)	21	33	56

Practitioners generally (i.e., 38 percent) try to keep the maximum warpage angle of the elements in the model smaller than 5 degrees. Also, some practitioners (i.e., 28 percent) accepted warpage angles as large as 10 degrees. The majority of practitioners (i.e., 48 percent) try to keep the percentage of elements with the biggest warpage angle in the model between zero and five percent. Also, a large number of practitioners (i.e., 45 percent) prefer an aspect ratio smaller than 3 to 1 followed by 5 to 1 (i.e., 23 percent) and 2 to 1 (i.e., 19 percent) when creating a meshing.

Contact Stability Issues

Practitioners usually choose (i.e., 38 percent) to refine the mesh in the contact area when contact instabilities occur during a simulation. A larger number of practitioners (i.e., 52 percent)

choose to modify the contact parameters like the penalty factors when they experience contact problems. There is not a clear answer from the practitioners on whether changing the contact type would solve the contact instability problem.

Energy Balance and Comparisons

Survey results show that as long as the variation in total energy and added mass are less than five percent practitioners (i.e., 52 percent) are generally not concerned about the energy balance and mass increase. Similarly, as long as the ratio between the hourglass energy and total energy is less than 10 percent practitioners (i.e., 42 percent) are generally not concerned.

Time Step Issues Regarding Element Size, Mesh Density and Mass Scaling

The majority of practitioners (i.e., 77 percent) prefer an initial time step in the range 1.0E-06 sec to 5.0E-06 sec. Very few (i.e., 20 percent) choose to accept initial time steps less than 1.0E-06 sec. To control the time step, all practitioners control both element dimensions and use the minimum time step option (i.e., mass scaling). Most practitioners (i.e., 60 percent) generally used some mass scaling in their models to keep the time step at a desirable level and prevent run times from becoming excessive. The majority of practitioners (i.e., 75 percent) agreed that they make sure the overall mesh is adequate for the contacts and the expected deformations. They use mass scaling to prevent the time step from getting too small.

VALIDATION

Almost all practitioners (i.e., 91 percent) agreed with the definition of validation given in the survey and taken from ASM V&V10-2006. When they were asked about the order of importance in validating a finite element simulation with a physical test, the results were very distinct. Other than the qualitative comparison of vehicle damage, which was chosen to be not so important, all other statements were deemed to be very important. Qualitative comparisons of barrier damage were favored most by the practitioners (i.e., 48 percent) followed by the quantitative comparison of displacement/rotation time histories (i.e., 39 percent) and qualitative comparison of crash sequence (i.e., 36 percent). Qualitative comparisons of velocity time histories, trajectories and quantitative comparison of acceleration time histories came next in the list (i.e., 32, 30 and 26 percent, respectively).

Practitioners agreed that they always use qualitative comparisons, such as hardware deformations, location/number of failed components, visual methods and phenomenological response to compare simulation results to the physical tests. They also agreed that they mostly use velocity-time histories, always use displacements and rotations and sometimes use stress/strain relationship to make quantitative comparisons. Responses on acceleration time histories were distributed evenly among always (i.e., 32 percent), mostly (i.e., 29 percent) and sometimes (i.e., 23 percent), while responses on energy balance comparisons were sometimes or rarely performed.

TRAP parameters like OIV and ORA were the most common metrics used by the practitioners (i.e., 64 percent) as shown in Appendix D. TRAP was by far the most commonly used metric in publications as discussed earlier in the literature review. Other metrics, such as Geer's MPC metrics, the NARD Validation Manual metrics and the ANOVA metrics were rarely used by the practitioners surveyed.

When asked about whether or not practitioners used a standard procedure for model verification and validation the most common answer was no (i.e., 59 percent). Similarly, when practitioners were asked about whether they used different validation methods according to specific roadside hardware studied, a majority answered "no" (i.e., 60 percent).

The majority of practitioners (i.e., 67 percent) used LS-PrePost to filter their simulation data followed by those who used SAE J211 (i.e., 47 percent). Some practitioners (i.e., 30 percent) reported using TRAP or other methods to filter simulation data.

The majority of practitioners (i.e., 81 percent) used LSDYNA as their analysis code for crash simulation. Finally, almost all practitioners (i.e., 94 percent) validate components or subassemblies of larger models whenever possible before validating the overall model.

CHAPTER 4 PROCEDURES

INTRODUCTION

The purpose of this Chapter is to present potential procedures for verification and validation for computer simulations in roadside safety applications. The procedures described herein apply primarily to incremental improvements to roadside safety hardware. For example, say that a particular type of guardrail terminal has been designed, crash tested and accepted by the Federal Highway Administration (FHWA) for use and has been in service for some years. The designer and manufacturer may be considering a small change that will either improve the performance, reduce the cost of the system or both. For example, perhaps the manufacturer has made some changes in the impact head of an energy absorbing terminal to reduce weight (e.g., primarily a cost savings but also some safety benefit) while making the impact area slightly taller (e.g., primarily a safety improvement). Another example might be using a different shape or material blockout in a strong-post w-beam guardrail. The designers may decide to investigate new incremental improvements like these using a finite element program like LSDYNA either in lieu of or in preparation for a crash test. How can the designer satisfy decision makers (i.e., the FHWA and the States) that the incremental design is acceptable according to the Report 350 or MASH crash testing recommendations based on the finite element simulations? What information does the designer need to provide to the decision maker to make the case that the new incremental improvement will also satisfy the crash testing guidelines as did the original design? Can the computer simulation provide all the necessary information for the decision maker such that additional crash tests are avoided? The purpose of this document is to provide answers to these questions. The focus of this chapter, therefore, is on providing information to decision makers that will allow them to make an acceptance decision for incremental improvements to roadside hardware.

These procedures are not intended for use on completely new hardware where there is little or no community experience but rather are intended for improvements to hardware whose performance is well known. On the other hand, however, these procedures are likely to be useful to hardware designers and crash test agencies in exploring new design options and evaluating them prior to a crash test even if the materials are not subsequently used in applying for acceptance of a design change.

As the community becomes more experienced and proficient with the use of numerical simulation technologies, however, it is likely that the *ad hoc* definition of what is a small incremental change will expand. A decision maker will always be free to require either more information or a new crash test if they feel that the increment is too large for their confidence. The procedures and recommendation herein primarily provide a language and a means of communication that will allow designers and decision makers to compare test and numerical analysis results in judging the performance of roadside safety systems.

DEFINITIONS

The definitions of verification, validation and calibration, as they are used in these procedures, were adopted with slight modifications from the definitions presented in the ASME “Guide for Verification and Validation in Computational Solid Mechanics,” ASME V&V 10-2006.(17) These definitions were discussed in detail in Chapter 2 but are summarized below.

Verification

Verification is concerned with how well the discrete numerical approximation (e.g., an LSDYNA simulation) agrees with the known mathematical solution (i.e., differential equation solution). Thus, *verification is the process of ensuring that the computational model provides results consistent with the developer’s conceptual description of the model and the underlying assumptions that form the basis of the mathematical model* (i.e., the model responds as the developer intends) and that computed results adhere to basic physical laws, such as conservation of energy and momentum.

There are no “known” solutions available in roadside safety in the sense that there is some closed-form differential equation that defines the mechanical and dynamic response of roadside hardware. Impacts with roadside hardware are complex since they involve a number of complicated mechanical structures (e.g., the vehicle, the barrier and even the terrain). While there are no “known” solutions, numerical solutions still must satisfy basic physical conservation laws: i.e. energy, momentum and mass must be conserved. The procedures developed in this chapter regarding model verification, as it relates to crash simulations of roadside safety hardware, include some solution verification criteria that help assure the analyst and decision maker that the numerical results are consistent with these basic conservation laws.

Other types of verification, for example code verification, are not directly discussed in this document. Generally, code developers have the ability and responsibility for performing code verification of a numerical method and it is generally presumed that a code used for roadside safety simulations has been independently verified.

Validation

While verification is primarily concerned with ensuring results adhere to basic physical laws, validation, on the other hand, is concerned exclusively with comparing the numerical solutions to real-world physical experiments. Validation, as used throughout this report, always implies that a numerical solution is being compared to some type of physical experiment. Validation, as it relates to crash simulations of roadside safety hardware, is defined in these procedures as the process of *determining the degree to which the computational model is an accurate representation of the real world crash tests from the perspective of accurately replicating (i) the NCHRP Report 350, MASH or EN 1317 crash test evaluation parameters, (ii) the structural performance of the barrier and (iii) the response of the vehicle.* It is important to keep in mind that the intended use of the model is to assess the results of the computer simulation in the same manner.

Calibration

Calibration is often confused with validation and verification. Verification and validation involve comparisons with physical experiments or known solutions that are independent of the model development, whereas calibration is *the use of physical experiments, the literature or analytical solutions to estimate the parameters needed to develop the model*. For example, if a material model is needed in a particular finite element simulation, the analyst may perform some physical tension tests in the laboratory to obtain the stress-strain response of the model. These physical test results can then be used to estimate the parameters needed for the computational material model. Such a material model has been “calibrated” by the physical tests. These same physical tests cannot be used to “validate” the material model since one is dependent on the other. On the other hand, the analyst might obtain the material properties from a handbook or the literature and use these literature parameters to build the model. A physical experiment in the laboratory can then be used to validate the material model because it is independent of the model development. Physical experiments, therefore, can be used to estimate parameters and thereby calibrate a model, or to validate a model, but not both.

PROCEDURES

Introduction

An informal procedure for verification and validation has evolved in roadside safety over the past decade as described in the Literature Review presented in Chapter 2. The procedures in this document formalize what many in the roadside safety community have been doing informally for a number of years. The intent is not to create a burdensome and difficult procedure but rather to standardize an already used *ad hoc* procedure such that decision makers can readily assess results from different laboratories and analysts. The procedure for the validation of roadside safety models is shown graphically in Figure 41 and includes the following seven steps:

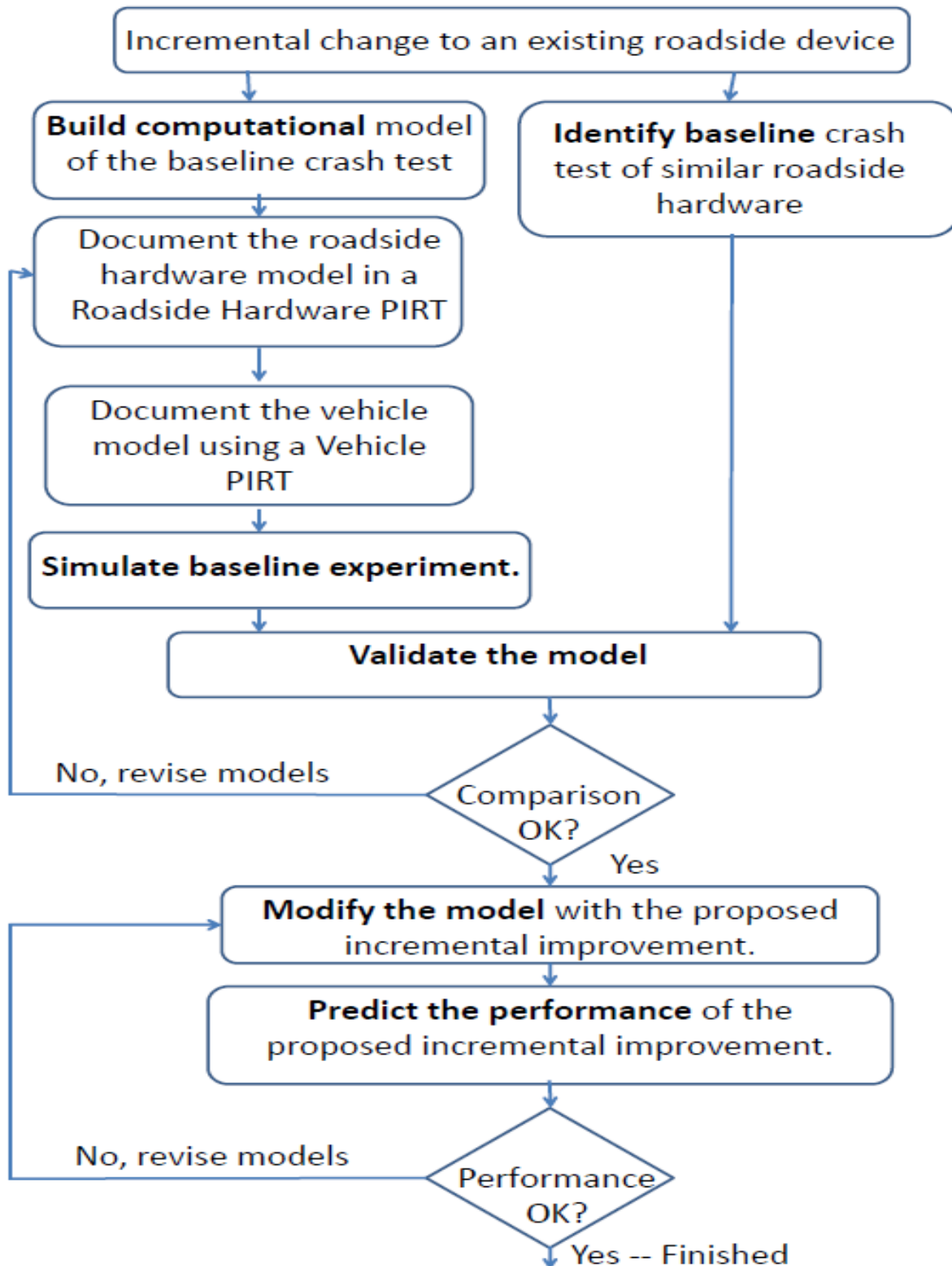


Figure 41. Roadside safety validation and incremental design process.

1. Identify the baseline experiment,
2. Build the computational model of the baseline experiment and document its characteristics in roadside hardware and vehicle PIRTS,
3. Use the model to simulate the baseline experiment,
4. Validate the model by comparing the simulation results to the physical test results,
5. Modify the model to represent incremental improvements of the baseline hardware design configuration,
6. Use the model to predict the performance of the incremental improvement, and
7. Evaluate the performance of the incrementally modified device to determine if the improvement satisfies the appropriate crash testing guidelines (e.g., Report 350 or MASH).

Each of these steps will be discussed in the following sections.

Identify the Baseline Experiment

The first step, shown at the top of Figure 41, involves identifying a baseline experiment for the comparison. Since these procedures are intended for incremental improvements to existing roadside hardware, it is presumed that there are already crash tests available that document the performance of the original roadside safety hardware and that the original design is fairly similar to the anticipated incremental improvement. For example, one of the examples presented later in Chapter 6 involves assessing the performance of a strong-post w-beam guardrail placed behind a curb. There are numerous crash tests of strong-post w-beam guardrails so one was chosen from the literature where the test report, electronic data and film/video data was available. This test from the literature did not have a curb placed in front of it but it was a standard strong-post w-beam guardrail. This test from the literature, therefore, was identified as the baseline test for the validation exercise.

As much documentation of the experiment should be obtained as possible. At a minimum, the time-histories (normally in the original raw electronic form) and a test report including the usual crash test evaluation criteria and photographs will be needed to perform the comparison in step four but video, additional photographs and other types of documentation may also be helpful in performing the comparison. There is no limit *per se* on the age of the experiment as long as all the needed data are available but as a practical matter vehicle models do not really exist for pre-Report 350 vehicles and test documentation including the electronic files may be difficult to find for older crash tests. The vehicle model used in the simulation must be a reasonable approximation of what was used in the crash test so for practical reasons baseline tests will generally be those that were performed for Report 350 (i.e., after about 1993). The result of this first step in the procedure should be complete documentation of the baseline crash test or tests.

Build the Model

Next in Figure 41 on the left hand side, models of the vehicle, barrier and support conditions are developed to exactly match the baseline experiments. The development of the models may involve calibration, verification or validation of parts, materials, subassemblies and assemblies of the complete model. Figure 42, for example, shows a schematic representation of a guardrail (e.g., the so-called European super rail) struck by a small passenger vehicle. The vehicle, barrier, and any boundary conditions constitute the whole model. Major independent portions of the model like the vehicle and barrier are “assemblies” in the model (note: generally the boundary or support conditions are presumed to be included in the roadside hardware model). By definition, an assembly is composed of a collection of subassemblies. The suspension system and the vehicle frame, for example, are sub-assemblies of the vehicle assembly and the rail, posts and anchor systems are subassemblies of the guardrail system. A subassembly is composed of a collection of parts. The post is a subassembly that is composed of parts representing the post, blockout, fasteners, spacers, stiffeners and soil. Each of these parts in turn is defined by its geometry and material properties.

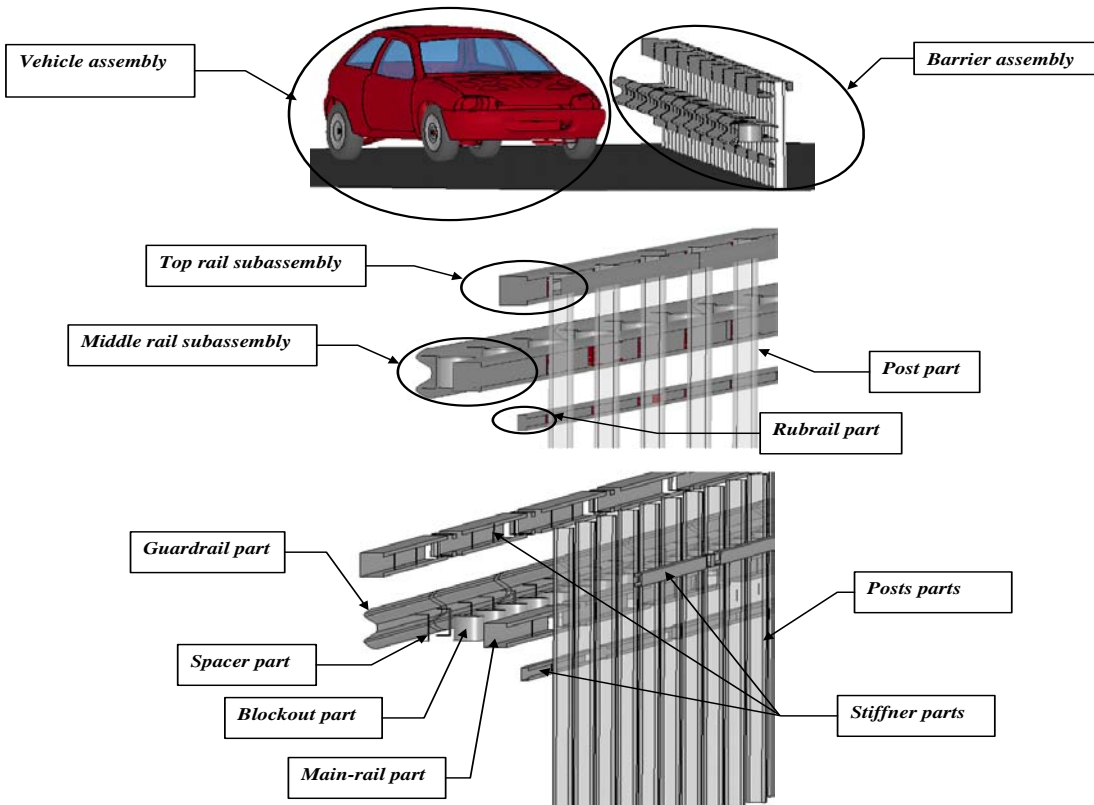


Figure 42. Hierarchy of a typical roadside hardware finite element model.

During the model development phase, each part, subassembly, and assembly should be calibrated, verified or validated if at all possible. Requiring validation of component at every

level of the model hierarchy would be unreasonably burdensome and may not even be possible in some cases. Calibrating and validating as many of the components as possible will, however, increase the overall confidence in the accuracy and robustness of the model predictions. For example, in developing the post subassembly the interaction of the steel guardrail post and the soil is an important step. The analyst may decide to perform some pendulum experiments of a typical guardrail post embedded in a typical soil. At the same time, the analyst would build a numerical model of the pendulum experiment and perform numerical calculations for the same impact conditions. Similarly, the rear suspension of a vehicle might be examined by performing some “bump” tests. A numerical model of the same suspension components and the same impact conditions could be performed and compared to the physical experiment. The results of the numerical pendulum test calculations and the physical pendulum tests can then be compared to see if the numerical results can be validated with the experimental results. Each part, subassembly and assembly that can be validated in the model development process will result in increased confidence in the model’s ability to correctly predict the crash performance.

Every roadside hardware simulation will contain a vehicle assembly and a roadside hardware assembly. It is important to document the capabilities of these two major assemblies in order to assess what the model reasonably can be expected to predict. For example, if the model does not include the possibility for the guardrail elements to fail, then it will never be able to replicate and be validated against an experiment where guardrail material failure was observed. The capabilities of the major assemblies (i.e., the vehicle model and the roadside hardware model) are documented in a so-call phenomena importance ranking table (PIRT).

Phenomena importance ranking tables (PIRT) are a technique that has been suggested by Oberkampf as a means of documenting, verifying and validating the types of phenomena a numerical model is intended to replicate.⁽¹⁶⁾ Since all mathematical models are abstractions of physical phenomena, all modelers are implicitly making assumptions about what is important in the model and what phenomena should be represented in the mathematical model. Unfortunately, these assumptions are generally not apparent to those reviewing the results of the model. For example, a modeler may build a vehicle model assuming that snagging of vehicle components is not an important phenomenon because the modeler’s intent is to investigate the response in a vertical rigid wall impact. In such a case, the modeler may not include contacts on the side of the vehicle to represent the door edges or edges of the body panels. Another modeler may take the vehicle model and use it in a guardrail simulation not knowing that snagging was not considered during model development. The simulations of the guardrail may be unlikely to predict or replicate snagging since this phenomenon was never included in the original model. In reviewing the results of the model, the second modeler may incorrectly believe that there are no snagging issues when, in fact, there are no snagging issues in the simulation because they were not accounted for in the model. Likewise, if a material is created without failure conditions, the physical system may experience failure in a test but this would not be observed in the model since failure was not included in the model. A PIRT provides a quick way of documenting the

phenomena that are included in the model so that subsequent users of the model or reviewers of the results will know what types of phenomena can reasonably be expected.

Examples of roadside hardware and vehicle PIRTS are included in Chapter 6 and Appendix C. In essence, the development of the PIRT is a validation exercise for subassemblies, components and parts of the overall assembly. When developing a numerical model, it is common practice to perform experiments for some of the important subassemblies and components and to compare the results to computational experiments from the model. For example, a material coupon test might be performed in the laboratory and compared to a numerical version of the coupon test in the model to ensure the results are compatible. Likewise, a timber guardrail post might be tested using a ballistic pendulum to investigate its impact performance and the results compared to the computational model of the timber post. If an experiment is being compared to a computation, the computation is being validated. It is sometimes not possible to validate all parts and subassemblies so the model behavior can also be calibrated or verified depending on the information available. For example, steering response should respond to the well-known Ackerman angles and comparing the model results in a steering simulation to the theoretical Ackerman angles would be a verification activity since the comparison is with a closed-form mathematical solution.

In the following discussion, the reader should refer to the example vehicle and roadside hardware PIRTs included in Appendices C6 through C7. Development of a PIRT for either a roadside device or vehicle involves three steps:

1. First, all comparisons to physical experiments or mathematical models that were performed during the development of the model should be listed and assigned a phenomena number (e.g., see Table C6-1, C7-1 or C8-1). These may include laboratory tests of materials, dynamic or static tests of components, full-model tests of suspension systems and any other type of comparison between a physical test and the computational model.
2. For each comparison between an experiment and calculation (e.g., row number 1 in Table C6-1), a “Comparison Metric Evaluation Table” should be developed (e.g., see Table C6-2). The metric evaluation can be performed using the program RSVVP which is described in Chapter 5. The results of the curve comparison should be entered into the table. There should be one “Comparison Metric Evaluation Table” for each comparison listed in list of experiments. It is also helpful to include some summary information about the comparison on the metric evaluation table although precisely what to include will depend on the particular comparison. For example, if an experiment is performed to validate the suspension deformations under various loads (e.g., see Table C7-2), a load-deformation plot and a photograph of the experimental set-up would be a useful item to include.
3. If the comparison in the “metric evaluation table” can be judged to be acceptable according to the criteria, the “phenomenon description” should be taken from the bottom

of each “Comparison Metric Evaluation Table” (e.g., Table C6-2) and entered into the PIRT (e.g., Table C6-8). The far right column allows the developer to indicate if the experiment was validated, verified or calibrated. Validation should be indicated only if the experimental results were compared to the analysis results and the two are independent (i.e., the experimental results were not used to establish properties of the analysis model). If the comparison is between an analytical theory and the analysis results, the model has been verified. Lastly, if the results of the experiment were used to determine material properties or some other characteristic of the model, the analysis result has been calibrated meaning the experiment and analysis are related to each other. The appropriate type of comparison should be indicated in the right column of the PIRT (e.g., see Table C6-8). Phenomena that did not result in acceptable comparisons for the “metric evaluation table” should not be entered in the PIRT.

A decision maker can very quickly determine what types of phenomena the vehicle or roadside hardware model is capable of replicating by examining the appropriate PIRT. If the decision maker feels that an important phenomenon is missing, the analyst may be asked to perform some tests and numerical simulations to validate, verify or calibrate that phenomenon and thereby add it to the PIRT. In this way, the PIRT also provides a way of keeping track of improvements to models that are re-used since new phenomena can be added as the model is used for an increasing variety of roadside hardware assessments.

The result of this second step in the procedure should be (1) a complete model of the roadside hardware simulation including the vehicle, roadside hardware and appropriate boundary conditions, (2) a PIRT describing the vehicle capabilities and (3) a PIRT describing the roadside hardware capabilities.

Compare the Baseline Test to the Computer Simulation

Once the model has been completely developed including the vehicle and roadside hardware PIRTS and the baseline tests have been identified, a computer simulation of the baseline test is then performed. The objective of this simulation is to as closely as possible match the impact conditions in the baseline test. The results of the computer simulation of the baseline condition are then compared to the results of the physical full-scale crash test by completing the “Validation Report.” Examples of several Verification and Validation Reports are provided in Appendices C1 through C5 and blank forms are included in Appendix E.

The validation/verification reports each have four parts:

1. Basic information,
2. Solution verification,
3. Time history comparison and
4. Domain specific evaluation.

The first part, basic information, lists important information about what the baseline test is, what organization performed the baseline test, what organization performed the numerical solution, the impact conditions, etc (see Appendix E).

The second part, solution verification, involves global checks to make sure the numerical solution appears to be stable and conforming to the conservation laws. The analyst should fill in the information shown in Table E-1. The table requires information about the total energy, energy balance, hourglass energy, shooting nodes and other computational characteristics of the model. The purpose of this part is to provide information to the decision maker that indicates that the numerical solution obeyed basic physical laws (e.g., conservation of energy, mass and momentum) and that the solution is numerically stable. The analyst can certainly add to the list shown in the examples but at least those items shown should be reported. All the criteria listed in Table E-1 must be satisfied.

In the third part, time history comparisons, the analyst performs a quantitative comparison of the time histories of the vehicle dynamics. The quantitative evaluation metrics can be easily generated by the RSVVP program, discussed in the next chapter, when comparing the time histories from the crash test to the numerical solution. The details of which quantitative metrics to use, how to calculate them and the appropriate acceptance criteria are discussed in Chapter 5 and illustrated in the examples shown in Chapter 6. The purpose of this general overview of the procedures, the objective of this third step in the process, is to compare the baseline crash test time histories to the numerical time histories in an objective, quantifiable manner. First the analyst should fill out Table E-2 using RSVVP to calculate the Sprague-Geers MPC metrics and the ANOVA metrics for each available time history (i.e., all the time histories collected in the full-scale crash test experiment). The time histories should be compared in the original units and orientation. For example, if the test vehicle was instrumented with accelerometers, accelerations should be compared and if the test data was collected in the local coordinate reference frame, the comparison should likewise use the local reference frame. If all the metrics satisfy the criteria in Table E-2, the time history comparisons can be considered acceptable and the analyst may continue on to the next step.

Sometimes, however, there may be one or two relatively unimportant channels that do not result in good quantitative comparisons. An example might be a small sign support test where the longitudinal acceleration has a much greater influence on the results of the impact event than do the lateral or vertical accelerations. The less important channels may not satisfy the criteria because they are essentially recording noise. The longitudinal channel in this example will probably be an order of magnitude greater than some of the other less important channels and the response is essentially determined by the one longitudinal channel. RSVVP includes a method for accounting for different levels of importance of channels. The procedure will be explained in more detail in Chapter 6 but it basically uses the change in momentum represented by each channel and weights the comparison metrics by the proportion of the momentum in each channel. For example, if the longitudinal channel in the sign support example accounts for 80

percent of the linear and angular momentum in the crash test, the longitudinal channel will have a weight of 0.8 and the other channels will have smaller weights summing to 0.2 Table E-3, the multi-channel option, has been included in the validation procedure to account for such cases. The user can use RSVVP in multi-channel mode to calculate the weighted Sprague-Geers and ANOVA metrics for the six channels of data that are typically collected in full-scale crash testing of roadside hardware; namely, 1) longitudinal, lateral and vertical accelerations; and the roll, pitch and yaw rotation rates. If the metrics satisfy the criteria in Table E-3, the time history comparison can be considered acceptable. In summary, the time history comparison is considered acceptable if (1) all the channels result in acceptable comparison metrics (i.e., Table E-2) or (2) the weighted channel results produce acceptable comparison metrics (i.e., Table E-3).

The fourth part of the verification and validation report compares the phenomena observed in both the crash test and the numerical solution. Table E-4 contains the Report 350/MASH crash test criteria with the applicable test numbers. The analyst should circle all the criteria that apply to the particular test being compared. For example, the small car test-level three longitudinal barrier test is test 3-10 so the analyst would circle criteria A, D, F, H, I and M since these are the criteria that Report 350 uses to evaluate test 3-10 (i.e., see the right column of Table E-4). Tables E-5a through E-5c contain an expanded list of these same criteria and provides space for the analyst to enter the observed crash test response and the observed numerical response. If the two agree, the analyst can indicate that there is agreement between the test and the numerical solution. For example, for test 3-10, criterion A1 in Table E-5a requires that the vehicle be contained and redirected. If both the numerical solution and the crash test resulted in redirection, the numerical solution and crash test would be judged to agree. If both did not redirect the vehicle, they would still agree. If the crash test vaulted over the barrier, however, and the numerical solution indicated redirection, then the two did not agree. The analyst should enter the result for each of the applicable criteria and indicate if there is agreement between the crash test and numerical solution or not in the right column of Table E-5.

Some of the phenomena in Table E-5 are binary (e.g., “did the barrier contain and redirect the vehicle?” requires a “yes” or “no” answer) while others are numerical. For the numerical comparison phenomena, the results for the experiment and analysis should be entered into Table E-5 and compared in both an absolute and relative sense. For example, the lateral occupant impact velocity in a test 3-10 crash test might be observed to be 9 m/s whereas the analysis solution predicts 10.5 m/s. The relative difference is the absolute value of the difference divided by the “true” (i.e., experimental) value so in this example the relative difference is 16 percent. In general, results must agree within 20 percent so this comparison would be judged acceptable. In some cases where the values are very small, the relative difference can give unreasonable results so the absolute difference must also be examined. For example, suppose the longitudinal ridedown acceleration in a test 3-10 crash test is 3 g’s and the analysis solution predicts 4 g’s. The relative difference in this case is 33 percent but clearly the values are very close since the absolute difference is only one g. To account for these situations, the Report

350/MASH limit on the criterion was taken and the value corresponding to 20 percent of the Report 350/MASH acceptance value was calculated. For example, Report 350 limits the ridedown accelerations to 20 g's so 20 percent of 20 g's is 4 g's. Any comparison where the absolute difference in occupant ridedown acceleration is less than 4 g's is, therefore, acceptable. Numerical comparisons are acceptable, therefore, if the relative difference is less than 20 percent or the absolute difference is less than the value indicated in Table E-5.

All the applicable criteria identified in Table E-4 should show acceptable agreement in the comparisons listed in Table E-5. If there is a case where one or two criteria do not agree and the analyst thinks the phenomenon is unimportant in that particular instance, the analyst should indicate that criteria with a footnote and explain why that criteria should be ignored in that particular instance. For example, in test 3-10 for criterion M4 in Table E-5 the analyst is asked if one or more vehicle tires failed or de-beaded. Say that there was a flat tire in the crash test but not in the numerical solution. If the analyst believes that the flat tire did not play a significant role in the dynamics of the crash (e.g., maybe the tire became flat during re-direction after losing contact with the barrier) then he may explain this in the footnote. Another example might be that the exit angle, criterion M2 in Table E-5c, did not agree because a suspension component failed in the experiment but not in the analysis leading to different dynamics after contact. In essence, this is a judgment call on the part of the analyst about how important the phenomena is and also whether it is a reasonable physical result. For example, if 10 full-scale crash tests were performed one may well observe a few where the suspension did not fail and resulted in a trajectory more similar to the analysis solution. Of course, the decision maker reviewing this information may or may not agree with the analyst's assessment but by footnoting it in the validation report the issue has been appropriately identified. In any case, the agreement should be indicated as "no" with an explanatory footnote and the comparison can be judged as valid "with exceptions" as shown at the bottom of Table E-5c.

If all the criteria in Tables E-1, E-2 or E-3 and E-5a-c are satisfied, the model can be considered "validated" and the appropriate check box can be marked on the cover sheet. This process should be repeated for each of the baseline tests. Four detailed examples with commentary are provided in Chapter 6 to illustrate the creation of all the PIRTS and documents needed for this step. Chapter 6 explains the process of developing the reports and the actual completed reports are included in Appendix C. Blank forms for all the reports are included in Appendix E.

Predict the Performance of the Incremental Improvement

Once the baseline model has been validated for all the baseline tests that are available, the model can be modified to explore incremental design changes. For example, the guardrail height might be changed or the connection type modified in an attempt to improve the guardrail performance. Generally this would involve two crash tests in Report 350 or MASH, one with the small car and another with the pickup. The simulations of both baseline tests (i.e., the small car

and the pickup truck) should be validated and documented in a validation report as described in the last section.

Once the modifications to the model have been made, a simulation of the new untested alternative is performed to predict the outcome of a crash test of the improved design. The improved design is evaluated based on the appropriate crash test evaluation criteria (e.g., Report 350, MASH or EN 1317 as appropriate). If the performance is satisfactory according to the crash testing guidelines, the design can be considered acceptable and the results can be presented to decision makers for acceptance. If the design does not perform satisfactorily, the design should be modified such that it results in acceptable performance. This step extrapolates the results of the validated baseline computer model to predict the performance of an untested configuration. There is no full-scale test corresponding to the extrapolated computation result so the presumption is that a model that correctly replicates the results of the baseline test should be able to predict the results of a new test with similar but slightly modified hardware.

The analyst should then document the results of the numerical simulation in a simulation report that is structured much like a traditional crash test report. The verification and validation report and PIRTS developed in Step 3 should be included as appendices to the simulation report of the incrementally improved hardware since it is the comparison to the baseline test that provides confidence in the un-tested result. This simulation report is the result of completing this fourth step in the process.

Provide Documentation to Decision Makers

The final step in the process is to provide the materials necessary for decision makers to make informed decisions about accepting the incremental improvement to the roadside hardware. The packet of material to be delivered to the decision makers is much the same as would be provided in the case of a roadside device developed entirely using crash tests except some additional material is provided showing that the method used to evaluate the incremental improvement is valid. Once the incremental design is complete, the analyst or inventor should provide the following materials to the decision makers:

1. A computer simulation report describing the computer simulation of the incremental improvement and providing a crash test assessment according to the appropriate crash test specification. This report was the product of step four and is much like a crash test report except the results are based on a computer simulation rather than a full-scale crash test.
2. A verification and validation report similar to the examples provided in Chapter 6 and Appendix C for each of the baseline tests showing a comparison between a similar physical crash test and a computational model of the baseline roadside hardware device. These validation reports were the result of completing step three in the process. Decision makers will review this report to satisfy themselves that the methods used to assess the incremental improvement are valid.

3. A vehicle PIRT similar to the examples provided in Chapter 6 and Appendices C7-C8. This document will provide evidence that the vehicle model is valid for its use in assessing the incremental improvement. A vehicle PIRT, which is one of the products produced in step two, should be provided for each type of vehicle used in the baseline test comparisons.
4. A roadside hardware PIRT similar to the examples provided in Chapter 6 and Appendix C6. Like the vehicle PIRT, this document will provide evidence that the roadside hardware model is valid for its intended use in assessing the incremental improvement.

Like any acceptance decision, be it based on physical crash tests or computations, decision makers may request additional information or documentation from the analyst to satisfy themselves that the incremental improvement is indeed acceptable and the methods used to assess it are valid. Providing the information listed above will not guarantee a positive acceptance but it will provide the minimum documentation required for a fair and impartial assessment of the acceptability of the incremental improvement.

IMPLEMENTATION

This report can serve a role in assessing roadside safety hardware performance. This report is the first attempt to standardize the evaluation of numerical analyses in roadside safety. This report explains how designers and analysts should perform V&V assessments and present those results to the appropriate decision-makers. Ideally, the crash test assessment procedure and the V&V assessment procedure could parallel each other as much as possible.

This project was focused primarily on making decisions on incremental hardware improvements. As discussed in the procedures section of the final report, a designer or analysis will be expected to provide the relevant decision-making authority (i.e., the FHWA or a State DOT) with the following information:

1. A V&V report that documents the comparison between a full-scale crash test and finite element analysis of that benchmark crash test. The benchmark crash test should involve a successful crash test of hardware that is the most similar to the retrofitted hardware. Since the goal is acceptance of design modifications to crash tested hardware, failed crash tests should be avoided.
2. A hardware PIRT for the benchmark case hardware.
3. A vehicle PIRT for the vehicle used in the benchmark crash test.
4. A simulation report documenting the results of the analysis of the extrapolated, untested design.

The V&V report, hardware PIRT and vehicle PIRT of the benchmark case should give the decision-maker enough information to be confident that the extrapolation to the new situation is reasonable and the simulation report of the extrapolated design provides the details. If the

decision-maker is satisfied with the documentation and the results, an acceptance letter can be written in exactly the same way as is currently done for crash tested hardware.

Another important implementation detail is providing access to the RSVVP code, user's manual, benchmark models and benchmark case documentation. All these materials should be available to analyst on the internet such that the RSVVP program can be obtained and used by roadside safety designers and analysts. Providing the actual benchmark models as well as the PIRTS and V&V reports associated with them will provide users learning the V&V process with actual examples that they can re-run and compare to the information published in this report. The FHWA-NHTSA National Crash Analysis Center (NCAC) website would be one logical place to archive this information. The NCAC already maintains a library of roadside safety and vehicle models as well as a database of crash test data so the addition of the V&V materials would be a natural extension to the materials it currently makes available to the roadside safety community.

CHAPTER 5 COMPARING TIME HISTORIES

INTRODUCTION

Comparing the correspondence between curves from physical experiments and mathematical models is a very important and common technique used by scientists and engineers to determine if the mathematical models adequately represent physical phenomena. Two common reasons for which shapes are compared are the verification or validation of computational results and the assessment of the repeatability of experimental tests. In the former case, an experimental and a numerical curve are compared in order to assess how well the numerical model predicts a physical phenomenon; while in the latter case, two or more experimental curves are compared in order to assess if they represent the same or similar physical events.

A traditional technique has been to visually compare curves by matching peaks, oscillations, common shapes, etc. Although this kind of comparison gives a subjective impression of how similar two curves are, it is based on a purely subjective judgment which could vary from one analyst to another. With subjective methods, validation is in the eye of the beholder. Validation and verification decisions need to be based as much as possible on quantitative criteria that are unambiguous and mathematically precise. In order to minimize the subjectivity, it is necessary to define objective comparison criteria based on computable measures. Comparison metrics, which are mathematical measures that quantify the level of agreement between simulation outcomes and experimental outcomes, can accomplish this goal.

Several comparison metrics have been developed in different engineering domains. Metrics can be grouped into two main categories: (i) deterministic metrics and (ii) stochastic metrics. Deterministic metrics do not specifically address the probabilistic variation of either experiments or calculation (i.e., for deterministic metrics the calculation results are the same every time given the same input), while stochastic metrics involve computing the likely variation in both the simulation and the experiment response due to parameter variations. Deterministic metrics found in literature can be further classified into two main types: (a) domain-specific metrics and (b) shape comparison metrics. The domain-specific metrics are quantities specific to a particular application. For example, the axial crush of a railroad car in a standard crash test might be a metric that is useful in designing rolling stock but has no relevance to other applications. Similarly, the occupant impact velocity in Report 350 is an important evaluation criterion in roadside safety but has no relevance in other domains of structural mechanics.

On the other hand, shape comparison metrics involve a comparison of two curves: a curve from a numerical simulation and a physical experiment in the case of validation. The curves may be time histories, force-deflection plots, stress-strain plots, etc. Shape comparison

metrics assess the degree of similarity between any two curves in general and, therefore, do not depend on the particular application domain.

In roadside safety, comparisons between several tests or between test and simulation results have mainly used domain-specific metrics (e.g. occupant severity indexes, changes in velocity, 10-msec average accelerations, maximum barrier deflection etc.).(132) The advantage of this method was that the user could use the same domain-specific metrics that are already used to evaluate experiments to compare test and simulations results. Although the comparison of domain-specific metrics can give an idea of how close two tests or a test and a simulation are, shape-comparison metrics would be another valuable tool since they can be used to directly evaluate the basic measured response of the structures like acceleration and velocity time histories. In roadside safety, many domain-specific metrics with numerical values (e.g., occupant risk, ride-down acceleration, change in velocity, etc) are derived from the acceleration time histories so if the acceleration time history information is valid, any metric derived from the time history data should also be valid.

A computer program is described in this chapter which automatically evaluates the most common shape-comparison metrics found in literature.(3,6,7,27, 35,133-139) The program, called Roadside Safety Simulation Validation Program (RSVVP) was developed to evaluate metrics used in the verification and/or validation of numerical models in the roadside safety field or for comparing repeated crash tests. In order to correctly evaluate the shape-comparison metrics, a series of preprocessing tasks are necessary to ensure a correct comparison of the two curves. These preprocessing tasks are implemented in the code before the actual metrics are calculated. The following sections describe the preprocessing steps implemented in the RSVVP code, the numerical implementation of the metrics and the post-processing operations implemented to present the results. In the second section, the results obtained comparing some simple analytical curves are presented and discussed. In the last section, the choice of metrics used in roadside safety and the acceptance criteria used to judge comparisons is presented.

The RSVVP code was written in Matlab; the user can input the data and select the various options using a series of intuitive graphical interfaces.(131) The user's manual for RSVVP, included in Appendix A, provides step-by-step instructions for using the program to compare time histories. The programmer's manual, included in Appendix B, documents the algorithms and structure of the program.

RSVVP

PREPROCESSING

Since the two curves being compared will come from different sources (e.g., a crash test and a finite element simulation), it is necessary to preprocess the curves in the same way to ensure that any differences are not the result of filtering, sampling rate, sensor bias or sensor

drift. Some pre-processing operations like re-sampling and trimming of the two curves are essential since the curves must have the same length and be comparable point-to-point. Other preprocessing steps like filtering and sensor bias adjustments, though not strictly necessary, can play an important role in the final comparison result. For example, two identical curves that are simply shifted in time with respect to each other because the data was recorded with a different start time could produce a poor result just because of the initial offset value between the curves. A synchronizing operation that ensures the two curves start at the same point in time is another important pre-processing step. While all these pre-processing steps could be performed prior to the comparison, they have been included in the RSVVP code to make an easy-to-use program that can perform all the steps needed to generate an accurate comparison starting from the raw electronic data.

The RSVVP program performs the following pre-processing operations:

- Filtering,
- Re-sampling (i.e., ensuring that the interval between data samples is the same in both curves),
- Synchronizing (i.e., ensuring that the two curves start at the same point) and
- Trimming (i.e., the curves are trimmed so they have the same length).

The user has the option of skipping any or all of these steps. For example, the input data for one curve may already be filtered so it would be unnecessary to re-filter the data. Similarly, if the user knows the two curves are sampled at the same frequency there is no need to re-sample the curves. A brief description of all the pre-processing tasks performed by the RSVVP code before evaluating the comparison metrics is presented in the following sections.

Filtering

Filtering the curves is the first preprocessing step. In the case of accelerations collected in crash tests, the data collected are characterized by some level of high-frequency noise (a.k.a. ringing) which does not reflect the true overall dynamics of the crash. The curves must be filtered before calculating the comparison metrics although the filtering may be done inside RSVVP or with some other program (e.g., TRAP).

RSVVP digitally filters the time-histories according to SAE J211, the same reference standard for filtering used in NCHRP Report 350.(140) The user can chose between the most common Channel Frequency Classes (CFC) and even define custom filter specifications if necessary. By default, the filter option is disabled to give the user the choice to filter data using an external program since most common crash test evaluation programs like TRAP perform filtering. The RSVVP filter function is a digital four-pole Butterworth low-pass filter. The algorithm uses a double-pass filtering option (i.e., forward and backward): data are filtered twice, once forward and once backward using the following difference equation in the time domain:

$$Y(t) = a_0 \cdot X(t) + a_1 \cdot X(t-1) + a_2 \cdot X(t-2) + b_1 \cdot Y(t-1) + b_2 \cdot Y(t-2) \quad (1)$$

where $X(t)$ = Input data sequence

$Y(t)$ = Filtered output sequence

The filter coefficients vary with the particular CFC value chosen and are calculated using the following formulas:

$$a_0 = \frac{\omega_a^2}{1 + \sqrt{2}\omega_a + \omega_a^2} \quad (2)$$

$$a_1 = 2a_0 \quad (3)$$

$$a_2 = a_0 \quad (4)$$

$$b_1 = \frac{-2(\omega_a^2 - 1)}{1 + \sqrt{2}\omega_a + \omega_a^2} \quad (5)$$

$$b_2 = \frac{-1 + \sqrt{2}\omega_a - \omega_a^2}{1 + \sqrt{2}\omega_a + \omega_a^2} \quad (6)$$

where,

$$\omega_d = 2\pi \cdot CFC \cdot 2.0775 \quad (7)$$

$$\omega_a = \frac{\sin(\omega_d \cdot T/2)}{\cos(\omega_d \cdot T/2)} \quad (8)$$

In order to avoid the typical scatter at both the beginning and the end of the filtered time histories due to the application of the difference equation (i.e., Eq. 1), a head and tail are added to the original data sets consisting of a simple repetition of the first and last data values. Once the modified data sets are filtered, the head and tail are deleted from the final filtered curve. The length of the head and tail is equal to the closest integer approximation of the curve frequency divided by 10.

Both Report 350 and MASH suggest using SAE J211 Part 1 in determining the appropriate filter specifications for electronic data from crash tests. In general, acceleration data used to document the rigid body motion of the vehicle and also intended for integration to obtain velocities should be filtered according to CFC Class 180. Since Report 350 and MASH

evaluation criteria like the occupant risk as based on velocities integrated from accelerations, the CFC 180 filter class should generally be used in performing V&V comparisons.

Re-Sampling

Since most shape-comparison metrics are based on point-to-point comparisons (i.e., the data at each sampling point is compared to the corresponding point in the other curve), the two curves must have the same sampling rate to ensure the points match up in time. After the time histories have been filtered, RSVVP checks the two sets of data to determine if they have been sampled at the same rate (note: while the curves can represent any type of data, this report generally refers to the curves as time histories since in roadside safety computational mechanics the curves being compared will generally be acceleration or velocity time histories).

The re-sampling operation is managed by a subroutine which checks if the sets of data corresponding to the two curves have the same sampling period within a fixed tolerance of 5E-6 sec. If the curves do not have the same sampling rate, RSVVP proceeds to resample the curve which has the lower sampling rate (i.e., the bigger difference in time between two contiguous data points) at the higher rate of the other curve. The resampling is performed by means of a simple linear interpolation between points.

Synchronizing

Usually the time history curves to be compared do not start at the same time and, hence, the two curves are shifted by a fixed value along the abscissa (i.e., the time axis). As the comparison metrics are generally point-to-point comparisons, the time shift between the two curves must be identified and corrected to ensure that corresponding start points are matched during the metric evaluation. For example, data from a crash test may begin to be recorded 20 msec before the initial impact whereas data from a computer simulation of the same impact may begin at first contact between the vehicle and barrier. The two curves must be adjusted in time to make sure that the actual impact point occurs at the same time in both curves. Figure 43 shows an example where a test and simulation curve is shifted by an amount “s.”

The user is given the option in RSVVP to choose between two different methods of synchronizing: (1) minimum area between the curves or (2) the least square error method. A Matlab function called *shift* was created which shifts either one of the two the curves by a value s with a positive value of s meaning a forward shift for the test curve and a negative value meaning a forward shift for the true curve. In both cases, positive or negative shift values, the tail of the curve which is shifted is cut by a length equal to the shift value s as well as the head of the other curve which is not shifted. This way, a positive shift value means a forward translation for the test curve while a negative value of the shift is equivalent to a backward translation of the test curve.

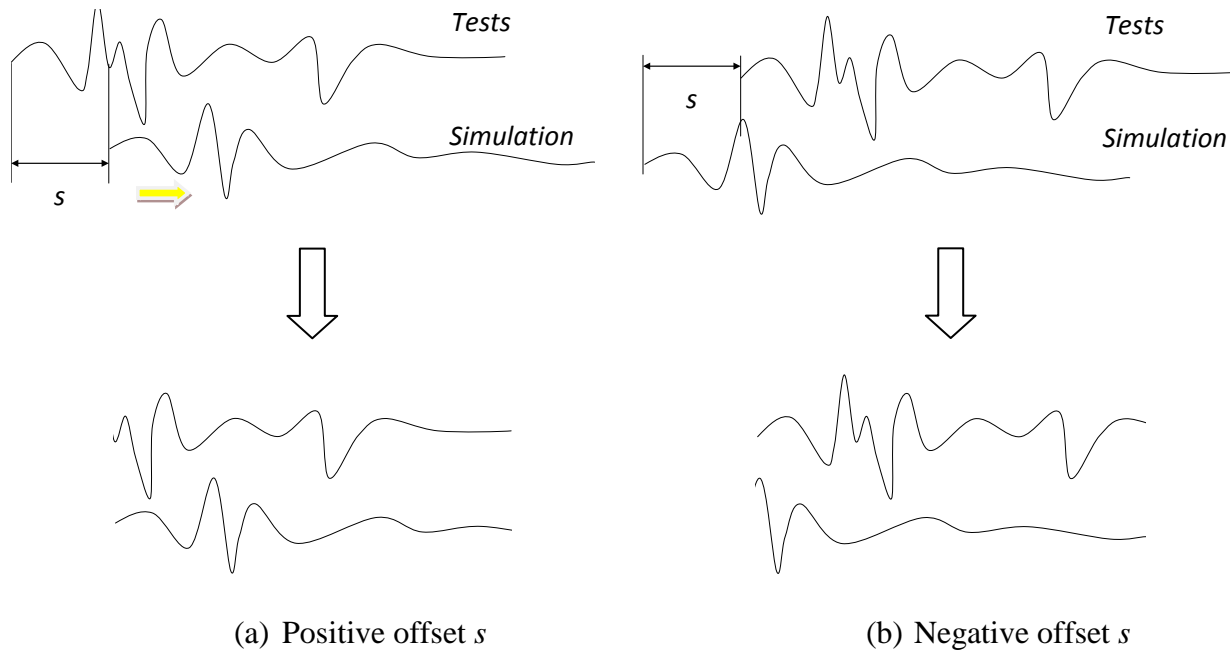


Figure 43. Shift between a test and simulation time history.

Once the *shift* function had been defined, two other Matlab functions were created which evaluate, respectively, the square root of the sum of the squared residuals (i.e., the difference between the value of the test and true curves at that instant in time) and the absolute area of residuals as a function of the shift value s . RSVVP identifies the shift value which minimizes either the absolute area of residuals (method 1) or of the sum of squared residuals (method 2); the shift value corresponding to the minimum error is the most probable matching point between the curves. Once the synchronization process is complete, the user can inspect the synchronized curves and, if the result is not satisfactory, the user can repeat the synchronization procedure using a different initial shift value for the minimization algorithm or using the other minimization method. The two methods are very closely related and generally give essentially the same result.

Trimming

After the two curves have been re-sampled, filtered and synchronized, RSVVP checks that they have the same length and, in the case of different lengths, the longer curve is trimmed to the same size of the shorter curve. At the conclusion of these preprocessing steps, the shape-comparison metrics can be calculated.

METRICS

A brief description of the shape-comparison metrics used in RSVVP is presented in this section. All fifteen metrics described are deterministic shape-comparison metrics. Details about

the mathematical formulation of each metric can be found in the cited literature. Conceptually, the metrics evaluated can be classified into three main categories: (i) magnitude-phase-composite (MPC) metrics, (ii) single-value metrics and (iii) analysis of variance (ANOVA) metrics.

RSVVP has two main parts: a generic shape-comparison tool and a roadside safety crash test specific comparison tool. The generic shape-comparison tool includes all 15 metrics described herein whereas the roadside safety analysis tool only uses the Sprague-Geers MPC and the ANOVA metrics. The rationale for selecting these metrics for roadside safety evaluations is presented in the last section of this chapter along with a discussion of appropriate acceptance criteria.

Analysts and researchers can use the first part of RSVVP to perform comparisons of any two shapes using any of the shape comparison metrics. The ability to perform general shape-metric comparisons was retained in RSVVP in order to provide a tool that can be used to validate parts, subassemblies and assemblies while developing roadside hardware or vehicle PIRTS. The second part of RSVVP is specially intended for comparing time histories that represent full-scale vehicle crash tests of roadside hardware.

MPC Metrics

MPC metrics treat the curve magnitude and phase separately using two different metrics (i.e., M and P, respectively). The M and P metrics are then combined into a single value comprehensive metric, C. The following MPC metrics are included in RSVVP and the formulations are shown in Table 14: (a) Geers (the original formulation and two variants), (b) Russell and (c) Knowles and Gear. (31, 32, 33, 133,134) Table 14 shows the mathematical definition of each metric. In this and the following sections, the terms m_i and c_i refer to the measured and computed quantities respectively with the “i” subscript indicating a specific instant in time. This symbology assumes that the measured data points (i.e., m_i) are the “true” data and the computed data points (i.e., c_i) are the data points being tested in the comparison.

In all MPC metrics, the phase component (P) should be insensitive to magnitude differences but sensitive to differences in phasing or timing between the two time histories. Similarly, the magnitude component (M) should be sensitive to differences in magnitude but relatively insensitive to differences in phase. These characteristics of MPC metrics allow the analyst to identify the aspects of the curves that do not agree. For each component of the MPC metrics, zero indicates that the two curves are identical. Each of the MPC metrics differs slightly in its mathematical formulation. The different variations of the MPC metrics are primarily distinguished in the way the phase metric is computed, how it is scaled with respect to the magnitude metrics and how it deals with synchronizing the phase. In particular, the Sprague and Geers metric uses the same phase component as the Russell metric. (33,134) Also, the magnitude component of the Russell metric is peculiar as it is based on a base-10 logarithm and it is the only MPC metrics among those considered in this paper to be symmetric (i.e., the order of the two curves is irrelevant). The Knowles and Gear metric is the most recent variation of

MPC-type metrics. (32, 135) Unlike the previously discussed MPC metrics, it is based on a point-to-point comparison. In fact, this metric requires that the two compared curves are first synchronized in time based on the so called Time of Arrival (TOA), which represents the time at which a curve reaches a certain percentage of the peak value. In this work the percentage of the peak value used to evaluate the TOA was five percent, which is the typical value found in literature. Once the curves have been synchronized using the TOA, it is possible to evaluate the magnitude metric. Also, in order to avoid creating a gap between time histories characterized by a large magnitude and those characterized by a smaller one, the magnitude component M has to be normalized using the normalization factor QS.

Table 14. Definition of MPC metrics.

	<i>Magnitude</i>	<i>Phase</i>	<i>Comprehensive</i>
Integral comparison metrics			
Geers	$M_G = \sqrt{\frac{\sum c_i^2}{\sum m_i^2} - 1}$	$P_G = 1 - \frac{\sum c_i m_i}{\sqrt{\sum c_i^2 \sum m_i^2}}$	$\sqrt{M_G^2 + P_G^2}$
Geers CSA	$M_G = \sqrt{\frac{\sum c_i^2}{\sum m_i^2} - 1}$	$P_{CSA} = 1 - \frac{ \sum c_i m_i }{\sqrt{\sum c_i^2 \sum m_i^2}}$	$sign(\sum c_i m_i) \sqrt{M_{CSA}^2 + P_{CSA}^2}$
Sprague & Geers	$M_G = \sqrt{\frac{\sum c_i^2}{\sum m_i^2} - 1}$	$P_{SG} = \frac{1}{\pi} \cos^{-1} \frac{\sum c_i m_i}{\sqrt{\sum c_i^2 \sum m_i^2}}$	$\sqrt{M_{SG}^2 + P_{SG}^2}$
Russell	$M_R = sign(m) \cdot \text{Log}_{10}(1 + m \frac{(\sum c_i^2 - \sum m_i^2)}{\sqrt{\sum c_i^2 \sum m_i^2}})$	$P_R = \frac{1}{\pi} \cos^{-1} \frac{\sum c_i m_i}{\sqrt{\sum c_i^2 \sum m_i^2}}$	$\sqrt{\frac{\pi}{4} (M_R^2 + P_R^2)}$
Point-to-point comparison metrics			
Knowles & Gear	$M_{KG} = \sqrt{\frac{\sum \left(\frac{ m_i }{m_{max}}\right)^p (\tilde{c}_i - m_i)^2}{\sum \left(\frac{ m_i }{m_{max}}\right)^p (m_i)^2}}$ where $\tilde{c} = c(t - \tau)$ (with $\tau = TOA_c - TOA_m$)	$P_{KG} = \frac{ TOA_c - TOA_m }{TOA_m}$	$\sqrt{\frac{10M_{KG}^2 + 2P_{KG}^2}{12}}$

Single-Value Metrics

Single-value metrics give a single numerical value that represents the agreement between the two curves. Eight single-value metrics are included in RSVVP:

1. The correlation coefficient metric,
2. The NARD correlation coefficient metric (NARD),
3. The Zilliacus error metric, The RSS error metric,
4. Theil's inequality metric,
5. Whang's inequality metric, the T statistic and
6. The regression coefficient metric. (27, 136 -139)

The first two metrics are based on integral comparisons while the others are point-to-point comparisons. The definition of each metric is given in Table 15 and in the discussion that follows.

Table 15. Definition of single-value metrics.

<i>Integral comparison metrics</i>			
<i>Correlation Coefficient</i>	$\frac{n \sum c_i m_i - \sum c_i \sum m_i}{\sqrt{n \sum c_i^2 - (\sum c_i)^2} \sqrt{n \sum m_i^2 - (\sum m_i)^2}}$	<i>Correlation Coefficient (NARD)</i>	$h \frac{\sum c_i m_i}{\sqrt{\sum c_i^2} \sqrt{\sum m_i^2}}$
<i>Weighted Integrated Factor</i>		$\sqrt{\frac{\sum \max(m_i^2, c_i^2) \cdot \left(1 - \frac{\max(0, m_i \cdot c_i)}{\max(m_i^2, c_i^2)}\right)^2}{\sum \max(m_i^2, c_i^2)}}$	
<i>Point-to-point comparison metrics</i>			
<i>Zilliacus error</i>	$\frac{\sum c_i - m_i }{\sum m_i }$	<i>RMS error</i>	$\frac{\sqrt{\sum (c_i - m_i)^2}}{\sqrt{\sum m_i^2}}$
<i>Theil's inequality</i>	$\frac{\sqrt{\sum (c_i - m_i)^2}}{\sqrt{\sum c_i^2} + \sqrt{\sum m_i^2}}$	<i>Whang's inequality</i>	$\frac{\sum c_i - m_i }{\sum c_i + \sum m_i }$
<i>Regression coefficient</i>		$\sqrt{1 - \frac{(n-1) \sum (c_i - m_i)^2}{n \sum (m_i - \bar{m})^2}}$	

ANOVA Metrics

ANOVA metrics are based on the assumption that if two curves represent the same event, then any differences between the curves must be attributable only to random experimental error. The analysis of variance (i.e., ANOVA) is a standard statistical test that assesses whether the

variance between two curves can be attributed to random error.(35, 36) When two time histories represent the same physical event, both should be identical such that the mean residual error and the standard deviation of the residual errors, are both zero. Of course, this is never the case in practical situations (e.g., experimental errors cause small variations between tested responses even in identical tests). The conventional T statistic provides an effective method for testing the assumption that the observed residual errors are close enough to zero to represent only random errors. Both Oberkampf and Ray independently proposed similar methods. In Ray's version of the ANOVA, the residual error and its standard deviation are normalized with respect to the peak value of the true curve. Using this method to compare six repeated frontal full-scale crash tests Ray proposed the following acceptance criteria:(36)

- The average residual error normalized by the peak response (i.e., \bar{e}^r) should be less than five percent.
- The standard deviation of the normalized residuals (i.e., σ^r) should be less than 20 percent.
- The t-test on the distribution of the normalized residuals should not reject the null hypothesis that the mean value of the residuals is null for a paired two-tail t-test at the five-percent level, $t_{0.005,\infty}$ (i.e., 90th percentile).

$$T = \frac{\sqrt{ne}^r}{\sigma^r} \quad (9)$$

Where n is the number of samples.

APPLICATION TO SIMPLE ANALYTICAL CURVES

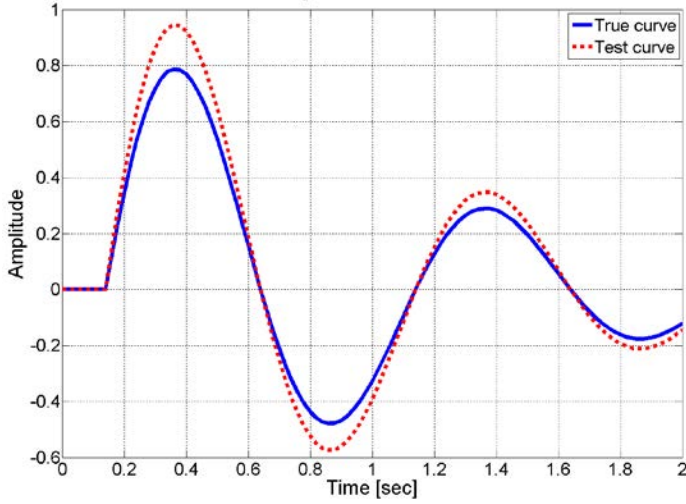
DEFINITION OF TEST FUNCTIONS

RSVVP was used to compare pairs of ideal analytical curves differing only in magnitude or phase as described in a recent work by Schwer.(32) These examples will illustrate the use of the RSVVP program and also provide some insight into the features of the different metrics calculated by RSVVP.

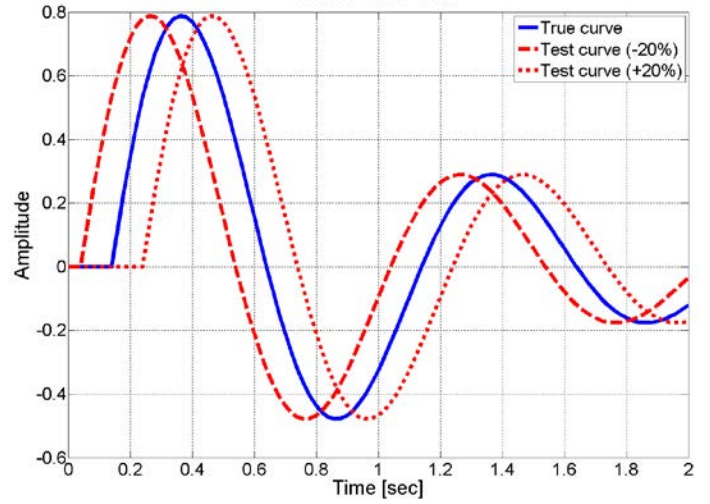
The baseline analytical curve used as a reference in both the magnitude and phase comparisons is referred to in Figure 44 as the “true” curve, while the curves differing respectively in phase or magnitude are referred to as the “test” curves. The true curve was defined by the following decayed sinusoidal curve:

$$m(t) = e^{-(t-\tau)} \sin 2\pi(t - \tau) \quad (10)$$

where the parameter τ was used to create a phase shift.



(a) Magnitude test



(b) Phase test

Figure 44. Analytical wave forms created for a (a) the magnitude test or (b) the phase test.

Following Schwer's work, two different tests were performed: (a) a curve with the same phase but an amplitude 20 percent greater than the true curve (i.e., the magnitude-error test) and (b) a curve with the same magnitude but out of phase by +/- 20 percent with respect to the true curve (i.e., the phase- error test). (32) The analytical forms used for the magnitude-error test were:

$$\begin{cases} m(t) = e^{-(t-0.14)} \sin 2\pi(t-0.14) \\ c(t) = 1.2 \cdot e^{-(t-0.14)} \sin 2\pi(t-0.14) \end{cases} \quad (11)$$

while the analytical forms used for the phase-error test were:

$$\begin{cases} m(t) = e^{-(t-0.14)} \sin 2\pi(t-0.14) \\ c(t) = e^{-(t-0.04)} \sin 2\pi(t-0.04) \end{cases} \quad (12)$$

and,

$$\begin{cases} m(t) = e^{-(t-0.14)} \sin 2\pi(t-0.14) \\ c(t) = e^{-(t-0.24)} \sin 2\pi(t-0.24) \end{cases} \quad (13)$$

In both cases, the sampling period was 0.02 sec, the start time was zero and the ending time was 2 sec. Figure 44 shows the graphs of the true and test curves used for the magnitude error and the phase error tests.

MPC METRIC RESULTS

The curves used for the magnitude test are shown in Figure 44 and the values for the 15 shape-comparison metrics evaluated using RSVVP are listed in Table 16. The M components of the MPC metrics are supposed to be insensitive to phase changes and sensitive to magnitude changes and this appears to be true according to the metric values shown in Table 16. An identical match would result in M, P and C scores of zero for all the MPC metrics. The Geers, Geers CSA, Sprague-Geers and Knowles-Gear M components are all 20 percent, as they should be, and the P components are near zero as they should be. The M component of the MPC metrics can, therefore, be considered to be an estimate of the percent difference in the magnitude. An M score of 20 can be interpreted as a magnitude difference of roughly 20 percent. The Russell M metric was found to be 13.6 with a P value of 0.0 so the Russell metric does not scale exactly with the percent of magnitude difference

Similarly, the P component of the MPC metrics should be insensitive to magnitude and sensitive to phase shift. As shown in the right two columns of Table 16, this also appears to be the case for the phase test of this simple analytical shape. The Geers, Geers CSA, Sprague-Geers and Russell phase components, P, all result in scores of around 20 percent (i.e., 18.2 to 19.5) so the phase component, P, of the MPC metrics can be interpreted as the percent of phase difference. The P value for the Knowles-Gear metric was 62.5 which indicates that magnitude and phase scores represent different levels of error for the Knowles-Gear metrics (i.e., a 20 percent magnitude shift results in an M of 20 and a 20 percent phase shift results in a P value of 62.5). The phase test was performed for both a leading and a lagging test curve. The results of the P component of the MPC metrics are exactly the same regardless of whether the test curve is leading or lagging the true curve. The P component, therefore, does not provide any information about the direction of the phase shift, only the amount of the phase shift. Table 16 also shows that there is very little difference between the values of each of the MPC metrics, particularly the Geers, Geers CSA and Sprague-Geers. Lastly, the C component of the MPC metrics is simply the vector combination of the M and P components. The C component is obtained by taking the square root of the sum of the squares of M and P.

The Geers, Geers CSA, Sprague-Geers and Russell metrics all produce similar results so there is no reason to use more than one of them. This is not surprising since the mathematical formulations for all of these metrics, as shown in Table 14, are very similar. Metrics that scale magnitude and phase similarly are easier to interpret so the Knowles-Gear metric is not preferred. One of the advantages of the Knowles-Gear metric is that it is formulated to account for unsynchronized signals. If a synchronization process provided in the pre-processing step of RSVVP is used prior to making the comparison calculations, there is no need to use the time-of-arrival technique in the Knowles-Gear metric. Likewise, metrics where the score directly represents the magnitude or phase shift are easier to interpret so the Russell metric is not

preferred. The Sprague-Geer MPC metric has gained some popularity in other areas of computational mechanics so it is the MPC metric recommended for roadside safety computational mechanics.

The only value of the C component of the MPC metric is to provide a single value for comparing the curves. Since there is useful diagnostic information in the M and P components, RSVVP calculates and reports both. The analyst can use the information in the M and P components to look for errors in their models but the C component has no direct diagnostic value. In roadside safety comparisons it is recommended that the Sprague-Geers M and P metrics be used to compare crash test time histories.

Table 16. Comparison metrics for the analytical curves for (1) the magnitude test and (2) the phase test.

RSVVP Metric Results	Magnitude +20%	Phase -20%	Phase +20%
MPC Metrics			
Geers Magnitude	20.0	0.1	-0.5
Geers Phase	0.0	18.2	18.2
Geers Comprehensive	20.0	18.2	18.2
Geers CSA Magnitude	20.0	0.1	-0.5
Geers CSA Phase	0.0	18.2	18.2
Geers CSA Comprehensive	20.0	18.2	18.2
Sprague-Geers Magnitude	20.0	0.1	-0.5
Sprague-Geers Phase	0.0	19.5	19.5
Sprague-Geers Comprehensive	20.0	19.5	19.5
Russell Magnitude	13.6	0.1	-0.4
Russell Phase	0.0	19.5	19.5
Russell Comprehensive	12.0	17.3	17.3
Knowles-Gear Magnitude	20.0	0.0	0.0
Knowles-Gear Phase	0.0	62.5	62.5
Knowles-Gear Comprehensive	18.3	25.5	25.5
Single Value Metrics			
Wang's Inequality	9.1	30.7	30.6
Theil's Inequality	9.1	30.2	30.2
Zilliacus Error Metric	20	61.8	60.4
RMS Error Metric	20	60.5	60.3
WiFAC	16.7	48.8	48.8
Regression Coefficient	97.9	78.9	79.1
Correlation Coefficient	100	81.0	80.9
NARD Correlation Coefficient	100	81.7	81.8
ANOVA Metrics			
Average Residual Error	0.02	0.0	0.0
Standard Deviation of Residuals	0.09	0.26	0.26

T Score	2.08	-0.17	0.35
---------	------	-------	------

SINGLE-VALUE METRICS RESULTS

The single value metrics are listed in the middle portion of Table 16. The correlation coefficient, NARD correlation coefficient and regression coefficient all result in a score of unity when the two curves are identical. For the magnitude test, the regression coefficient is 97.9 and both forms of the correlation coefficient are 100. Correlation suggests that two curves can be linearly transformed into each other. It does not mean that they are identical curves. Two straight lines with different slopes, for example, have a 100 percent correlation. The magnitude test results show that the two correlation coefficients and the regression coefficients are not sensitive to changes in magnitude since all three result in either perfect or nearly perfect scores (i.e., 100). The results are similar though not as good in the phase tests. The three correlation-type single value metrics result in values between 78.9 and 81.8 indicating fairly high correlation. If the scores in the phase test for these three metrics is subtracted from 100, a value near 20 is obtained indicating that these metrics are fairly direct measures of phase shift. The correlation-type metrics appear to be insensitive to magnitude shifts and directly sensitive to the amount of phase shift.

It should also be pointed out that the NARD version of the correlation coefficient is identical to one minus the P component of the Geers and Geers CSA metrics and also closely related to the Sprague-Geers P component. Since the phase information detected by the correlation, NARD correlation and regression coefficients is captured equally well in the P component of the Sprague-Geers metrics, there is no reason to routinely calculate these metrics in roadside safety verification and validation activities.

The RMS is the root-mean squared error, another standard mathematical technique for comparing signals. The RMS for the magnitude test as shown in Table 16 is 20, the amount of the magnitude shift. The RMS score for the phase shift, however, is about 60, much greater than the 20 percent phase shift. While the RMS yields the percent shift in the magnitude test, the fact that it yields a large value in the phase test limits its diagnostic utility since for a general shape comparison it would not be clear if the difference is due to an error in magnitude or phase. The Zilliacus error metric shares a similar formulation to the RMS and results in similar values. Neither the RMS or Zilliacus Error Factor are suggested for use in roadside safety verification and validation activities because the information they provide is adequately covered in the MPC metrics.

As shown in Table 15, Wang's and Theil's inequalities are very similar formulations (i.e., one using a square root of a square and the other the absolute value). In the magnitude test both yield values of 9.1 and in the phase tests values of just over 30. The two different formulations, therefore, generally will produce very similar results so there is no need to use both. Both inequalities are essentially measures of the point-to-point error between the signals as shown in

their formulations in Table 15. As will be shown in the next section, the average residual error component of the ANOVA metric is essentially the same as both Wang's and Thiel's error metrics. Since these metrics are redundant with each other and the average residual error, they are not preferred for roadside safety verification and validation comparisons.

The weighted integrated factor (WiFac) value for the magnitude test was 16.7 and 48.8 for the phase test. The diagnostic value of the WiFac is not apparent to the authors so this metric is also not recommended.

ANOVA METRICS RESULTS

With the exception of Theil's and Wang's inequality factors and the Zilliacus error factor, all the metrics discussed so far are assessments of the similarity of the magnitudes or phase of the two curves being compared. The metrics proposed by Theil, Wang and Zilliacus, on the other hand are point-to-point estimates of the residual error between the two curves. Each of these methods subtracts the test from the true signal at each point in time to find the instantaneous difference between the two curves. These differences are then summed and in some fashion normalized. Both Ray and Oberkampf independently developed a more direct assessment of the residual error. Ray and Oberkampf's methods are essentially identical except Ray normalizes by the peak value of the true curve whereas Oberkampf normalized by the mean of the peaks of the test and true curves. While the other types of metrics compare the phase or magnitude of the two curves, these point-to-point error methods examine the residual error.

Ray's method has an additional advantage since it uses both the average residual error and the standard deviation of the residual error. In essence, the ANOVA method proposed by Ray examines the shape of the residual error curve resulting from a point-to-point comparison of the curves. Random experimental error by definition is normally distributed about a mean of zero and there are standard statistical tests to test the assumption that the error fits a normal distribution. The analytical shape test presented herein is not really a particularly good test of the ANOVA metric since there is no random experimental error – the differences between the curves result from the fact that the curves are in fact different though very similar analytical curves (i.e., there is a very intentional systematic error between the test and true curves in this case).

Nonetheless, the results of the magnitude and phase test are shown at the bottom of Table 16. The average residual error for both the magnitude and phase tests was near zero indicating that the average value of the error between the curves was zero. A review of the curves in Figure 44 shows that the curves have a symmetric oscillation above and below zero so the average distance between points on the two curves should be close to zero. The standard deviation is 0.9 in the magnitude test and 0.26 in the two phase tests.

Based on an assessment of repeated crash tests, Ray has proposed that the average residual error should be less than five percent and the standard deviation of the residual error should be less than 20 percent. By those criteria the values in Table 16 would indicate that the two curves could represent the same event. The third component of the ANOVA procedure is the T test which is a standard statistical test of the hypothesis that the observed error is normally distributed. For large numbers of samples, as is the case in this test and most full-scale crash tests, and 90 percent confidence, the critical value for the T test is 2.67. The magnitude test is close but under this critical value whereas the phase tests are well inside the acceptance range. The ANOVA test is recommended for use in roadside safety computational mechanics because it provides a direct assessment of the residual errors between the test and true curves and, thereby, provides additional useful diagnostic information about the degree of similarity or difference between the curves.

APPLICATION TO REPEATED CRASH TESTS

REPEATED CRASH TESTS

While exploring the characteristics of deterministic shape comparison metrics using an analytical curve, as was done in the last section, is an informative verification exercise, the performance of the metrics for real-world crash test data is of more practical importance since real time histories are not nearly as well behaved as simple analytical functions. The objective of this section is to examine the performance of the Sprauge-Geers MPC metrics and the ANOVA metrics in a series of identical crash tests.

If a particular physical phenomena (e.g., a crash test) is documented using some type of sensors (e.g., accelerometers) and the physical experiment is repeated many times, we would expect that the response would be similar between all the experiments although not identical. Any experiment will experience random experimental error and there is a limit to the precision which sensor data can be collected and processed. If a numerical analysis is performed for the same

conditions as the physical experiment and it is not possible to distinguish the physical experiment from the numerical analysis then performing the numerical analysis is as good as another physical experiment. The question of validating computer analyses of roadside hardware collisions, then, is essentially one involving the repeatability of crash tests and quantifying the normal variation that is typically observed in such tests. If the time history from



Figure 45. Full-scale crash test set up for the repeated ROBUST crash tests.(43)

a numerical analysis cannot be distinguished from the time histories of physical experiments, then the numerical analysis is a valid representation of the physical phenomena.

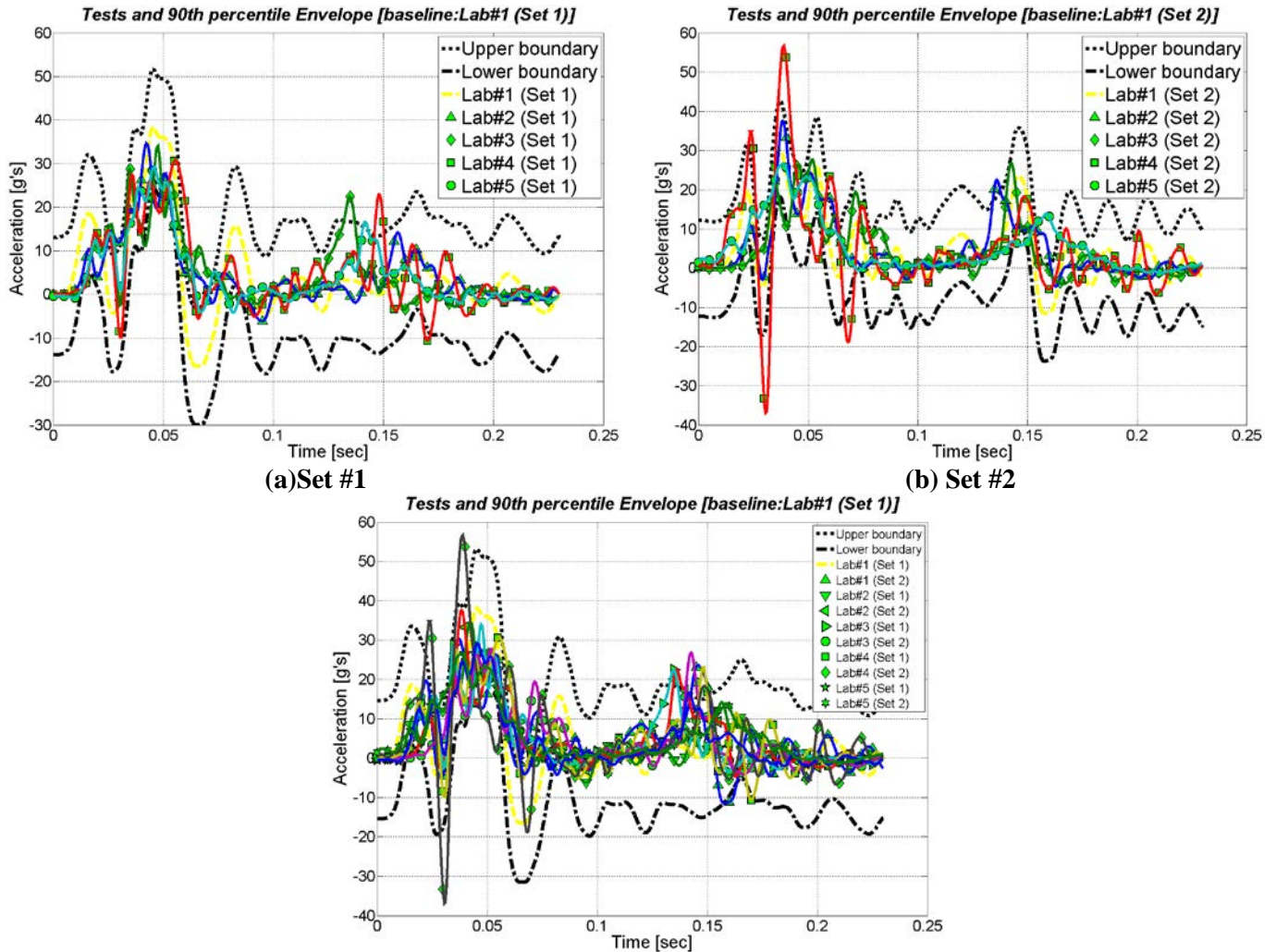


Figure 46. 90th percentile envelope and acceleration time histories for (a) set #1, (b) set #2 and (c) sets #1 and #2 combined.

A series of five crash tests (i.e., Set #1) with new model year 2000 Peugeot 106 vehicles and a rigid concrete barrier were performed as a part of the ROBUST project. (43) The basic test conditions are shown in Figure 45. The tests were independently carried out by five different test laboratories in Europe, labeled laboratories one through five in this report, with the purpose of assessing the repeatability of full-scale crash tests. As the main intent was to see if experimental curves representing the same physical test resulted in similar time-history

responses, a rigid barrier was intentionally chosen in order to limit the scatter of the results which is presumably greater in the case of deformable barriers. A second series of five tests (i.e., Set #2) was performed using the same barrier but with vehicles of different brands and models. All the vehicles used in the second series, however, corresponded to the standard 900-kg small test vehicle specified the European crash test standards, EN 1317.(11) The second set of tests was performed to investigate influences arising from different vehicle models on the repeatability of crash tests. In all cases, the three components of acceleration, including the lateral acceleration used in this paper, were measured at the center of gravity of the vehicles. Only lateral accelerations and velocities are discussed in this paper for the purpose of conciseness; the lateral response is thought to be the more critical in this type of re-directional barrier test. In order to compare the different time histories, it was necessary to prepare them in exactly the same way. All the time history curves were pre-processed in exactly the same way using the RSVVP program described earlier in this chapter.

One common method for assessing the validity of a simulation result or the repeatability of multiple impact experiments in the biomechanics field is to develop response envelopes. If multiple experiments are available, the time histories for all the experiments can be plotted together. If the responses are average and standard deviations are calculated at each instant in time, the $\pm 90^{\text{th}}$ percentile envelope indicating the likely response corridor can be plotted. After the ten curves were preprocessed, the 90^{th} percentile envelope for each of the two sets of tests (i.e., set #1 with the same new vehicle and set #2 with similar vehicles) was computed considering the response from Lab #1 to be the “true” curve (note: the results from Lab #1 were chosen arbitrarily as the “true” curve). The 90^{th} percentile envelope for each set was evaluated by adding and subtracting to the respective “true” curve the average of the standard deviations of the residuals for each specific set of tests multiplied by 1.6449. Figure 46 shows the preprocessed curves and the respective envelopes for sets #1 and #2. Also, all ten tests from both sets were compared together considering the response of test Lab#1/Set #1 as the “true” curve and the results are shown in the bottom portion of Figure 46.

As expected, there is considerable scatter between the acceleration time histories shown in Figure 46 although there is also a clear trend. Any test response that falls within the response corridors shown in Figure 46 would be considered to be identical or at least equivalent impact events. As shown by the response envelopes, all ten experiments tend to remain inside the response envelopes although the test from Lab #4 in Set #2 has several peaks that are outside the response corridor. While calculating response corridors is a very useful technique, at least five experiments must be available before a corridor can be constructed and the level of confidence (i.e., the width of the corridor) will be wider the smaller the number of samples is. In roadside safety the normal situation is that there is generally only one experiment. A response corridor cannot be obtained from just one or two experiments so if an analyst desires to compare a single

computational result to a single crash test experiment, the response corridor method is not an option.

ACCEPTANCE CRITERIA

When comparing a computational result to an experiment, the analyst must decide what constitutes a reasonable acceptance criterion. While the metrics themselves are deterministic a subjective judgment still has to be made about how close to zero (i.e., zero is a perfect match for all the metrics considered in this section) is “good enough.” Since all ten of the experiments discussed in this paper represent identical tests, the range of metric values observed should be an indicator of the acceptable range of scores for more or less identical tests. One of the purposes of this work, therefore, is to provide insight on acceptance criteria when using the Sprague-Geers and ANOVA metrics.

Results Using Acceleration Time Histories

Once the time histories for the ten experiments were preprocessed, each was compared to the “true” curve by evaluating the Sprague-Geers and ANOVA metrics calculated using the RSVVP program, described in Chapter 5. Initially, the two sets of tests, Set #1 with the same new vehicle and Set#2 with similar vehicles, were considered separately using the response from the Lab #1 test in each set as the “true” curve. The choice of Lab #1 to represent the “true” curve was arbitrary and certainly the results would be slightly different if another test set was used as the “true” baseline curve. The question being evaluated in this section is, therefore, “are the results from Lab #1 the same as those reported by Labs #2 through #5?” The resulting metric values for set #1, Set #2 and the combination of both sets are shown in Table 17 in the top, middle and bottom portions, respectively.

Sprague-Geers MPC Metrics

The upper portion of Table 17 shows the values for the Sprague-Geers MPC metrics. The magnitude component of the metric is negative for all four of the comparison experiments indicating that the “true” experiment (i.e., the result from Lab #1) general experienced a higher magnitude. The amount of the magnitude score is roughly equal to the percent difference in magnitudes and in the case of Set #1 varies between 14 and almost 26 percent. The last column in Table 17 is a possible acceptance criterion which is based on calculating the 90th percentile value of the observed metrics (i.e., the mean plus 1.67 times the standard deviation). Even when the same make and model of vehicle is used, the acceleration time histories under identical impact conditions can vary as much as nearly 30 percent in magnitude. The results for Set #2, where different vehicles meeting the EN 1317 small car test vehicle criteria were used, are similar although the experiment from Lab #4 experienced a much higher magnitude score indicating that Labs #2, #3 and #5 tended to have smaller magnitudes than the Lab #1 true test and Lab #4 had a much higher magnitude. This is actually confirmed by the time history graphs

in Figure 46 where the results for Lab #4 are clearly higher and even cross outside the response corridor. The large difference between Lab #4 and the other tests is reflected in the much larger standard deviation (i.e., 4.85 versus 21.35). It is not clear whether the differences between Sets #1 and #2 are due to the differences in the vehicles or the one unusual test from Lab #4 in Set #2.

When the magnitude component of the Sprague-Geers metric is combined for all ten tests, as shown in the bottom portion of Table 17, the mean score is -17.2 showing that on average the tests have smaller magnitudes than the true test. The standard deviation of the results is nearly 12. If the 90th percentile value were used to establish an acceptance criterion for the magnitude component, a value of 37.1 would be the result.

Table 17. Comparison metrics for Set #1, Set #2 and the combination of both sets.

Metric	Lab #2	Lab #3	Lab #4	Lab #5	Mean	Std.	Possible
DATA SET #1							
Sprague-Geers							
Magnitude	-23.0	-21.4	-14.4	-25.8	-21.2	4.85	± 29.2
Phase	22.6	36.3	31.2	24.9	28.8	6.21	39.1
ANOVA							
Avg. Residual Error	0.00	-0.01	-0.01	0.00	-0.01	0.01	± 0.01
Std Dev. Of Residuals	0.19	0.24	0.23	0.20	0.22	0.02	0.25
DATA SET #2							
Sprague-Geers							
Magnitude	-2.6	-8.2	35.6	-9.3	3.9	21.35	± 39.3
Phase	21.3	22.8	25.4	26.7	24.0	2.49	28.2
ANOVA							
Avg. Residual Error	-0.01	0.00	0.00	-0.02	-0.01	0.01	± 0.02
Std Dev. Of Residuals	0.21	0.22	0.31	0.25	0.25	0.05	0.32
DATA SETS #1 and #2 COMBINED							
Sprague-Geers							
Magnitude	See above for individual scores				-17.2	11.94	± 37.1
Phase					34.9	8.44	33.2
ANOVA							
Avg. Residual Error					-0.01	0.01	± 0.02
Std Dev. Of Residuals	See above for individual scores				0.24	0.04	0.31

The result for the phase component is similar as shown in Table 17. Due to the formulation, the values for the phase component must always be positive so it is not possible to determine from the metric value whether the test curve is leading or lagging the true curve in phase. For Set #1, the values varied from just above 22 to just over 36 with a mean and standard

deviation of 28.8 and 6.21, respectively. The phase component of the metric can be interpreted as being the percent out of phase of the signal. The results for Set #2 were very similar and actually resulted in a smaller standard deviation than Set #1 possibly indicating that the difference between vehicles does not appear to play a major role at least in this test with this type of vehicle. Combining both sets of data and calculating the 90th percentile indicates that a phase score of about 33 would be appropriate.

Based on the results of the ten essentially identical full-scale crash tests summarized in Table 17, an absolute upper bound value of 40 could be used as acceptance criteria for both the magnitude and phase components of the Sprague-Geers MPC metrics when evaluating acceleration time histories from full-scale crash tests because 90 percent of identical crash tests should have a response that falls within these limits.

ANOVA Metrics

While the Sprague-Geers metrics assess the magnitude and phase of two curves, the ANOVA examines the differences or residual errors between two curves. The average and standard deviation of the residuals were evaluated for each time history in both sets of data and the results are shown in Table 17. For all ten experiments, the average residual error was always close to zero. The standard deviations of the residual errors were always under 31 percent and in all cases but one less than 25 percent. Since the time histories for all the crash tests represented essentially identical physical events, the residuals for each curve should be attributable only to random experimental error or noise. Statistically speaking, this means that the residuals should be normally distributed around a mean residual error equal to zero. As shown in the cumulative density function in Figure 47, the shape of the residual accelerations distribution is typical of a normal distribution for both sets of crash tests when taken separately or combined. Since the cumulative distribution is an “S” shaped curve centered on zero, the distribution of the residuals is consistent with random experimental error as would be expected in these series of repeated crash tests. This is a very strong indicator that the ten tests are, in fact, similar impact events.

Ray applied the ANOVA criteria to a set of six identical frontal rigid pole impacts and reported the results in a paper published in 1996.(35) Ray proposed an acceptance criteria based on these six tests of a mean residual error less than or equal to five percent and a standard deviation of the residual less than 20 percent. Since the tests used in this earlier study were of a type that are presumed to be highly repeatable (i.e., the same type of vehicle was used, the same crash test facility was used, the barrier was a rigid instrumented pole and the impact was a center-on full-frontal impact) it was not known if these criteria would be reflective of more general roadside hardware crash tests performed under less ideal conditions. The data in Table 17 indicate that the mean residual error criterion of less than five percent appears to be adequate since none of the comparisons for these ten tests resulted in a mean residual greater than two percent. The standard deviation of the residuals, however, was higher in this test series than in the one reported by Ray in 1996. The highest standard deviation of the residuals (i.e., 31

percent) was found for Lab #4 in Set #2, the same test that resulted in an unusually high magnitude score. With that exception, the standard deviations were generally between 20 and 25 percent, a little higher than Ray originally proposed.

Based on these eight comparisons and Ray’s 1996 work, the average residual error should be less than five percent and the standard deviation of the error should be less than 35 percent.

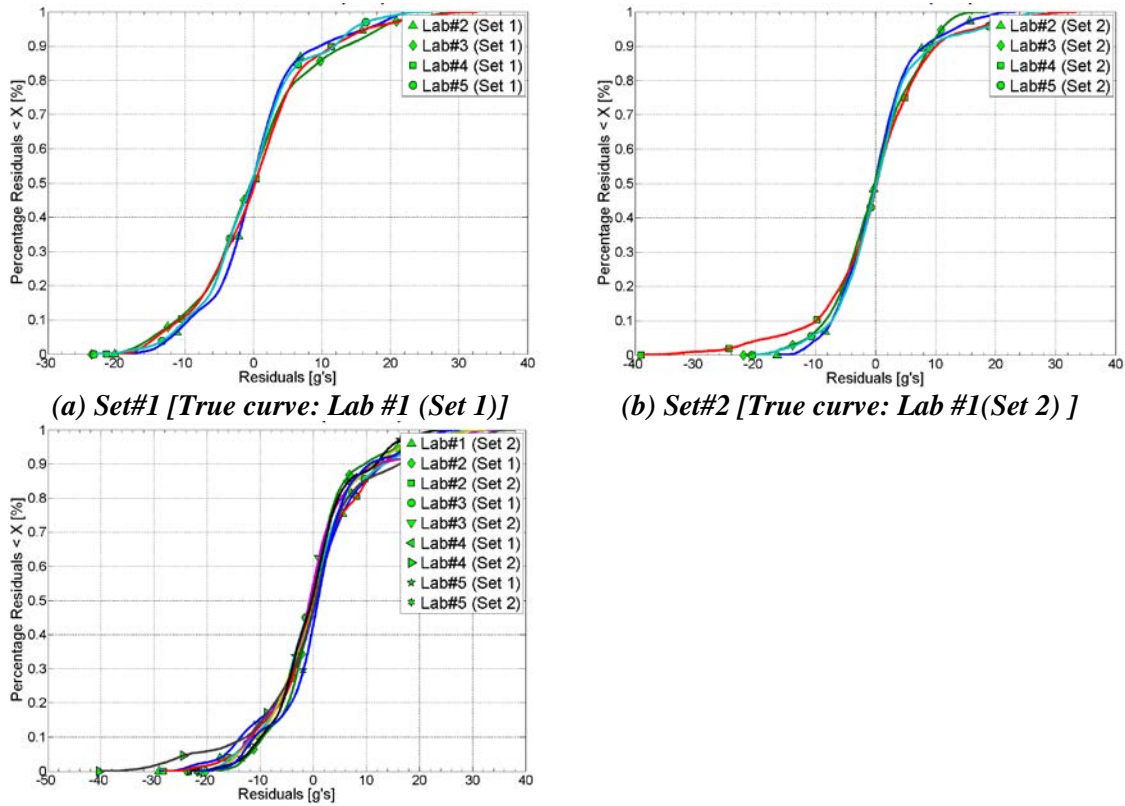


Figure 47. Cumulative density function of the residual accelerations for (a) Set #1, (b) Set #2 and (c) the combination of Sets #1 and #2.

RESULTS USING VELOCITY TIME HISTORIES

Sometimes velocity time histories are used to visually compare curves rather than acceleration time histories because they are less noisy and the trends are more easily apparent. The acceleration histories for the ten experiments were integrated to obtain the lateral velocities and the velocity time histories and the 90th percentile response corridors as shown in Figure 48 for Set #1. The velocity corridor is much narrower and smoother than the corresponding acceleration time history response corridor shown in Figure 48.

Just as the Sprague-Geers MPC metrics can be used to compare the shapes of acceleration time histories, exactly the same procedure can be used to evaluate the velocity time

histories. Table 18 shows the values of the metrics calculated for Set #1. As shown in Table 18, the Sprague-Geers magnitude and phase metrics are much smaller for the velocity time history comparison than was the case for the acceleration time history comparison. The maximum magnitude score was 5.1 and the maximum phase score was 3.1. Using these values to compute the 90th percentile range results in an acceptance value of less than 10 for both magnitude and phase, much less than the 35 recommended for acceleration time histories.

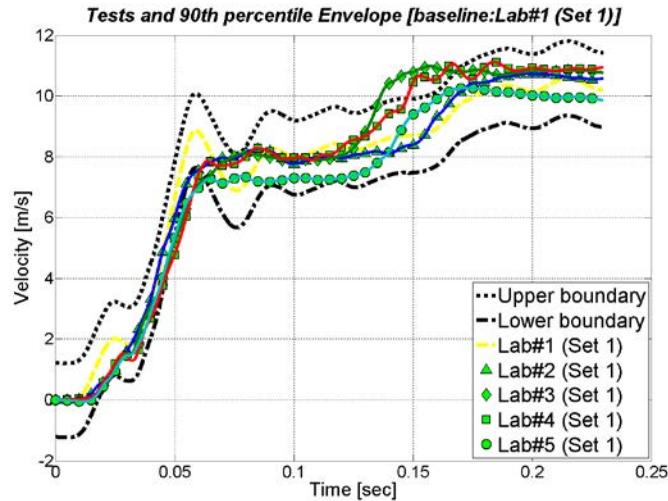


Figure 48. 90th percentile envelope and velocity time histories for Set#1.

Table 18. Values of the comparison metrics using velocity time histories for Set#1.

Metric	Lab #2	Lab #3	Lab #4	Lab #5	Mean	Std.	Upper
Sprague-Geers							
Magnitude	0.5	5.1	4.5	4.0	1.5	4.21	8.5
Phase	2.0	3.5	3.1	2.8	2.9	0.64	3.9
ANOVA							
Avg. Residual Error	0.0	-0.02	-0.02	0.04	0.00	0.03	0.05
Std Dev. Of Residuals	0.05	0.09	0.08	0.06	0.07	0.02	0.10

While the Sprague-Geers metrics improve as the acceleration time history is integrated to a velocity time history, the ANOVA metrics becomes much worse. While the average residual errors are still around zero, the standard deviation increases by a factor of four or five. The reason for this poor performance with the velocity curves is that the integration process in essence masks the residual acceleration errors. When using an ANOVA technique, the

evaluation of metrics should always be performed using time histories directly measured and not derived using either integration or differentiation. For example, if accelerations are measured experimentally, accelerations should be the basis of the ANOVA comparison. Velocities and displacements obtained by integrating the acceleration curve will accumulate error with each subsequent integration. This is shown graphically in Figure 49 where the distribution of the residuals is more spread out and the mean is not as close to zero as was the case for Figure 49.

While the Sprague-Geers MPC metrics can be used with either raw data (i.e., accelerations) or integrated data (i.e., velocities), it is recommended that the comparison be made based on the data the way it was collected (i.e., raw data). Using processed data adds a mathematical layer of complexity that can introduce its own errors. For example, in this case local lateral velocities were compared but if all six channels of data were integrated using a coupled numerical integration to obtain the global velocities, errors from various channels would “seep” into the other data channels. For example, say the lateral accelerations were identical but the yaw rate gyros for the test and simulation were quite different. A coupled integration of such data would result in errors in every channel since the yaw rate data is coupled to every other channel. For this reason, it is suggested that data be compared the way it was collected without any subsequent processing. For example, if local acceleration data is collected, local acceleration data should be the basis of the comparison in order to avoid errors due to post-processing the data into some other form.

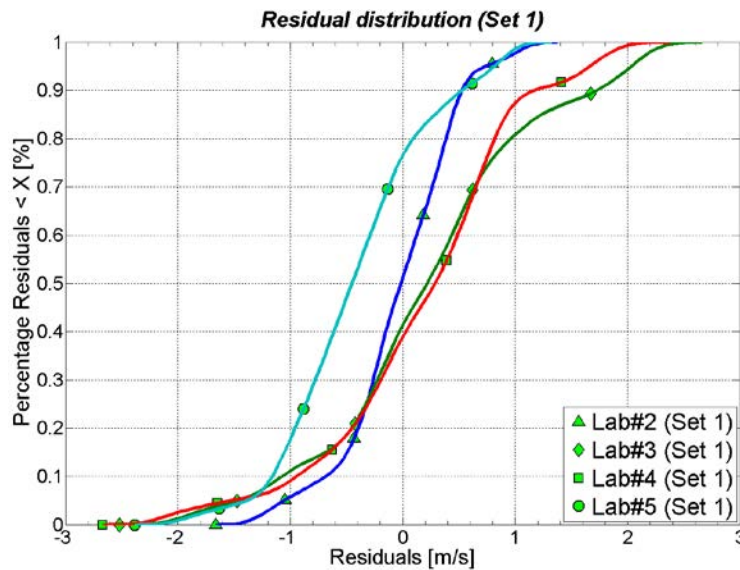


Figure 49. Cumulative density functions of the residual velocities for Set #1.

For the ANOVA metrics, the comparison must take place based on the accelerations if the original data was collected with accelerometers. It is recommended that when using an ANOVA procedure, the results be computed based on the time histories collected in the physical

experiments; normally this would be accelerations and rate gyros in crash tests. In evaluating the ANOVA metrics for a series of six identical frontal rigid pole impacts, Ray proposed an acceptance criterion of a mean residual error less than five percent of the peak and a standard deviation of less than 20 percent of the peak test acceleration.(35) As shown in Table 19 and discussed above, this is probably a bit too restrictive and should be changed to a average residual error of less than five percent and a standard deviation of less than 35 percent.

The purpose of examining these repeated crash tests was to explore how repeatable similar full-scale crash tests would be and identify sources of possible discrepancies between test organizations. (43) As discussed earlier, the magnitude results for Lab #4 Set #2 represent a departure from most of the other test results. The ROBUST team, in fact, examined all the test procedures and techniques used by the different test agencies and actually identified several differences that could explain some of the discrepancies. For example, the ROBUST team discovered that each test organization used a different technique to mount the accelerometer block to the test vehicle and the mounting technique had a measurable effect on the acceleration time histories. They designed and tested a new light-weight more rigid composite block that significantly improved the consistency of the testing results. This illustrates an important point: while two tests may be performed at the same impact conditions and use the same vehicle and barrier, the way data is collected and processed will also affect the results. The shape-comparison metrics will be sensitive not only to differences in the impact conditions and test results, but also to the way data was collected and processed.

ACCEPTANCE CRITERIA

A comparison of ten repeated essentially identical crash tests was presented above. The Sprague-Geers MPC metrics and the ANOVA metrics were used to quantitatively make comparisons between eight pairs of crash tests. Two sets of data were available, the first set of five tests used the same make, model and year of vehicle whereas the second set of five tests used different vehicles that met the requirements for the small car defined by EN 1317. The original raw time histories from the 10 tests were filtered, re-sampled and synchronized in order generate accurate comparison results. The statistics derived from the analysis of the residuals confirmed the hypothesis that the errors were normally distributed and could, therefore, be attributed to normal random experimental error.

Using the data from these ten tests, recommendations for acceptance criteria for evaluation metrics for comparing repeated crash tests were recommended. Namely:

- The Sprague-Geers magnitude and phase metrics should be strictly less than 40.
- The average residual error when comparing two acceleration time histories from a crash test should be less than five percent. The standard deviation of the residual errors should be less than 35.

INDEPENDENT ACCEPTANCE CRITERIA ASSESSMENT

Abu-Odeh and Ferdous performed their own unpublished independent examination of the acceptance criteria described in the previous sections using four similar crash tests performed at Texas Transportation Institute. Four crash tests of strong-post w-beam guardrails were used as repeated crash tests. In all four cases, the only difference between the guardrail systems was the type of material used for the blockout. Test 1 used a typical timber blockout whereas tests 2 and 3 used recycled polymer blockouts and test 4 used a composite blockout. All four tests used C2500 Chevrolet pickup trucks between model years 1989 and 1996 and the nominal impact conditions were essentially the same as shown in Table 19. Since differences between the blockout materials are unlikely to change the results of the test as long as the blockout does not split and break (which they did not in these tests), the tests are essentially repeated instances of the same test of a strong-post w-beam guardrail.

Table 19. Comparison metrics for four essentially identical crash tests of a strong-post w-beam guardrail with different blockouts.

Test Characteristics	Test						
	#1	#2	#3	#4			
Vehicle Model Year	1989	1996	1990	1996			
Impact Speed (km/hr)	101.5	101.4	100.9	101.4			
Impact Angle (deg)	25.5	25.4	25.2	23.8			
MPC Metrics	M	P	M	P	M	P	
X acceleration channel	19	36	10	35	5	39	
Y acceleration channel	17	31	23	40	1	35	
Z acceleration channel	4	46	13	46	37	56	
Roll rate channel	1	35	38	38	34	38	
Pitch rate channel	16	37	38	38	8	32	
Yaw rate channel	13	13	16	16	9	11	
ANOVA Metrics	Residual	SD	Residual	SD	Residual	SD	
X acceleration channel	0.01	0.22	0.01	0.22	0.02	0.23	
Y acceleration channel	0.01	0.13	0.00	0.18	0.00	0.14	
Z acceleration channel	0.00	0.26	0.00	0.25	0.05	0.27	
Roll rate channel	0.03	0.29	0.02	0.29	0.06	0.29	
Pitch rate channel	0.04	0.32	0.03	0.31	0.02	0.29	
Yaw rate channel	0.06	0.15	0.07	0.18	0.09	0.08	

Note: All tests used Chevrolet C2500 pickup trucks with the same nominal impact conditions.

Abu-Odeh and Ferdous used the RSVVP program to calculate the Sprague-Geer and ANOVA metrics for these four tests using the results of test 1 as the “true” curve and each of the other tests as the test cases. The results are summarized in Table 19. As shown in Table 19, the acceptances recommended in the last section were always satisfied with the exception of the Z accelerations for tests 3 and 4. In these cases, the Z acceleration is a relatively unimportant channel since most of the vehicle kinematics are described by the X and Y accelerations and the Yaw rotation. As discussed earlier, there is a procedure in RSVVP to account for weighting relatively unimportant channels in RSVVP and when this procedure was used by Abu-Odeh and

Ferdous the weighted comparison was acceptable. The results also show that, with the exception of the Z channel in comparisons 3 and 4, some of the results are near the acceptance criteria indicating that the values chosen are reasonable for this type of re-directional guardrail crash test. Abu-Odeh and Ferdous's examination confirms that the acceptance criteria recommended in the last section are indeed reflective of the values of repeated crash tests and so are therefore meaningful acceptance criteria for comparing full-scale crash test results and numerical simulation results.

CONCLUSIONS

This chapter described the features of the RSVVP program, provided an example of its application to simple analytical curves and provided examples of developing acceptance criteria based on repeated identical full-scale crash tests. RSVVP pre-processes the two input curves. Data can be filtered, adjusted for any bias, re-sampled to the same data acquisition frequency and synchronized to the same equivalent initial time. Pre-processing is an important step because poor metric scores can result just because the curves might have been processed differently. For this reason, it is preferable that raw (i.e., unprocessed) data is used in RSVVP rather than crash test data that has already been processed.

RSVVP includes fifteen separate metrics that can be used to compare and analyze the differences between the test and true curves. The formulations of these metrics are summarized in Table 14 and Table 15 and full details are available in the literature. A test case using a simple analytical function was performed and the results for the 15 metrics were shown in Table 16. A review of the results and formulations of these metrics show that there are really just three basic features of a shape comparison that are assessed: similarities in magnitude, similarities in phase and the shape of the residual error curve. Since many of the metrics share similar formulations, their results are often identical or very similar and there is no reason to include all the variations. The Sprague-Geers MPC metrics are recommended to assess the similarity of magnitude (i.e., the M metric) and phase (i.e., the P metric) and the ANOVA metric is recommended to assess the characteristics of the residual errors.

The RSVVP program will provide a convenient platform for engineers to explore the similarities and differences between both physical test and computational results in validation efforts as well as comparing the repeatability of physical experiments. The program provides all the tools needed to quickly perform the assessments between two curves.

Acceptance criteria for comparing full-scale crash tests and numerical simulations were developed using comparisons with analytical curves and a set of 10 essentially identical crash tests. Based on the results of comparing these 10 identical crash tests, the Sprague-Geers magnitude and phase metrics should be strictly less than 40, the average residual error should be less than five percent, and the standard deviation of the residual errors should be less than 35 for acceptable results. Lastly, the acceptance criteria were used by Abu-Odeh and Ferdous to

examine four nearly identical crash tests and the results showed that, with the exception of some of the Z accelerations, the acceptance criteria resulted in the correct assessment – that is, that the crash tests were identical.

CHAPTER 6 BENCHMARK CASES

INTRODUCTION

Chapter 4 described the recommended procedures for validating roadside safety simulations of crash tests and Chapter 5 discussed the comparison of time histories, the development of comparison metric acceptance criteria and the use of RSVVP. This chapter provides several examples of the validation process including documentation of the capabilities of the vehicle and roadside hardware models in phenomena importance ranking tables (PIRTs) and the documentation of the comparison in the validation and verification report. The following four benchmark test cases are presented:

1. A C2500 pickup truck striking a strong-post w-beam guardrail (see Appendices C1, C6 and C8),
2. A C2500 pickup truck striking a strong-post w-beam guardrail with a six-inch curb (see Appendix C2, C6 and C8),
3. A Geo Metro striking a vertical concrete barrier (i.e., the ROBUST Tests) (see Appendices C3 and C4) and
4. A tractor Trailer Striking a Concrete Median Barrier (see Appendix C5 and C7).

The complete PIRTS and V&V reports for each of these test cases are provided in Appendix C.

TEST CASE 1: PICKUP TRUCK STRIKING A GUARDRAIL

INTRODUCTION

The first test case involves a ¾-ton pickup truck impacting the most commonly installed strong-post w-beam guardrail system in the U.S. (i.e., the modified G4(1S) with wood blockouts). The purpose of the research leading to the development of this finite element model was to evaluate the effects of installing curbs in combination with guardrail systems.(141) Since there were no physical tests of a curb installed in combination with the G4(1S) at the time when this model was developed, the research approach used in validating the model was to first develop a model of the guardrail, validate the model using existing full-scale crash test data of the system without a curb, then modify the model by including various curbs placed in combination with the guardrail to evaluate their effects on crash performance based on safety criteria in Report 350. This first test case, therefore, involves the validation of the original strong-post w-beam guardrail model without a curb in an impact with a pickup truck. This model was used to assess the effects of several types of curbs placed in combination with the guardrail system, as well as the lateral offset distance of the curb relative to guardrail position. The results of these extrapolated simulations with the model were ultimately validated with subsequent full-scale crash tests of select curb-guardrail combinations. The validation of one of those extrapolated cases is the subject of Test Case 2 in this chapter.

The G4(1S) guardrail with routed wood blockouts is composed of 12-gauge w-beam rails supported by W150x13.5 steel posts with 150x200 mm wood blockouts, as shown in Figure 50. The posts are spaced at 1.905 m center-to-center. The w-beam rails are spliced together using eight 16-mm diameter bolts at each splice connection and the rails are connected to the posts and blockouts using a single bolt at each post location.



Figure 50. Modified G4(1S) guardrail with routed wood blockouts.

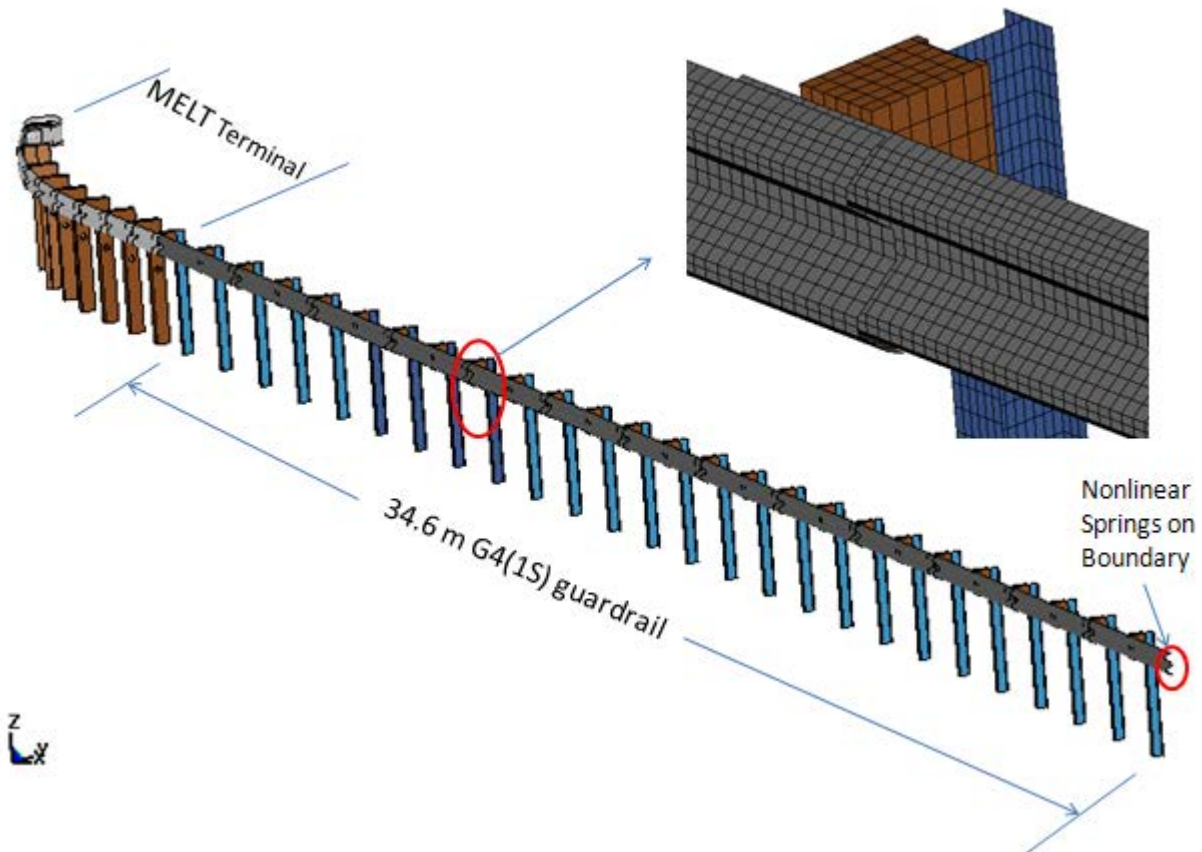


Figure 51. Finite element model of the G4(1S).

The complete guardrail model, shown in Figure 51, consists of 34.6 m of the guardrail system with thirteen 3.81-m sections of w-beam rail, twenty-six W150x13.5 steel posts spaced at 1.905 m, and twenty-six 150 x 200-mm wood blockouts. At the up-stream end of the model a MELT guardrail terminal, validated in a previous study, was used to simulate the anchor system used in the test.(40, 89) The downstream anchor was modeled using nonlinear springs representative of the longitudinal stiffness of the MELT guardrail terminal model.

PIRT FOR THE G4(1S)

When a model is validated for a particular application it may not be appropriate for use in other applications that vary significantly from the original application. In many cases, models are developed and validated by one analyst and then obtained and used by others for entirely different purposes. Because a model was considered “valid” by its developer, subsequent users may inadvertently use the models inappropriately if they do not understand the modeler’s original intent. It is always the user’s responsibility to verify the results of the model. Therefore, the user must ensure that the various components of the model accurately simulate the phenomena that are important to their application. The PIRT provides a means of communicating to other users the specific phenomena that the model was validated for during its development. The PIRT lists all the physical tests that were used to validate the various components and subassemblies of the model and provides a quantified assessment of their validity.

The G4(1S) model was developed for use in crash simulations of Report 350 test 3-11 (e.g., a 2000-kg pickup truck impacting the guardrail at a speed of 100 km/hr and 25 degrees at a specified critical impact point along the length-of-need section of the guardrail). In the development of the model, several components were validated by simulating physical tests that were conducted on those components (or subassembly of components) and comparing the results. The specific components of the guardrail model that were validated include the steel post, the splice connection, the rail-to-post connection, and the post-soil interaction/response.

Table 20 lists the six laboratory tests that were used in validating specific phenomena of the model and indicates whether they were considered valid. The validity of each phenomenon should be quantified in much the same way as validating the complete model against full-scale crash tests. That is, the time-history data collected from the simulation are compared to a physical test using RSVVP to calculate the validation metrics. If the Sprague and Geers metrics are less than 40 and the ANOVA metrics are less than 0.5 and 0.35 for the mean residual error and the standard deviation of the mean residual error, respectively, then the phenomenon is considered valid. Unfortunately, much of the electronic data that were collected from the physical tests in the validation of the G4(1S) are no longer accessible. In those cases, validity was determined based on a qualitative assessment of data presented in the project reports.

Table 20. Phenomena Importance Ranking Table (PIRT) for the G4(1S).

	Validated Phenomenon	Validated? Verified? Calibrated?
1.	Three-Point Bend Test of W150x13.5 Post About Weak Axis	Validated
2.	Load-to-rupture of splice connection under quasi-static axial loading	Qualitative Validation
3.	Pull-through of post-bolt-head connection to w-beam using axial load machine	Qualitative Validation
4.	Full-scale bogie impact tests of the W150x13.5post embedded in 1,980 kg/m ³ soil	Qualitative Validation
5.	Full-scale bogie impact tests of the W150x13.5post embedded in 2,110 kg/m ³ soil	Qualitative Validation
6.	Full-scale bogie impact tests of the W150x13.5post embedded in 2,240 kg/m ³ soil	Validated

An example of documenting the validity of a particular phenomenon is shown in Figure 52. In this case, phenomenon number one in Table 20 is documented in Figure 52. A weak-axis quasi-static bending test was performed on a W150x13.5 steel post in order to validate the finite element model of the guardrail post. The force-displacement response was measured in the physical test and compared to the prediction from the finite element model as shown in the lower left portion of Figure 52. The two curves, one from the physical experiment and the other from the finite element simulation, were compared using RSVVP and the results are tabulated in the upper portion of Figure 52. The comparison, in this particular case, was very good resulting in satisfactory values for all the metrics. Since the curve comparisons were acceptable, the results of this aspect of the model can be considered validated such that users can be confident that the model will provide accurate results in similar applications.

Some of the phenomena in Table 20 could only be validated qualitatively in this case because the original data was no longer available. In these cases, the experimental and finite element curves were compared visually but since the data files were not available, the metrics could not be calculated. Sometimes physical tests are used to calibrate the model. This can also be indicated in the PIRT in the right column by indicating “calibrated” rather than “validated.” The complete PIRT report for the strong-post w-beam guardrail is included in Appendix C6.

PIRT FOR THE C2500R VEHICLE MODEL

The vehicle model used in the analysis was a modified version of the NCAC C2500R finite element model, which is a reduced element model of a 1995 Chevrolet 2500 pickup truck. (83, 144) The C2500R model has been used by several research organizations over the years and each organization has made changes/improvements to the model. As a result, the model has become very efficient and robust for use in crash analyses.

PHENOMENA # 1: Plastic deformation of guardrail posts due to bending about weak axis			
Sprague-Geers Metrics List all the data channels to be compared below. Using RSVVP calculate the M and P metrics comparing the experiment and the simulation. Values less than or equal to 20 are acceptable.	M	P	Pass?
• <i>Force-Displacement</i>	3.6	1.1	Yes
ANOVA Metrics List all the data channels to compare in the rows below. Use RSVVP to calculate the ANOVA metrics and enter the values below. The following criteria must be met: <ul style="list-style-type: none"> The mean residual error must be less than or equal to five percent of the peak acceleration ($\bar{e} \leq 0.05 \cdot a_{Peak}$) The standard deviation of the residuals must be less than or equal to 25 percent of the peak acceleration ($\sigma \leq 0.25 \cdot a_{Peak}$) 	Mean Residual	Standard Deviation of Residuals	Pass?
• <i>Force-Displacement</i>	0.03	0.03	Yes
PHENOMENA <i>Three-Point Bend Test of W150x13.5 Post About Weak Axis</i>			

Figure 52. Example of a validation sheet from a roadside hardware PIRT.

The research team at WPI made several modifications to the model in order to improve its accuracy in simulating vehicle interaction with curbs, with particular emphasis on the suspension system.(83) A list of the modifications and the extent of verification, calibration, and validation of each component model is shown in Table 21. The development of a comprehensive PIRT for the vehicle model was not possible since the majority of information regarding model development is no longer available. In order to compute the quantitative comparison metrics, time-history data from both the physical test and simulation is needed. All validation assessments reported in Table 21 were based on qualitative comparison of test and simulation data, as

reported in the literature.(83) The vehicle PIRT for the C2500 pickup truck is shown in Appendix C8.

VALIDATION OF THE G4(1S) GUARDRAIL MODEL

Part I – Basic Information

The first step in the validation procedure is to document basic information about the test and simulation on the cover page and in Part I of the validation report as shown in Appendix C1. The full-scale crash test used for validation of the G4(1S) model was TTI test No. 405421-1, conducted by TTI on November 16, 1995.(143) The simulation was conducted by WPI in January 2002 with model No. TTI-405421-1_SIM-2002_01. The impact conditions for the simulation matched exactly those from the full-scale test (i.e., a 2000-kg pickup impacting the guardrail system at 101.5 km/hr at an angle of 25.5 degrees, at an impact point just upstream of post 12 in the guardrail system). These impact conditions correspond to NCHRP Report 350 test 3-11. The complete validation and verification report for this test case is shown in Appendix C1.

Table 21. Partial PIRT for the NCAC C2500R pickup truck. (83)

Phenomena	Summary	Valid?
Front suspension coil springs	Properties calibrated with physical test data	Calibration
Front suspension dampers	Properties verified with physical test data obtained from external source and calibrated with laboratory tests conducted at WPI	Calibration
Suspension stops on front A-arms	Response verified through visual observation of computer model results	Verification
Stabilizer bar	Response verified through visual observation of computer model results	Verification
Rear leaf spring suspension	Spring properties for vertical stiffness calibrated with physical test data. Lateral and torsional stiffness properties obtained analytically.	Calibration
Steering system properties	Properties calibrated with physical tests	Calibration
Steer stops on steering system	Response verified through visual observation of computer model results	Verification
Inertial Properties	Properties calibrated through data obtained from NHTSA and TTI	Calibration
Vertical front suspension response	Roll-off drop tests	Validation*
Vertical rear suspension response	Roll-off drop tests	Validation*
Front and rear suspension response	90-degree curb traversal tests – 6-inch AASHTO type B curb	Validation*
Front and rear suspension response and steer response	25-degree curb traversal tests – 6-inch AASHTO type B curb	Validation*

* *Qualitative assessment only*

A qualitative assessment of the response of the vehicle behavior in the full-scale test and numerical simulation was quite good as shown in Figure 53. The model results replicated the basic timing and phenomenological events that occurred in the full-scale test. Sequential views of TTI Test 405421-1 and the simulation are shown in Figure 53 from a downstream perspective. In the past, the analyst may have been satisfied with a comparison of views like those shown in Figure 53 but the objective of the procedures discussed in chapter 4 is to develop a much more quantitative procedure for assessing the validation.

Part II - Solution Verification

After documenting the basic information on the cover page and in Part I, the next step in the validation process is to perform global checks of the analysis to verify that the numerical solution is stable and is producing physical results (e.g., results conform to the basic laws of conservation). This analysis is modeled as a closed system, which means that energy is not being added or removed during the analysis. Consequently, the total energy should remain constant throughout the analysis and should be equal to the initial kinetic energy of the impacting vehicle. The one exception in this case is any kinetic energy generated due to the gravity load which should be minimal during the short time period of the crash event relative to the initial kinetic energy of the vehicle. There are, however, several opportunities for non-physical energy to be added during the analysis, resulting from numerical inaccuracies in element formulation, contact definitions, mass-scaling, etc. It is typical to expect some error in the analysis due to these deficiencies; however, it is the responsibility of the analyst to ensure that the errors are sufficiently small so that they have minimal effect on the solution. Table 22 shows a summary of the global verification assessment based on criteria recommended in the procedures for verification and validation discussed in Chapter 4. Figure 54 shows a plot of the global energy-time histories from the analysis.

As shown in Table 22, all the solution verification parameters were satisfied so the analyst can be reasonably sure that the solution represents a physically plausible impact event that obeys basic conservation laws. This is confirmed as well by Figure 54 which shows that the total energy remains fairly constant during the simulated event. The solution meets all the recommended global energy balance criteria and appears to be free of any major numerical problems. This does not indicate that the simulation is necessarily valid, only that the results adhere to the basic laws of physics and that the solution is numerically stable. The validation assessment for Step I was entered as “Yes” on the cover page of the validation report in Appendix C1.

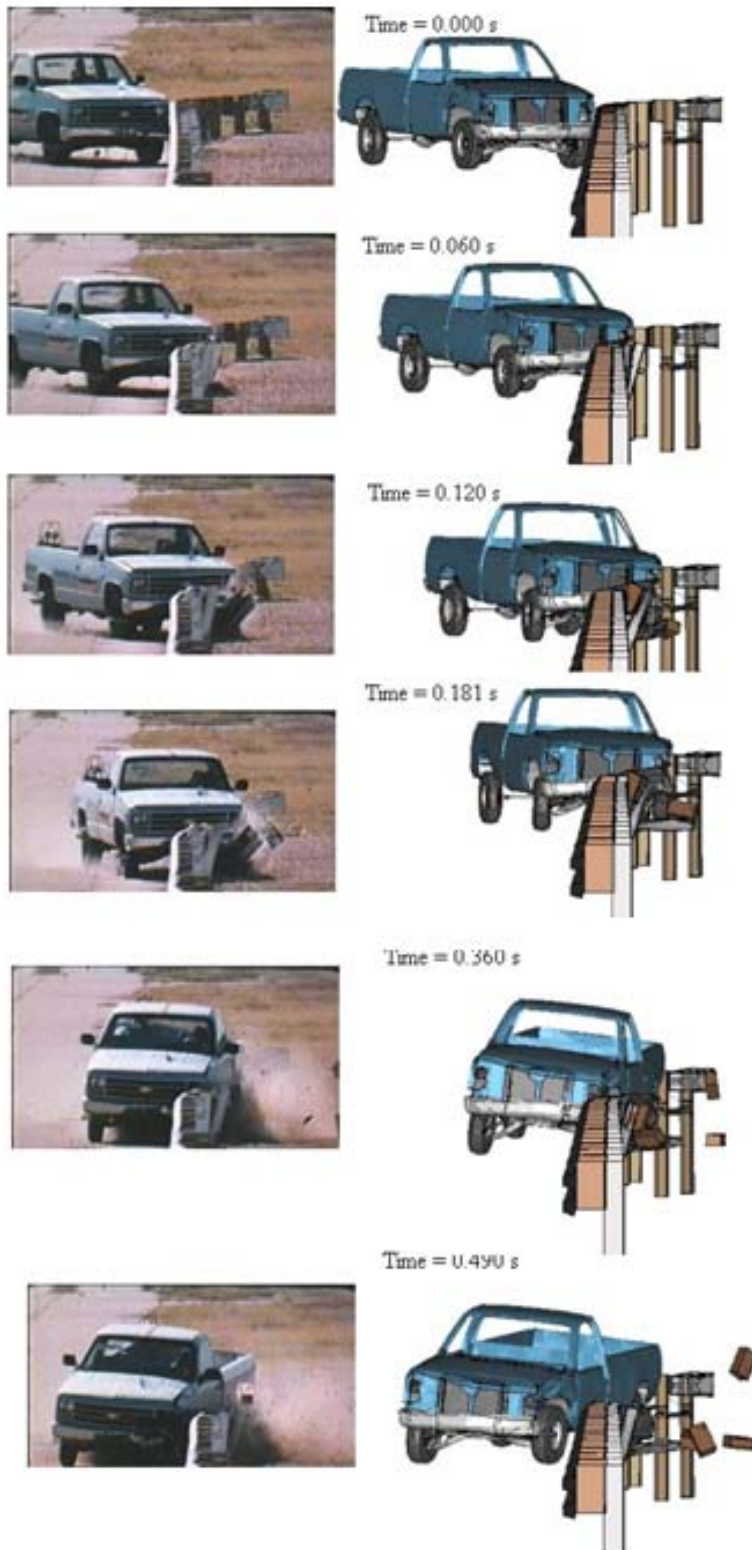


Figure 53. Sequential views of TTI Test 405421-1 and the finite element simulation from a downstream perspective, test case 1. (146)

Table 22. Analysis solution verification table for test case 1.

Verification Evaluation Criteria	Change (%)	Pass?
Total energy of the analysis solution (i.e., kinetic, potential, contact, etc.) must not vary more than 10 percent from the beginning of the run to the end of the run.	1.3	YES
Hourglass Energy of the analysis solution at the end of the run is less than <i>five percent</i> of the total <i>initial energy</i> at the <i>beginning</i> of the run.	0	YES
Hourglass Energy of the analysis solution at the end of the run is less than <i>ten percent</i> of the total <i>internal energy</i> at the <i>end</i> of the run.	0	YES
The part/material with the highest amount of hourglass energy at any time during the run is less than five percent of the total initial energy at the beginning of the run.	0	YES
Mass added to the total model is less than five percent of the total model mass at the beginning of the run.	0	YES
The part/material with the most mass added had less than 10 percent of its initial mass added.	0	Yes
The moving parts/materials in the model have less than five percent of mass added to the initial moving mass of the model.	0	Yes
There are shooting nodes in the solution?	No	Yes
There are solid elements with negative volumes?	No	Yes

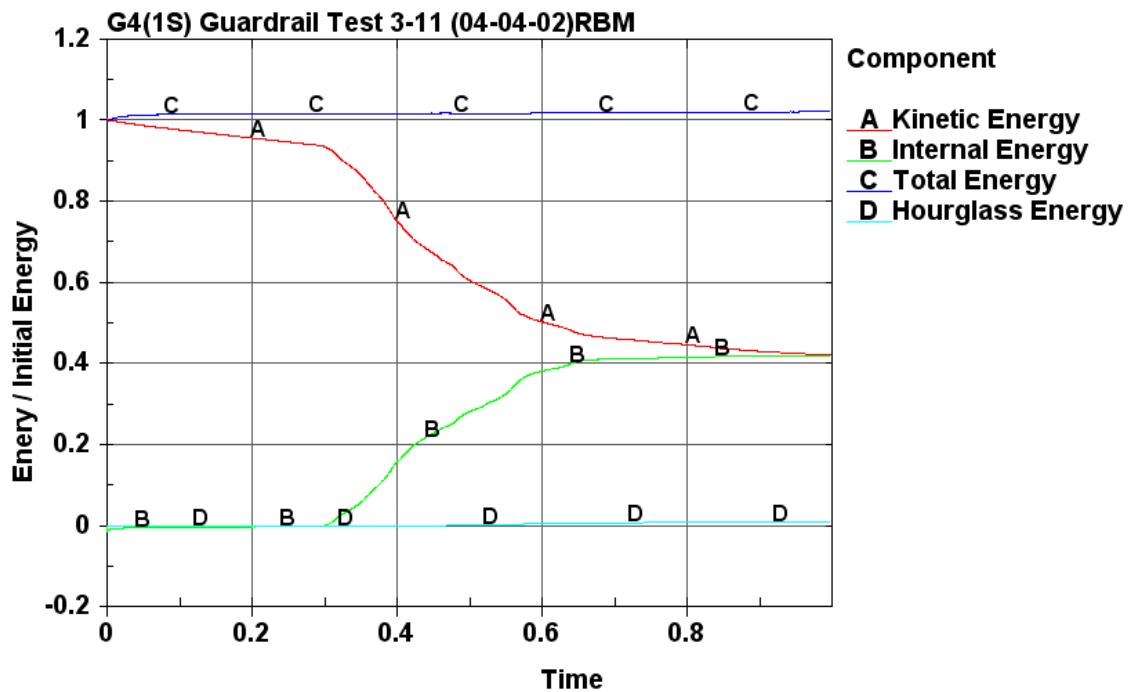


Figure 54. Plot of global energy-time histories for test case 1.

Part III - Quantitative Evaluation

Next, the RSVVP computer program was used to compute the Sprague-Geer metrics and ANOVA metrics using time-history data from the physical test (i.e., true curve) and analysis data (i.e., test curve). The multi-channel option in RSVVP was used since this option computes metrics for each individual channel as well as for the weighted composite of the combined channels. The data from each of the six data channels, which were located at the center of gravity of the vehicle, were input into RSVVP. These data included the x-acceleration, y-acceleration, z-acceleration, roll-rate, pitch-rate and yaw-rate. From Chapter 4, it was recommended that the raw data be used as input into the program; however, only pre-filtered data was available for this test case. The data was pre-filtered using a SAE class 180 filter. The data was then filtered in RSVVP using a CFC class 180 filter, which resulted in essentially no change to the curves. The shift and drift options in RSVVP were used for the physical test data (i.e., true curves) for the x-, y-, and z-channels, but not used for the roll-, pitch- and yaw-channels. From visual inspection, the physical test data appeared to show no initial offset of acceleration magnitude and experienced very little drift. Consequently, the shift and drift options had minimal effect on the shape of the curves, as illustrated in Figure 55 which shows the results of preprocessing of the x-channel data.

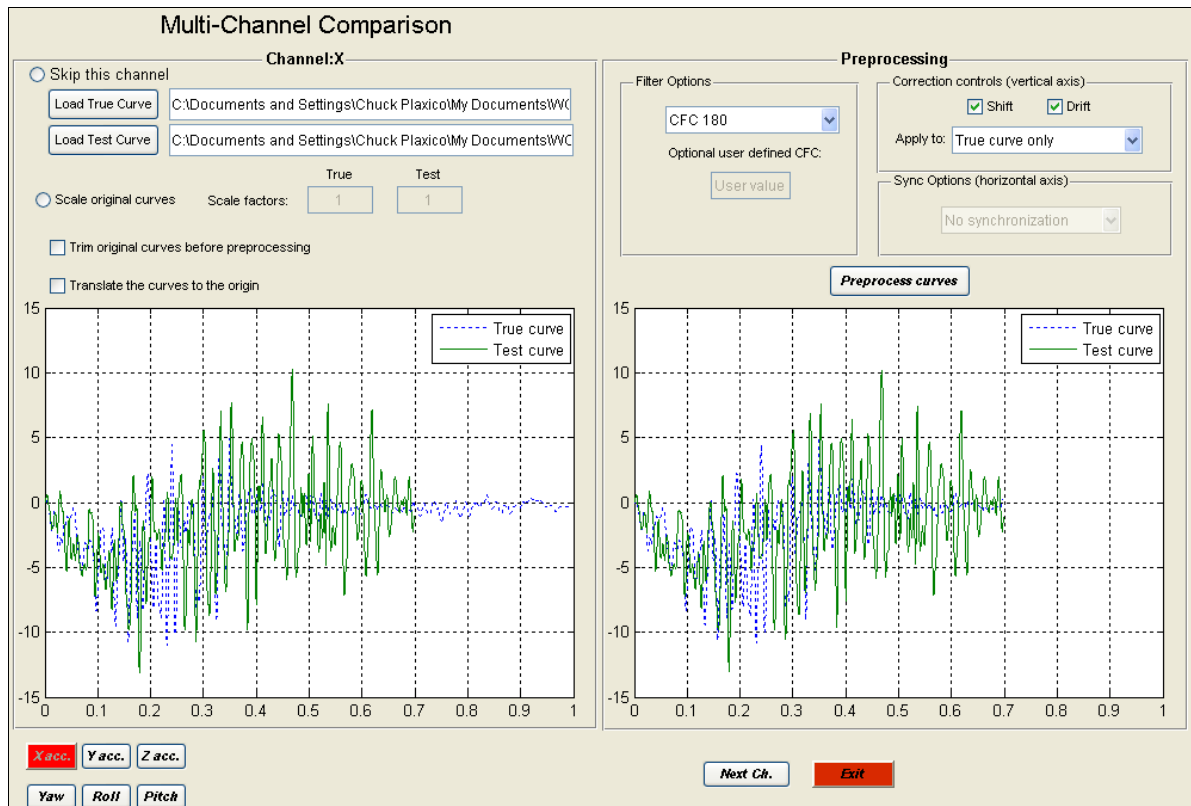


Figure 55. RSVVP preprocessing input and results for the x-channel data, test case 1.

Each of the curve pairs (i.e., true and test) were synchronized using the minimum absolute area of residuals option in RSVVP. For the metrics evaluation options in RSVVP, the default metrics were selected, which included the Sprague and Geers and the ANOVA metrics, as shown in Figure 56. The “Whole Time Window Only” option was also selected which directed RSVVP to evaluate the curves over the complete time history of available data, which in this case was 0.7 seconds.

Metric profile: NCHRP 22-24 (suggested) ▼

Metrics

MPC metrics

- Geers
- Geers CSA
- Sprague & Geers
- Russell
- Knowles & Gear

Single-value metrics

- Whang's inequality
- Theil's inequality
- Ziliacus error
- RSS error
- Weighted Integrated Factor
- Regression coefficient
- Correlation Coefficient
- Correlation Coefficient (NARD)

ANOVA metric

- Average & Stand. deviation

Time window

Whole time window only ▼

Figure 56. RSVVP metrics evaluation selection for test case 1

The results of the evaluation for the individual channels are shown in Table 23. Figure 57 through Figure 62 show the time histories for each pair of data that were used to compute the metrics. Based on the Sprague & Geers metrics, the x-, roll- and yaw-channels indicated that the numerical analysis was in agreement with the test, and that the y-, z-, and pitch-channels were not. The ANOVA metrics indicated that the simulation was in good agreement with the test for all channels except the pitch-channel.

Table 23. Roadside safety validation metrics rating table for test case 1 – (single channel option).

Evaluation Criteria							Time interval [0 sec; 0.7 sec]		
O Sprague-Geer Metrics List all the data channels being compared. Calculate the M and P metrics using RSVVP and enter the results. Values less than or equal to 40 are acceptable.									
	Filter Option	Sync. Option	Shift		Drift		M	P	Pass?
			True Curve	Test Curve	True Curve	Test Curve			
X acceleration	CFC 180	Min. area of Residuals	Y	N	Y	N	21.5	33.3	Y
Y acceleration	CFC 180	Min. area of Residuals	Y	N	Y	N	43.9	35.7	N
Z acceleration	CFC 180	Min. area of Residuals	Y	N	Y	N	21.1	43.0	N
Roll rate	CFC 180	Min. area of Residuals	N	N	N	N	35.3	32.7	Y
Pitch rate	CFC 180	Min. area of Residuals	N	N	N	N	13.3	48.0	N
Yaw rate	CFC 180	Min. area of Residuals	N	N	N	N	11.7	8.7	Y
P ANOVA Metrics List all the data channels being compared. Calculate the ANOVA metrics using RSVVP and enter the results. Both of the following criteria must be met: <ul style="list-style-type: none"> The mean residual error must be less than five percent of the peak acceleration ($\bar{e} \leq 0.05 \cdot a_{Peak}$) and The standard deviation of the residuals must be less than 35 percent of the peak acceleration ($\sigma \leq 0.35 \cdot a_{Peak}$) 									
							Mean Residual	Standard Deviation of Residuals	Pass?
X acceleration/Peak							0.02	0.34	Y
Y acceleration/Peak							0.05	0.27	Y
Z acceleration/Peak							0.02	0.32	Y
Roll rate							0.02	0.27	Y
Pitch rate							0.05	0.36	N
Yaw rate							0.04	0.12	Y

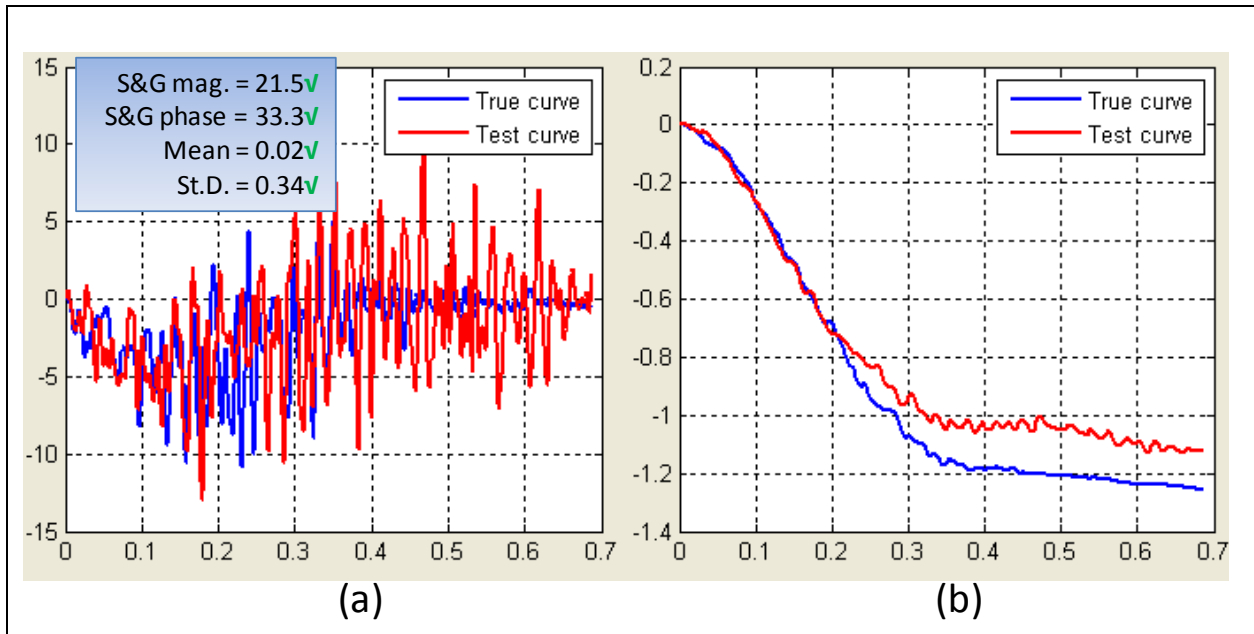


Figure 57. X-channel (a) acceleration-time history data used to compute metrics and (b) integration of acceleration-time history data, test case 1.

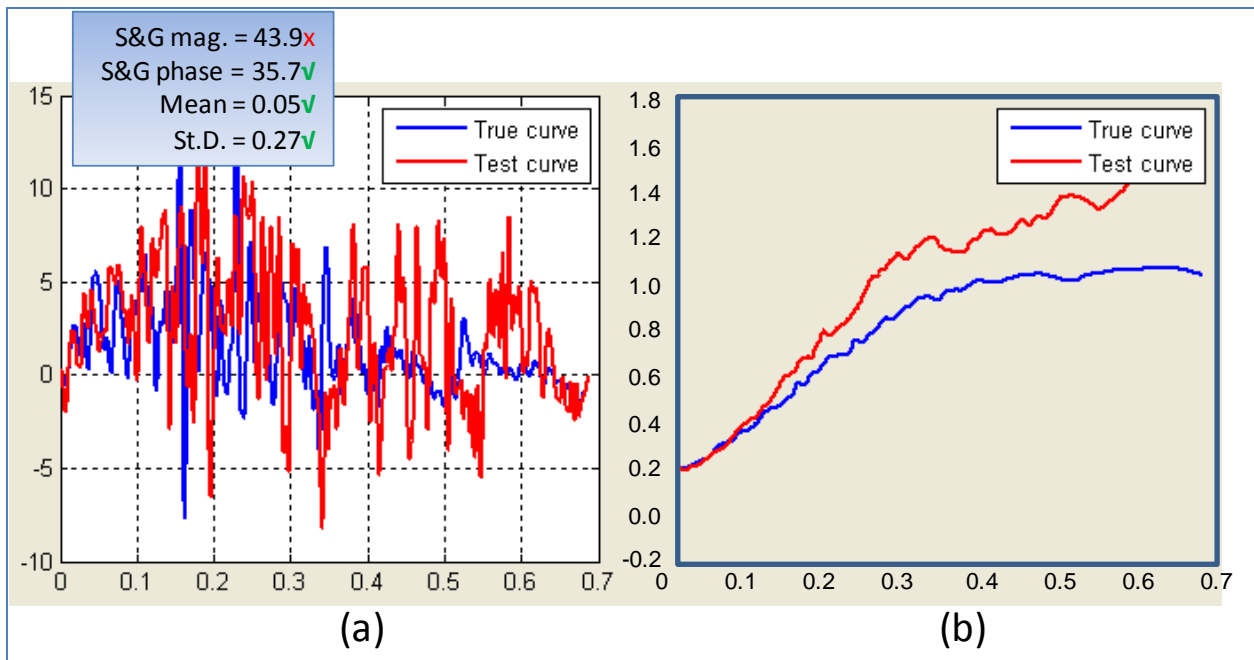


Figure 58. Y-channel (a) acceleration-time history data used to compute metrics and (b) integration of acceleration-time history data, test case 1.

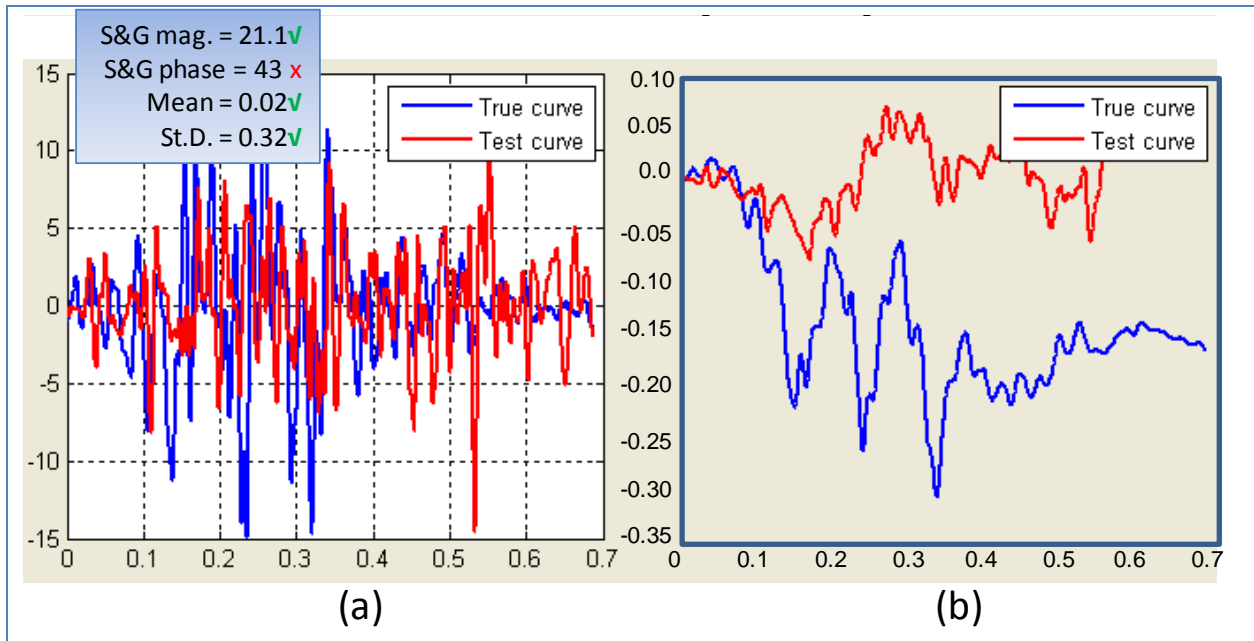


Figure 59. Z-Channel (a) acceleration-time history data used to compute metrics and (b) integration of acceleration-time history data, test case 1.

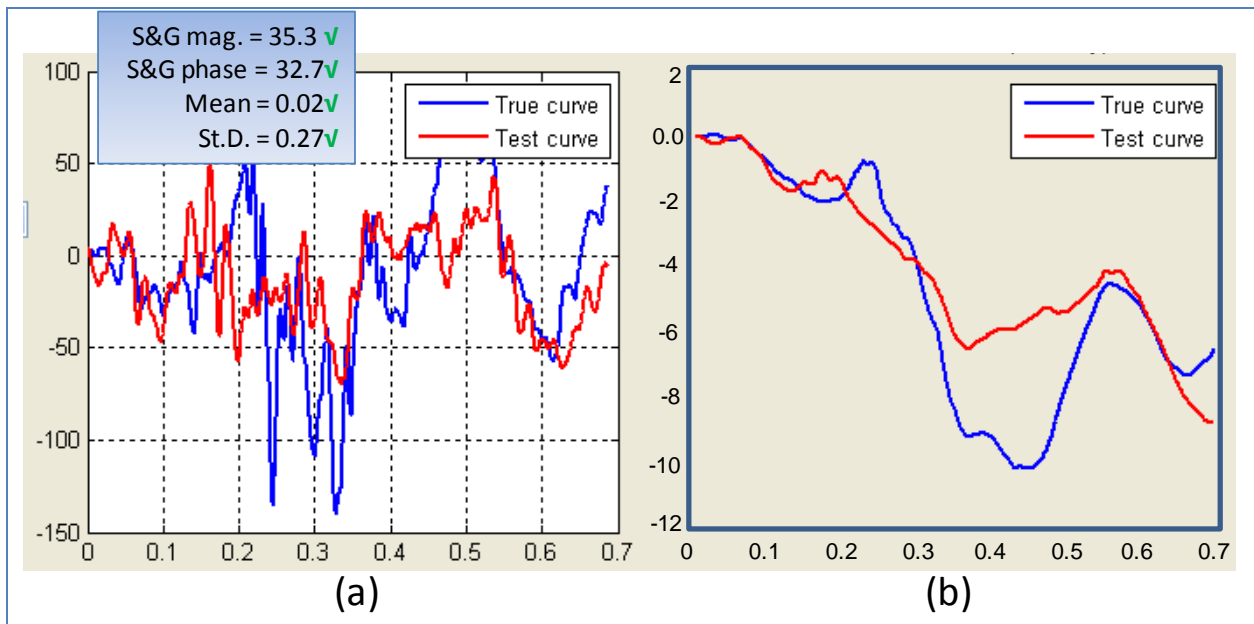


Figure 60. Roll-Channel (a) angular rate-time history data used to compute metrics and (b) integration of angular rate-time history data, test case 1.

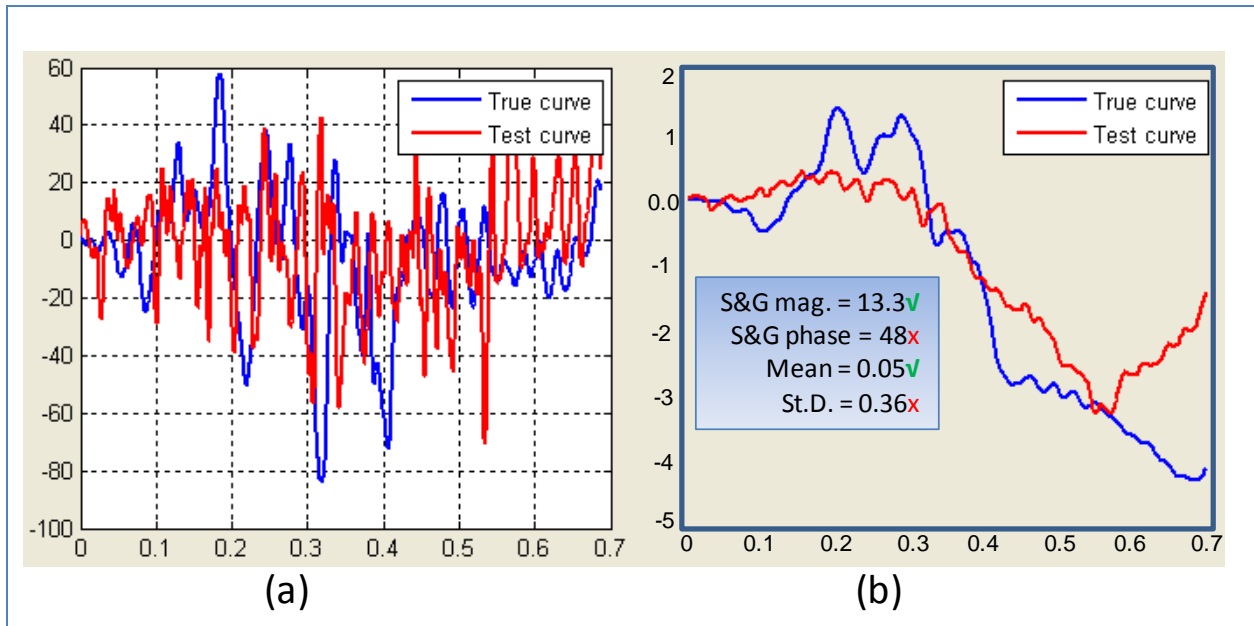


Figure 61. Pitch-Channel (a) angular rate-time history data used to compute metrics and (b) integration of angular rate-time history data, test case 1.

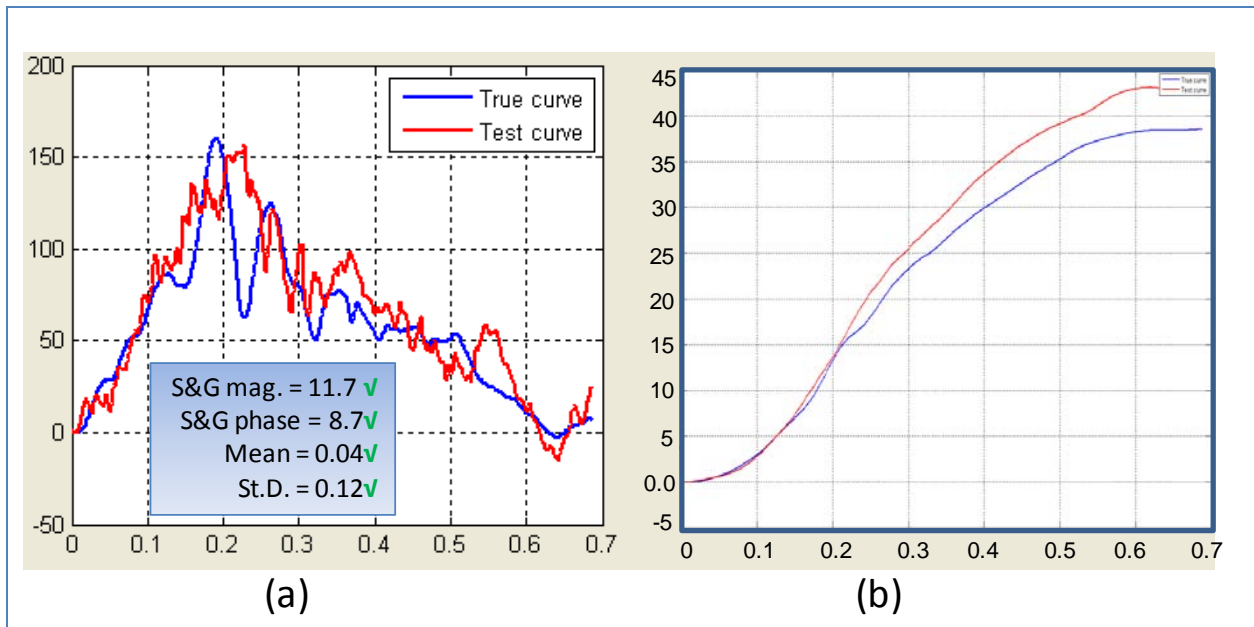


Figure 62. Yaw-Channel (a) angular rate-time history data used to compute metrics and (b) integration of angular rate-time history data, test case 1.

Since the metrics computed for the individual data channels did not all satisfy the acceptance criteria, the multi-channel option in RSVVP was used to calculate the weighted Sprague-Geer and ANOVA metrics for the six channels of data. Two weighting methods were used in the multi-channel evaluation: (1) the Area II method and (2) the inertia method.

The Area II method is the default method used in RSVVP. The Area (II) method determines the *weight* for each channel based on a pseudo momentum approach using the area under the curves. The Inertia method, on the other hand, determines the *weight* for each channel by computing the actual linear and rotational momentum from the six channels of data. The Inertia method provides the most accurate *weight* value for each channel but requires that the mass of the vehicle and the three angular inertia properties be input into RSVVP. As is typical especially for the rotary moments of inertia, the exact inertial properties for the test vehicle were not known. It is also important that the data from the six channels be collected at the center of gravity of the vehicle. The inertia properties that were input into the RSVVP program were obtained from the NHTSA website* for a 1991 Chevrolet 1500 Silverado, where:

- Mass = 1999 kg
- $I_{xx} = 705 \text{ kg}\cdot\text{m}^2$
- $I_{yy} = 4802 \text{ kg}\cdot\text{m}^2$
- $I_{zz} = 4924 \text{ kg}\cdot\text{m}^2$

Table 2 and Table 3 show the results from RSVVP for the multi-channel option using the Area (II) method and the Inertia method, respectively. The resulting weight factors computed for each channel are shown in both tabular form and graphical form in the tables. The results from both methods indicate that the x-, y-, and yaw rate-channels dominate the kinematics of the impact event. A visual assessment of the magnitudes of the integrated acceleration-time history curves for the x-, y-, and z-channels, show that the velocity change in the z-direction is insignificant compared to the change in velocity in the x- and y-directions. Similarly, visual inspection of the integrated angular-rate channels indicates that the yaw-channel is much more important than the roll- and pitch-channels.

*http://www.nhtsa.dot.gov/staticfiles/DOT/NHTSA/IRD/Multimedia/PDFs/VRTC/ca/nhtsa_inertia_database_metrics.pdf

Table 24. Roadside safety validation metrics rating table for test case 1 – (multi-channel option using Area II method).

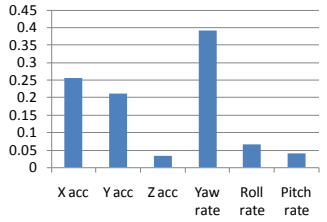
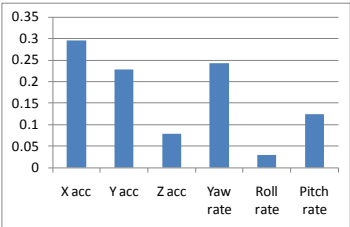
Evaluation Criteria (time interval [0 sec; 0.7 sec])			
Channels (Select which were used)			
<input checked="" type="checkbox"/> X Acceleration	<input checked="" type="checkbox"/> Y Acceleration	<input checked="" type="checkbox"/> Z Acceleration	
<input checked="" type="checkbox"/> Roll rate	<input checked="" type="checkbox"/> Pitch rate	<input checked="" type="checkbox"/> Yaw rate	
Multi-Channel Weights -Area (II) Method-	X Channel – 0.255116		
	Y Channel – 0.210572		
	Z Channel – 0.034312		
	Yaw Channel – 0.392648		
	Roll Channel – 0.06581		
	Pitch Channel – 0.041542		
O	Sprague-Geer Metrics Values less or equal to 40 are acceptable.	M	P
		22.9	25
P	ANOVA Metrics Both of the following criteria must be met: <ul style="list-style-type: none"> The mean residual error must be less than five percent of the peak acceleration ($\bar{e} \leq 0.05 \cdot a_{peak}$) The standard deviation of the residuals must be less than 35 percent of the peak acceleration ($\sigma \leq 0.35 \cdot a_{peak}$) 	Mean Residual	Standard Deviation of Residuals
		0.03	0.24
		Pass?	Pass?
		Y	Y

Table 25. Roadside safety validation metrics rating table for test case 1– (multi-channel option using Inertia method).

Evaluation Criteria (time interval [0 sec; 0.7 sec])				
Channels (Select which were used)				
<input checked="" type="checkbox"/> X Acceleration	<input checked="" type="checkbox"/> Y Acceleration	<input checked="" type="checkbox"/> Z Acceleration		
<input checked="" type="checkbox"/> Roll rate	<input checked="" type="checkbox"/> Pitch rate	<input checked="" type="checkbox"/> Yaw rate		
Multi-Channel Weights -Inertia Method-	X Channel – 0.296345 Y Channel – 0.227346 Z Channel – 0.079612 Yaw Channel – 0.242396 Roll Channel – 0.030312 Pitch Channel – 0.123988			
	Multi-Channel Weights -Inertia Method-			
O	Sprague-Geer Metrics Values less or equal to 40 are acceptable.	M	P	Pass?
		23.6	30.4	Y
P	ANOVA Metrics Both of the following criteria must be met: <ul style="list-style-type: none"> The mean residual error must be less than five percent of the peak acceleration ($\bar{e} \leq 0.05 \cdot a_{peak}$) The standard deviation of the residuals must be less than 35 percent of the peak acceleration ($\sigma \leq 0.35 \cdot a_{peak}$) 	Mean Residual	Standard Deviation of Residuals	Pass?
		0.04	0.27	Y

The two methods do not result in the exact same weights for each channel, as shown graphically in Figure 63 although they are similar, especially considering that the inertial properties are not known exactly. Given that the inertial properties are not always known for the test vehicles, the Area (II) method appears to provide acceptable values for the weight factors in this case and should for most typical cases. The value for the Sprague and Geers Magnitude was 22.9 for the Area II method compared to 23.6 for the Inertia method. The value for the Sprague and Geers Phase was 25 for the Area II method compared to 30.4 for the Inertia method. The value for the mean residual error was 0.03 for the Area II method compared to 0.4 for the Inertia method. The value for the standard deviation of residual errors was 0.24 for the Area II method compared to 0.27 for the Inertia method. In general, unless the actual inertial properties are known from the crash test, the Area (II) method should be used.

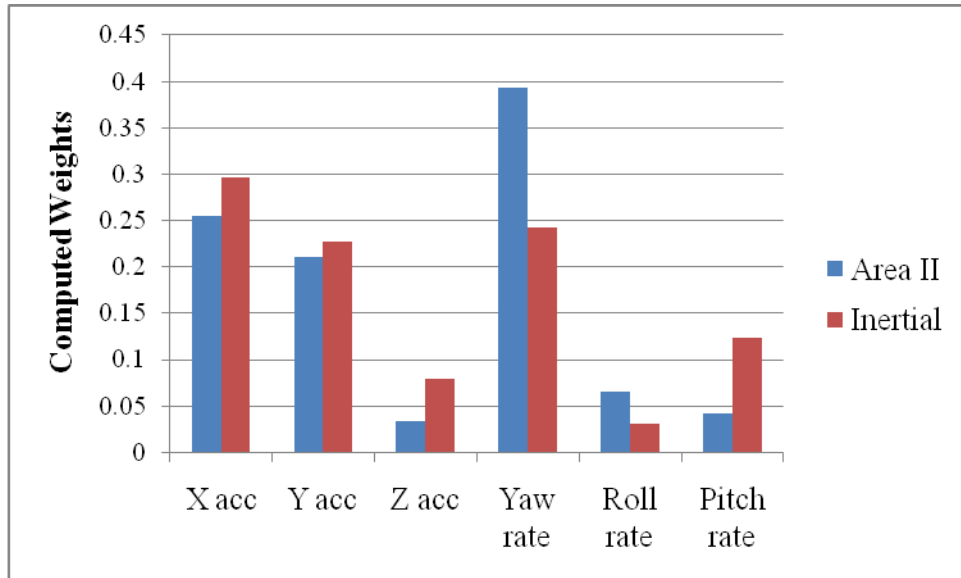


Figure 63. Comparison of multi-channel weight values computed using the Area II and the Inertia methods, test case 1.

The weighted metrics computed in RSVVP using both the Area II and the Inertia methods in the multi-channel mode all satisfy the acceptance criteria, and therefore the time history comparison can be considered acceptable. The validation assessment for Part II should be entered as “Yes” on the cover page of the validation report.

Part IV - Validation of Crash Specific Phenomena

The last step in the validation procedure is to compare the phenomena observed in both the crash test and the numerical solution. Table 26 contains the Report 350 crash test criteria with the applicable test numbers. The criteria that apply to test 3-11 (i.e., corresponding to this particular test case) are marked with a red square. These include criteria A, D, F, L and M.

Table 27 through Table 29 contain an expanded list of these same criteria including additional specific phenomena that were measured in the test and that could be directly compared to the numerical solution. Table 27 contains a comparison of phenomena related to structural adequacy, Table 28 contains a comparison of phenomena related to occupant risk, and Table 29 contains a comparison of phenomena related to vehicle trajectory.

Table 26. Evaluation criteria test applicability table for test case 1.

Evaluation Factors	Evaluation Criteria			Applicable Tests	
Structural Adequacy	A	Test article should contain and redirect the vehicle; the vehicle should not penetrate, under-ride, or override the installation although controlled lateral deflection of the test article is acceptable.		10, 11, 12, 20, 21, 22, 35, 36, 37, 38	
	B	The test article should readily activate in a predictable manner by breaking away, fracturing or yielding.		60, 61, 70, 71, 80, 81	
	C	Acceptable test article performance may be by redirection, controlled penetration or controlled stopping of the vehicle.		30, 31,, 32, 33, 34, 39, 40, 41, 42, 43, 44, 50, 51, 52, 53	
Occupant Risk	D	Detached elements, fragments or other debris from the test article should not penetrate or show potential for penetrating the occupant compartment, or present an undue hazard to other traffic, pedestrians or personnel in a work zone.		All	
	E	Detached elements, fragments or other debris from the test article, or vehicular damage should not block the driver's vision or otherwise cause the driver to lose control of the vehicle. (Answer Yes or No)		70, 71	
	F	The vehicle should remain upright during and after the collision although moderate roll, pitching and yawing are acceptable.		All except those listed in criterion G	
	G	It is preferable, although not essential, that the vehicle remain upright during and after collision.		12, 22 (for test level 1 – 30, 31, 32, 33, 34, 35, 36, 37, 38, 39, 40, 41, 42, 43, 44)	
	H	Occupant impact velocities should satisfy the following:			10, 20, 30,31, 32, 33, 34, 36, 40, 41, 42, 43, 50, 51, 52, 53, 80, 81
		Occupant Impact Velocity Limits (m/s)			
		Component	Preferred	Maximum	
Longitudinal and Lateral	9	12			
Longitudinal	3	5	60, 61, 70, 71		
I	Occupant ridedown accelerations should satisfy the following:			10, 20, 30,31, 32, 33, 34, 36, 40, 41, 42, 43, 50, 51, 52, 53, 60, 61, 70, 71, 80, 81	
	Occupant Ridedown Acceleration Limits (g's)				
	Component	Preferred	Maximum		
Longitudinal and Lateral	15	20			
L	The occupant impact velocity in the longitudinal direction should not exceed 40 ft/sec and the occupant ride-down acceleration in the longitudinal direction should not exceed 20 G's.		11,21, 35, 37, 38, 39		
Vehicle Trajectory	M	The exit angle from the test article preferable should be less than 60 percent of test impact angle, measured at the time of vehicle loss of contact with test device.		10, 11, 12, 20, 21, 22, 35, 36, 37, 38, 39	
	N	Vehicle trajectory behind the test article is acceptable.		30, 31, 32, 33, 34, 39, 42, 43, 44, 60, 61, 70, 71, 80, 81	

Note: The squares around the letters indicate the criteria that are applicable to this case.

Table 27. Structural adequacy phenomena for test case 1.

		Evaluation Criteria	Known Result	Analysis Result	Difference Relative/ Absolute	Agree?	
Structural Adequacy	A	A1	Test article should contain and redirect the vehicle; the vehicle should not penetrate, under-ride, or override the installation although controlled lateral deflection of the test article is acceptable. (Answer Yes or No)	Yes	Yes	X	YES
		A2	Maximum dynamic deflection: - Relative difference is less than 20 percent or - Absolute difference is less than 0.15 m	1.0 m	0.985m	1.5% 0.02 m	YES
		A3	Length of vehicle-barrier contact: - Relative difference is less than 20 percent or - Absolute difference is less than 2 m	0.691 s	0.690 s	0.1%	YES
		A4	The relative difference in the number of broken or significantly bent posts is less than 20 percent.	3	3	0	YES
		A5	Did the rail element rupture or tear (Answer Yes or No)	No	No	X	YES
		A6	Were there failures of connector elements (Answer Yes or No).	Yes	Yes	X	YES
		A7	Was there significant snagging between the vehicle wheels and barrier elements (Answer Yes or No).	Yes	Yes	X	YES
		A8	Was there significant snagging between vehicle body components and barrier elements (Answer Yes or No).	No	No	X	YES

Table 28. Occupant risk phenomena for test case 1.

Evaluation Criteria		Known Result	Analysis Result	Difference Relative/ Absolute	Agree?		
Occupant Risk	D	Detached elements, fragments or other debris from the test article should not penetrate or show potential for penetrating the occupant compartment, or present an undue hazard to other traffic, pedestrians or personnel in a work zone. (Answer Yes or No)	Pass	Pass		YES	
	F	F1	The vehicle should remain upright during and after the collision although moderate roll, pitching and yawing are acceptable. (Answer Yes or No)	Pass	Pass		YES
		F2	Maximum roll of the vehicle: - Relative difference is less than 20 percent or - Absolute difference is less than 5 degrees.	-8.7	-10.1	16% 1.4 deg	YES
		F3	Maximum pitch of the vehicle is: - Relative difference is less than 20 percent or - Absolute difference is less than 5 degrees.	-3.3	-4.3	30% 1.0 deg	YES
		F4	Maximum yaw of the vehicle is: - Relative difference is less than 20 percent or - Absolute difference is less than 5 degrees.	41	42.8	4% 1.8 deg	YES
	L		The occupant impact velocity in the longitudinal direction should not exceed 12 m/sec and the occupant ridedown acceleration in the longitudinal direction should not exceed 20 G's.				
		L1	• Longitudinal OIV (m/s)	5.4	4.7	13% 0.7m/s	YES
		L2	• Lateral OIV (m/s)	4.4	5.0	13.6% 0.6 m/s	YES
		L3	• THIV (m/s)	6.3	6.4	1.6% 0.1 m/s	YES
		L4	Occupant accelerations: - Relative difference is less than 20 percent or - Absolute difference is less than 4 g's.				
		L5	• Longitudinal ORA	7.9	8.9	12.7% 1.0 G	YES
		L6	• Lateral ORA	8.4	10.0	19.0% 1.6 G	YES
			• ASI	0.68	0.72	5.9% 0.04	YES

Table 29. Vehicle trajectory phenomena for test case 1.

		Evaluation Criteria	Known Result	Analysis Result	Difference Relative/Absolute	Agree?
Vehicle Trajectory		M1 The exit angle from the test article preferable should be less than 60 percent of test impact angle, measured at the time of vehicle loss of contact with test device.	15.5° 61%	17.3° 68%	X	YES
	M	M2 Exit angle at loss of contact: - Relative difference is less than 20 percent or - Absolute difference is less than 5 degrees.	15.5°	17.3°	11.6% 1.8 deg	YES
		M3 Exit velocity at loss of contact: - Relative difference is less than 20 percent or - Absolute difference is less than 5 degrees.	55 km/h	62 km/h	12.7% 7.0 km/hr	YES
		M4 One or more vehicle tires failed or de-beaded during the collision event (Answer Yes or No).	Yes	N.A.	X	

All the applicable criteria in Table 27 through Table 29 agree (i.e., the relative difference between the numerical solution and the test was less than 20%) except for the comparison of maximum pitch angle, which resulted in a relative difference of 30%. However, the magnitude of pitch was relatively small for both the test (i.e., 3.3 degrees) and the numerical solution (i.e., 4.3 degrees) compared to the other angular components, and therefore could be considered negligible. Recall that the weight factor computed for the pitch channel in RSVVP, as shown in Table 2, also indicated that the effects of pitch were of little significance in the crash event.

In general, as the magnitudes of the measured quantities get smaller and smaller, the use of the relative percent difference as a validation criterion may not be appropriate. For example, according to NCHRP Report 350 it is preferred that the occupant ridedown acceleration (ORA) remains below 12 G's and that it should not exceed 15 G's. If the ORA from the physical test was, for example, 1.0 G and the ORA from the numerical solution was 1.4 G, the absolute difference would be 40 percent. Whereas from a qualitative view point, based on crash test experience, there is essentially no difference between these two acceleration values. To account for this problem, the quantitative phenomena in Table 27 through Table 29 also include *absolute* acceptance criteria. For example, the criterion F3 in Table 28 requires that the maximum pitch in the simulation must either be within 30 percent of the true pitch in the crash test, or else the absolute difference between them must be less than 5 degrees.

The validation assessment for Part IV for Case 1 can be entered as “Yes” on the cover page of the validation report since all the phenomena agree. Since the model has been validated for each part of the validation procedure, it can now be considered valid for use in assessing the

effects of incremental modifications to the system. The comparison documented in the verification and validation report (i.e., Appendix C1) shows that the finite element model accurately replicates the results of the baseline crash test. The analyst and policy maker can have confidence that the model will produce good predictions for crashes that are reasonably similar to the baseline crash. The analyst could now use this model to explore incremental variations to the roadside hardware system represented by the baseline crash. For example, in this case, the analyst could use this model to explore slightly different guardrail heights, different blockout configurations, or the affect of curbs placed in front of the guardrail.

In fact, this particular model was used to explore the performance of a variety of curbs placed in front of the guardrail system as described in NCHRP Report 537. (141) The research team in NCHRP Report 537 used the model to parametrically vary the location of the curb (i.e., three different offset locations), the type and height of the curb (i.e., five different types) and the speed and angle of the pickup truck when it left the road (i.e., three angles and three speeds). Altogether, simulations of 33 different combinations were performed to determine the likely Report 350 performance of the curb-guardrail combinations. Clearly, running 33 finite element simulations was far less expensive than performing 33 full-scale crash tests but establishing the validity of the model was, therefore, very important.

In order to further validate the whole parametric range of the finite element simulations, seven full-scale crash tests were performed at critical points in the parameter space. A validation of one of those simulations with one of these crash tests is the subject of Case 2 presented in the next section.

TEST CASE 2: PICKUP TRUCK STRIKING A GUARDRAIL WITH A CURB

INTRODUCTION

The validated model of the G4(1S) described in Case I was used to assess the effects of installing various types of curbs in combination with the G4(1S) guardrail system. The objective of the study was to investigate the effects of curb type, curb placement and impact speed on the performance of the barrier system, regarding structural adequacy of the barrier, occupant risk (e.g., OIV, ORA, etc.) and vehicle trajectory.⁽¹⁴¹⁾ The results from the parametric study were subsequently confirmed by conducting full-scale tests on a subset of the curb-barrier combination scenarios. One of those tests involved the same impact conditions that were used in one of the numerical simulations; i.e., a 2000-kg pickup impacting a G4(1S) guardrail with a 6-inch AASHTO type B curb placed underneath the rail.⁽¹⁴⁵⁾ The finite element model is shown in Figure 64 which illustrates the placement of the curb relative to the barrier system. In the following sections, the results from the numerical solution are compared to the full-scale test using the validation procedures presented in Chapter 4.

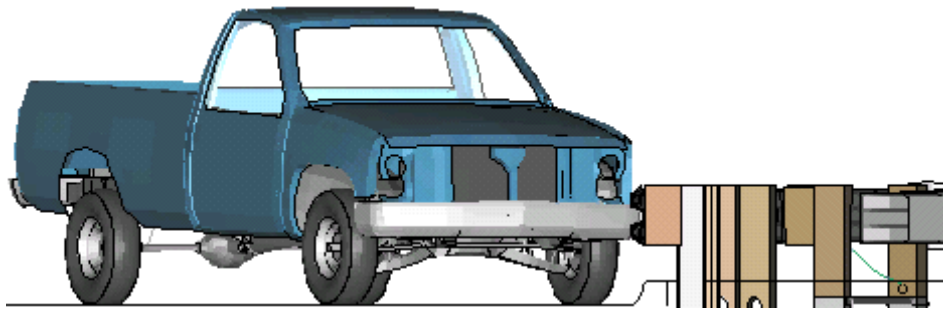


Figure 64. Finite element model for the analysis of the G4(1S) and AASHTO B curb. ⁽¹⁴⁶⁾

PIRT FOR THE CURB AND VEHICLE MODELS

The finite element models of the curbs were modeled with rigid material properties in the Worcester Polytechnic Institute (WPI) curb-guardrail combination study.⁽¹⁴¹⁾ It was assumed that the curb does not deform or suffer damage during “tracking” impacts with passenger vehicles. The curb dimensions were consistent with those specified for the 6-inch tall AASHTO type B curb.⁽¹⁴²⁾ Since there were no tests used to validate the accuracy of the curb model, the only information included in the PIRT was verification of the curb dimensions. The PIRT for the guardrail used in Case 1 and shown in Appendix C6 was also used for this case.

Similarly, the same vehicle model was used in Case 2 as in Case 1 so the same PIRT for the C2500 pickup truck shown in Appendix C8 applies to this case as well.

VALIDATION OF THE G4(1S) GUARDRAIL WITH CURB MODEL

The basic information about the test and simulation was documented on the Cover Page and in Part I of the validation report as shown in Appendix C2. The full-scale crash test, test No. 52-2556-001, was conducted by E-TECH Testing Services, Inc. on June 6, 2003.(141, 145, 146) The simulation was conducted by WPI in July 2002 with model No. B-0m-85-FEA_2002-0708 and is documented in NCHRP Report 537.(141) The impact conditions for the test were similar to those used in the numerical simulation. The test vehicle was a 1998 GMC 3/4 –ton pickup with a gross mass of 1,993-kg. The impact speed and angle of the test vehicle were 85.6 km/hr and 25 degrees, respectively. The impact point in the test was 0.6 m upstream of post 14. The simulation vehicle was the modified C2500R with a total mass of 2,000 kg. The impact conditions for the numerical simulation were 85 km/hr and 25 degrees. The impact point in the numerical simulation was 0.49 m upstream of post 14. A summary of the test and simulation information is provided in Table 30. Sequential views of the full-scale test and simulation are shown in Figure 65 from a downstream perspective and Figure 66 from an over-head view.

Table 30. Summary of the test and simulation impact conditions for Case 2.

General Information	Known Solution	Analysis Solution
Performing Organization	ETECH	WPI
Test/Run Number:	52-2556-001 (6/5/2003)	B-0m-85-FEA (7/8/2002)
Vehicle:	1998 GMC 3/4-ton	WPI modified (NCAC C2500R)
Impact Conditions		
Vehicle Mass:	1,993 kg	2,000 kg
Speed:	85.6 km/hr	85.0 km/hr
Angle:	25 degrees	25 degrees
Impact Point:	0.6 m upstream of post 14	0.49 m upstream of post 14

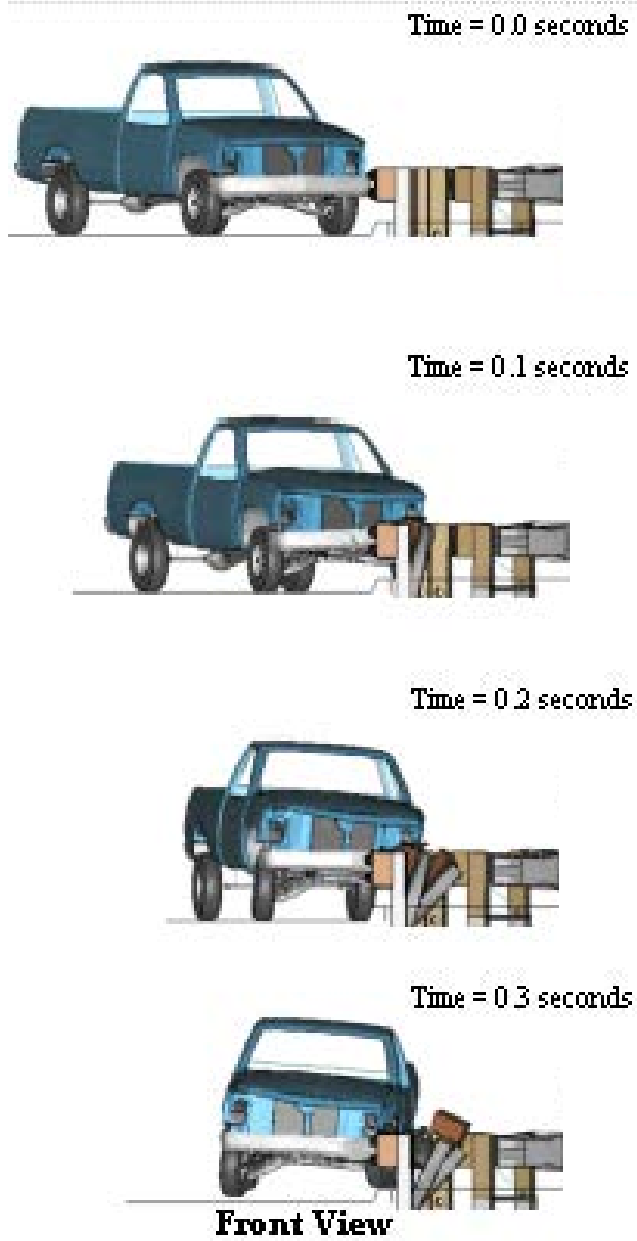


Figure 65. Sequential views from E-TECH test 52-2556-001 and simulation from a downstream perspective for Case 2.(146)

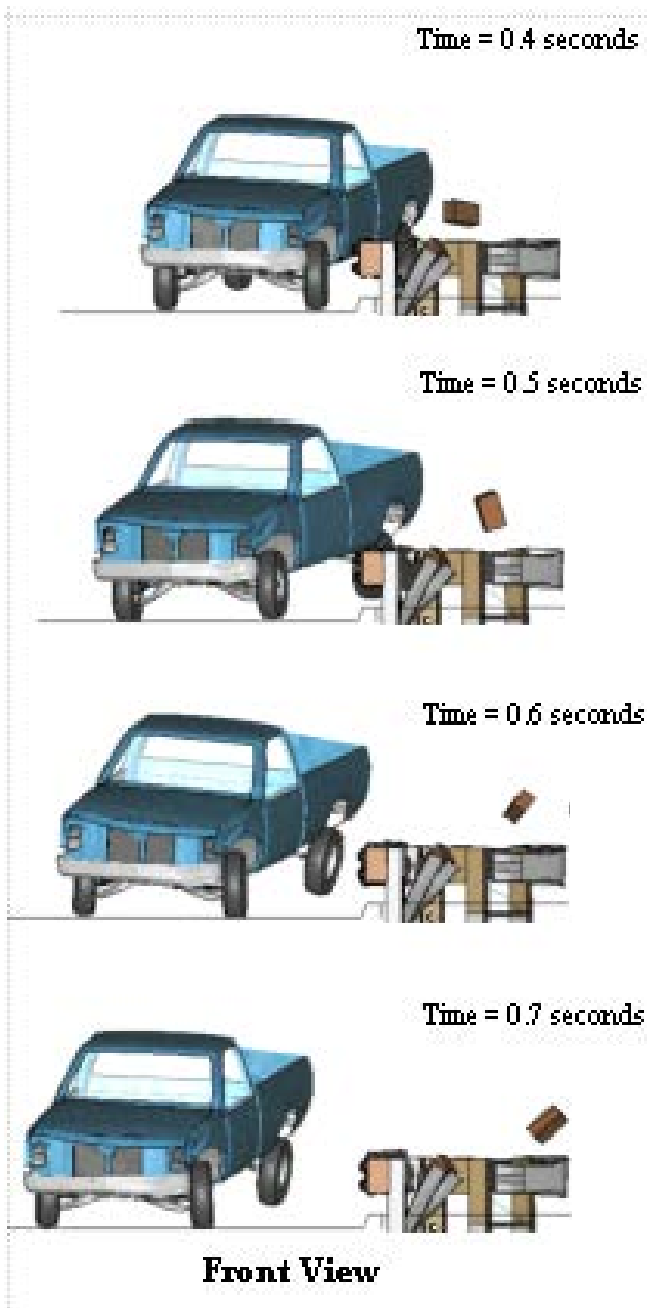


Figure 65. Sequential views from E-TECH test 52-2556-001 and simulation from a downstream perspective for Case 2. (continued).*(146)*

Time = 0.0 seconds



Time = 0.1 seconds



Time = 0.2 seconds



Time = 0.3 seconds



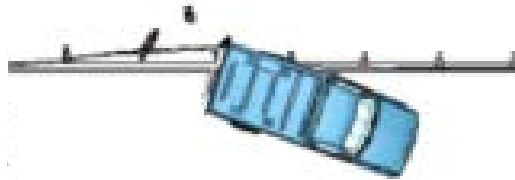
Top View

Figure 66. Sequential views from E-TECH test 52-2556-001 and simulation from an overhead perspective for Case 2.(146)

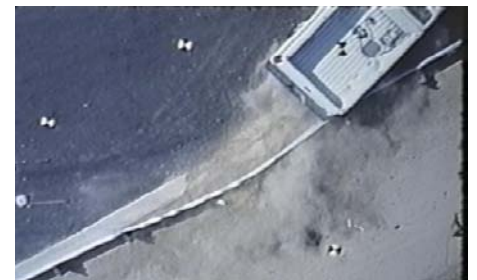
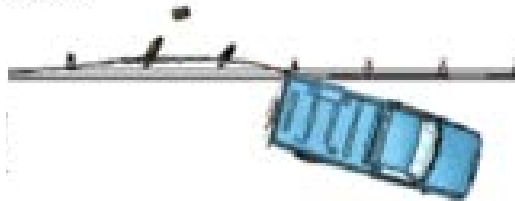
Time = 0.4 seconds



Time = 0.5 seconds



Time = 0.6 seconds



Time = 0.7 seconds



Top View

Figure 66. Sequential views from E-TECH test 52-2556-001 and simulation from an overhead perspective for Case 2. (continued).(146)

Part I - Solution Verification

The next step in the validation process is to perform global checks of the analysis to verify that the numerical solution is stable and is producing physical results. (e.g., results that conform to the basic laws of conservation). This analysis was modeled as a closed system so the total energy should remain constant throughout the analysis and should be equal to the initial

kinetic energy of the impacting vehicle. There are, however, several opportunities for non-physical energy to be added during the analysis, resulting from numerical inaccuracies in element formulation, contact definitions, mass-scaling, etc. It is typical to expect some error in the analysis due to numerical inaccuracies in element formulation, contact definitions, mass-scaling, etc.; however, it is necessary to ensure that the errors are sufficiently small so that they have minimal effect on the solution.

Table 31. Summary of Global Energy Checks for Case 2.

Verification Evaluation Criteria	Change (%)	Pass?
Total energy of the analysis solution (i.e., kinetic, potential, contact, etc.) must not vary more than 10 percent from the beginning of the run to the end of the run.	0.3	Yes
Hourglass Energy of the analysis solution at the end of the run is less than <i>five percent</i> of the total <i>initial energy</i> at the <i>beginning</i> of the run.	2.1	Yes
Hourglass Energy of the analysis solution at the end of the run is less than <i>ten percent</i> of the total <i>internal energy</i> at the <i>end</i> of the run.	5.5	Yes
The part/material with the highest amount of hourglass energy at any time during the run is less than five percent of the total initial energy at the beginning of the run.	0.8	Yes
Mass added to the total model is less than five percent of the total model mass at the beginning of the run.	3.4e-4	Yes
The part/material with the most mass added had less than 10 percent of its initial mass added.	0.3	Yes
The moving parts/materials in the model have less than five percent of mass added to the initial moving mass of the model.	0.006	Yes
There are shooting nodes in the solution?	No	Yes
There are solid elements with negative volumes?	No	Yes

The solution meets all the recommended global energy balance criteria and appears to be free of any major numerical problems. The validation assessment for Part I should be entered as “Yes” on the cover page of the validation report.

Part II - Quantitative Evaluation

Next, the RSVVP computer program was used to compute the Sprague-Geers metrics and ANOVA metrics using time-history data from the known (i.e., physical test) and analysis data. The multi-channel option in RSVVP was used since this option computes metrics for each individual channel as well as for the weighted composite of the combined channels. The raw data from each of the six data channels collected at the center of gravity of the vehicle were input into RSVVP. These data included the x-acceleration, y-acceleration, z-acceleration, roll-rate, pitch-rate and yaw-rate. The data was then filtered in RSVVP using a CFC class 180 filter. The *shift* and *drift* options in RSVVP were used for the *true curves* (i.e., physical test data) for the x-, y-,

and z-channels, but not used for the roll-, pitch- and yaw-channels. In general, numerical solutions are not subject to shift and drift since these are sensor (e.g., accelerometer) phenomena.

Each of the curve pairs were synchronized using the *minimum absolute area of residuals* option in RSVVP. For the metrics evaluation options in RSVVP, the default metrics were selected, which included the Sprague and Geers and the ANOVA metrics. The *Whole Time Window Only* option was also selected which directed RSVVP to evaluate the curves over the complete time history of available data, which in this case was 1.22 seconds.

The results of the evaluation for the individual channels are shown in Table 32. Figures 67 through 72 show the time histories for each pair of data that were used to compute the metrics. Based on the Sprague & Geers metrics, the pitch- and the yaw-channels from the numerical analysis were in agreement with the test, with the metrics for the x- and y-channels falling just outside the acceptable values. The z-channel and the roll-channel were not in good agreement. The ANOVA metrics indicated that the simulation was in good agreement with the test for all channels except the roll- and pitch-channels.

The x-, y-, and yaw rate-channels dominate the kinematics of the impact event, which can be verified by simple inspection of the integrated time-history traces. A visual assessment of the magnitudes of the integrated acceleration-time history curves for the x-, y-, and z-channels, indicate that the velocity change in the z-direction is insignificant compared to the change in velocity in the x- and y-directions. Similarly, visual inspection of the integrated angular-rate channels indicates that the yaw-channel is much more important than the roll- and pitch-channels.

Since the metrics computed for the individual data channels did not all satisfy the acceptance criteria, the multi-channel option in RSVVP was used to calculate the weighted Sprague-Geers and ANOVA metrics for the six channels of data. Two weighting methods were used in the multi-channel evaluation: 1) Area II method (default method) and 2) Inertial method. The Inertial method, as discussed previously in Test Case 1 and in Chapter 4, provides the most accurate *weight* value for each channel but requires that the mass of the vehicle and the three angular inertial properties be input into RSVVP. The inertial properties used in the multi-channel evaluation were the same as the properties used in Test Case 1 (see Test Case 1 for more details).

Table 32. Roadside safety validation metrics rating table for Case 2– (single channel option).

Evaluation Criteria							Time interval [0 sec; 1.22 sec]						
O	Sprague-Geer Metrics List all the data channels being compared. Calculate the M and P metrics using RSVVP and enter the results. Values less than or equal to 40 are acceptable.												
	Filter Option	Sync. Option	Shift		Drift		M	P	Pass?				
			True Curve	Test Curve	True Curve	Test Curve							
	X acceleration	CFC 180	Min. area of Residuals	Y	N	Y	N	1.2	41.6	N			
	Y acceleration	CFC 180	Min. area of Residuals	Y	N	Y	N	5.7	43.1	N			
	Z acceleration	CFC 180	Min. area of Residuals	Y	N	Y	N	0.5	48.6	N			
	Roll rate	CFC 180	Min. area of Residuals	N	N	N	N	1.5	44.5	N			
	Pitch rate	CFC 180	Min. area of Residuals	N	N	N	N	9.7	25.2	Y			
Yaw rate	CFC 180	Min. area of Residuals	N	N	N	N	9.6	10.4	Y				
P	ANOVA Metrics List all the data channels being compared. Calculate the ANOVA metrics using RSVVP and enter the results. Both of the following criteria must be met: <ul style="list-style-type: none"> The mean residual error must be less than five percent of the peak acceleration ($\bar{e} \leq 0.05 \cdot a_{Peak}$) and The standard deviation of the residuals must be less than 35 percent of the peak acceleration ($\sigma \leq 0.35 \cdot a_{Peak}$) 							Mean Residual	Standard Deviation of Residuals	Pass?			
	X acceleration/Peak										0.00	0.17	Y
	Y acceleration/Peak										0.02	0.17	Y
	Z acceleration/Peak										0.01	0.23	Y
	Roll rate										0.02	0.51	N
	Pitch rate										0.07	0.36	N
	Yaw rate										0.06	0.14	Y

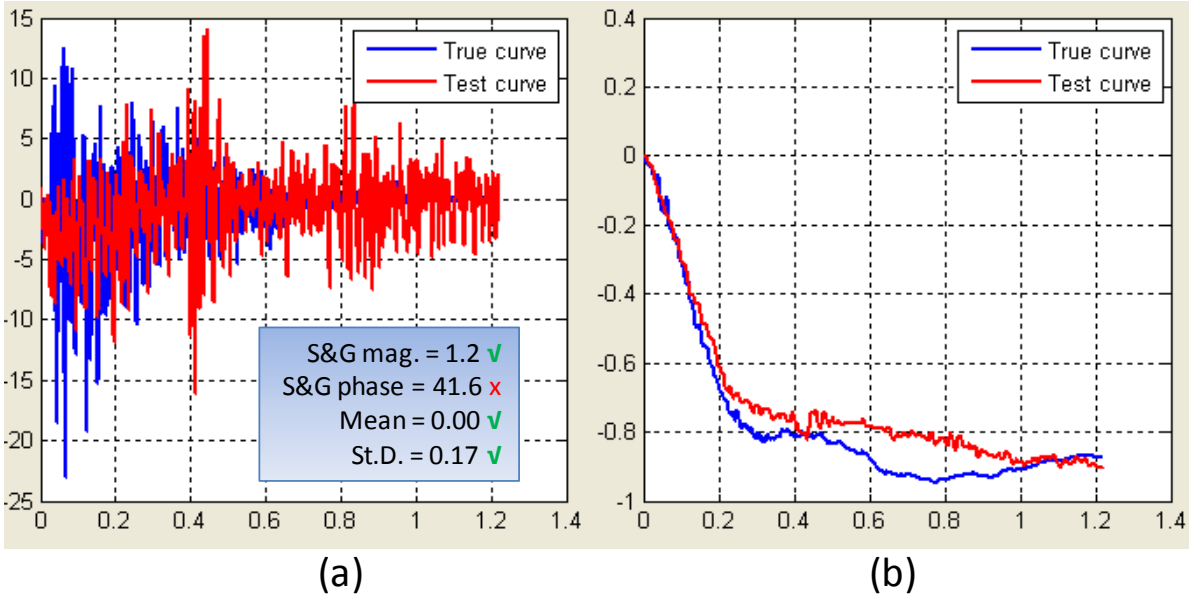


Figure 67. X-channel (a) acceleration-time history data used to compute metrics and (b) integration of acceleration-time history data for Case 2.

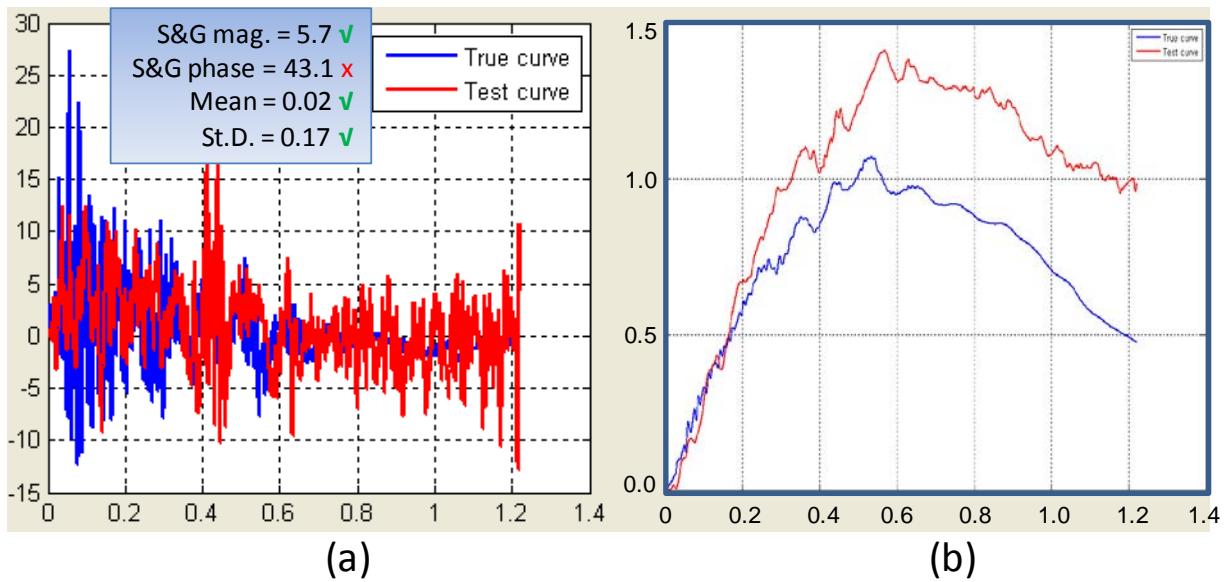


Figure 68. Y-channel (a) acceleration-time history data used to compute metrics and (b) integration of acceleration-time history data for Case 2.

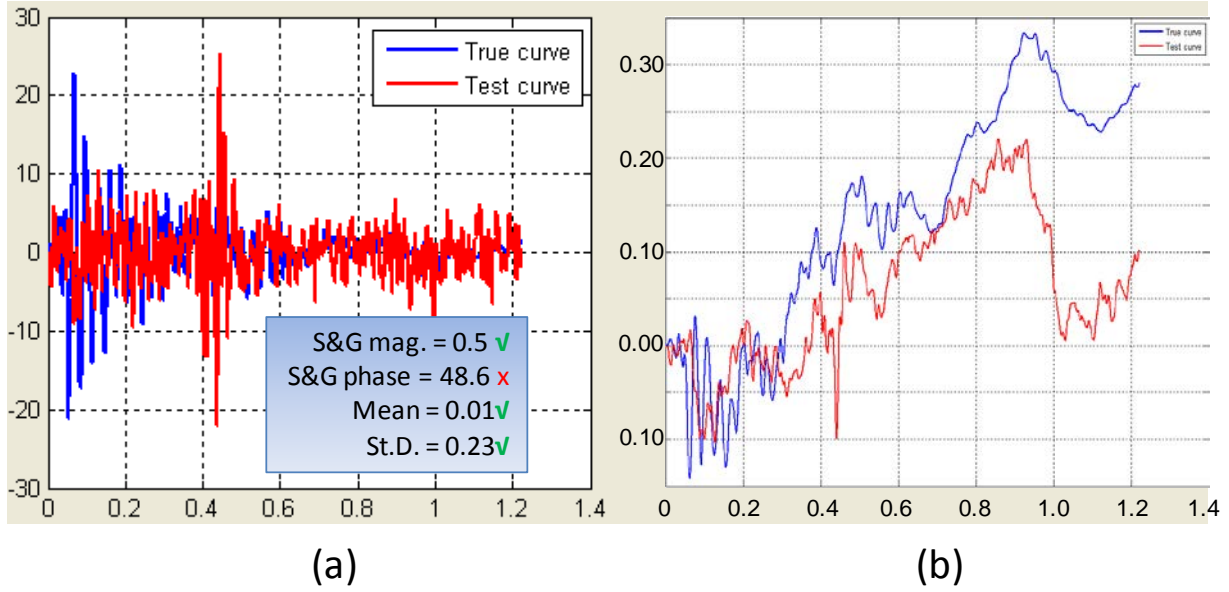


Figure 69. Z-Channel (a) acceleration-time history data used to compute metrics and (b) integration of acceleration-time history data for Case 2.

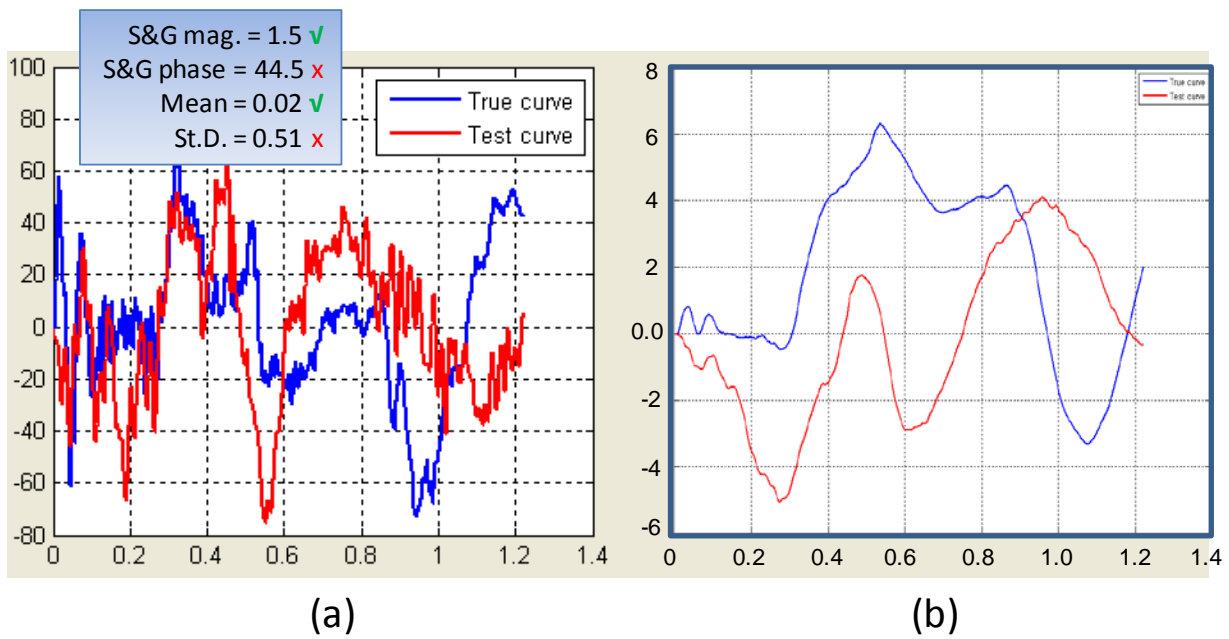


Figure 70. Roll-Channel (a) angular rate-time history data used to compute metrics and (b) integration of angular rate-time history data for Case 2.

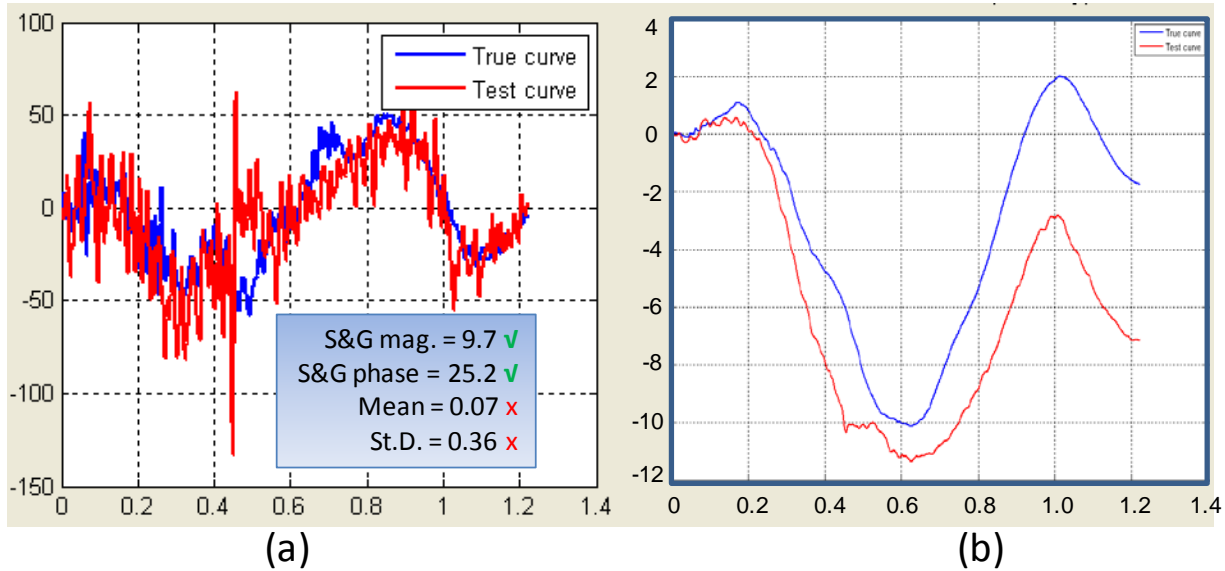


Figure 71. Pitch-Channel (a) angular rate-time history data used to compute metrics and (b) integration of angular rate-time history data for Case 2.

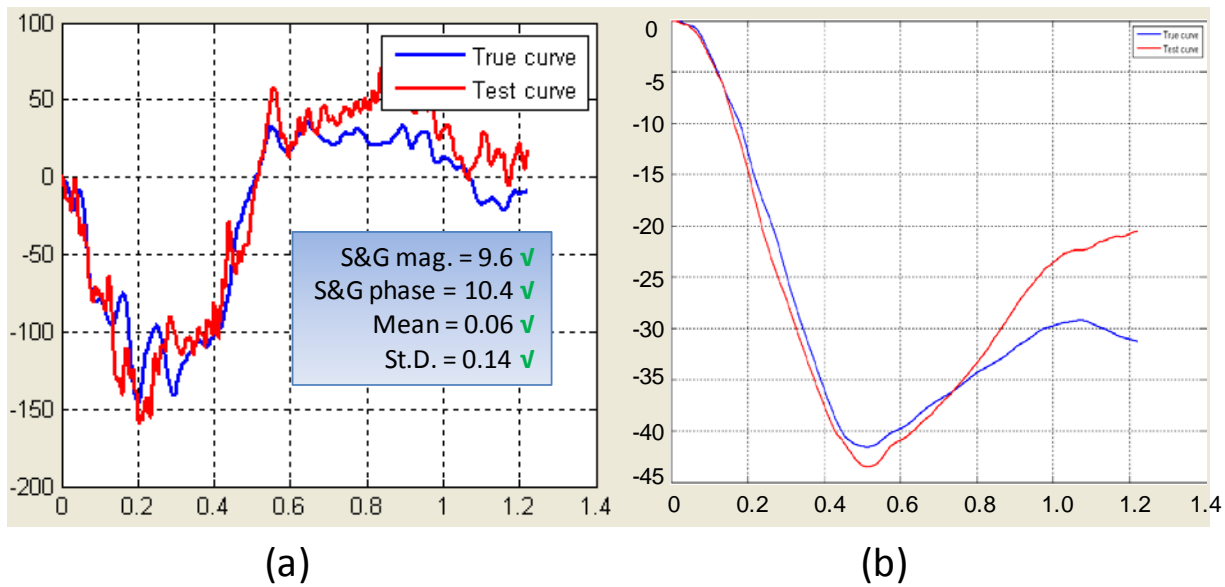
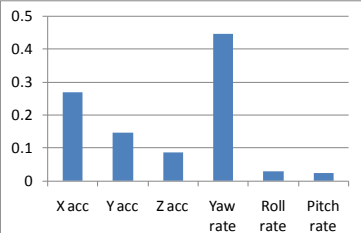


Figure 72. Yaw-Channel (a) angular rate-time history data used to compute metrics and (b) integration of angular rate-time history data for Case 2.

Table 33 and Table 34 show the results from RSVVP for the multi-channel option using the Area (II) method and the Inertial method, respectively. The resulting weight factors computed for each channel are shown in both tabular form and graphical form in the tables. The two methods disagree considerably on the weight given to the x-channel and the pitch-channel, however, all other weight factors are very similar for both methods, as shown in Figure 73, the end results, as shown in Table 33 and Table 34, agree that the comparison is adequate.

Table 33. Roadside safety validation metrics rating table for Case 2 – (multi-channel option using Area II method).

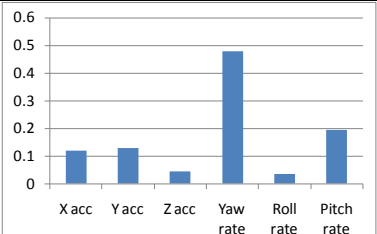
Evaluation Criteria (time interval [0 sec; 1.22 sec])			
Channels (Select which was used)			
<input checked="" type="checkbox"/> X Acceleration	<input checked="" type="checkbox"/> Y Acceleration	<input checked="" type="checkbox"/> Z Acceleration	
<input checked="" type="checkbox"/> Roll rate	<input checked="" type="checkbox"/> Pitch rate	<input checked="" type="checkbox"/> Yaw rate	
Multi-Channel Weights - Area II Method -	X Channel – 0.268011 Y Channel – 0.145893 Z Channel – 0.086096 Yaw Channel – 0.446323 Roll Channel – 0.028886 Pitch Channel – 0.02479		
	Sprague-Geer Metrics Values less or equal to 40 are acceptable.		M 5.7
ANOVA Metrics Both of the following criteria must be met: <ul style="list-style-type: none"> The mean residual error must be less than five percent of the peak acceleration ($\bar{e} \leq 0.05 \cdot a_{peak}$) The standard deviation of the residuals must be less than 35 percent of the peak acceleration ($\sigma \leq 0.35 \cdot a_{peak}$) 	Mean Residual 0.03	Standard Deviation of Residuals 0.18	Pass? Y

The weighted metrics computed in RSVVP using both the Area II and the Inertial methods in the multi-channel mode all satisfy the acceptance criteria, and therefore the time history comparison can be considered acceptable. The validation assessment for Part II should be entered as “Yes” on the cover page of the validation report.

Part III - Validation of Crash Specific Phenomena

The last step in the validation procedure is to compare the phenomena observed in both the crash test and the numerical solution. Since, like Case 1, this case is an example of Report 350 Test 3-11, the same phenomena previously identified in Table 26 apply to this case as well, namely: criteria A, D, F, L and M.

Table 34. Roadside safety validation metrics rating table for Case 2 – (multi-channel option using Inertia method).

Evaluation Criteria (time interval [0 sec; 1.22 sec])			
Channels (Select which was used)			
<input checked="" type="checkbox"/> X Acceleration	<input checked="" type="checkbox"/> Y Acceleration	<input checked="" type="checkbox"/> Z Acceleration	
<input checked="" type="checkbox"/> Roll rate	<input checked="" type="checkbox"/> Pitch rate	<input checked="" type="checkbox"/> Yaw rate	
Multi-Channel Weights - Inertia Method -	X Channel – 0.119486 Y Channel – 0.129217 Z Channel – 0.04426 Yaw Channel – 0.477606 Roll Channel – 0.034208 Pitch Channel – 0.195224		
	Sprague-Geer Metrics Values less or equal to 40 are acceptable.		M 7.3
ANOVA Metrics Both of the following criteria must be met: <ul style="list-style-type: none"> The mean residual error must be less than five percent of the peak acceleration ($\bar{e} \leq 0.05 \cdot a_{Peak}$) The standard deviation of the residuals must be less than 35 percent of the peak acceleration ($\sigma \leq 0.35 \cdot a_{Peak}$) 	Mean Residual 0.02	Standard Deviation of Residuals 0.21	Pass? Y

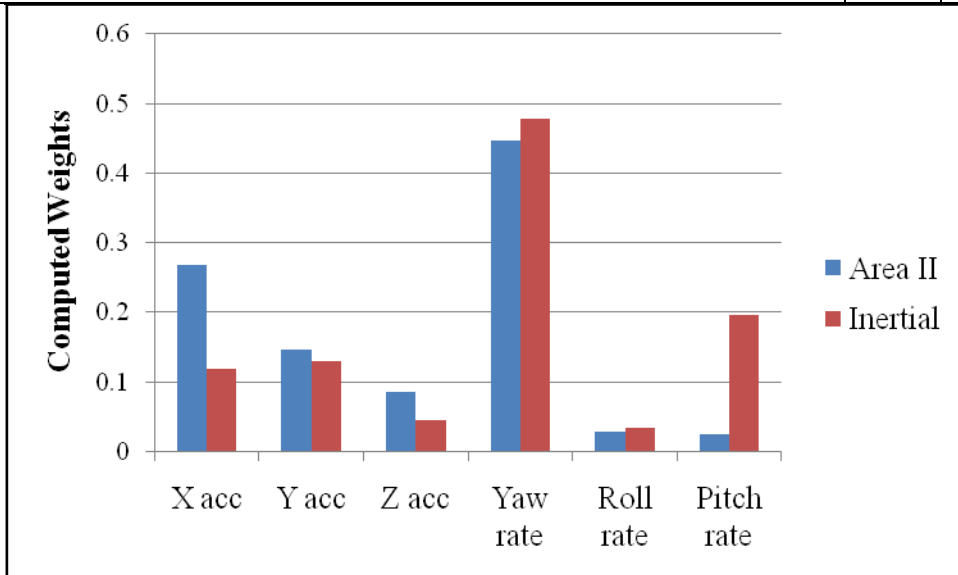


Figure 73. Comparison of multi-channel weight values computed using the Area II and the Inertial methods for Case 2.

Table 35 through Table 37 contain expanded lists of these same criteria including additional specific phenomena that were measured in the test and that could be directly compared to the numerical solution. Table 35 contains a comparison of phenomena related to structural adequacy, Table 36 contains a comparison of phenomena related to occupant risk, and Table 37 contains a comparison of phenomena related to vehicle trajectory.

As shown in Table 35, the comparison between all the structural adequacy phenomena was acceptable both in relative and absolute comparison terms. For example, the dynamic deflection in the full-scale crash test was 0.5 m whereas it was 0.6 m in the finite element simulation. This corresponds to an absolute difference of 0.1 m and a relative difference of 20%. Since the absolute difference is less than 0.15 m, the comparison is judged to be good (i.e., even though the relative difference was 20 percent, which is at the limit, the absolute difference was well below the limit). The finite element simulation and full-scale test agreed exactly with respect to the number of bent/broken posts, number of rail elements detached from the post and the number of blockouts broken or detached.

Table 35. Structural Adequacy Phenomena for Case 2.

		Evaluation Criteria	Known Result	Analysis Result	Difference Relative/ Absolute	Agree?	
Structural Adequacy	A	A1	Test article should contain and redirect the vehicle; the vehicle should not penetrate, under-ride, or override the installation although controlled lateral deflection of the test article is acceptable. (Answer Yes or No)	Yes	Yes	X	YES
		A2	Maximum dynamic deflection: - Relative difference is less than 20 percent or - Absolute difference is less than 0.15 m	0.5 m	0.6 m	20% 0.1 m	YES
		A3	Length of vehicle-barrier contact: - Relative difference is less than 20 percent or - Absolute difference is less than 2 m	~6.32 m	~6.19 m	2.1% 0.13 m	YES
		A4	The relative difference in the number of broken or significantly bent posts is less than 20 percent.	2	2		YES
		A5	The rail element ruptured or failed (Answer Yes or No)	No	No	X	YES
		A6	There were failures of connector elements (Answer Yes or No).	Yes	Yes	X	YES
		A6a	Number of detached posts from rail	2	2	X	YES
		A6b	Number of detached blockouts from posts	1	1	X	YES

As shown in Table 36, a comparison of the finite element and full-scale crash test results for all the occupant risk phenomena result in good comparisons except the lateral ridedown acceleration (i.e., criterion L6). The maximum lateral ORA predicted in the simulation was 4.3 g's higher than the value measured in the test. The absolute limit for differences in acceleration is 4 g's so the lateral ORA is just barely over the limit. Both the test and simulation agree that the ORA is lower than the suggested limits specified in Report 350 (i.e., < 12 G's) and the

simulation is being over conservative (predicting too high) so this result will be considered a pass although a marginal one.

An examination of criterion F3 in Table 36 illustrates the importance of using absolute as well as relative differences. The relative difference in the maximum pitch rotation was 25.5 percent (i.e., 12.8 versus 10.2 degrees) which is an unacceptably high relative difference. The absolute difference, however, is only 1.2 degrees which, given the relatively small maximum pitch is considered acceptable since it is less than 5 degrees of absolute difference.

Table 36. Occupant Risk Phenomena for Case 2.

Evaluation Criteria		Known Result	Analysis Result	Difference Relative/Absolute	Agree?		
Occupant Risk	D	Detached elements, fragments or other debris from the test article should not penetrate or show potential for penetrating the occupant compartment, or present an undue hazard to other traffic, pedestrians or personnel in a work zone. (Answer Yes or No)	Pass	Pass	X	YES	
		F1	The vehicle should remain upright during and after the collision although moderate roll, pitching and yawing are acceptable. (Answer Yes or No)	Pass	Pass	X	YES
	F	F2	Maximum roll of the vehicle: - Relative difference is less than 20 percent or - Absolute difference is less than 5 degrees.	6.5	4.9	24.6% 1.6 deg.	YES
		F3	Maximum pitch of the vehicle is: - Relative difference is less than 20 percent or - Absolute difference is less than 5 degrees.	10.2	12.8	25.5% 2.6 deg	YES
		F4	Maximum yaw of the vehicle is: - Relative difference is less than 20 percent or - Absolute difference is less than 5 degrees.	42.0	43.2	2.9% 1.2 deg	YES
		L1	Occupant impact velocities: - Relative difference is less than 20 percent or - Absolute difference is less than 2 m/s.				
	L	L1	• Longitudinal OIV (m/s)	4.9	4.2	14.3% 0.7 m/s	YES
		L2	• Lateral OIV (m/s)	4.7	4.1	12.8% 0.6 m/s	YES
		L3	• THIV (m/s)	24.1	26.8	11.2% 2.7 m/s	YES
		L2	Occupant accelerations: - Relative difference is less than 20 percent or - Absolute difference is less than 4 g's.				
		L5	• Longitudinal ORA	8.1	8.1	0.0	YES
		L6	• Lateral ORA	6.3	10.6	68.3% 4.3 G	NO
			ASI	0.7	0.67	4.3% 0.03	YES

Table 37. Vehicle Trajectory Phenomena for Case 2.

		Evaluation Criteria	Known Result	Analysis Result	Difference Relative/Absolute	Agree?
Vehicle Trajectory		M1 The exit angle from the test article preferable should be less than 60 percent of test impact angle, measured at the time of vehicle loss of contact with test device.	Yes 14 deg	No 16 deg	X	NO
		M2 Exit angle at loss of contact: - Relative difference is less than 20 percent or - Absolute difference is less than 5 degrees.	14 deg	16 deg	5.1	YES
	M	M3 Exit velocity at loss of contact: - Relative difference is less than 20 percent or - Absolute difference is less than 10 m/s.	41.3* 53.1** km/hr	56.7 km/hr	37.3 6.8	YES
		M4 One or more vehicle tires failed or de-beaded during the collision event (Answer Yes or No).	Yes	N/A	X	-
		M5 One or more tires separated from the vehicle (Answer Yes or No).	No	N/A	X	-

* Velocity reported in the test report computed by integrating the raw x-acceleration channel

** Velocity computed by integrating the x-channel data processed by RSVVP (e.g., with drift and shift)

Criterion M1, shown in Table 37, which is related to the exit angle of the vehicle when the vehicle loses contact with the guardrail, did not agree although the exit angle predicted in the simulation agreed very well with the yaw angle measured in the test. This criterion states that the exit angle of the vehicle should be less than 60 percent of the impact angle (i.e., < 15 degrees). The exit angle computed in the simulation was one degree over this limit and the exit angle measured in the test was one degree below this limit so the standard Report 350 criterion M would be right on the limit. As shown by criterion M2, however, the difference between the test and simulation was only two degrees which is quite good. In this particular case, the “NO” result for criterion M1 can be ignored since the two results fall right on the limit and criterion M2 shows that the agreement in terms of the angles, is quite good.

In general, the simulation agrees fairly well with the full-scale test results with the small exceptions noted. Criteria L6 and M1 did not compare well but on closer examination it is clear that the results are actually either conservative or right on the limit. The simulation, therefore, can be considered validated with these exceptions. The fact that this case was validated with crash tests gives the community more confidence that the results of the 33 simulations in Report 537 are, in fact, good predictions.(141)

TEST CASE 3: GEO METRO STRIKING A RIGID BARRIER

INTRODUCTION

This test case involves a 900-kg small car impacting a rigid concrete barrier. The simulation was originally performed to reproduce the ten repeated full-scale crash tests performed during the ROBUST project.(43) The main purpose of this task of the ROBUST project was twofold: (1) assessing the typical scatter of results which characterizes experimental tests in roadside safety by performing the same full-scale crash test at different test houses and (2) reproducing numerically the test in order to assess the reliability of numerical simulations using the model of a generic small car. The simulation was performed using an improved version of the publicly available LSDYNA numerical model of the Geo Metro vehicle originally developed by the NCAC.

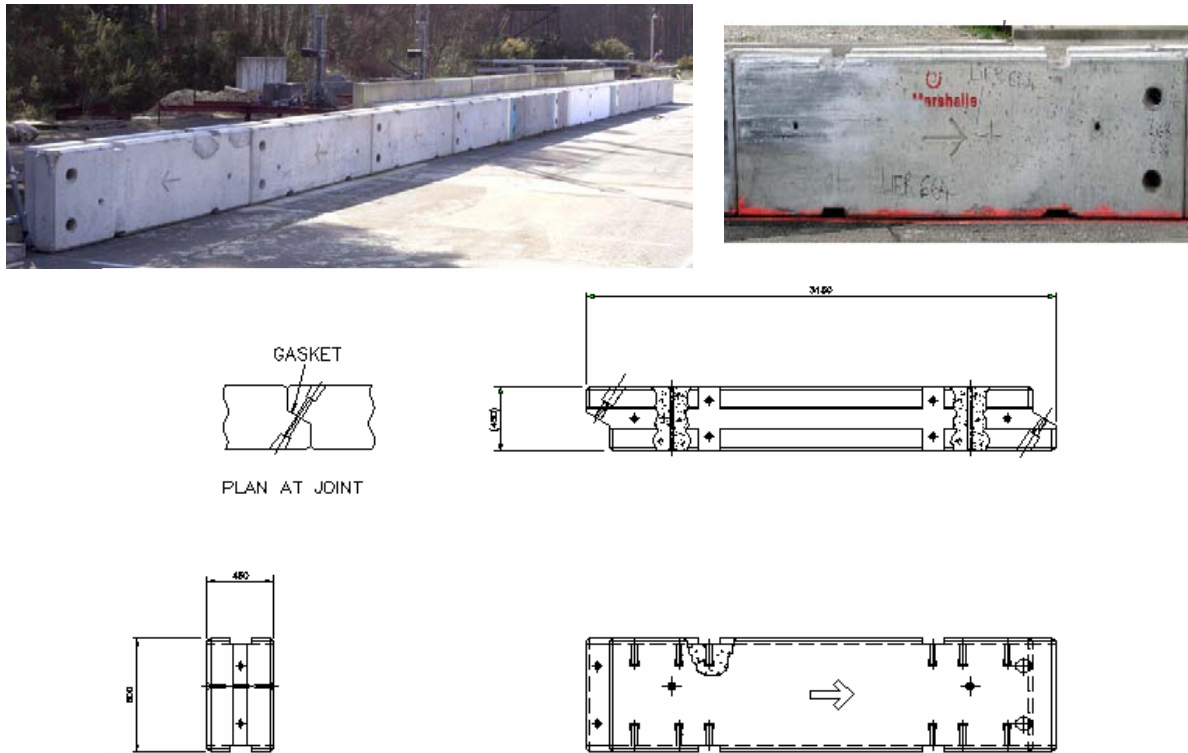


Figure 74. Temporary vertical concrete barrier.

The concrete barrier used in the Round Robin tests was a temporary vertical concrete barrier (Figure 74) produced by the British company Marshall RC Products Company and is usually employed as a modular lane divider. It is constructed with independent, precast concrete units. Each unit has a mass of 2,600 kg (5,732 lb) is 3.150 m (10.3 ft) long, 0.450 m (1.5 ft) wide and 0.816 m (2.7 ft) high. They were placed end to end on the track and were connected by two M24 bolts passing through holes in the vertical scarf-joints at the ends of the units. To prevent damage to the joints, a 5-mm thick non-cellular rubber gasket was placed in the gap between the ends of the units. The total length of the barrier installation during the test was 30 m.

The validation of the numerical model was carried out by comparing the simulation results against the outcomes of two different full-scale experimental tests performed using the same type of barrier and similar vehicles. In the following sections, the various steps of the validation process are separately described with respect to each of the two experimental tests, which will be referred to as Test 1 and Test 2 accordingly. The verification and validation reports for the comparisons using Tests 1 and 2 are contained in Appendices C3 and C4, respectively.

The vehicles used in Test 1 and Test 2 were, respectively, a Fiat UNO (Figure 75a) and a Peugeot 206 (Figure 75b). In both the tests the vehicle complied with the requirements of the EN1317 standard for the 900-kg small car category.

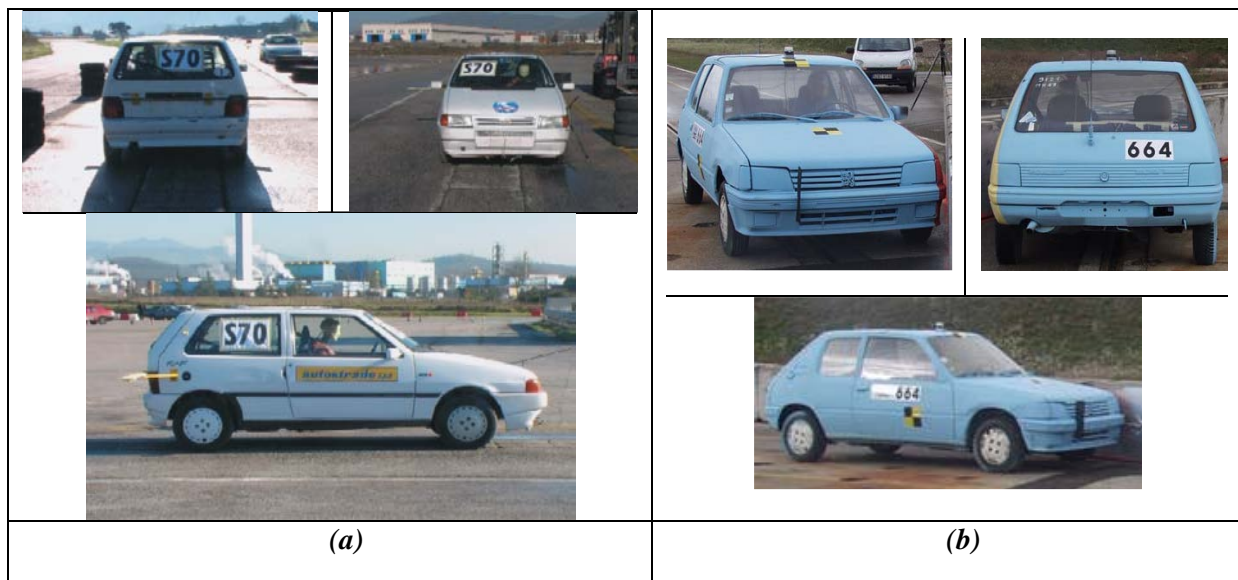


Figure 75. Vehicle used in (a) Test 1 and (b) Test 2.

PIRT FOR THE GEO METRO VEHICLE MODEL

The vehicle used in the numerical analysis was a modified version of the Geo Metro reduced finite element model originally developed by the NCAC. (77) Although this numerical model does not represent in full detail the actual vehicle used during the full-scale test (e.g., the model was based on a Geo Metro whereas neither test used that particular brand), it has similar geometrical and inertial properties and falls into the same category of small cars. The original vehicle model was modified by a team of researchers from Politecnico di Milano in Italy. (77) The primary changes and improvements involved both the front and rear suspensions and the steering system. For the details of the modifications made to these components of the model, refer to the ROBUST reports.(43, 77) Furthermore, other minor improvements were made to the original model such as re-meshing of the tires and the wheel rims.

The total mass of the model was increased in order to comply with the specifications of the European standard EN 1317 for a small vehicle (i.e., a 900-kg car impacting barriers at a

speed of 100 km/hr and 20°). (11) Table 38 shows a list of the modifications made to the original model. As no data regarding any experimental component tests relative to the actual Geo Metro car were available at the time the model was improved, only a partial PIRT of the vehicle model could be filled out.

Table 38. Partial PIRT for the Geo Metro model. (43)

Phenomena	Summary	Valid?
Front suspension system (independence from steering system)	Response verified through visual observation of computer model results	Verification
Steering system properties i) Ackerman principle ii) Steep stop	Response verified through visual observation of computer model results	Verification
Front suspensions and steer stability (curb response)	Response verified through visual observation of computer model results	Verification
Rear suspension system i) Correct kinematics ii) Curb response	Response verified through visual observation of computer model results	Verification

PIRT FOR THE CONCRETE BARRIER

The model of the concrete barrier developed in the study is shown in Figure 76. Due to the simplicity of the geometry of the actual design and its strength, the barrier has been modeled as a monolithic wall made of solid elements (Figure 76). In order to improve the contact between the vehicle and the barrier model, the external surfaces of the solid elements facing the front side of the barrier model were overlapped by shell elements defined with the LSDYNA null material (i.e., Mat_009). As experienced during the various tests independently carried out by various test agencies, the barrier was always firmly held in its position by placing it against concrete parapets or massive concrete blocks so the corresponding model was rigidly anchored to the ground. The total length of the barrier model is 15 m.

Considering the simple nature of the concrete barrier, which can be considered for its full extent a rigid wall, no tests were performed to validate any of its components (i.e., concrete blocks and connections). As a consequence, the PIRT table for the barrier model could not be filled out.

VALIDATION OF THE GEO METRO MODEL

This section describes the steps followed in the validation process of the finite element model of the Geo Metro vehicle. The detailed validation report for this case can be found in Appendix C3 for the test using a Fiat (Test 1) and Appendix C4 for the test using a Peugeot (Test 2).

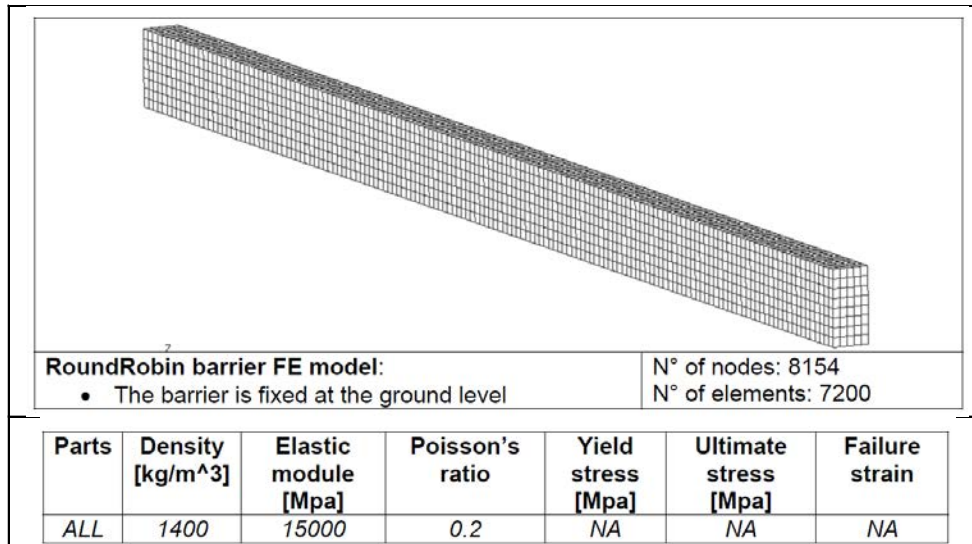


Figure 76. Finite element model of the concrete barrier.

Part I – Basic Information

The first step of the validation procedure is to document basic information about the test and simulation on the Cover Page and in Part I of the validation report.

The validation of the improved Geo Metro model was performed by comparing the outcomes of the experimental tests against the corresponding numerical results. In this case, two sets of experimental data were obtained from the full-scale crash test No S70 (Test 1) and ROU/ROB -02/664 (Test 2) performed by two of the test agencies involved in the Robust Project. (43) The tests were conducted according to the testing guidelines of the European standard EN 1317 for the test level TB11. Test 1 involved a 922-kg (2,033-lb) small car vehicle while in Test 2 the vehicle mass was 862 kg (1,900 lb). In both tests the vehicle impacted against a concrete barrier at 100 km/hr (62 mph) and an impact angle of 20 degrees. In particular, the test vehicle used in Test 1 was a Fiat UNO (2nd edition) and the test vehicle used in Test 2 was a Peugeot 206. The test article, which was of the same exact type in both the two tests, was a 0.816 m (32 inches) high concrete barrier with an installation length of 30 m (98 ft).

The numerical model of the vehicle and the barrier used in the simulation were the modified version of the Geo Metro and the monolithic barrier model described in the previous sections. Table 39 summarizes the information about the vehicle and the test/simulations conditions.

Table 39. Vehicle type and impact conditions for the two tests in Case 3.

General Information	Known Solution (Test 1)	Known Solution (Test 2)	Analysis Solution
Performing Organization	Robust test agency 1	Robust test agency 2	Politecnico di Milano
Test/Run Number:	S 70	ROU/ROB-02/664	GM_R5
Vehicle:	F i a t U N O	Peugeot 205	Geo Metro (GM_R5)
Impact Conditions			
Vehicle Mass:	922 kg (2,033 lb)	862 kg (1,900 lb)	860 kg (1,896 lb)
Speed:	100.33 km/h (62 mph)	100.4 km/h (62 mph)	100 km/h (62 mph)
Angle:	20deg	20deg	20 deg.
Impact Point:	10 m (33 ft) from beginning	10.7 m (35 ft) from beginning	4.5 m (15 ft) from beginning

The qualitative assessment of the vehicle response obtained from the numerical simulation compared well with both of the two full-scale tests. In both cases, the numerical model was able to replicate the general vehicle kinematics and the timing of the actual experimental test during the first phase of the impact. Figure 77 shows a sequential comparison of the vehicle behavior between Test 1 (left side of Figure 77) and Test 2 (right side of Figure 77), and the numerical analysis (middle column of Figure 77) .

In the second phase of the impact, a different behavior in the vehicle kinematics occurred between the numerical solution and the two experimental tests. In the numerical model, the vehicle tended to remain parallel to the barrier during the entire test while in the actual tests it was redirected back toward the roadway. In Test 1, the vehicle eventually settled back parallel to the barrier. The reason for this difference in the vehicle trajectory of the numerical model is probably due to the turning of the right front wheel towards the barrier in the simulation caused by the failure of the steering system when the opposite wheel hits against the rigid barrier. Although suspension failure did not happen in these two particular experimental tests, this phenomenon is not unusual in such a small car impact. The comparison of the experimental and numerical curves was performed on a time interval smaller than the entire period which was simulated and is shown in the sequence in Figure 77.

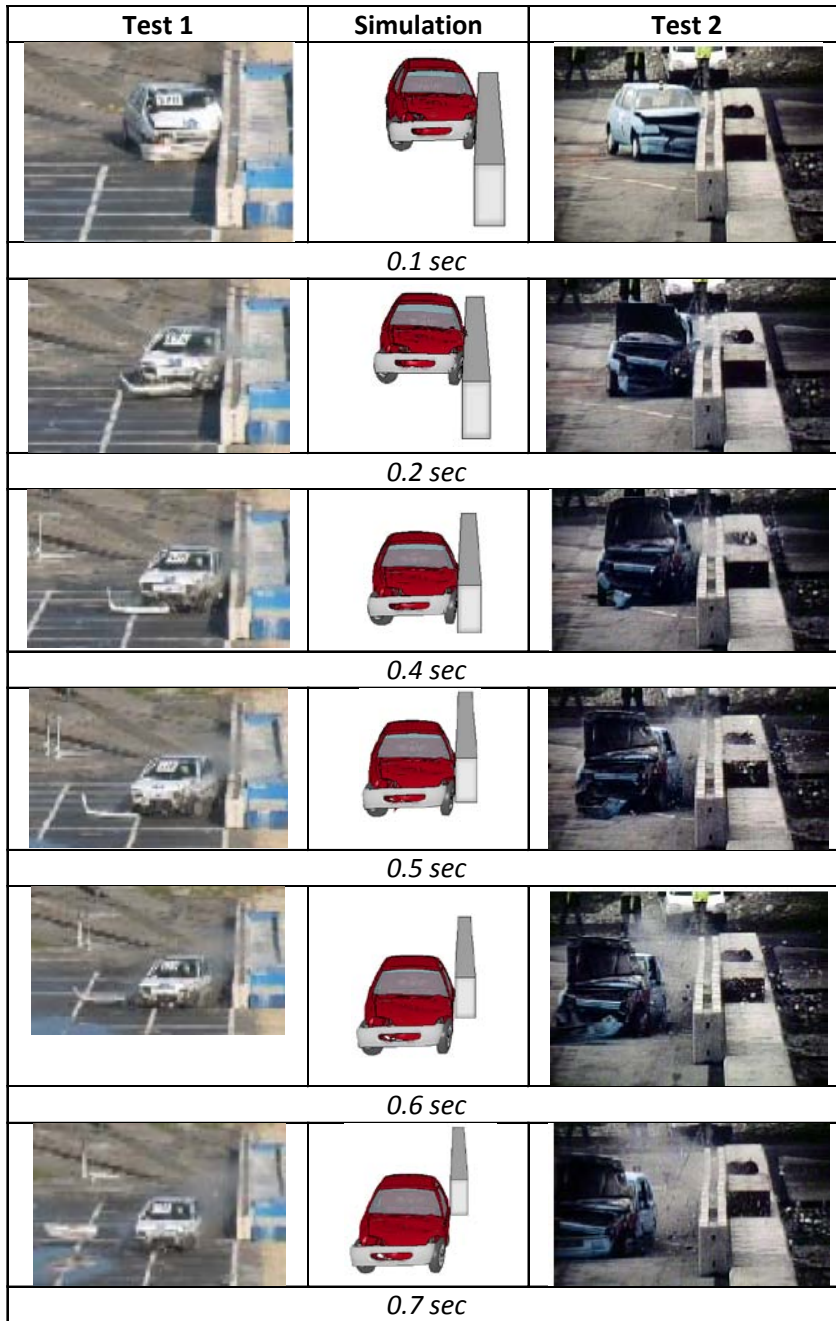


Figure 77. Sequential views of experimental tests and the finite element simulation for Case 3.

Part II - Solution Verification

The first step in the validation of the numerical analysis involves simple checks to ensure that the model is stable and capable of producing physically reasonable results. This first set of criteria serve to make sure that the model does not contain any numerical errors and it complies with the basic general physics laws; hence, passing these checks is considered a *conditio sine qua non* which it is necessary to comply with but not yet sufficient to consider the model as validated. In fact, these early controls are made independently from the results of the experimental tests.

This step is performed by checking that the global energies and mass involved in the simulation vary within a reasonable range. From the energy point of view, as no external energy is added to the system, the total energy should remain essentially constant. The time histories of the global energies, normalized with respect to the initial energy, involved in the simulation are shown in Figure 78. As can be seen, the total initial energy stays constant for the duration of the simulation. At the beginning of the simulation, the total energy of the system is purely the initial kinetic energy of the vehicle. The decrease of the kinetic energy during the impact is compensated by an equivalent increase of the internal energy and the energy dissipated by the frictional forces. Also, the fictitious hourglass energy can be considered practically null. Similarly, the total mass of the system should stay constant and any increase of the total mass of the model due to the application of the mass-scaling technique during the simulation should be negligible with respect to the initial mass. Table 40 shows the verification of the energy and mass conservation performed according to the criteria recommended in the procedures for verification and validation proposed in this research.

Table 40. Analysis Solution Verification Table for Case 3.

Verification Evaluation Criteria	Change (%)	Pass?
Total energy of the analysis solution (i.e., kinetic, potential, contact, etc.) must not vary more than 10 percent from the beginning of the run to the end of the run.	-1	YES
Hourglass Energy of the analysis solution at the end of the run is less than five percent of the total initial energy at the beginning of the run.	0.5	YES
The part/material with the highest amount of hourglass energy at any time during the run is less than five percent of the total initial energy at the beginning of the run.	0.5	YES
Mass added to the total model is less than five percent of the total model mass at the beginning of the run.	0	YES
The part/material with the most mass added had less than 10 percent of its initial mass added.	0	YES
The moving parts/materials in the model have less than five percent of mass added to the initial moving mass of the model.	0	YES
There are shooting nodes in the solution?	No	YES
There are solid elements with negative volumes?	No	YES

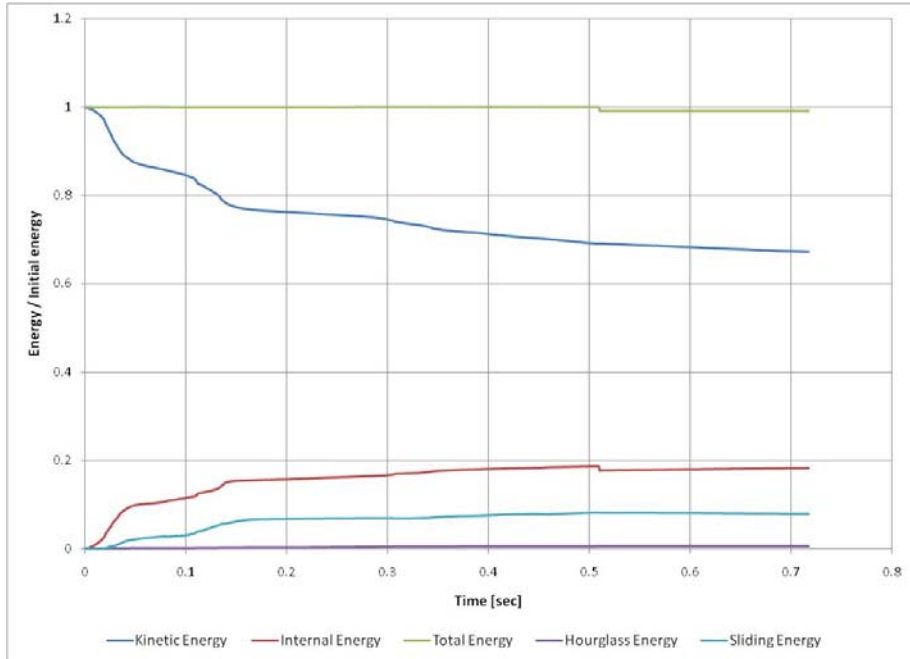


Figure 78. Plot of normalized global energy time histories for Case 3.

As all the criteria listed in Table 40 are considered acceptable, the simulation can be considered verified with respect to the conventional conservation laws. The assessment for Part I was entered as “Yes” on the cover page of the validation report for both Test 1 and Test 2.

Part III - Quantitative Evaluation

The next step of the validation procedure was the quantitative comparison of the time histories using the Sprague & Geers and ANOVA comparison metrics which were computed using the RSVVP computer program described in Chapter 5. The two full-scale crash tests used different instrumentation setups. Test 1 used X, Y and Z accelerometers and a Yaw rate gyro whereas Test 2 used three accelerometers (i.e., X, Y and Z) and three rate gyros (i.e., roll, pitch and yaw). The data were collected for both tests and the simulation at the vehicle center of gravity. According to the RSVVP nomenclature, the experimental curve is defined as the “true” curve while the numerical curve is the “test” curve.

The original numerical input curves had already been initially filtered using an SAE 180 class filter. Before the metrics were calculated, both the experimental and numerical curves were preprocessed using the RSVVP preprocessing options. The units and, for certain channels also the sign, of the numerical time histories needed to be adjusted to be consistent with the experimental curves. In particular, the numerical acceleration channels were converted from mm/s^2 to g's and the sign of the Y, Z acceleration and the Yaw and Pitch rates (for Test 2) were inverted due to a different reference system between Report 350 and EN 1317. The experimental time histories from both Test 1 and Test 2 were manually trimmed as they were characterized by a considerably long flat head due to very early triggering and an excessively long flat tail. After the experimental curves were manually trimmed, RSVVP automatically shifted the time vector to the origin (i.e., the beginning of the impact event started at time zero). The tails of the simulation time histories were manually trimmed after 0.4 sec, in order to consider only the interval of impact. Eventually, both the experimental and numerical curves were re-filtered in RSVVP using the SAE J211 CFC180 Class filter option and each channel was synchronized using the minimization of the area of the residuals method in RSVVP. Figure 79 and Figure 80 show comparisons of the original and preprocessed curves for each of the input channels for Test 1. From the graph of the preprocessed yaw rate in Figure 80 it is clearly evident that the time interval on which the true and test curves were compared was large enough to adequately cover all the phases of the impact. In fact, the selected interval completely contained the curve since the velocity increased from zero until the time it was stabilized back to a null value. Similar conclusions can be drawn considering the six channels when using the time histories from Test 2. The comparisons between the original and preprocessed curves for the six channels considering Test 2 are shown in Figure 81 and Figure 82.

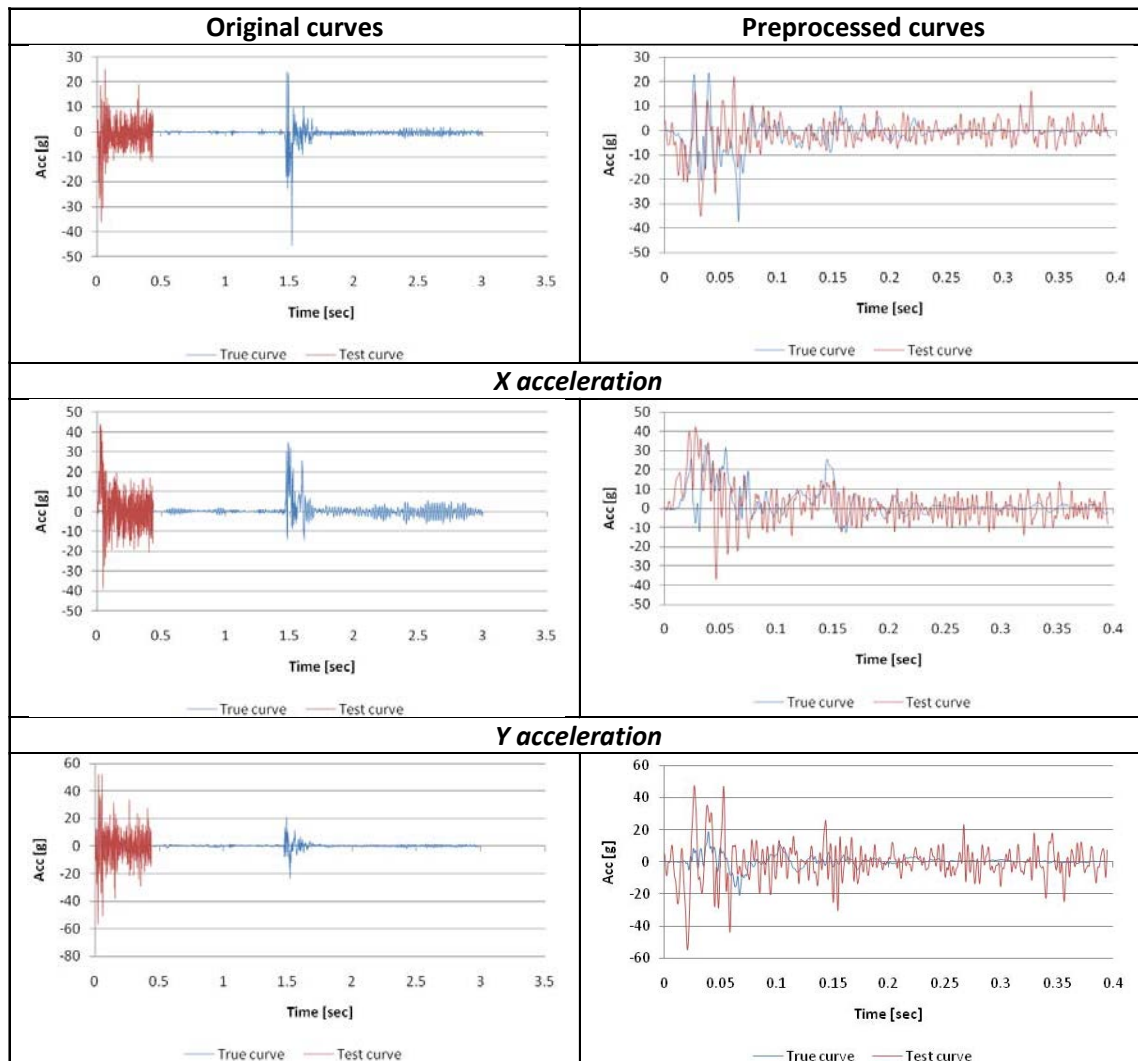


Figure 79. Original and preprocessed acceleration curves for Case 3 with Test 1.

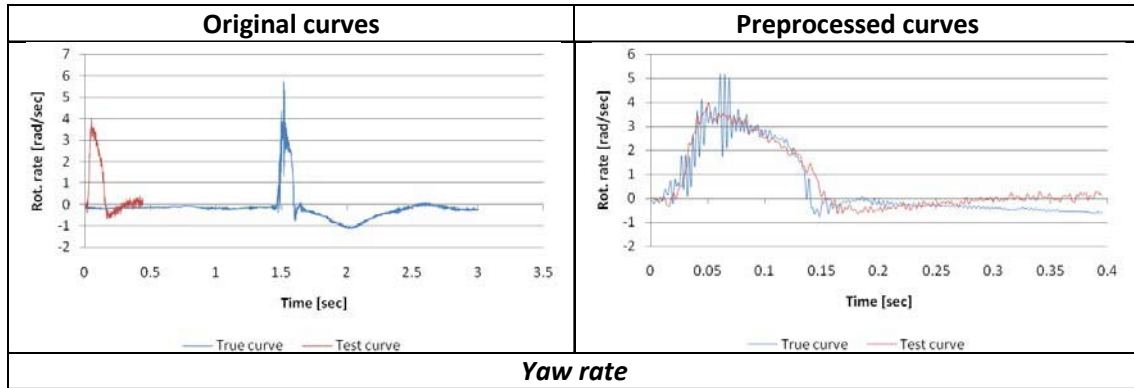


Figure 80. Original and preprocessed Yaw rate curve for Case 3 with Test 1.

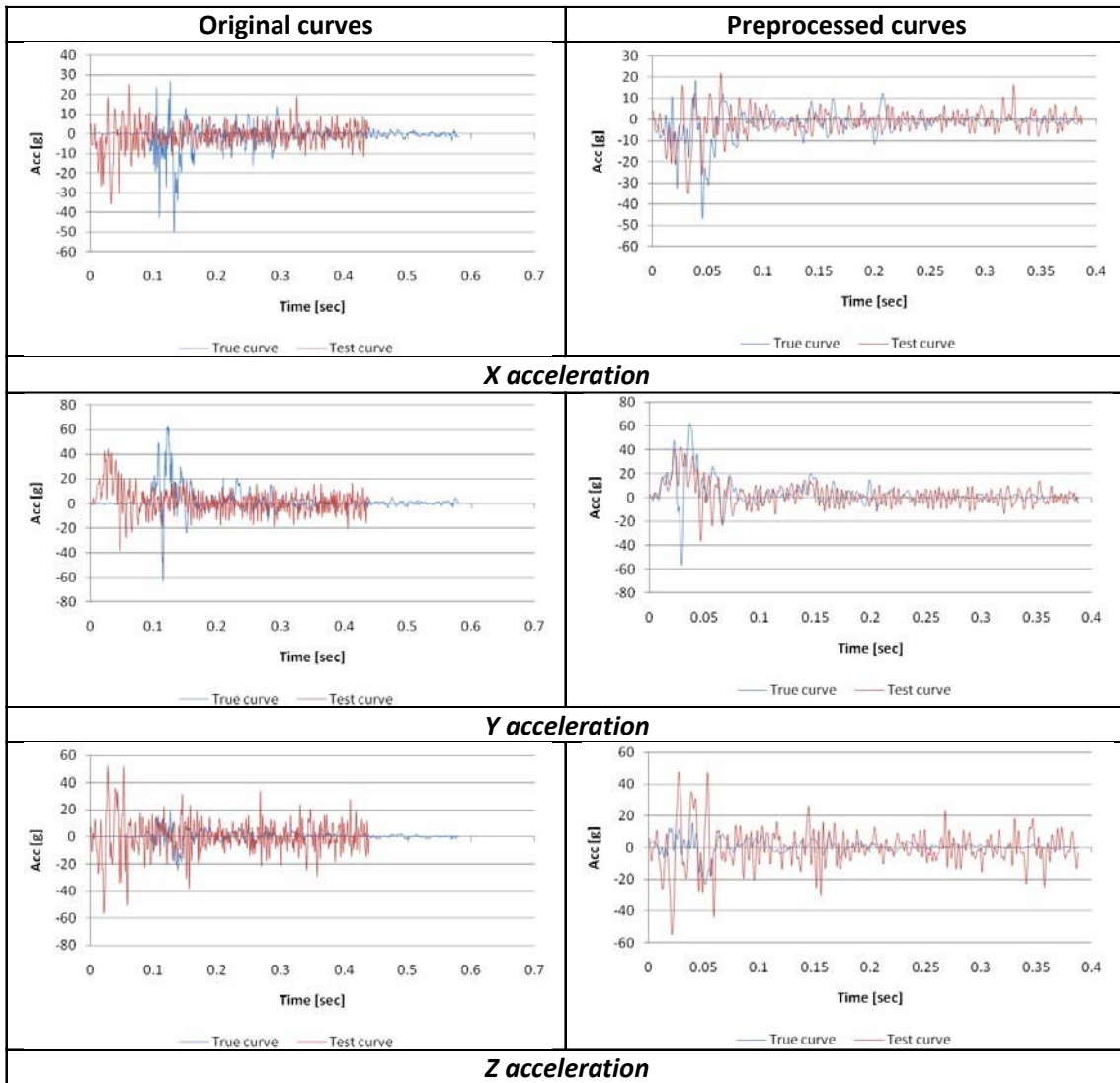


Figure 81. Original and preprocessed acceleration curves for Case 3 with Test 2.

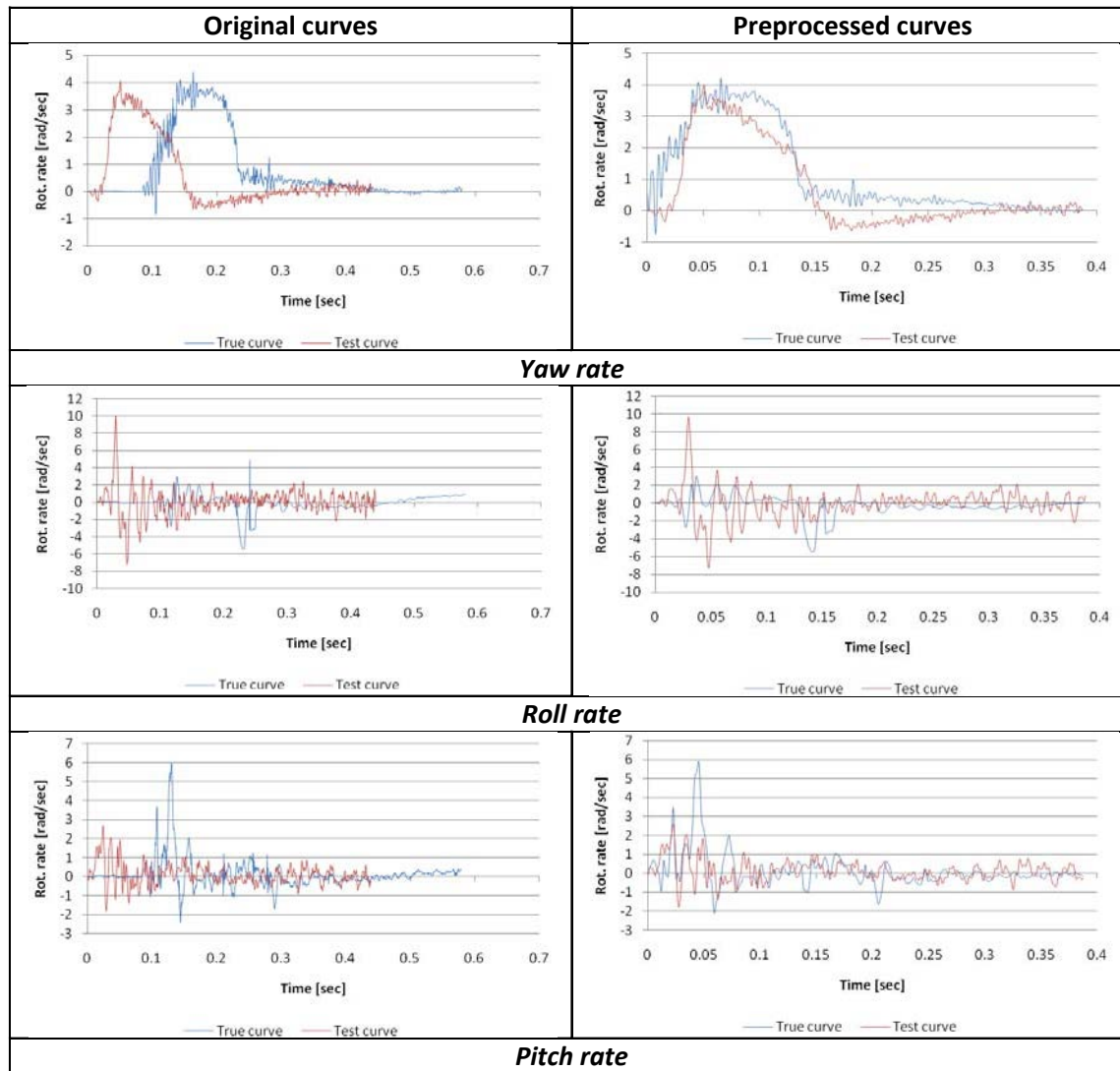


Figure 82. Original and preprocessed rotational rate curves for Case 3 with Test 2.

The time histories were compared over the complete time history of the preprocessed data, which was 0.4 seconds. The comparison metrics were computed for each individual channel using the single channel option in RSVVP and they were also computed using the multi-channel weighting option in RSVVP. In particular, the weights were assessed automatically by RSVVP based on the area of the time history of the experimental curve for each channel. The results of the evaluation for the individual channels are shown in Table 41.

For Test 1, the only channel that was outside the acceptance criterion for both the Sprague & Geers and the ANOVA metrics was the acceleration along the vertical axis (i.e., Z). In particular, the magnitude component of the Sprague & Geers was significantly greater than the proposed criterion of 40 percent indicating that, for this channel, the numerical curve had a

considerable difference in magnitude respect to the corresponding experimental curve. The vertical acceleration in this type of redirectional crash test is likely negligible with respect to the other channels, in particular the lateral acceleration along the Y axis. All the other input channels (i.e., X and Y accelerations and Yaw rate) were acceptable according to the acceptance criteria.

The comparison of the six individual channels in the case of Test 2 confirms the disagreement between the vertical acceleration time histories from the experimental test and the numerical analysis. As was the case for Test 1, the magnitude component of the Sprague & Geers metric is slightly above the acceptance value (i.e., 41.4 %) for the X channel and even higher for the Z channel. As for the rotational rates, the yaw rate time histories were a good match, but the less important pitch and roll rates did not result in good comparisons.

A visual confirmation of the results obtained from the values of the comparison metrics from each input channel can be found in the analysis of the integrated time histories which are shown in Figure 83 and Figure 84. Considering the acceleration channels, the integral functions of the Z-acceleration time histories are clearly the ones with the worst match for both the cases with Test 1 and test 2. Furthermore, the comparison of the integral functions from the accelerations along the X axis denotes that the case with Test 1 has a slightly better agreement than with Test 2, especially the magnitude. This is in agreement with the fact that the value of the M component of the Sprague & Geers metric which is computed using the acceleration time histories, in the case with Test 2, presents a slightly worse magnitude correlation between the curves. As for the rotational rate channels, also in this instance, the visual inspection of the corresponding integral functions shows a better agreement in the comparison involving Test 1.

Table 41. Roadside safety validation metrics rating table for Case 3 (single channel option).

Evaluation Criteria							Time interval [0 sec; 0.4 sec]						
O	Sprague-Geers Metrics List all the data channels being compared. Calculate the M and P metrics using RSVVP and enter the results. Values less than or equal to 40 are acceptable.						Simulation vs. Test 1			Simulation vs. Test 2			
	RSVVP Curve Preprocessing Options						M [%]	P [%]	Pass?	M [%]	P [%]	Pass?	
	Filter Option	Sync. Option	Shift		Drift								
			True Curve	Test Curve	True Curve	Test Curve							
	X acceleration	CFC 180	Min. area of Residuals	N	N	N	N	7.7	36.8	Y	6.8	41.3	N
	Y acceleration	CFC 180	Min. area of Residuals	N	N	N	N	24.5	38.5	Y	12.3	39.7	Y
	Z acceleration	CFC 180	Min. area of Residuals	N	N	N	N	218	41.5	N	181	47.8	N
	Yaw rate	N/A	N/A	N/A	N/A	N/A	N/A	0.7	11.1	Y	16.4	12	Y
	Roll rate	N/A	N/A	N/A	N/A	N/A	N/A	N/A	N/A	N/A	46.2	50.1	N
	Pitch rate	N/A	N/A	N/A	N/A	N/A	N/A	N/A	N/A	N/A	38.7	40.2	N
P	ANOVA Metrics List all the data channels being compared. Calculate the ANOVA metrics using RSVVP and enter the results. Both of the following criteria must be met: <ul style="list-style-type: none"> The mean residual error must be less than five percent of the peak acceleration ($\bar{e} \leq 0.05 \cdot a_{Peak}$) and The standard deviation of the residuals must be less than 35 percent of the peak acceleration ($\sigma \leq 0.35 \cdot a_{Peak}$) 						Mean Residual [%]	Standard Deviation of Residuals [%]	Pass ?	Mean Residual [%]	Standard Deviation of Residuals [%]	Pass ?	
	X acceleration/Peak	0.82	17.4	Y	0.9	16.7							Y
	Y acceleration/Peak	-2.32	30.5	Y	-1	20	Y						
	Z acceleration/Peak	-2.84	54.2	N	-3	53	N						
	Yaw rate	3.3	9.5	Y	-11	11.8	N						
	Roll rate	N/A	N/A	N/A	6.2	36.7	N						
	Pitch rate	N/A	N/A	N/A	0.11	16.1	Y						

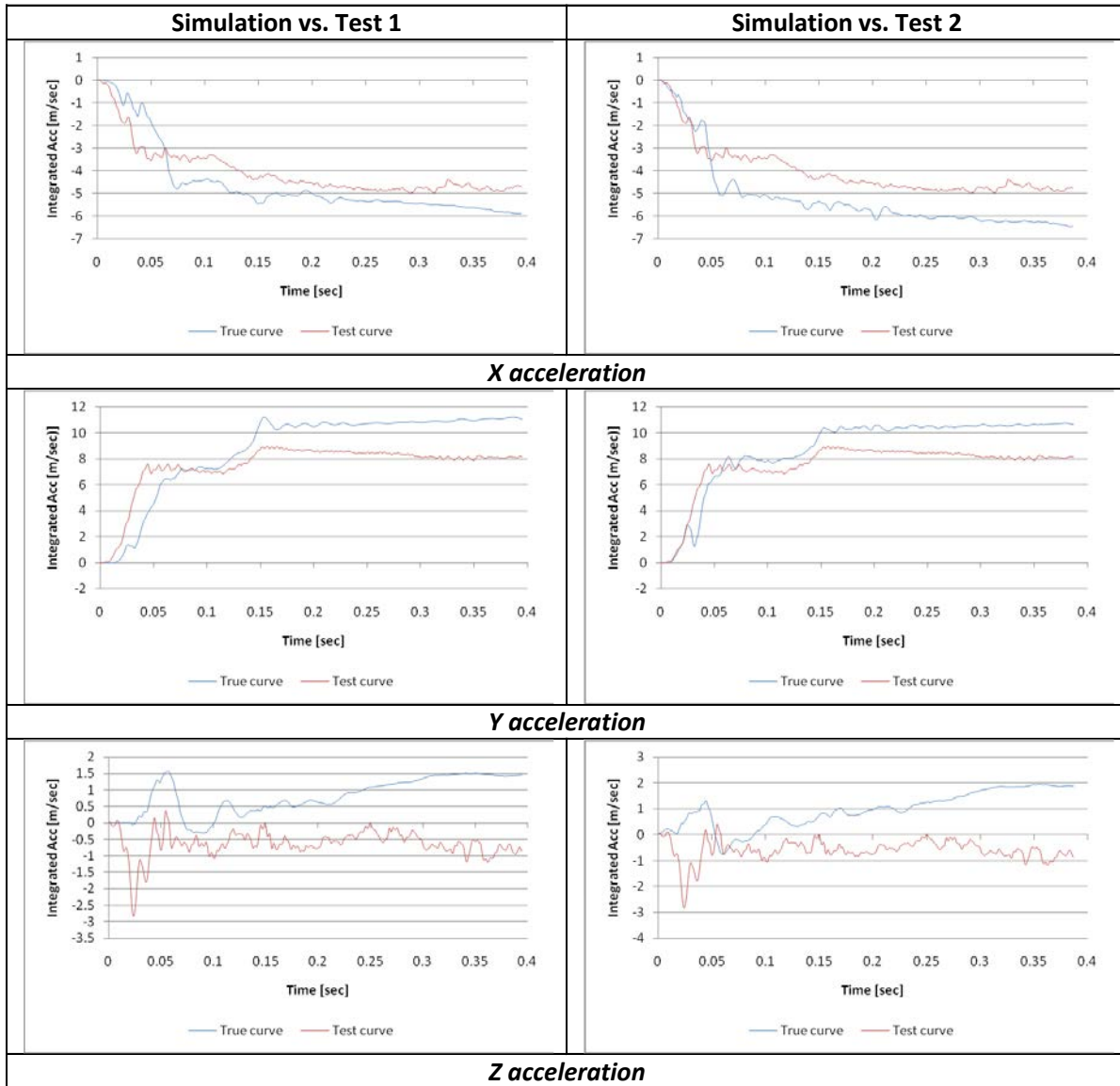


Figure 83. Comparison of the integral functions for each of the acceleration channels for Case 3.

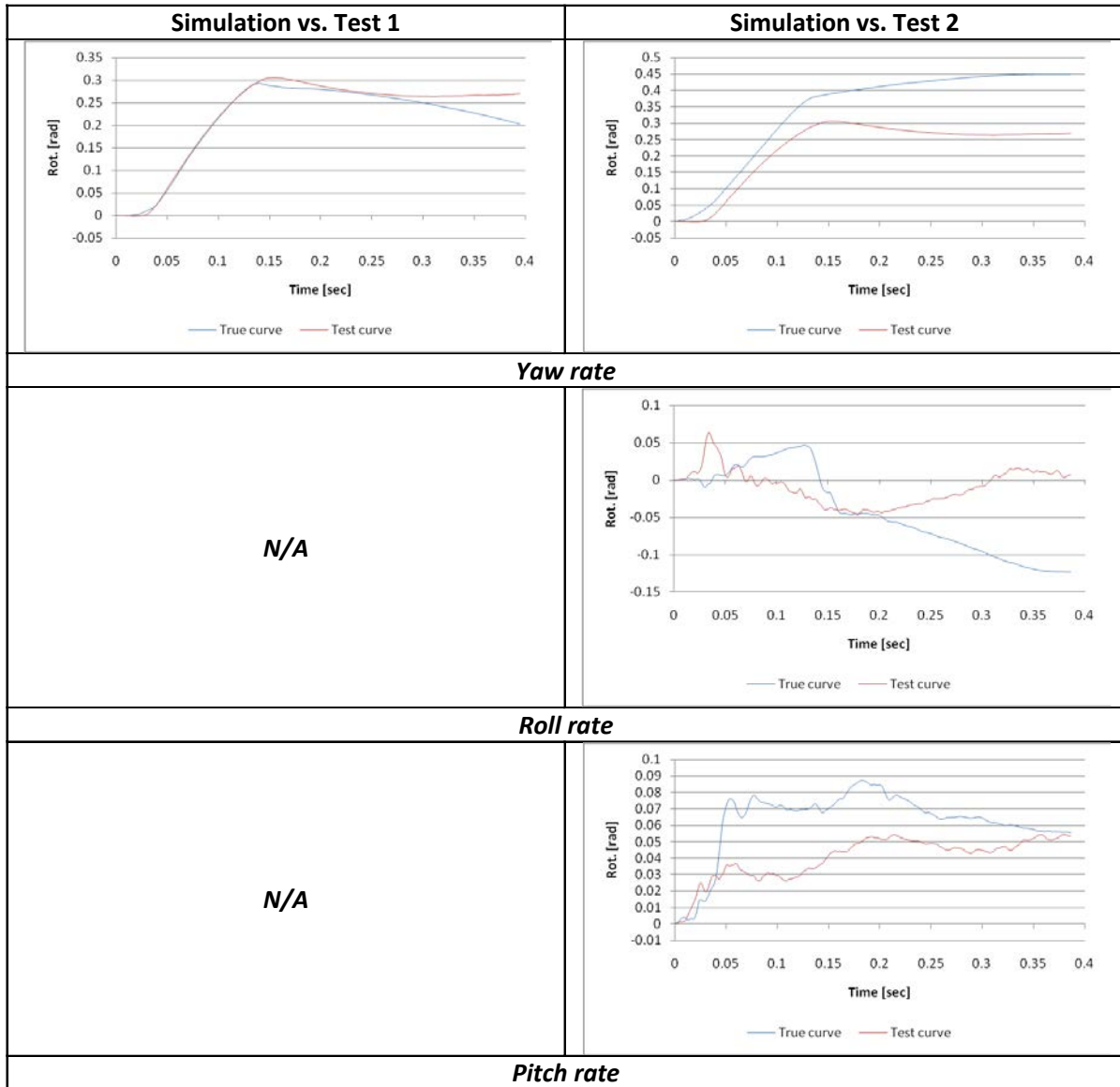


Figure 84. Comparison of the integral functions for each of the rotational rate channels for Case 3.

Since not all the channels satisfied the single-channel acceptance criteria, Test 1 and Test 2 were further compared using the multi-channel option in RSVVP in order to calculate the weighted Sprague & Geers and ANOVA metrics. The weighting factors were automatically calculated based on the area of the true curves (i.e., method Area II in RSVVP).

Table 42. Roadside safety validation metrics rating table for the Case 3 (multi-channel option).

Evaluation Criteria (time interval [0 sec; 0.4 sec])																				
Channels (Select which was used)																				
Simulation vs. Test 1																				
<input checked="" type="checkbox"/> X Acceleration	<input checked="" type="checkbox"/> Y Acceleration	<input checked="" type="checkbox"/> Z Acceleration																		
<input checked="" type="checkbox"/> Roll rate	<input type="checkbox"/> Pitch rate	<input type="checkbox"/> Yaw rate																		
Multi-Channel Weights -Area (II) Method-	X Channel – 0.16 Y Channel – 0.30 Z Channel – 0.04 Yaw rate Channel – 0.5		<table border="1"> <caption>Simulation vs. Test 1 Weights</caption> <tr><th>Metric</th><th>Weight</th></tr> <tr><td>X acc</td><td>0.16</td></tr> <tr><td>Y acc</td><td>0.30</td></tr> <tr><td>Z acc</td><td>0.04</td></tr> <tr><td>Yaw rate</td><td>0.5</td></tr> </table>				Metric	Weight	X acc	0.16	Y acc	0.30	Z acc	0.04	Yaw rate	0.5				
	Metric	Weight																		
X acc	0.16																			
Y acc	0.30																			
Z acc	0.04																			
Yaw rate	0.5																			
Simulation vs. Test 1																				
<input checked="" type="checkbox"/> X Acceleration	<input checked="" type="checkbox"/> Y Acceleration	<input checked="" type="checkbox"/> Z Acceleration																		
<input checked="" type="checkbox"/> Roll rate	<input checked="" type="checkbox"/> Pitch rate	<input checked="" type="checkbox"/> Yaw rate																		
Multi-Channel Weights -Area (II) Method-	X Channel – 0.17 Y Channel – 0.28 Z Channel – 0.05 Yaw rate Channel – 0.36 Roll rate Channel – 0.10 Pitch rate Channel – 0.04		<table border="1"> <caption>Simulation vs. Test 1 Weights</caption> <tr><th>Metric</th><th>Weight</th></tr> <tr><td>X acc</td><td>0.17</td></tr> <tr><td>Y acc</td><td>0.28</td></tr> <tr><td>Z acc</td><td>0.05</td></tr> <tr><td>Yaw rate</td><td>0.36</td></tr> <tr><td>Roll rate</td><td>0.10</td></tr> <tr><td>Pitch rate</td><td>0.04</td></tr> </table>				Metric	Weight	X acc	0.17	Y acc	0.28	Z acc	0.05	Yaw rate	0.36	Roll rate	0.10	Pitch rate	0.04
	Metric	Weight																		
X acc	0.17																			
Y acc	0.28																			
Z acc	0.05																			
Yaw rate	0.36																			
Roll rate	0.10																			
Pitch rate	0.04																			
			Simulation vs. Test 1		Simulation vs. Test 2															
O	Sprague-Geer Metrics Values less or equal to 40 are acceptable.	M [%]	P [%]	Pass?	M [%]	P [%]	Pass?													
		17.6	24.7	Y	25.7	31.5	Y													
P	ANOVA Metrics Both of the following criteria must be met: <ul style="list-style-type: none"> The mean residual error must be less than five percent of the peak acceleration ($\bar{e} \leq 0.05 \cdot a_{Peak}$) The standard deviation of the residuals must be less than 35 percent of the peak acceleration ($\sigma \leq 0.35 \cdot a_{Peak}$) 	Mean Residual	Standard Deviation of Residuals	Pass?	Mean Residual	Standard Deviation of Residuals	Pass?													
		1%	18.8%	Y	-3.7	19.6	Y													

The weighted composite value of both the Sprague & Geers and the ANOVA metrics, and the weighting factors are shown in Table 42. In this case, all the values meet the acceptance criteria. As can be seen from the column diagrams of the weighting factors for the comparison

case with Test 1, the yaw rate channel is given 50 percent of the total weight. This happens because RSVVP assumes that the weights are equally distributed between the acceleration and the rotational rate groups and, in the case with Test 2, the yaw rate is the only channel in the latter group so it is weighted by half the total (i.e., 50 percent). In any case, also in the case with Test 2 where all the six channels were involved, the yaw rate channel was the one with the highest weighting factor which is reasonable for this type of re-directional longitudinal barrier crash test. For both tests, the channel with the highest weight in the acceleration group is the Y acceleration (i.e., lateral direction). This is also reasonable considering the type of impact: a 20-degree re-directional impact. In particular, the Z acceleration channel was considered negligible for comparisons to both tests as expected. In the case of Test 2, the roll- and pitch-rate channels are negligible as well.

Another confirmation of the low weighting factor assigned to the Z-acceleration channel can be obtained by analyzing the integrated acceleration time histories of the X, Y, and Z channels shown in Figure 83 for Case 3. It can be clearly seen that the change in velocity along the Z direction (i.e., the integral of the Z-acceleration curve) is insignificant with respect to the other two acceleration channels. Similar conclusions can be drawn also for the roll- and pitch-rate channels for Test 2 (Figure 84).

Considering the results obtained from the calculation of the comparison metrics in the multichannel case, the quantitative evaluation of the time histories can be regarded as passed for both comparisons with Test 1 and Test 2. Hence, the validation assessment for Part III was entered as “Yes” on the cover page of the respective validation report.

Part IV - Validation of Crash Specific Phenomena

This section describes the last section of the verification and validation report, the comparison of the phenomena characterizing both the experimental test and the numerical simulation. Referring to the phenomena selection table shown earlier in Table 26, the phenomena that apply to this type of crash test (i.e., a Report 350 test 3-10) are criteria A, D, F, H, I and M. Table 43 through Table 45 show, respectively, the phenomena related to structural adequacy, occupant risk and vehicle trajectory for the comparison with Test 1. In each of the three tables, the criteria applicable to this particular case are indicated with a red square. Similar results and conclusions were obtained in the PIRT tables for the comparison involving Test 2. For the sake of conciseness, the tables for Test 2 are not shown here although they are included in Appendix C4.

As shown in Table 43, all the structural adequacy criteria agree with the exception of criterion A3. As explained earlier, the reason is that the vehicle in the simulation steered into the wall due to suspension damage whereas in Test 1, the vehicle was re-directed away from the wall. The absence of agreement for criterion A3 points out the need to model the suspension accurately. In fact, the difference may well be the differences between the actual vehicles used in the tests (i.e., a Fiat and a Peugeot) and the vehicle model (i.e., a Geo Metro).

Table 43. Structural Adequacy Phenomena for Case 3 with Test 1.

		Evaluation Criteria	Known Result	Analysis Result	Relative Diff. (%)	Agree?
Structural Adequacy	A	A1 Test article should contain and redirect the vehicle; the vehicle should not penetrate, under-ride, or override the installation although controlled lateral deflection of the test article is acceptable. (Answer Yes or No)	Yes	Yes	X	YES
	A2	Maximum dynamic deflection: - Relative difference is less than 20 percent or - Absolute difference is less than 0.15 m	0	0	0 % 0 m	YES
	A3	Length of vehicle-barrier contact: - Relative difference is less than 20 percent or - Absolute difference is less than 2 m	7 m	10 m	30% 3 m	NO
	A4	The relative difference in the number of broken or significantly bent posts is less than 20 percent.	0	0	0	YES
	A5	The rail element ruptured or failed (Answer Yes or No)	No	No	X	YES
	A6	There were failures of connector elements (Answer Yes or No).	No	No	X	YES
	A7	There was significant snagging between the vehicle wheels and barrier elements (Answer Yes or No).	No	No	X	YES
	A8	There was significant snagging between vehicle body components and barrier elements (Answer Yes or No).	No	No	X	YES

The occupant risk phenomena comparisons for Test 1 and the simulation are shown in Table 44. There is good agreement for all aspects of criterion H in both relative and absolute terms, but the lateral ORA and PHD of criterion I both exceed the absolute and relative acceptance criteria. In both cases, the experimental response is stiffer than the simulated one. This may be a result of the difference between vehicles as well but it is an issue that should be further examined by the analyst.

The severity indexes for criteria H and I were computed using exactly the same preprocessed curves used to calculate the comparison metrics by RSVVP. Initially, the preprocessed time histories were considered for their total length (i.e., 0 sec, 0.4 sec) but this created an inconsistency in the time at which TRAP evaluated the maximum longitudinal Occupant Ridedown Acceleration (ORA) for the experimental and simulation results. Also, because of the different ORA time, the values of the longitudinal ORA resulted in opposite signs. Figure 85 shows 10-ms averaged time histories of the X-acceleration channel and the time of the maximum ORA for the test and true curves. Although the curves of the longitudinal acceleration for the experimental and numerical case were in good agreement on the time interval during which the impact occurred, the presence of a some smaller peaks in the numerical curve, which did not appear in the actual test, affected the time at which the maximum ORA was calculated. Considering only the time interval on which the impact occurred (i.e., 0sec, 0.2 sec) allowed

TRAP to solve this inconsistency as shown in Figure 85b. Limiting the interval of the curves did not affect the value for any of the other severity indexes evaluated by TRAP.

Criterion M2 in Table 45 did not compare well. This is a result of the vehicle steering into the barrier in the simulation and away from it in both the tests. Although the comparisons were acceptable for most of the criteria in Table 43 through Table 45, a few of them were not within the criteria indicating that this result should not be considered valid as yet. The analyst should re-examine the model and determine why the suspension components failed in so different a manner. Resolving the suspension failure issue should improve the failed results for criteria M2 and I.

Table 44. Occupant Risk Phenomena for the Case 3 with Test 1.

		Evaluation Criteria	Known Result	Analysis Result	Relative Diff. (%)	Agree?	
Occupant Risk	D	Detached elements, fragments or other debris from the test article should not penetrate or show potential for penetrating the occupant compartment, or present an undue hazard to other traffic, pedestrians or personnel in a work zone. (Answer Yes or No)	Pass	Pass	X	√	
	F	F1	The vehicle should remain upright during and after the collision although moderate roll, pitching and yawing are acceptable. (Answer Pass or Not pass)	Pass	Pass	X	√
		F2	The relative difference between the maximum roll of the vehicle is less than 20 percent.	≈3 ^{o(1)}	2.5°	16	√
		F3	The relative difference between the maximum pitch of the vehicle is less than 20 percent.	N/A	N/A	N/A	N/A
		F4	The relative difference between the maximum yaw of the vehicle is less than 20 percent.	16.8°	17.5°	4	√
	H	H1	Occupant impact velocities: - Relative difference is less than 20 percent or - Absolute difference is less than 2 m/s. ⁽²⁾ : • Longitudinal OIV (m/s) • Lateral OIV (m/s)	4.5	3.3	-27% 1.2 m/s	YES
				-7.2	-7.2	0 % 0 m/s	YES
		H2	• Longitudinal OIV	4.5	3.3	-27% 1.2 m/s	YES
		H3	• THIV (m/s)	7.9	7.6	-3.8 % 0.3 m/s	YES
	I		Occupant accelerations: - Relative difference is less than 20 percent or - Absolute difference is less than 4 g's. ⁽²⁾ : • Longitudinal ORA (g) • Lateral ORA (g) • PHD (g) • ASI				
				-5	-3.5	30 % 1.5 g's	YES
				19.8	10	-49.5 % 9.8 g's	NO
				20.4	11.2	-45 % 9.2 g's	NO
				1.59	1.78	11% 0.2	YES

⁽¹⁾ The value was visually assessed from the image sequence of the test.

⁽²⁾ The severity indexes were computed considering the curves preprocessed by RSVVP on the time interval [0 sec, 0.2 sec].

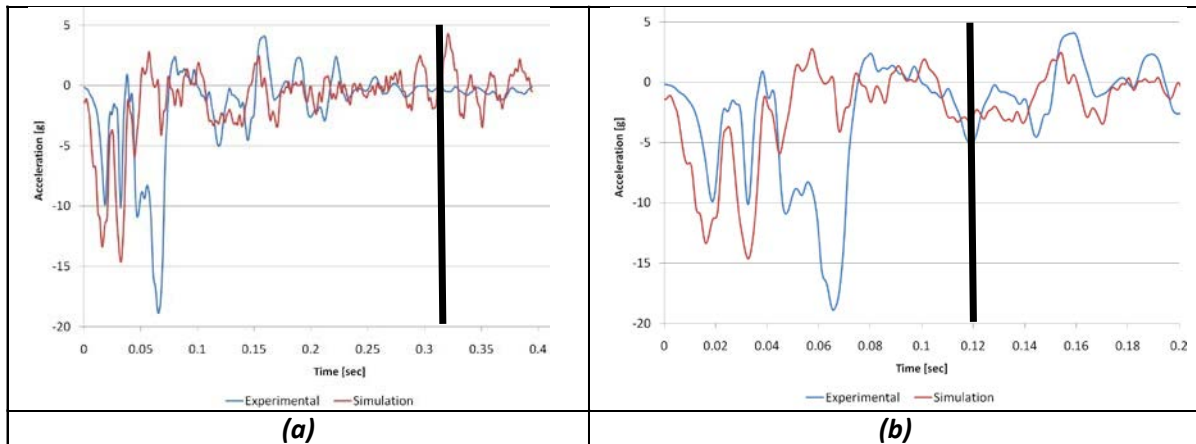


Figure 85. X-acceleration: time of max longitudinal ORA considering the intervals (a) [0, 0.4] and (b) [0, 0.2] for Case 3 with Test 1.

Table 45. Vehicle Trajectory Phenomena for the Case 3 with Test 1.

Evaluation Criteria			Known Result	Analysis Result	Relative Diff. (%)	Agree?	
Vehicle Trajectory	M	M1	The exit angle from the test article preferable should be less than 60 percent of test impact angle, measured at the time of vehicle loss of contact with test device.	$\approx 10^{(1)}$ Yes	$0^{(2)}$ Yes		YES
		M2	The relative difference in the exit angle at loss of contact is less than 20 percent or 5 degrees	10	$0^{(2)}$	-100% 10°	NO
		M3	The relative difference in the exit velocity at loss of contact is less than 20 percent or 10 km/hr	78.8 km/h	82 ^(2,3) km/h	4% 3.2 km/hr	YES
		M4	One or more vehicle tires failed or de-beaded during the collision event (Answer Yes or No).	Yes	Yes	X	YES
		M5	One or more tires separated from the vehicle (Answer Yes or No).	No	No	X	YES

⁽¹⁾ The value was visually assessed from the image sequence of the test.

⁽²⁾ The vehicle slid along the whole length of the barrier and never lost contact.

⁽³⁾ The exit velocity was considered at the same time the vehicle lost contact w/ barrier in the experimental test ($t = 0.35$ sec).

TEST CASE 4: TRACTOR AND SEMITRAILER FE MODEL

INTRODUCTION

This fourth test case involves the NCAC/Battelle tractor-semitrailer finite element model impacting a “rigid” 42-inch tall median barrier at 80 km/hr and at an impact angle of 15 degrees. The National Transportation Research Center, Inc. (NTRCI), in collaboration with the Turner Fairbanks Highway Research Center (TFHRC), sponsored the research team of Battelle, Oak Ridge National Laboratory (ORNL) and the University of Tennessee at Knoxville (UTK) to conduct a three-phase investigation to enhance and refine a finite element model (the beta version of the tractor model was developed by the NCAC) for simulating tractor-semitrailer crash events involving roadside safety barriers such as bridge rails and median barriers. A quantitative evaluation of the model results is presented here based on the procedures outlined in Chapter 4. The project is currently in its third phase and is not yet complete; therefore, the data presented in the following sections are tentative for this model.

The tractor-semitrailer model, shown in Figure 86, is based on a 1992 Freightliner FLD120 with integral sleeper cabin and the semitrailer model is based on a 1990 Stoughton box semitrailer. The model consists of 417,550 nodes, 348,700 elements, and 541 parts. More details regarding the development of the model can be found in the project reports.(147, 148, 149)

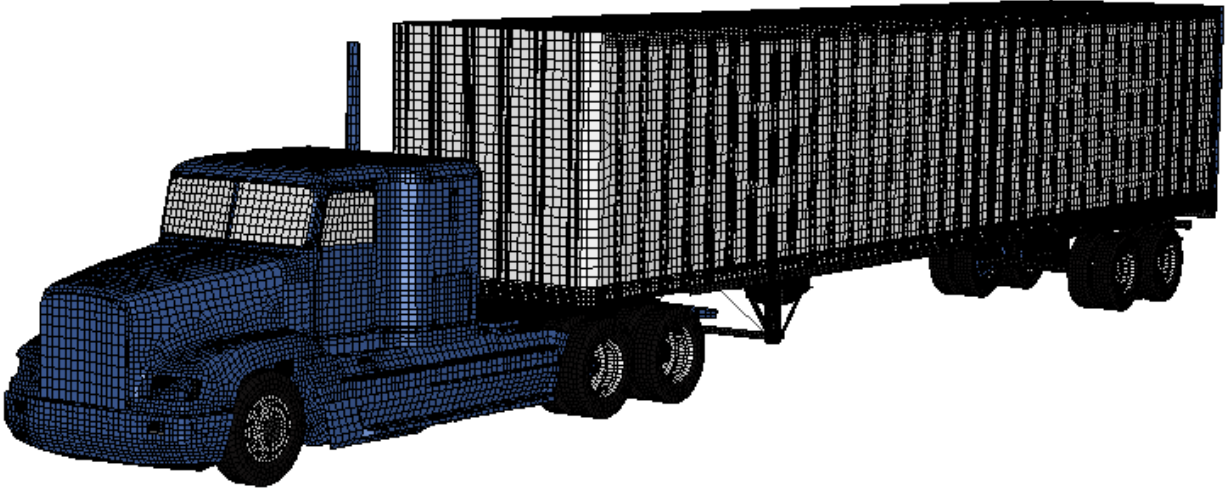


Figure 86. NCAC/Battelle tractor-semitrailer model. (147)

PIRT FOR THE TRACTOR-SEMITRAILER MODEL

The use of this model has so far been limited to re-directive impacts into rigid barriers (e.g., Report 350 Test 5-12 through about 1.70 seconds of impact). The research team believes that this tractor-semitrailer model is reasonably valid for this type of crash simulation and that it

will provide useful results in general barrier design evaluation work regarding impact loads and general vehicle-barrier interaction. The model has not been assessed for use in other applications, such as high-energy impacts (e.g., full frontal impact with bridge pier), vehicle dynamics (e.g., vehicle response due to steer maneuvers), or vehicle-to-vehicle impacts to name a few. The model user must critically assess the results obtained from the model in all cases, but especially for applications that the model has not been validated for.

In the development of the model, several components were validated by simulating physical tests that were conducted on those components (or subassembly of components) and comparing results. The components of the tractor that have been validated are all related to the front and rear suspension components and are listed in the preliminary PIRT shown in Table 46.

Table 46. Phenomenon Importance Ranking Table for Tractor-Semitrailer Model (Case 4).

No.	Validated Phenomenon	Test Description	Validated? Verified? Calibrated?
1.	Front Leaf-Spring Suspension	Uniaxial load vs. displacement	Validated
2.	Suspension Displacement Limiter	Uniaxial load/unload vs. displacement	Validated
3.	Rear Shock Absorbers	Uniaxial sinusoidal displacement tests to measure load-velocity time history data at various displacement rates	Calibrated
4.	Front Shock Absorbers	Uniaxial sinusoidal displacement tests to measure load-velocity time history data at various displacement rates	Calibrated
5.	Rear "Air-Bag" Suspension	Compression/extension tests at various load rates and bag pressures	Validated
6.	Front Suspension U-Bolts	Uniaxial load vs. displacement to failure	Calibrated

For example, in the development of the front leaf spring model, a leaf spring assembly for a 1992 Freightliner FLD120 tractor was purchased from a local Freightliner dealer. A laboratory test was conducted to measure the force/velocity response of the leaf spring assembly using a MTS uni-axial machine. The test and test setup are shown in Figure 87.



Figure 87. Laboratory Test of a 1992 Freightliner FLD120 Leaf-spring Suspension (Case 4).

The modeled geometry of the components of the leaf spring assembly was created by digitizing the physical components and generating a three dimensional rendering of the part using Pro-Engineer™ CAD software, as shown in Figure 88.

The leaf spring was then meshed using thin shell elements. The taper of the leaves was accounted for in the model in a piecewise manner, as shown in the exploded view in Figure 89. Each colored segment was defined as a separate part in the model and a representative thickness was assigned to each segment based on the average thickness of the segment (measured from the physical component).

An analysis was conducted to validate the stiffness of the leaf-spring model based on a comparison with the laboratory test results. The boundary and loading conditions were modeled based on the test fixture used in the laboratory test, as shown in Figure 91.



Figure 88. Digitized three dimensional geometry of the 1992 Freightliner FLD 120 suspension (Case 4).

Thin Shell Approach

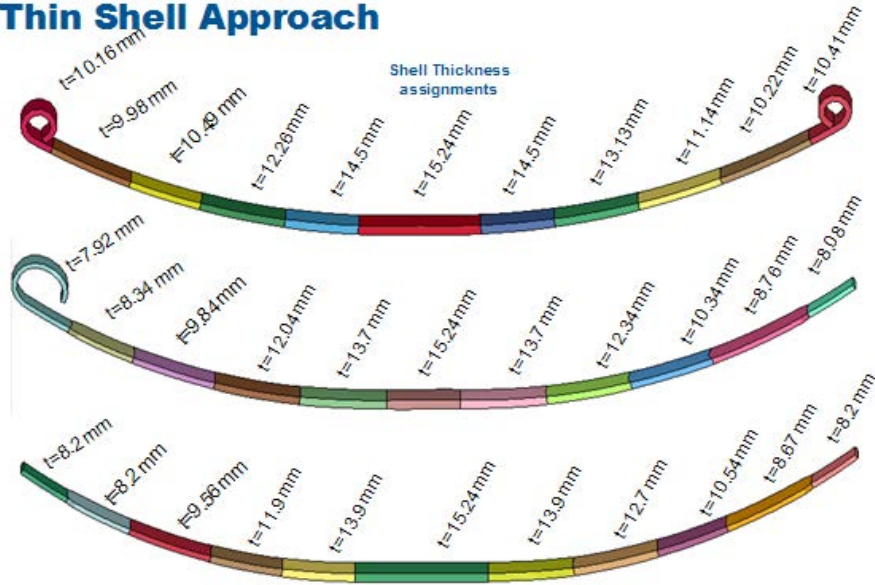


Figure 89. Exploded view of leaf-spring thin shell model (Case 4).

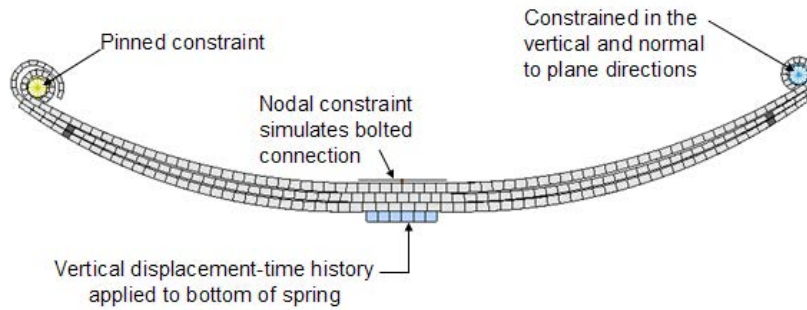


Figure 90. Finite element model for validating leaf-spring stiffness response.

The finite element model of the leaf-spring was modeled with two different mesh densities for comparison: 1) nominal element size = 20 mm and 2) nominal element size = 10 mm. The load was applied to the model in the finite element analysis dynamically, whereas the load was applied at a quasi-static rate in the physical test. Consequently, the results of the simulation were somewhat “noisy” at the beginning of the analysis but tended to damp out as the load increased. A comparison of the model results to the experimental results are shown in Figure 91.

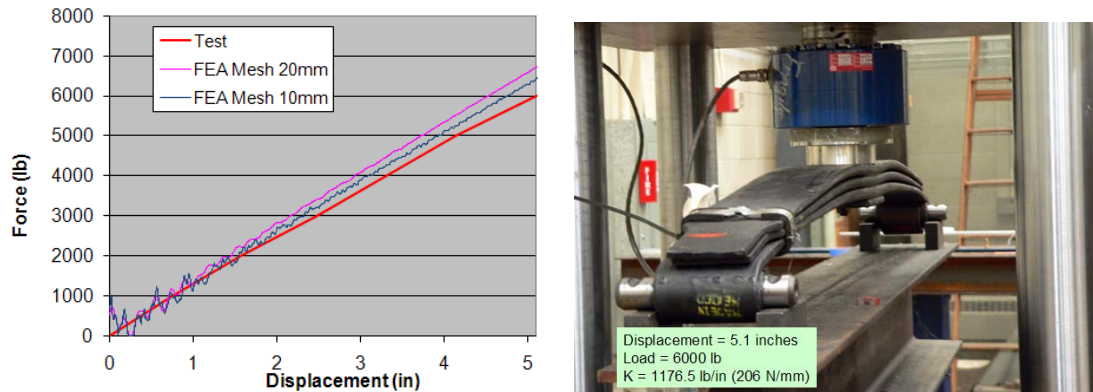


Figure 91. Force-displacement Response of Leaf Spring from Test and FEA

The RSVVP program was used to quantify the similarity between the test and simulation. The results for the quantitative assessment of the leaf spring suspension are shown in Table 47. The more refined mesh yielded better agreement, although the ANOVA metric for the mean residual error was higher than the recommended maximum value of 0.05. It is assumed that the difference in load rate between the test and simulation significantly affected the ANOVA metrics since the ANOVA is sensitive to “noise.” The overall response of the models was slightly more stiff than the response measured in the physical test. The more refined mesh (i.e., 10-mm elements) yielded better agreement with the test and it is expected that the response would continue to approach that of the test with further mesh refinement. This indicates that the material properties, geometric dimensions, and element thicknesses were accurate, and that the error was due to mesh refinement.

Table 47. Metric Evaluation Table for Leaf Spring Response (Case 3 Vehicle PIRT).

<i>Sprague-Geers Metrics</i>	M	P	Pass?
• <i>Force-Displacement History (Element Size 20 mm)*</i>	11.3	0.9	Y
• <i>Force-Displacement History (Element Size 10 mm)</i>	5.9	1.1	Y
<i>ANOVA Metrics</i>	Mean	Std.D.	Pass?
• <i>Force-Displacement History (Element Size 20 mm)*</i>	0.06	0.04	N
• <i>Force-Displacement History (Element Size 10 mm)</i>	0.03	0.03	Y
General Comparisons	Test	FEA	Error
• Stiffness (lb/in) – Element Size 20 mm*	1176	1317	12%
• Stiffness (lb/in) – Element Size 10 mm	1176	1262	7.3%

* Element size used in tractor model

The details of the component validation for the remaining phenomena listed in Table 46 can be found in the NTRCI project reports. A summary of the validation of each phenomenon in the tractor-trailer vehicle PIRT can be found in Appendix C7.

PIRT FOR THE MEDIAN BARRIER MODEL

In this case the objective was to validate the vehicle model. As such, the test selected for the validation was one that involved minimal or zero deflection of the barrier during impact, which ensured that any discrepancies between the simulated and test results were due to errors in the vehicle model and not the barrier model. Considering the simple nature of the rigid concrete barrier there were no tests were performed to validate any of its components (i.e., concrete blocks and connections); the geometric dimensions of the barrier model, however, were verified to be consistent with those of the test article. As a consequence, the PIRT table for the barrier model could not be filled out. The top of the concrete barrier was not flat, but shaped as shown in Figure 93.

VALIDATION OF THE TRACTOR-SEMITRAILER FINITE ELEMENT MODEL

The performance of the tractor-semitrailer finite element model was evaluated by comparing simulation results to data obtained from full-scale crash test No. TL5CMB-2 conducted at the Midwest Roadside Safety Facility on July 12, 2007.(148) The crash test was conducted according to the testing guidelines of NCHRP Report 350 for Test Level 5 impact conditions. The test involved a 36,153-kg (79,705-lb) tractor-semitrailer vehicle impacting a concrete median barrier at 84.9 km/hr (52.7 mph) and an impact angle of 15.4 degrees. The test vehicle was a 1991 White GMC tractor with a 1988 Pines 14.6-m (48-ft) semitrailer. The test article was a 1.067 m (42 inches) tall concrete median barrier with an installation length of 60.9 m (200 ft).

The simulation was conducted by Battelle in May 2009 with model No. TT090518_RUN1_200ms-approach-SP. The impact conditions for the numerical analysis were consistent with those used in the full-scale crash test. The simulation vehicle was the tractor model, Trac_Day_v1a_090506, and the semitrailer model, SemiTrailer48_090520. A summary of the test and simulation information is provided in Table 48 . This information was also documented on the Cover Page and in Part I of the validation report shown in Appendix C7.

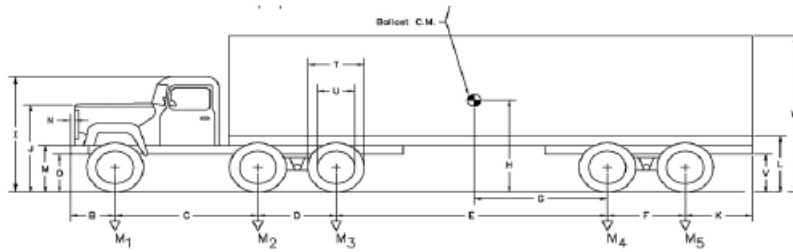
Table 48. Summary of the test and simulation impact conditions for Case 4.

General Information	Known Solution	Analysis Solution
Performing Organization	MwRSF	WPI/Battelle
Test/Run Number:	TL5CMB-2	TT090518_RUN1_200ms-approach-SP
Vehicle:	1991 White/GMC Tractor 1988 Pines 48-ft Trailer	01aTrac_Day_v1a_090506.k 02aSemiTrailer48_090520.k
Impact Conditions		
Vehicle Mass:	36,154 kg	36,200 kg
Speed:	84.9 km/hr	84.9 km/hr
Angle:	15.5 degrees	15.5 degrees

This version of the tractor model was modified from the original model. The geometry of the tractor finite element model was modified such that the wheelbase of the model was the same as the wheelbase of the test vehicle used in MwRSF Test No. TL5CMB-2. In particular, a section of the sleeper-cabin was removed to make the tractor model a day-cab style tractor, and the wheelbase length of the model was adjusted by removing a section of the frame rails (along with other components in this section of the model). The geometric and mass inertial properties of the modified tractor-semitrailer model are compared to those of the test vehicle in Figure 92. The most notable differences between the test vehicle and modified finite element model are listed below:

- The length dimensions of the finite element model were all within two percent of the test vehicle dimensions, except for the distance from the front bumper to the center of the front wheel (e.g., dimension “B” in Figure 92.), which was 13.5% shorter in the finite element model.
- The trailer floor in the finite element model was 148 mm (5.8 inches) higher than the test vehicle (e.g., dimension “L” in Figure 92.), and the top of the trailer in the finite element model was 169 mm (6.7 inches) lower than the test vehicle (e.g., dimension “W” in Figure 92.).
- The center of gravity of the ballast in the finite element model was located 600 mm (23.6 inches) rearward of and 188 mm (4.6 inches) higher than the c.g. location of the ballast in the test vehicle.
- The suspension system on the finite element trailer model was the Airide™ design, and the suspension on the trailer test vehicle was a leaf-spring design.

In the qualitative assessment, the general response of the modified finite element model compared well to test TL5CMB-2; the model results replicated the basic timing and magnitudes of phenomenological events that occurred in the full-scale test. Figure 93 shows a comparison of sequential views of the test and simulation.



Vehicle Geometry -mm

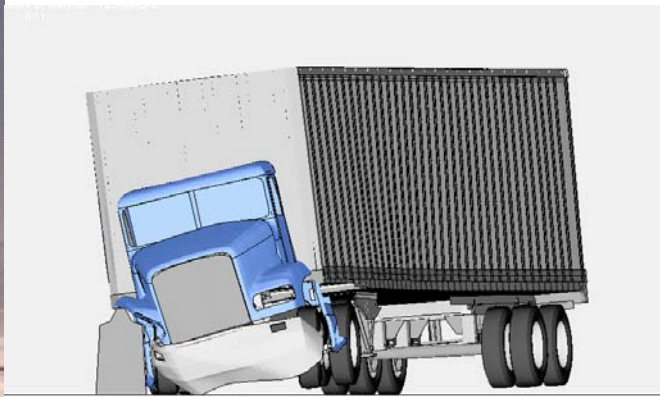
Test Vehicle	FE Model	Error %	Test Vehicle	FE Model	Error %	Test Vehicle	FE Model	Error %	Test Vehicle	FE Model	Error %				
A	2,604	2,636	1.2	G	5,906	5,307	-10.1	N	584	518	-11.3	T	1,016	1,004	-1.2
B	1,314	1,136	-13.5	H	1,831	1,949	6.4	O	2,007	1,929	-3.9	U	597	592	-0.8
C	3,270	3,280	0.3	J	1,746	1,734	-0.7	P	1,842	1,906	3.5	V	781	926	18.6
D	1,334	1,265	-5.2	K	1,575	1,552	-1.5	Q	1,981	2,045	3.2	W	4,064	3,895	-4.2
E	10,185	10,188	0.0	L	1,156	1,304	12.8	R	533	460	-13.7				
F	1,257	1,245	-1.0	M	902	726	-19.5	S							

Mass -Properties

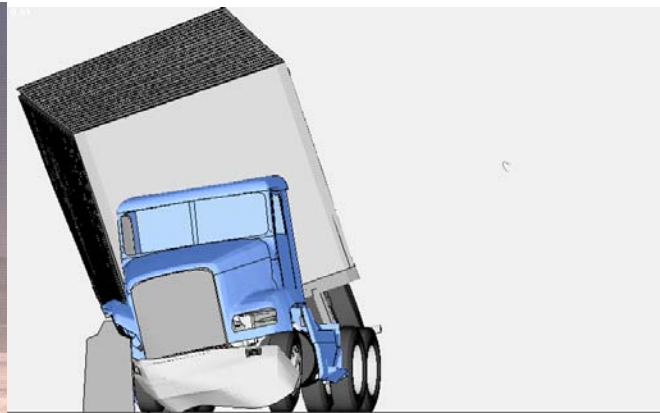
		Curb			Test Inertial			Gross Static		
		Test Vehicle	FE Model	Error %	Test Vehicle	FE Model	Error %	Test Vehicle	FE Model	Error %
M_1	(kg)	3,973	-	-	4,441	4,040	-9.0	4,441	4,040	-9.0
$M_2 + M_3$	(kg)	5,144	-	-	17,017	17,570	3.2	17,017	17,570	3.2
$M_4 + M_5$	(kg)	3,955	-	-	14,696	14,590	-0.7	14,696	14,590	-0.7
M_{Total}	(kg)	13,073	13,100	0.2	36,154	36,200	0.1	36,154	36,200	0.1
I_{11}	(kg - m ²)	-	16,020	-	-	31420	-	-	31420	-
I_{22}	(kg - m ²)	-	474,300	-	-	863,200	-	-	863,200	-
I_{33}	(kg - m ²)	-	473,800	-	-	866,300	-	-	866,300	-

Figure 92. Comparison of finite element vehicle model dimensions to those of the test vehicle for Case 4.

Time = 0.4 seconds



Time = 0.8 seconds

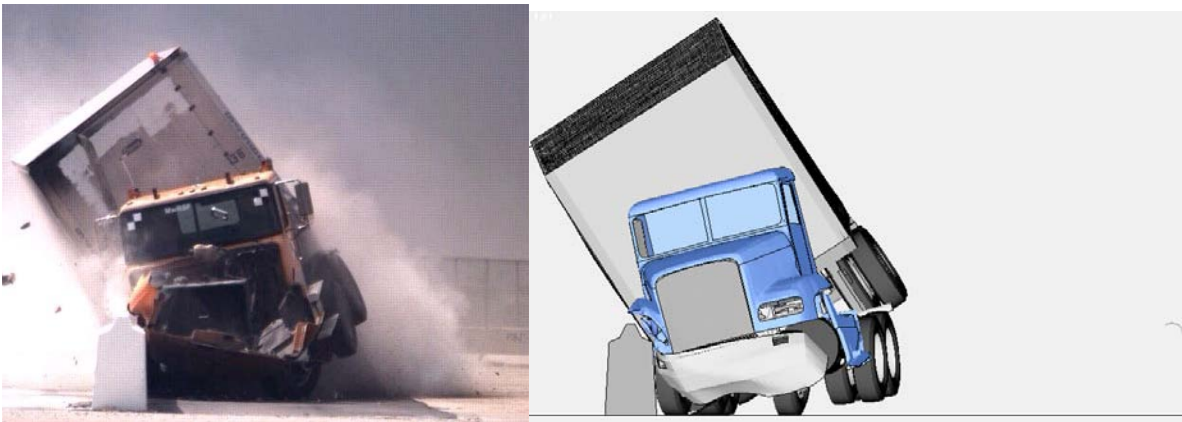


Time = 1.2 seconds



Figure 93. Summary of Phenomenological Events that Occurred during Full-scale Test and Finite Element Model Simulation in Case 4.

Time = 1.4 seconds



Time = 1.7 seconds



Figure 93. Summary of Phenomenological Events that Occurred during Full-scale Test and Finite Element Model Simulation in Case 4. (continued)

Part I - Solution Verification

The next step in the validation process is to perform global checks of the analysis to verify that the numerical solution is stable and is producing physical results. (e.g., results conform to the basic laws of conservation). The analysis was modeled as a closed system; therefore, the total energy should remain constant throughout the analysis and should be equal to the initial kinetic energy of the impacting vehicle. It is typical to expect some error in the analysis due to numerical inaccuracies in element formulation, contact definitions, mass-scaling, etc. It is therefore necessary to ensure that the errors are sufficiently small so that they have minimal effect on the solution. Table 49 shows a summary of the global verification assessment based on criteria recommended in the procedures for verification and validation discussed in Chapter 4.

Table 49. Summary of Global Energy Checks for Case 4.

Verification Evaluation Criteria	Change (%)	Pass?
Total Energy of the analysis solution (i.e., kinetic, potential, contact, etc.) must not vary more than 10 percent from the beginning of the run to the end of the run. <ul style="list-style-type: none"> Sliding Interface Energy was the source of the increase in total energy 	10	YES
Hourglass Energy of the analysis solution at the end of the run is less than 5 percent of the total initial energy at the beginning of the run.	0.1	YES
Hourglass Energy of the analysis solution at the end of the run is less than <i>ten percent</i> of the total <i>internal energy</i> at the <i>end</i> of the run.	0.6	Yes
The part/material with the highest amount of hourglass energy at any time during the run is less than five percent of the total initial energy at the beginning of the run.	0.02	Yes
Mass added to the total model is less than five percent of the total model mass at the beginning of the run.	0.0	Yes
The part/material with the most mass added had more than 10 percent of its initial mass added*. <ul style="list-style-type: none"> - Weld elements connecting trailer side panels to vertical posts - 200 kg (added) /50 kg (initial) 	400	NO*
The moving parts/materials in the model have less than five percent of mass added to the initial moving mass of the model.	0.0	Yes
There are shooting nodes in the solution?	No	Yes
There are solid elements with negative volumes?	No	Yes

* Part 7803 are weld elements used to connect the trailer's outer side panels to the vertical support posts. These connector elements are relatively "rigid" and the mass added is considered insignificant to the overall mass of the parts to which they connect.

The additional mass added to the weld elements was considered acceptable by the model developers. The solution meets all other recommended global energy balance criteria and appears to be free of any major numerical problems. Thus, the verification assessment for Part I was entered as "Yes" on the cover page of the validation report.

Part II - Quantitative Evaluation

Next, the RSVVP computer program was used to compute the Sprague & Geers metrics and ANOVA metrics using time-history data from the known (i.e., physical test) and analysis data. The number, type, and location of the electronic data recorders (EDRs) vary from test to test. The most common EDR locations are: 1) inside the tractor cabin near the center of gravity

of the tractor, 2) on the tractor near the fifth-wheel, 3) at the front of the trailer near the king-pin, 4) at the center of gravity of the trailer ballast, and 5) on the trailer near the trailer tandem axle.

The translational accelerations and rotational velocities of the vehicle model were collected at 16 locations on the tractor-semitrailer. The test vehicle was instrumented with only two triaxial accelerometers: one located near the tractor fifth-wheel and another located on the floor of the semitrailer near the trailer's tandem axle. Due to technical issues that caused the EDR on the tractor's fifth-wheel to start recording prematurely, the only quantitative data recorded in the full-scale test was from the accelerometer set located at the rear of the trailer. This location is consistent with accelerometer No. 16 in the numerical model, as illustrated in Figure 94.

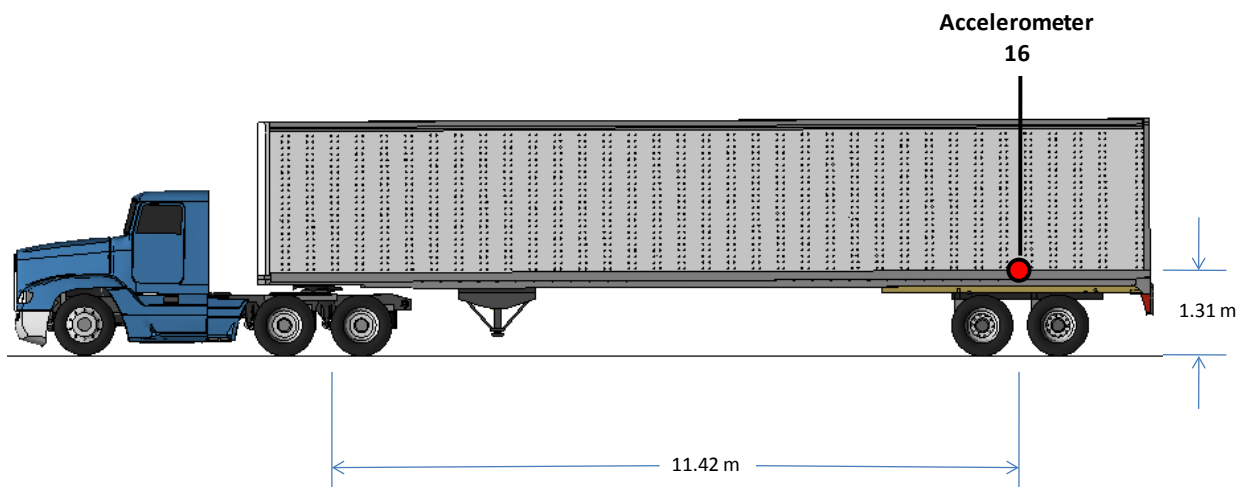


Figure 94. EDR locations and nomenclature used in test report for Case 4.

The multi-channel option in RSVVP was used to compute metrics for each individual channel as well as for the weighted composite of the combined channels. The raw acceleration data from each of the three data channels collected on the semitrailer were input into RSVVP. The data was then filtered in RSVVP using a CFC class 180 filter. The shift and drift options in RSVVP were not used. Each of the curve pairs were synchronized using the minimum absolute area of residuals option in RSVVP.

For the metrics evaluation options in RSVVP, the default metrics (i.e., Sprague & Geers and ANOVA) were selected. The “Whole Time Window Only” option was also selected which directed RSVVP to evaluate the curves over the complete time history of available data, which in this case was 1.54 seconds. The time-history data collected in the analysis was actually for a time period 1.67 seconds, but due to the synchronization of the curves in RSVVP, the analysis time was shifted back slightly.

Figure 95 through Figure 98 show the time histories that were used to compute the metrics and the 50-millisecond average acceleration-time history for each pair of data. The results of the evaluation for the individual channels are shown in Table 50. Based on the Sprague & Geers metrics, the x-acceleration and z-acceleration were out of phase with the test, but the magnitudes of acceleration were in very good agreement with the test for all channels. The ANOVA metrics also indicated that the simulation was in good agreement with the test for all channels.

Table 50. Roadside safety validation metrics rating table for Case 4 – (single channel option).

Evaluation Criteria							Time interval [0 sec; 1.54 sec]					
O <i>Sprague-Geer Metrics</i> List all the data channels being compared. Calculate the M and P metrics using RSVVP and enter the results. Values less than or equal to 40 are acceptable.												
	RSVVP Curve Preprocessing Options						M	P	Pass?			
	Filter Option	Sync. Option	Shift		Drift							
			True Curve	Test Curve	True Curve	Test Curve						
X acceleration	CFC 180	Min. area of Residuals	N	N	N	N	12.4	48.5	N			
Y acceleration	CFC 180	Min. area of Residuals	N	N	N	N	13.5	31.4	Y			
Z acceleration	CFC 180	Min. area of Residuals	N	N	N	N	12.8	47.1	N			
P <i>ANOVA Metrics</i> List all the data channels being compared. Calculate the ANOVA metrics using RSVVP and enter the results. Both of the following criteria must be met: <ul style="list-style-type: none"> The mean residual error must be less than five percent of the peak acceleration ($\bar{e} \leq 0.05 \cdot a_{Peak}$) and The standard deviation of the residuals must be less than 35 percent of the peak acceleration ($\sigma \leq 0.35 \cdot a_{Peak}$) 							Mean Residual	Standard Deviation of Residuals	Pass?			
X acceleration/Peak										0.02	0.10	Y
Y acceleration/Peak										0.0	0.08	Y
Z acceleration/Peak										0.0	0.14	Y

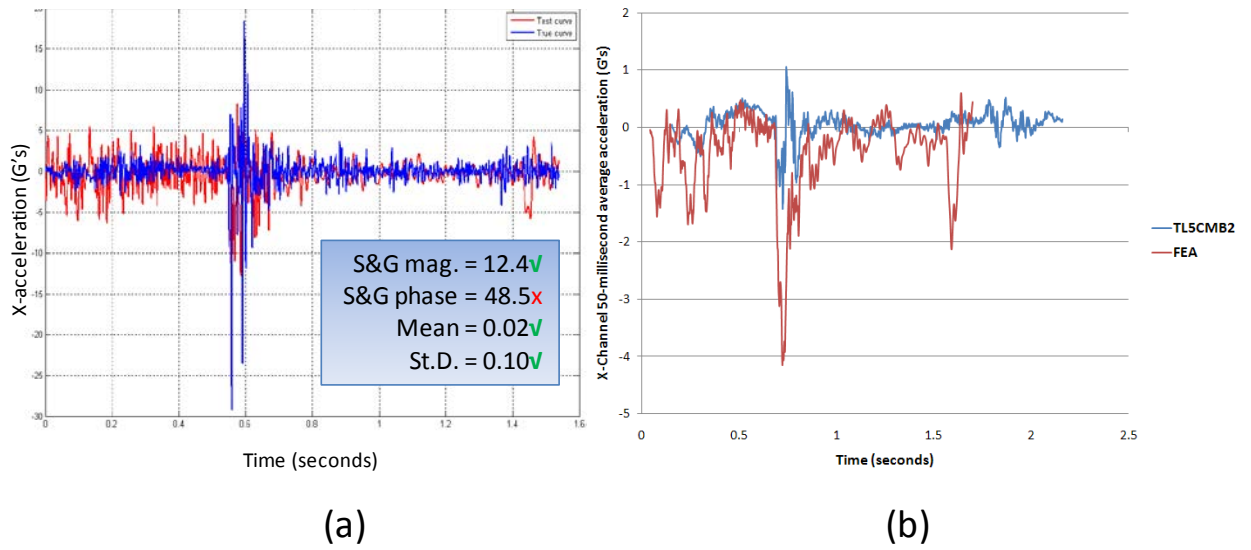


Figure 95. X-channel (a) acceleration-time history data used to compute metrics and (b) 50-millisecond average acceleration -time history data for Case 4.

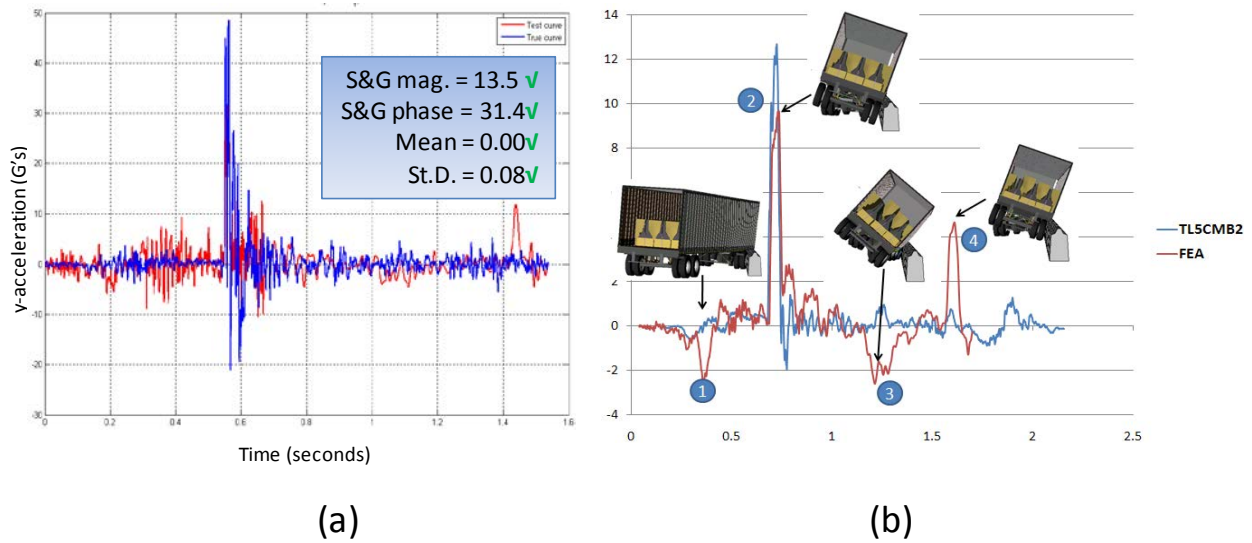


Figure 96. Y-channel (a) acceleration-time history data used to compute metrics and (b) 50-millisecond average acceleration -time history data for Case 4.

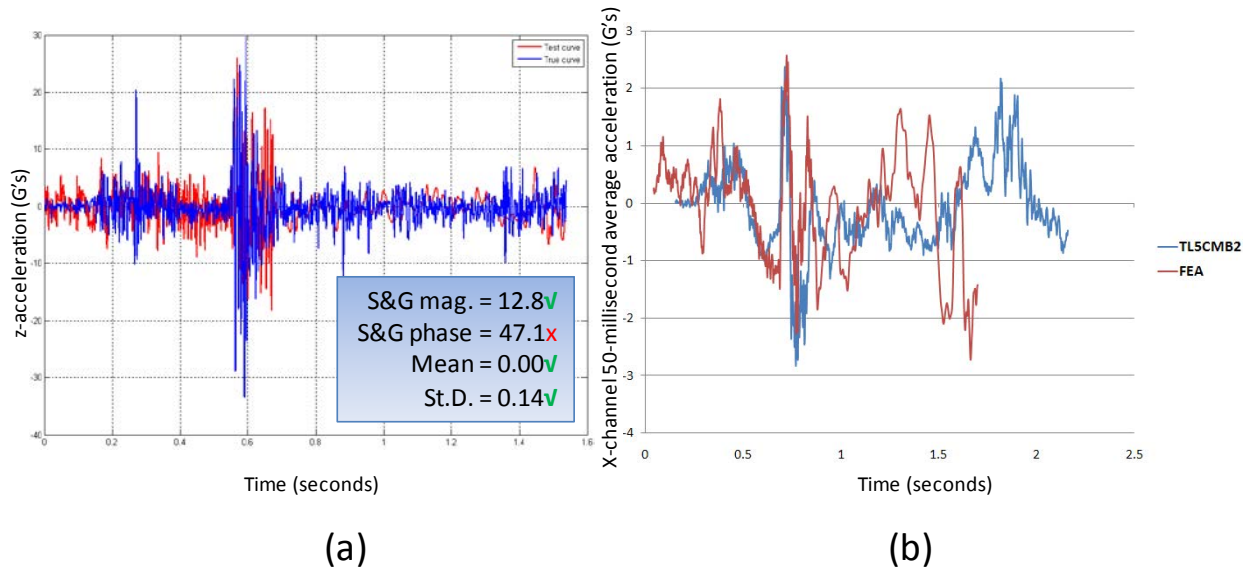


Figure 97. Z-channel (a) acceleration-time history data used to compute metrics and (b) 50-millisecond average acceleration-time history data for Case 4.

Since the metrics computed for the individual data channels did not all satisfy the acceptance criteria, the multi-channel option in RSVVP was used to calculate the weighted Sprague & Geers and ANOVA metrics for the six channels of data. Table 50 shows the results from RSVVP for the multi-channel option. RSVVP weights the relative importance of each channel based on the total area under the curve. The resulting weight factors computed for each channel are shown in both tabular form and graphical form in Table 51. The y-channel dominates the kinematics of the impact event, which can be verified by comparison of the acceleration magnitudes from the 50-ms average acceleration-time history plots.

Table 51. Roadside safety validation metrics rating table for the Case 4 – (multi-channel option).

Evaluation Criteria (time interval [0 sec; 1.54 sec])									
Channels (Select which was used)									
<input checked="" type="checkbox"/> X Acceleration	<input checked="" type="checkbox"/> Y Acceleration	<input checked="" type="checkbox"/> Z Acceleration							
<input type="checkbox"/> Roll rate	<input type="checkbox"/> Pitch rate	<input type="checkbox"/> Yaw rate							
Multi-Channel Weights -Area (II) Method-	X Channel – 0.038 Y Channel – 0.640 Z Channel – 0.322								
	O <i>Sprague-Geer Metrics</i> Values less or equal to 40 are acceptable.			<table border="1"> <thead> <tr> <th>M</th> <th>P</th> <th>Pass?</th> </tr> </thead> <tbody> <tr> <td>13.2</td> <td>37.1</td> <td>Y</td> </tr> </tbody> </table>	M	P	Pass?	13.2	37.1
M	P	Pass?							
13.2	37.1	Y							
P	<i>ANOVA Metrics</i> Both of the following criteria must be met: <ul style="list-style-type: none"> The mean residual error must be less than five percent of the peak acceleration ($\bar{e} \leq 0.05 \cdot a_{Peak}$) The standard deviation of the residuals must be less than 35 percent of the peak acceleration ($\sigma \leq 0.35 \cdot a_{Peak}$) 		<table border="1"> <thead> <tr> <th>Mean Residual</th> <th>Standard Deviation of Residuals</th> <th>Pass?</th> </tr> </thead> <tbody> <tr> <td>0.00</td> <td>0.10</td> <td>Y</td> </tr> </tbody> </table>	Mean Residual	Standard Deviation of Residuals	Pass?	0.00	0.10	Y
	Mean Residual	Standard Deviation of Residuals	Pass?						
0.00	0.10	Y							

The weighted metrics computed in RSVVP in the multi-channel mode all satisfy the acceptance criteria, and therefore the time history comparison can be considered acceptable. The validation assessment for Part II should be entered as “Yes” on the cover page of the validation report.

Part III - Validation of Crash Specific Phenomena

The last step in the validation procedure is to compare the phenomena observed in both the crash test and the numerical solution. Table 52 contains the Report 350 crash test criteria with the applicable test numbers. The criteria that apply to test 5-12 (e.g., corresponding to this particular test case) are marked with a red square. These include criteria A, D, F, L and M.

Table 52. Evaluation Criteria Test Applicability Table for Case 4.

Evaluation Factors	Evaluation Criteria			Applicable Tests	
Structural Adequacy	A	Test article should contain and redirect the vehicle; the vehicle should not penetrate, under-ride, or override the installation although controlled lateral deflection of the test article is acceptable.		10, 11, 12, 20, 21, 22, 35, 36, 37, 38	
	B	The test article should readily activate in a predictable manner by breaking away, fracturing or yielding.		60, 61, 70, 71, 80, 81	
	C	Acceptable test article performance may be by redirection, controlled penetration or controlled stopping of the vehicle.		30, 31,, 32, 33, 34, 39, 40, 41, 42, 43, 44, 50, 51, 52, 53	
Occupant Risk	D	Detached elements, fragments or other debris from the test article should not penetrate or show potential for penetrating the occupant compartment, or present an undue hazard to other traffic, pedestrians or personnel in a work zone.		All	
	E	Detached elements, fragments or other debris from the test article, or vehicular damage should not block the driver’s vision or otherwise cause the driver to lose control of the vehicle. (Answer Yes or No)		70, 71	
	F	The vehicle should remain upright during and after the collision although moderate roll, pitching and yawing are acceptable.		All except those listed in criterion G	
	G	It is preferable, although not essential, that the vehicle remain upright during and after collision.		12, 22 (for test level 1 – 30, 31, 32, 33, 34, 35, 36, 37, 38, 39, 40, 41, 42, 43, 44)	
	H	Occupant impact velocities should satisfy the following:			10, 20, 30,31, 32, 33, 34, 36, 40, 41, 42, 43, 50, 51, 52, 53, 80, 81
		Occupant Impact Velocity Limits (m/s)			
		Component	Preferred	Maximum	
Longitudinal and Lateral	9	12	60, 61, 70, 71		
Longitudinal	3	5	10, 20, 30,31, 32, 33, 34, 36, 40, 41, 42, 43, 50, 51, 52, 53, 60, 61, 70, 71, 80, 81		
Occupant ridedown accelerations should satisfy the following:					
Occupant Ridedown Acceleration Limits (g’s)					
Component	Preferred	Maximum			
Longitudinal and Lateral	15	20	11,21, 35, 37, 38, 39		
L	The occupant impact velocity in the longitudinal direction should not exceed 40 ft/sec and the occupant ride-down acceleration in the longitudinal direction should not exceed 20 G’s.				
Vehicle Trajectory	M	The exit angle from the test article preferable should be less than 60 percent of test impact angle, measured at the time of vehicle loss of contact with test device.		10, 11, 12, 20, 21, 22, 35, 36, 37, 38, 39	
	N	Vehicle trajectory behind the test article is acceptable.		30, 31, 32, 33, 34, 39, 42, 43, 44, 60, 61, 70, 71, 80, 81	

Angular-rate data was not collected in test TL5CMB-2. However, the high-speed videos, TL-5 CMB-2 aos3.avi and TL-5 CMB-2 aos-4.avi, from the full-scale test were used to measure the approximate roll-time history of the trailer at time intervals of 0.2 seconds. The roll-time history of the trailer in the simulation compares very well to the roll-time history measured from the high-speed test video, regarding both timing and magnitude, as shown in Figure 98. The

analysis terminated prematurely at 1.67 seconds of the impact event, but at the time of termination the simulation was showing approximately the same behavior (e.g., roll position and roll-rate) of the trailer as was measured from the test videos.

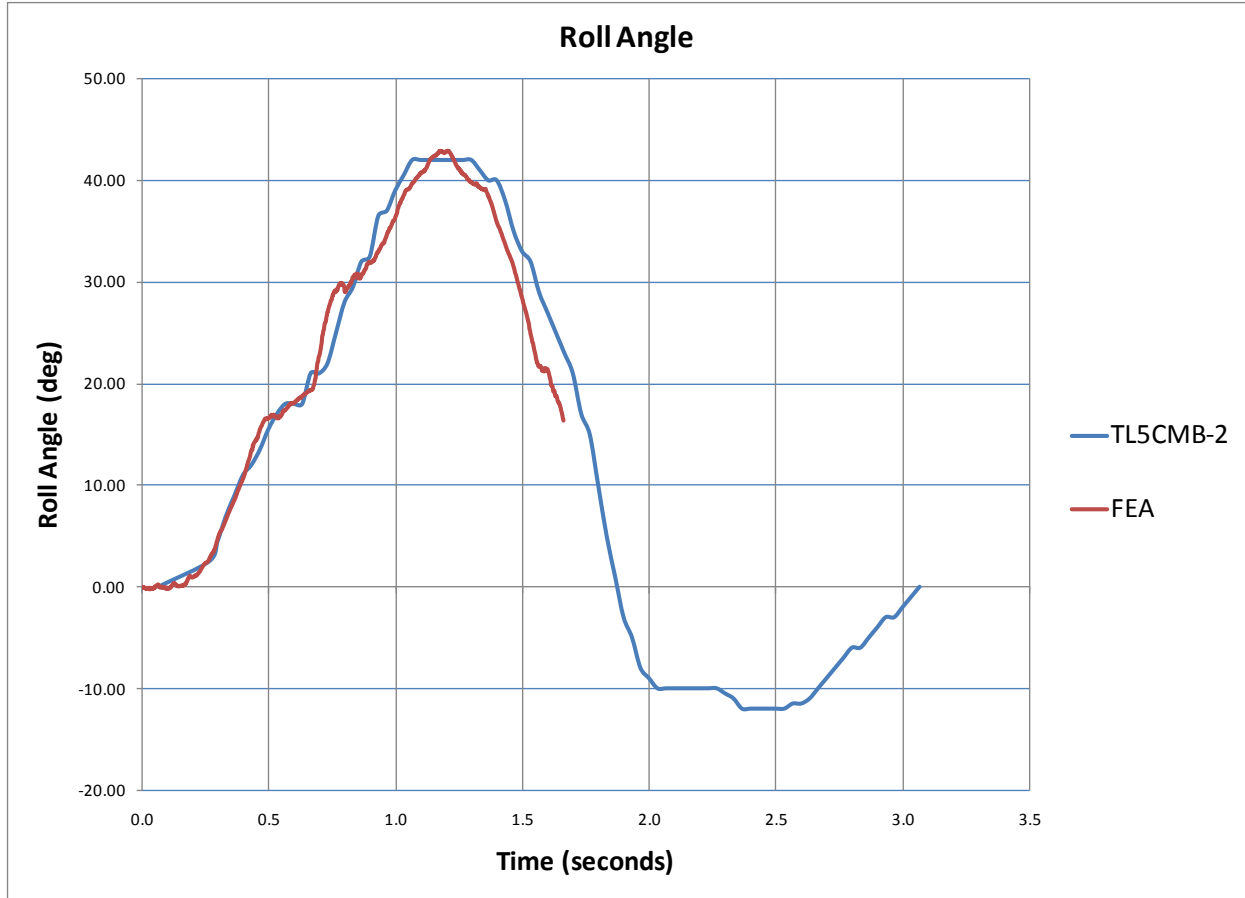


Figure 98. Roll angle-time history plot for the tractor-semitrailer test case.

Table 53 through Table 55 contain a list of the crash test evaluation phenomena including additional specific phenomena that were measured in the test and that could be directly compared to the numerical solution. Table 53 contains a comparison of phenomena related to structural adequacy. Table 54 addresses occupant risk and phenomena related to vehicle trajectory. Table 55 provides a list of other phenomenological events and their time of occurrence for both the full-scale crash test and the finite element simulation.

In this particular analysis, structural adequacy (e.g., ability of barrier to contain and redirect the vehicle) was not really an issue. The primary focus of the analysis was to assess the performance of the tractor model for simulating the impact load and kinematic response of the vehicle. The deflection of the barrier in the test was negligible; therefore, the barrier was modeled as rigid to ensure no deflection of the barrier during the crash event. Since the barrier was modeled as rigid, criterion D could not be assessed (i.e., occupant compartment penetration

and hazard to other traffic, pedestrians or personnel in a work zone caused by detached elements, fragments or other debris from the barrier).

All the applicable criteria in Table 53 through Table 55 agree. The timing of phenomenological events in Table 55 also compared very well between the simulation and test with only a few exceptions. The validation assessment for Part III should, therefore, be entered as “Yes” on the cover page of the validation report. Since the model has been validated for each part of the validation procedure, it can now be considered valid for use in assessing the performance of longitudinal barriers, regarding impact loads and general vehicle-barrier interaction.

Table 53. Structural Adequacy Phenomena for Case 4.

		Evaluation Criteria	Known Result	Analysis Result	Relative Diff. (%)	Agree?	
Structural Adequacy	A	A1	Test article should contain and redirect the vehicle; the vehicle should not penetrate, under-ride, or override the installation although controlled lateral deflection of the test article is acceptable. (Answer Yes or No)	Yes	Yes	X	YES
		A2	Maximum dynamic deflection: - Relative difference is less than 20 percent or - Absolute difference is less than 0.15 m	0	0	0 % 0 m	YES
		A3	Length of vehicle-barrier contact: - Relative difference is less than 20 percent or - Absolute difference is less than 2 m	full-barrier	N.A.*	30% 3 m	N.A.
		A4	The relative difference in the number of broken or significantly bent posts is less than 20 percent.	N.A.	N.A.	0	N.A.
		A5	The rail element ruptured or failed (Answer Yes or No)	N.A.	N.A.	X	N.A.
		A6	There were failures of connector elements (Answer Yes or No).	N.A.	N.A.	X	N.A.
		A7	There was significant snagging between the vehicle wheels and barrier elements (Answer Yes or No).	No	No	X	YES
		A8	There was significant snagging between vehicle body components and barrier elements (Answer Yes or No).	No	No	X	YES

* FE vehicle was still in contact with the barrier at time of analysis termination

Table 54. Occupant Risk Phenomena for Case 4.

Evaluation Criteria		Known Result	Analysis Result	Difference Relative/Absolute	Agree?		
Occupant Risk	D	Detached elements, fragments or other debris from the test article should not penetrate or show potential for penetrating the occupant compartment, or present an undue hazard to other traffic, pedestrians or personnel in a work zone. (Answer Yes or No)	Pass	Pass		N.A.*	
	G1	It is preferable, although not essential, that the vehicle remain upright during and after collision. (Answer Yes or No)	Pass	Pass		YES	
	G	G2	Maximum roll of the vehicle: - Relative difference is less than 20 percent or - Absolute difference is less than 5 degrees.	42°	42.8°	2 % 0.8°	YES
		G3	Maximum pitch of the vehicle is: - Relative difference is less than 20 percent or - Absolute difference is less than 5 degrees.	Not measured			
	G4	Maximum yaw of the vehicle is: - Relative difference is less than 20 percent or - Absolute difference is less than 5 degrees.	15.5°	15.5°	0% 0°	YES	
Vehicle Trajectory	M1	The exit angle from the test article preferable should be less than 60 percent of test impact angle, measured at the time of vehicle loss of contact with test device.	Yes	Yes		YES	
	M2	Exit angle at loss of contact: - Relative difference is less than 20 percent or - Absolute difference is less than 5 degrees.	15.5°	15.5°	0% 0°	YES	
	M	M3	Exit velocity at loss of contact: - Relative difference is less than 20 percent or - Absolute difference is less than 10 m/s.				
		M4	One or more vehicle tires failed or de-beaded during the collision event (Answer Yes or No).	Yes	N/A		-
	M5	One or more tires separated from the vehicle (Answer Yes or No).	No	N/A		-	

*The barrier was modeled as rigid; therefore criterion D could not be assessed.

Table 55. Comparison of Phenomenological Events for Case 4.

Event	Test Time (seconds)	FE model Time (seconds)	Relative Diff. (%)	Agree?
Tractor begins to yaw	0.024	0.02 - 0.03	0	YES
U-bolt connecting front axle to right-side leaf spring broke	unknown	0.09 – 0.1		
Left-front tire lifts off pavement	0.144	0.10 - 0.11	24	NO
Right-front corner of trailer contacted the top protrusion of the barrier	0.186	0.17 - 0.18	3	YES
Trailer started to roll toward the barrier	0.190	0.19 - 0.200	0	YES
Left-rear tires were lifted off the ground	0.2	0.21 - 0.22	0	YES
The right front corner of the trailer was vertically coincident with the back face of the barrier	0.260	0.26 - 0.27	0	YES
Both left-rear trailer tires were lifted off the ground	0.356	0.25 - 0.26	27	NO
Tractor was parallel to barrier	0.394	0.32 - 0.33	16	YES
Tractor reached peak roll and began to roll back from the barrier	0.290 – 0.364 (≈15 deg.)	0.29 - 0.30 (14.6 deg.)	0	YES
Left-front tractor tires returned to roadway surface	0.468	0.34 - 0.35	25	NO
U-bolt connecting front axle to left-side leaf spring broke	unknown	0.34 - 0.35		
Trailer was parallel to barrier	0.648	0.63 - 0.64	1	YES
Tractor rolled back to level position	0.650	0.74 - 0.75	14	YES
Rear trailer tandem contacts barrier	0.656	0.65 - 0.66	0	YES
Time of maximum impact force between trailer tandem and barrier	0.72	0.71 - 0.72	0	YES
Tractor started to roll toward the barrier	0.776	0.80 - 0.81	3	YES
Tractor left-front tire again lifted from the roadway	0.956	N/A (u-bolts broken)		
Trailer reached maximum roll and began to roll back from the barrier All left side tires were off the ground	1.150 (≈42 deg.)	1.19 - 1.20 (42.8 deg.)	3	YES
Tractor again reached peak (maximum) roll angle	0.994 (≈19 deg.)	1.16 - 1.17 (23.8 deg.)	17	YES
Left-front tire returned to the roadway surface	1.294	N/A		
Tractor left side tandems returned to roadway surface	1.652	1.52 - 1.53	7	YES
Analysis Terminated		1.67		
Trailer left side tires returned to roadway surface	1.800	-		

CONCLUSION

The four test cases described in this chapter provide step-by-step examples for how to document the capabilities of the roadside hardware and vehicle models in a PIRT and how to make the comparison between a full-scale test and simulation and document the results of the comparison in a verification and validation report. These examples have also shown that comparing real tests to finite element simulations can sometimes be a challenge. Sometimes all the data from the full-scale test is not available, sometimes it was not collected or the instrumentation failed. In some cases, the differences between the actual vehicle models and the vehicles used in the test may be too different for a good comparison. The purpose of performing the comparison is to develop a quantifiable assessment of the validity and utility of the models. Some of the comparisons described in the chapter were very good, whereas some others could not be considered validated. For the cases where validation could not be established, the analyst can go back and re-examine the model knowing exactly what aspect of the model is not predicting the results of the crash test correctly. Improvements and modifications can be made to the model and a new comparison with the improved model can then be made. Similarly, sometimes the experimental data is not complete or the post-processing methods are unclear. The analyst and test engineer should work to resolve the differences if at all possible. It may sometimes be necessary to run a full-scale crash test experiment in order to ensure that all the needed data is collected for the comparison.

The purpose of the procedures described in this report and the examples provided in this chapter is to establish a common language for discussing the degree of similarity between tests and numerical results. There will also be “grey” areas or phenomena and criteria that require some engineering judgment to resolve but these procedures place the comparison task on a firm foundation of quantifiable and objective criteria.

CHAPTER 7 CONCLUSIONS

Computational analysis tools and capabilities have expanded rapidly in the last decade making analyses that were considered too large, costly and complex only a few years ago to be economically feasible. While crash test costs have continued to increase, computational analysis costs have remained more stable while the fidelity and complexity that can be addressed in numerical solutions has increased many fold. Computational analyses are expected to continue to be a valuable tool in assessing roadside hardware designs; in fact, the use of computational analyses is today a standard feature of most roadside hardware design and crash testing activities. The same trend is taking place all across the mechanical design field from fields as diverse as automotive and aircraft design to the design of consumer products like cell phones, razor blades and packaging.

As computational analyses have become more integrated into the design process so too is the importance of establishing objective, quantifiable validation methods and criteria. While analysts have always compared numerical and experimental results, the techniques used have generally been visual and subjective. For the results of computational analysis to be used in acceptance decisions, it is necessary to use methods that are objective, numerical and quantifiable in order that decisions may be fair, impartial and consistent. The objective of this project was to develop objective procedures for assessing the validity of computational analyses in the area of roadside hardware performance and, in particular, for cases where incremental improvements are being assessed for possible acceptance. Chapters 1 and 2 reviewed the literature regarding verification and validation in the general computational mechanics literature as well as a detailed description of the roadside safety computer simulation literature. Validation and verification processes were discussed and compared and metrics for validation and verification were described, compared and contrasted. A survey was performed to elicit the opinions of practitioners and researchers with experience in the use of LS-DYNA in roadside safety research and the results were presented as a representation of best practices currently used in computational roadside safety in Chapter 3. Chapter 4 presented general procedures that can be used to perform these types of acceptance assessments, Chapter 5 discussed the development and use of a computer tool, RSVVP, which largely automates much of the assessment work. Examples of how the procedures would work using real-life practical cases were presented in Chapter 6.

The findings in this report are a starting point for establishing a way to talk about validation of computational models in roadside safety and the repeatability of full-scale crash testing. The findings in this report and the RSVVP software will help to encourage analysts to examine and present their analysis results in this standardized format. Crash testing procedures have evolved over the past 50 years resulting in five or six potential procedures for performing and analyzing full-scale crash tests. As testing and sensor technology improved and the range of activities requiring testing expanded, changes to the crash testing guidelines were made accordingly. The same will undoubtedly occur with these validation procedures as the roadside safety computational mechanics community gains experience and confidence in analyzing roadside hardware impacts. Likewise, decision makers will gain insight and experience that will likely improve these procedures further. What is important, however, is to start the process by using these procedures so that community experience can be captured, refined and incorporated in roadside hardware acceptance decisions.

REFERENCES

- 1 Turner, M. J., Clough, R.W., Martin, H. C., and Topp, L. J., "Stiffness and Deflection Analysis of Complex Structures," *Journal of the Aeronautical Sciences*, Vol. 23 (1956) pp. 805-823.
- 2 Argyris, J. H., "Energy Theorems and Structural Analysis," Butterworth Publications, London, U.K. (1954).
- 3 Clough, R.W., and Wilson, E., "History of the Finite Element Method at Berkeley," in *Proceedings of the Fifth U.S. National Congress on Computational Mechanics*, Boulder (CO), USA (Aug. 4-6, 1999).
- 4 Belytschko, T., Liu, W. K., and Moran, B., "Nonlinear Finite Elements for Continua and Structures", John Wiley & Sons, LTD, Chichester, UK (2000).
- 5 Argyris, J. H., "Elasto-Plastic Matrix Displacement Analysis of Three-Dimensional Continua," *Journal of the Royal Aeronautical Society*, Vol. 69 (1965) pp. 633-635.
- 6 Powell, G.H., "General Computer Program for Analysis of Automobile Barriers," in *Highway Research Record No. 343*, Highway Research Board, Washington, D.C. (1971).
- 7 Giavotto, V., Puccinelli, L., and Astori, P. C., "Vehicle Dynamics and Crash (Vedyac)," SPAT, Milan, (1972).
- 8 Hallquist, J. O., "Preliminary User's Manuals for DYNA3D and DYNAP (Nonlinear Dynamic Analysis of Solids in Three Dimensions)," *Report No. UCID-17268*, University of California, Lawrence Livermore National Laboratory, (1976).
- 9 Ray, M. H., "The Use of Finite Element Analysis in Roadside Hardware Design," *International Journal of Crashworthiness*, Vol. 2, No 4 (1997) pp. 333 - 348, Woodhead Publishing, London, UK.
- 10 Plaxico, C.A., Ray, M.H., Hiranmayee, K., "Impact Performance of the G4(1W) and G4(2W) Guardrail Systems Comparison Under NCHRP Report 350 Test 3-11 Conditions", *Transportation Research Record 1720*, Transportation Research Board, Washington, D.C. (2000) pp 7-18.
- 11 European Committee of Standardization, "European Standard EN 1317-1 and EN 1317-2: Road Restraint Systems," CEN (1998).
- 12 Sango, F., and Haukass, M., "Evaluation of Small car vehicle model – GM_R2," *Robust Document No. ROBUST-5-005/TR-2004-0107*, Norwegian Public Roads Administration, January 2006.

- 13 Federal Aviation Administration, "Methodology for dynamic seat certification by analysis for use in parts 23, 25, 27 and 29 airplanes and rotorcraft," *Advisory Circular No. 20-146*, FAA, Washington, D.C. (19 May 2003).
- 14 European Committee of Standardization, "Railway Applications – Crashworthiness Requirements for Railway Vehicles Bodies," *European Standard prEN 1527 (Draft)* (April 2005).
- 15 American Institute of Aeronautics and Astronautics, "Guide for the Verification and Validation of Computational Fluid Dynamics Simulations," *AIAA-G-077-1998*, AIAA, Reston, VA (1998).
- 16 Oberkampf, W. L., Trucano, T. G., and Hirsch, C., "Verification, Validation and Predictive Capability in Computational Engineering and Physics," *In the Proceedings of Verification and validation for Modeling and Simulation in Computational Science and Engineering Applications*, Johns Hopkins University, Applied Physics Laboratory, Laurel, MD (October 22, 2002).
- 17 American Society of Mechanical Engineers (Performance Test Code Committee, PTC-60), "Guide for Verification and Validation in Computational Solid Mechanics," *American National Standard V&V 10-2006*, ASME, New York (2006).
- 18 Johnson, W., "Impact Strength of Materials," Edward Arnold Publishers LTD, London, UK (1972).
- 19 Kolsky, H., "Stress Waves in Solids", Clarendon Press, Oxford, UK (1953).
- 20 Ross, H. E. Jr., Sicking, D. L., Zimmer, R. A., and Michie, J. D., "Recommended Procedures for the Safety Performance Evaluation of Highway Features," *National Cooperative Highway Research Program (NCHRP) Report 350*, Transportation Research Board, Washington, D.C. (1993).
- 21 Invernizzi, F., Poggi, S., Tirelli, M., "Helicopter Fuel Tank Crashworthiness: Numerical Approach for the Design," Politecnico di Milano, Milano, Italy (2007).
- 22 Kokkins, S., Kong, W., and Kasturi, K., "Locomotive Crashworthiness Research: Modeling, Simulation, and Validation," Foster-Miller, Incorporated, Federal Railroad Administration (2001).
- 23 Zhao, Y., *et al.*, "The use of FEA Nonlinear Model to Determine the In-vivo Cardiac Pacing Lead Coils for Fatigue Analysis", *In Proceedings of 2003 Summer Bioengineering Conference*, Sonesta Beach Resort in Key Biscayne, Florida (June 25-29, 2003).
- 24 McMahan, C., and Zhao, Y., "Modeling Implantable Medical Device-Interactions," *In Proceedings of 2003 ABAQUS User's Conference*, Vienna, Austria (2003).
- 25 Didoszak, J. M., Shin, Y. S., and Lewis, D. H., "Shock Trial Simulation for Naval Ships," Naval Postgraduate School, Monterey, CA (2003).

- 26 Plaxico, C.A., Kennedy, J.C. Jr., and Miele, C.R., "Analysis of Plastic Safety System's CrashGard Sand Barrel System," *Final Report*, Battelle Memorial Institute, Columbus, OH (January 2007).
- 27 Basu, S., Haghghi, A., "Numerical Analysis of Roadside Design (NARD) vol. III: Validation Procedure Manual," *Report No. FHWA-RD-88-213*, Federal Highway Administration, Virginia (1988).
- 28 Ray, M. H., and Hiranmayee, K., "Quantitative Evaluation of the Fidelity of Public-Domain Vehicle Models for Roadside Hardware Research," *unpublished paper*, (1998).
- 29 Tabiei, A., and Wu, J., "Validated Crash Simulation of the Most Common Guardrail System in the USA," *International Journal of Crashworthiness*, Vol. 5, No. 2 (2000) pages 153 - 168.
- 30 Atahan, A.O., and Cansız, Ö.F., "Impact Analysis of a Vertical Flared Back Bridge Rail-to-Guardrail Transition Using Simulation," *Finite Elements in Analysis and Design*, Vol. 41, No. 4 (2005) pp. 371-396.
- 31 Geers, T. L., "An Objective Error Measure for the Comparison of Calculated and Measured Transient Response Histories," *The Shock and Vibration Bulletin Part 2 – Ship Shock, shock and Blast and Ground Shock*, The shock and vibration center at Naval Research Laboratory, Washington D.C. (June 1984).
- 32 Schwer, L. E., "Validation Metrics for Response Histories: Perspectives and Case Studies," *Engineering with Computers*, Vol. 23, No. 4 (Special issue in Verification and Validation) (2007) pp. 295 - 309, Springer-Verlag, London, UK.
- 33 Russell, D. M., "Error Measures for Comparing Transient Data: part I: Development of a Comprehensive Error Measure," *In Proceedings of the 68th shock and vibration symposium*, Hunt Valley, MD (1997) pp 175–184.
- 34 Shin, Y. S., and Schneider, N., "Ship Shock Trial Simulation of USS Winston S. Churchill (DDG81): Modeling and Simulation Strategy and Surrounding Fluid Volume Effects," *In Proceedings of the 74th Shock and Vibration Symposium*, San Diego CA (27-31 October, 2003).
- 35 Ray, M. H., "Repeatability of Full-Scale Crash Tests and a Criteria for Validating Finite Element Simulations," *Transportation Research Record No. 1528*, Transportation Research Board, Washington, D.C. (1996).
- 36 Oberkampf, W. L., and Barone, M. F., "Measures of Agreement Between Computation and Experiment: Validation Metrics," *Journal of Computational Physics*, Vol. 217, No. 1 (Special issue: Uncertainty quantification in simulation science) (2006) pp 5–36.
- 37 Bayarri, M. J., Berger, J. O., Kennedy, M. C., Kottas, A., Paolo, R., and Sacks, J., "Bayesian Validation of a Computer Model for Vehicle Crashworthiness", *Technical Report 163*, National Institute of Statistical Sciences, (July 23, 2005).

- 38 Mahadevan, S., and Rebba, R., "Validation of Reliability Computational Models Using Bayesian Networks," *Reliability Engineering and System Safety*, Vol. 87, No. 5 (2005) pp. 223-232.
- 39 Favarelli, L., "Stochastic Finite Elements for Crash Problems," *Structural Safety*, Vol. 8, No. 1-4 (July 1990) pp. 113–130.
- 40 Patzner, G.S., Plaxico, C.A., and Ray, M.H., "Effects of Post and Soil Strength on Performance of Modified Eccentric Loader Breakaway Cable Terminal," *Transportation Research Record 1690*, Transportation Research Board, Washington D.C. (1999).
- 41 Ray, M.H., and Silvestri, C., "Development of a Finite Element Model of the Knee-Thigh-Hip of a 50th Percentile Male Including Ligaments and Muscles," *International Journal of Crashworthiness*, (pending) (2007).
- 42 Ray, M.H., Hiranmayee, K., and Kirkpatrick, S., "Performance Validation of two Side Impact Dummies," *International Journal of Crashworthiness*, Vol. 4, No. 3 (1999) pp. 287-303, Woodhead Publishing Limited, London, UK.
- 43 Anghileri, M., Mongiardini, M., "Round Robin Concrete Barrier," *Robust Document No. ROBUST-05-012*, Politecnico di Milano, October 2005.
- 44 Brown, C. M., "Ford Festiva Center Impacts with a Narrow Fixed Object (Rigid Pole)," *Report FHWA-RD-95-040*, Federal Highway Administration, U.S. Department of Transportation (1995).
- 45 Orengo, F., Ray M. H., and Plaxico, C. A., "Modeling Tire Blow-out in Roadside Hardware Simulations Using LSDYNA," *In Proceedings IMECE'03, 203 ASME International Mechanical Engineering Congress and Exposition*, Paper IMECE2003-44057 (November 2003).
- 46 Wright, A. E., and Ray, M. H., "Characterizing Guardrail Steel for LSDYNA3D Simulations," *Transportation Research Record No. 1528*, Transportation Research Board, Washington, D.C. (1996) pp 138-145.
- 47 Gentry, T.R., and Bank, L.C., "Finite-Element Modeling and Model Verification of Steel W-Beam Guardrails Subject to Pendulum Impact Loading," *Transportation Research Record 1647*, Transportation Research Board, Washington, D.C. (1998).
- 48 Tabiei, A., "Experimental and Numerical Simulation of the Use of Fiber Reinforced Composite Materials for Roadside Safety Applications," *Publication no FHWA-RD-96-026*, US Department of Transportation, McLean, VA, (1997).
- 49 Eskandarian, A., Marzougui, D., and Bedewi, N. E., "Finite Element Model and Validation of a Surrogate Crash Test Vehicle for Impacts with Roadside Objects," *International Journal of Crashworthiness*, Vol. 2, No. 3 (1997) pp. 239 - 258.
- 50 Langseth, M., Hopperstad, O. S., and Berstad, T., "Crashworthiness of Aluminum Extrusions: Validation of Numerical Simulation, Effect of Mass Ratio and Impact

- Velocity,” *International Journal of Impact Engineering*, Volume 22, No. 9-10 (October 1999) pp. 829-854.
- 51 Borvik, T., “Finite Element Analysis of Ductile Failure in Structural Steel Subjected to Multiaxial Stress States and High Strain rates,” *In Proceedings of the 3th European LSDYNA User's Conference*, Paris, France (2001).
- 52 Du Bois, P. A., Kolling, S., and Fassnacht, W., “Modeling of Safety Glass for Crash Simulation,” *Computational Materials Science*, Volume 28, No 3-4, (November 2003) pp. 675-683.
- 53 Timmel, M., Kolling, S., Osterrieder, P., and Du Bois, P. A., “A Finite Element Model for Impact Simulation with Laminated Glass,” *International Journal of Impact Engineering*, Volume 34, No 8 (August 2007) pp. 1465-1478.
- 54 Du Bois, P. A., Koesters, M., Frank, T., and Kolling, S., “Crashworthiness Analysis of Structures Made from Polymers,” *In Proceedings of the 3th LSDYNA Forum*, Bamberg, Germany (2004).
- 55 Sun, D.Z., Andrieux, F., Ockewitz, A., Klamser, H., and Hogenmüller, J., “Modeling of the Failure Behaviour of Windscreens and Component Tests,” *In Proceedings of the 4th LSDYNA Forum*, Bamberg, Germany (2005).
- 56 Atahan, A.O., and Ross, H.E. Jr., “Computer Simulation of Recycled Content Guardrail Post Impacts,” *ASCE Journal of Transportation Engineering*, Vol. 130, No. 6 (2004) pp. 485-496.
- 57 Lewis, B.A., “Manual for LSDYNA Soil Material Model 147,” *Report No. FHWA-HRT-04-095*, Federal Highway Administration, Washington, D.C. (2004).
- 58 Murray, Y.D., “Theory and Evaluation of Concrete Material Model 159,” *In Proceedings of the 8th International LSDYNA User's Conference*, Dearborn, Michigan, (2004).
- 59 Murray, Y.D., Reid, J.D., Faller, R.K., Bielenberg, B.W., and Paulsen, T.J., “Evaluation of LSDYNA Wood Material Model 143,” *Report No. FHWA-HRT-04-096*, Federal Highway Administration, Washington D.C. (2005).
- 60 Reid, J. D., Coon, B. A., Lewis, B. A., Sutherland, S. H., and Murray, Y. D., “Evaluation of LSDYNA Soil Material Model 147,” *Report No. FHWA-HRT-04-094*, University of Nebraska, Lincoln; APTEK, Incorporated; Federal Highway Administration, Washington, D.C. (2004).
- 61 Tong, X., and Tuan, C. Y., “Viscoplastic Cap Model for Soils under High Strain Rate Loading,” *J. of Geotechnical and Geoenvironmental Engineering*, Vol. 133, No. 2 ((February 2007) pp. 206-214.
- 62 Murray, Y. D., “Users Manual for LSDYNA Concrete Material Model 159,” *Publication No. FHWA-HRT-05-062*, US Department of Transportation, Federal Highway Administration National Transportation Systems Center; Federal Highway Administration (May 2007).

- 63 Miele, C. R., Plaxico, C. A., Kennedy, J. C., Simunovic, S., and Zis, N., "Heavy Vehicle Infrastructure Asset Interaction and Collision," *Cooperative Agreement No. DTFH61-03-X-00030*, Federal Highway Administration, Washington, D.C. (September 2005).
- 64 Haufe, A., Du Bois, P. A., Kolling, S., and Feucht, M., "On the Development, Verification and Validation of a Semi-Analytical Model for Polymers Subjected to Dynamic Loading," *In Proceedings of the International Conference on Adaptive Modeling and Simulation*, ADMOS, Barcelona, Spain (2005).
- 65 Wood, P. K., Schley, C. A., Kenny, S., and Dutton, T., "Validating Material Information for Stochastic Crash Simulation Part 1 - Quasi static properties," *In Proceedings of the 5th European LSDYNA Conference*, Birmingham, UK (2005).
- 66 Dietemberger, M., Büyük, M., and Kan, C.D., "Development of a High Strain-Rate Dependent Vehicle Model," *In Proceedings of the 4th LSDYNA Forum*, Bamberg, Germany (2005).
- 67 Gerhard, S., Gavin, V., and Virenda, C., "Model Material Validation of a High Efficiency Energy Absorbing Foam," *In Proceedings of the 5th German LSDYNA Forum*, Ulm, Germany (2006).
- 68 Blankenhorn, G., Muller, I., Siebert, A., and Schweizerhof, K., "On the Numerical Analysis of a Carillon Bell Using LSDYNA with a Specific View on Model Validation," *In Proceedings of the 5th German LSDYNA Forum*, Ulm, Germany (2006).
- 69 Walker, B., "A New Generation of Crash Barrier Models for LSDYNA," *In Proceedings of the 9th International LSDYNA Users Conference*, Dearborn, Michigan (2006).
- 70 Wood, P. K., Buckley, M., Walker, B., and Dutton, T., "Validating Dynamic Tensile Mechanical Properties of Sheet Steels for Automotive Crash Applications," *In Proceedings of the 6th European LSDYNA Conference*, Gothenburg, Sweden (2006).
- 71 Sheikh, N.M., Bligh, R.P., Bullard, D.L., Buth, C.E., Alberson, D.C., Abu-Odeh, A.Y., and Ross, H.E. Jr., "Development of an Energy Absorbing End Terminal for Open Box Beam Guardrail," *In Proceedings of the 9th International LSDYNA Users Conference*, Dearborn, Michigan (2006).
- 72 Shoukry, S. N., and Fahmy, M., "Validation of 3D FE Analysis of Rigid Pavement Dynamic Response to Moving Traffic and Nonlinear Temperature Gradient Effects," *International Journal of Geomechanical Engineering*, Vol. 7, No. 1 (January/February 2007) pp. 16-24.
- 73 Horstemeyer, M. F., Li, H., Siervogel, J., Kwasniewski, L., Wekezer, J. W., Christian, B., and Roufa, G., "Material Characterization and Connection Testing for Crash Analysis of Paratransit Buses," *International Journal of*

- Crashworthiness*. In press (manuscript number: IJCR.184, accepted: March 12, 2007).
- 74 Mendis, K, Mani, A, and Shyu, S-C, "Finite Element Crash Models of Motor Vehicles," *Report FHWA-RD-94-151*, Federal Highway Administration, Washington, D.C. (July, 1994).
- 75 Cofie, E., and Ray, M. H., "Finite Element Model of a Small Automobile Impacting a Rigid Pole," *Report FHWA-RD-94-151*, Federal Highway Administration, Washington, D.C. (1995).
- 76 Thacker, J. G., Reagan, S. W., Pellettiere, J. A., Pilkey, W. D., Crandall, J. R., and Sieveka, E. M. "Experiences During the Development of a Dynamic Crash Response Automobile Model," *Finite Elements in Analysis and Design*, Vol. 30, No. 4 (1998) p. 279-295.
- 77 Anghileri, M., and Mongiardini, M., "Geo Metro Finite Element Model (GM_R3): Improvements of Steering System and Suspensions," *Robust Document No. ROBUST-05-006*, Politecnico di Milano (January 2005).
- 78 Sango, F., "Evaluation of Small Car – RM_R1 – Prepared by Politecnico di Milano," *Robust Document No. ROBUST-5-002/TR-2004-0039*, Norwegian Public Roads Administration (January 2006).
- 79 Zaouk, A.K., and Marzougui, D., "Development and Validation of a US Side Impact Moveable Deformable Barrier FE Model," *In Proceedings of the 3th European LSDYNA User's Conference*, Paris, France (2001).
- 80 Zaouk, A.K., Bedewi, N.E., Kan, C.D., and Marzougui, D., "Validation of a Non-Linear Finite Element Vehicle Model Using Multiple Impact Data," *In Proceedings of the 1996 ASME International Mechanical Engineering Congress and Exposition*, Atlanta, GA (1996) pp. 91–106.
- 81 Zaouk, A. K., Bedewi, N. E., Kan, C. D., and Marzougui, D., "Development and Evaluation of a C-1500 Pickup Truck Model for Roadside Hardware Impact Simulation," *Report Number FHWA-RD-96- 212*, FHWA Vehicle Crash Analysis, Federal Highway Administration, Washington, D.C. (1997).
- 82 Marzougui, D., Zaouk A., and Kan, C.D., "Development of a C-2500 Pick-Up Truck Model for Roadside Hardware Impact," *Transportation Research Board Annual Conference*, 1996.
- 83 Tiso, P., Plaxico, C. A., and Ray, M. H., "An Improved Truck Model for Roadside Safety Simulations: Part II -- Suspension Modeling," *Transportation Research Record No. 1797*, Transportation Research Board, Washington, D.C. (2002).
- 84 Marzougui, D., Zink, M., Zaouk, A..K, Kan, C. D., and Bedewi, N. E., "Development and Validation of a Vehicle Suspension Finite Element Model for

- Use in Crash Simulations,” *International Journal of Crashworthiness*, Vol. 9, No. 6 (2004) pp. 565-576.
- 85 Mohan, P., Marzougui, D., and Kan, C. D. S., “Validation of a Single Unit Truck Model for Roadside Hardware Impact,” *International Journal of Vehicle Systems Modelling and Testing*, Vol. 2, No.1 (2007) pp. 1-15.
- 86 Perneti, M, and Scalera, S., "Development of a Validated Finite Element Model of a Rigid Truck Suitable to Simulate Collisions Against Road Safety Barriers," *In Proceedings of the 6th European LSDYNA Conference*, Gothenburg, Sweden (2007).
- 87 Wekezer, J. W., Oskard, M. S., Logan, R. W., and Zywicz, E., "Vehicle Impact Simulation," *Journal of Transportation Engineering*, Vol. 199, No. 4 (July/August, 1993) pp. 598-617, New York, N.Y.
- 88 Ray, M. H., "Using Finite Element Analysis in Designing Roadside Hardware," *Public Roads*, Vol. 57, No. 4, Federal Highway Administration, Washington, D.C. (1994).
- 89 Ray, M. H., and Patzner, G. A., “A Finite Element model of the Modified Eccentric Loader Breakaway Cable Terminal (MELT),” *Report Number FHWA-RD-96- 212*, FHWA Vehicle Crash Analysis, Federal Highway Administration, Washington, D.C. (1997).
- 90 Munz, T., and Willam, K., “Finite Element Modeling of Vehicular Collision with Transformer Base Luminaire Support,” *Report FHWA-RD-96-212*, FHWA Vehicle Crash Analysis, Federal Highway Administration, Washington, D.C. (1997).
- 91 Plaxico, C. A., Hackett, R. M., and Uddin, W., “Finite Element Simulation of Vehicle Impact Against a Modified Thrie-Beam Guardrail,” *Report FHWA-RD-96-212*, FHWA Vehicle Crash Analysis, Federal Highway Administration, Washington, D.C. (1997).
- 92 Reid, J. D., “Simulation of Four Roadside Safety Applications,” *Report Number FHWA-RD-96- 212*, FHWA Vehicle Crash Analysis, Federal Highway Administration, Washington, D.C. (1997).
- 93 Abu-Odeh, A. Y., Bligh, R. P., and Ross, H. E. Jr., “Finite Element Analysis of a Slip-Base Luminaire Support,” *Report FHWA-RD-96-212*, FHWA Vehicle Crash Analysis, Federal Highway Administration, Washington, D.C. (1997).
- 94 B.F. Hendricks, Martin, O.S. and Wekezer, J. W., “Impact Simulation of the 820C Vehicle with the G2 Guardrail,” *Report FHWA-RD-96-212*, FHWA Vehicle Crash Analysis, Federal Highway Administration, Washington, D.C. (1996).
- 95 Martin, O. S., and Wekezer, J. W., “Crash Impact Analysis of the G2 Guardrail: a Validation Study,” In *Proceedings of the 77th Transportation Research Board Meeting*, Transportation Research Board (1998), Paper No. 98-0184.

- 96 Ray, M.H., Engstrand, K., Plaxico, C.A., and McGinnis, R.G., "Improvements to the Weak-Post W-Beam Guardrail," *Transportation Research Record 1743*, Transportation Research Board, Washington, D.C. (2001) pp 88-96.
- 97 Eskandarian, A., Marzougui, D., and Bedewi, N. E., "Impact Finite Element Analysis of Slip-Base Sign Support Mechanism," *Journal of Transportation Engineering*, Vol. 126, No. 2 (2000) pp. 143-153.
- 98 Marzougui, D., Kan, C. D., and Eskandarian, A., "Safety Performance Evaluation of Roadside Hardware Using Finite Element Simulation," *In Proceedings of the ASCE Fourteenth Engineering Mechanics Conference*, Austin, Texas (May 24, 2000).
- 99 Reid, J. D., Sicking, D. L., and Paulsen, G. W., "Design and Analysis of Approach Terminal Sections using Simulation," *Journal of Transportation Engineering*, Vol. 122, No 5 (1996) pp. 399-405.
- 100 Paulsen, G.W., and Reid, J.D., "Nonlinear Finite-Element Analysis of Dual Support Breakaway Sign," *Transportation Research Record 1528*, Transportation Research Board, Washington D.C. (1996) pp 146-154.
- 101 Ray, M. H., and Patzner, G. S., "Finite Element Model of a Modified Eccentric Loader Breakaway Guardrail Terminal," *Transportation Research Record 1599*, Transportation Research Board, Washington, D.C. (1997) pp 11-21.
- 102 Plaxico, C.A., Patzner, C.S., and Ray, M.H., "Finite Element Modeling of Guardrail Timber Posts and the Post-Soil Interaction," *Transportation Research Record 1647*, Transportation Research Board, Washington D.C. (1998) pp 139-146.
- 103 Reid, J. D., Sicking, D. L., Faller, R. K., Pfeifer, B. G., "Development of a New Guardrail System," *Transportation Research Record 1599*, Transportation Research Board, Washington, D.C. (1997).
- 104 Reid, J.D., and Sicking, D.L., "Design and Simulation of a Sequential Kinking Guardrail Terminal," *International Journal of Impact Engineering*, Vol. 21, No. 9 (1998) pp. 761-772.
- 105 Reid, J.D., and Bielenberg, B.W., "Using LSDYNA Simulation to Solve a Design Problem: Bullnose Guardrail Example," *Transportation Research Record 1690*, Transportation Research Board, Washington, D.C. (1999).
- 106 Marzougui, D., Mohan, P., Kan, S., and Opiela, K., "Evaluation of Rail Height Effects on the safety Performance of W-Beam Barriers," *In Proceedings of the 6th European LSDYNA User's Conference*, Gothenburg, Sweden (2007).
- 107 Marzougui, D., Bahouth, G., Eskandarian, A., Meczowski, L., and Taylor, H., "Evaluation of Portable Concrete Barriers Using Finite Element Simulation," *Transportation Research Record 1720*, Transportation Research Board, Washington, D.C. (2000) pp 1-6.

- 108 Bielenberg, B., Reid, J.D., Faller, R.K., "Compliance Testing of a Bullnose
Median Barrier System," *Transportation Research Record 1743*, Transportation
Research Board, Washington, D.C. (2001) pp 60-70.
- 109 Marzougui, D., Meczkowski, L., Taylor, H., and Bedewi, N. E., "Sign Support
Height Analysis Using Finite Element Simulation," *International Journal of
Crashworthiness*, Vol. 6, No. 1 (2001) pp. 33-41.
- 110 Engstrand, K., Jansson, M., and Nilsson, L., "On Vehicle Impact on Roadside
Barrier," *In Proceedings of the 3th European LSDYNA User's Conference*, Paris,
France (2001).
- 111 Atahan, A.O., "Finite Element Simulation of a Strong-Post W-beam Guardrail
System," *Society for Computer Simulations*, Vol. 78, No. 10 (2002) pp 587-599.
- 112 Reid, J. D., Faller, R. K., Holloway, J. C., Rohde, J. R., and Sicking, D. L., "New
Energy-Absorbing High-Speed Safety Barrier," *Transportation Research Record
1851*, Transportation Research Board, Washington D.C. (2003) pp 53-64.
- 113 Bielenberg, R.W., "Modeling Crushable Foam for the SAFER Racetrack Barrier,"
In Proceedings of the 8th International LSDYNA User's Conference, Deaborn,
Michigan, (2004).
- 114 Ray, M. H., Oldani, E., and Plaxico, C. A., "Design and Analysis of an Aluminum
F-Shape Bridge Railing," *International Journal of Crashworthiness*, Vol. 9, No. 4
(2004) pp. 349-363.
- 115 Whitworth, H. A., Bendidi, R, Marzougui, D., and Reiss, R., "Finite Element
Modeling of the Crash Performance of Roadside Barriers," *International Journal
of Crashworthiness*, Vol. 9, No.1 (2004) pp. 35-43.
- 116 Mohan, P., Marzougui, D., Meczkowski, L., and Bedewi, N. E., "Finite Element
Modeling and Validation of a 3-Strand Cable Guardrail System," *International
Journal of Crashworthiness*, Vol. 10, No 3 (2005) pp. 267-273.
- 117 Tahan, F., Marzougui, D., Zaouk, A., Bedewi, N. E., Eskandarian, A., and
Meczkowski, L., "Safety Performance Evaluation of Secure Mailboxes Using
Finite Element Simulations and Crash Testing," *International Journal of
Crashworthiness*, Vol. 10, No. 4 (2005) pp. 341-349.
- 118 Sheikh, N.M., Alberson, D.C., and Bullard, D.L., "Development of a Hybrid
Energy Absorbing Reusable Terminal (HEART) for Roadside Safety
Applications," *In proceedings of the 84th Transportation Research Board
Meeting*, Washington, D.C. (2005), Paper No. 05-2571.
- 119 Atahan, A.O., "Finite Element Simulation of the New York Portable Concrete
Barrier with I-Shaped Connector," *Journal of Structural Engineering*, Vol. 132,
No. 3 (2006) pp 430-440.
- 120 Bonin, G., Cantisani, G., Loprencipe, G., and Ranzo, A., "Improvement of
Portable Concrete Barrier Design Using Computational Mechanics," *In*

- Proceedings of the 85th Transportation Research Board Meeting*, Washington, D.C. (2006), Paper No. 06-1797.
- 121 Plaxico, C. A., Kennedy, J. C. Jr., and Miele, C. R., “Evaluation and Design of ODOT’s Type 5 Guardrail with Tubular Backup,” *Report No. FHWA/OH-2006/4*, Battelle Memorial Institute, Columbus, Ohio, (February 2006).
- 122 Plaxico, C. A., Kennedy, J. C. Jr., and Miele, C. R., “Development of an NCHRP Report 350 TL-3 New Jersey Shape 50-inch Portable Concrete Barrier,” *Report No. FHWA/OH- 2006/16*, Battelle Memorial Institute, Columbus, Ohio (February 2006).
- 123 Anghileri, M., “Numerical Evaluation of Severity Indices for Finite Element Analysis,” *In proceedings of the 85th Transportation Research Board Meeting*, Washington, D.C. (2006)
- 124 Marzougui, D., Mohan, P., Kan, C.D.,and Opiela, K., “Performance Evaluation of Low Tension Three Strand Cable Median Barriers,” *In proceedings of the 86th Transportation Research Board Meeting*, Washington, D.C. (2007), Paper No. 07-3275.
- 125 Roh, Y. S., “Scaling Study of LS-DYNA MPP on High Performance Servers,” *In Proceedings of the 6th International LSDYNA User’s Conference*, Dearborn, Michigan (2000).
- 126 Roh, Y. S., Fong, H. F., “LS-DYNA Performance of UltraspacTM-II Servers and Workstations,” *In Proceedings of the 7th International LSDYNA User’s Conference*, 2001.
- 127 Cook, Robert D., *Finite Element Modeling for Stress Analysis*, John Wiley & Sons, Inc., New York, 1995.
- 128 Du Bois, Paul, NOTES, 1998
- 129 Plaxico, Chuck A., Design Guidelines for the Use of Curbs and Curb/Guardrail Combinations Along High-Speed Roadways, Ph.D. Dissertation, Worcester Polytechnic Institute, Worcester, MA, 2002.
- 130 Larsson, A., Pettersson, M. and Svensson, H., “User Manual: CurveAnalyzer v1.0,” Autoliv, 11 June 2003.
- 131 *MATLAB. User Guide*. The MathWorks Inc, The MathWorks, Inc., 3 Apple Hill Drive, Natick, MA 01760-2098, 1994-2008.
- 132 Ray, M. H., C.A. Plaxico, and K. Hiranmayee. Impact Performance of the G4(1W) and G4(2W) Guardrail Systems Comparison Under NCHRP Report 350Test 3-11 Conditions. *In Transportation Research Record: Journal of the Transportation Research Board, No. 1720*, Transportation Research Board of the National academies, Washington, D.C., 2000, pp. 7-18.

- 133 *Comparative Shock Analysis (CSA) of Main Propulsion Unit (MPU)*. Validation and Shock Approval Plan, SEAWOLF Program, Contract No. N00024-90-C-2901, 9200/SER: 03/039, September 20, 1994.
- 134 Sprague, M. A., and T. L. Geers. Spectral elements and field separation for an acoustic fluid subject to cavitation. *Journal of Computational Physics*, Vol. 162, 2003, pp. 184:149.
- 135 Knowles, C. P., and C.W. Gear. Revised validation metric, unpublished manuscript, 16 June 2004 (revised July 2004).
- 136 Cohen, J., P. Cohen, S. G. West and L. S. Aiken. *Applied multiple regression/correlation analysis for the behavioral sciences*. Lawrence Erlbaum Associates, Hillsdale, NJ, 2003 (3rd ed.).
- 137 Whang, B., W. E. Gilbert, and S. Zilliachus. *Two Visually Meaningful Correlation Measures for Comparing Calculated and Measured Response Histories*. Report, CARDEROCKDIV-U-SSM-67-93/15. Carderock Division, Naval Surface Warfare Center, Survivability, Structures and Materials Directorate, Research and Development, Bethesda, Maryland, September, 1993.
- 138 Theil, H. *Economic Forecasts and Policy*. North-Holland Publishing Company, Amsterdam, 1975.
- 139 Russell, D. M. Error Measures for Comparing Transient Data: Part II: Error Measures Case Study. In Proceedings of the 68th Shock and Vibration Symposium, 2006, pp. 185-198.
- 140 SAE J211-1 (R) *Instrumentation for Impact Test—Part 1—Electronic Instrumentation*. SAE International, Warrendale PA, USA, July 1, 2007.
- 141 M. H. Ray, C. A. Plaxico, J. A. Weir, F. Council, Recommended Guidelines for Curb and Curb-Barrier Combinations, National Cooperative Highway Research Program Report No. 537, ISBN 0-309-08920-8, National Academy of Sciences, Washington, D.C., 2005.
- 142 AASHTO, “A Policy on the Geometric Design of Highways and Streets,” American Association of State Highway and Transportation Officials, Washington, D.C., 2001.
- 143 Bullard, D., W. Menges, and D. Alberson, " NCHRP Report 350 Compliance Test 3-11 of the Modified G4 (1S) Guardrail with Timber Blockouts," FHWA contract DTFH61-95-C-00090, Research Project 405421-1, Texas Transportation Institute, College Station, Texas, January 1996.
- 144 Tiso, Paolo, “Improvements to the Suspension of the NCAC C2500 Pickup Truck Finite Element Model,” Master’s Thesis, Worcester Polytechnic Institute, August 2001.

- 145 LaTurner, J. F., "NCHRP Report 350 Crash Test Results for Curb-Barrier Combinations," Project No. 52-2556, Report 231, E-Tech Testing Services, Inc., Rocklin, CA, February, 2004
- 146 Plaxico, C., Kennedy, J., Miele, C., Simunovic, S. and Zisi, N., "Enhanced Finite Element Analysis Crash Model of Tractor-Trailers (Phase B)," National Transportation Research Center, Inc., Knoxville, TN, 2009.
- 147 Rosenbaugh, S.K, Sicking, D.L., and Faller, R.K., "Development of a TL-5 Vertical Faced Concrete Median Barrier Incorporating Head Ejection Criteria," Test Report No. TRP-030194-07, Midwest Roadside Safety Facility, University of Nebraska-Lincoln, 10 December 2007.
- 148 Plaxico, C., Kennedy, J., Simunovic, S. and Zisi, N., Enhanced Finite Element Analysis Crash Model of Tractor-Trailers (Phase A), National Transportation Research Center, Inc., Knoxville, TN, 2008.
- 149 Bligh, R. P., Ross, H. E. Jr., and Epperson, B. and Sherry, K., "Test Risk Assessment Program (TRAP): Version 2.1," Texas Transportation Institute, Report No. 472540-F, College Station, TX, January 2000.

Appendix A

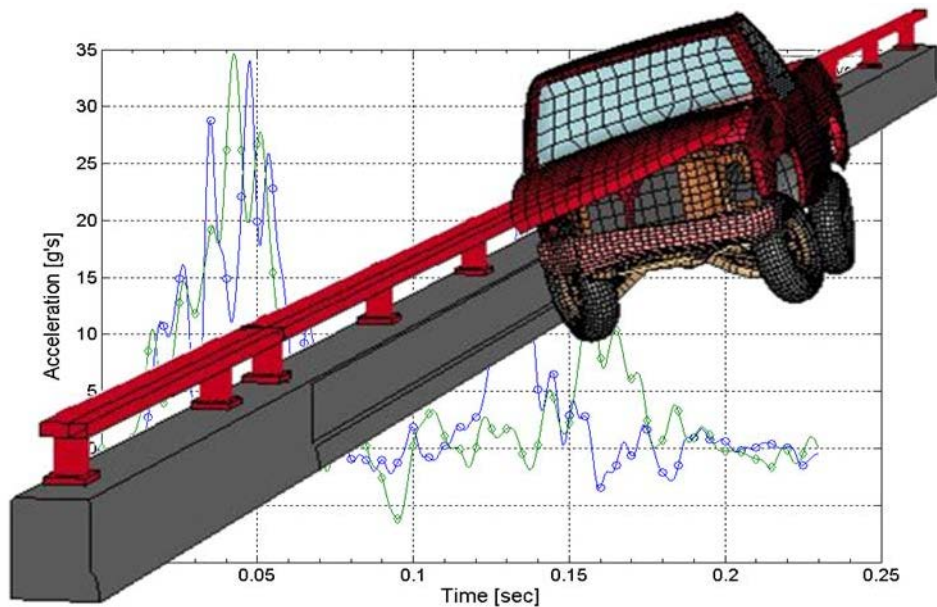
Roadside Safety Verification and Validation Program (RSVVP)

User's Manual

December 2009 (Revision 1.4)

Mario Mongiardini

Malcolm H. Ray



CONTENTS

INTRODUCTION TO RSVVP	4
INSTALLATION	5
System requirements	5
Installation of the MATLAB Component Runtime	5
Starting RSVVP	6
EVALUATION METHODS AND DATA ENTRY PROCEDURE	7
General Discussion	7
Format of input curves	8
Copy of the original input curves.....	9
Loading a configuration file.....	9
<i>Procedure for Selecting Evaluation Methods</i>	10
<i>Procedure for Data Entry</i>	12
<i>Procedure for Initial Preprocessing</i>	13
PREPROCESSING	16
Filtering.....	17
<i>Procedure for Filtering Data</i>	18
Shift/Drift controls	19
<i>Procedure for Applying Shift and Drift</i>	20
Curve Synchronization (Single-channel mode)	20
<i>Procedure for Applying Synchronization</i>	21
<i>Procedure for defining input for Multiple Channels</i>	22
<i>Procedure for Performing Additional Preprocessing in Multiple-Channel Mode</i>	23
METRICS SELECTION	26
Metrics selection	26
<i>Procedure for Metrics selection</i>	27
Time interval.....	29
<i>Procedure for Selecting Time Window</i>	29
<i>Procedure for Compression of Image Files</i>	30
METRICS EVALUATION	31
<i>Procedure for Metrics Evaluation</i>	31
<i>Procedure for Defining the Whole-Time Window</i>	32
<i>Procedure for Defining User-Defined-Time Window(s)</i>	32
SCREEN OUTPUT	34
OUTPUT OF RESULTS	36
<i>Procedure for Exiting and Saving Results</i>	36
Table of results (Excel [®] worksheet)	37
Graphs.....	40
Time Histories Results	40
EXAMPLES	41
Example 1: Single-Channel Comparison.....	41
<i>Analysis Type</i>	42
<i>Data Entry and Preprocessing</i>	42
<i>Metric selection and evaluation</i>	46
<i>Save Results</i>	50

Example 2: Multiple-Channel Comparison	52
<i>Analysis Type</i>	53
<i>Data Entry and Preprocessing</i>	53
<i>Metric selection and evaluation</i>	56
REFERENCES	63
APPENDIX A1: Comparison Metrics in RSVVP	64
APPENDIX A2: Multi-Channel Weight Factors.....	69

List of Figures

Figure A-1: Format of the test and true curves.	9
Figure A-2: Input of the test and true curves.	13
Figure A-3: Synchronization of the channel/resultant.	25
Figure A-4: Select the metric profile from the drop-down menu.	28
Figure A-5: Example of a metrics selection using the ‘ <i>User selected metrics</i> ’ profile.	28
Figure A-6: Time window(s) selection.	29
Figure A-7: Option to compress/uncompress the image files created by RSVVP.	30
Figure A-8: Press the ‘ <i>Evaluate metrics</i> ’ button to begin the metrics calculations.....	31
Figure A-9: Pop-up window for saving the configuration file.	32
Figure A-10: Defining data range in the user defined time window.	33
Figure A-11: Screen output for the NCHRP 22-24 profile.....	35
Figure A-12: Screen output for the ‘ <i>All metrics</i> ’ or ‘ <i>User defined</i> ’ profiles	35
Figure A-13: Pop-up browse window for selecting output folder for RSVVP results.	37
Figure A-14: Message shown while RSVVP creates results folder.	37
Figure A-15: Excel table containing the metrics results for the various time intervals.....	38
Figure A-16: Summary of preprocessing options and separate sheets for each input channel in the Excel file.....	39

List of Tables

Table A1: Acceptance criteria suggested for the NCHRP 22-24 metrics profile.	71
---	----

INTRODUCTION TO RSVVP

The Roadside Safety Verification and Validation Program (RSVVP) quantitatively compares the similarity between two curves, or between multiple pairs of curves, by computing comparison metrics. Comparison metrics are objective, quantitative mathematical measures of the agreement between two curves. The comparison metrics calculated by RSVVP can be used to validate computer simulation results against experimental data, to verify the results of a simulation against the results of another simulation or analytical solution, or to assess the repeatability of a physical experiment. Although RSVVP has been specifically developed to aid in the verification and validation of roadside safety computational models, it can generally be used to provide a quantitative comparison of essentially any pair of curves. The comparison metrics calculated by RSVVP are deterministic, meaning they do not specifically address the probabilistic variation of either experiments or calculations (i.e., the calculation results are the same every time given the same input). For a description of each metric calculated by the RSVVP see Appendix A1.

In order to ensure the most accurate comparison between the curves, RSVVP allows the user to select among several preprocessing tasks prior to calculating the metrics. The interactive graphical user interface of RSVVP was designed to be as intuitive as possible in order to facilitate the use of the program. Throughout each step of the program, RSVVP provides warnings to alert the user of possible mistakes in their data and to provide general guidance for making proper selection of the various options.

The interpretation of the results obtained using RSVVP is solely the responsibility of the user. The RSVVP program does not presuppose anything about the data; it simply processes the data and calculates the metrics. The user must verify that the data input into the program is appropriate for comparison and that the appropriate options in RSVVP are used for their specific case.

INSTALLATION

SYSTEM REQUIREMENTS

RSVVP has been written and compiled using Matlab[®]. In order to run the RSVVP program either the full Matlab[®] (version 2009a or higher) software or the free distributable *MATLAB Component Runtime* (MCR 7.10) software must be installed on the user's system. The minimum hardware requirements to run RSVVP are shown below in Table A1:

Table A1. Minimum hardware requirements for running RSVVP

	32 bit version	64-bit version
CPU	Intel [®] Pentium 4 (and above), Intel Celeron, Intel Xeon, Intel Core, AMD Athlon 64, AMD Opteron, AMD Sempron	Intel [®] Pentium 4 (and above), Intel Celeron, Intel Xeon, Intel Core, AMD64,
RAM	512 MB	1024 MB
Disk space	510 MB (MATLAB [®] only)	510 MB (MATLAB [®] only)

INSTALLATION OF THE MATLAB COMPONENT RUNTIME

The source code for RSVVP was written in Matlab[®] (version R2007b) and then compiled as an executable file for Windows[®] XP/Vista in order to create a standalone program that can be run on computers with or without Matlab[®] installed on them. However, before running RSVVP on a machine without Matlab[®] it is first necessary to install Matlab[®] *Component Runtime* (MCR 7.10), which is free software distributed by Matlab[®]. MCR provides all the necessary Matlab[®] functional support to ensure proper execution of the RSVVP software. (Note: the MCR environment only has to be installed once). The latest version of RSVVP and the MCR

environment can be downloaded from:

http://civil-ws2.wpi.edu/Documents/Roadsafe/NCHRP22-24/RSVVP/RSVVP_1_7.zip

To install MCR, perform the following steps:

1. Extract the content of the *RSVVP.zip* file in the folder on your PC where you want to install RSVVP (for example: *C:\RSVVP*).
2. Open the folder where you extracted the files and double-click on the *Installer.bat* file.
3. Follow the instructions of the installation wizard. It may take several minutes to complete the installation. This installs the free Matlab[®] MCR environment that is used in conjunction with RSVVP.
4. Reboot your PC.

At this point RSVVP should be installed on your computer.

STARTING RSVVP

After MCR and RSVVP have been installed, simply double-click the *RSVVP.exe* file located in the installation folder (e.g., *C:\RSVVP*) to start the program. Once started, a series of graphical user interfaces will guide the user through the preprocessing, the evaluation of the comparison metrics and saving the results. The following sections describe the features and use of the program.

EVALUATION METHODS AND DATA ENTRY PROCEDURE

GENERAL DISCUSSION

In RSVVP, the baseline curve or reference curve is called the “true curve” as it is assumed to be the correct response, whereas the curve that is to be verified or validated, say from a model or experiment, is called the “test curve.” For example, in validating a computer simulation against a full-scale crash test, the time history data from the physical crash test would be input as the “true curve” in RSVVP and the computer simulation time history would be input as the “test curve”. Since the comparison metrics assess the degree of similarity between any pair of curves in general, the input curves may represent various physical entities (e.g., acceleration time histories, force-deflection plots, stress-strain plots, etc.). RSVVP does not presuppose anything about the curves being compared so it is the user’s responsibility to ensure that the units, for example, are consistent. The only restriction on the input data is that the abscissa values must increase monotonically. Curves representing loading/unloading cycles or, in general, curves which are characterized by more than one data point with the same abscissa value cannot be managed in RSVVP at the moment. As a note of caution: when using RSVVP to compare force-deflection data or stress-strain data, the user must ensure that the abscissa data is monotonically increasing. It may be more appropriate to compare force-time history data and deflection-time history data separately to avoid this problem.

Comparison metrics provide an objective measure of how well two curves match each other and can thus be applied to essentially any monotonically increasing pair of curves. A typical application of the metrics evaluated by RSVVP is the validation of a numerical model by comparing the numerical results with the experimental results. Another application could be to check the repeatability of an experiment by comparing the results obtained from several repetitions of the same experiment. Yet another application is to verify the results of one numerical simulation with the results of another numerical simulation.

Two general types of comparison can be performed in RSVVP:

1. Single Channel - A single pair of curves are compared
2. Multiple Channels- Multiple pairs of curves are compared (i.e., up to three acceleration-time histories and/or three angular rate-time histories).

In the ‘Single Channel’ option, comparison metrics are based on the comparison of a single pair of input curves, while in the ‘Multiple Channel’ option the comparison metrics are computed by either, 1) calculating the metrics for the individual channels (i.e., curve pairs) and then computing composite metrics based on a weighted average of the individual channels, or 2) calculating the resultant of the various channels and then computing the comparison metrics based on the resulting single curve pair. In either case, the ‘Multiple Channel’ option is intended to provide an overall assessment of multiple data channels by computing a single set of composite metrics.

The *multiple channel* option in RSVVP was created for the specific purpose of comparing numerical simulations of vehicle impacts into roadside barriers to the results from a full-scale crash test. An example might be a small sign support test where the longitudinal acceleration has a much greater influence on the results of the impact event than do the lateral or vertical accelerations. The less important channels may not satisfy the criteria because they are essentially recording noise. The longitudinal channel in this example will probably be an order of magnitude greater than some of the other less important channels and the response is essentially completely determined by the one longitudinal channel. The weighting factors used to compute the composite metrics are based on the area under the true curve for that respective channel, and thereby account for the different levels of importance of the various channels.

FORMAT OF INPUT CURVES

The input curve files must be in ASCII format but can have any extension (or no extension) in the file name. The abscissa and ordinate data of the input curves must be tabulated into two columns as shown in Figure A-1. Each line in the input file represents a single data point (e.g., time and corresponding acceleration). If a data file includes a header, RSVVP will automatically detect and skip it. In such case, RSVVP will warn that a header was detected and will ask the user for confirmation of the number of lines to be skipped before starting data entry.

Abscissa	Ordinate
0.00000000	0.10000000
0.02000000	0.09900000
0.04000000	0.09800000
0.06000000	0.09700000
0.08000000	0.09600000
0.10000000	0.09500000
0.12000000	0.09400000
0.14000000	0.09300000
.....	

Figure A-1: Format of the test and true curves.

Although no limitation is imposed or assumed for the units of both the abscissa and ordinate columns, the use of some preprocessing features like the SAE filtering option may only make sense for time history data (i.e., the first column represents time). It is the user's responsibility to ensure that the units of the input curves are consistent, especially when comparing multiple pairs of curves in the Multichannel mode.

COPY OF THE ORIGINAL INPUT CURVES

A copy of the original input curves is automatically saved into the folder '\Input_curves' in both the main directory of RSVVP and the 'Result_XX' folder. Any file saved into the '\Input_curves' folder located in the main directory is deleted at the beginning of each new run of RSVVP.

LOADING A CONFIGURATION FILE

The user can also load a configuration file from a previous run of RSVVP. This configuration file contains all the necessary information to retrieve the files containing the original input curves and all the selected options for the preprocessing of the curves and the evaluation of the metrics. This configuration file can be loaded into two different ways:

- *Run Completely* mode, or
- *Edit Curves/Preprocessing* mode.

When the *run completely* mode is selected, RSVVP reads the configuration file and automatically evaluates the comparison metrics using the options stored in to the configuration file (e.g. preprocessing, metrics selection time intervals, etc.). This option is a useful tool for providing documentary proof of the values of the comparison metrics obtained during the verification/validation process or to simply enable the user to re-run a previously saved session. Using the *run completely* mode, RSVVP provides the user three options:

1. Reproduce comparison metrics using all the user time intervals from the original run,
2. Reproduce comparison metrics from a portion of the original time intervals (but with the constraint to follow the original sequence of the intervals) or
3. Compute comparison metrics on new user-defined time intervals.

The original configuration file can be updated with the new user defined time intervals at the end of the calculation.

Likewise, in *edit curves/preprocessing* mode, RSVVP loads the original input curves and automatically preprocesses them according to the options saved in the configuration file. In this mode, however, once the curves have been preprocessed, the user can go back and modify any of the preprocessing options or replace any of the original input curves. This option can be very useful when the analyst wants to assess, for example, how the various pre-processing options affect the values of the comparison metrics.

Procedure for Selecting Evaluation Methods

At the startup of RSVVP, first select a maximum re-sampling rate using the drop-down menu, 'Re-sampling rate limit', as illustrated in Figure A-2. By default, RSVVP limits the rate at which the curves are re-sampled to a maximum of 10 kHz. If a higher limit is desired, the user can choose from the available options in the drop-down menu.

Then choose between 'Single Channel', 'Multiple Channel', or 'Load a Configuration' File options.

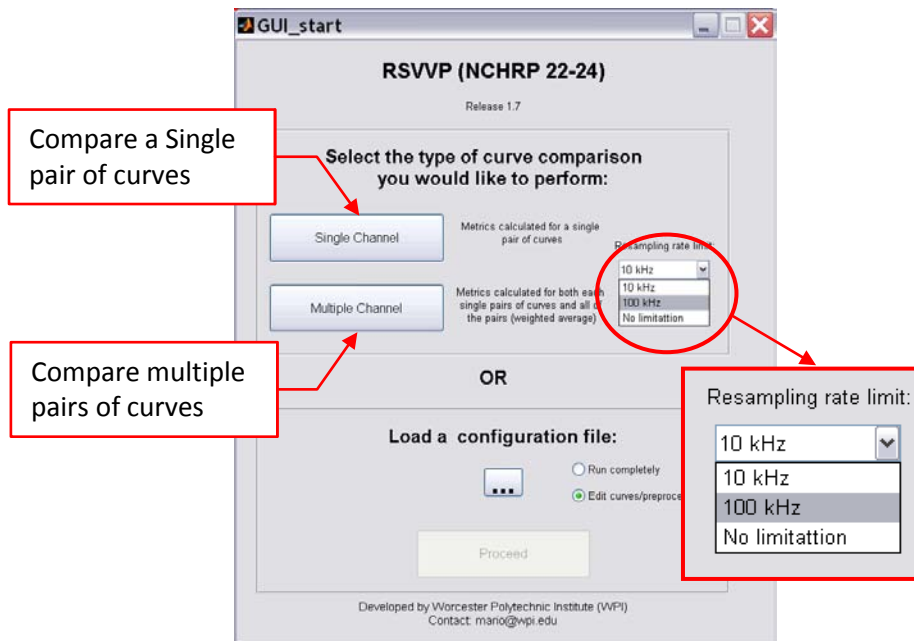


Figure A-2: Selection of the type of comparison and re-sampling limit.

To Load the configuration file, click the button with three dots (i.e., ). This will open a browse window that can be used to search/select the desired configuration file, as shown in Figure A-3. Once the configuration file has been loaded, the button 'Proceed' becomes active.

Before proceeding, select the desired mode for running the configuration file (i.e., 'Run completely' or 'Edit curves/preprocessing') The default option is to load the configuration file in *Edit* mode; to change to 'Run completely' mode, select the corresponding radio button

Note: When a configuration file has been loaded in 'run completely' mode, any selection made by the user to limit the re-sampling rate is overridden by the configuration file. In order to change the re-sampling limit, load the configuration file in 'edit' mode.

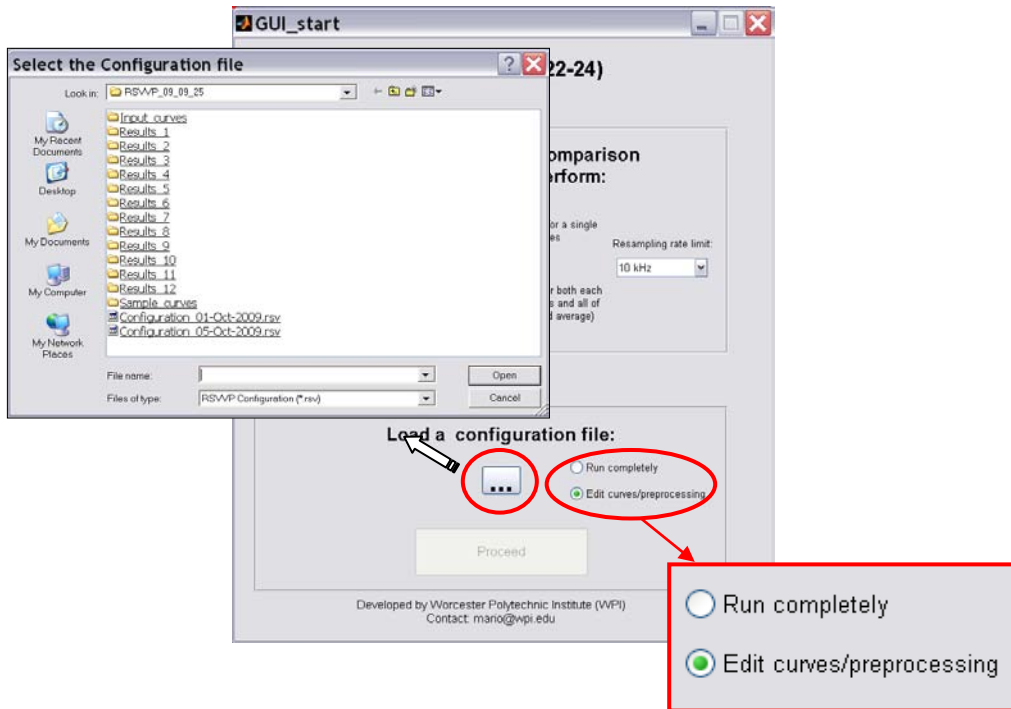


Figure A-3: Selection of the configuration file.

Procedure for Data Entry

After the analysis options have been selected, RSVVP closes the window and opens another graphical user interface that will be used for loading and preprocessing the input curves.

Clicking on the buttons, '*Load True Curve*' and '*Load Test Curve*', opens a browse window that can be used to search/select the corresponding curves, as illustrated in Figure A-4. Recall from the discussion section that the '*True Curve*' is the baseline curve or reference curve and is assumed to be the correct response; the '*Test Curve*' is the data from a model or experiment that is to be verified or validated.

After each input file is loaded, RSVVP will show a preview of the raw curves in the graphics area on the left side of the main window, as shown in Figure A-4.

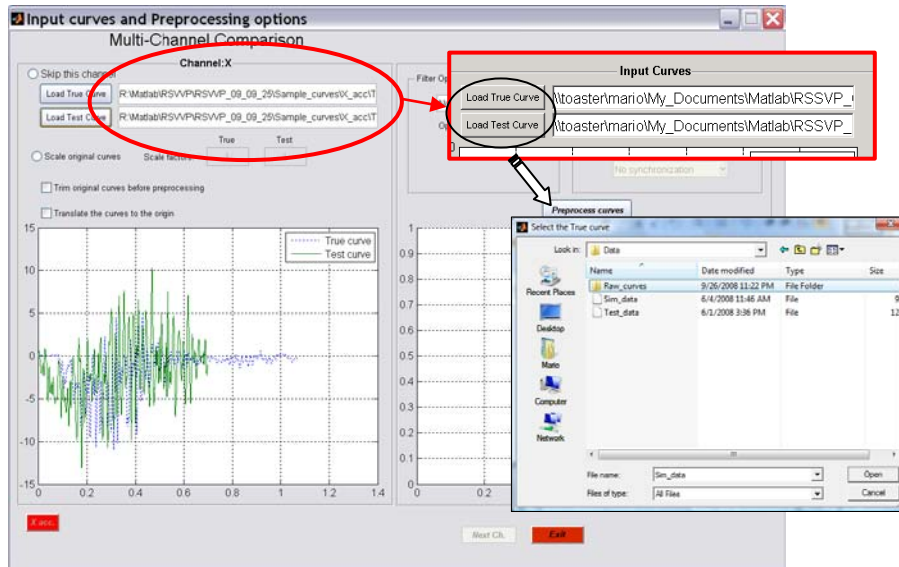


Figure A-4: Input of the test and true curves.

Procedure for Initial Preprocessing

The user is given the option to perform initial adjustments of the data, including scaling, trimming, and translating the curves, prior to applying additional preprocessing options, as shown in Figure A-5. The radio button to scale the input curves and the checkboxes to activate the option to trim and/or translate the curves to the origin can be selected only after both the test and true curves have been input.

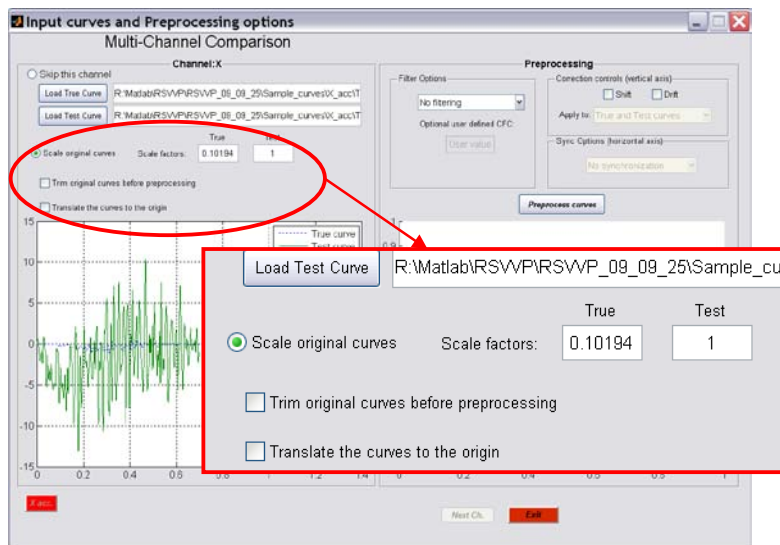


Figure A-5: Checkboxes for the manual trim and the translation of the raw curves.

Curve scaling

The ‘*scale*’ option allows the user to scale the original time histories using user-defined scale factors. The true and test curves can be scaled by separate scale factors. This option may be used, for example, to invert the sign of time histories or to convert units (e.g., accelerations can be converted from m/s^2 to g 's).

To scale either the true curve or test curve or both, check the radio button ‘*Scale original curves*’ shown in Figure A-5. Input the scale factor for the true and/or test curves into the respective fields ‘*True*’ and ‘*Test*’ located beside the radio button. Each time a new scale factor is defined for either the true or the test curve (or the scaling option is deselected), the graphs are automatically updated.

Curve trimming

The ‘*trim*’ option allows the user to trim the beginning and/or the end of the raw data *before* preprocessing the curves. This option can be used, for example, to remove the pre- and post-impact data from the curves to ensure that the comparison evaluation is applied only to the impact portion of the data. The ‘*trim*’ option can also be used, for example, to trim the input data at a point where the true and test curves start diverging to allow for better synchronization of the curves in the preprocessing phase. Although it is possible to specify a *user defined time interval* over which to evaluate the comparison metrics (see section [Time Interval](#)), it is advisable to trim the input curves when they have a ‘null head’ or ‘null tail’ in order to improve data synchronization during the preprocessing operations.

To trim the original data, check the box ‘*Trim original curves before preprocessing*’. This action will open the pop-up window shown in Figure A-6. The ‘*trim*’ option is applied to the true and test curves independently. The fields ‘Lower limit’ and ‘Upper limit’ show the boundary values for the curve selected using the radio buttons for either the test or true curve. Only one curve at a time can be selected in order to allow for independent trimming of each of the two curves. The curve selection is performed using the radio buttons located at the bottom left of the window. A straight and dotted line respectively indicates the lower and upper limit in the graph area. Both the lines move according to the value input in the user fields (blue and green color are used for the true and test curves, respectively). By default, both the test and true curves are shown in the graph area; however, RSVVP provides an option to only show the curve being trimmed, which is useful when the curves cannot easily be distinguished.

If the raw data curves are characterized by a high level of noise, the *trim window* also provides an option for the user to filter the curves before performing the trim operation. The user can select the desired CFC value from the drop-down menu located in the ‘*Filter option*’ box. While it is not recommended, if the user wants to use filter

specifications different from the standard SAE J211 filter, user defined filters parameters can be specified.

Note: If data is filtered during the trimming process, the user will not be allowed to change the filtering option during subsequent preprocessing operations. If a different filtering option is desired, it will be necessary to return to the ‘trimming’ box to make any change in the choice of filtering.



Figure A-6: Window for trimming input curves.

Curve translation

The ‘*translate*’ option allows the user to shift the input curves along the abscissa. This may be used, for example, to ensure that the beginning of the abscissa vector starts at zero (e.g., if time histories are input, the time vector can be shifted to start at time zero). This option works for either positive or negative value.

If the ‘*trim*’ option has been used, then the curves are automatically translated to the origin so there is no need to perform the ‘*curve translation*’ procedure. In fact, the checkbox to translate the original raw curves is not active when the ‘*trim*’ option has been selected. This option is useful whenever one or both the original input curves are shifted with respect to the origin. A typical application is shown in Figure A-7.

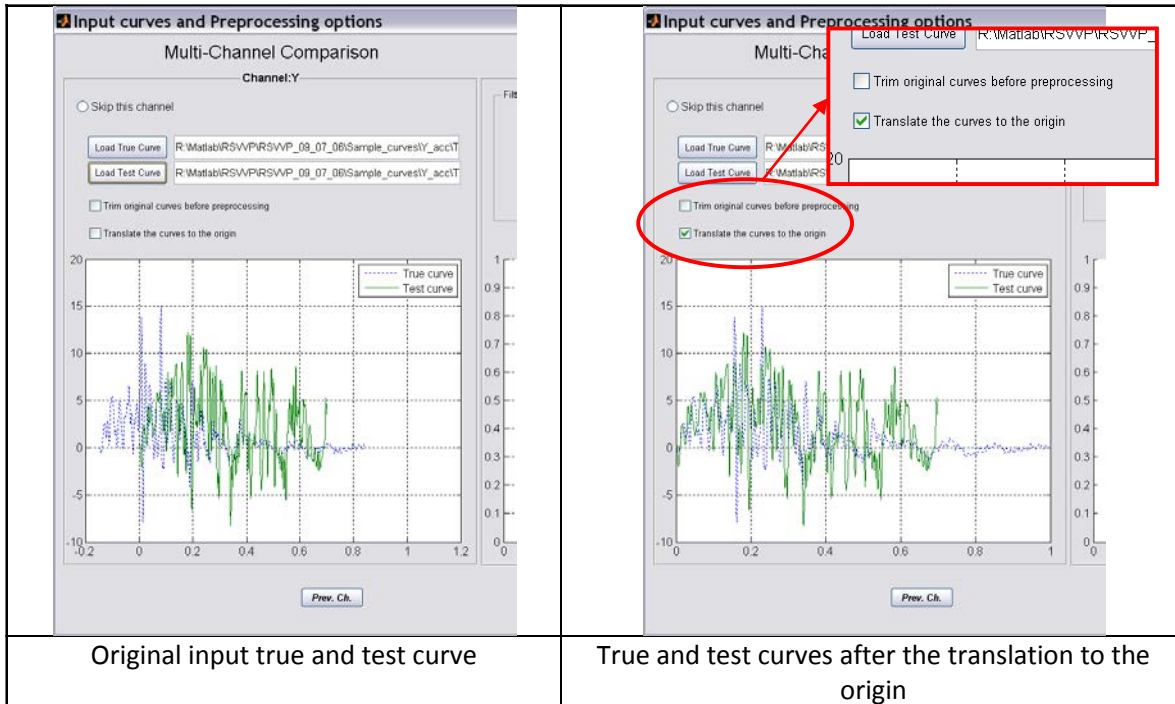


Figure A-7: Shift of one of the two input curves to the origin.

Note: If the option to scale the original curves is changed or if the scaling factors are changed, RSVVP will automatically update the graph of the original input curves as well as the graph of the preprocessed curves.

Note: If the ‘trim’ option or the ‘translate’ option is changed, or if an input curve is changed, then all the preprocessing operations applied to the curves are reset by RSVVP.

Note: The *copies* of the original input curves (automatically saved by RSVVP) do not include any of these initial preprocessing results.

PREPROCESSING

RSVVP is now ready to perform some basic and necessary pre-processing operations on the input curves, as well as some optional preprocessing operations that can be selected by the user based on qualitative visual assessment of the original data. In order to calculate the comparison metrics, all the curves must all have the same sampling rate and the same number of data points. Because these operations are necessary for subsequent calculations, they are performed automatically by RSVVP and do not permit user control. When the ‘*multiple channel*’

option has been selected, RSVVP trims each individual channel of data based on the shortest curve in each curve pair; then, after all the data has been input and preprocessed, the curves are further trimmed to the length of the shortest channel.

If the original sampling rate of one of the curves is larger than the '*re-sampling rate limit*', the data will be re-sampled to the chosen limit value (see Figure A-2). Note that higher sampling rates result in more data points and will therefore increase computation time. When the '*multiple channel*' option has been selected, the sampling rate determined for the first pair of curves is used for all subsequent data pairs.

In order to proceed to the next step (i.e., metrics selection) it is necessary to press the '*Preprocess curves*' button even if no optional preprocessing options have been selected.

RSVVP provides three optional pre-processing operations, including:

- Filtering,
- Shift/drift control and
- Synchronization.

Each of these three preprocessing operations is optional and can be selected independently from each other. After selecting the desired preprocessing options, press the '*Preprocess curves*' button located immediately below the *Preprocessing box* to preview results. If the results are not satisfactory, any of the previous options can be changed until satisfactory results are obtained.

Note: When the '*multiple channel*' option has been selected, the synchronization option will not be active in the preprocessing window. For multiple channels, the option for data synchronization, as well as other preprocessing operations, will be made available in an additional/secondary preprocessing step.

FILTERING

RSVVP gives the user the option of filtering the two input curves. This option can be very useful when the original input curves are noisy (e.g., noise created by the transducer during the acquisition process of experimental curves or undesired high-frequency vibrations). In order to obtain a value of the comparison metrics that is as reliable as possible, it is very important to remove noise from both the test and true curves. While noise derives from different sources in

physical experiments and numerical simulations, the true and test curves should be filtered using the same filter to ensure that differences in the metric evaluation are not based on the difference in frequency content in the true and test signals.

The filter options in RSVVP are compliant with the SAE J211/1 specification. It is recommended that raw data be used whenever possible in the evaluation to avoid inconsistent processing of the two curves. It is also important that both the test and true curves are filtered in the same way to avoid errors due to different filtering techniques. Although there is no general limitation to the type of units used for the input to RSVVP, the SAE filtering option presumes that the curves are time histories with time values expressed in units of seconds. In a future release of RSVVP, the option to use different units for the time vector of the time histories will be implemented.

The user can select between the following SAE J211 Channel Frequency Class (CFC) filters: 60, 180, 600 and 1000. Table shows the specifications of each CFC value as defined by SAE J211/1.

Table 2: Specifications for typical CFC values.

CFC value	3 dB limit frequency [Hz]	Stop damping [dB]
60	100	-30
180	300	-30
600	1000	-40
1000	1650	-40

While it is not recommended, if the user wants to use filter specifications different from the standard SAE J211 filters, user defined filters parameters can be specified.

Procedure for Filtering Data

By default RSVVP does NOT filter the input curves. To apply the filter option, click on the drop-down menu in the ‘Filter Options’ box (Figure A-8a) and select the desired CFC value

If it is necessary to specify a CFC value that is not listed in the menu, select the option ‘User defined CFC...’ at the end of the list and input the desired CFC parameters in the ‘Optional user defined CFC’ field located right below (Figure A-8b).

Note: This field is active only if the ‘User defined CFC’ option is selected from the drop-down menu.

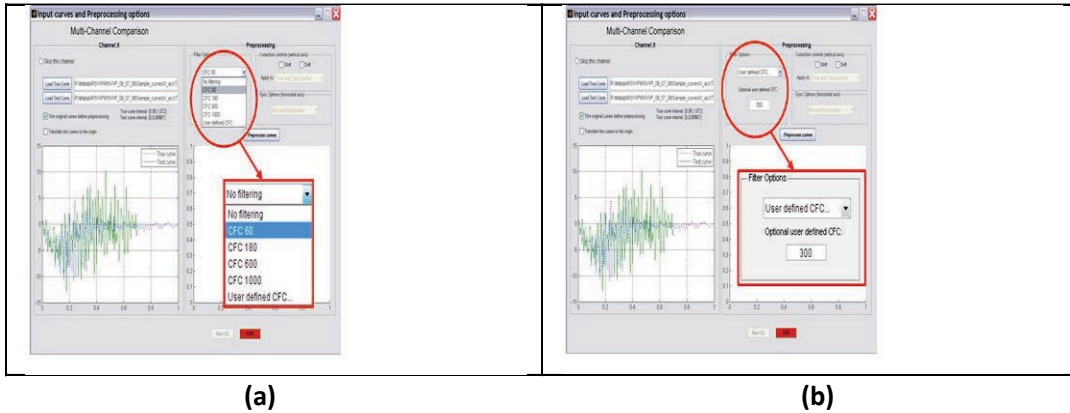


Figure A-8: Filter Options’ box - (a) drop down menu and (b) ‘Optional user defined CFC’ field.

Note: If the original curves have already been filtered during the optional trimming process, the ‘Filter Options’ box will show the filtering option chosen at that time without allowing the user to make any change. If a different filtering option is desired, it is necessary to go back to the trimming box to make any change to the previous choice.

SHIFT/DRIFT CONTROLS

Another preprocessing option supported by RSVVP is the possibility to correct any initial shift and/or drift in the curves. Experimental data sometimes contain shift and/or drift effects due to the change of temperature immediately before or during the test. The shift effect is an initial vertical shift of the curve due an increase of the temperature after the measurement gauges have been zeroed while the drift effect is a linear drift of experimental curve typical of the increase of the temperature during the test. The shift and drift controls of RSVVP correct the above mentioned effects and, therefore, can be very useful in case one or both the two input curves have been recorded from experimental tests and present either or both these data acquisition problems. As either the initial shift or drift of the test and/or the true curve are caused by an incorrect acquisition of the experimental data, these pre-processing options are important for an accurate evaluation of the comparison metrics. In generally, curves resulting

from numerical solution should not need to use these options since shift and drift are features of sensor characteristics in physical tests. The use of the shift and drift options is, therefore, not recommended for curves resulting from computer simulations.

Procedure for Applying Shift and Drift

Both the *shift* and *drift* controls can be activated independently from each other by checking the respective boxes. Once one or both of them have been checked, the user has the choice to apply the selected control/s to the true curve, the test curve or both the true and test curves (Figure A-9). By default these controls are inactive.

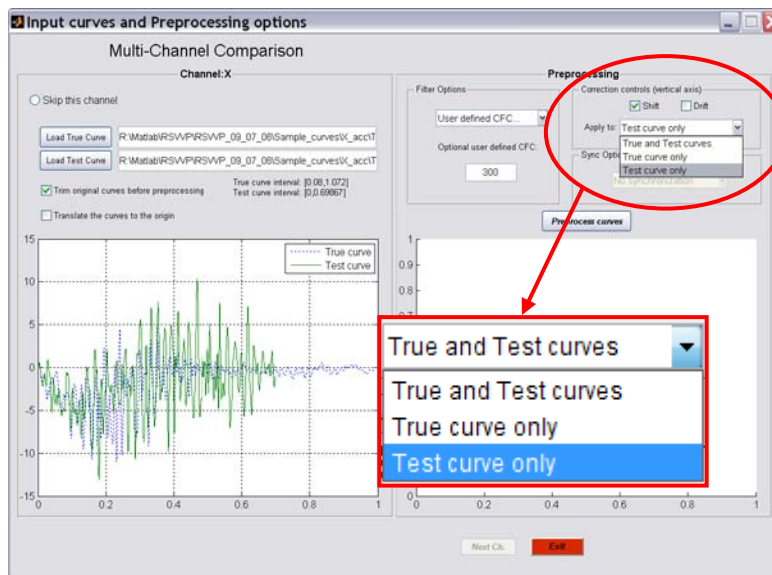


Figure A-9: Shift and Drift controls.

CURVE SYNCHRONIZATION (SINGLE-CHANNEL MODE)

RSVVP allows the user to optionally synchronize the two input curves before evaluating the comparison metrics. This option can be very useful if the original test and true curves have not been acquired starting at exactly the same instant (e.g., the test and true curve represent respectively a numerical simulation and an experimental test of the same crash test but the instant at which data collection was started is not the same). The synchronization of the two input curves is very important as any initial shift in the time of acquisition between the test and true curves could seriously affect the final value of the comparison metrics. For example, two

identical input curves with an initial phase difference due to a different starting point in the acquisition process would probably lead to poor results of some of the comparison metrics.

Two different synchronization options are available in RSVVP: (1) the absolute area between the two curves (i.e., the area of the residuals) and (2) the squared error between the two curves. Both options are based on the minimization of a target function. Although these two methods are similar, they sometimes give slightly different results. Selecting one of these methods will result in the most probable pairing point for the two curves. Once the original curves have been preprocessed, the user is given the option to further refine the synchronization of the data.

Procedure for Applying Synchronization

By default RSVVP does NOT synchronize the input curves. To apply the synchronization option, click on the drop-down menu in the 'Sync Options' box, shown in Figure A-10, and select one of the two available synchronization methods: (1) Minimum absolute area of residuals or (2) Least Square error. As previously noted: when the '*multiple channel*' option has been selected, the option for data synchronization, as well as other preprocessing operations, will be made available in an additional/secondary preprocessing step.

Once the curves have been preprocessed by pressing the '*Preprocess curves*' button, a pop-up window will ask the user to verify that the synchronization is satisfactory. If the '*No*' button is selected, another pop-up window with a slider will appear, as illustrated in Figure A-11. Moving the slider changes the initial starting point of the minimization algorithm on which the synchronization process is based.

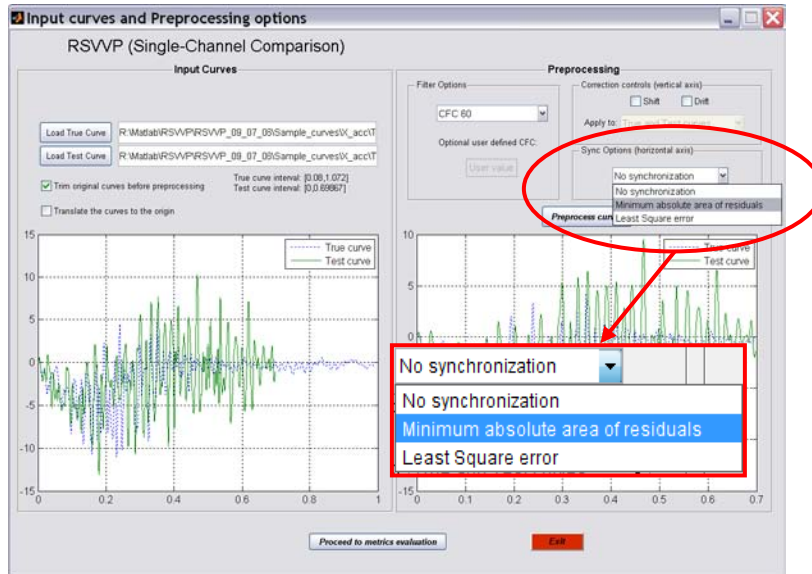


Figure A-10: Drop down menu of the ‘Sync Options’ box.

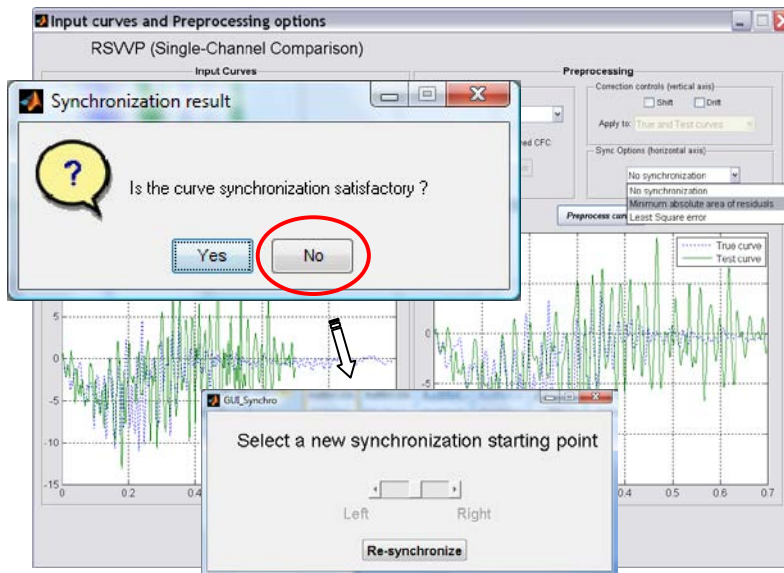


Figure A-11: Option for selecting new starting point for synchronization.

Procedure for defining input for Multiple Channels

For the *multiple channel* option, selecting the ‘Next Ch.’ button located at the bottom of the screen advances the input selection to the next channel (note: the name of the current channel appears at the top of the window). If data is not available for a particular channel, the radio button, ‘Skip this channel,’ (located at the top of the window) may be used to skip any of the six available channels.

In the multichannel mode, six tabs are located at the bottom, left corner of the GUI window, as shown in Figure A-12. The tab corresponding to the current channel's input/preprocessing page is highlighted in red. If the user wants to return to a previous channel, for instance, to change the input files or to modify preprocessing options, the user can simply select the corresponding tab and RSVVP will display the selected channel's input/preprocessing page.

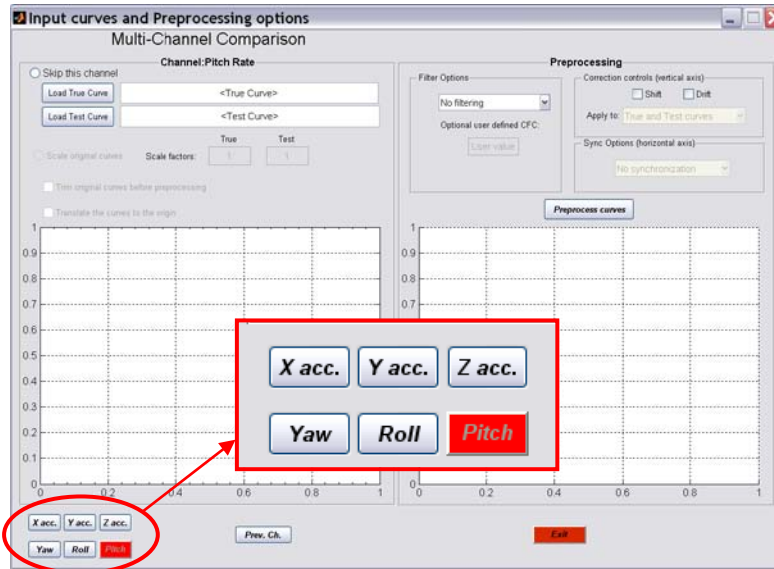


Figure A-12: Tabs linked to the input/pre-processing page for each channel

Procedure for Performing Additional Preprocessing in Multiple-Channel Mode

RSVVP provides two methods for evaluating the multiple channels of data: 1) weighting factors method and 2) resultant method. The *weighting factors* method calculates the metrics for the individual channels (i.e., curve pairs) and then computes composite metrics based on a weighted average of the individual channels. The 'resultant' method, on the other hand, calculates the resultant of the various channels and then computes the comparison metrics based on the resulting single curve pair. In either case, the 'Multiple Channel' option is intended to provide an overall assessment of the multiple data channels by computing a single set of composite metrics.

After the preprocessing has been completed for each data channel, press the button 'Proceed to curves synchro.' This opens a second window that will be used to select the *Evaluation Method* and synchronize the curves.

Note: If the last channel is skipped, RSVVP will automatically proceed to this second GUI.

In the *Evaluation method* box, select the desired method for the evaluation of the multiple data channels using the dropdown menu, as illustrated in Figure A-13. The default method is to use ‘Weighting Factors.’ If this method is selected, the graph on the left side of the window will show the curves for the first available channel. To switch to the resultant method, click on the drop down menu and select ‘*Resultant*’. Once the method has been changed, the button ‘*Update*’ becomes red (refer to Figure A-13). Press this button in order to update to the new selected method. The graph will now show the resultant of the first three channels.

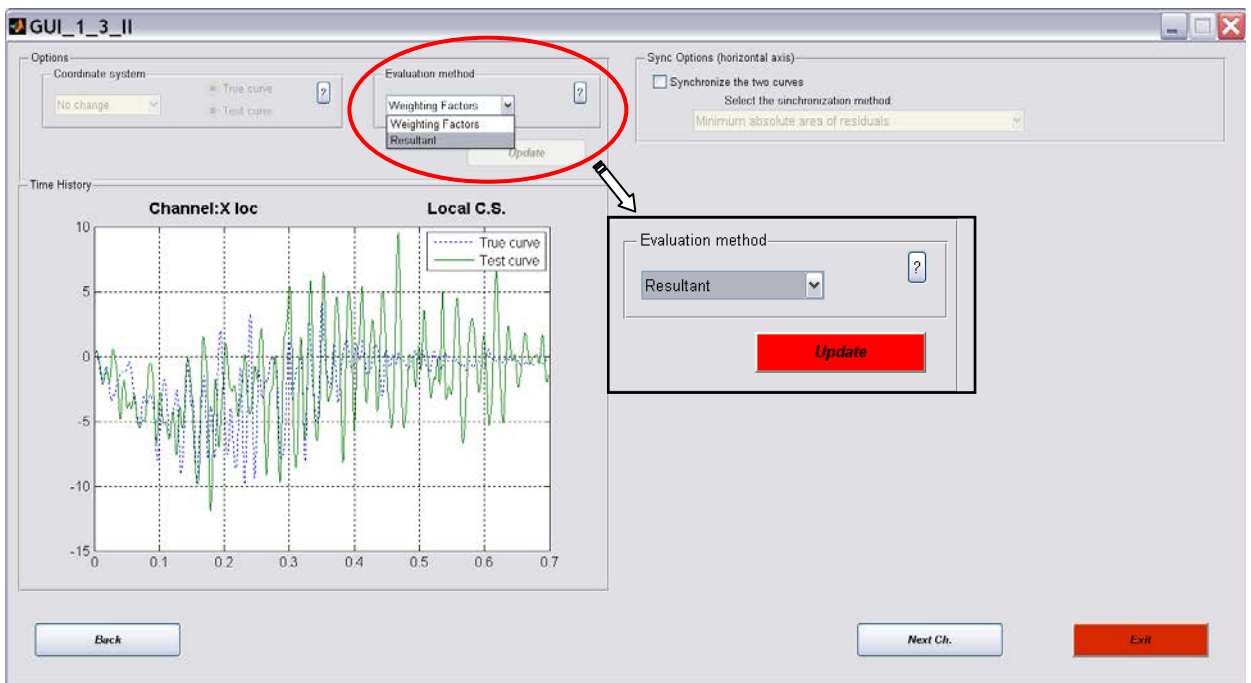


Figure A-13: Selection of the method for the computation of the multichannel metrics.

After the evaluation method has been selected, RSVVP is now ready to synchronize the curves. To begin the synchronization process, select the checkbox ‘*Synchronize the two curves*’ located in the *Sync options* box on the left side of the GUI, as shown in Figure A-14 (Note: Synchronization starts automatically). Synchronization of the curves is optional, and leaving the checkbox unselected will allow the user to skip this operation.

As in the single channel mode, two different synchronization methods are available: (1) minimum area of residuals and (2) least square error. Both options are based on the minimization of a target function. Although these two methods are similar, they sometimes give slightly different results. Selecting one of these methods will result in

the most probable pairing point for the two curves. However, if the user is not satisfied with the synchronization, he has the option of changing the initial starting point used in the minimization algorithms.

To proceed to the next channel, press the button, 'Next Ch.'

Note: If the *resultant method* has been selected, pressing the 'Next Ch.' button then displays the resultant curves computed from the second group of channels (i.e., the angular rate channels).

Note: Each time the evaluation method is changed, it is necessary to select the 'Update' button to make the change effective.

Note: Changing the evaluation method resets all curve synchronizations.

When the last channel/resultant has been reached, the button 'Proceed to metrics selection' will become active. Pressing it will advance RSVVP to the next phase of the program.

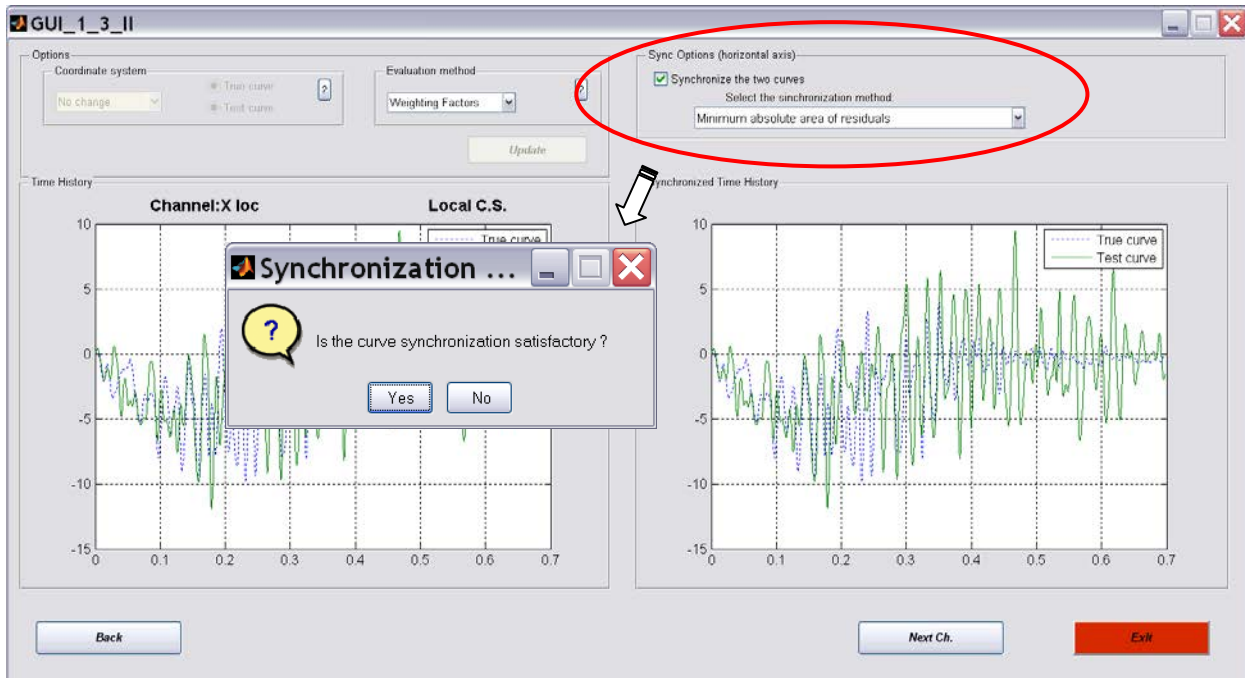


Figure A-2: Synchronization of the channel/resultant.

METRICS SELECTION

METRICS SELECTION

The metrics computed in RSVVP provide mathematical measures that quantify the level of agreement between the shapes of two curves (e.g., time-history data obtained from numerical simulations and full-scale tests). There are currently fourteen metrics available in RSVVP for computing quantitative comparison measures; all are deterministic shape-comparison metrics and are classified into three main categories:

1. Magnitude Phase Composite (MPC) metrics

- a) Geers
- b) Geers CSA
- c) Sprague & Geers
- d) Russell
- e) Knowles & Gear

2. Single Value Metrics

- f) Whang's inequality
- g) Theil's inequality
- h) Ziliacus error
- i) RSS error
- j) Weighted Integrated Factor
- k) Regression coefficient
- l) Correlation Coefficient
- m) Correlation Coefficient (NARD)

3. Analysis of Variance (ANOVA)

- n) Ray

A description of each metric is provided in Appendix A1.

The MPC metrics treat the magnitude and phase of the curves separately and combine them into a single value comprehensive metric. The single-value metrics give a single numerical value that represents the agreement between two curves. The ANOVA metric is a statistical assessment of whether the variance between two curves can be attributed to random error.

The recommended metrics are the Sprague & Geers metrics and the ANOVA metrics. The Sprague & Geers metrics assess the magnitude and phase of two curves while the ANOVA

examines the differences of residual errors between them. Of the fourteen different metrics available in RSVVP, the Sprague-Geers MPC metrics were found to be the most useful metrics for assessing the similarity of magnitude and phase between curves and the ANOVA metrics were found to be the best for examining the characteristics of the residual errors. For more details regarding the definitions of these metrics refer to Appendix A1.

Procedure for Metrics selection

Select the desired *Metric profile* from the drop down menu at the top of the metrics window, as illustrated in Figure A-15. There are three metrics profiles available:

1. NCHRP 22-24 (default),
2. All metrics, and
3. User selected metrics.

The '*NCHRP 22-24*' profile is the default profile and it is suggested that this profile be used when validating numerical simulations against full-scale crash tests (e.g., NCHRP Report 350 crash tests).

The second profile '*All metrics*' automatically selects all fourteen different comparison metrics that are available in RSVVP. If the '*User selected metrics*' profile has been selected, the checkbox beside each available metric will become active and allow the user to select any number of the available metrics by selecting the corresponding checkboxes, as shown in Figure A-16.

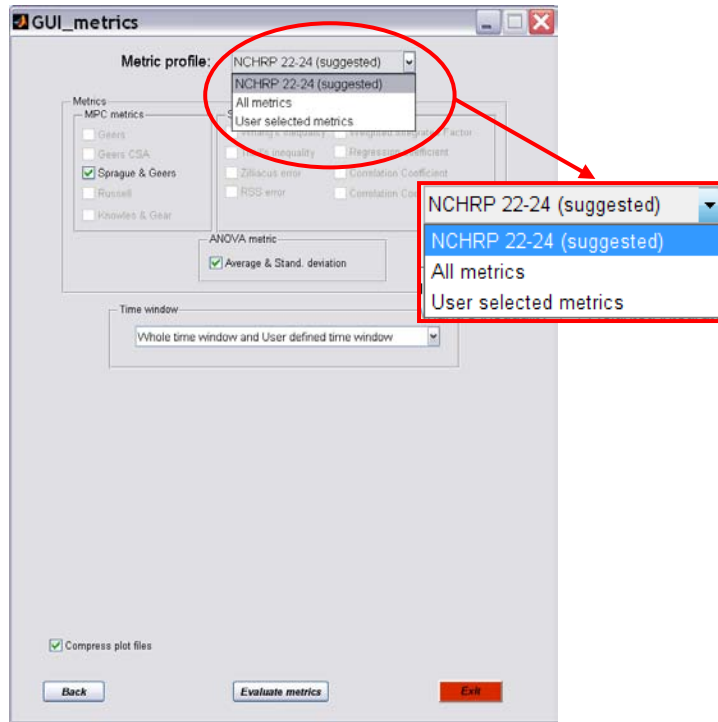


Figure A-3: Select the metric profile from the drop-down menu.



Figure A-4: Example of a metrics selection using the 'User selected metrics' profile.

TIME INTERVAL

In RSVVP, metrics can be evaluated over the complete length of the curve (e.g., whole time interval) and/or over one or more user defined time intervals.

Procedure for Selecting Time Window

From the drop-down menu in the *Time window* box shown in Figure A-17, select from one of the three available options:

- 1) *Whole time window and User defined time window*,
- 2) *Whole time window only* and
- 3) *User defined time window only*.

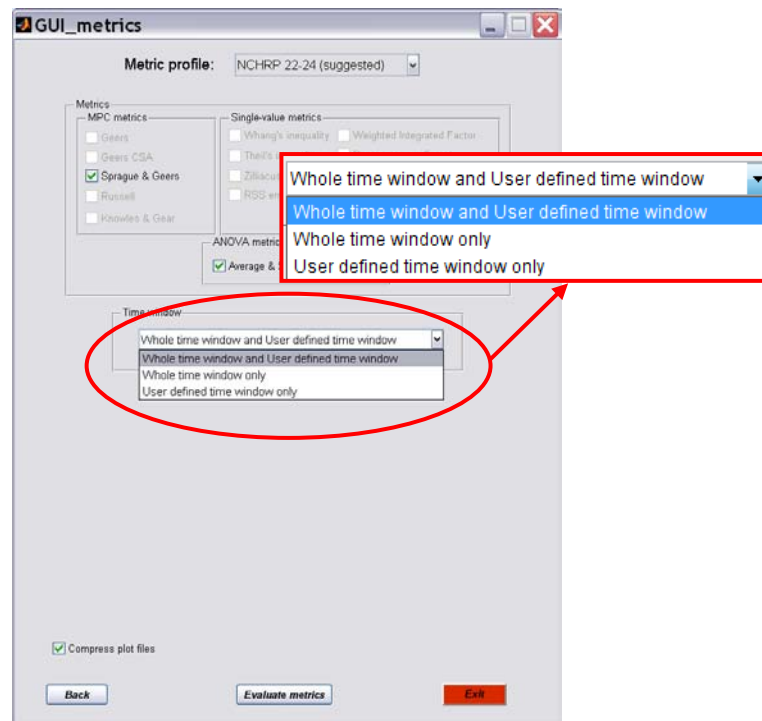


Figure A-5: Time window(s) selection.

If the “Whole time window” option is selected, the metrics are computed using all the available data (i.e., the complete length of the curves). If the “User defined time window” option is selected, the metrics will be computed for one or more arbitrary user defined intervals of data.

By default RSVVP evaluates the selected metrics on both the *whole time interval* and *user selected time interval(s)*. If this option is selected, RSVVP will first compute the comparison metrics over the ‘*Whole Time interval,*’ then, after displaying the results, it will prompt the user to define an arbitrary ‘*User Defined Time interval*’ over which to calculate the metrics.

Procedure for Compression of Image Files

During the computation of the metrics, RSVVP creates several graphs and saves them as bitmap images (.bmp). Since the cumulated size of these entire image files may exceed several megabytes, the default option in RSVVP is to compress them in .zip format. RSVVP provides an option for overriding file the file compression by unchecking the box ‘*Compress plot files*’ at the bottom of the window, as shown in Figure A-18.

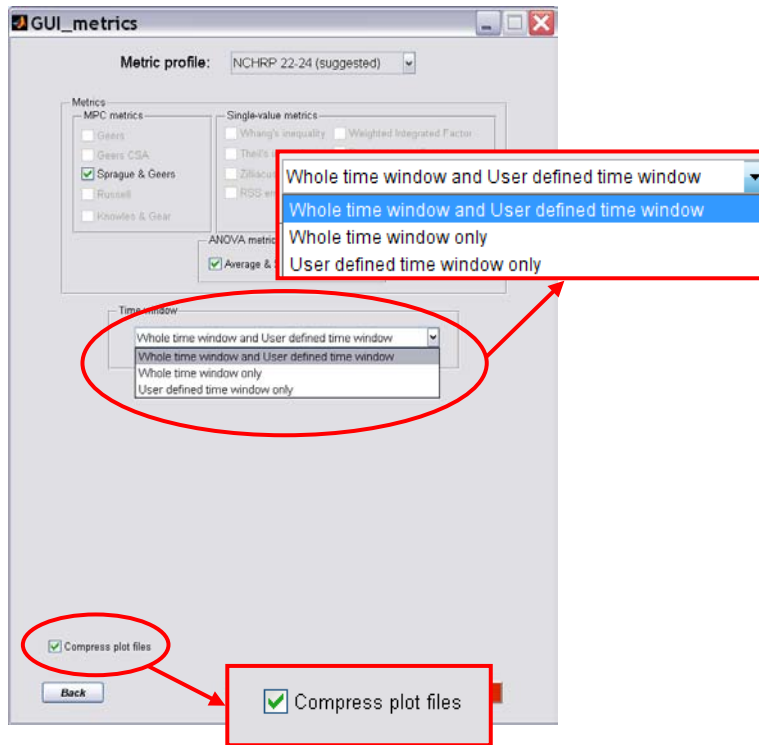


Figure A-6: Option to compress/uncompress the image files created by RSVVP.

METRICS EVALUATION

Once the desired metrics have been selected, and the time intervals over which the metrics will be calculated have been defined by the user, RSVVP begins the metrics calculation process. In the multichannel mode, RSVVP first calculates the value of the metric for each individual channel (or channel resultants if the *resultant method* was selected) and then computes single metric value based on a weighted average of the results. For details regarding the weighting scheme refer to Appendix A2.

Procedure for Metrics Evaluation

To start the metrics evaluation, press the ‘*Evaluate metrics*’ button located at the bottom of the window, as shown in Figure A-19. Note: It is possible to go back to the main graphical interface to change any of the selected input curves and /or modify any of the preprocessing options by clicking the ‘Back’ button.



Figure A-7: Press the ‘*Evaluate metrics*’ button to begin the metrics calculations.

Before the metrics are evaluated, a pop-up window appears, as shown in Figure A-20, asking the user to indicate a location and file name for saving the configuration file. The

configuration file contains all the information that has been input in RSVVP, including all the preprocessing options as well as the metrics selection. Thus, the configuration file contains all the information necessary to repeat the analysis. By default, the location of the configuration file is in the “working” directory and the name of the configuration file is ‘Configuration_Day-Month-Year.rsv’, where Day, Month and Year correspond to the data that the file is being created.

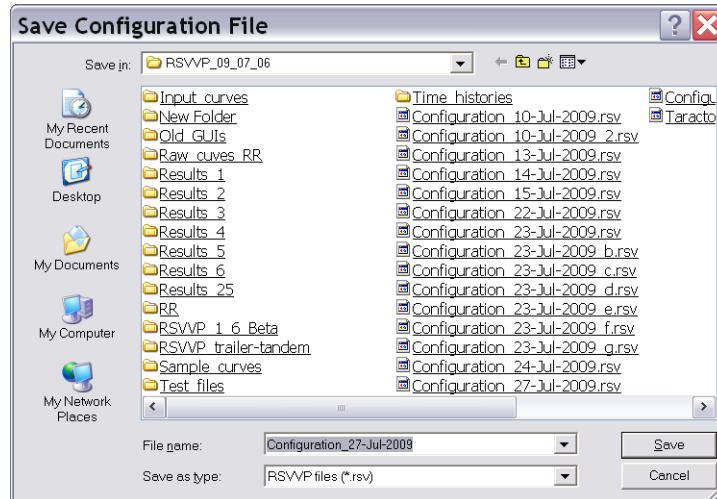


Figure A-8: Pop-up window for saving the configuration file.

Note: A copy of the configuration file is also saved in the subfolder .../Results_x that is created by RSVVP at the end of the run (see section [Output of Results](#) for more details about the result folder).

Note: The configuration file can be used, for example: (i) to quickly re-input a set of curves and configurations and then modify any of the previously selected options or (ii) to *exactly* repeat a previous run.

Procedure for Defining the Whole-Time Window

No action is needed to define the time interval for the ‘*Whole time window*’ option (i.e., options 1 and 2 from the *time interval* box) as RSVVP will automatically consider the maximum time interval possible for the data.

Procedure for Defining User-Defined-Time Window(s)

If a ‘*User defined time window*’ was selected (i.e., options 1 and 3 from the *time interval* box), RSVVP will prompt the user to select the upper and lower boundaries of the local time interval on which the comparison metrics will be evaluated. RSVVP shows a window with a graph of the test and true curves and two blank fields at the bottom which

are used to define respectively the time value of the lower and upper boundary, as shown in Figure A-21. Fill in the desired values and press the 'Evaluate metrics' button to start the evaluation of the metrics on the defined interval.



Figure A-9: Defining data range in the user defined time window.

When the limits are input into the fields, the upper and lower limits are shown as vertical lines in the graph. For multichannel input, a drop-down menu located at the bottom of the window allows the user to select the desired channel to use for defining the limits.

Note 1: The selected upper and lower boundaries do not change when a new channel is plotted as they share the same interval for each channel in the multi-channel option.

It is possible to evaluate the metrics on as many user defined time windows as desired; after the results of the user defined time window have been shown, RSVVP will prompt

the user for a new *User Defined* time window. The results obtained for each time interval will be saved separately.

SCREEN OUTPUT

For each of the time intervals on which the comparison metrics were evaluated, RSVVP shows various screen outputs to present the results:

- Graph of the true curve and test curve,
- Graphs of the time-integration of the curves,
- Values of the comparison metrics,
- Graph of residual time history,
- Graph of the residual histogram and
- Graph of the residual cumulative distribution.

Note: Comparison metrics are always computed using the curves shown in the graph of the true and test curves. The time-integrated curves are shown only to provide additional interpretation of the curves. For example, if acceleration data is being compared, it is often quite noisy and difficult to visually interpret. The time-integration of acceleration, however, yields a velocity-time history plot that is much easier for the user to interpret.

Figure A-11 and Figure A-12 show the typical output screen for the *NCHRP 22-24 profile* and the other two metric selection profiles, respectively (i.e., 'All metrics' or 'User defined' profiles). If the *NCHRP 22-24 profile* was selected, only the Sprague & Geers and ANOVA metrics are shown. The word 'Passed' and a green square beside the value of each metric indicate that the metric value meets the NCHRP 22-24 acceptance criterion for that specific metric; the word 'Not passed' and a red square indicate that the value does not meet the suggested acceptance criterion.

When either of the other two metrics profiles is selected, the results of all fourteen metrics are shown in the window and the word N/A appears beside any metrics that were not calculated (i.e., metrics not checked by the user in the '*User defined*' profile). In these cases, no acceptance criteria have been defined and the user must use their own judgment regarding acceptable values. Also, only the graph of the true curve and test curve is shown.

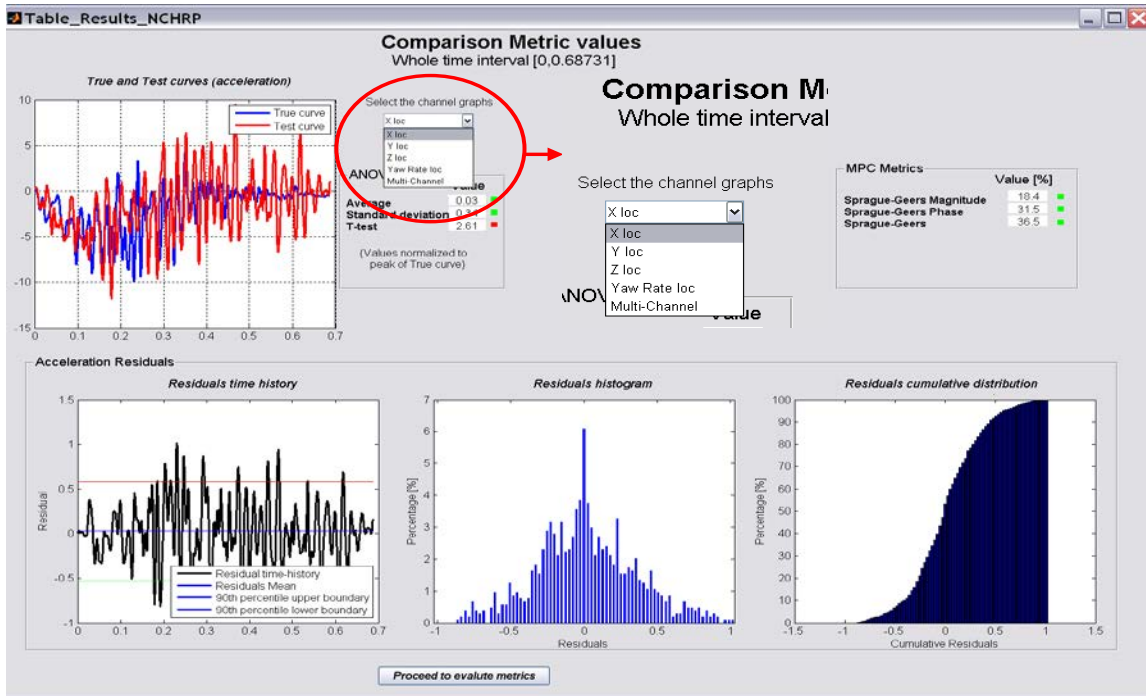


Figure A-10: Screen output for the NCHRP 22-24 profile

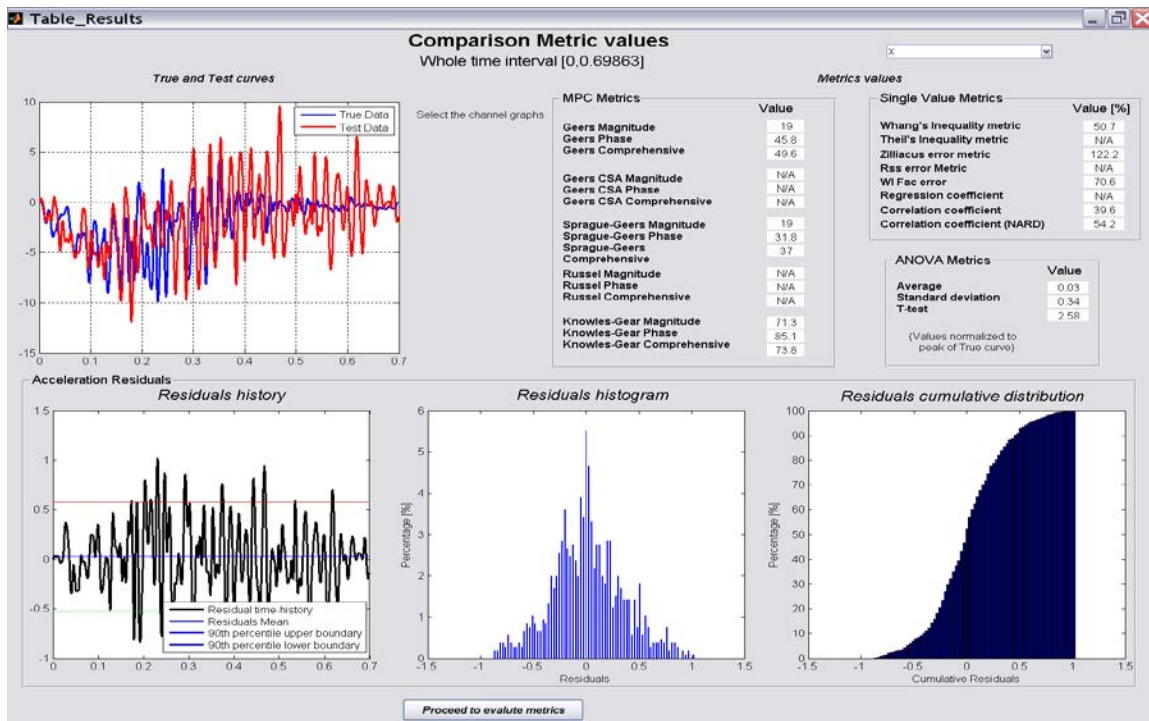


Figure A-11: Screen output for the 'All metrics' or 'User defined' profiles

For multichannel input, if the *weighting factors method* has been selected, the user can view the results for any of the individual channels or the multi-channel weighted results by selecting the desired option from the drop-down menu beside the time-history graph. When the *Multi-channel* results is selected from the drop-down menu, a histogram graph of the weighting factors used to compute the metric values in the multichannel mode is plotted. This gives an immediate understanding of the weight of each input channel with respect to the others in the evaluation of the multichannel metrics.

Note: It may be necessary to wait a few seconds before the metric values and the graphs are updated to a new selected channel.

The next step in RSVVP depends on whether or not the option for *User time intervals* was selected in the Metrics Selection GUI. If so, the user has the option to: (1) proceed to the evaluation of a new interval and/or (2) to save the results and quit the program. Select the button corresponding to the desired action. If the option ‘*whole and user defined time interval*’ was selected, RSVVP requires the user to go through the process of defining at least one user-defined time interval before they will have the option to save the results and quit RSVVP.

OUTPUT OF RESULTS

During the curve preprocessing and evaluation of the metrics, RSVVP generates several types of output, which are saved in the output-folder location defined by the user. If no output-folder was selected, RSVVP automatically saves the results in a folder called ‘\Results_X’, where X is an incremental numbering (i.e., 1, 2, etc). The folder ‘\Results_X’ is created in the folder where RSVVP was executed. At the beginning of the run, RSVVP checks to see if there is a previous sequence of folders named “\Results_X”, and creates a new Results folder with the suffix corresponding to the next number in the sequence. For example, if there is already a previous folder named ...Results_3, the new output folder will be named ...Results_4).

Procedure for Exiting and Saving Results

Pressing the button ‘Save results and Exit’ will open a browse window, as shown in Figure A-24, for the user to select where to save the results.

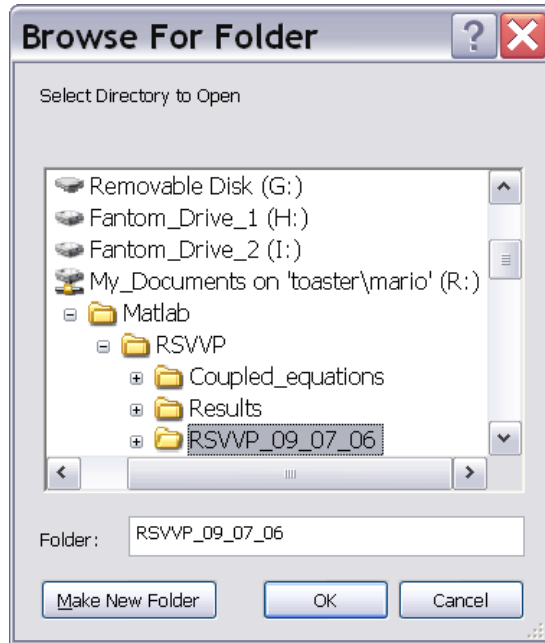


Figure A-12: Pop-up browse window for selecting output folder for RSVVP results.

The user has the option of creating a new folder by selecting the tab 'Make New Folder' in the browse window. If no selection has been made or if the cancel button has been pressed, RSVVP will automatically create a folder named 'Results_X' in the current directory.

Note: The process of saving of the results may take a few minutes. During this period, RSVVP displays the message shown in Figure A-25.

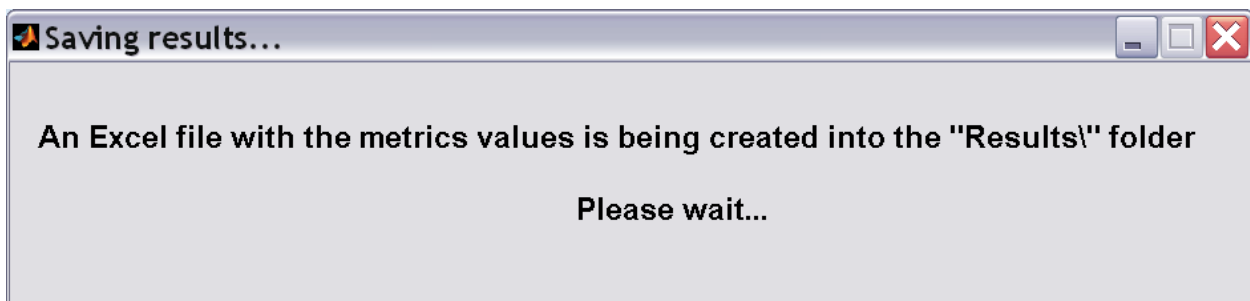


Figure A-13: Message shown while RSVVP creates results folder.

TABLE OF RESULTS (EXCEL[®] WORKSHEET)

The results of the comparison metrics are saved in the Excel file '*Comparison Metrics.xls*'. This spreadsheet contains the results for all the comparison metrics computed for

the *whole time interval* and all *user defined time intervals*, as shown in Figure A-26. The time interval used in each evaluation is indicated in the heading of each column.

	Whole time interval [0,0.5474]	User time interval #1 [0.08005,0.19995]	User time interval #2 [0.12005,0.21995]
MPC Metrics			
	Value [%]	Value [%]	Value [%]
<i>Geers Magnitude</i>	7.1	4.7	10.5
<i>Geers Phase</i>	23.9	22.1	21.4
<i>Geers Comprehensive</i>	24.9	22.6	23.8
<i>Geers CSA Magnitude</i>	N/A	N/A	N/A
<i>Geers CSA Phase</i>	N/A	N/A	N/A
<i>Geers CSA Comprehensive</i>	N/A	N/A	N/A
<i>Sprague-Geers Magnitude</i>	N/A	N/A	N/A
<i>Sprague-Geers Phase</i>	N/A	N/A	N/A
<i>Sprague-Geers Comprehensive</i>	N/A	N/A	N/A
<i>Russell Magnitude</i>	5.6	3.8	7.9
<i>Russell Phase</i>	22.5	21.6	21.2
<i>Russell Comprehensive</i>	20.5	19.4	20.1
<i>Knowles-Gear Magnitude</i>	58	101.1	1573.2
<i>Knowles-Gear Phase</i>	1.8	0	0
<i>Knowles-Gear Comprehensive</i>	53	92.3	1436.2
Single Value Metrics			
	Value [%]	Value [%]	Value [%]
<i>Whang's inequality metric</i>	38.5	36.5	38.1
<i>Theil's inequality metric</i>	N/A	N/A	N/A
<i>Zilliacus error metric</i>	76.8	76.5	85.9
<i>RSS error metric</i>	N/A	N/A	N/A
<i>WIFac_Error</i>	N/A	N/A	N/A
<i>Regression Coefficient</i>	66.7	49.9	65.2
<i>Correlation Coefficient</i>	N/A	N/A	N/A
<i>Correlation Coefficient(NARD)</i>	76.1	77.9	78.6
ANOVA Metrics			
	Value	Value	Value
<i>Average</i>	0.01	0.04	0.05
<i>Std</i>	0.15	0.25	0.16
<i>T-test</i>	7.21	7.39	14.43
<i>T/T_c</i>	2.81	2.88	5.63

Figure A-14: Excel table containing the metrics results for the various time intervals.

A summary of the input files and preprocessing options for each channel is written at the end of the Excel file, as shown in Figure A-27. If RSVVP is run in multichannel mode using the *weighting factors* method, the weighting factors and the metrics values calculated for each separate channel are provided in the Excel file on separate sheets, as indicated in Figure A-27.

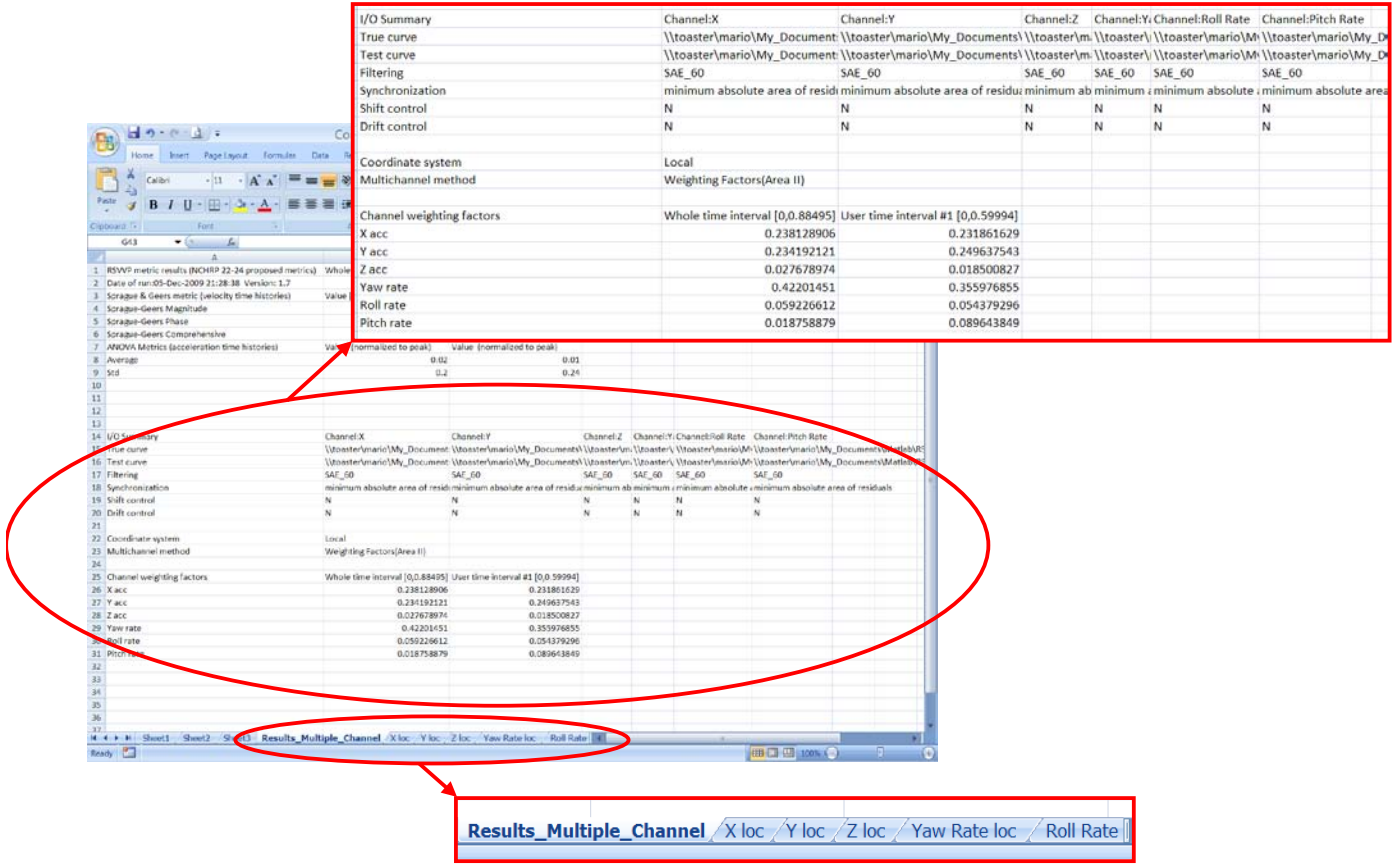


Figure A-15: Summary of pre-processing options and separate sheets for each input channel in the Excel file.

GRAPHS

RSVVP creates several graphs during the evaluation of the metrics and saves them as *bitmap* image files. For each time interval evaluated in RSVVP, the following graphs are created in the folder *.../Results/Time-histories/*:

- a) Time histories of the true and test curves,
- b) Time histories of the metrics and
- c) Residuals time histories, histogram and cumulative distribution.

For multichannel input, the time histories of the metrics represent the weighted average of the time histories of the metrics from each channel. Similarly, the residuals time history, histogram and distribution are plotted using the weighted average from the residual histories of each channel. The graphs are saved in separate directories corresponding to each time interval.

TIME HISTORIES RESULTS

Time-history data generated by RSVVP is saved in a convenient format (ASCII or Excel) so that the user has ready access to the data. For example, the user may want to conduct additional post processing of the data, or to simply recreate the graphs produced by RSVVP so that they can be reformatted for inclusion in a report.

RSVVP generates time history files for the following:

- a) Original input curves
- b) Preprocessed curves
- c) Calculated metrics

Each of the original input curves is saved as an ASCII file in the subfolder *.../results_X/Input_curves*. Likewise, the preprocessed curves used in the metrics calculations are saved ASCII files in the subfolder *.../Results/Preprocessed_curves*. The time histories of the metrics are saved in Excel format; a separate metrics-time history file is created for each time interval evaluated (e.g., *Metrics_histories_whole.xlsx*).

EXAMPLES

Two examples are presented in the following sections in order to illustrate the step-by-step procedure for using RSVVP. In Example 1, an acceleration-time history from a full-scale crash test is compared to that of another “essentially” identical full-scale crash test using the *single channel* option in RSVVP. In Example 2, data from multiple data channels (including three acceleration channels and three rotational rate channels) from a numerical simulation are compared to those from a full-scale crash test using the *multiple channels* option.

EXAMPLE 1: SINGLE-CHANNEL COMPARISON

In this example, RSVVP is used to compare the longitudinal acceleration-time history between two full-scale crash tests. The tests involved a small car impacting a rigid longitudinal barrier at 100 km/hr at a 25-degree impact angle. Both tests were performed using new vehicles of the same make and model and the *same* longitudinal barrier. The acceleration-time history data was collected from the center-of-gravity of the vehicle in each case.

Although, theoretically, the results from two essentially identical crash tests should be the same, in practice, results from supposedly identical tests will always show some variations due to random differences in material make-up and experimental procedure. In fact, in complex experiments such as full-scale crash tests, it is practically impossible to *completely* control parameters such as the initial impact speed, impact angle, point of impact, or especially the behavior of the vehicle’s mechanical components. As such, perfect agreement between experiments is rarely achieved; however, the agreement should be within an acceptable range of expected differences that are typical of such experiments (e.g., tolerances determined from experience).

The steps of the evaluation process in this example will include 1) data entry, 2) preprocessing, 3) selection of comparison metrics, 4) calculation of the metrics and 5) interpretation of the results based on recommended acceptance criteria for these types of full-scale crash tests.

Analysis Type

The first step is to select the type of curve comparison that will be performed. In this example, only a single pair of curves is being compared, so the option ‘*single channel*’ is selected in the GUI window, as shown in Figure A-17.

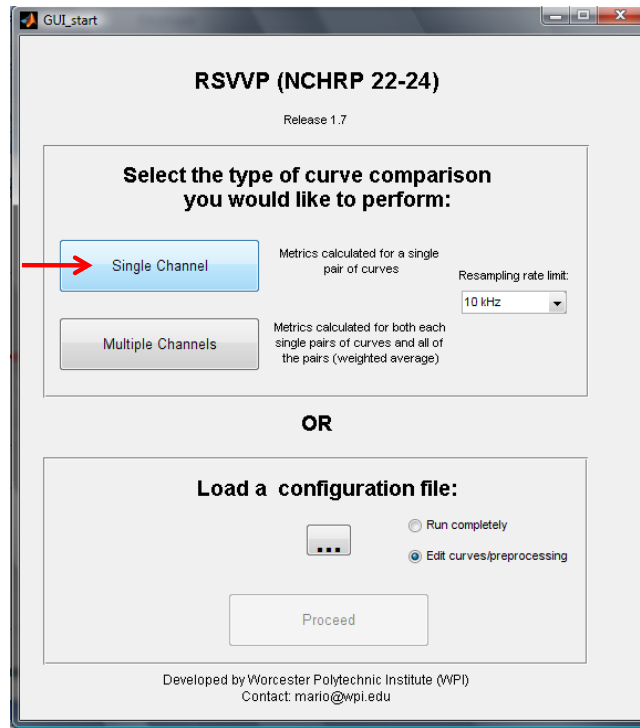


Figure A-17: The *Single Channel* option is selected in the GUI window

Data Entry and Preprocessing

The next step is to load the two acceleration time histories (i.e., curve 1 and 2) into RSVVP. Note that when comparing results from a numerical computation to those from a physical experiment, the experimental data will *always* be considered the *true curve* and the numerical data will be the *test curve*. In this case, however, both curves are from physical experiments, thus the choice of *true curve* and *test curve* is irrelevant. In this example, curve 1 is arbitrarily designated as the *true curve*, as shown in Figure A-18.

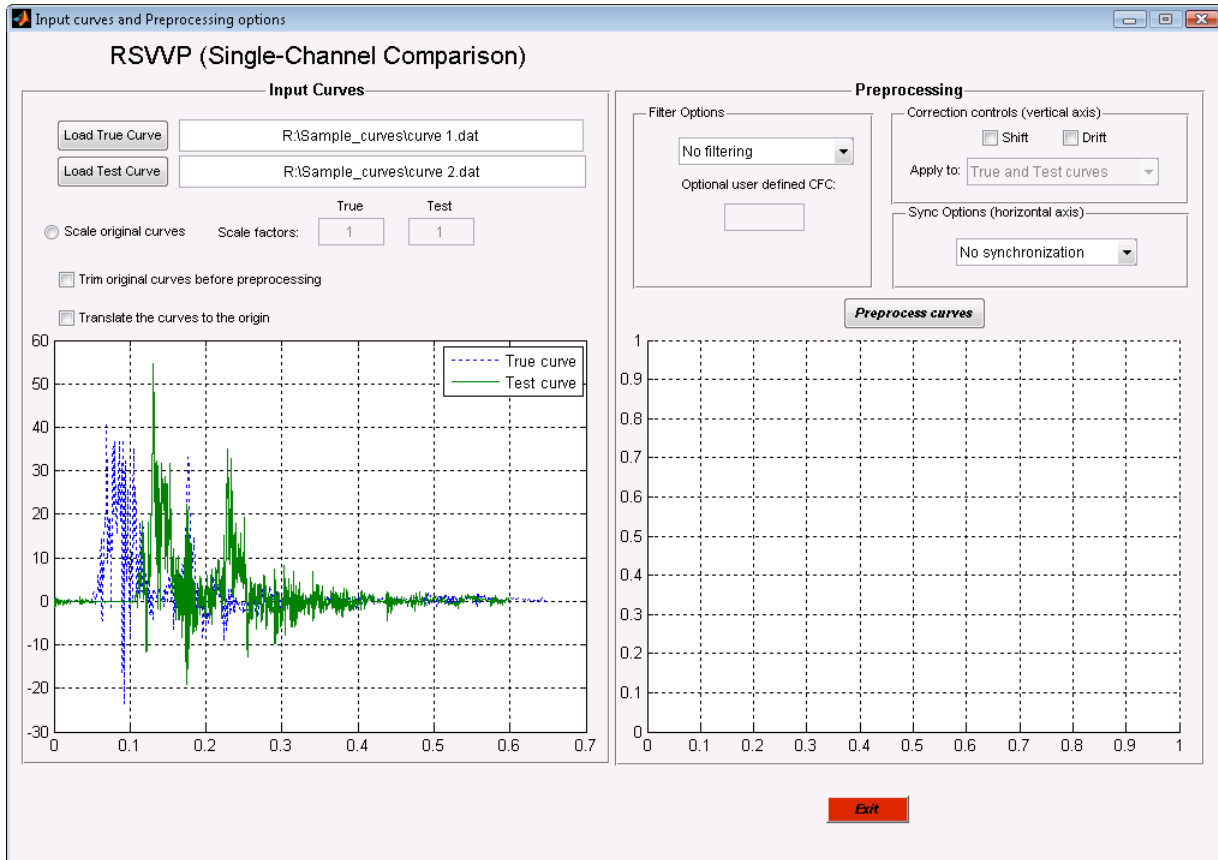


Figure A-18: GUI-preview of original input data loaded into RSVVP.

The various preprocessing operations are applied incrementally in this example in order to demonstrate how each operation contributes to the general improvement of the input curves. Note, however, that these preprocessing operations can be applied simultaneously.

From the graph shown in the GUI window (Figure A-18), it is obvious that both curves include some pre- and post-impact data. That is, the curves have an initial “flat” section at the beginning (pre-impact data) and a relatively flat section at the end starting at approximately 0.4 seconds (post impact data). To trim the heads and tails of the curves, select the checkbox beside the option ‘*trim original curves before preprocessing*’, as shown in Figure A-19. Note: this option opens a pop-up window (not shown) that permits the user to perform the trim operation.

The tails of the two curves were trimmed starting at 0.4 seconds, and the results are shown in the graphics display in the GUI window in Figure A-19. In this example, only the tail of the each curve is trimmed in order to demonstrate the effectiveness of the *synchronization*

option, which will be used in a later step. Note: It is typically desirable to also trim the head of the curves to eliminate any pre-impact data from the curve comparison.

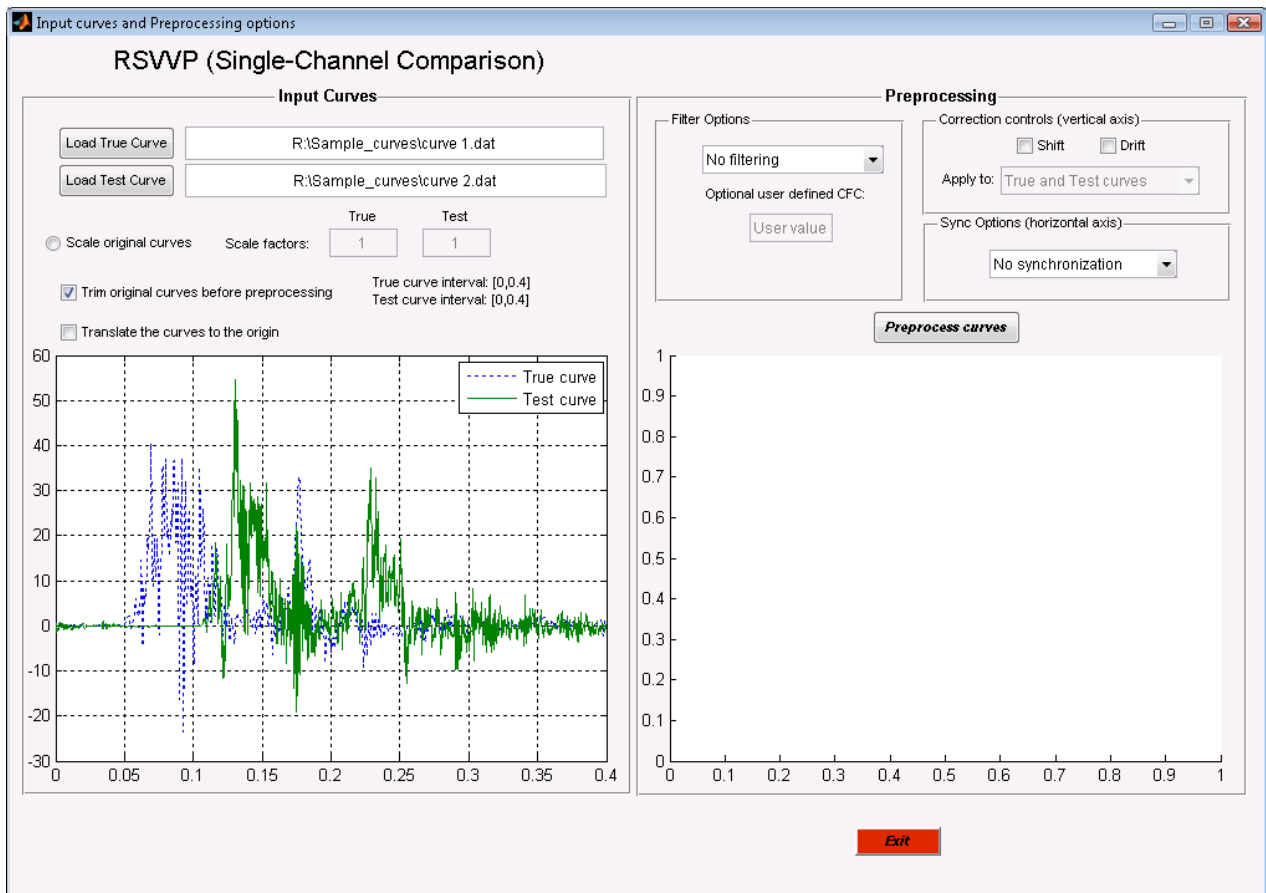


Figure A-19: Input curves after the manual trimming operation.

The input curves are characterized by a certain level of high frequency vibrations (as is typical of most acceleration data), which are not generally important in overall response of the vehicle, and should be filtered before computing the comparison metrics. In this example, the CFC 60 filter is selected and the results of the filtering operation are shown in the graph on the right side of the GUI-window in figure A-20.

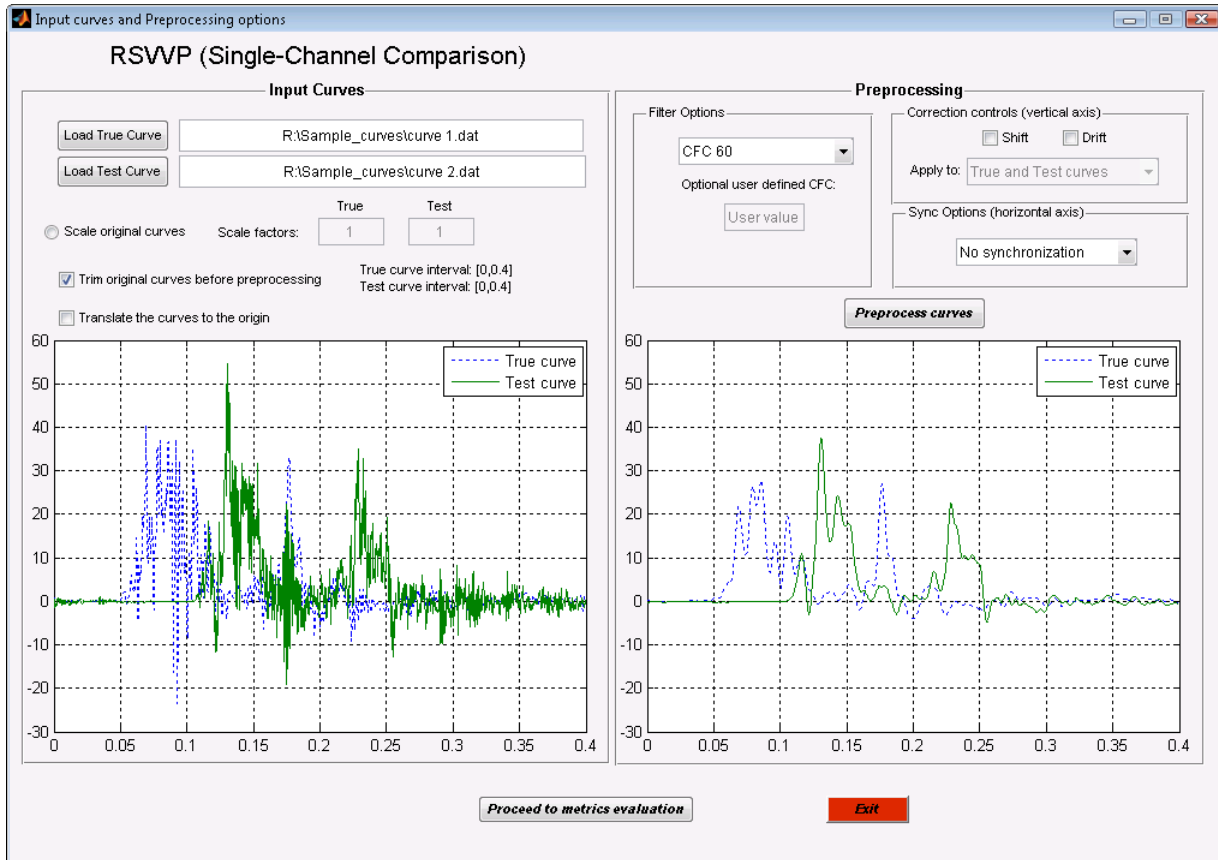


Figure A-20: Original and filtered acceleration time histories.

It is apparent from the graphs in Figure A-20 that the two curves are not synchronized with each other, as each curve demonstrates a different start-time at which the acceleration data started recording.

There are two methods available in RSVVP for performing the synchronization operation: one based on the ‘*Least squares*’ and the other based on ‘*Minimum area of residuals*’. The results from both methods are shown in Figure A-21. Both of these methods typically give good results, especially if the pre- and post-impact data is trimmed appropriately. In this case, however, the method of ‘*Minimum area of residuals*’ provides the best results.

Note: RSVVP shows a warning message if no filtering and/or synchronization options were selected.

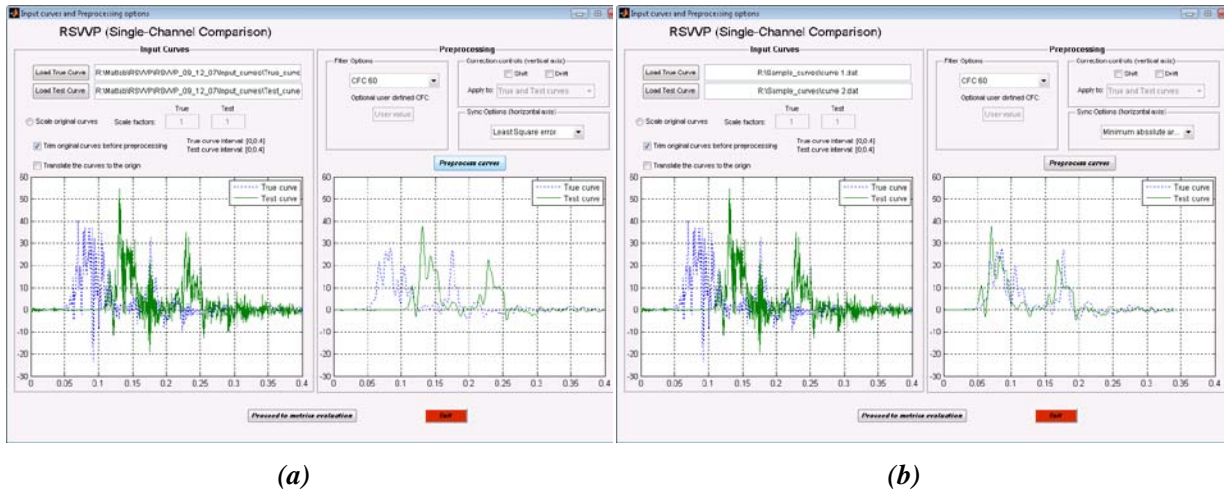


Figure A-21: Data synchronization results using (a) the *Least squares* method and (b) the *Minimum Area of Residuals* method.

After the test and true curves have been preprocessed, the next step is the selection of the metrics and time intervals.

Metric selection and evaluation

There are three *metrics profiles* available in RSVVP: 1) *NCHRP 22-24*, 2) *All Metrics* and 3) *User Selected Metrics*. In this example, the *NCHRP 22-24* metrics profile is selected, which is the recommended profile for comparing full-scale crash test data. This profile calculates Sprague & Geers MPC metrics and the ANOVA metrics and provides an interpretation of the data based on recommended acceptance criteria.

The option ‘*Whole time window and user-defined time window*’ was selected from the drop-down list in the *Time Window* box. For this option, RSVVP first computes the metrics based on all the available data from the preprocessed curves (i.e., complete length of curves) and then computes the metrics on a select interval of the data defined by the user.

The metric evaluation is initiated by pushing the ‘*Evaluate metrics*’ button shown in Figure A-22.

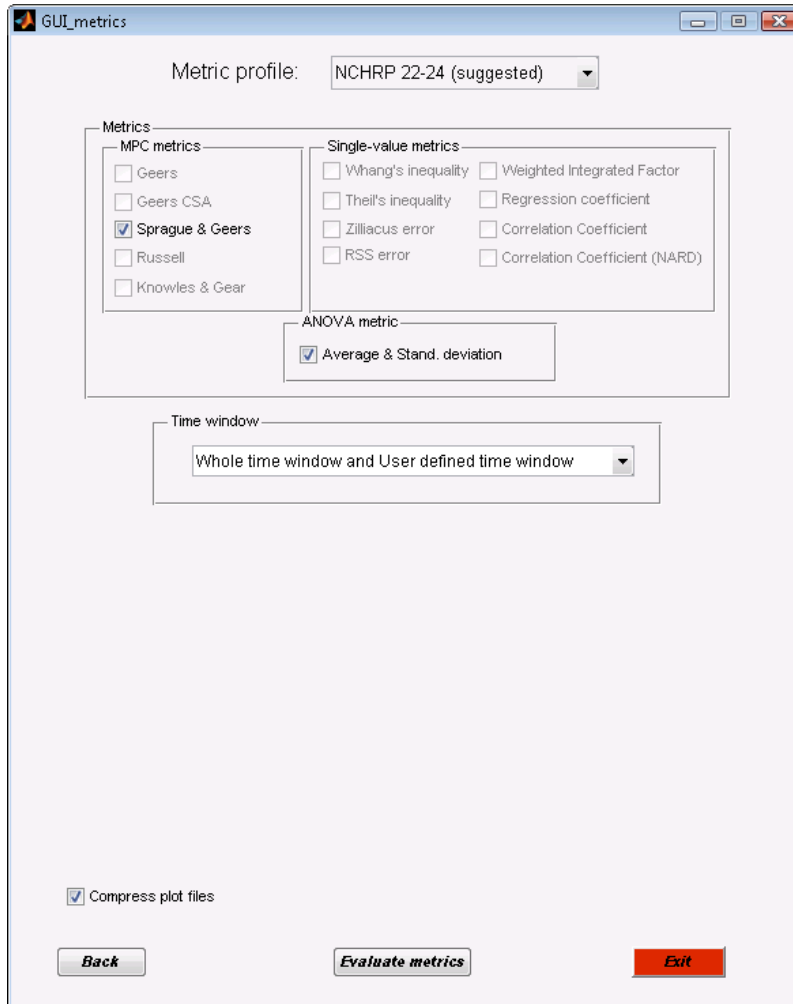


Figure A- 22: Selection of the metrics profile and time interval.

During the calculations of the metrics, various graphs appear and disappear on the computer screen. Screen-captures of these graphs are taken during this process and the files are saved in the output directory defined by the user. When the metrics calculations are completed, the results are displayed in the GUI-window shown Figure A-23. Note that beside each metric value RSVVP indicates whether or not the result meets the recommended acceptance criteria.

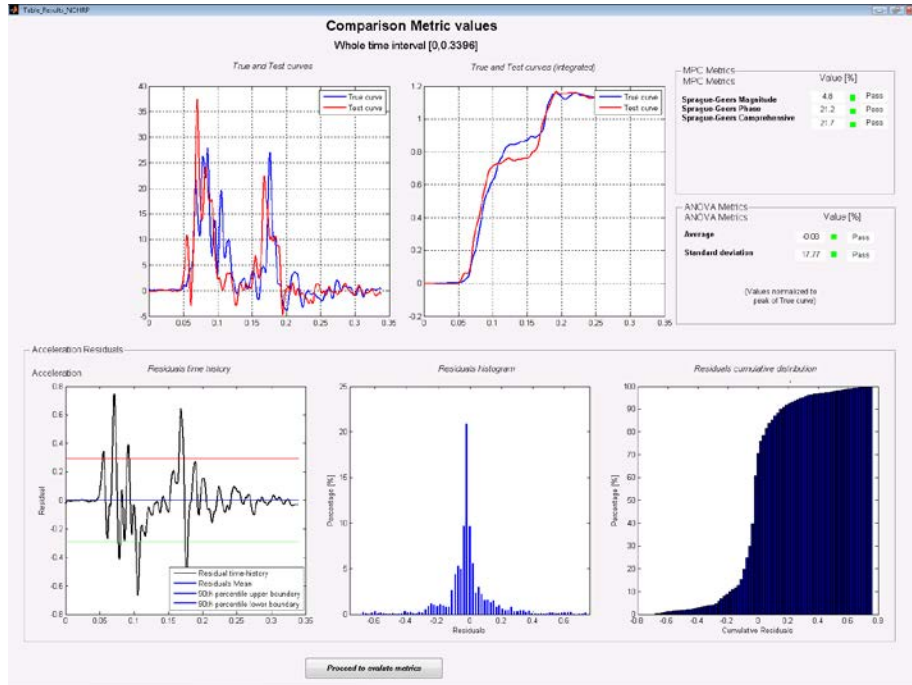


Figure A-23: GUI-window displaying results from *whole time interval* metrics calculations

Clicking the 'Proceed to evaluate metrics' button, opens a GUI-window, as shown in Figure A-24, that will allow the user to define *upper* and *lower* boundaries for a new time interval over which to calculate the metrics. The interval selected for this example is 0.05 seconds to 0.15 seconds.

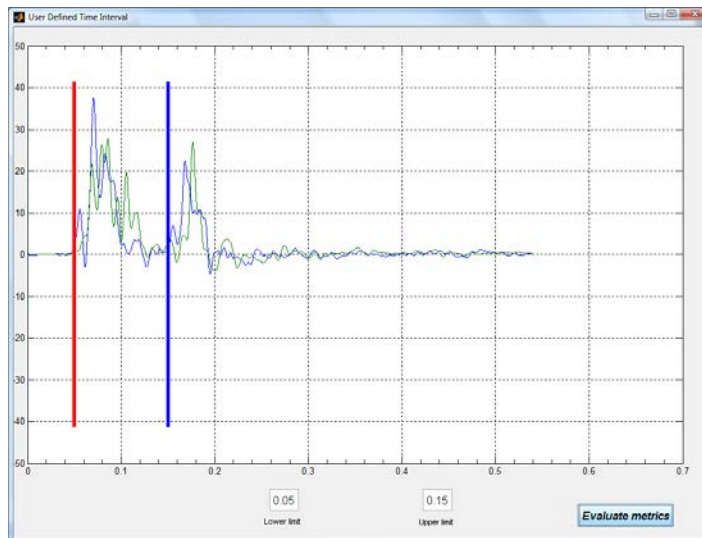
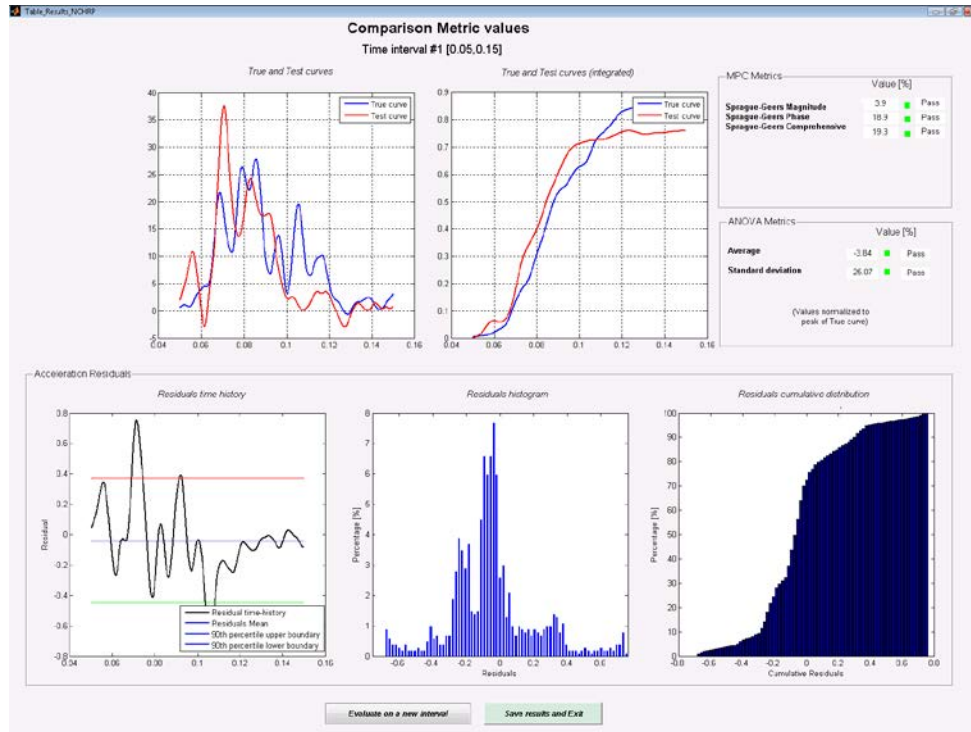


Figure A-24: GUI window for setting *user defined time interval*.

Once the user time window has been defined, the button ‘*Evaluate metrics*’ is pressed to start the calculations of the metrics based on the data within the user defined interval. As before, various graphs appear and disappear on the computer screen, as RSVVP captures and saves the data. The results of the metrics calculations for the user defined window are shown in the GUI-window shown in Figure A-25.



FigureA-25: Metrics results for user-defined *time interval* [0.05 sec, 0.15 sec]

At this point we have the option to save results and exit or to evaluate metrics on another time interval. For this example, we will select the ‘*Evaluate on a new interval*’ button and define another time interval over which to compute the metrics following the same procedure used in defining the first time interval. In this case, the time interval 0.15 seconds to 0.20 seconds is defined, as shown in Figure A-26; the resulting metrics calculations are shown in Figure A-27.

Note: The preceding procedure can be repeated indefinitely to compute comparison metrics for as many user-defined time intervals as desired.

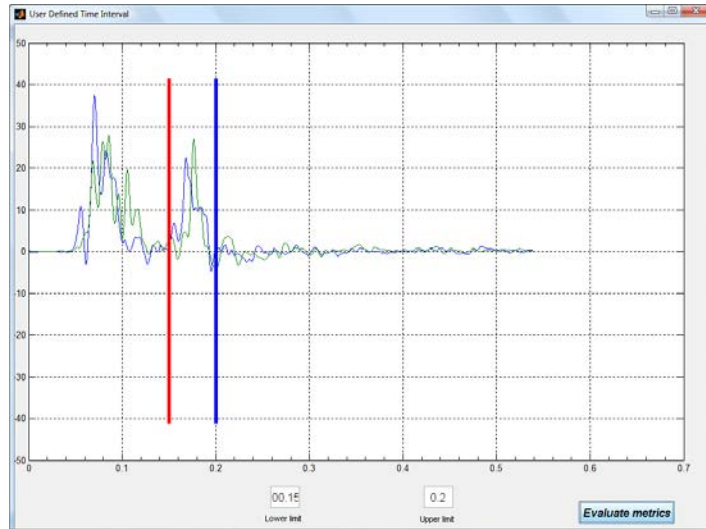


Figure A-26: Time interval 0.15 seconds to 0.20 seconds defined using GUI window

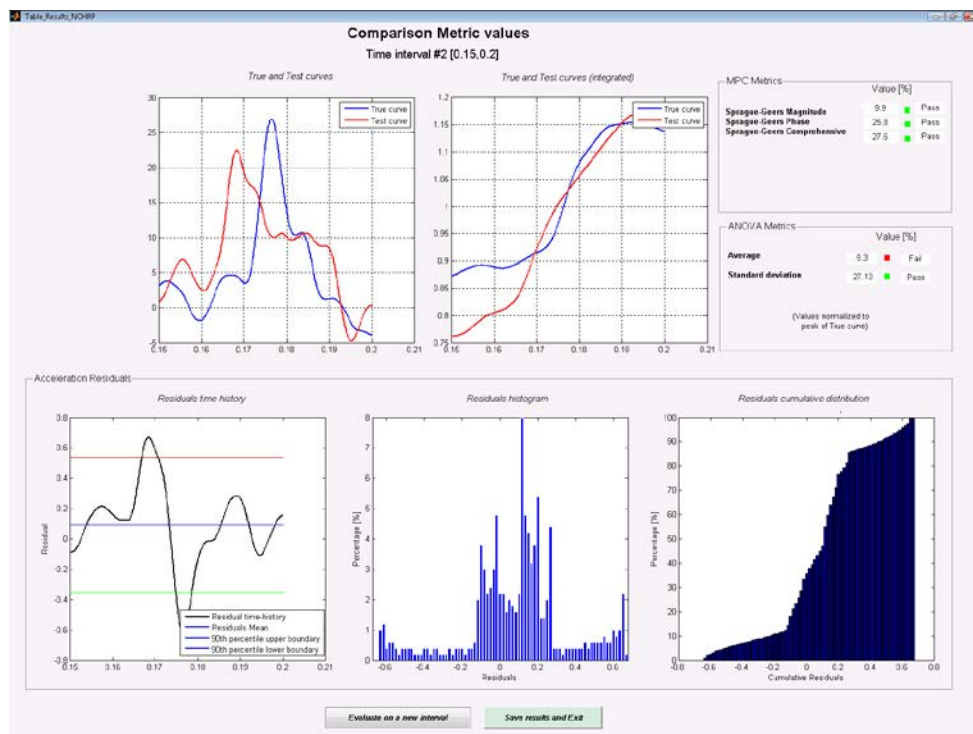


Figure A-27: Metrics computed for time interval [0.15 sec, 0.20 sec]

Save Results

To save results and exit, simply press the button ‘*Save results and Exit*’. RSVVP creates a folder called `\Results\` in the ‘working’ directory and creates subfolders for each time interval

evaluated during the metrics calculations. For this example, three different subfolders were created:

- Whole_time_Interval,
- User_defined_interval_1_[0.05 , 0.15] and
- User_defined_interval_2_[0.15005 , 0.19995].

Also, an Excel file named *Comparison Metrics.xls* is created that contains a summary of the metrics values for each interval.

Table A-3 summarizes the results of the comparison metrics for each of the three time intervals (i.e., whole time and two user defined time intervals). The values of the metrics computed using the whole time interval of data are all within the recommended acceptance criteria for these types of data, which indicates that they are similar enough to be considered “*equivalent*”. The metric values computed for the data between 0.5 seconds and 0.15 seconds also indicate that the two curves are effectively “*equivalent*.” The metric values calculated for the data between 0.15 seconds and 0.20 seconds, however, yield mixed results. For this section of the curves, the values for Sprague & Geers indicate that they are more or less “*Equivalent*,” while the ANOVA metrics indicate that the differences between the curves are at least not likely to be attributable to random experimental errors. This result should not be surprising, since any differences that occur during the crash event are cumulative and will continuously alter the response of the vehicle. Thus, the similarity of the curves should be expected to diminish as the test progresses, especially towards the end of the test.

Table A-3: Summary of the metrics values for each of the time intervals evaluated.

Calculated Metric	Whole Time Interval [0, 0.3396]	User Time Interval [0.05, 0.15]	User Time Interval [0.15, 0.20]
Sprague & Geers Magnitude	4.8% [pass]	3.9% [pass]	9.9% [pass]
Sprague & Geers Phase	21.2% [pass]	18.9% [pass]	25.8% [pass]
Sprague & Geers Comprehensive	21.7% [pass]	19.3% [pass]	27.6% [pass]
ANOVA Average Residual Error	-.08% [pass]	-3.84% [pass]	9.3% [fail]
ANOVA Standard Deviation of Residual Errors	17.77% [pass]	25.07% [pass]	27.13% [pass]

EXAMPLE 2: MULTIPLE-CHANNEL COMPARISON

In this second example, the *multiple channel option* in RSVVP is used to compare the results from a finite element analysis to the results of a full-scale crash test. Six data channels are compared: three acceleration channels and three rotational rate channels.

Although each of these channels could be compared independently using the *single channel option* in RSVVP, the *multiple channel option* provides an additional analysis feature. That is, in addition to computing the metrics for each individual channel, the program also computes a *single set of metrics* that provide a comprehensive assessment of the combined data. The basic concept of this comprehensive assessment is to calculate a *weight factor* for each channel that is representative of its importance with respect to the other channels. Once the weighting factors have been evaluated, the multi-channel comprehensive metrics are calculated from a weighted average of the individual channel metrics.

Analysis Type

The first step is to select the type of curve comparison that will be performed. In this example, six pairs of curves are being compared, so the option ‘*multiple channel*’ is selected in the GUI window, as shown in Figure A-28.

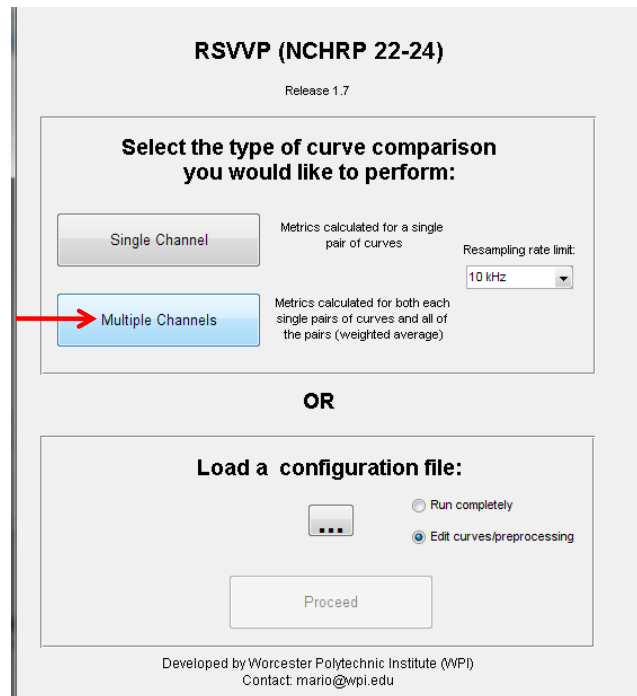
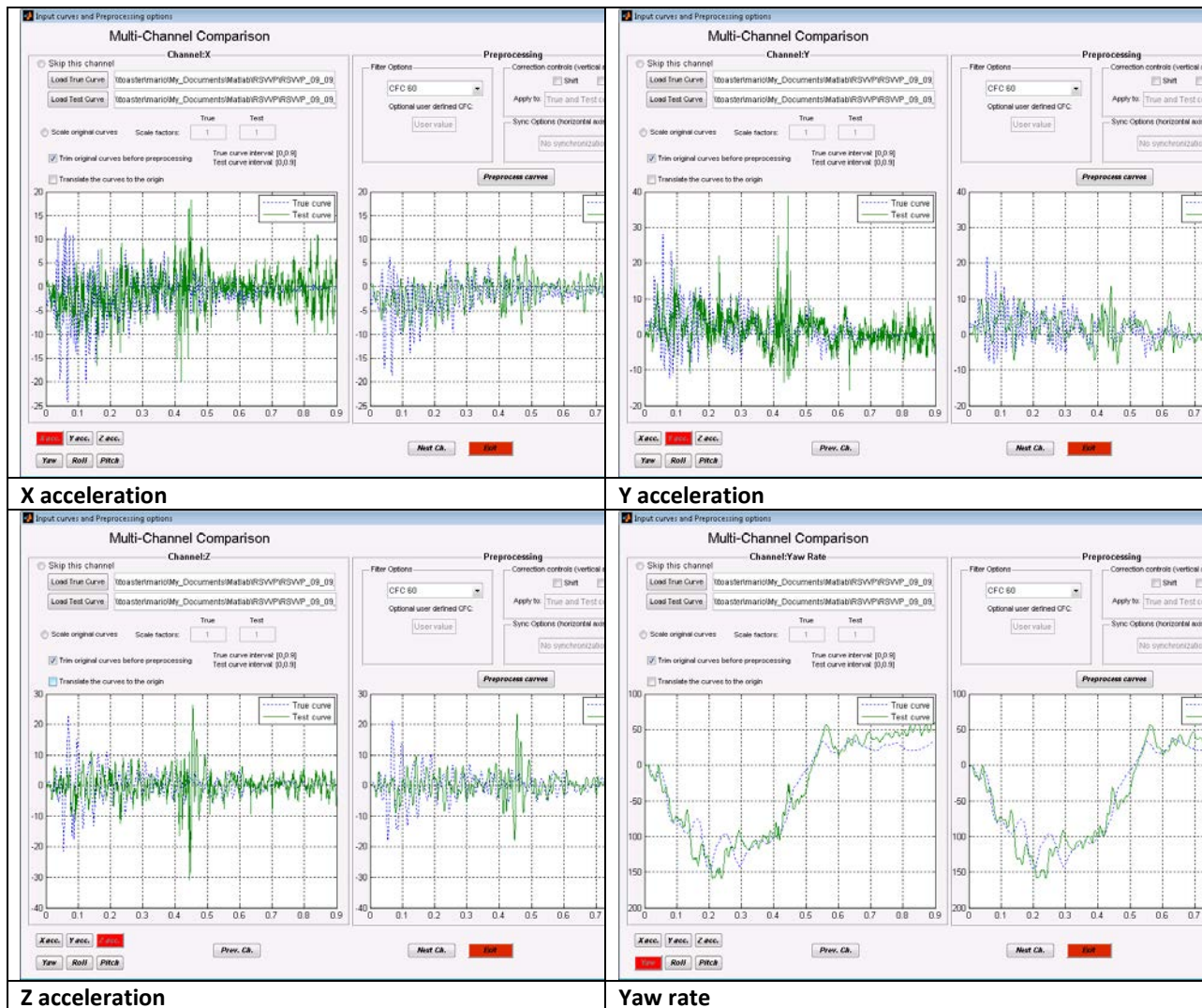


Figure A-28: The *Multiple Channel* option is selected in the GUI window

Data Entry and Preprocessing

The data entry for the *multiple channel* option is accomplished by loading and preprocessing each pair of data channels one at a time, using the same basic procedure described in Example 1. In fact, the GUI for the *multiple channel* option is the same basic GUI used in the *single channel* option. Since each pair of curves is processed independently, it is possible to select different preprocessing options for each channel. In this example, however, the same preprocessing options are used for each of the six pairs of data. In particular, all curves were trimmed using the ‘*trim original curves before preprocessing*’ option (i.e., lower limit = 0.0 and upper limit = 0.9

seconds), and filtered using SAE 60 filter. Figure A-29 shows the original and preprocessed curve pairs for each of the acceleration and rotational rate channels.



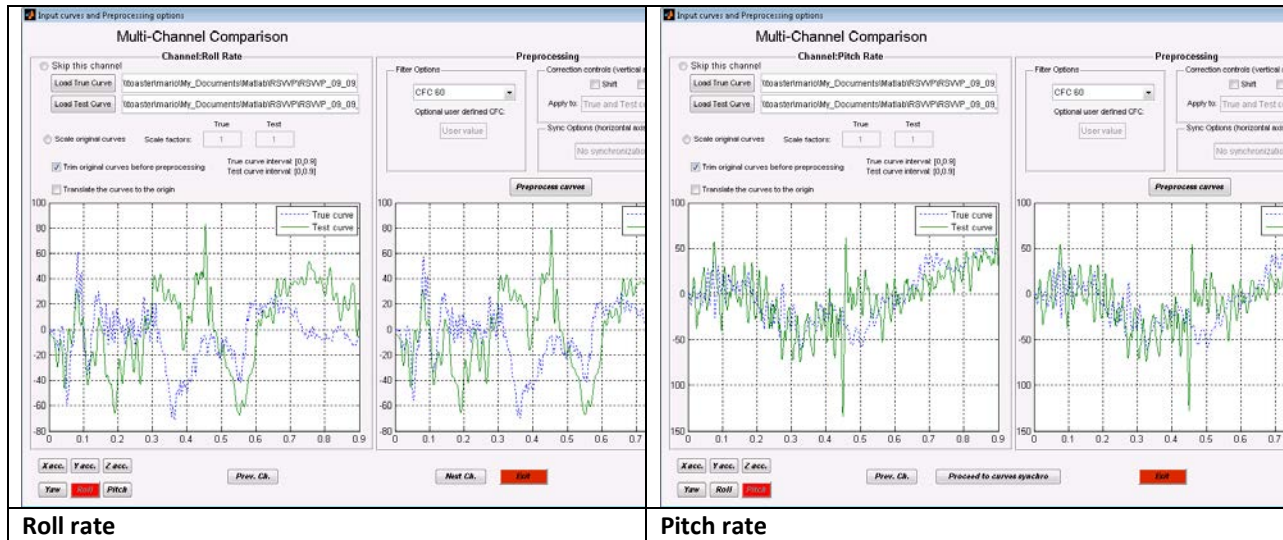
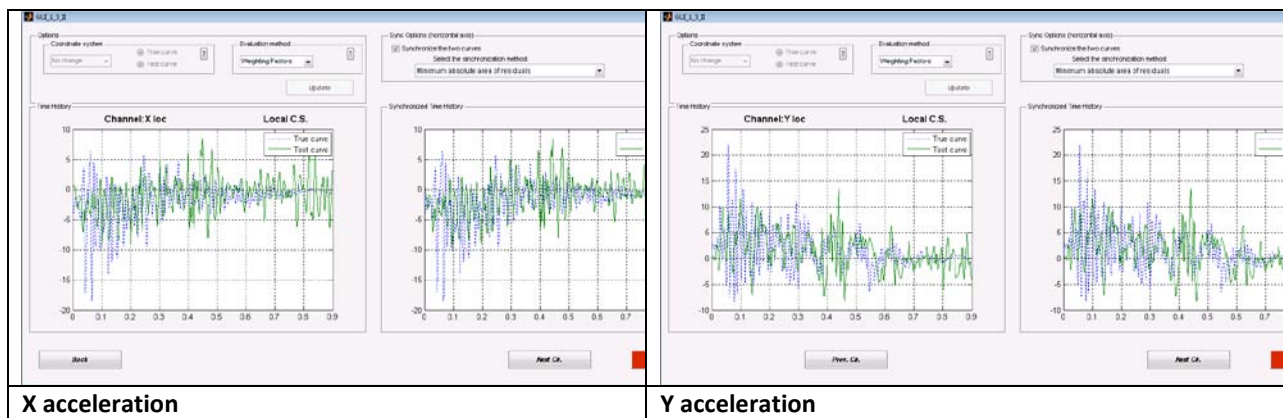


Figure A-29: Original and pre-processed curve pairs for each data channel

Note that, in the multi-channel case, the synchronization is performed in an intermediate step, after all the channels have been input. Once all the curve pairs have been entered into RSVVP and preprocessed, the *'Proceed to curves syncho'* option at the bottom of the GUI window will open a new GUI for synchronizing the curves. The default evaluation method, *'Weighting Factors,'* will be used in this example (see Appendix A2 for more details regarding the Weighting Factor method). The default synchronization method, *'Minimum absolute area of residuals,'* is then used to synchronize each of the curve pairs. The results of the synchronization operation are shown in Figure A-30.



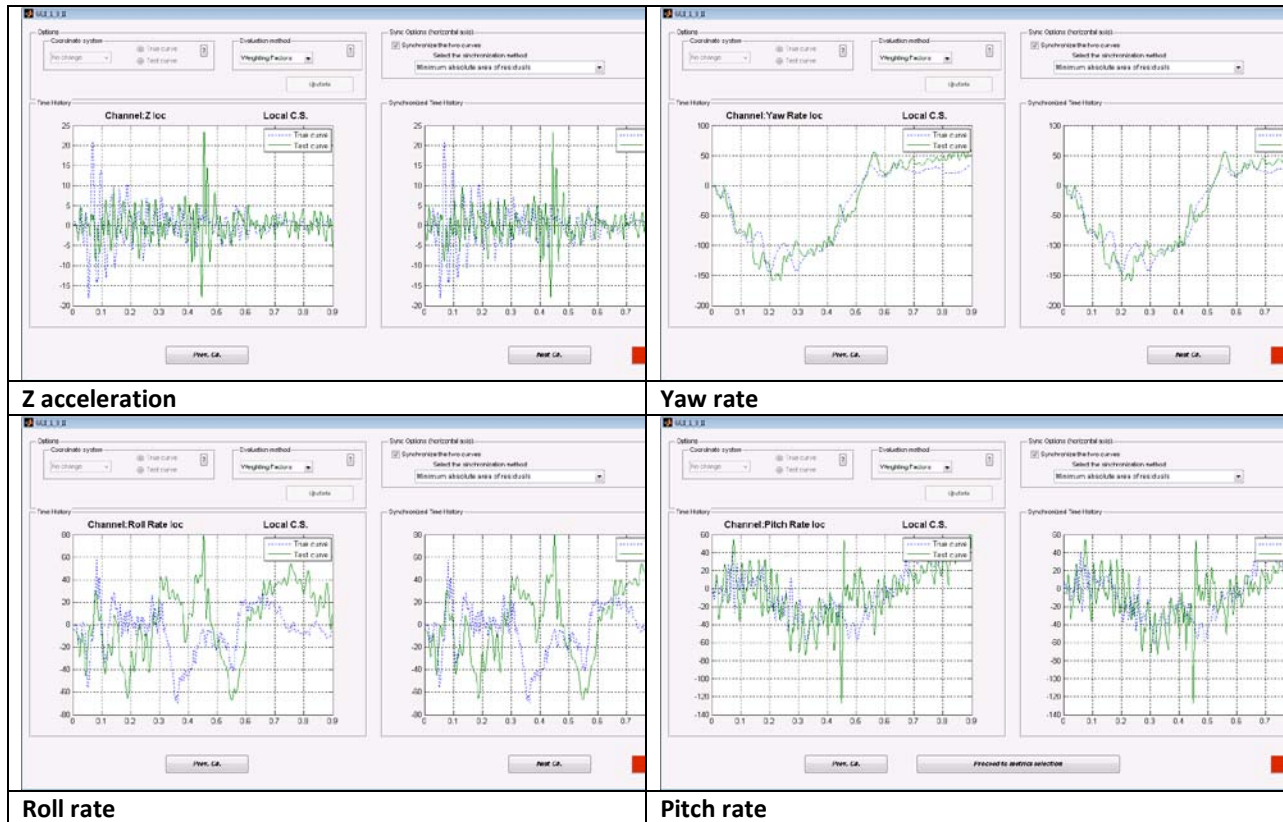


Figure A-30: Synchronization results

Metric selection and evaluation

After the synchronization process is completed, RSVVP automatically opens another GUI for selecting the desired metrics. For this example, the NCHRP 22-24 metrics profile (i.e., ANOVA metrics and the Sprague & Geers MPC metrics) was selected from the *Metrics Box* and the option *Whole time window only* was selected from the drop-down menu in the *Time Window Box*.

The metrics calculations are initiated by pressing the *Evaluate metrics* button at the bottom of the GUI window. RSVVP then calculates the metrics for each individual channel, computes a weight factor for each channel based on a pseudo momentum approach (see Appendix A2), and computes the multi-channel comprehensive metrics from a weighted average of the individual channels. During the calculations of the metrics, various graphs appear and disappear on the computer screen. Screen-captures of these graphs are taken during this process and the files are saved in the output directory defined by the user. When the metrics calculations

are completed, RSVVP displays the results of the first channel on the screen. Note that beside each metric value RSVVP indicates whether or not the result meets the recommended acceptance criteria. To view the results for the other five channels or to view the weighted average results, use the drop-down menu at the left of the *True and Test curves* graph to select the corresponding option. Note that when the *weighted average of the results* is selected from the drop-down menu, RSVVP displays a bar graph of the weight factors for each channel. Figures A-31 through A-36 show the results obtained for each channel, and Figure A-37 shows the weighted average results.

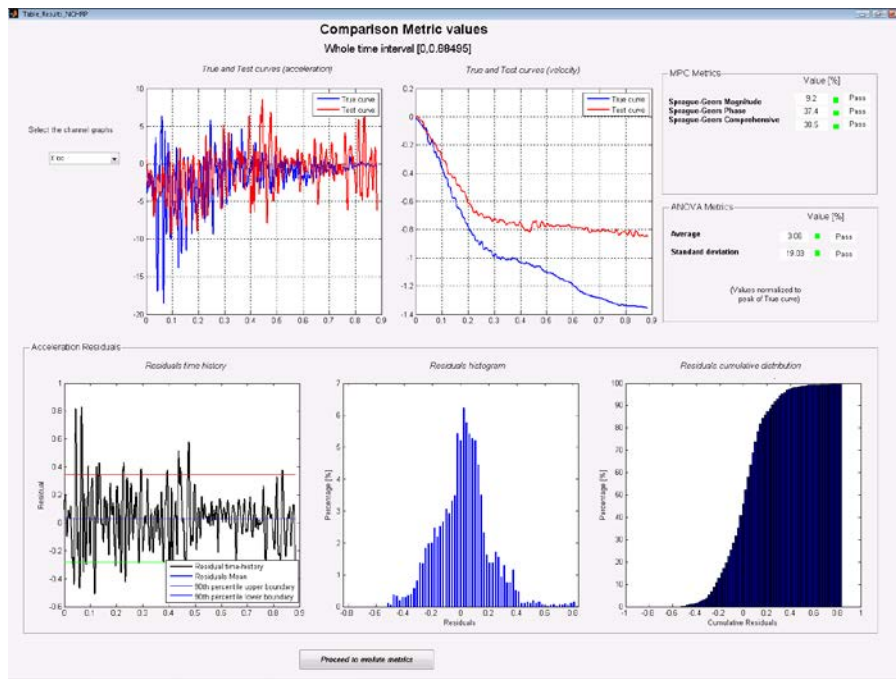


Figure A-31: Screen output of the results for the X channel.

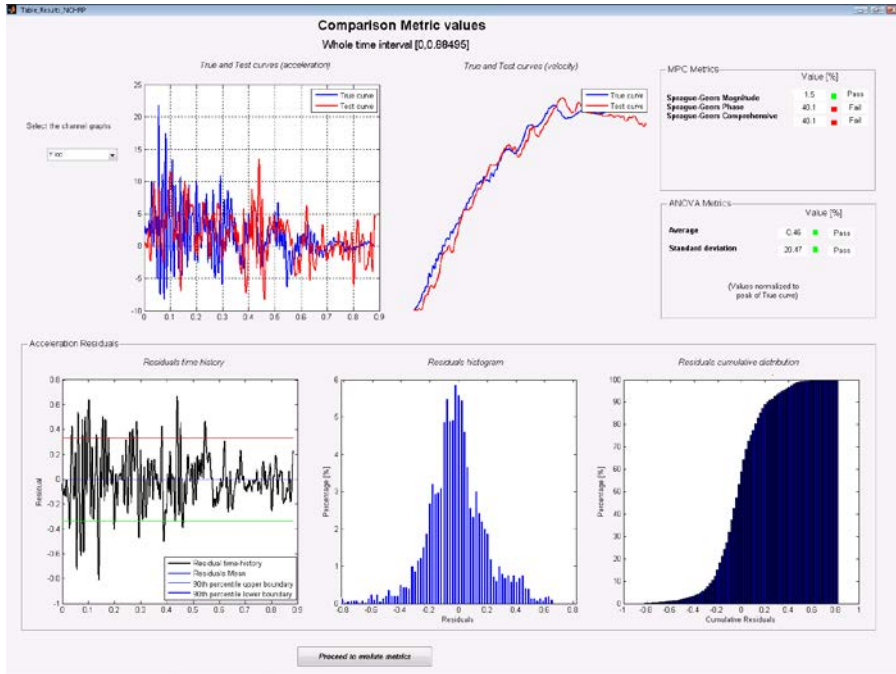


Figure A-32: Screen output of the results for the Y channel.

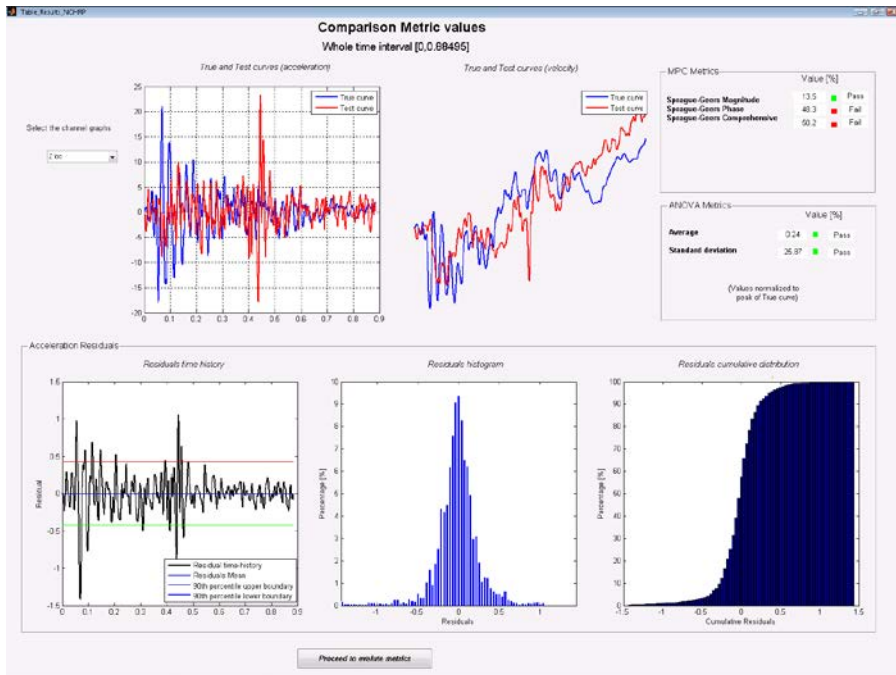


Figure A-33: Screen output of the results for the Z channel.

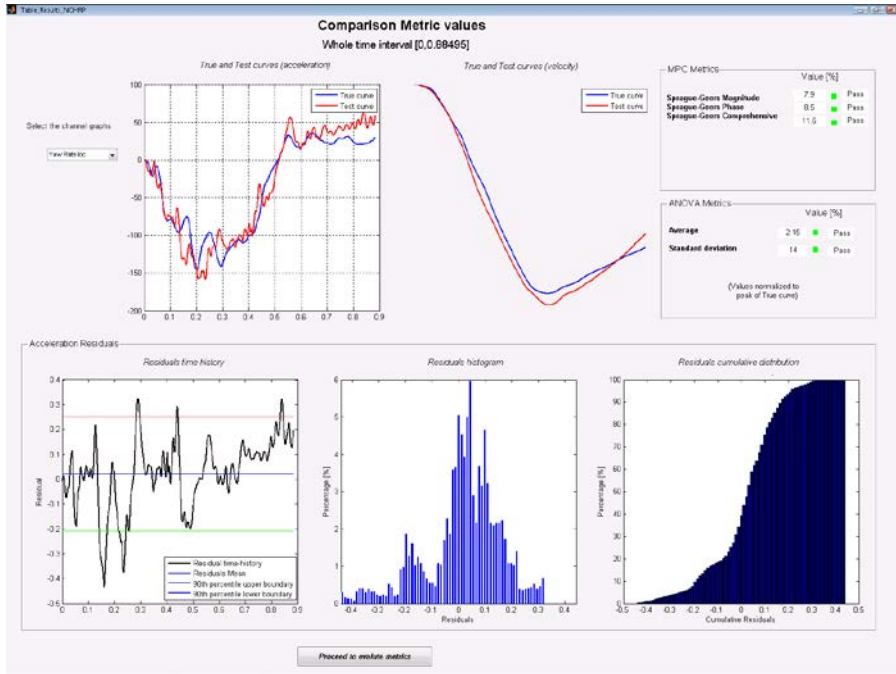


Figure A-34: Screen output of the results for the Yaw channel.

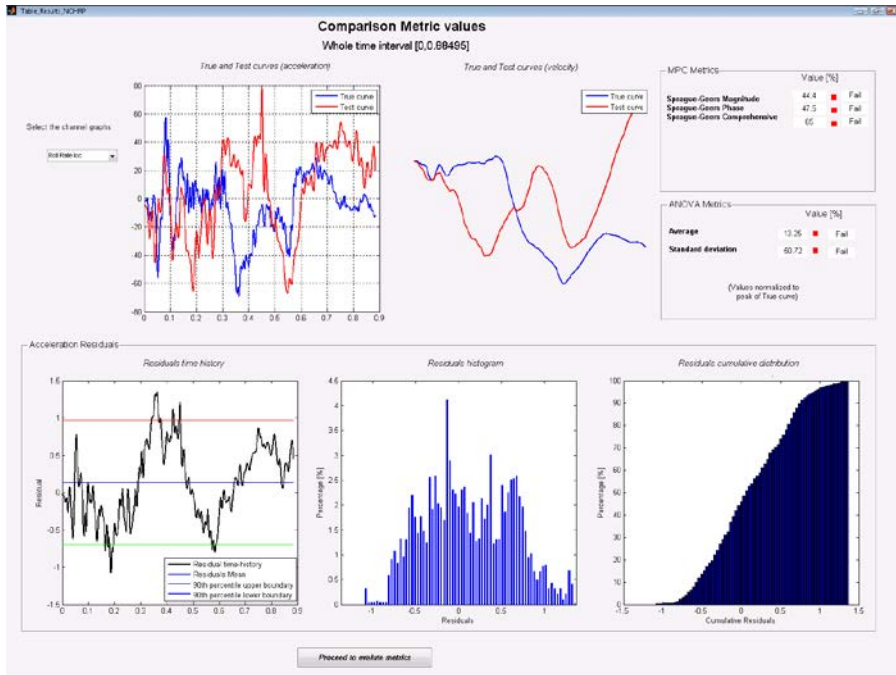


Figure A-35: Screen output of the results for the Roll channel.

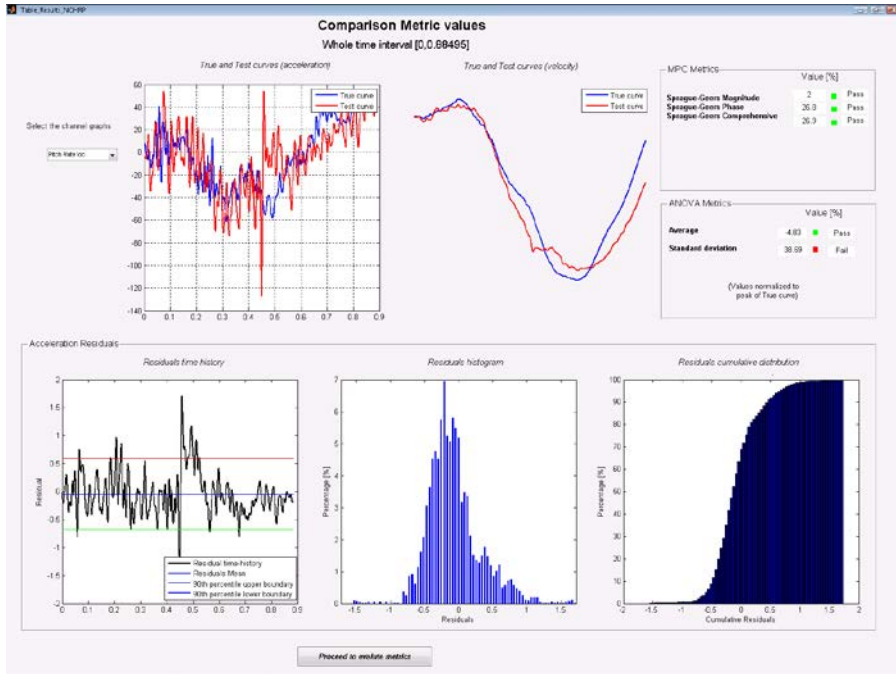


Figure A-36: Screen output of the results for the Pitch channel.

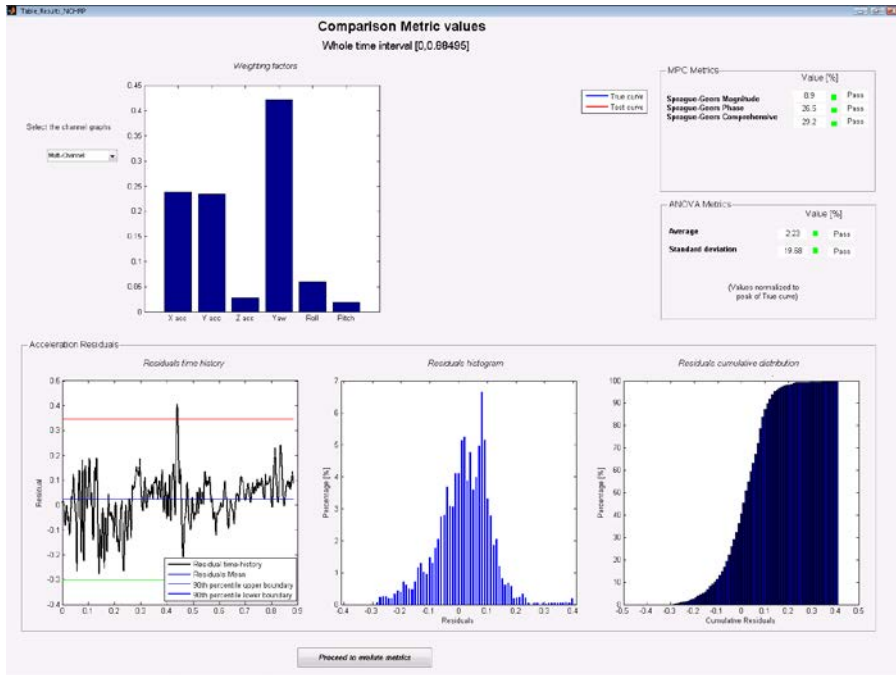


Figure A-37: Screen output of the results for the weighted average.

Table A-4 shows a summary of the comparison metrics computed for each data channel and the weighted average. The values that exceed the NCHRP 22-24 recommended acceptance criterion for that metric are displayed with a red background in the table.

The comparison of the roll-channel shows that the simulation results were not similar to those measured in the test. The magnitudes of the z-channel accelerations in the numerical simulation are consistent with the test data, but they are out of phase with each other. The pitch-channel data from the simulation was of similar magnitude and phase, but failed to meet the criterion for the standard deviation of residual errors. Thus, based on the comparison metrics for the individual channels, the numerical model cannot be deemed valid.

Taking into consideration the weighted contribution of each channel to the overall response of the vehicle in the test event, however, yields a set of comprehensive metrics which indicate that, in fact, the simulation and test are in agreement. The weighting factors for each channel are shown in Figure A-37, which indicate that the response of the vehicle was dominated by the x-acceleration, y-acceleration and yaw-rate. It should not be surprising that the numerical simulation and the test were not in agreement with respect to the z-, roll-, and pitch-channels; since there is such low energy involved in these channels, compared to the other channels, the agreement would not be expected to be in any better had we been comparing two identical full-scale crash tests.

Table A-4: Summary of the calculated metrics for the multi-channel data

Data Channel	Sprague & Geers		ANOVA	
	(M)	(P)	(average)	(std)
x	9 %	37 %	3 %	19 %
y	2 %	40 %	0 %	2 %
z	14 %	48 %	0 %	26 %
Yaw	8 %	9 %	2 %	14 %
Roll	44 %	48%	13 %	51 %
Pitch	2 %	27 %	-5 %	39 %
Weighted Average	9 %	27 %	0 %	2 %

REFERENCES

- [1] M.H. Ray, “Repeatability of Full-Scale Crash Tests and a Criteria for Validating Finite Element Simulations”, *Transportation Research Record*, Vol. 1528, pp. 155-160, (1996).
- [2] W.L. Oberkampf and M.F. Barone, “Measures of Agreement Between Computation and Experiment: Validation Metrics,” *Journal of Computational Physics* Vol. 217, No. 1 (Special issue: Uncertainty quantification in simulation science) pp 5–36, (2006).
- [3] T.L. Geers, “An Objective Error Measure for the Comparison of Calculated and Measured Transient Response Histories”, *The Shock and Vibration Bulletin*, The Shock and Vibration Information Center, Naval Research Laboratory, Washington, D.C., Bulletin 54, Part 2, pp. 99-107, (June 1984).
- [4] *Comparative Shock Analysis (CSA) of Main Propulsion Unit (MPU), Validation and Shock Approval Plan*, SEAWOLF Program: Contract No. N00024-90-C-2901, 9200/SER: 03/039, September 20, 1994.
- [5] M.A. Sprague and T.L. Geers, “Spectral elements and field separation for an acoustic fluid subject to cavitation”, *J Comput. Phys.*, pp. 184:149, Vol. 162, (2003).
- [6] D.M. Russell, “Error Measures for Comparing Transient Data: Part I: Development of a Comprehensive Error Measure”, *Proceedings of the 68th shock and vibration symposium*, pp. 175–184, (2006).
- [7] L.E. Schwer, “Validation Metrics for Response Time Histories: Perspective and Case Studies”, *Engng. with Computers*, Vol. 23, Issue 4, pp. 295–309, (2007).
- [8] C.P. Knowles and C.W. Gear, “Revised validation metric”, unpublished manuscript, 16 June 2004 (revised July 2004).
- [9] J. Cohen, P. Cohen, S.G. West and L.S. Aiken, *Applied multiple regression/correlation analysis for the behavioral sciences*, Hillsdale, NJ: Lawrence Erlbaum, (3rd ed.), 2003.
- [10] S. Basu and A. Haghghi, “*Numerical Analysis of Roadside Design (NARD) vol. III: Validation Procedure Manual*”, Report No. FHWA-RD-88-213, Federal Highway Administration, Virginia, 1988.
- [11] B. Whang, W.E. Gilbert and S. Zilliagus, *Two Visually Meaningful Correlation Measures for Comparing Calculated and Measured Response Histories*, Carderock Division, Naval Surface Warfare Center, Bethesda, Maryland, Survivability, Structures and Materials Directorate, Research and Development Report, CARDEROCKDIV-U-SSM-67-93/15, September, 1993.
- [12] H. Theil, *Economic Forecasts and Policy*, North-Holland Publishing Company, Amsterdam, 1975.
- [13] D.M. Russell, “Error Measures for Comparing Transient Data: Part II: Error Measures Case Study”, *Proceedings of the 68th shock and vibration symposium*, pp. 185–198, (2006).

APPENDIX A1: Comparison Metrics in RSVVP

A brief description of the metrics evaluated by RSVVP is presented in this section. All fourteen metrics available in RSVVP are deterministic shape-comparison metrics. Details about the mathematical formulation of each metric can be found in the cited literature. Conceptually, the metrics evaluated can be classified into three main categories: (i) magnitude-phase-composite (MPC) metrics, (ii) single-value metrics and (iii) analysis of variance (ANOVA) metrics.

MPC METRICS

MPC metrics treat the curve magnitude and phase separately using two different metrics (i.e., M and P, respectively). The M and P metrics are then combined into a single value comprehensive metric, C. The following MPC metrics are included in RSVVP: (a) Geers (original formulation and two variants), (b) Russell and (c) Knowles and Gear. [3-8] Table A1-1 Table A1-1 shows the analytical definition of each metric. In this and the following sections, the terms m_i and c_i refer to the measured and computed quantities, respectively, with the “i” subscript indicating a specific instant in time.

In all MPC metrics the phase component (P) should be insensitive to magnitude differences but sensitive to differences in phasing or timing between the two time histories. Similarly, the magnitude component (M) should be sensitive to differences in magnitude but relatively insensitive to differences in phase. These characteristics of MPC metrics allow the analyst to identify the aspects of the curves that do not agree. For each component of the MPC metrics, zero indicates that the two curves are identical. Each of the MPC metrics differs slightly in its mathematical formulation. The different variations of the MPC metrics are primarily distinguished in the way the phase metric is computed, how it is scaled with respect to the magnitude metric and how it deals with synchronizing the phase. In particular, the Sprague & Geers metric [5] uses the same phase component as the Russell metric [6]. Also, the magnitude component of the Russell metric is peculiar as it is based on a base-10 logarithm and it is the only MPC metric that is symmetric (i.e., the order of the two curves is irrelevant). The Knowles

and Gear metric [7,8] is the most recent variation of MPC-type metrics. Unlike the previously discussed MPC metrics, it is based on a point-to-point comparison. In fact, this metric requires that the two compared curves are first synchronized in time based on the so called Time of Arrival (TOA), which represents the time at which a curve reaches a certain percentage of the peak value. In RSVVP the percentage of the peak value used to evaluate the TOA was 5%, which is the typical value found in literature. Once the curves have been synchronized using the TOA, it is possible to evaluate the magnitude metric. Also, in order to avoid creating a gap between time histories characterized by a large magnitude and those characterized by a smaller one, the magnitude component M has to be normalized using the normalization factor QS .

Table A1-1: Definition of MPC metrics.

	Magnitude	Phase	Comprehensive
Integral comparison metrics			
Geers	$M_G = \sqrt{\frac{\sum c_i^2}{\sum m_i^2} - 1}$	$P_G = 1 - \frac{\sum c_i m_i}{\sqrt{\sum c_i^2 \sum m_i^2}}$	$\sqrt{M_G^2 + P_G^2}$
Geers CSA	$M_G = \sqrt{\frac{\sum c_i^2}{\sum m_i^2} - 1}$	$P_{CSA} = 1 - \frac{ \sum c_i m_i }{\sqrt{\sum c_i^2 \sum m_i^2}}$	$\text{sign}(\sum c_i m_i) \sqrt{M_{CSA}^2 + P_{CSA}^2}$
Sprague & Geers	$M_G = \sqrt{\frac{\sum c_i^2}{\sum m_i^2} - 1}$	$P_{SG} = \frac{1}{\pi} \cos^{-1} \frac{\sum c_i m_i}{\sqrt{\sum c_i^2 \sum m_i^2}}$	$\sqrt{M_{SG}^2 + P_{SG}^2}$
Russell	$M_R = \text{sign}(m) \cdot \text{Log}_{10}(1 + m)$ $\text{where } m = \frac{(\sum c_i^2 - \sum m_i^2)}{\sqrt{\sum c_i^2 \sum m_i^2}}$	$P_R = \frac{1}{\pi} \cos^{-1} \frac{\sum c_i m_i}{\sqrt{\sum c_i^2 \sum m_i^2}}$	$\sqrt{\frac{\pi}{4} (M_R^2 + P_R^2)}$
Point-to-point comparison metrics			
Knowles & Gear	$M_{KG} = \sqrt{\frac{\sum \left(\frac{ m_i }{m_{max}}\right)^p (\tilde{c}_i - m_i)^2}{\sum \left(\frac{ m_i }{m_{max}}\right)^p (m_i)^2}}$ $\text{where } \tilde{c} = c(t - \tau)$ $\text{(with } \tau = TOA_c - TOA_m)$	$P_{KG} = \frac{ TOA_c - TOA_m }{TOA_m}$	$\sqrt{\frac{10M_{KG}^2 + 2P_{KG}^2}{12}}$

SINGLE-VALUE METRICS

Single-value metrics give a single numerical value that represents the agreement between the two curves. Seven single-value metrics were considered in this work: (1) the correlation coefficient metric, (2) the NARD correlation coefficient metric (NARD), (3) Zilliacus error metric, (4) RSS error metric, (5) Theil's inequality metric, (6) Whang's inequality metric and (7) the regression coefficient metric. [9-12] The first two metrics are based on integral comparisons while the others are based on point-to-point comparisons. The definition of each metric is shown in Table A1-2.

Table A1-2: Definition of single-value metrics.

Integral comparison metrics			
Correlation Coefficient	$\frac{n \sum c_i m_i - \sum c_i \sum m_i}{\sqrt{n \sum c_i^2 - (\sum c_i)^2} \sqrt{n \sum m_i^2 - (\sum m_i)^2}}$	Correlation Coefficient (NARD)	$\frac{\sum c_i m_i}{\sqrt{\sum c_i^2} \sqrt{\sum m_i^2}}$
Weighted Integrated Factor		$\sqrt{\frac{\sum \max(m_i^2, c_i^2) \cdot \left(1 - \frac{\max(0, m_i \cdot c_i)}{\max(m_i^2, c_i^2)}\right)^2}{\sum \max(m_i^2, c_i^2)}}$	
Point-to-point comparison metrics			
Zilliacus error	$\frac{\sum c_i - m_i }{\sum m_i }$	RSS error	$\frac{\sqrt{\sum (c_i - m_i)^2}}{\sqrt{\sum m_i^2}}$
Theil's inequality	$\frac{\sqrt{\sum (c_i - m_i)^2}}{\sqrt{\sum c_i^2} + \sqrt{\sum m_i^2}}$	Whang's inequality	$\frac{\sum c_i - m_i }{\sum c_i + \sum m_i }$
Regression coefficient	$\sqrt{1 - \frac{(n-1) \sum (c_i - m_i)^2}{n \sum (m_i - \bar{m})^2}}$		

ANOVA METRICS

ANOVA metrics are based on the assumption that two curves do, in fact, represent the same event such that any differences between the curves must be attributable only to random experimental error. The analysis of variance (i.e., ANOVA) is a standard statistical test that assesses whether the variance between two curves can be attributed to random error.[1,2] When two time histories represent the same physical event, both should be identical such that the mean residual error, \bar{e} , and the standard deviation of the residual errors, σ , are both zero. Of course, this is never the case in practical situations (e.g., experimental errors cause small variations between tested responses even in identical tests). Ray proposed a method where the residual error and its standard deviation are normalized with respect to the peak value of the true curve and came to the following acceptance criteria based on six repeated frontal full-scale crash tests [1]:

- The average residual error normalized by the peak response (i.e., \bar{e}^r) should be less than five percent.

$$\bar{e}^r = \frac{\sum (c_i - m_i) / m_{\max}}{n} < 0.05 \cdot m_{\max}$$

- The standard deviation of the normalized residuals (i.e., σ^r) should be less than 35 percent.

$$\sigma^r = \sqrt{\frac{\sum (e^r - \bar{e}^r)^2}{n-1}} < 0.35 \cdot m_{\max}$$

APPENDIX A2: Multi-Channel Weight Factors

The multi-channel mode in RSVVP was created for the specific purpose of comparing numerical simulations of vehicle impact into roadside barriers to the results from a full-scale crash test. The data that are typically collected in such tests include (at a minimum) three acceleration channels (i.e., longitudinal, transverse and vertical directions) and three rotational rate channels (i.e., roll, pitch and yaw angular rates). These data are collected at the center of gravity of the vehicle and are used to measure vehicle response (e.g., stability) and are also used to estimate occupant risk factors (e.g., occupant impact velocity and occupant ride-down acceleration). It is desired to have as much time history data as possible available from the physical experiment for use in validating the numerical model; however, it is more often the case that only the six aforementioned channels of data are collected in the full-scale tests. As such, all these data should be used in the validation process.

Sometimes, however, there may be one or two relatively unimportant channels that do not result in good quantitative comparisons. An example might be a small sign support test where the longitudinal acceleration has a much greater influence on the results of the impact event than do the lateral or vertical accelerations. The less important channels may not satisfy the criteria because they are essentially recording noise. The longitudinal channel in this example will probably be an order of magnitude greater than some of the other less important channels, and the response would essentially be determined by a single channel, i.e., the longitudinal channel.

In such case, the analyst may want to ignore any of the channels that appear to be less meaningful to the outcome of the crash event, or at least to rank those channels with less importance. The issue then is how to make the decision *objective*, since it is not likely that everyone will have the same opinion on how to rank each channel.

The RSVVP program calculates a *weight* for each channel that corresponds to the importance that each channel had in the overall response in the physical test. The methods available in RSVVP for computing these *weight factors* include:

1. Inertial Method – weighted momentum approach and

2. Area Method (default) – pseudo momentum approach
3. Kinetic Energy Approach – (not available in current version of RSVVP)

The *Inertial method* determines the *weight* for each channel by computing the linear and rotational momentum of the six channels of data. The weight factors correspond to the proportion of the momentum in each channel. This method provides the most accurate weight value for each channel but requires that the mass of the vehicle and the three angular inertial properties be input into RSVVP. In many cases, however, the exact inertial properties for the test vehicle are not known.

The *Area method*, on the other hand, calculates a *weight* for each channel based on a *pseudo* momentum approach using the area under the curves. In this method, the inertial properties of the vehicle are not used in the calculations and therefore the weight values will not be an exact representation of the momentum change associated with each channel. The *Area Method* has been shown, however, to provide values *similar* to those computed using the *Inertial Method* for cases involving vehicle impact into longitudinal roadside barriers (e.g., concrete median barrier).

AREA METHOD WEIGHT FACTORS

In this section, a brief description of how the weighting factors are calculated in RSVVP for the Area Method is presented. Note: The weight factors are calculated in all cases using the data from the *true curve* input.

Using the Area Method, RSVVP computes weight factors for each individual channel based on a ‘pseudo’ momentum approach. The basic concept of this weighting scheme is to calculate a local index for each channel that is representative of its importance (or weight) with respect to the other channels. Once these indexes have been computed, the weighting factors are calculated by simply dividing the index calculated for each channel by the sum of all the channels indexes. Thus the total sum of the weight factors equals unity.

Because the units differ between linear and rotational momentum, each of these two groups of channels will be treated separately. The weighting factors for each channel are calculated using the following procedure:

- Evaluation of the area of the *True curve* for each acceleration channel, a_i , and rotational channel, v_i .
- Evaluation of the sum of the acceleration areas, a_{Sum} , and rotational areas, v_{Sum} .
- Evaluation of the local weight of each acceleration channel, $lw_i^{(a)} = \frac{a_i}{a_{Sum}}$, and rotational

$$\text{channel } lw_i^{(v)} = \frac{v_i}{v_{Sum}}$$

- Evaluation of the channel weight factors,

$$w_i^{(a)} = \frac{lw_i^{(a)}}{\sum lw_i^{(a)} + \sum lw_i^{(v)}}$$

$$w_i^{(v)} = \frac{lw_i^{(v)}}{\sum lw_i^{(a)} + \sum lw_i^{(v)}}$$

Once the weighting factors have been evaluated, the multi-channel metrics are calculated using a weighted average of the individual channel metrics. Note that the combination of the time histories is performed for each of the metrics selected at the beginning of the run by the user.

Table A2-1 shows the acceptance criteria proposed for the verification and validation of finite element models in roadside safety using the NCHRP 22-24 metrics profile.

Table A2-1: Acceptance criteria suggested for the NCHRP 22-24 metrics profile.

Sprague & Geers metrics		ANOVA metrics	
Magnitude (M)	≤ 40	Mean	≤ 0.05
Phase (P)	≤ 40	Standard deviation	≤ 0.35
Composite (C)	≤ 40		

Apart from the value of the comparison metrics, it is important that the graphs of the cumulative distribution and histogram of the residual errors have the following typical characteristics of a normal distribution:

- The histogram should have a normal or bell shaped distribution and the
- Cumulative distribution should have an “S” shape

If the histogram and the cumulative distribution do have these shape characteristics, the residuals between the two curves are most likely due to some systematic error which should be identified and corrected.

Appendix B:

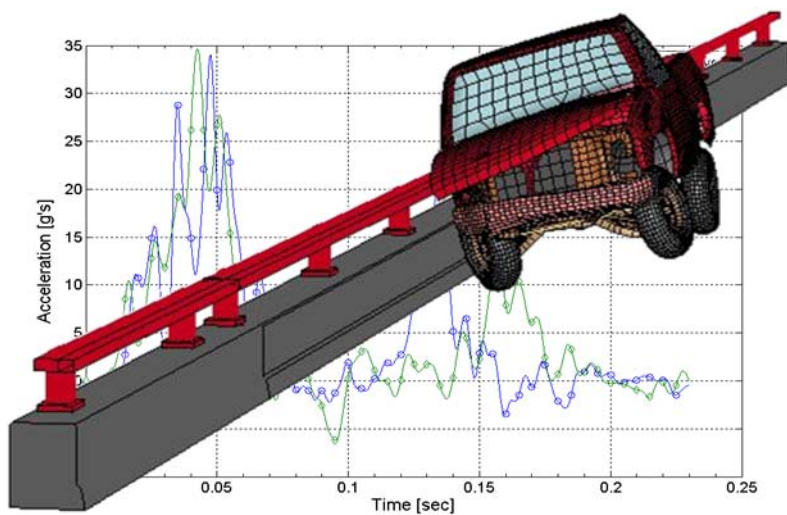
Roadside Safety Verification and Validation Program (RSVVP)

Programmer's Manual

December 2009 (Revision 1.4)

Mario Mongiardini

Malcolm H. Ray



CONTENTS

FOREWORD	1
INTRODUCTION	2
DESCRIPTION OF TASKS	3
Input of data	3
Preprocessing	3
Scaling	4
Manual trimming and/or shift of the origin	4
Filtering	4
Shift/drift correction	6
Re-sampling and Trimming	7
Synchronization	8
Metrics evaluation	9
Post-processing	11
Output of results	12
PROGRAM STRUCTURE	13
<i>Notation used for the flow charts</i>	15
Graphical User Interfaces	16
Block A (Initialization)	19
<i>Opening (Block A.1)</i>	20
<i>Initialization (Block A.2)</i>	20
Block B (Input and Option selection)	24
<i>Input/Preprocessing (Block B.1)</i>	27
<i>Preprocessing 2 (Block B.2)</i>	33
<i>Metrics selection (Block B.3)</i>	36
Block C (Curve preparation)	38
<i>Curves preparation (Block C.1)</i>	39
<i>Curves histories (Block C.2)</i>	41
<i>Curve plotting (Block C.3)</i>	42
Block D (Metrics evaluation)	43
<i>Whole time (Block D.1)</i>	45
<i>User time (Block D.2)</i>	52
Block E (Output)	56
<i>Configuration file (E.1)</i>	58
<i>Excel results (Block E.2)</i>	58
<i>Folder selection (Block E.3)</i>	65
REFERENCES	66
APPENDIX B-1: CODE VERIFICATION	68
APPENDIX B-2: COMPILING RSVVP	72
APPENDIX B-3: Type of Variables Used in the Code	73
APPENDIX B-4: Preprocessing Algorithms	75
APPENDIX B-5: Metrics Algorithms	83

List of Figures

Figure B-1: Representation of (a) Shift and (b) drift effects.	6
Figure B-2: The behavior of the shift subroutine for a (a) positive or (b) negative offsets.....	9
Figure B-3: Diagram of the five main blocks of the RSVVP code	14
Figure B-4: Symbols used for the flowcharts in this manual.....	15
Figure B-5: Structure of a Matlab® GUI.....	17
Figure B-6: Structure of the variable <i>handles</i>	18
Figure B-7: Representation of the workspace of the Main and Objective functions of a GUI....	19
Figure B-8: Diagram of Block A.	20
Figure B-9: Fields of the variable <i>Selection</i>	21
Figure B-10: Flow chart of the algorithm of sub-block A.2 (Initialization).	21
Figure B-11: Flow chart of the scripts <i>Load configuration</i> (left) and <i>Load preprocess</i> (right) (sub-block A.2).	23
Figure B-12: Diagram of Block B.	24
Figure B-13: Scheme of the loop which forms Block B.....	25
Figure B-14: Flow chart of the main algorithm of Block B.	26
Figure B-15: Flow chart of the algorithm of sub-block B.1 (Input/Preprocessing).....	27
Figure B-16: Flow chart of the script <i>Load_Preprocess</i> (sub-block B.1) – part A.	30
Figure B-17: Flow chart of the script <i>Load_Preprocess</i> (sub-block B.1) – part B.	31
Figure B-18: Flow chart of the script <i>Load_curves</i> (sub-block B.1).	32
Figure B-19: Diagram of sub-block B.2 (Preprocessing2).	33
Figure B-20: Flow chart of the script <i>Preprocessing_2</i> (sub-block B.2).	35
Figure B-21: Diagram of sub-block B.3 (Metrics selection).	37
Figure B-22: Flow chart of the script <i>Metrics_selection</i> (sub-block B.3).	38
Figure B-23: Diagram of Block C.	39
Figure B-24: Data organization of the matrix variables <i>True</i> and <i>Test</i>	40
Figure B-25: Diagram of sub-block C.1 (Curves preparation).	40
Figure B-26: Diagram of sub-block C.2 (Curves histories) (center) and the two invoked scripts, <i>Save_curves_original</i> (left) and <i>Save_curves_preprocessed</i> (right).	41
Figure B-27: Flow chart of the script <i>Whole_plot_curves</i> (sub-block C.3).	43
Figure B-28: Diagram of Block D.	44
Figure B-29: Main structure Block D.	44
Figure B-30: Diagram of sub-block D.1 (Whole time).....	46
Figure B-31: Flow chart of the script <i>Weighting_scheme_whole</i> (sub-block D.1).....	47
Figure B-32: Flow chart of the scripts <i>Whole_time_evaluation</i> (left) and <i>Whole_time_postprocessing</i> (right) (sub-block D.1).	48
Figure B-33: Data organization of the variables <i>Output_xls</i> and <i>Output_channel_xls</i>	51
Figure B-34: Data organization of the variables <i>Output_single_history_xls</i> and <i>Output_channel_history_xls</i>	52
Figure B-35: Diagram of sub-block D.2 (User time).....	54
Figure B-36: Data organization of the variables <i>Output_xls</i> and <i>Output_channel_xls</i>	56
Figure B-37: Diagram of Block E.....	57
Figure B-38: Main structure Block E.....	57
Figure B-39: Diagram of sub-block E.1 (Configuration file).	58

Figure B-40: Diagram of sub-block E.2 (Excel results).	59
Figure B-41: Flow chart of the script <i>Excel_results</i> (sub-block E.2).	61
Figure B-42: Flow chart of the script <i>Excel_results_MPC</i>	62
Figure B-43: Data extraction from the variable <i>Output_channel_xls</i> .	63
Figure B-44: Flow chart of the script <i>Excel_time_histories</i> (sub-block E.2).	64
Figure B-45: Diagram of sub-block E.3 (Folder selection).	65
Figure B-46: Idealized time histories used for the case of (a) 20% magnitude and (b) time of arrival.	69
Figure B-47: Sprague-Geers component metric vs. time for the magnitude-difference test.	70
Figure B-48: Sprague-Geers component metric vs. time for the phase-difference tests: (a) +20% and (b)-20%.	71
Figure B-49: Example of a Matlab structure variable [1].	73
Figure B-50: Example of a Matlab structure variable [1].	74
Figure B-51: Algorithm of the SAE filtering.	76
Figure B-52: Main algorithm of the script <i>Shift_drift</i> .	77
Figure B-53: User-defined functions <i>shift_value</i> (left) and <i>drift_value</i> (right) Algorithms.	78
Figure B-54: Algorithm of the script <i>Resampling_trimming</i> .	79
Figure B-55: Algorithm of the script <i>Curve_synchronizing</i> .	80
Figure B-56. Algorithm of the user-defined functions <i>area_res</i> (left) and <i>sre</i> (right).	81
Figure B-57: Algorithm of the user-defined function <i>shift</i> .	82
Figure B-58. Algorithm of the Sprague & Geers metric implemented in RSVVP.	84
Figure B-59. Algorithm of the ANOVA metrics implemented in RSVVP.	85

List of Tables

Table B-1: Definition of MPC metrics.	10
Table B-2: Definition of single-value metrics.	11
Table B-3: Definition of ANOVA metrics.	11
Table B-4: Value of the Sprague & Geers metric components calculated using the RSVVP program.	70

FOREWORD

This guide describes the implementation of the Roadside Safety Verification and Validation Program (RSVVP) developed under the NCHRP 22-24 project. The main intent of the guide is to provide the programmer with a comprehensive description of the various parts which compose the RSVVP code and their corresponding algorithms. For this reason, this programmer's manual has the form of a "service" manual. The programmer can refer to this manual to retrieve all the information necessary to locate the section of the code which performs a specific operation and understand the implemented algorithms or, vice versa, i.e., given a specific section of the code, the programmer can go back to the task that part of the code performs. This information may be useful for future improvements, modifications or customization of the original code.

The manual is organized in the following manner. First an initial overview of the different tasks performed by RSVVP along with an explanation of the theory behind the implementation. Then, both a general and detailed description of the structure of the code and the algorithms used to implement each task is described.

RSVVP is written in Matlab[®] (version R2009 a) [1] and the source code can be either executed directly from the Matlab[®] environment or compiled as an executable application. In the latter case, it is necessary to have the Matlab[®] Compiler Runtime (MCR) component installed on the machine on which it is desired to run the executable. See 0-1 for further detail about how to compile and run RSVVP as an executable application.

INTRODUCTION

RSVVP quantitatively compares one or multiple pairs of curves by computing comparison metrics which are objective, quantitative mathematical measures of the agreement between two curves. The comparison metrics calculated by RSVVP can be used to accomplish one or more of the following operations:

- Validate computer simulation models using data obtained from experimental tests
- Verify the results of a simulation with another simulation or analytical solution
- Assess the repeatability of a physical experiment

Although RSVVP has been specifically developed to perform the verification and validation of roadside safety simulations and crash tests, it can be used to generally perform a comparison of virtually any pair of curves. All the comparison metrics evaluated by RSVVP are deterministic, meaning they do not specifically address the probabilistic variation of either experiments or calculations (i.e., the calculation results are the same every time given the same input).

In order to ensure a correct comparison of the curves, RSVVP gives the user the option to perform various preprocessing tasks before the metrics are calculated.

The intuitive and interactive graphical user interface of RSVVP allows the user to effortlessly input the curves to be compared and easily perform any of the existing preprocessing operations. Also, a series of automatic warnings alert the user about possible mistakes during the preprocessing phase.

For programmers interested in modifying or improving the original code, The Matlab[®] source code of RSVVP can be downloaded from:

http://civil-ws2.wpi.edu/Documents/Roadsafe/NCHRP22-24/RSVVP/Source_code.zip

DESCRIPTION OF TASKS

This section gives a description of the operations performed by RSVVP, and when possible the theoretical background behind the operations. The tasks performed by RSVVP can be categorized into six main categories:

- 1) Input of data
- 2) Preprocessing
- 3) Selection of metrics/time interval
- 4) Metrics evaluation
- 5) Post-processing
- 6) Output of results

Each task may be further divided into various steps or subtasks. A description of the steps performed for each of the above mentioned tasks is given in this section.

INPUT OF DATA

Data are input by loading ASCII files containing the data points of the curves. Each curve must be defined by a distinct file containing two columns; the first column representing the time (or x coordinate) and the second one the value of the curve at the corresponding time (i.e., y coordinate). After the sets of data have been loaded, the program automatically calculates the minimum sampling rate and the maximum time value based on the time vector of each curve. These values are used to perform some of the preprocessing operations.

PREPROCESSING

The program performs various preprocessing operations. Some of them are necessary and automatically executed, while others are optional and the user can decide whether to accomplish them or not. The following preprocessing tasks are implemented in the code:

- Scaling
- Manual trimming and/or Shift of the origin
- Filtering
- Shift/Drift

- Re-sampling and Trimming
- Synchronization

The re-sampling and trimming operations are performed by default as they are necessary to correctly compare any pair of curves because both curves must match point-to-point.

In the next sections, a brief description of each preprocessing operation and the theory/method implemented are given. For a description of the algorithms used to implement each preprocessing feature, see 0.

Scaling

The original input curves can be scaled by an arbitrary user defined factor. This operation may be useful when the true and test curves have been collected using different units. The scaling of the original curves is performed multiplying the vector containing the data point by the user-defined scale factors. In case the user has not input any of the two optional scale factors, one for each of the two curves of the pair, the default values are automatically set to the unity.

Manual trimming and/or shift of the origin

The manual trimming of the original curves is performed after the rescaling operation. After the user has defined the minimum and maximum extreme values for either one or both the two curves, the value of the index corresponding to (or approximating, in case the sampling rate does not allow the exact fit) these values are calculated. The vectors containing the data point for each curve are then trimmed using the index values previously found. After being trimmed, the time vectors are shifted in order to start from the origin, by subtracting the corresponding initial value.

Note that, at this point, the two curves may be still characterized by different sampling periods as the trimming operation is performed independently for each of them.

Filtering

Filtering the time histories is the first step of data preprocessing and is a very common operation in preprocessing time history data. The filtering operation is performed by

implementing a digital filter which complies with the specifications of the SAE J211 standard [2], the reference in the matter of filtering for the NCHRP Report 350 [3] and EN1317 [4]. A digital four-pole Butterworth low-pass filter is implemented using an algorithm which uses a double-pass filtering option (i.e., forward/backward): data are filtered twice, once forward and once backward using the following difference equation in the time domain:

$$Y(t) = a_0 \cdot X(t) + a_1 \cdot X(t-1) + a_2 \cdot X(t-2) + b_1 \cdot Y(t-1) + b_2 \cdot Y(t-2) \quad (\text{B1})$$

Where: $X(t)$ is the input data sequence and $Y(t)$ is the filtered output sequence.

The filter coefficients vary with the CFC value and are calculated using the following formulas:

$$a_0 = \frac{\omega_a^2}{1 + \sqrt{2}\omega_a + \omega_a^2} \quad (\text{B2})$$

$$a_1 = 2a_0 \quad (\text{B3})$$

$$a_2 = a_0 \quad (\text{B4})$$

$$b_1 = \frac{-2(\omega_a^2 - 1)}{1 + \sqrt{2}\omega_a + \omega_a^2} \quad (\text{B5})$$

$$b_2 = \frac{-1 + \sqrt{2}\omega_a - \omega_a^2}{1 + \sqrt{2}\omega_a + \omega_a^2} \quad (\text{B6})$$

where,

$$\omega_d = 2\pi \cdot \text{CFC} \cdot 2.0775 \quad (\text{B7})$$

$$\omega_a = \frac{\sin(\omega_d \cdot T/2)}{\cos(\omega_d \cdot T/2)} \quad (\text{B8})$$

In order to avoid the typical scatter at both the beginning and the end of the filtered time histories due to the application of the difference equation (B1), a head and tail are added to the original data sets consisting respectively of a simple repetition of the first and last data value. Once the modified data sets are filtered, the head and tail are deleted from the final filtered

curve. The length of the head and tail is equal to the closest integer approximation of the curve frequency divided by 10.

Shift/drift correction

The shift and drift effects are generally due to the heating of sensors during an experiment. In particular, the shift effect is homogeneous vertical translation of the entire experimental curve due to the change of the sensor temperature between the time it has been zeroed and the time the test has been performed (Figure B-1 a). Instead, the drift effect is a linearly increasing translation of the experimental curve due to a change in the temperature of the sensor between the beginning of the test and the end (Figure B-1 b).

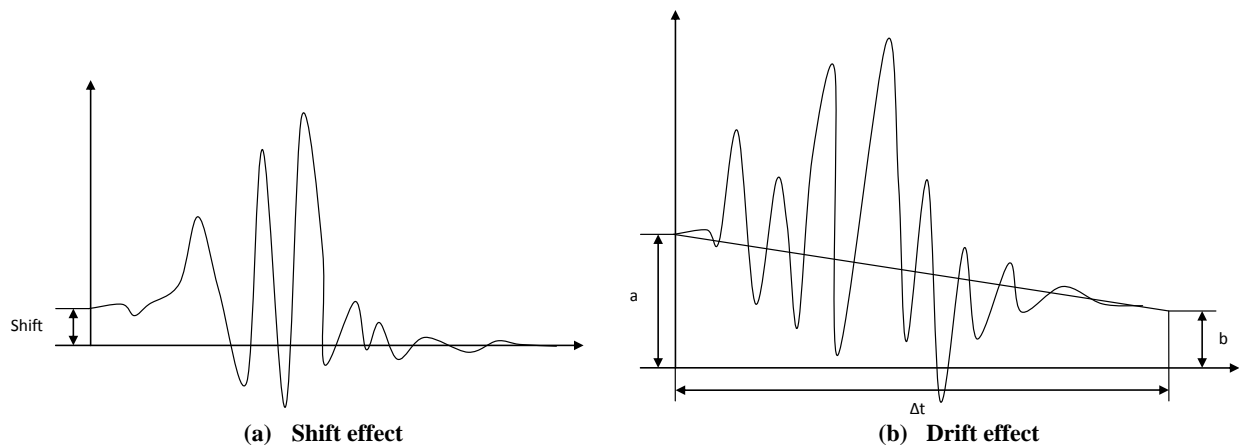


Figure B-1: Representation of (a) Shift and (b) drift effects.

The drifted curve is basically shifted by a value which linearly increases/decreases in the time according to the following simple formula:

$$\Delta = m \cdot t \quad (\text{B9})$$

where m is the slope of the linear drift and can be easily computed as:

$$m = (b - a) / \Delta t \quad (\text{B10})$$

with a and b representing respectively the initial and final values of the linear drift function and Δt its total length as shown in Figure B-1(b).

The correction of the shift effect can be easily achieved by translating the whole curve by the shift value a . As for the drift effect, once the value of the slope m has been calculated from Equation (10), it is possible to correct it by translating each point of the curve by the opposite of the corresponding values obtained from the drift baseline function (Equation (9)). Note that, as the drift baseline is not a constant function, the correction value is different for each sample point of the original curve.

In order to calculate the shift or drift values by which the input curves have to be translated, it is necessary to consider the mean values at the beginning and the end of each curve. In particular, it is important to ensure that the values at the beginning and the end of the vector containing the data points (i.e., head and tail) are sufficiently constant to guarantee that the mean values of these sub-vectors effectively represent the shift/drift values. An initial guess for the point until the head of the curve can be considered as constant (or from which the tail of the curve is considered constant) is the time at which the curve reaches 5 percent of the peak value (or from which the curve is less than 5 percent of the curve's peak). In order to check that the initially guessed head or tail sub-vectors are constant, their standard deviation must be under a critical value, which was defined to be 0.1. In case the initial sub-vectors do not satisfy the above mentioned criterion, the algorithm iteratively decreases the initial length of the head and tail sub-vectors till the standard deviation of the new reduced sub-vectors is less than the proposed critical value.

Re-sampling and Trimming

As most of the metrics which quantify the agreement between the test and simulation curves are based on the evaluation of the point-to-point error, in order to correctly calculate the residuals, it is mandatory that the two curves have the same sampling rate. The original curves, however, may have been sampled at different frequencies so it could be necessary to re-sample them in order to compute a point-to-point difference. The program checks if the two sets of data have the same sampling period within a tolerance of $5E-6$ sec. If the two curves do not have the same sampling frequency, RSVVP proceeds to re-sample the curve which has the lower sampling rate (i.e., the bigger difference in time between two contiguous data points) at the higher rate of the other curve. The re-sampling is performed by mean of a linear interpolation, assuming that the time vector starts from zero. Also, when the two curves are re-sampled, the

smaller of the end values between the two original time vectors is considered, in order to trim them to the same interval. Note that, because of the new sampling rate the end value of the new time vector may be approximated by defecting the maximum time of the original curve.

Synchronization

Usually the experimental and numerical time histories do not start at the same time and, hence, the two curves are shifted by a certain value in the time direction. In this case, the curves should be shifted back or forth so that the impact time in each of them is synchronized. As the comparison metrics are mostly based on the evaluation of the residual error, it is necessary to delete or at least reduce as much as possible any time shift between the test and simulation curves; otherwise, even if the two curves are exactly the same, this gap in time would negatively affect the final metric result. The last preprocessing operation performed by the RSVVP before the metric evaluation is synchronizing the test and simulation curves.

Two different methods of synchronizing have been implemented in RSVVP, based on (1) the minimum area between the curves or (2) the least square error of the residuals. The main idea in both the cases is to find the shift value which minimizes the target function.

In order to implement these two methods of synchronization, a specific function shifts along the time direction either one of the two curves by a value s , with a positive value of s meaning a forward shift for the test curve and a negative value being equivalent to a backward shift for the simulation curve (Figure B-2). RSVVP identifies the shift value which minimizes either the absolute area of residuals (method 1) or the sum of squared residuals (method 2). The shift value corresponding to the minimum error is the most probable matching point between the curves. In case the result is not satisfactory, the user can repeat the synchronization procedure using a different initial shift value at the beginning of the minimization algorithm or using the other minimization method.

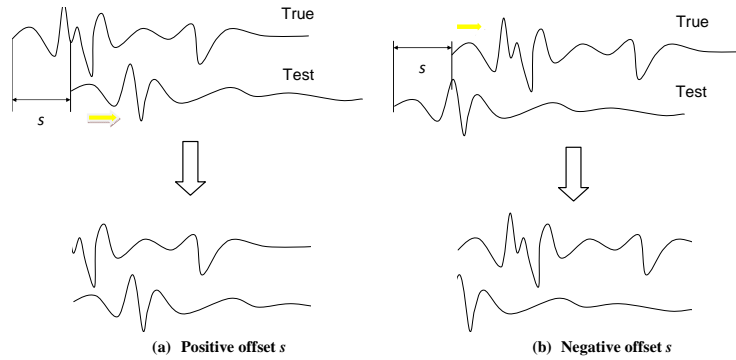


Figure B-2: The behavior of the shift subroutine for a (a) positive or (b) negative offsets.

METRICS EVALUATION

Various comparison metrics have been implemented into the code. The mathematical formulation of the metrics is shown in Table B-1 through Table B-3, where the measured and computed data points are indicated respectively as m_i and c_i . For more details about the comparison metrics implemented in RSVVP refer to the Appendix A-1 in the User's Manual.

For a description of the algorithms used to implement each metric, see 0B-5.

Although all the metrics by definition give a scalar value (i.e., a simple number), they are implemented in order to be evaluated on various time intervals characterized by an increasing size. The smaller time interval on which the input curves are compared is ten percent of the total time and, at each step, it is increased in size till it becomes the total interval. In this way, it is possible to reconstruct a time history of the metrics indicating how the values evolve comparing the curves on increasing portions of their total time interval.

Table B-1: Definition of MPC metrics.

	<i>Magnitude</i>	<i>Phase</i>	<i>Comprehensive</i>
<i>Integral comparison metrics</i>			
<i>Geers</i> [5]	$M_G = \sqrt{\frac{\sum c_t^2}{\sum m_t^2}} - 1$	$P_G = 1 - \frac{\sum c_t m_t}{\sqrt{\sum c_t^2 \sum m_t^2}}$	$\sqrt{M_G^2 + P_G^2}$
<i>Geers CSA</i> [6]	$M_G = \sqrt{\frac{\sum c_t^2}{\sum m_t^2}} - 1$	$P_{CSA} = 1 - \frac{ \sum c_t m_t }{\sqrt{\sum c_t^2 \sum m_t^2}}$	$\text{sgn} \left(\sum c_t m_t \right) \sqrt{M_{CSA}^2 + P_{CSA}^2}$
<i>Sprague&Geers</i> [7,8]	$M_G = \sqrt{\frac{\sum c_t^2}{\sum m_t^2}} - 1$	$P_{SG} = \frac{1}{\pi} \cos^{-1} \frac{\sum c_t m_t}{\sqrt{\sum c_t^2 \sum m_t^2}}$	$\sqrt{M_{SG}^2 + P_{SG}^2}$
<i>Russell</i> [9]	$M_R = \text{sgn}(m) \cdot \text{Log}_{10}(1 + m)$ where $\frac{(\sum c_t^2 - \sum m_t^2)}{\sqrt{\sum c_t^2 \sum m_t^2}}$	$P_R = \frac{1}{\pi} \cos^{-1} \frac{\sum c_t m_t}{\sqrt{\sum c_t^2 \sum m_t^2}}$	$\sqrt{\frac{\pi}{4} (M_R^2 + P_R^2)}$
<i>Point-to-point comparison metrics</i>			
<i>Knowles&Gear</i> [8]	$M_{KG} = \sqrt{\frac{\sum \left(\frac{ m_t }{m_{max}} \right)^p (\xi_t - \tau)}{\sum \left(\frac{ m_t }{m_{max}} \right)^p (m_t)}}$ where $\xi = c(t - \tau)$ (with $\tau = TOA_c - TOA_m$)	$P_{KG} = \frac{ TOA_c - TOA_m }{TOA_m}$	$\sqrt{\frac{10M_{KG}^2 + 2P_{KG}^2}{12}}$

Table B-2: Definition of single-value metrics.

<i>Integral comparison metrics</i>			
<i>Correlation Coefficient</i> [10]	$\frac{n \sum c_i m_i - \sum c_i \sum m_i}{\sqrt{n \sum c_i^2 - (\sum c_i)^2} \sqrt{n \sum m_i^2 - (\sum m_i)^2}}$	<i>Correlation Coefficient (NARD)</i> [11]	$h \frac{\sum c_i m_i}{\sqrt{\sum c_i^2} \sqrt{\sum m_i^2}}$
<i>Weighted Integrated Factor</i> [12]		$\sqrt{\frac{\sum \max(m_i^2, c_i^2) \cdot \left(1 - \frac{\max(0, m_i \cdot c_i)}{\max(m_i^2, c_i^2)}\right)^2}{\sum \max(m_i^2, c_i^2)}}$	
<i>Point-to-point comparison metrics</i>			
<i>Zilliacus error</i> [13]	$\frac{\sum c_i - m_i }{\sum m_i }$	<i>RMS error</i> [13]	$\frac{\sqrt{\sum (c_i - m_i)^2}}{\sqrt{\sum m_i^2}}$
<i>Theil's inequality</i> [14]	$\frac{\sqrt{\sum (c_i - m_i)^2}}{\sqrt{\sum c_i^2} + \sqrt{\sum m_i^2}}$	<i>Whang's inequality</i> [13]	$\frac{\sum c_i - m_i }{\sum c_i + \sum m_i }$
<i>Regression coefficient</i> [10]		$\sqrt{1 - \frac{(n-1) \sum (c_i - m_i)^2}{n \sum (m_i - \bar{m})^2}}$	

Table B-3: Definition of ANOVA metrics.

<i>Average residual error*</i> [15,16]	$\bar{e} = \frac{\sum (c_i - m_i) / m_{\max}}{n}$
<i>Standard deviation of the residuals*</i> [15, 16]	$\sigma^r = \sqrt{\frac{\sum (e^r - \bar{e})^2}{n-1}}$
(*) normalized to the peak of the measured values	

POST-PROCESSING

The post-processing of data consists of the following operations:

- Compute the weighted average of the metrics,
- Plot the time history of the metrics and
- Prepare the variable to output results in Excel files.

The program can evaluate metrics considering either a single couple of curves or multiple pairs simultaneously. In the latter case, the results obtained from each pair of curves (channels) are combined together during the post-processing of data by computing a weighted average. The weighting factors are automatically calculated by the user based on the area of the true curve for each channel. Following is a description of the procedure implemented to calculate the weighting factors:

- Evaluation of the area of the true curve for each acceleration channel, a_i , and rotational channel, v_i .
- Evaluation of the sum of the acceleration areas, a_{Sum} , and rotational areas, v_{Sum} .
- Evaluation of the local weight of each acceleration channel, $lw_i^{(a)} = \frac{a_i}{a_{Sum}}$, and rotational

$$\text{channel } lw_i^{(v)} = \frac{v_i}{v_{Sum}}$$

- Evaluation of the channel weight factors,

$$w_i^{(a)} = \frac{lw_i^{(a)}}{\sum lw_i^{(a)} + \sum lw_i^{(v)}}$$

$$w_i^{(v)} = \frac{lw_i^{(v)}}{\sum lw_i^{(a)} + \sum lw_i^{(v)}}$$

Apart from calculating the weighted values of the metrics, the post-processing operation also consists in plotting the time histories of the metrics and preparing the variables with a complex data structure which contain the time histories and results for the output in Excel files.

OUTPUT OF RESULTS

Results are output in various formats:

- ASCII files,
- Excel files and
- Graphs (bmp. pictures).

In particular, the output of the results in Excel format requires the results be stored in variables characterized by particular data structures which will be discussed in detail in the following section.

PROGRAM STRUCTURE

The information presented herein is intended to illustrate the basic structure and organization of the RSVVP program so that users can easily locate where and how each specific task is programmed. In each of the following sections a general overview of the organizational structure of the code is given, followed by a detailed description of each programmed task.

The code has a modular structure; it is divided into five main blocks (i.e., subroutines), where each *block* performs one or more of the operations described in the previous section. The five main blocks (i.e., groups of operations) are:

- Block A – Initialization
- Block B – Input & Options selection
- Block C – Curve Preparation
- Block D – Metrics Evaluation
- Block E – Output

Each of the five blocks is invoked systematically by the principal script (*Main.m*) which is executed at the start of the program. Each of the blocks then invokes one or more secondary scripts that perform the various tasks. Both the principal and secondary scripts may recall either specific functions from various Matlab[®] libraries (toolboxes) or user-defined functions programmed *ad hoc* to perform specific operations. Each operation may be performed by one or more scripts, and in some cases, a secondary script may also recall one or more subscripts. Figure B-3 illustrates the five organizational blocks in RSVVP and the respective operations performed in each.

Every *block* is divided into two or three sub-blocks, each performing specific operations. In most cases these *blocks* are accessed via graphical user interfaces. The general concepts behind the implementation of the graphical interfaces in Matlab[®], and a detailed description of the algorithms and data structures making up the various sub-blocks are presented in the

following sections. Due to various reasons which will be explained later in this manual, in general, it was not possible to implement each of the programmed tasks into a specific corresponding block (i.e., a one to one correspondence between the tasks and the blocks).

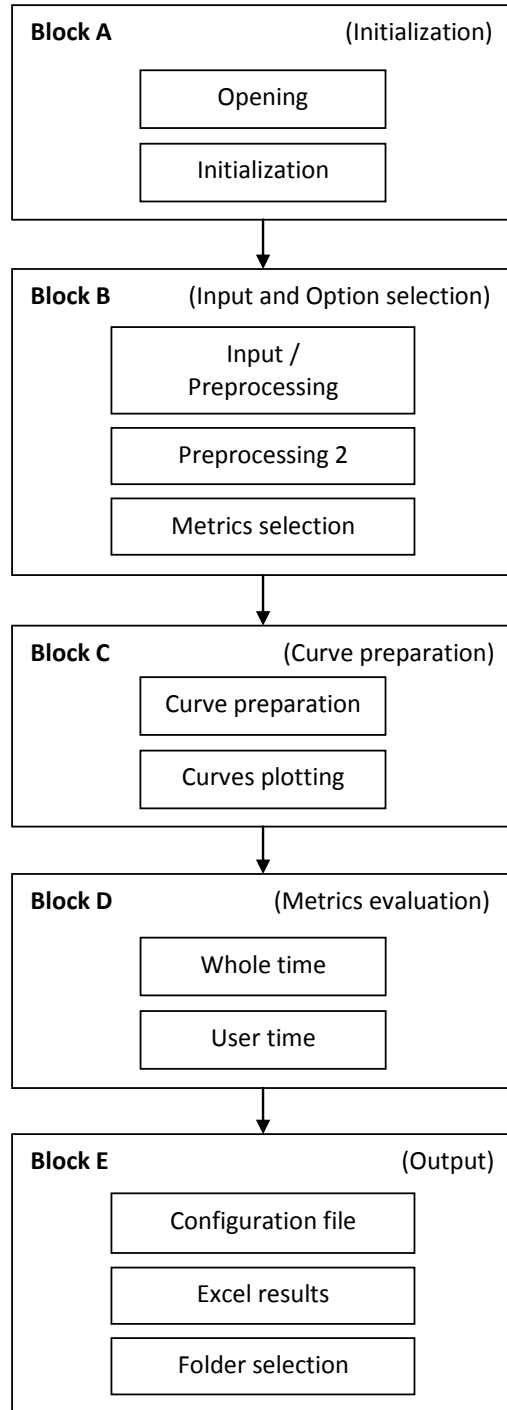


Figure B-3: Diagram of the five main blocks of the RSVVP code

Because of the complexity of the code, the algorithms implemented in each block are described at different levels of detail, starting from a general overview and going more into details at each further level of the flowcharts. In particular, each block is described using flowcharts at three different levels:

1. Block level

Delineates the main frame of the block and the relations between the various sub-blocks.

2. Sub-block level

Describes the implementation of each sub-block.

3. Script level

Provides a detailed description of the specific scripts invoked by a sub-block.

Notation used for the flow charts

The flowchart diagrams presented in the next sections of this manual have been drawn using a set of standard symbols. Figure B-44 displays the symbols used in the flowcharts and their related meaning.

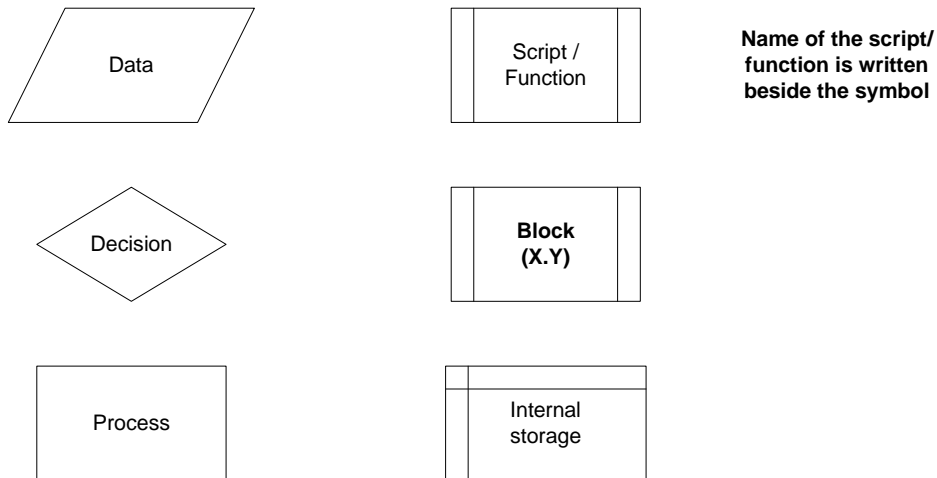


Figure B-4: Symbols used for the flowcharts in this manual.

Note that the filename containing a specific script/function which performs the operation indicated by each 'predefined' shape is shown beside the shape in bold characters.

GRAPHICAL USER INTERFACES

The interaction between the program and the user is achieved using various Graphical User Interfaces (GUI's). A graphical interface in Matlab[®] is regarded as a function, which means it is possible to define both input and output variables. The possibility to input variables allows a GUI to load information about the configuration saved during the previous instance or a default configuration in case the GUI is opened for the first time. In fact, some of the GUIs are implemented into iterative loops and, after being invoked for the first time, they may be opened again. In this case, the new instance of a GUI is given as input a variable which contains all the information about the configuration previously saved. In order to organize all the configuration information in a single variable which is easy to pass through the GUI functions, the Matlab[®] structure type has been adopted. A structure variable is composed of multiple fields which can store an array of any available Matlab[®] data type. The fields of a structure variable can be heterogeneous, thus allowing to store in the same variable different type of information. For more information see 0.

In Matlab[®], each GUI is composed of two main components: (1) a figure which includes all the various graphical objects (checkbox, radio button, drop-down menu, plot area, etc.) and (2) an M-file which recalls the figure and manages the various components. The development and modification of the figure can be achieved only in Matlab[®] by using the command “*guide*” (GUI Developer), which opens a graphical interface for the creation/modification of the GUI figure. The M-file of each GUI is a Matlab[®] script containing a set of functions and is basically composed of the following main parts (Figure B-5):

- Main function
- Opening function
- Output functions
- Object functions

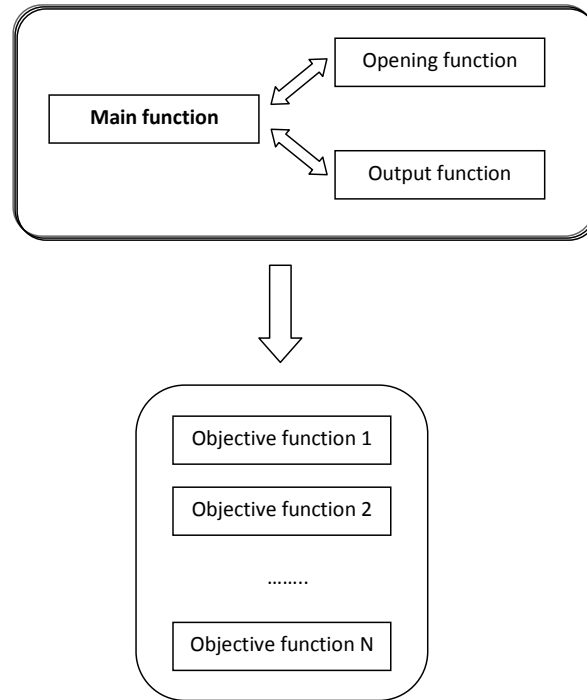


Figure B-5: Structure of a Matlab® GUI.

The **Main function** has the same name as the GUI and is the function which is recalled in the code to start the GUI itself. This function invokes in sequence the **Opening function** and the **Output function** and is then set into “wait” mode in order to make the GUI wait for user response before returning to the code where it has been invoked. The Opening function performs all the necessary operations to initialize the GUI immediately before it appears on the screen. In particular, it may receive the structure variable passed to the Main function which contains the configuration saved during a previous instance of that GUI. In this case, the fields of the input structure variable are used to properly configure the GUI. The Output function, instead, manages the data passed back by the GUI function when it is closed.

Once the GUI has appeared, the user can select the different objects. To each object of the GUI corresponds a specific **Object function**, which implements the operations to be performed for that particular object. During the period in which the Main function is in wait mode, each time the user interacts with an object of the GUI, the corresponding function is invoked from the local workspace of the Main function. In general, each Object function receives as input the three variables “*hObject*”, “*eventdata*”, “*handles*” from the workspace of

the Main function and may return the variable “*handles*” to the same local workspace. In most cases, except in some rare exceptions, the exchange of information between an Object function and the Main function is achieved using the field ‘output’ of the structure variable “*handles*” (i.e., *handles.output*).

The field “*handles.output*” is usually further structured into various subfields (Figure B-6) according to specific GUI and is the one which, eventually, is passed back by the Main function to the principal code of the program.

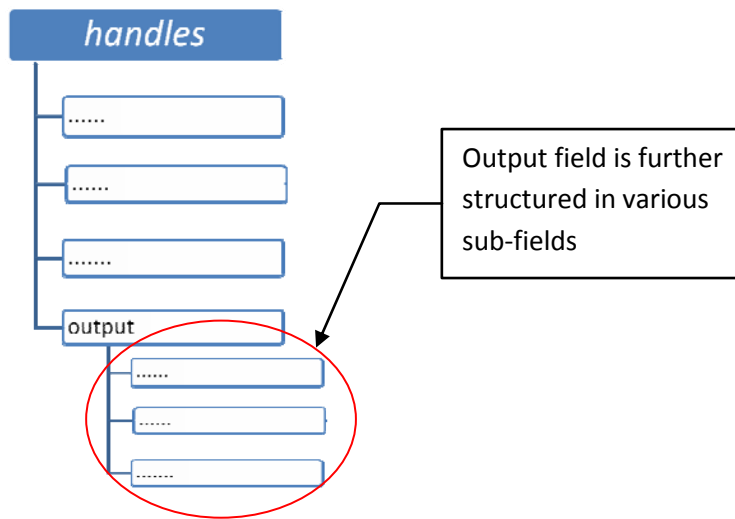


Figure B-6: Structure of the variable *handles*.

In case the GUI is iteratively recalled, the values of this structure variable are repeatedly passed back and forth from the main code to the GUI and vice versa (Figure B-7).

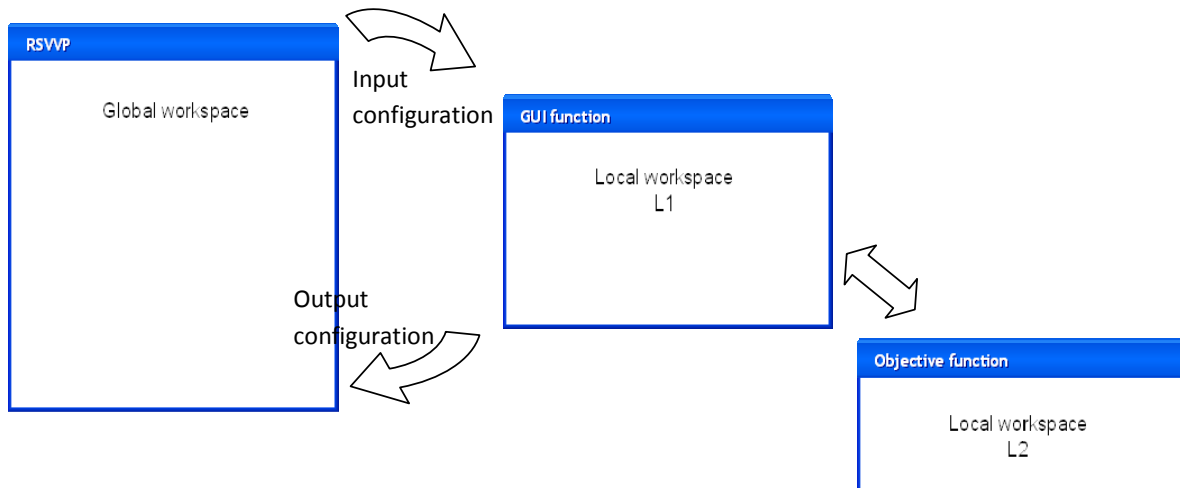


Figure B-7: Representation of the workspace of the Main and Objective functions of a GUI.

When the GUI main function closes and returns to the main invoking code, the related figure is not automatically closed by Matlab[®]. Thus, in order to close the figure, it is necessary to add into the main code the command “*close all*” immediately after the command which recalled the GUI.

BLOCK A (INITIALIZATION)

Block A is the first of the blocks in which the program code is subdivided; it performs the initial operations necessary to start the program. The functions performed by this block are: defining the type of comparison, selecting between some basic choices and performing the initialization of the major variables used during the execution of RSVVP. Moreover, in case a configuration file is input, this block performs the following tasks: (i) input of data and (ii) preprocessing.

As shown in Figure B-8, Block A is divided into two sub-blocks:

- Opening and
- Initialization.

A detailed description of each sub-block is given in the following sections.

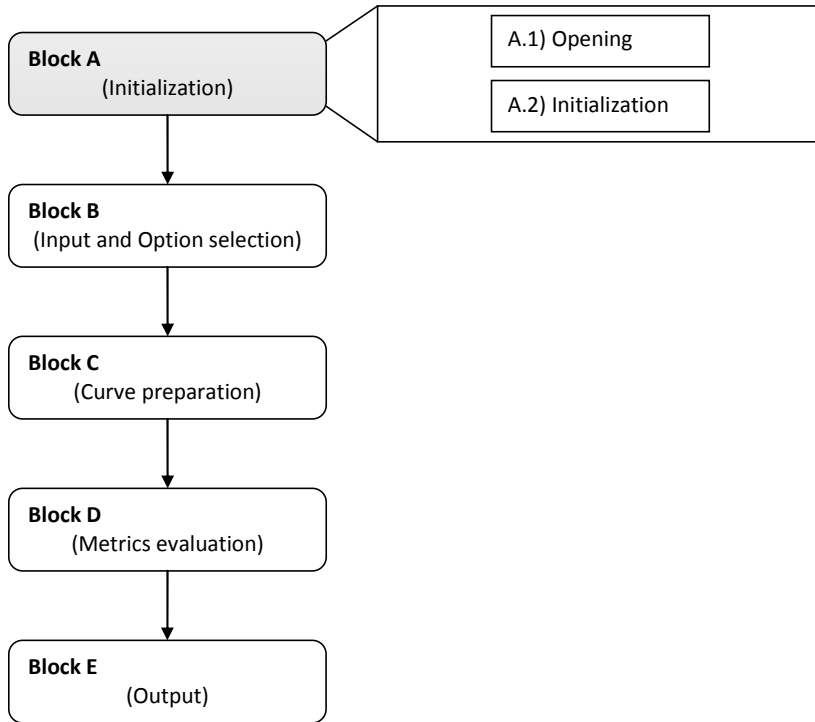


Figure B-8: Diagram of Block A.

Opening (Block A.1)

The sub-block *Opening* contains the first interactive Graphical User Interface (GUI) of the code. This GUI, which is called *GUI_Start*, manages the user choice for the following options:

- Single / Multiple channel
- Re-sampling rate limit
- Configuration file

When the GUI function *GUI_Start* closes, the options selected by the user are passed to the variable *Selection* which is used afterwards in the code. Figure B-9 B-9 shows the fields of the structured variable *Selection* which are used to store the options.

Initialization (Block A.2)

The sub-block *Initialization* performs an initialization of most of the variables used by RSVVP or, in case a configuration file has been loaded, it reads the variables containing information about the preprocessing options from the file and performs the necessary

input/preprocessing operations. Figure B-10 shows the main structure of the sub-block *Initialization*. As can be seen from the flow chart, different operations are performed according to whether a configuration file has been input or not.

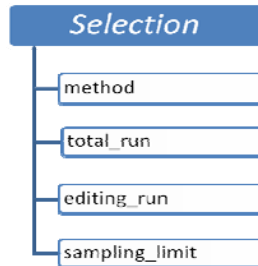


Figure B-9: Fields of the variable *Selection*.

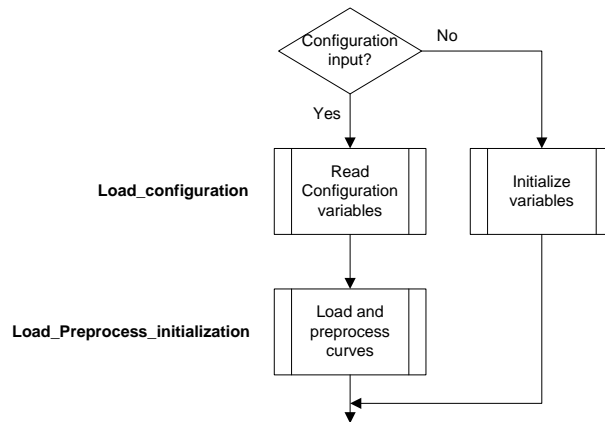


Figure B-10: Flow chart of the algorithm of sub-block A.2 (Initialization).

In the case where no configuration file is input, the sub-block A.2 initializes most of the variables used during the execution of the code. Although in Matlab[®] there is no need to statically allocate memory for the definition of variables, the way RSVVP has been implemented requires that an initial default value is assigned to the variables which control the input/preprocessing options. Following is a list of the variables initialized:

- *Reply* (*v*)
- *Reply_2* (*v*)
- *Procedure*
- *Channel_list*
- *Time_interval* (*v*)
- *Time_interval_total_run* (*v*)

In the case of multiple channels, most of the option values for each input channel are stored in vectors instead of scalar variables (The variables which become vectors are indicated with “(v)” in the previous list). In this case, each element of the vector represents the default option for the corresponding channel.

In case a configuration file has been loaded, the input curves are read from the original data files and then preprocessed according to the options obtained from the configuration file.

Figure B-11 describes in detail the algorithms used to implement respectively the two scripts *Load configuration* and *Load preprocess* recalled by the main algorithm of Block A.2.

Load configuration

This script implements the operations necessary to load the variables contained in the configuration file. As can be seen in the flowchart of the algorithm, if the user has selected to load the configuration in edit mode, a copy of the input re-sampling rate is saved at the beginning in order to be overwritten to the value of the corresponding variable once it has been loaded from the configuration file.

The algorithm checks if the file name of the configuration file is correct and, if it is correct, loads the variables; otherwise, a warning message is displayed and the program quits.

In order to avoid a crash of RSVVP in the case where no channel has been manually trimmed, it is also necessary to delete the corresponding flag variable *Manual_trim_config*.

Load preprocess initialization

This script manages the loading of the data from the input curves and the preprocessing operations according to the information obtained from the configuration file. The two branches clearly visible in the flowchart diagram of this script indicate the two main sections in which it can be divided. These two sections of the algorithm run in series, one after the other, and each of them contains a loop (both indicated by a red rectangle).

The first branch is a loop which cycles over the total number of channels (i.e., one for the case of a single channel or six for the case of multiple channels). Each iteration of the loop loads the input curves and performs the preprocessing operations according to the information read from the configuration file. For more details about the scripts or part of the code which perform

the loading and the specific preprocessing operations, refer to the next section (Block B). Before concluding each iteration, the preprocessed curves are saved in the matrix variable *Preprocessed* (refer to Section Block B in this manual for more details about the structure of this variable) and the variable *Ch_num* is incremented.

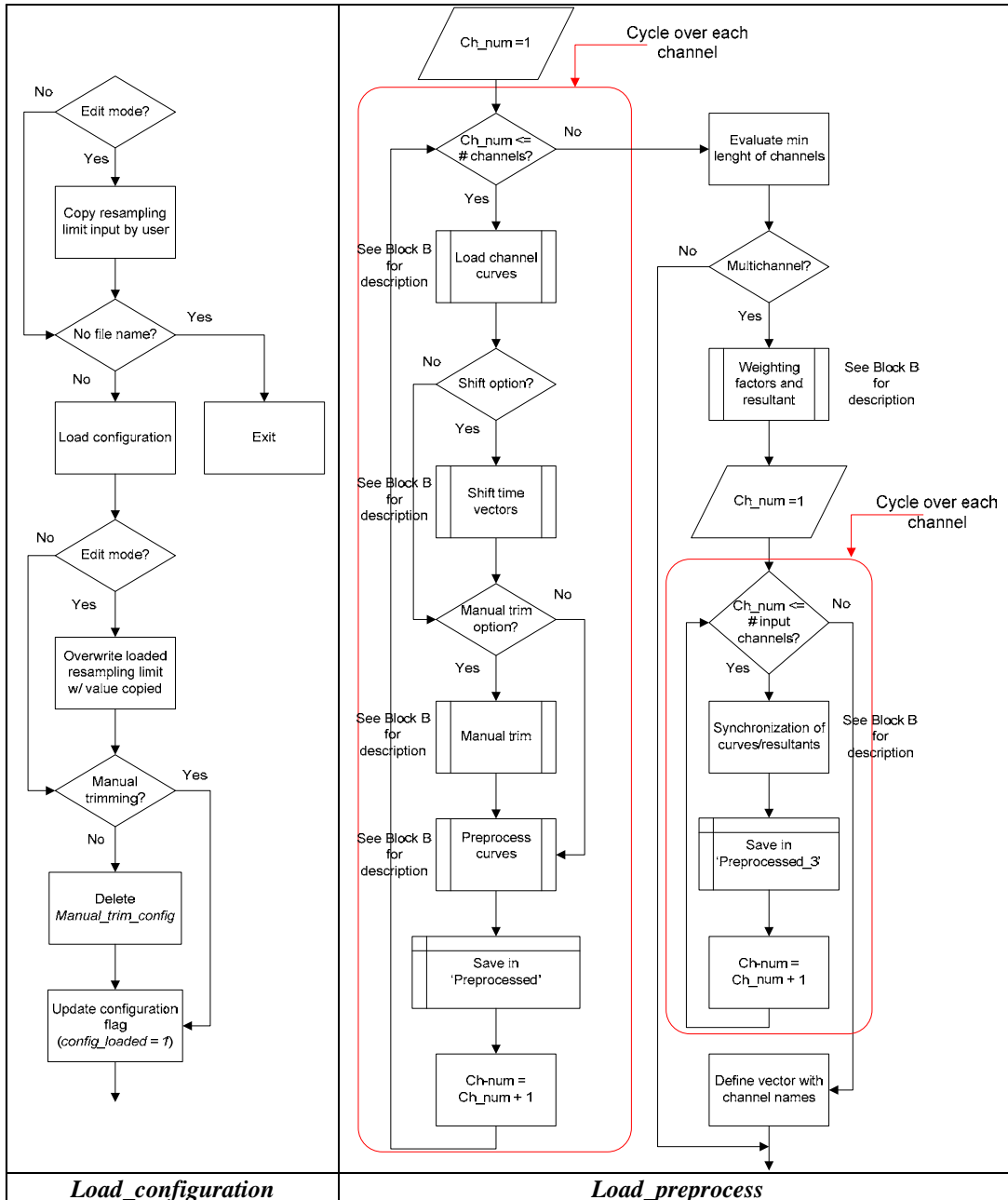


Figure B-11: Flow chart of the scripts *Load configuration* (left) and *Load preprocess* (right) (sub-block A.2).

After the cycle has concluded and all the channels have been input and preprocessed, the minimum length between all the couple of channels is computed. In case of multiple channels, first the weighting factors or the resultants are calculated and, then, the program cycles over the channels/resultants to perform the synchronization of the curves in case it is requested by the configuration file. Eventually, a vector with the names of the specific input channels (or the resultants) is created to be used during during the postprocessing operations for the output of results.

BLOCK B (INPUT AND OPTION SELECTION)

Block B implements most of the interaction activity with the user. In fact, this block manages three different graphical interfaces which respectively perform three different tasks: (i) input of data, (ii) preprocessing and (iii) selection of metrics/time intervals. The diagram of Block B is shown in Figure B-12; the block is divided into three sub-blocks:

- Input/Preprocessing (GUI_1_3),
- Preprocessing 2 (GUI_1_3_II) and
- Metrics selection (GUI_metrics).

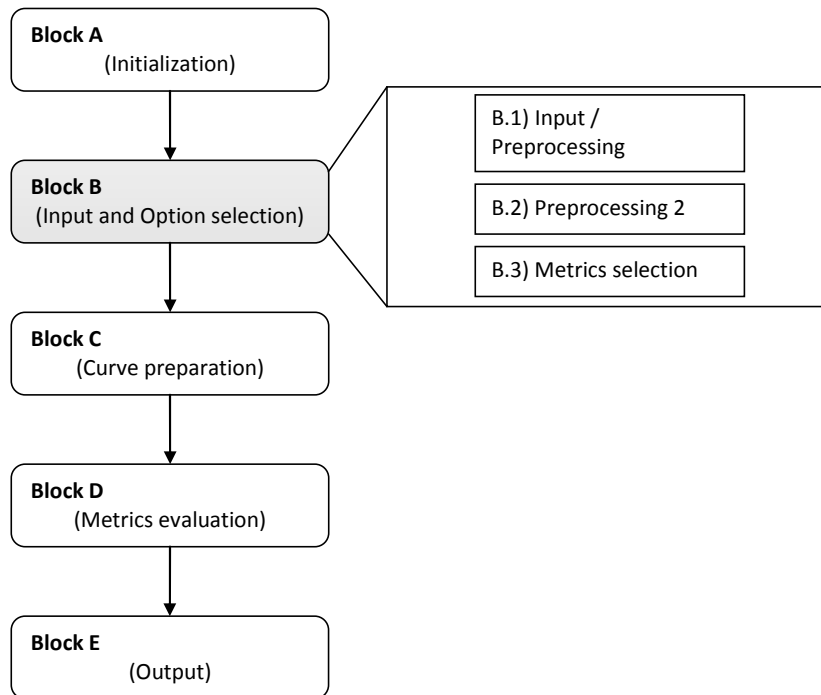


Figure B-12: Diagram of Block B.

The main characteristic of Block B is that the three sub-blocks are implemented in sequence into a loop which terminates only when the user decides to proceed to the evaluation of metrics (Figure B-13).

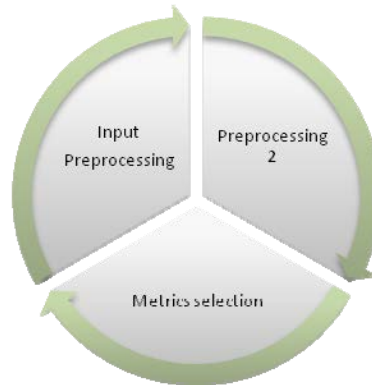


Figure B-13: Scheme of the loop which forms Block B.

Figure B-14 shows the main algorithm of Block B. The implementation of the three sub-blocks into a loop allows the possibility to go back to the previous sub-block to apply any further change to the options selected in the previous instance. In fact, by skipping directly to the next iteration of the loop, it is possible to go back to the first sub-block (i.e., B.1). In case the user is executing operations implemented in the sub-block B.3 (i.e., the last of the three blocks), it is also possible to skip directly to the second sub-block, B.2, during the new iteration of the loop by defining a flag variable and a conditional statement at the beginning of the first block. In this case, given a particular value of the flag variable, the conditional statement for the execution of the first block would skip it and start the new iteration of the loop directly from sub-block B.2.

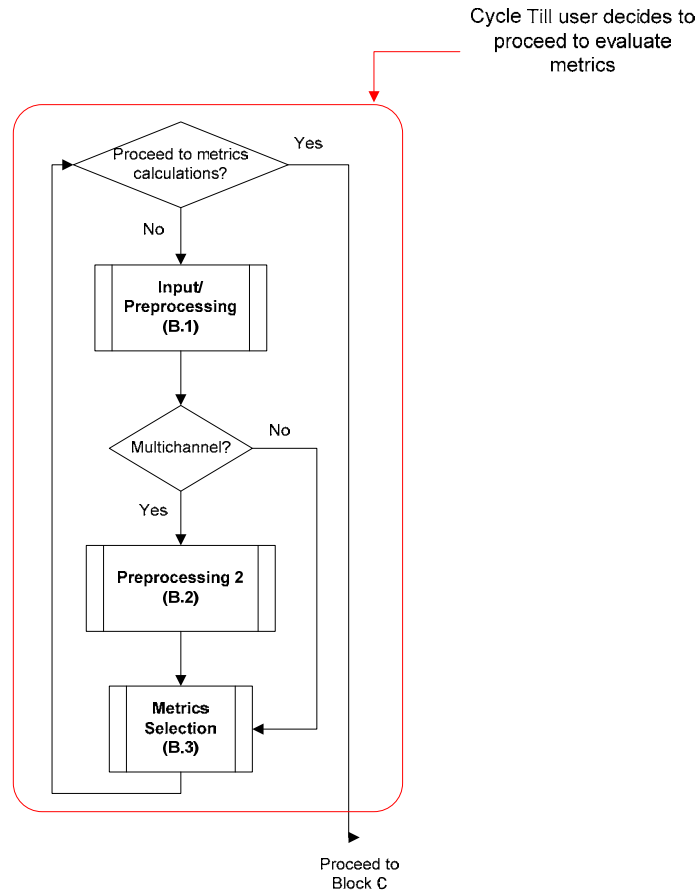


Figure B-14: Flow chart of the main algorithm of Block B.

Any time they open, the graphical interfaces of each of the three sub-blocks load the options and the various data input by the user during the previous iteration of the main loop. This information is read from variables whose structure and content will be specifically discussed ahead in this section. Using such a structure, whenever the user goes back to the previous sub-block, the graphical interface which is reopened shows the same information of the previous iteration. In the case where a configuration file has been loaded, the input/preprocessing operations performed by Block B are skipped as they have already been performed in Block A. A detailed description of each sub-block is given in the following sections.

Input/Preprocessing (Block B.1)

This sub-block is the first of Block B and implements the GUI which handles the input of the curves and their preprocessing (GUI_1_3).

The flow chart in Figure B-15 shows the general implementation of this sub-block. As can be seen from the flow chart, the core of sub-block B.1 is the script *Load_preprocess*, which is invoked only under the condition that both no configuration file has been input (*config_loaded* = 0) and that GUI_1_3 is set to be open (*open_GUI_1_3* = 1). The former condition avoids that curves are input and preprocessed when a configuration file has been loaded, while the latter condition is used to skip the execution of this block in order to go directly to the next sub-block during the new iteration of the main loop defined by the cycle in Figure B-14. In either the case the script *Load_Preprocess* has been invoked or not, before proceeding to the sub-block B.2, a copy of the original input curves is saved.

If the *Exit* button has been pressed during the execution of GUI_1_3, the algorithm terminates the program.

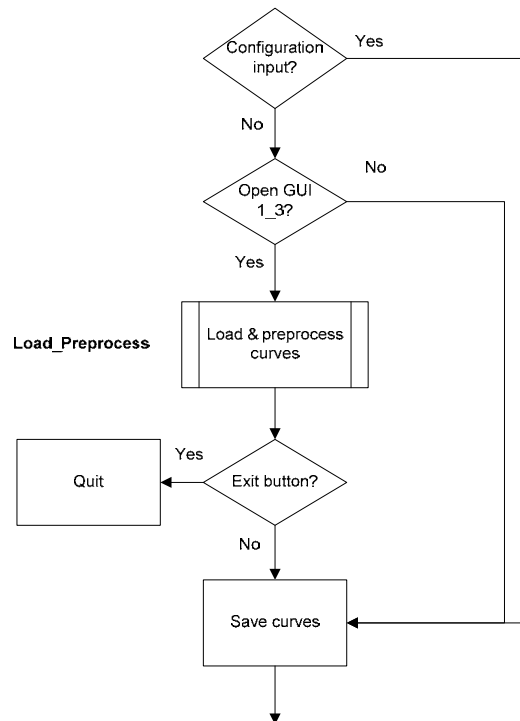


Figure B-15: Flow chart of the algorithm of sub-block B.1 (Input/Preprocessing).

Load Preprocess

As previously mentioned, this script is the core of Block B.1 which manages the input of the channel/s and the corresponding preprocessing. The algorithm of the script is shown in Figure B-16 and Figure B-17.

The script is embedded into a loop which stops only when, after the last channel has been input and preprocessed, the user decides to proceed to the selection of metrics. Using a loop it is possible to move back and forth through any of the available channels by incrementing/decrementing the variable *ch_num* which is used to define the specific channel. This allows the user to go back to a previously input channel and make any modification also after this channel has already being input.

The flag variable which controls the loop is *Reply.flag* and the condition to keep cycling is either the value 0 or 4. Initially, before starting the cycle, this flag variable is assigned the null value; while the value 4 means that the preprocessing options of the specific channel have been reset and a new iteration has to be performed on that channel. When the user pushes the button to proceed to the selection of metrics in the corresponding GUI (*GUI_1_3*), *Reply.flag* becomes unity and the cycle terminates. The variable *ch_num* specifies the channel which is considered at each iteration of the loop. The value of this variable is by default equal to 1 in case of a single channel or is assigned by the variable *Reply.channel_id* (written by the *GUI_1_3*) in case of multiple channels.

At the beginning of each iteration of the loop, *GUI_1_3* opens. The first time *GUI_1_3* is opened for each channel indicated by the variable *ch_num*, the default values created during the initialization are recalled. When the GUI closes, the algorithm proceeds to load the curves from the selected files and perform the preprocessing according to the selection made by the user. At the beginning of the next iteration, the GUI is opened again and shows the preprocessed curves. In case the GUI has already been opened for a specific channel before, it reloads any previous option or data and, if the user has modified/reset any of the preprocessing options, when the GUI closes the algorithm proceeds to reload the curves and modify the preprocessing according to the new options. In case the last channel has been skipped, the algorithm automatically ends the loop.

Apart from the scaling operation, which is performed by the script *Load_curves*, and the manual trimming of the curves, which is implemented in the script *Manual_trim_shift*, all the other preprocessing operations are invoked by the script *Preprocessing*.

The scaling option is implemented by simply multiplying the vector containing the data points by the scaling factor defined by the user for that specific channel and curve.

Data vectors are manually trimmed by limiting the original vectors within the indexes which are closer to either the lower or upper boundary values, respectively; while, the shift of the time vector is obtained by subtracting the initial time value from the time vectors of the curves. The other preprocessing operations are performed by recalling the script *Preprocessing* which, on its turn, recalls one or more of the following scripts according to the specific options selected for each channel:

- Filtering
- Shift_drift
- Resampling_trimming
- Curve_synchronizing

The algorithms for these pre-processing operations are described in 0.

The preprocessed curves are saved into the variable *Preprocessed* which is a matrix of cells. As shown in Figure B-18, the i^{th} row contains respectively the time, true data and test data vectors of the corresponding channel i . Note that the possibility to store vectors for each of the element of the matrix *Preprocessed* is achieved by first converting the vector into a cell. In case of a single channel comparison, this matrix reduces to a horizontal vector.

After the loop ends, the pairs of curves from the various input channels are trimmed to the length of the shortest and the algorithm proceeds to the next block.

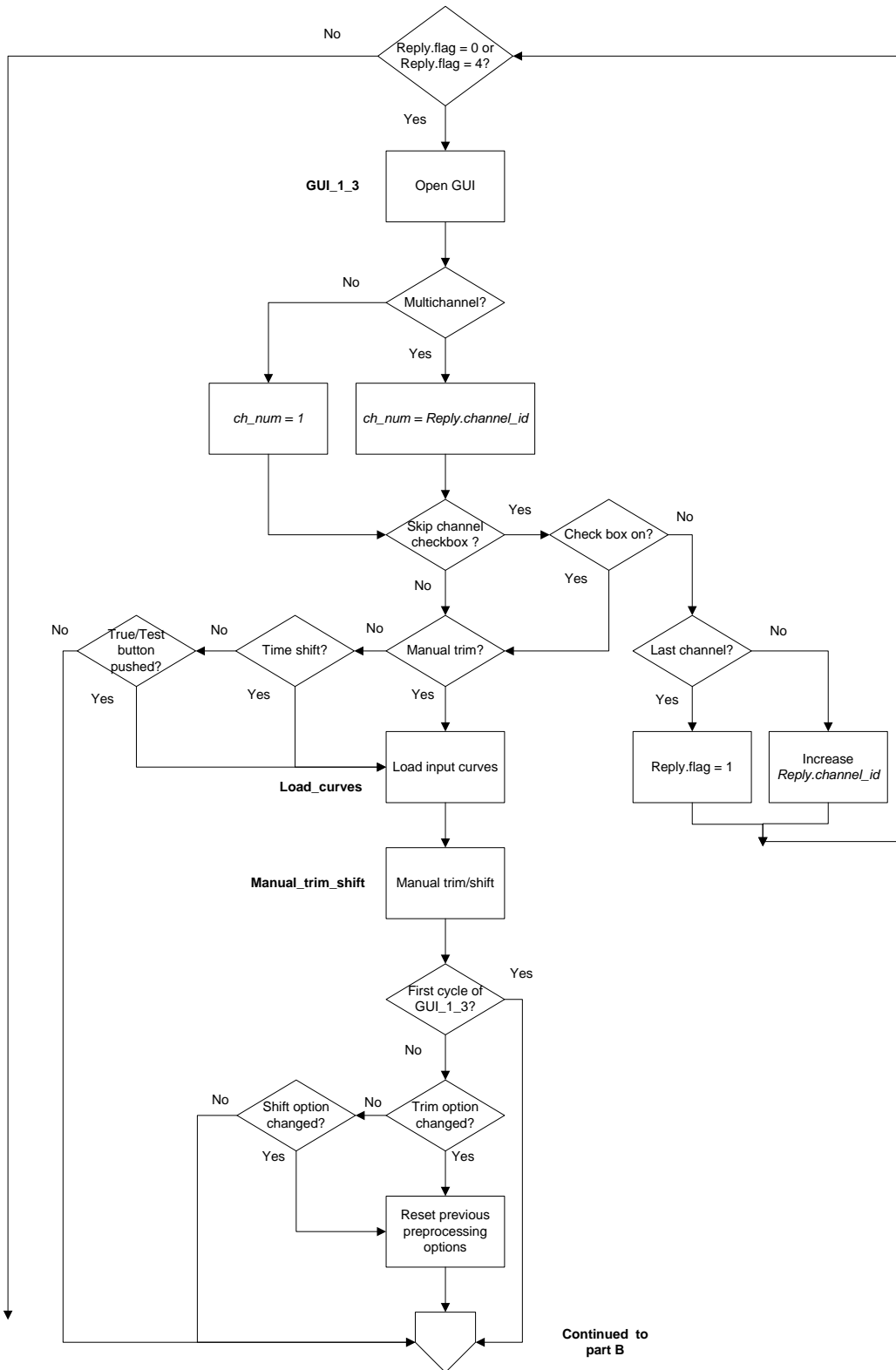


Figure B-16: Flow chart of the script *Load_Preprocess* (sub-block B.1) – part A.

Continued
from part A

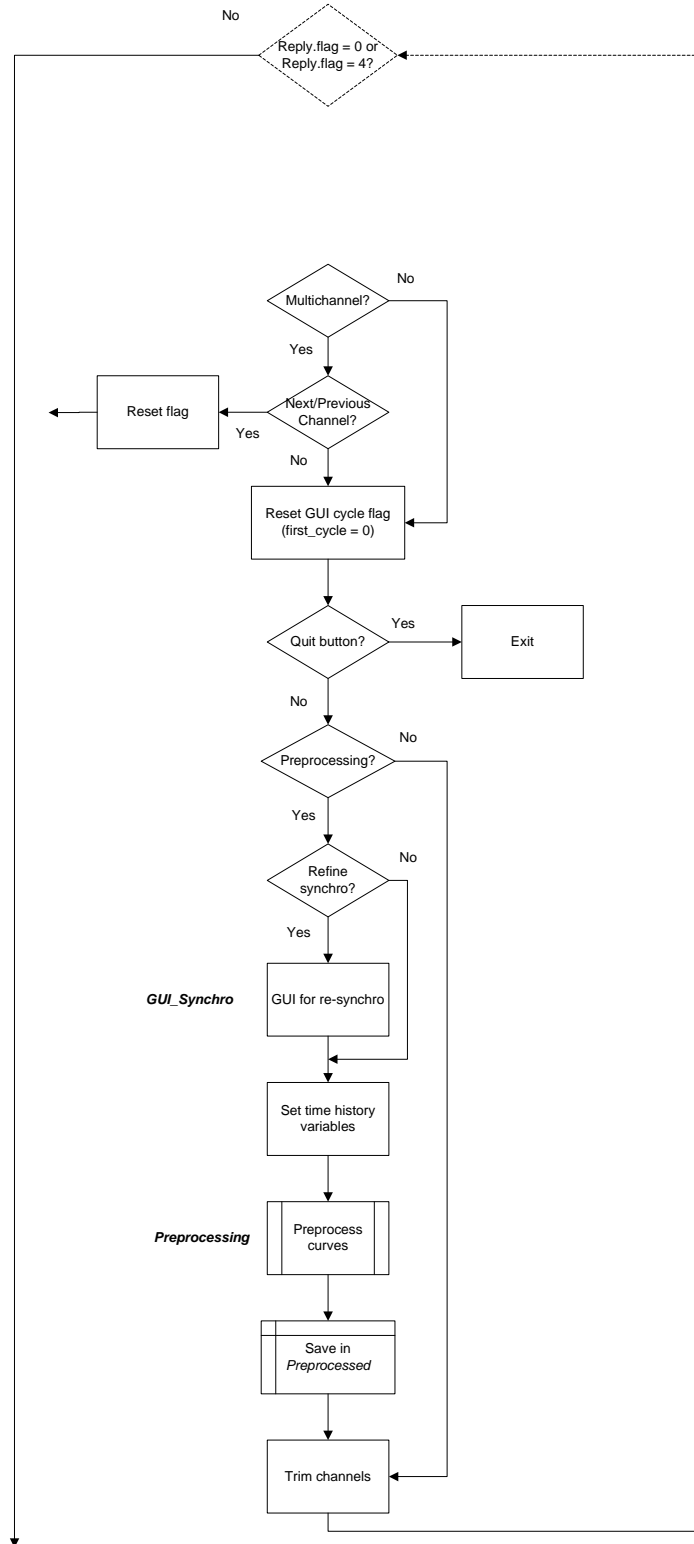


Figure B-17: Flow chart of the script *Load_Preprocess* (sub-block B.1) – part B.

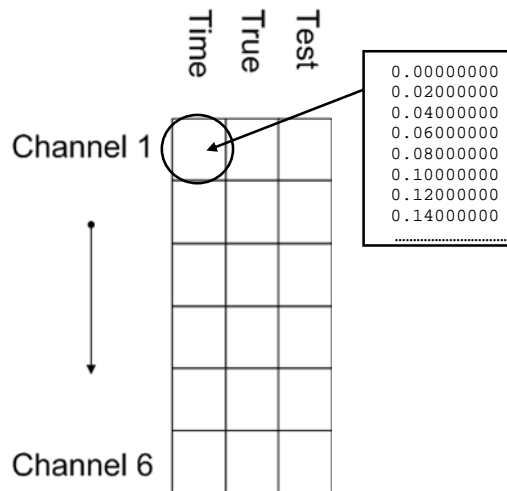


Figure B-18: Sketch of the structure of the variable *Preprocessed*.

Load curves

This script manages the load of the input curves from the ASCII files provided by the user. In particular, it skips any of the initial rows containing non-numeric characters and scales the data point by the user defined factors. The algorithm of this script is shown in Figure B-18. The same algorithm is repeated of both the test and true curves.

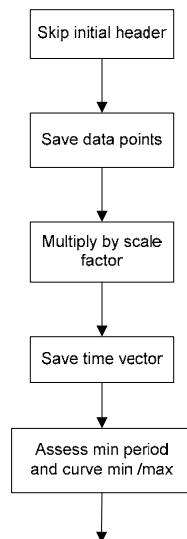


Figure B-18: Flow chart of the script *Load_curves* (sub-block B.1).

Preprocessing 2 (Block B.2)

This sub-block implements the synchronization of the curves in case multiple channels are input. In this case, the synchronization is performed after the single channels have been input and partially preprocessed in order to allow the user the option to compute the resultants from the acceleration and rotational rate channels. In fact, if the resultant option is selected, the true and test curves from the input channels are combined together in order to first obtain the corresponding resultant curves which are then synchronized.

The flow chart in Figure B-19 shows the general implementation of this sub-block. It is recalled only in the case multiple channels are input (*comparison_type* = 2) and is completely skipped in the case of a single channel. At the beginning, the sub-block B.2 initializes some variables and then proceeds to the core script *Preprocess_2* which manages *GUI_1_3_II*. In case the Exit or the Back button has been pressed in *GUI_1_3_II*, the sub-block B.2 respectively quits the program or goes back to *GUI_1_3* by forcing a new iteration of the loop described by the flow chart in Figure B-14.

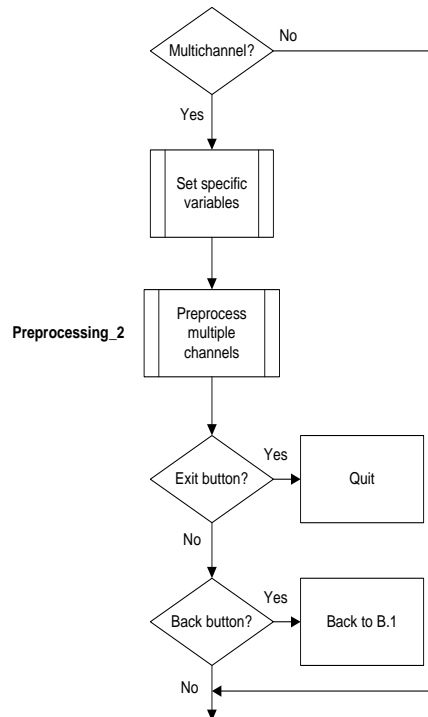


Figure B-19: Diagram of sub-block B.2 (Preprocessing2).

Preprocessing 2

This script is the core of sub-block B.2. It manages the synchronization of the multiple channels and the selection of the method to use for computing the equivalent metrics (weighting factors or resultant). Similarly to the previous sub-block, also in this case the script is mostly contained into a loop in order to implement the possibility to move back and forth through any of the available channels by incrementing/decrementing the variable *ch_num* which is used to define the specific channel.

The algorithm of the script is shown in Figure B-20. Before entering the loop, the variable *Preprocessed_2* is initialized as a copy of the variable *Preprocessed*. In this way, the curves originally preprocessed by the previous sub-block are always available in case the user decides to reset the preprocessing performed by this sub-block.

At the beginning of each iteration of the loop, the GUI called *GUI_1_3_II* is opened. Similarly to *GUI_1_3*, also the first time that *GUI_1_3_II* is opened for each channel the default values created during the initialization are recalled and, as soon as the GUI closes, the algorithm performs the preprocessing operations. When the GUI is opened again at the beginning of the next iteration, both the initial and preprocessed curves are shown.

If the synchronization option has been selected in the GUI (indicated by the variable *Reply_2.synchro*) the specific channel is synchronized. Also, in case the user decided to re-synchronize the curves, a new GUI is invoked (*GUI_Synchro*) to define a new starting point for the synchronization procedure. Note that in this case, after the re-synchronization, the algorithm will go to the next iteration of the loop where *GUI_1_3_II* will be invoked to show the new synchronized curves.

The default option for the computation of multichannel (weighting factors/resultant) is set to weighting factors. In case this option is changed (identified by the variable *Reply_2.update*) in the GUI, the algorithm proceeds to re-initialize the variable *Preprocessed_2* accordingly by recalling the script *Initialization_2*.

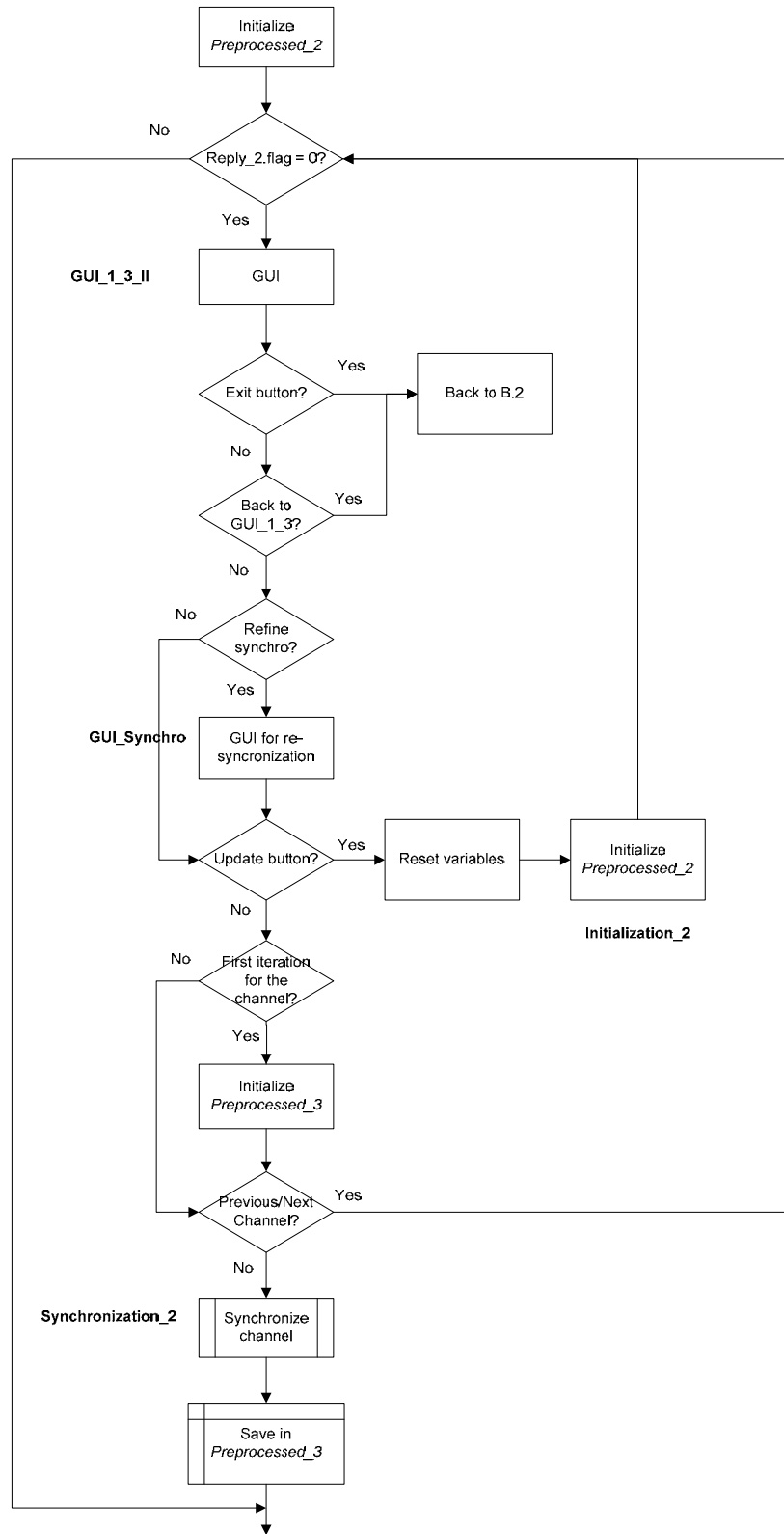


Figure B-20: Flow chart of the script *Preprocessing_2* (sub-block B.2).

In case the iteration of the loop is the first for that channel (*Reply_2.first_iteration = 1*), the variable *Preprocessed_3* is initialized. If the next or previous buttons have been pushed in the *GUI_1_3_II*, a new iteration of the loop is forced and *GUI_1_3_II* is invoked showing the next or previous channels.

Metrics selection (Block B.3)

Metrics selection is the last of the sub-blocks of Block B. It implements the GUI for the selection of the metrics and time intervals on which compare the input curves (whole time and/or user defined intervals).

The flow chart in Figure B-21 shows the general implementation of this sub-block. The first action performed is set the value of the variable *procedure* according to the type of multichannel comparison (i.e., weighting factors or resultant). This variable is then used in subsequent parts of the program code.

In case multiple channels are input, a script checks if any channel has been skipped, and in case, null vectors are added to the corresponding row in the variable *Preprocessed_3*. Also, the algorithm creates a configuration file relative to the RSVVP run. Note that, if a previous configuration file has been loaded without editing (total-run mode), the creation of the configuration file is skipped.

Metrics_selection

This script is the core of sub-block B.3 and manages the GUI for the selection of the metrics and the type of time intervals on which to compare the curves (whole and/or user-defined time intervals).

The algorithm of the script is shown in Figure B-22. The script manages the GUI for the selection of metrics (*GUI_metrics*). In case a configuration file is loaded in ‘run mode’, the GUI is not opened as the information is taken directly from the configuration file and RSVVP automatically re-runs the comparison. Also in this case, once the GUI has collected the information entered by the user, it is closed and the algorithm proceeds according to the selected option/s.

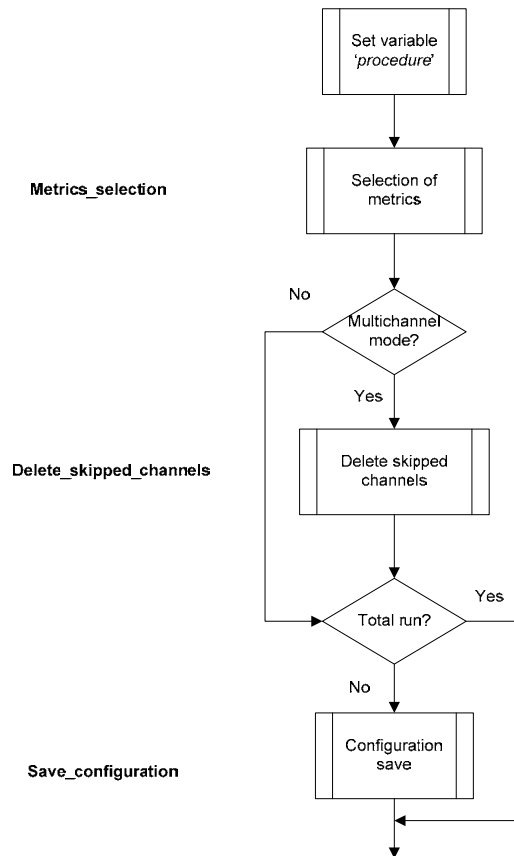


Figure B-21: Diagram of sub-block B.3 (Metrics selection).

If the back button has been pressed in the GUI, the algorithm set the variables *open_GUI_1_3* and *config_loaded* equal to zero and then a new iteration of the main loop of Block B is forced. The values assigned to these variables skip the opening of *GUI_1_3* at the next iteration of the main loop.

In case the user has selected the metrics and time intervals, the algorithm sets the variable *Metrics_list* according to the metrics selected in the GUI. Note that, in this case, the variable *Metrics.flag* is set to the unity in order to quit the main loop of Block B and proceed to Block C.

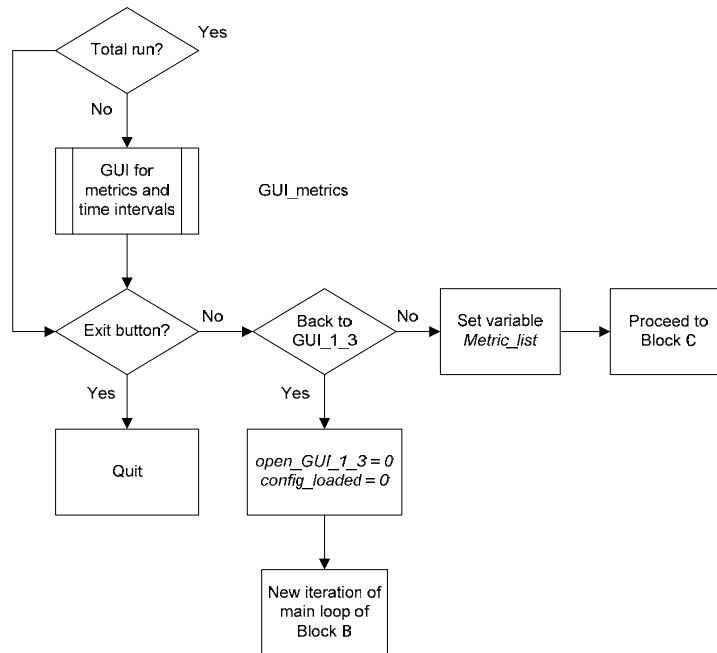


Figure B-22: Flow chart of the script *Metrics_selection* (sub-block B.3).

BLOCK C (CURVE PREPARATION)

Block C finalizes the preprocessing activities and creates the plots of the input curves after the preprocessing. Figure B-23 shows the diagram of this block, which is composed of three sub-blocks:

- Curve preparation,
- Curves histories and
- Curves plotting.

A detailed description of each sub-block is given in the following sections.

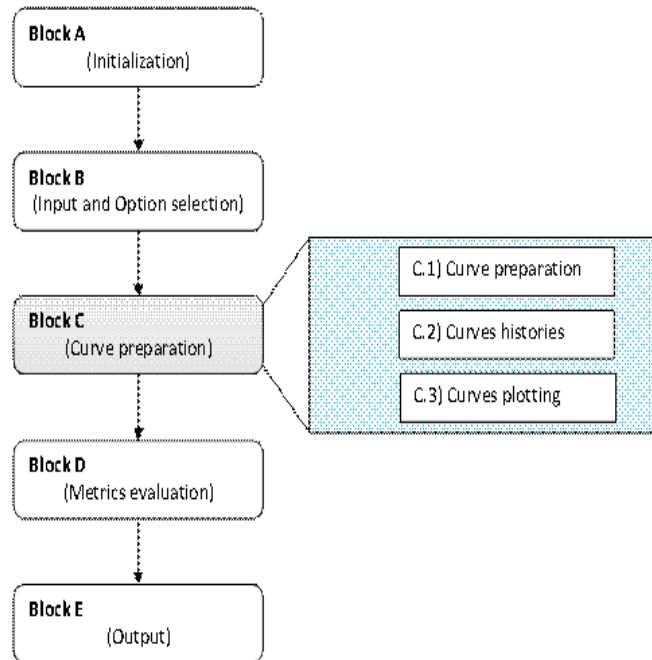


Figure B-23: Diagram of Block C.

Curves preparation (Block C.1)

The sub-block *Curves preparation* refines the preprocessing by trimming the couples of curves from the various channels to the length of the shortest channel. This operation is performed only in multi-channel mode ($comparison_type = 2$).

Data points of the input channels are initially stored in the variable *Preprocessed_3*, which is a matrix of cell (for details about the structure of this variable, refer to section Block C). The vectors of the true and test curves of each channel are extracted from the respective cells structures, trimmed and stored in the matrix variable *True* or *Test* correspondingly. As the length of the vectors is the same for all the channels after the trimming, it is possible to store the data in a simple matrix structure without the need to use a cell configuration, like required before the trimming operation.

The organization of the matrices *True* and *Test* is represented in Figure B-24. For both the matrices, the vectors of the data points for the channel i is saved in the i^{th} column. The flow chart in Figure B-25 shows the general implementation of this sub-block.

Curves histories (Block C.2)

This sub-block saves the time histories of both the original and preprocessed input curves. The original and preprocessed time histories are managed respectively by the script *Save_curves_original* and *Save_curves_preprocessed*. The main implementation of this sub-block and the two mentioned scripts are shown in Figure B-26.

As usual, in case of multiple channels, in the algorithm of both the scripts a loop cycles over the total number of input channels.

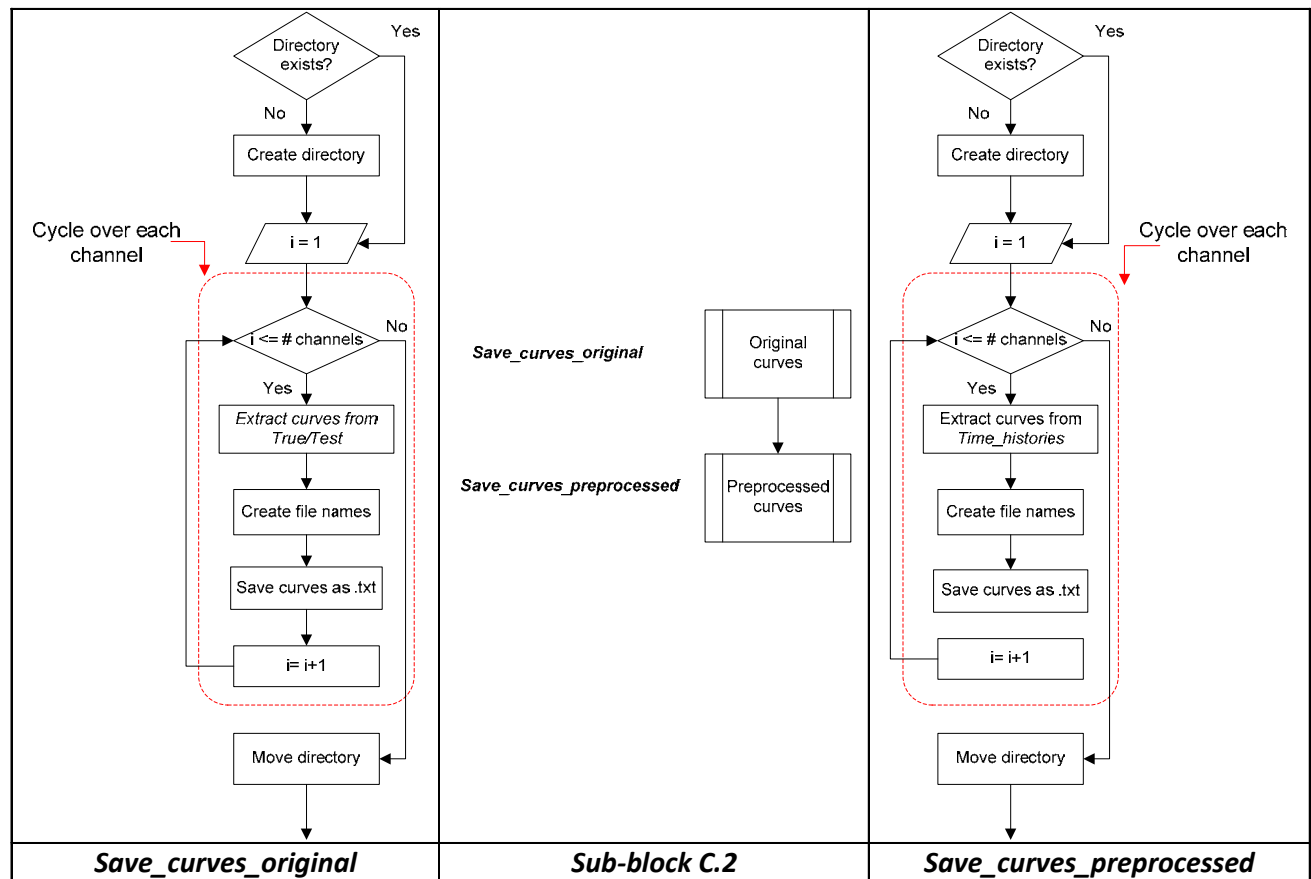


Figure B-26: Diagram of sub-block C.2 (Curves histories) (center) and the two invoked scripts, *Save_curves_original* (left) and *Save_curves_preprocessed* (right).

Curve plotting (Block C.3)

The sub-block *Curves plotting* performs two main operations: (i) plot the preprocessed curves after they have been finalized by the previous sub-block (*Curve preparation*) and (ii) evaluate the area of the true curve for each channel.

Before plotting the curves, the code creates the destination folder where the corresponding bitmap files are saved. In case the NCHRP 22-24 profile has been chosen, also the integrals of the original input curves are plotted. In both the cases, a conditional statement based on the value of the variable *zip_flag* handles the possibility to compress the bitmap files.

The evaluation of the area of each channel is implemented at the end of the block and the corresponding values are saved in the vector variable *Channel_area*. This vector is used in the following part of the code (Block D) to evaluate the weighting factors for the whole time interval. Note that, for each user-defined time interval, the values of the channel areas are evaluated again in a following part of the code located in Block D.

The flow chart in Figure B-27 shows the general implementation of this sub-block.

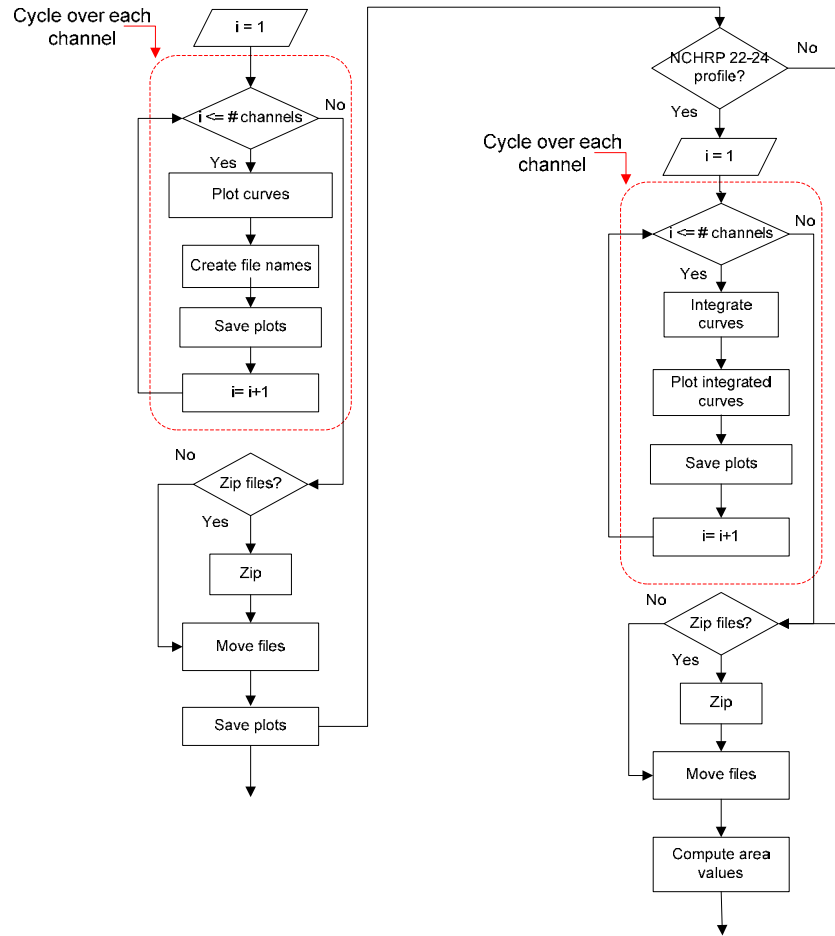


Figure B-27: Flow chart of the script *Whole_plot_curves* (sub-block C.3).

BLOCK D (METRICS EVALUATION)

Block D implements the computation of the comparison metrics and the corresponding post-processing operations necessary to evaluate the weighted average of the metrics obtained from the single channels. As can be seen in Figure B-28, Block D is composed of two sub-blocks which handles the evaluation and post-processing of metrics respectively on the whole time interval and the user defined time interval/s.

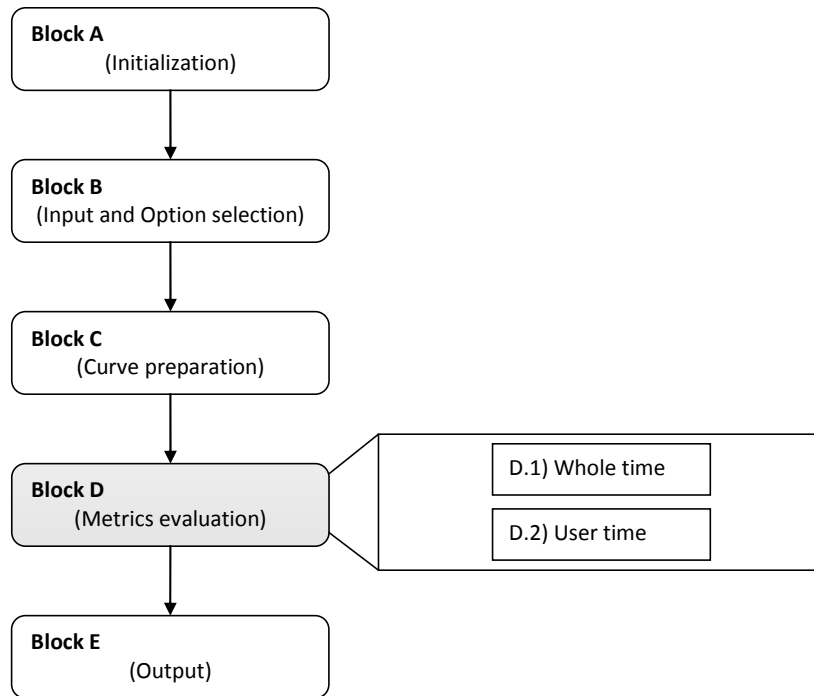


Figure B-28: Diagram of Block D.

The main structure of Block D is shown in Figure B-29. The sub-blocks Whole time (D.1) and User time (D.2) are invoked respectively in the case the curves are compared on the whole time or a user time interval. In particular, in case the whole time option is not selected, a void vector/matrix is created for the corresponding output in the Excel file.

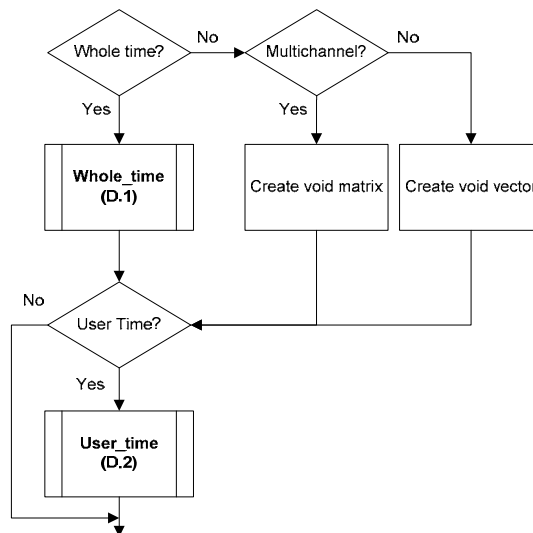


Figure B-29: Main structure Block D.

Whole time (Block D.1)

The sub-block *Whole time* calculates the metrics in the full time interval on which the curves are defined. The flow chart in Figure B-30 shows the general implementation of this sub-block.

If RSVVP is running in single channel mode, the weight assigned to the channel is the unity. In multichannel mode, at the beginning of its execution, the sub-block computes the weighting factors according to the specific method selected by the user. In case the resultants for the accelerations and rotational rates have been computed, each of them is assigned a weight equal to 50 percent of the total; otherwise, the weighting factors for each channel are computed based on the area of the true curves. In the latter case, the script *Weighting_scheme_whole* is invoked.

The calculation of the metrics is performed by invoking the script *Metrics_evaluation* which is cycled over each of the input channels (the loop in the flowchart is indicated by the red rectangle). After the metrics have been computed for each channel, the sub-block D.1 also performs two main post-processing operations:

- Computation of the weighted average (multiple channels)
- Creation of variables for the Excel output

The post-processing is executed by the script *Whole_time_postprocessing*.

Eventually, the sub-block D.1 displays the results (metrics values and various graphs) through a GUI which is managed by the script *Table_output_whole*.

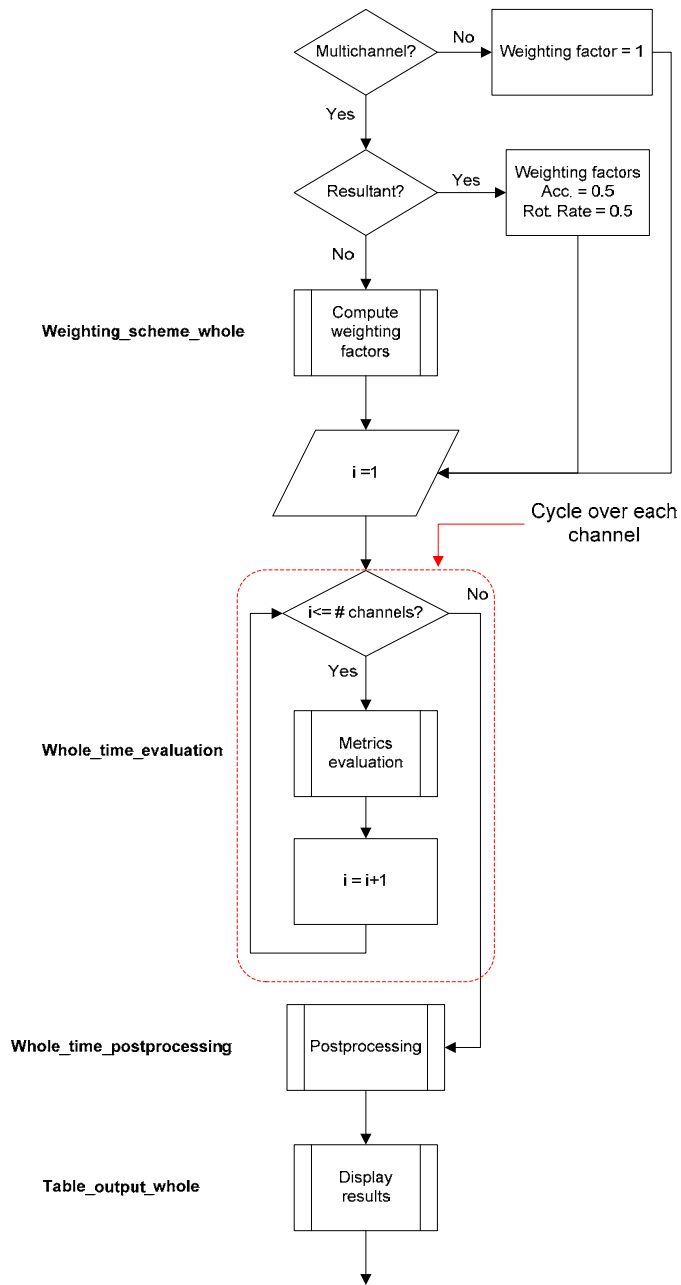


Figure B-30: Diagram of sub-block D.1 (Whole time).

Weighting scheme whole

This script calculates the weighting factors in case of multiple channels. The steps followed to compute the weighting factors are shown in the flowchart in Figure B-32.

The method is based on the computation of the area of the true curve for each channel and the areas of the accelerations and rotational rates are considered separately because, otherwise, the different units may lead to a disproportion in the evaluation of the weighting factors.

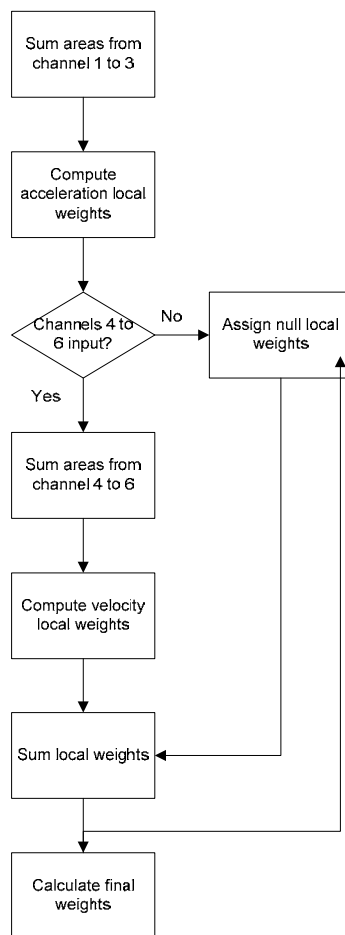


Figure B-31: Flow chart of the script *Weighting_scheme_whole* (sub-block D.1).

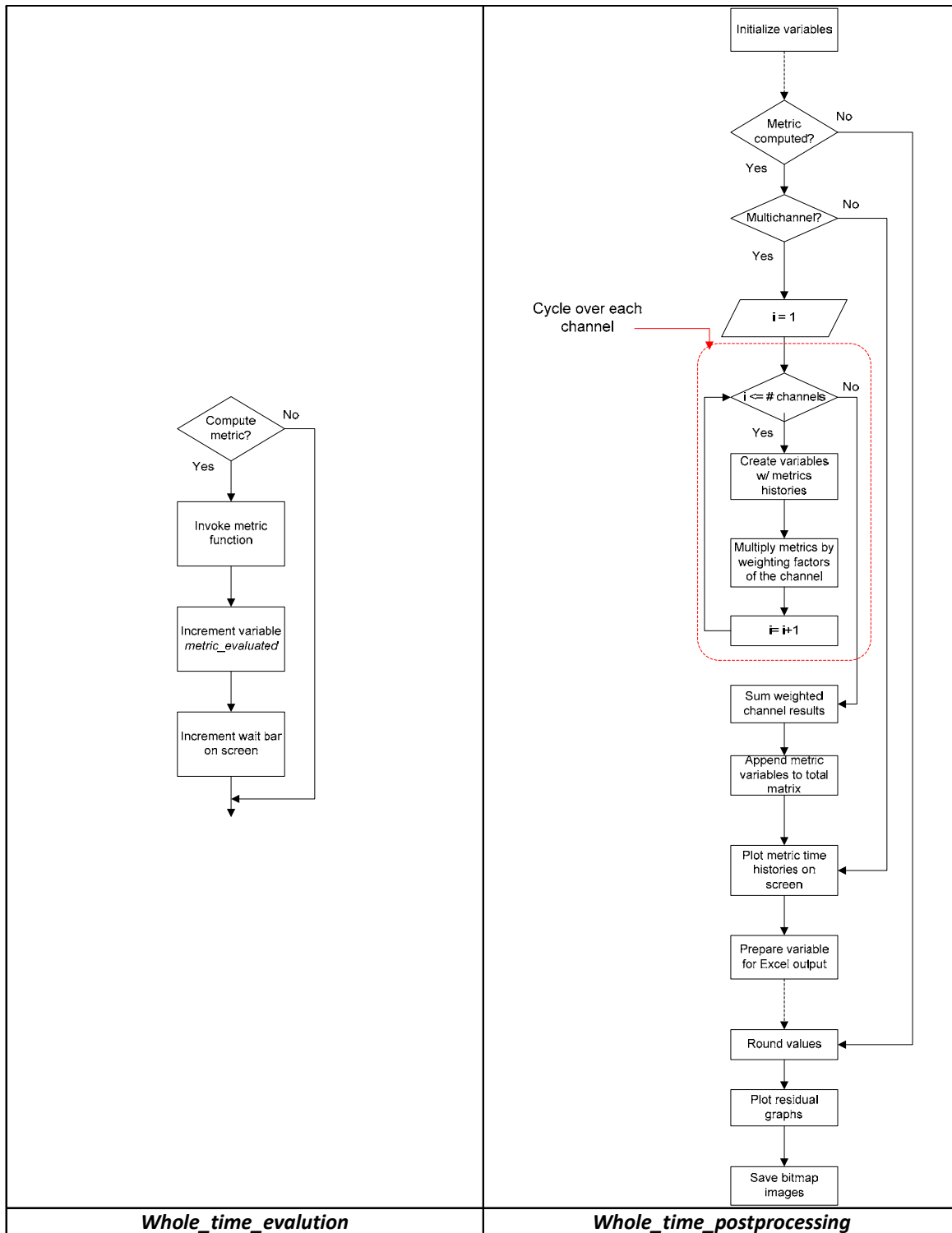


Figure B-32: Flow chart of the scripts *Whole_time_evaluation* (left) and *Whole_time_postprocessing* (right) (sub-block D.1).

Whole time evaluation

This script manages the computation of the metrics according to the selection made by the user in the corresponding GUI. The variable used to store the metric flags is *Metrics*. The algorithm of this script is composed of a series of conditional blocks, one for each of the metrics implemented in the code. The generic flowchart of these blocks is shown in Figure B-32 (left).

If it has been selected, a metric is evaluated by invoking the corresponding function. Metric functions are programmed in Matlab[®] and, generally, they receive as input the preprocessed curves corresponding to a specific channel and give as output one or more vectors containing the time history/ies of the metric. Once the metric values have been computed, a counter variable (*metric_evaluated*) is incremented which then is used to add a bar to an on-screen waiting bar used to inform the user about how many metrics have been calculated/remain.

Whole time postprocessing

This script is the core of sub-block D.1. It manages the following four operations:

- calculation of the weighted average of metrics (multiple channels)
- creation of the variables containing the metrics values and time histories (for the output both on screen and using Excel files)
- round-off of the metrics values
- residuals plotting (time histories, histogram and cumulative distribution)

The flowchart of the whole script is shown in Figure B-32 (right). Similarly to the previous script, also the algorithm of this script is mainly composed of a series of conditional blocks, one for each of the metrics implemented in the code.

The generic structure of each of these conditional blocks is delimited in the dotted rectangle in the flowchart. In the whole flowchart, each block is related to a specific metric and is performed only if that metric has been computed. In case of multiple channels, a loop is defined which cycles over each of the input channels. For each iteration of the loop, a local variable is created which contains the metric values for that specific channel. Also, the values for each channel are then multiplied by the corresponding weighting factors previously computed

by the script *Weighting_scheme_whole*. These weighted values are then summed up immediately after the loop ends in order to obtain a weighted average.

Once variables with metrics values and time histories have been created for a specific metric, they are appended to a corresponding global variable which cumulates the results for the various metrics computed during the run.

After the script has post-processed all the metrics, it proceeds to round the values and plot the graphs of the residuals, histogram and cumulative distribution. Note that, during the rounding of the values, the algorithm checks if any of the implemented metrics has been computed and, in case it has not, it automatically adds the word 'N/A'.

Eventually, the script creates the following variables containing the various values to be output by Block E: in Excel format.

- *Output_channel_history_xls*
- *Output_single_history_xls*
- *Output_xls*
- *Output_channel_xls*

The diagrams in Figure B-33 and Figure B-34 show how data are organized in each of the above mentioned variables.

Sprague&Geers M Sprague&Geers P T-test		Sprague&Geers M Sprague&Geers P T-test	
<i>Output_xls</i>		<i>Output_channel_xls</i>	

Figure B-33: Data organization of the variables *Output_xls* and *Output_channel_xls*.

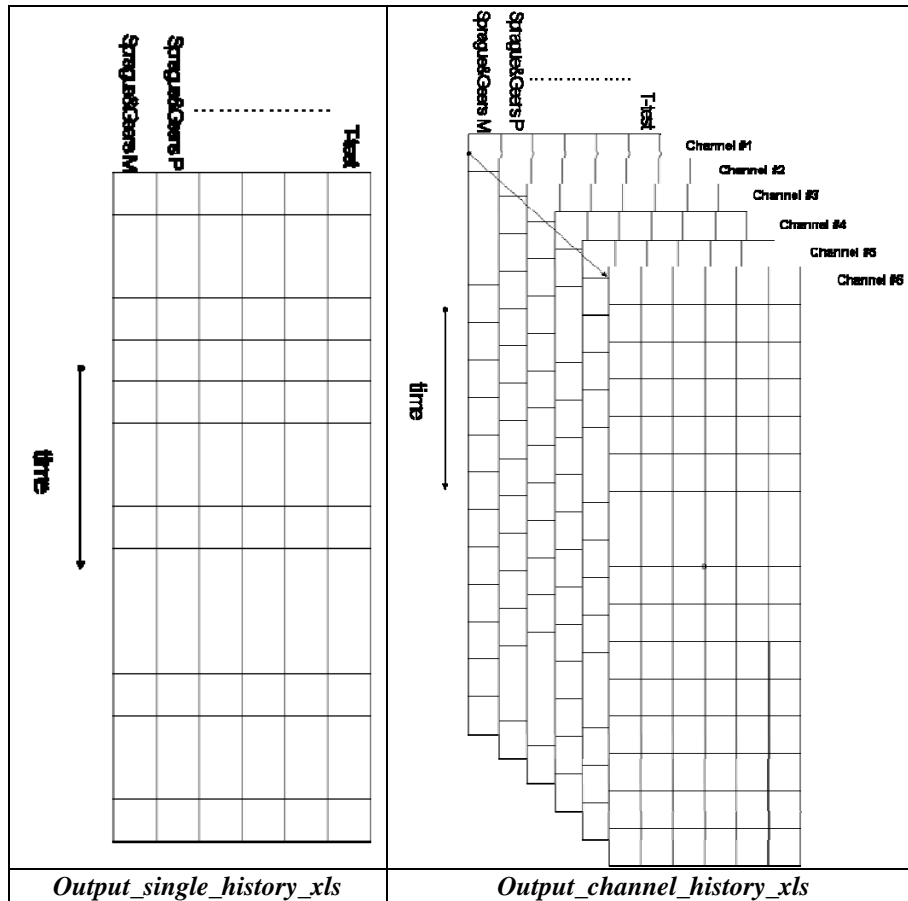


Figure B-34: Data organization of the variables *Output_single_history_xls* and *Output_channel_history_xls*.

Table_output_whole

This script is the last recalled by sub-block D.1 and contains commands to create a summary table with graphics and the values of the metrics. The summarizing table is a GUI managed by the function *Table_Results_NCHRP* or *Table_Results* according to which type of metric profile has been selected at the beginning of the run.

User time (Block D.2)

The sub-block *User time* calculates the metrics on the time interval/s defined by the user during the execution of RSVVP. The flow chart in Figure B-35 shows the general implementation of this sub-block. The main characteristic of the algorithm for this sub-block is that it is implemented in a loop (indicated by the bigger red rectangle in the flow chart) in order to allow to cycle over an arbitrary number of user-defined time intervals.

Because the scripts used in the following sub-blocks have a structure similar to the corresponding scripts used in the preceding sub-block, D.1, the reader can refer to the description already given in the previous section. The only script which is described next in this section is *Store_results*, as it is peculiar of sub-block D.2.

At the beginning of each iteration of the loop, the script *User_time_interval* is invoked which manages a GUI for the definition of time intervals and the curves are plotted on that interval by the script *User_plot_curves*. After the time interval has been defined, the weighting factors and the comparison metrics are calculated using two algorithms (respectively *Weighting_scheme_user* and *User_time_evaluation*) similar to those used to compute the metrics for each channel in sub-block D.1. Similarly to sub-block D.1, also for the user-defined time interval, after the metrics have been computed for each channel, they are post-processed by the script *User_time_postprocessing*. The variables containing the final values of the metrics have the same structure of those earlier described

Also, the various results for each user-defined time interval (i.e., each iteration of the loop) are appended to the corresponding variables which are used in Block E to write the results in Excel format. In fact, as multiple user time intervals may be defined, at the end of each iteration the matrices containing the results for the specific time interval considered are stored before being rewritten for the next time interval (see the description of script *Store Results* for details).

Similarly to sub-block D.1, before concluding the iteration, the results for the specific time interval are displayed on the screen through a GUI which is managed by the script *Table_output_user*. In case the user decides to define a new time interval, the variable *Time_interval* which is used to count the number of user-defined time intervals is incremented and a new iteration of the cycle starts.

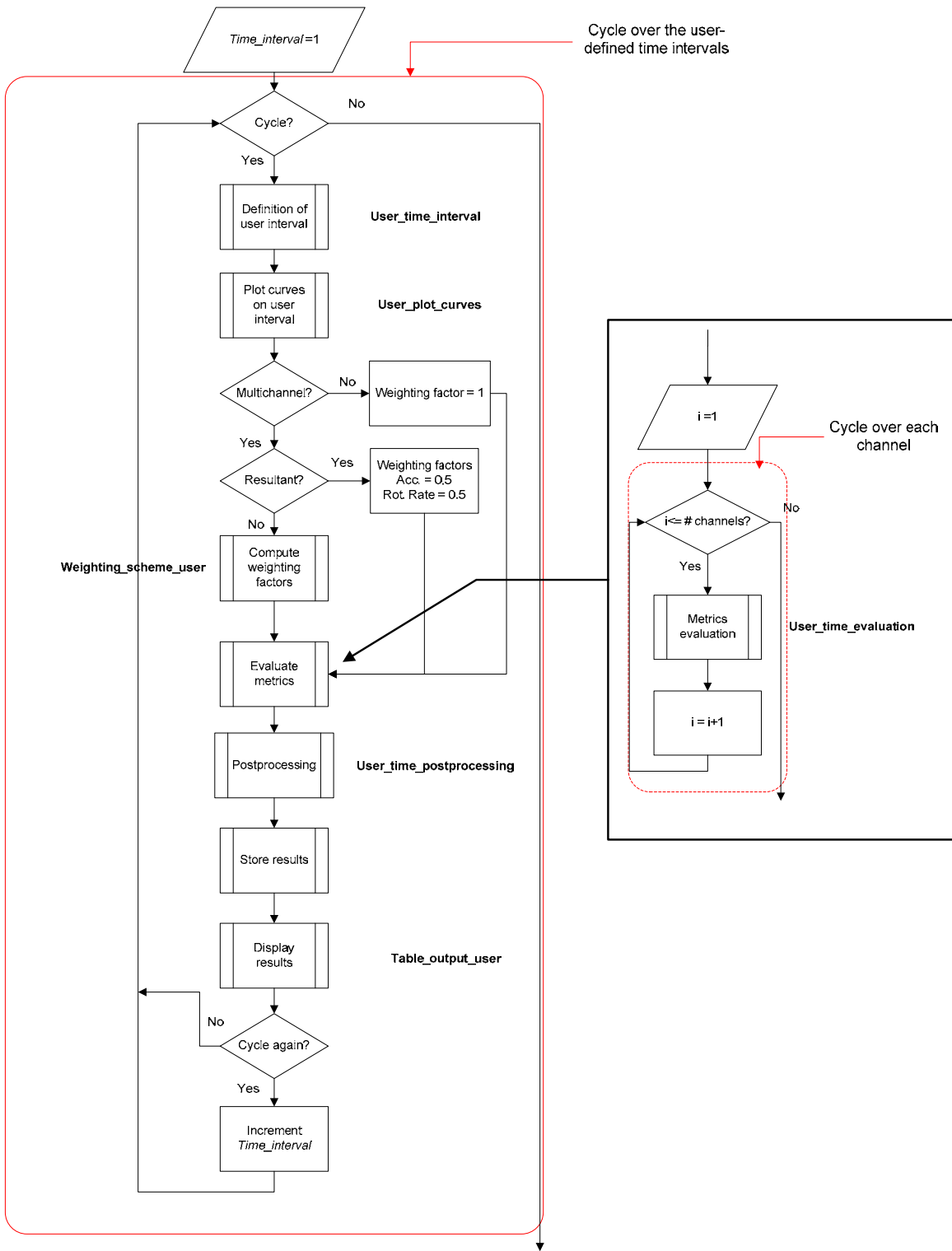


Figure B-35: Diagram of sub-block D.2 (User time).

Save Results

This script manages the storage of the results obtained for each iteration of the main loop of sub-block D.2 (i.e., for each user-defined time interval on which the comparison metrics are computed). In fact, because the various variables in which the script *User_time_postprocessing* saves the results are rewritten during each iteration, this script appends the results obtained for every specific time interval to the corresponding global variables.

Eventually, the following global variables are created which will be used by the following block (Block E):

- *Time_history_channel_xls_user*
- *Time_history_single_xls_user*
- *Output_xls*
- *Output_channel_xls*

The diagrams in Figure B-36 show the data organization of the variables *Output_xls* and *Output_channel_xls*.

The column vector containing the final metrics values for the specific time interval (*Output_xls_user*) is appended to the end of the matrix *Output_xls*, which has been previously created by sub-block D.1 and already contains the final results for the whole time interval. Note that, in case, the whole time interval has not been considered, the results will be appended to an originally null matrix. In case of multiple channels, the final metrics values for the actual time interval have been previously saved in the matrix *Output_channel_xls*. In this case, in a manner similar to that used to append the single/weighted results, the matrix containing the results for the current time interval is appended to the third dimension of the 3D matrix *Output_channel_xls*.

As for the matrices containing the time histories of the metrics for the single/weighted channel (*Output_single_history*) and each of the input channels (*Output_channel_history*), they are transformed in a single cell and appended to respectively the vector *Time_history_channel_xls_user* and *Time_history_single_xls_user*.

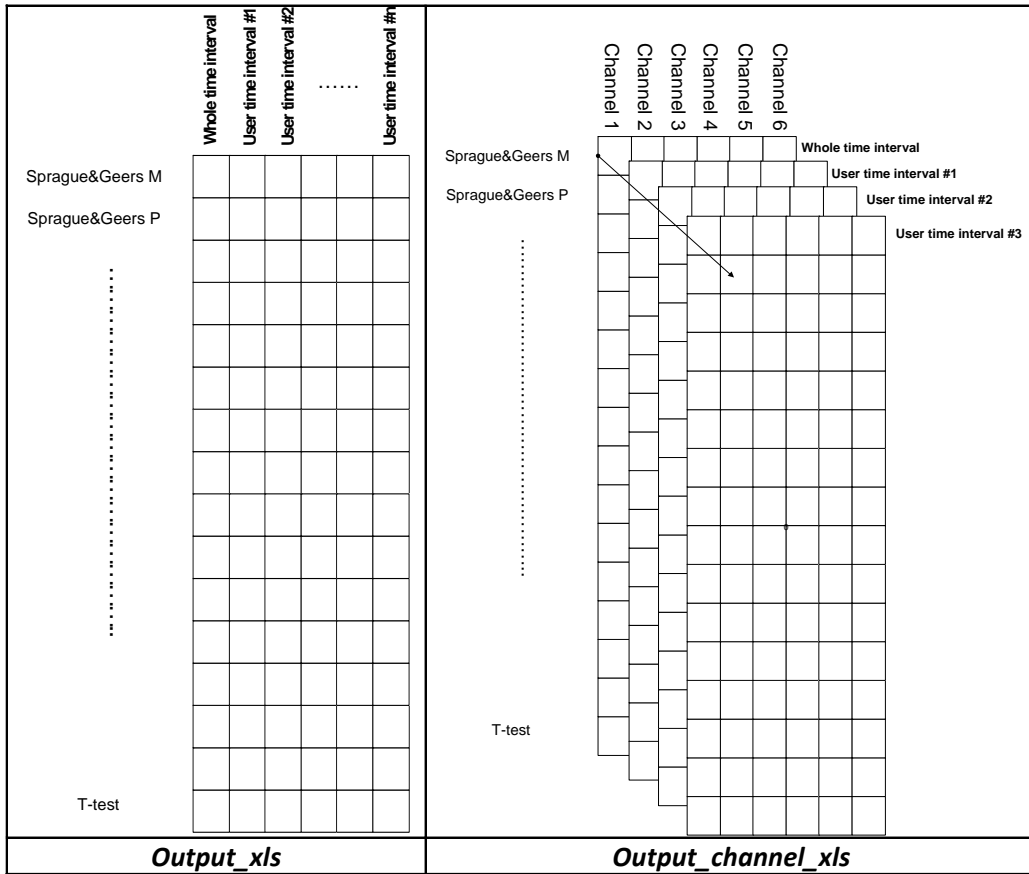


Figure B-36: Data organization of the variables *Output_xls* and *Output_channel_xls*.

BLOCK E (OUTPUT)

Block E is the last block implemented in the program code. It handles the various results output by RSVVP. As can be seen in **Error! Reference source not found.**, this block is composed of three sub-blocks: Configuration file, Excel results and Folder selection. The main structure of Block E is shown in **Error! Reference source not found.**

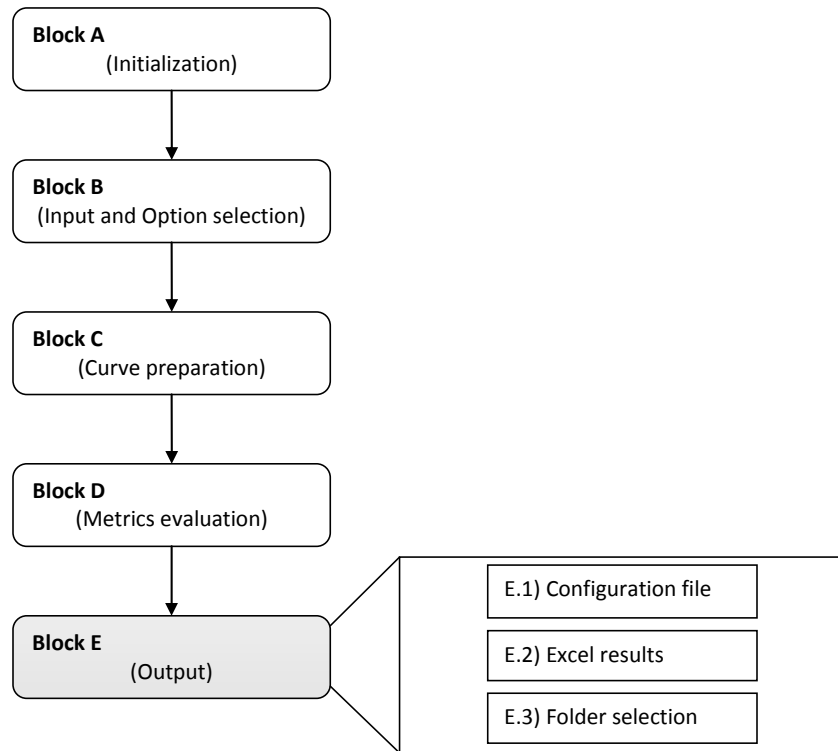


Figure B-37: Diagram of Block E.

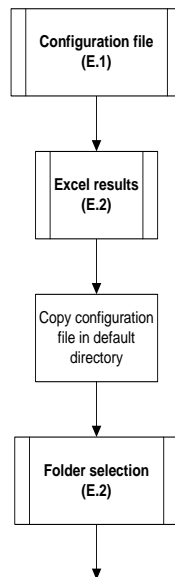


Figure B-38: Main structure Block E.

Configuration file (E.1)

The sub-block *Configuration file* manages the possibility to update the configuration file with the information about any time interval defined by the user during the execution of RSVVP.

The flow chart in Figure B-35 shows the general implementation of this sub-block. The option to update the configuration file is given for any case the user has defined any time interval during the execution of the program. The algorithm skips the update only in two cases: (1) a previous configuration file has been loaded in total run mode and no new user intervals have been defined or (2) in case the user does not want to update the previous configuration file.

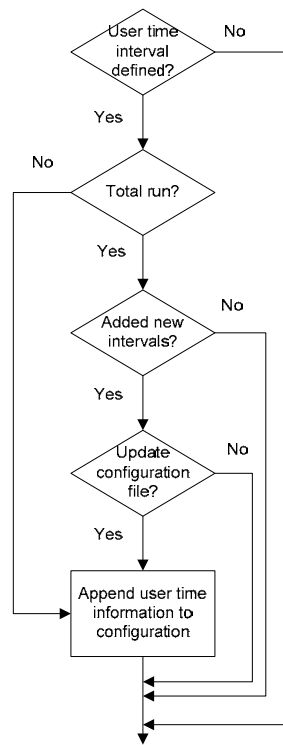


Figure B-39: Diagram of sub-block E.1 (Configuration file).

Excel results (Block E.2)

This sub-block is the core of the Block E as it creates the Excel files containing respectively the metrics values and time histories.

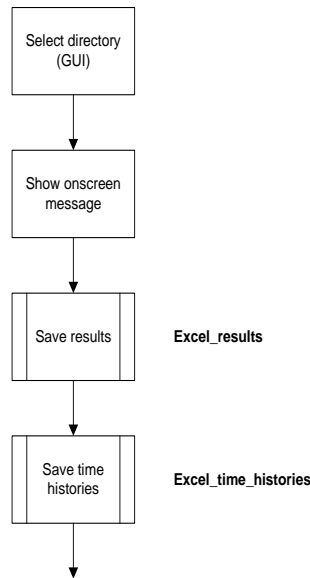


Figure B-40: Diagram of sub-block E.2 (Excel results).

As can be seen from the algorithm shown in Figure B-40, after the GUI for the selection of the destination folder where to save all the results, the code performs the scripts *Excel_results* and *Excel_time_histories*.

Excel_results

This script manages the creation of the Excel file containing the metrics values for the various time intervals considered during the run of RSVVP. The flowchart of this script is shown in Figure B-41. In case of multiple channels, the algorithm also cycles over the total number of input channels and creates specific sheets containing the results for each of them. The writing of the results for the MPC, Single-value and ANOVA metrics is managed by separate scripts, respectively *Excel_results_MPC*, *Excel_results_Single* and *Excel_results_ANOVA*. Note that, in case the NCHRP 22-24 profile has been selected, the single metrics are not computed and, hence, the corresponding script is skipped as they do not appear in the Excel file.

Excel_results_MPC

Figure B-42 shows the flowchart of the script *Excel_results_MPC*. The first step performed by this script is to create the headers for each of the time interval considered during the run of the program and write them in the main sheet of the Excel file. In case of multiple

channels, a new sheet is written for each channel and the same headers are written also for any of the channel sheets. This operation is implemented in a loop which cycles over the number of input channels.

As this script is focused on managing and writing only the values for the MPC metrics, after the headers have been created, the script proceeds to extracting the metrics values from the variable *Output_xls* which has been created during the post-processing in Block D. The values corresponding to the MPC metrics are extracted by considering only a certain range of rows of the matrix *Output_xls*. Note that, according to the metric profile chosen, the number of computed metrics varies and, hence, also the corresponding number of rows extracted. In case of multiple channels, a similar extraction procedure is applied on the 3-D matrix *Output_channel_xls* in order to extract only the desired metrics values. Also, in this particular case, the results for each channel are extracted by cycling over their total number. See Figure B-43 for a graphical visualization of the extraction procedure.

The other two scripts which manage the writing of the results for the single-value and the ANOVA metrics (*Excel_results_Single* and *Excel_results_ANOVA*) are implemented in a similar manner and, hence, the corresponding flowcharts are not shown for the sake of conciseness.

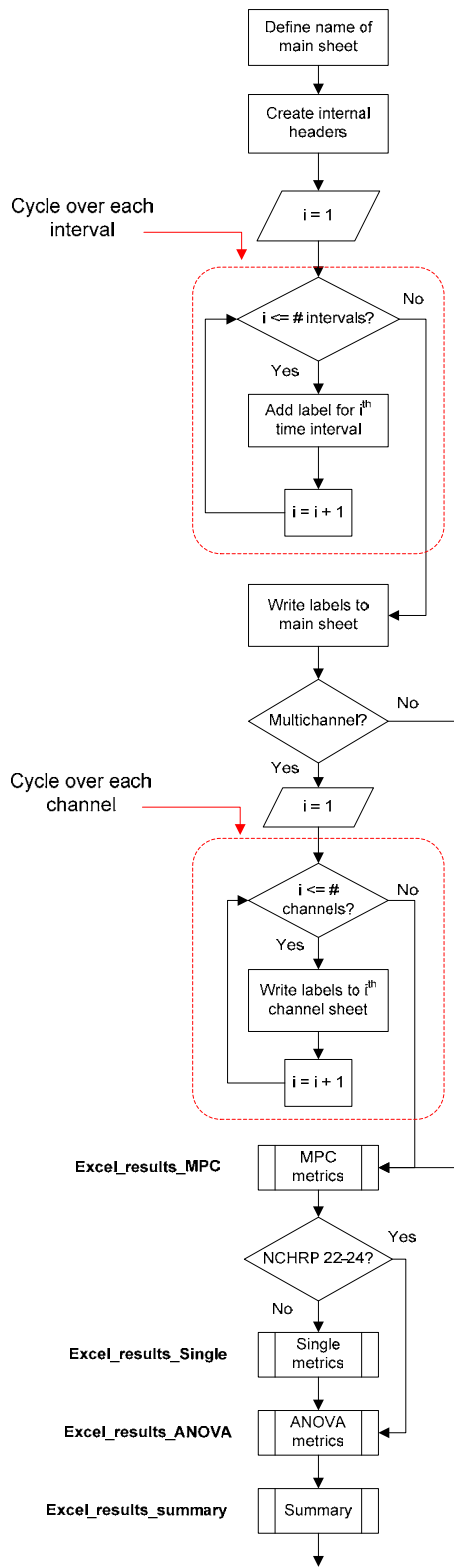


Figure B-41: Flow chart of the script *Excel_results* (sub-block E.2).

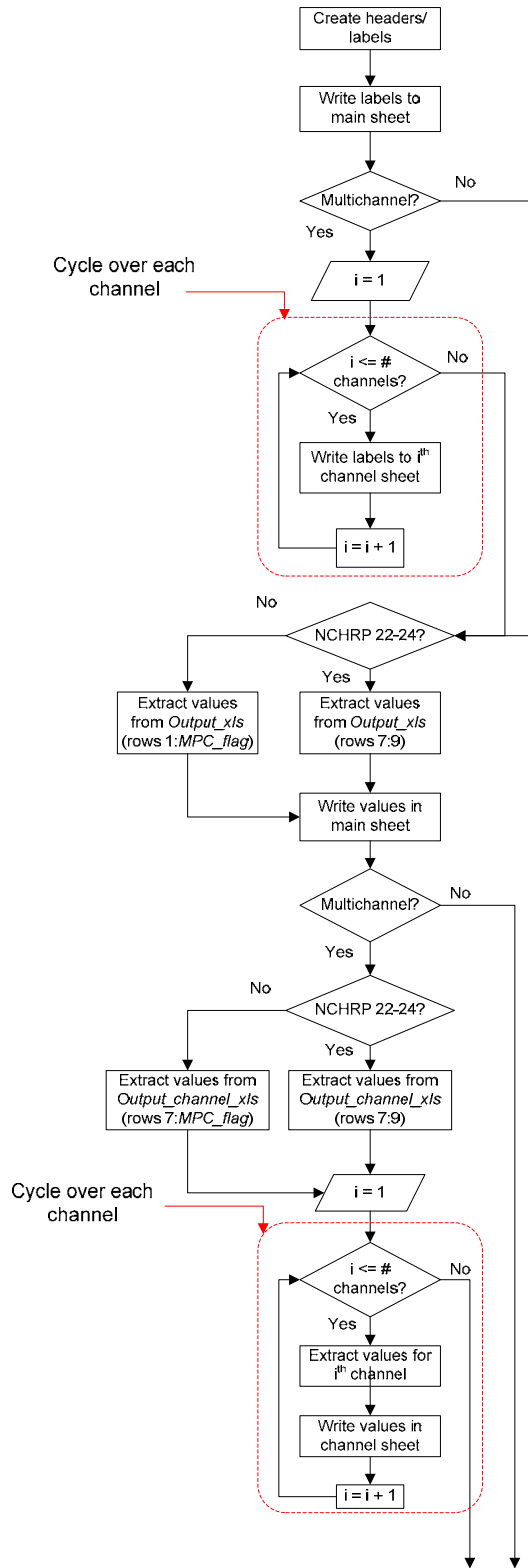


Figure B-42: Flow chart of the script *Excel_results_MPC* (recalled by the script *Excel_results*).

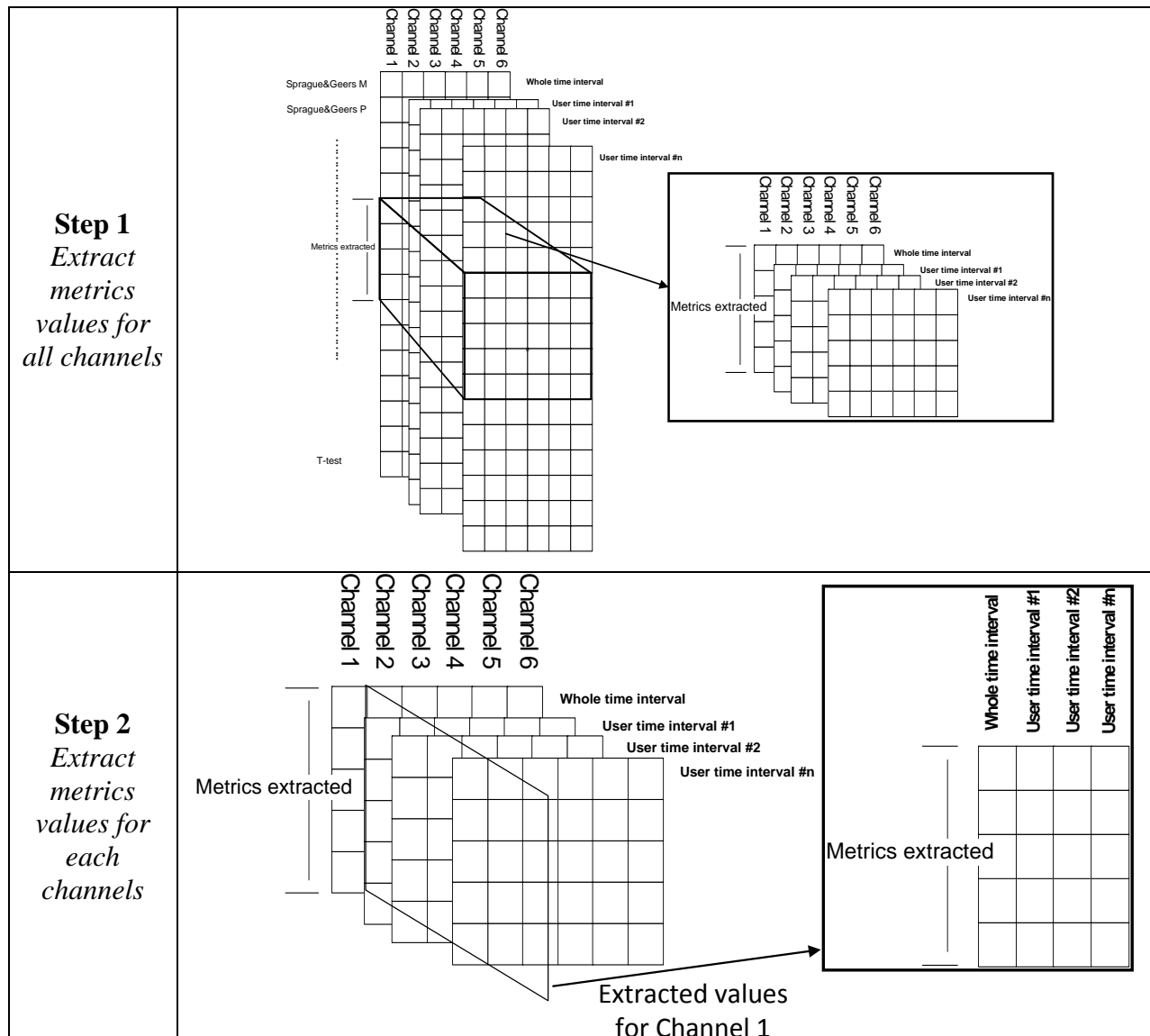


Figure B-43: Data extraction from the variable *Output_channel_xls*.

Excel time histories

This script manages the creation of Excel files containing the time histories for the metrics computed by RSVVP. Figure B-44 shows the algorithm of the script. The first step performed is the selection of the name to be given to the sheet containing accordingly the metrics time histories for either the single channel or the weighted mean from the multiple channels. The algorithm then creates an Excel file containing the results for the comparison between the curves on the whole time interval and/or separate Excel files for each of the user-defined time intervals, depending on which selection was made during the run of the program. In the latter

case, a loop cycles over the number of time intervals defined by the user and creates an Excel file during each iteration. Also, if multiple channels were input, in either the case the comparison was performed on the whole time interval or user defined time interval/s the algorithm cycles over each of the input channels in order to save them in separate sheets of the same Excel file.

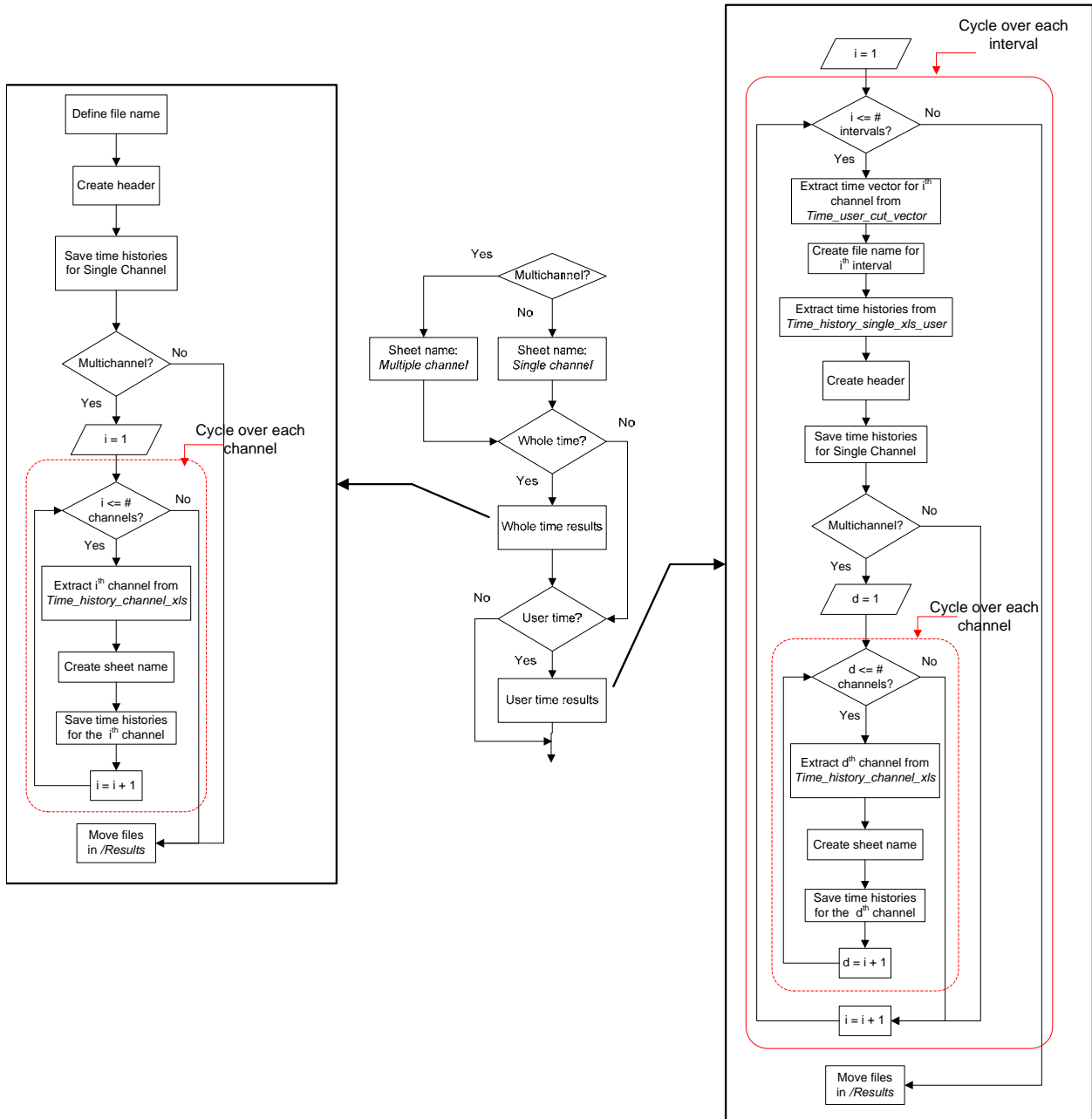


Figure B-44: Flow chart of the script *Excel_time_histories* (sub-block E.2).

Folder selection (Block E.3)

This sub-block (Figure B-45) checks if the user defined a directory where to save the output files and, in case, moves all the previously created files from the default directory */Results_XX* to that folder. In any case, at the end, a message is shown on the screen indicating to the user that the results have been saved in the selected directory.

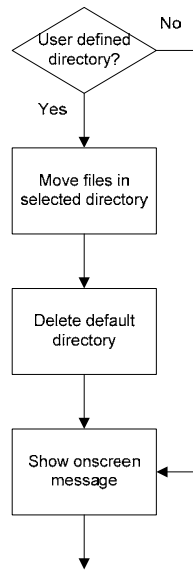


Figure B-45: Diagram of sub-block E.3 (Folder selection).

REFERENCES

- [1] MathWorks, “Matlab[®] User Guide – high performance numeric computation and visualization Software”, The MathWorks Inc., 3 Apple Hill Drive, Natick, MA, USA, 2008.
- [2] Society of Automotive Engineers, “SAE J211-1 (R) Instrumentation for Impact Test—Part 1—Electronic Instrumentation. SAE International”, Warrendale PA, USA, Jul 1, 2007.
- [3] H.E. Ross, D.L. Sicking, R.A. Zimmer, and J.D. Michie, “*Recommended Procedures for the Safety Performance Evaluation of Highway Features*”, National Cooperative Highway Research Program (NCHRP) Report 350, Transportation Research Board, Washington, D.C., 1993.
- [4] European Committee of Standardization, “European Standard EN 1317-1 and EN 1317-2: Road Restraint Systems”, CEN (1998).
- [5] T.L. Geers, “An Objective Error Measure for the Comparison of Calculated and Measured Transient Response Histories”, *The Shock and Vibration Bulletin*, The Shock and Vibration Information Center, Naval Research Laboratory, Washington, D.C., Bulletin 54, Part 2, pp. 99-107, (June 1984).
- [6] *Comparative Shock Analysis (CSA) of Main Propulsion Unit (MPU), Validation and Shock Approval Plan*, SEAWOLF Program: Contract No. N00024-90-C-2901, 9200/SER: 03/039, September 20, 1994.
- [7] M.A. Sprague and T.L. Geers, “Spectral elements and field separation for an acoustic fluid subject to cavitation”, *J Comput. Phys.*, pp. 184:149, Vol. 162, (2003).
- [8] L.E. Schwer, “Validation Metrics for Response Time Histories: Perspective and Case Studies”, *Engng. with Computers*, Vol. 23, Issue 4, pp. 295–309, (2007).
- [9] D.M. Russell, “Error Measures for Comparing Transient Data: Part I: Development of a Comprehensive Error Measure”, *Proceedings of the 68th shock and vibration symposium*, pp. 175–184, (2006).
- [10] J. Cohen, P. Cohen, S.G. West and L.S. Aiken, *Applied multiple regression/correlation analysis for the behavioral sciences*, Hillsdale, NJ: Lawrence Erlbaum, (3rd ed.), 2003.
- [11] S. Basu and A. Haghghi, “*Numerical Analysis of Roadside Design (NARD) vol. III: Validation Procedure Manual*”, Report No. FHWA-RD-88-213, Federal Highway Administration, Virginia, 1988.
- [12] D. Twisk and A. Ritmeijer, “A Software for Demonstrating Validation of Computer Dummy Models Used in the Evaluation of Aircraft Seating Systems”, SAE Paper No. 2007-01-3925, Society of Automotive Engineers, Warrendale, PA, 2007.
- [13] B. Whang, W.E. Gilbert and S. Zilliacus, *Two Visually Meaningful Correlation Measures for Comparing Calculated and Measured Response Histories*, Carderock Division, Naval Surface Warfare Center, Bethesda, Maryland, Survivability, Structures and Materials Directorate, Research and Development Report, CARDEROCKDIV-U-SSM-67-93/15, September, 1993.
- [14] H. Theil, *Economic Forecasts and Policy*, North-Holland Publishing Company, Amsterdam, 1975.

[15] M.H. Ray, “Repeatability of Full-Scale Crash Tests and a Criteria for Validating Finite Element Simulations”, *Transportation Research Record*, Vol. 1528, pp. 155-160, 1996.

[16] W.L. Oberkampf and M.F. Barone, “Measures of Agreement Between Computation and Experiment: Validation Metrics,” *Journal of Computational Physics* Vol. 217, No. 1 (Special issue: Uncertainty quantification in simulation science) pp 5–36, 2006.

APPENDIX B-1: CODE VERIFICATION

The implementation of the following main features of RSVVP has been verified:

- Sprague & Geers metrics
- Knowles & Gear metrics

In order to verify the correct implementation of the Sprague & Geers metric, a comparison of ideal analytical wave forms differing only in magnitude or phase was performed and the results were compared with the outcomes obtained by Schwer [8] using the same benchmark curves.

The baseline analytical wave form was given by the following decayed sinusoidal curve:

$$m(t) = e^{-(t-\tau)} \sin 2\pi(t - \tau) \quad (\text{B1-1})$$

where the parameter τ was used to create a phase in time or “time of arrival”.

Following Schwer’s work, two different tests were performed, considering respectively as the test function: (a) a wave form with the same time of arrival of (B1-1), but an amplitude 20% greater than the original wave form (*magnitude-error test*) and (b) a wave form with the same amplitude of (B1-1) but a time of arrival such that the phase was about $\pm 20\%$ respect to the original wave form (*phase-error test*). The analytical forms used for the magnitude-error test were:

$$\begin{cases} m(t) = e^{-(t-0.14)} \sin 2\pi(t - 0.14) \\ c(t) = 1.2 \cdot e^{-(t-0.14)} \sin 2\pi(t - 0.14) \end{cases} \quad (\text{B1-2})$$

while the analytical wave forms used for the phase-error test were defined as:

$$\begin{cases} m(t) = e^{-(t-0.14)} \sin 2\pi(t - 0.14) \\ c(t) = e^{-(t-0.04)} \sin 2\pi(t - 0.04) \end{cases} \quad (\text{B1-3})$$

and,

$$\begin{cases} m(t) = e^{-(t-0.14)} \sin 2\pi(t - 0.14) \\ c(t) = e^{-(t-0.24)} \sin 2\pi(t - 0.24) \end{cases} \quad (\text{B1-4})$$

In both cases, the sampling period was $\Delta t = 0.02 \text{ sec}$ and $0 \text{ sec} \leq t \leq 2 \text{ sec}$.

Figure B-46 shows the graphs of the analytical curves used respectively for the magnitude error and the phase error tests.

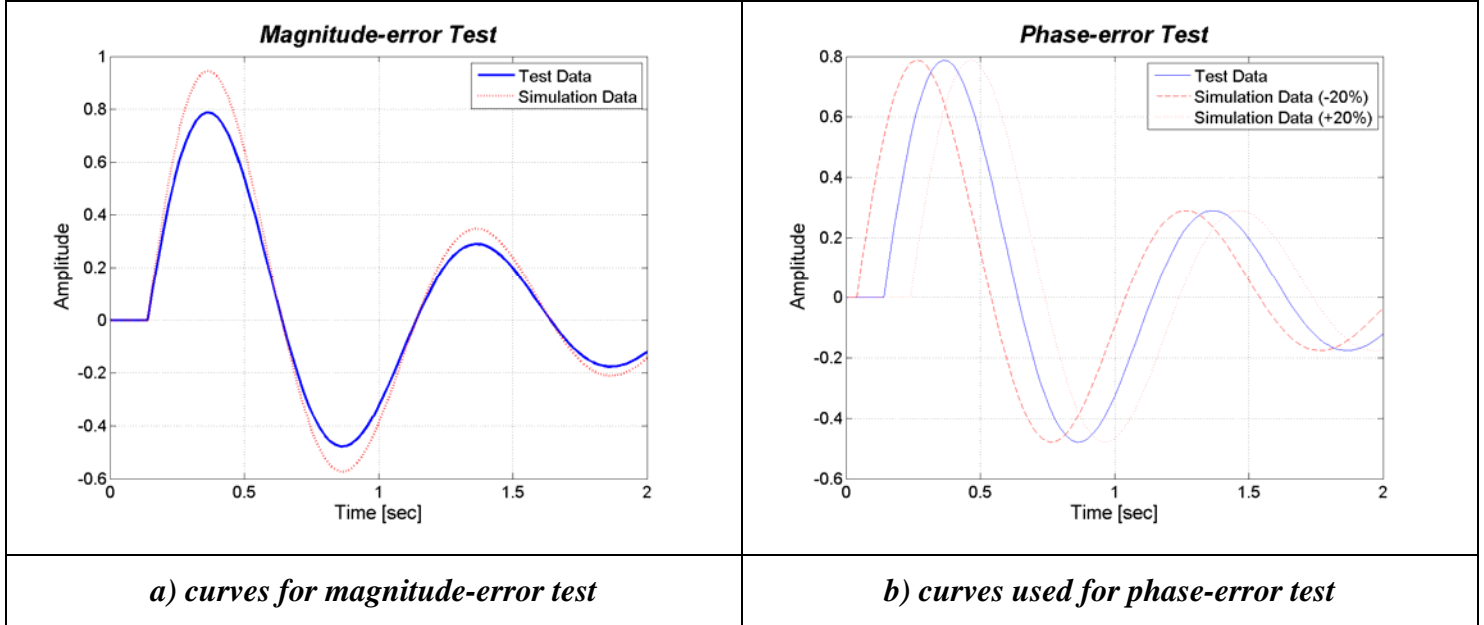


Figure B-46: Idealized time histories used for the case of (a) 20% magnitude and (b) time of arrival.

As in this case, the phase shift between the baseline and the test curves was a wanted characteristic, the metrics was applied without synchronizing the two time histories in the preprocessing phase. The results obtained using the Sprague & Geers metric implemented in RSVVP for the difference in magnitude and the difference in time of arrival are shown respectively in Figure B-47 and Figure B-48. Table B-4 shows the value of the metric component obtained considering a time interval equal to the total length of the time histories. These values match completely with those obtained by Schwer, thus confirming the correct implementation of this metric.

Table B-4: Value of the Sprague & Geers metric components calculated using the RSVVP program.

<i>Metric component</i>	<i>20 % Magnitude difference</i>	<i>Phase difference</i>	
		<i>+20%</i>	<i>-20%</i>
Magnitude	0.2	≈ 0	≈ 0
Phase	0	0.195	0.195
Combined	0.2	0.195	0.195

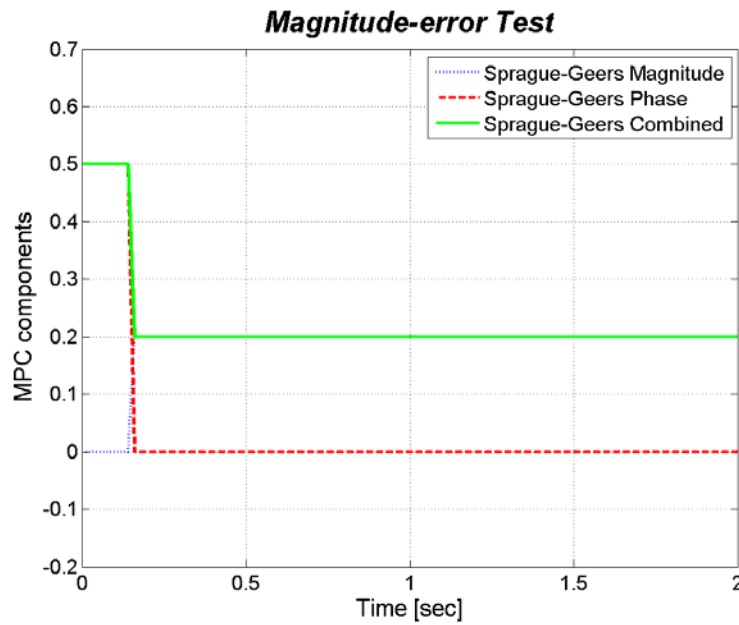


Figure B-47. Sprague & Geers component metric vs. time for the magnitude-difference test.

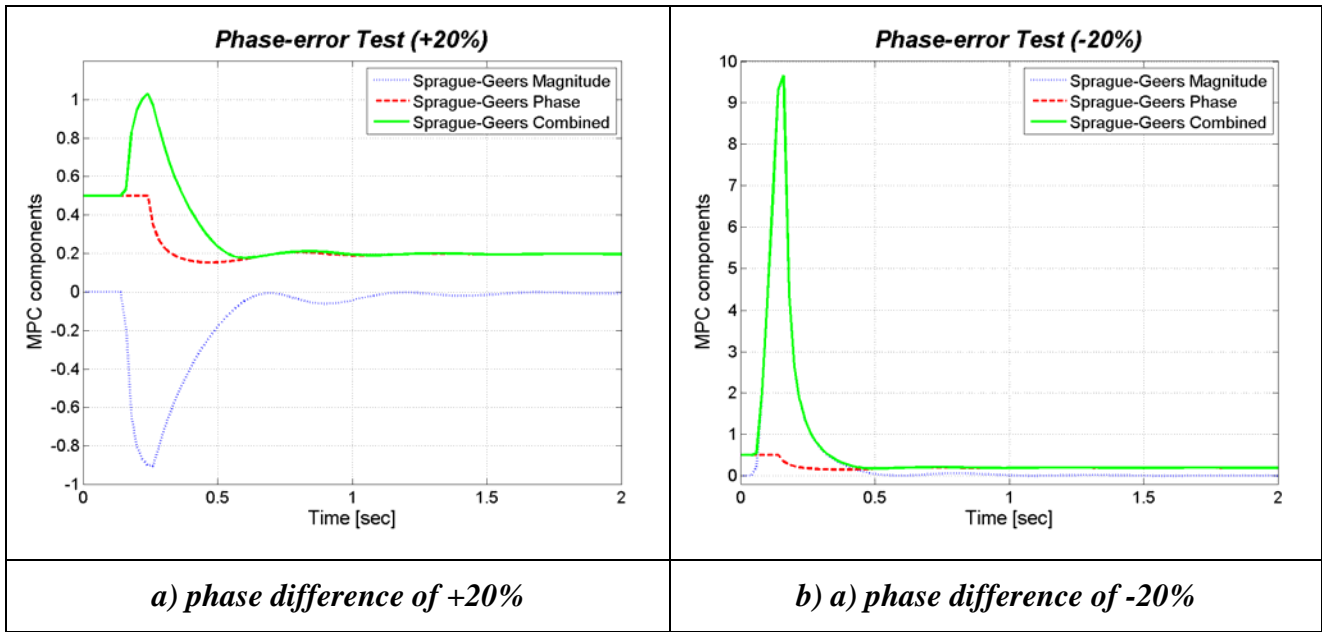


Figure B-48: Sprague & Geers component metric vs. time for the phase-difference tests: (a) +20% and (b)-20%.

APPENDIX B-2: COMPILING RSVVP

The Matlab[®] code of RSVVP can be compiled as a standalone executable. This allows users who do not have Matlab[®] installed on their machine to be able to run RSVVP.

The standalone application of RSVVP is compiled using Matlab[®] Compiler, a Matlab[®] toolbox which requires a specific license. In order to create an executable version of RSVVP, set the current directory of Matlab[®] to the folder where the RSVVP files are located and launch the following command:

```
mcc -m -v RSVVP
```

Note 1: In order to compile the standalone application, it is first necessary to indicate to Matlab[®] which compiler to use by launching the following command:

```
mbuild -setup
```

The 32-bit Windows version of Matlab[®] has a built-in C compiler called 'Lcc-win32'. In case other third-party C/C++ compilers are installed on the machine, it is also possible to select any of them.

Note 2: the previous versions of Matlab[®] Compiler allowed the user to create a standalone application only from functions and it was not possible to directly compile scripts. As the principal file of RSVVP (*Main.m*) is a script, in order to compile the first versions of the program, the code was originally invoked from a function called RSVVP. While this trick made it possible to compile RSVVP, a side effect was that a few local variables created in specific functions of the code had to be saved to the Matlab[®] base space. This was necessary in order to permit a sharing of these specific local variables among different functions. Although the latest versions of Matlab[®] Compiler can now directly compile a script, making the conversion of these local variables into global variables no more necessary, these conversions may still appear in some part of the code.

APPENDIX B-3: Type of Variables Used in the Code

The main typologies of variables available in Matlab[®] and used in the implementation of the code of RSVVP are:

- Matrices and arrays (floating-point/integer data, characters and strings)
- Structures
- Cell arrays

Matrices and arrays are used to store both numbers and text characters. These data type includes also scalar numbers or single characters which are considered to be a 1x1 matrix.

Numbers can be either stored as floating-point or integer data.

Structures and cell arrays provide a way to store dissimilar types of data in the same array. A Matlab[®] **structure** is a data type that provides the means to store selected data together in a single entity. A structure consists mainly of data containers, called fields, and each of these fields stores an array of some Matlab[®] data type. Figure B-49 shows an example of structure variable, *s*, which has three fields: *a*, *b*, and *c*.

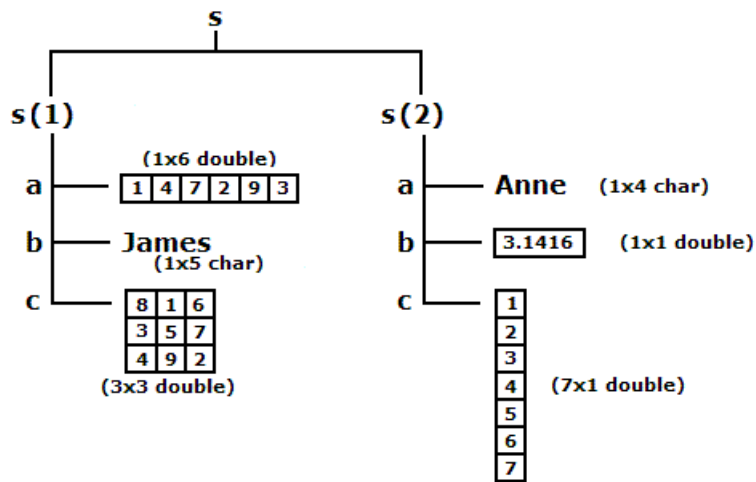


Figure B-49: Example of a Matlab structure variable [1].

A Matlab[®] **cell array** is a collection of containers called cells in which different types of data can be stored. As an example, Figure B-50 shows a 2-by-3 cell array in which the cells in row one hold an array of unsigned integers, an array of strings, and an array of complex

numbers, while row two holds three other types of arrays, the last being a second cell array nested in the outer one.

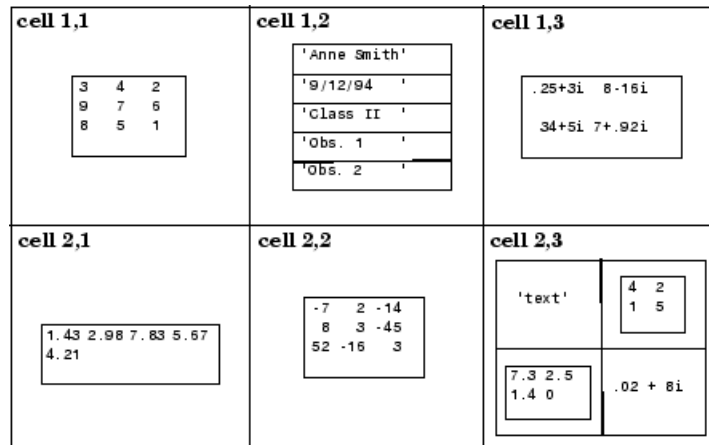


Figure B-50: Example of a Matlab structure variable [1].

Structure-type variables are used to store in an organized manner the several options selected by the user in the various graphical interfaces while cell-type variables are used to conveniently store in a single variable all the data vectors (or matrices) which are characterized by different dimensions and would have otherwise required singular specific array (or matrix) variables.

APPENDIX B-4: Preprocessing Algorithms

This appendix describes the general algorithms used to perform the following preprocessing operations:

- Filtering
- Shift/drift
- Resampling & trimming
- Synchronization

Filtering

The filter process is implemented in the function *sae_filter*, whose algorithm is shown in Figure B-51. The function receives as input the following three variables: (i) *CFC*, (ii) *T* and (iii) *X*. *CFC* and *T* are scalar variables containing respectively the value of the filter class and the sampling period of the input curves, while *X* is a vector containing the data points of the curve. The algorithm assumes that the sampling period is constant and, hence, the time vector is not necessary.

Before filtering the data a head and a tail vectors are created by repeating respectively the first and last value of the vector containing the data points. These vectors are then appended at the beginning and end of the vector containing the original data, correspondingly. The modified vector is then filtered by applying equation (B1) a first time forward and a second time backward in order to have a two-pass filter. The filter coefficients are calculated using the formulas indicated in equations (B2) through (B6).

Once the data are filtered, the added head and tail are trimmed and the filtered vector *Y* is given as the function output.

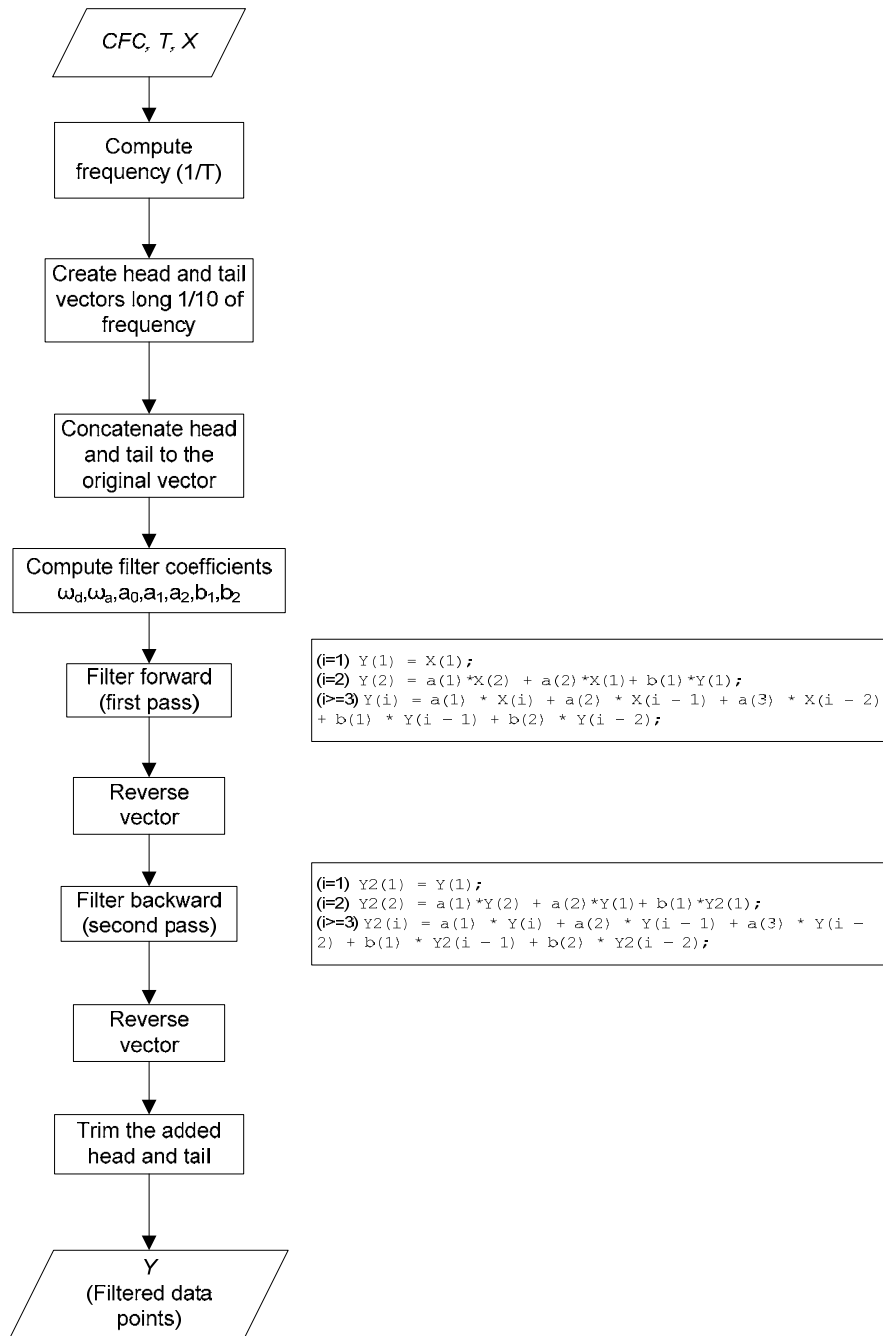


Figure B-51: Algorithm of the SAE filtering.

Shift/drift

The shift and drift corrections are implemented in the script *Shift_drift*. The main steps followed to perform this preprocessing task are shown in the algorithm in Figure B-52. The

steps described in the algorithm are performed on either the true or test curves or both of them, according to the user selection.

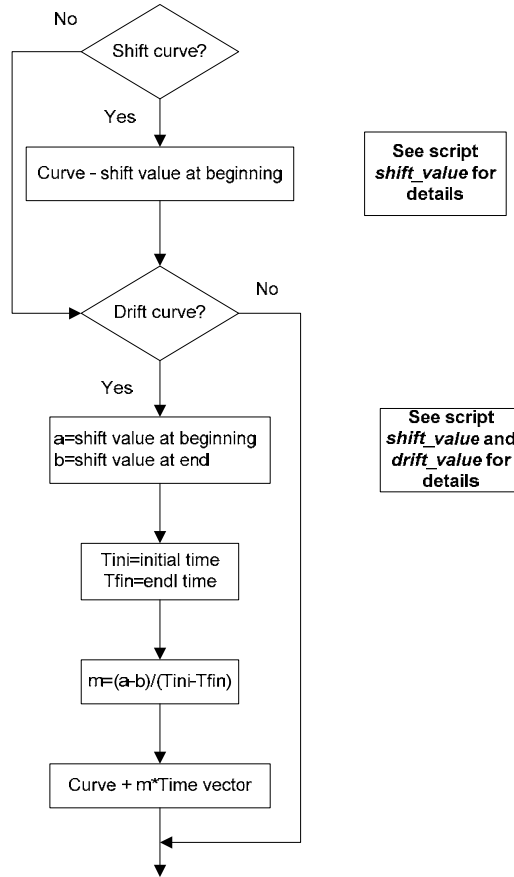


Figure B-52: Main algorithm of the script *Shift_drift*.

The shift values at the beginning and the end of the curve are computed respectively by the user-defined functions *shit_value* and *drift_value* (Figure B-53). The former function evaluates the vertical shift at the beginning of the curve, while the *drift* function at the end of the curve. The algorithms of both the two functions are very similar; the shift values are computed as the mean of respectively the initial and final portion of the data vector till/from 5 percent of the peak value. Also, if the standard deviation of the sub-vector is greater than 0.1, the algorithm iteratively decreases the size till the standard deviation drops within this value.

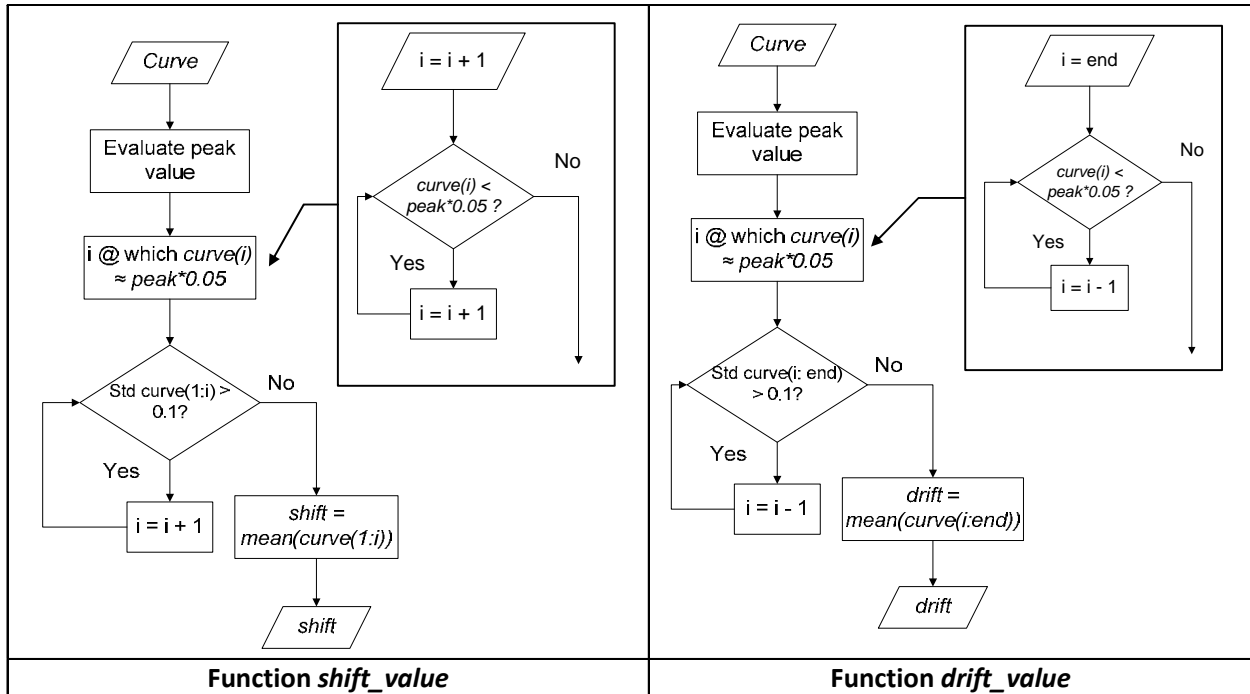


Figure B-53: User-defined functions *shift_value* (left) and *drift_value* (right) Algorithms.

Re-sampling & trimming

The re-sampling and trimming operations are implemented simultaneously in the script *Resampling_trimming* whose algorithm is shown in Figure B-54. In fact, the curves are resampled on a trimmed time interval which considers respectively the maximum between the initial time values of the two curves and the minimum of the final time values. The Resampling is performed using a linear polynomial whose coefficients are evaluated using the predefined Matlab[®] function *interp1*.

The sampling period (i.e., the minimum time between the collection of two consecutive data points) is defined as the minimum between that of the two curves and, in any case, it cannot be smaller than a minimum limit value (defined by the user at the beginning of the calculation). The minimum sampling period is determined by considering the first input channel; the same period is then used to resample also any of the other channels.

Eventually, both the true and test curves are interpolated on the trimmed time interval using their respective polynomial coefficients through the Matlab[®] function *ppval*. In case of multiple channels, the same procedure is repeated for each of them.

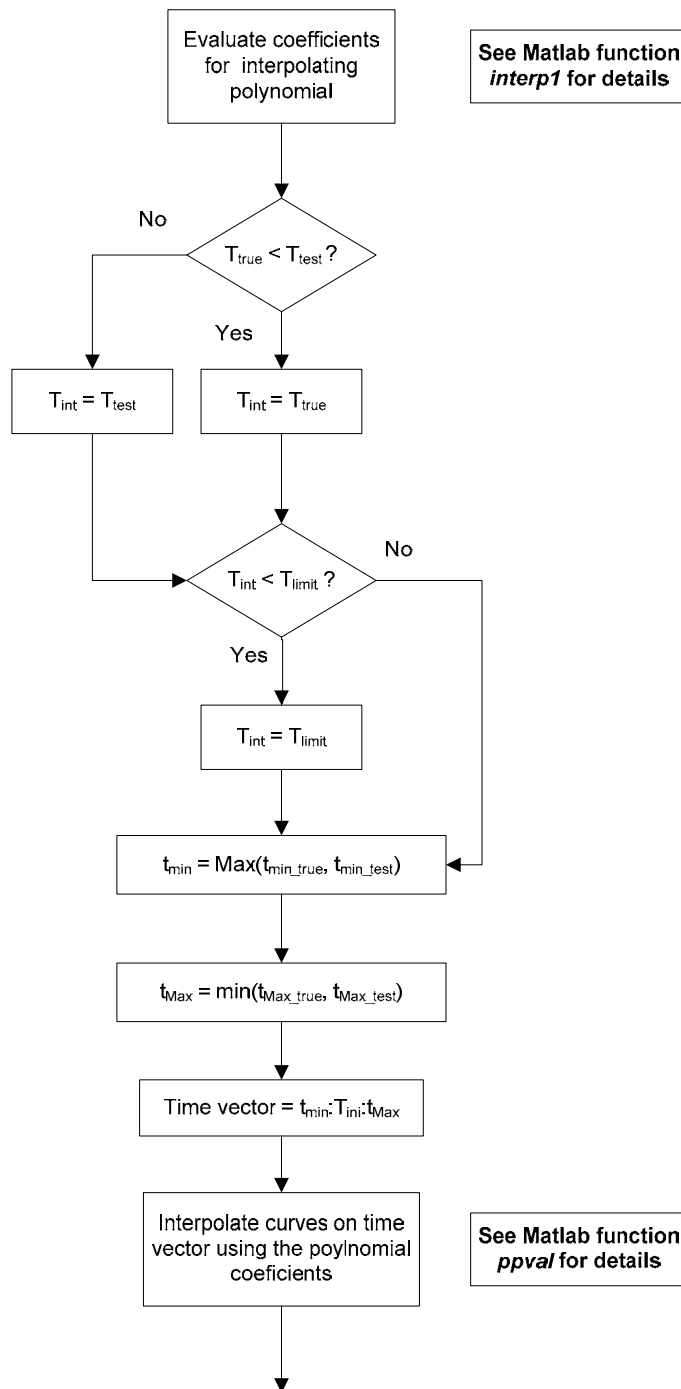


Figure B-54: Algorithm of the script *Resampling_trimming*.

Synchronization

The automatic synchronization of the curves is implemented in the script *Curve_synchronizing* whose algorithm is shown in Figure B-55. This script calculates the shift value which minimizes a target function, which can be either the area between the two curves (area of the residuals method) or the square error (lest square error method). The two target functions are recalled by user-defined Matlab[®] functions, respectively *area_res* and *rse*. In both the two functions, the couple of curves can be shifted respect to each other by an arbitrary value *s*. The minimization process is performed using a Matlab[®] function (*fminsearch*) which iteratively calculates the values of the selected target function (area of residual or square-root error) varying the value of the shift variable in order to find the optimal solution. Eventually, the algorithm shifts the two input curves by the optimal value obtained from the minimization process.

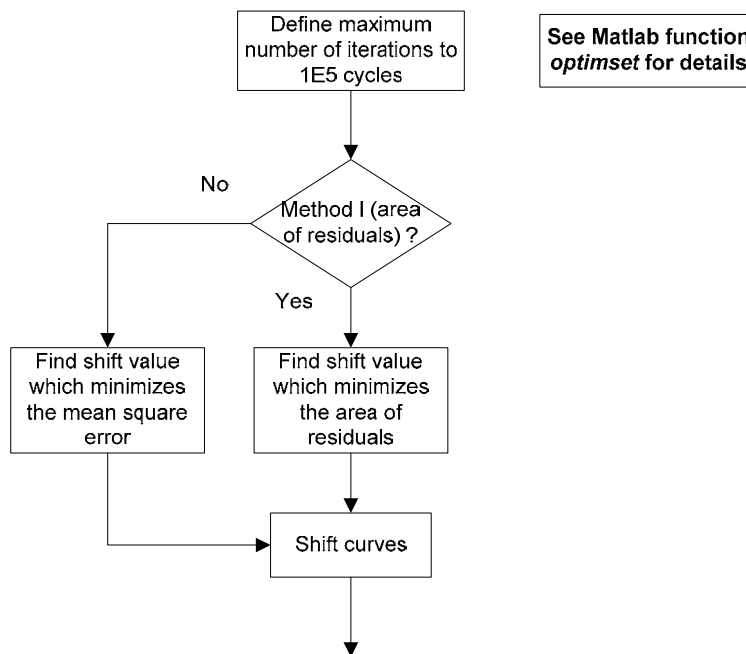


Figure B-55: Algorithm of the script *Curve_synchronizing*.

Both the user-defined functions *are-res* and *sre* require as input only the value by which to shift the two curves before calculating respectively the area between them or the square-root error. The algorithms of these two functions are shown in Figure B-56. For either of these two

functions, the shifting of the two curves is performed by invoking the user-defined function *shift* whose algorithm is shown in Figure B-57.

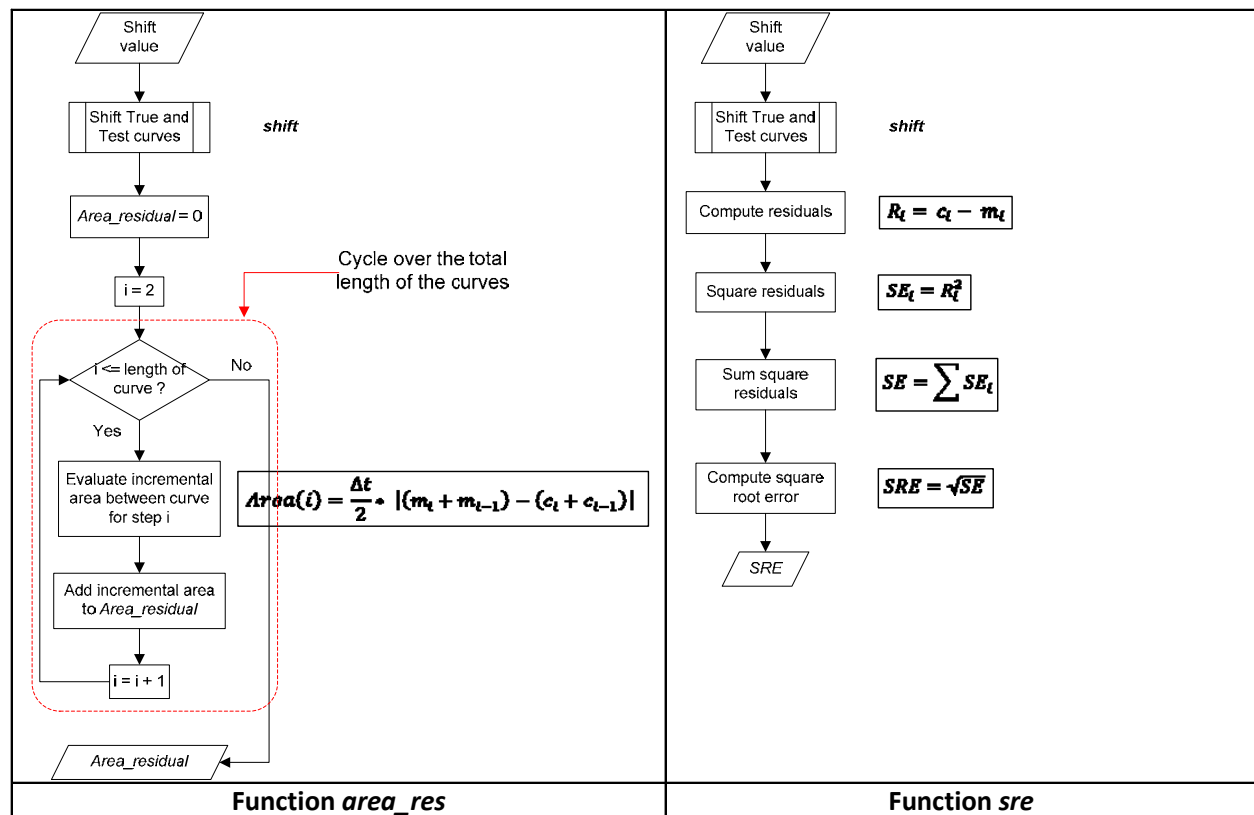


Figure B-56. Algorithm of the user-defined functions *area_res* (left) and *sre* (right).

The function *shift* has only one input, the value by which to shift the two curves respect to each other. In fact, the data points of the two curves are read directly from the global space of Matlab®. This allows the shift function to be recalled also within the local space *area_res* and *sre*, where the data points of the input curves would not otherwise be available. Based on the sign of the input shift value, the algorithm of the function *shift* creates a shifted time vector for either the test or the true curve and a vector trimmed at the end for the other curve. In particular, a positive shift value corresponds to a time vector for the true curve which starts at the shift value and a time vector for the test curve which is trimmed at the end by the same shift value, in order to have two vectors with the same length. Vice versa happens in case of a negative shift value. Once the appropriate time vectors have been defined, the shifted curves are obtained by computing the corresponding interpolating polynomials on these time points. Eventually, a

common time vector is used for both the interpolated true and test curves, which starts at time zero and is trimmed at the end by a value equal to the shift.

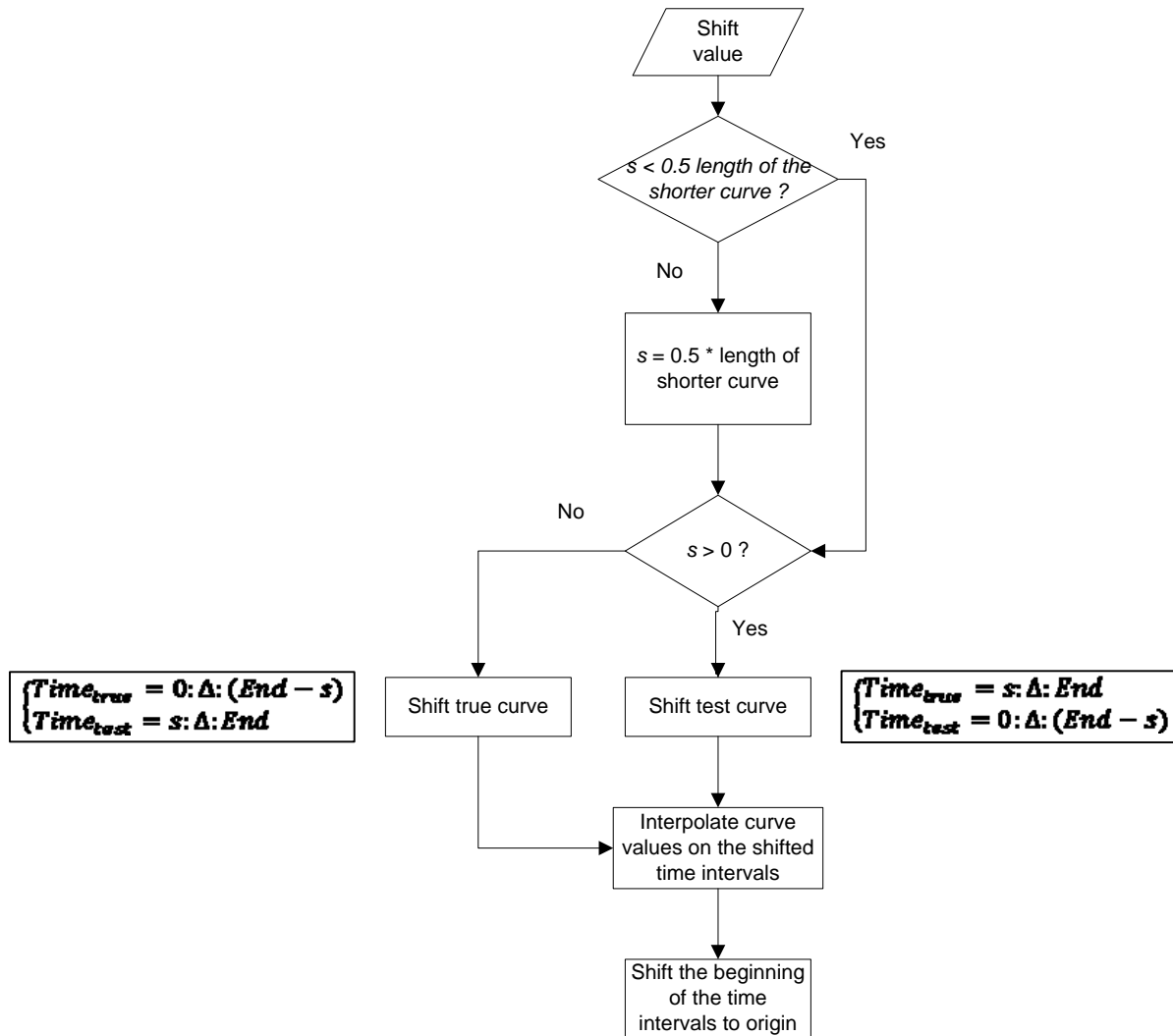


Figure B-57: Algorithm of the user-defined function *shift*.

APPENDIX B-5: Metrics Algorithms

This appendix gives a detailed description of the algorithms used to implement the various comparison metrics available in RSVVP. Note that each metric implemented in RSVVP is repeatedly evaluated considering time intervals increasing in size in order to track the behavior of the metrics when the two curves are compared on a limited portion of the time domain. The starting interval has a dimension equal to 10 percent of the total time interval and the final time interval is the entire time domain on which the true and test curves are compared. In the following sections, the measured and the computed curves are indicated respectively as m and c .

Sprague & Geers

The analytical definition of the magnitude and phase component of the Sprague & Geers metric is defined by the following formulas:

$$M_{SG} = \sqrt{I_{cc} / I_{mm}} - 1 \quad (B5-1)$$

$$P_{SG} = \frac{1}{\pi} \cos^{-1} (I_{mc} / \sqrt{I_{mm} I_{cc}}) \quad (B5-2)$$

where I_{mm} , I_{cc} and I_{mc} are respectively defined as:

$$I_{mm} = (t_2 - t_1)^{-1} \int_{t_1}^{t_2} m^2(t) dt \quad (B5-3)$$

$$I_{cc} = (t_2 - t_1)^{-1} \int_{t_1}^{t_2} c^2(t) dt \quad (B5-4)$$

$$I_{mc} = (t_2 - t_1)^{-1} \int_{t_1}^{t_2} m(t) \cdot c(t) dt \quad (B5-6)$$

The comprehensive error is defined as the vector whose two components are M_{SG} and P_{SG} :

$$C_{SG} = \sqrt{M_{SG}^2 + P_{SG}^2} \quad (B5-7)$$

Assuming that the two curves are characterized by a uniform and common sampling rate, the integrals defined by equations B5-3 through B5-6 reduces to the following summation:

$$I_{mm} = \sum m^2 \quad (\text{B5-8})$$

$$I_{cc} = \sum c^2 \quad (\text{B5-9})$$

$$I_{mc} = \sum mc \quad (\text{B5-10})$$

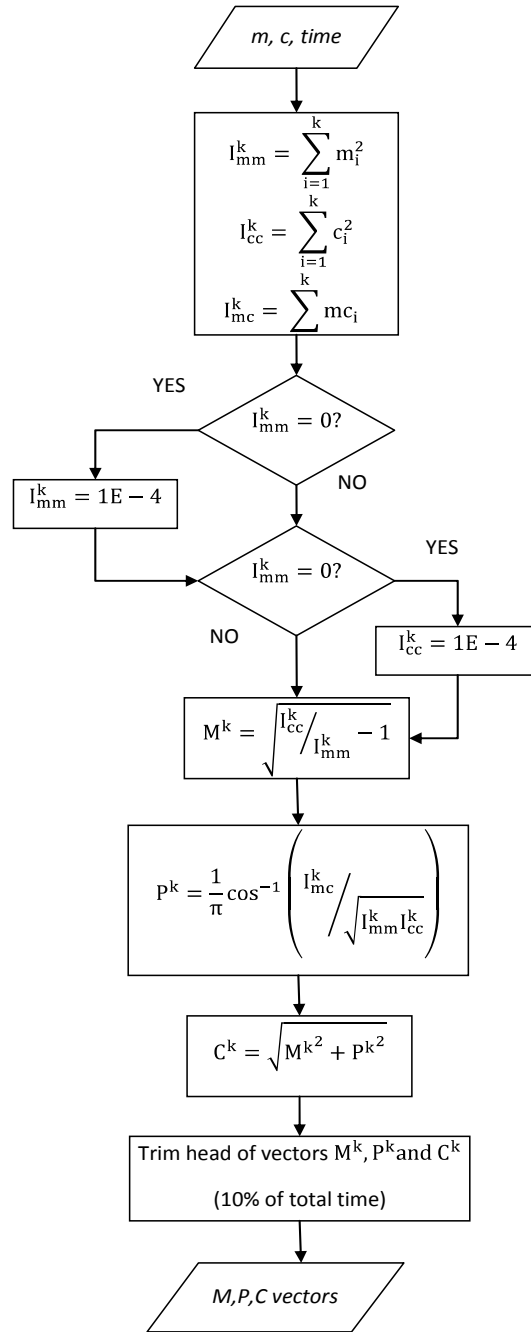


Figure B-58. Algorithm of the Sprague & Geers metric implemented in RSVVP.

ANOVA

The Analysis of Variance metrics are based on the residuals between the measured and the computed curves. In particular, the residuals are normalized to the peak value of the measured curve. The algorithm of the ANOVA metrics (mean, standard deviation, and t-test of the residuals) is shown in Figure B-59.

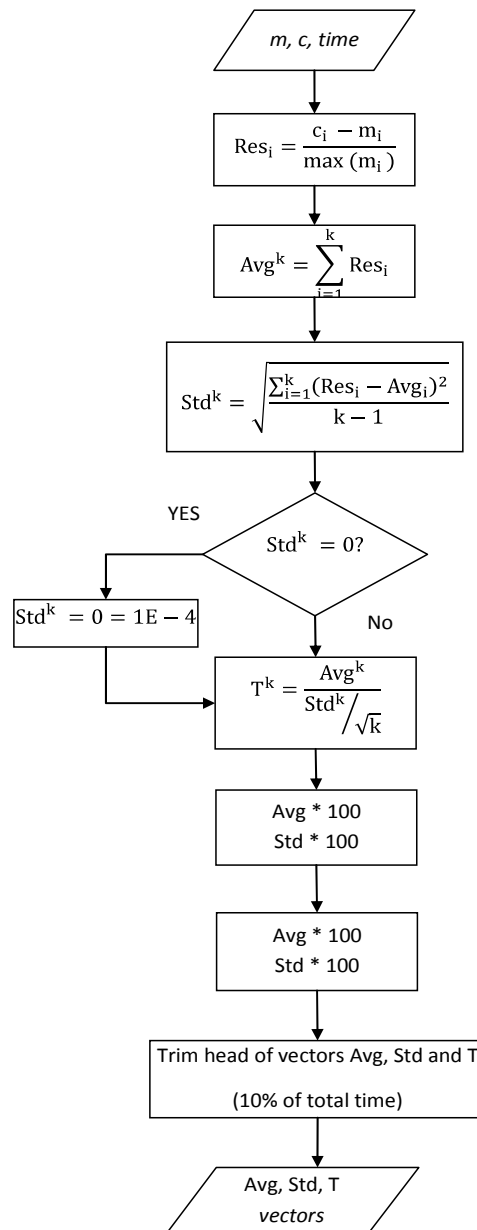


Figure B-59. Algorithm of the ANOVA metrics implemented in RSVVP.

APPENDIX C : BENCHMARK CASE EXAMPLE FORMS

The following sections include the filled-out forms and reports corresponding to the benchmark cases described in Chapter 6. The blank forms with instructions are included in Appendix E. The instructions are omitted from the forms in this Appendix to conserve space and reduce repetition.

APPENDIX C1: TEST CASE 1: PICKUP TRUCK STRIKING A STRONG-POST W-BEAM GUARDRAIL WITHOUT A CURB

VALIDATION/VERIFICATION REPORT

FOR

A Report 350 2000P Pickup Truck

(Report 350 or MASH or EN1317 Vehicle Type)

Striking a Steel deformable barrier G4(1S) with Wood Blockouts

(roadside hardware type and name)

Report Date: 11-30-2009

Type of Report (check one)

Verification (known numerical solution compared to new numerical solution) or

Validation (full-scale crash test compared to a numerical solution).

General Information	Known Solution	Analysis Solution
Performing Organization	TTI	WPI/Battelle
Test/Run Number:	TTI 405421-1	TTI-405421-1_SIM-2002_01
Vehicle:	1989 Chevrolet 2500	WPI modified (NCAC C2500R)
Impact Conditions		
Vehicle Mass:	2000 kg	2000 kg
Speed:	101.5 km/hr	101.5 km/hr
Angle:	25.5 degrees	25.5 degrees
Impact Point:	Upstream of post 12	Upstream of post 12

Composite Validation/Verification Score

List the Report 350/MASH or EN1317 Test Number		T3-11
Part I	Did all solution verification criteria in Table 1 pass?	Yes
Part II	Do all the time history evaluation scores from Table C1-2 result in a satisfactory comparison (i.e., the comparison passes the criterion)? If all the values in Table C1-2 did not pass, did the weighted procedure shown in Table C1-3 result in an acceptable comparison. If all the criteria in Table C1-2 pass, enter “yes.” If all the criteria in Table C1-2 did not pass but Table C1-3 resulted in a passing score, enter “yes.”	Yes
Part III	All the criteria in Table C1-4 (Test-PIRT) passed?	Yes
	Are the results of Steps I through III all affirmative (i.e., YES)? If all three steps result in a “YES” answer, the comparison can be considered validated or verified. If one of the steps results in a negative response, the result cannot be considered validated or verified.	Yes

The analysis solution (check one) is is NOT verified/validated against the known solution.

PART I: BASIC INFORMATION

1. What type of roadside hardware is being evaluated (check one)?
 - Longitudinal barrier or transition
 - Terminal or crash cushion
 - Breakaway support or work zone traffic control device
 - Truck-mounted attenuator
 - Other hardware: _____

2. What test guidelines were used to perform the full-scale crash test (check one)?
 - NCHRP Report 350
 - MASH
 - EN1317
 - Other: _____

3. Indicate the test level and number being evaluated (fill in the blank). 3-11

4. Indicate the vehicle type appropriate for the test level and number indicated in item 3 according to the testing guidelines indicated in item 2.

NCHRP Report 350/MASH

- | | | |
|---|---------------------------------|--------------------------------|
| <input type="checkbox"/> 700C | <input type="checkbox"/> 820C | <input type="checkbox"/> 1100C |
| <input checked="" type="checkbox"/> 2000P | <input type="checkbox"/> 2270P | |
| <input type="checkbox"/> 8000S | <input type="checkbox"/> 10000S | |
| <input type="checkbox"/> 36000V | | |
| <input type="checkbox"/> 36000T | | |

EN1317

- | | | |
|---|---|---|
| <input type="checkbox"/> Car (900 kg) | <input type="checkbox"/> Car (1300 kg) | <input type="checkbox"/> Car (1500 kg) |
| <input type="checkbox"/> Rigid HGV (10 ton) | <input type="checkbox"/> Rigid HGV (16 ton) | <input type="checkbox"/> Rigid HGV (30 ton) |
| <input type="checkbox"/> Bus (13 ton) | | |
| <input type="checkbox"/> Articulated HGV (38 ton) | | |

PART II: ANALYSIS SOLUTION VERIFICATION

Table C1-1. Analysis Solution Verification Table.

Verification Evaluation Criteria	Change (%)	Pass?
<i>Total energy</i> of the analysis solution (i.e., kinetic, potential, contact, etc.) must not vary more than 10 percent from the beginning of the run to the end of the run.	1.3	YES
<i>Hourglass Energy</i> of the analysis solution at the end of the run is less than <i>five percent</i> of the total <i>initial energy</i> at the <i>beginning</i> of the run.	0	YES
<i>Hourglass Energy</i> of the analysis solution at the end of the run is less than <i>ten percent</i> of the total <i>internal energy</i> at the <i>end</i> of the run.	0	YES
The part/material with the highest amount of hourglass energy at the end of the run is less than ten percent of the total internal energy of the part/material at the end of the run.	0	YES
Mass added to the total model is less than five percent of the total model mass at the beginning of the run.	0	YES
The part/material with the most mass added had less than 10 percent of its initial mass added.	0	Yes
The moving parts/materials in the model have less than five percent of mass added to the initial moving mass of the model.	0	Yes
There are no shooting nodes in the solution?	Yes	Yes
There are no solid elements with negative volumes?	Yes	Yes

The Analysis Solution (check one) passes does NOT pass all the criteria in Table C1-1
with without exceptions as noted.

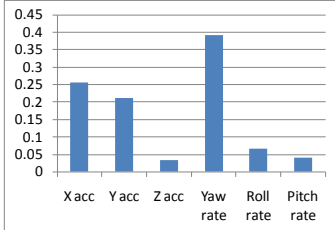
PART III: TIME HISTORY EVALUATION TABLE

Table C1-2. Roadside Safety Validation Metrics Rating Table – Time History Comparisons (single channel option).

Evaluation Criteria							Time interval [0 sec; 0.7 sec]						
O	Sprague-Geers Metrics List all the data channels being compared. Calculate the M and P metrics using RSVVP and enter the results. Values less than or equal to 40 are acceptable.						M	P	Pass?				
	RSVVP Curve Preprocessing Options												
		Filter Option	Sync. Option	Shift		Drift							
				True Curve	Test Curve	True Curve				Test Curve			
	X acceleration	CFC 180	Min. area of Residuals	Y	N	Y				N	21.5	33.3	Y
	Y acceleration	CFC 180	Min. area of Residuals	Y	N	Y				N	43.9	35.7	N
	Z acceleration	CFC 180	Min. area of Residuals	Y	N	Y				N	21.1	43.0	N
	Roll rate	CFC 180	Min. area of Residuals	N	N	N				N	35.3	32.7	Y
Pitch rate	CFC 180	Min. area of Residuals	N	N	N	N	13.3	48.0	N				
Yaw rate	CFC 180	Min. area of Residuals	N	N	N	N	11.7	8.7	Y				
P	ANOVA Metrics List all the data channels being compared. Calculate the ANOVA metrics using RSVVP and enter the results. Both of the following criteria must be met: <ul style="list-style-type: none"> The mean residual error must be less than five percent of the peak acceleration ($\bar{e} \leq 0.05 \cdot a_{peak}$) and The standard deviation of the residuals must be less than 35 percent of the peak acceleration ($\sigma \leq 0.35 \cdot a_{peak}$) 						Mean Residual	Standard Deviation of Residuals	Pass?				
	X acceleration/Peak									0.02	0.34	Y	
	Y acceleration/Peak									0.05	0.27	Y	
	Z acceleration/Peak									0.02	0.32	Y	
	Roll rate									0.02	0.27	Y	
	Pitch rate									0.05	0.36	N	
	Yaw rate									0.04	0.12	Y	

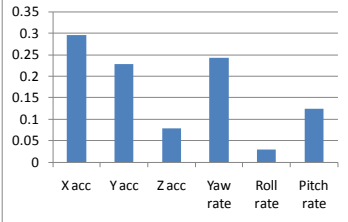
The Analysis Solution (check one) passes does NOT pass all the criteria in Table C1-2.

Table C1-3(a). Roadside Safety Validation Metrics Rating Table – Time History Comparisons
(multi-channel option using Area II method).

Evaluation Criteria (time interval [0 sec; 0.7 sec])					
Channels (Select which were used)					
<input checked="" type="checkbox"/> X Acceleration	<input checked="" type="checkbox"/> Y Acceleration	<input checked="" type="checkbox"/> Z Acceleration			
<input checked="" type="checkbox"/> Roll rate	<input checked="" type="checkbox"/> Pitch rate	<input checked="" type="checkbox"/> Yaw rate			
Multi-Channel Weights -Area (II) Method-		X Channel – 0.255116 Y Channel – 0.210572 Z Channel – 0.034312 Yaw Channel – 0.392648 Roll Channel – 0.06581 Pitch Channel – 0.041542			
O	Sprague-Geer Metrics Values less or equal to 40 are acceptable.		M	P	Pass?
			22.9	25	Y
P	ANOVA Metrics Both of the following criteria must be met: <ul style="list-style-type: none"> The mean residual error must be less than five percent of the peak acceleration ($\bar{e} \leq 0.05 \cdot a_{peak}$) The standard deviation of the residuals must be less than 35 percent of the peak acceleration ($\sigma \leq 0.35 \cdot a_{peak}$) 		Mean Residual	Standard Deviation of Residuals	Pass?
			0.03	0.24	Y

The Analysis Solution (check one) passes does NOT pass all the criteria in Table C1-3.

Table C1-3(b). Roadside Safety Validation Metrics Rating Table – Time History Comparisons (multi-channel option using Inertia method).

Evaluation Criteria (time interval [0 sec; 0.7 sec])				
Channels (Select which were used)				
<input checked="" type="checkbox"/> X Acceleration	<input checked="" type="checkbox"/> Y Acceleration	<input checked="" type="checkbox"/> Z Acceleration		
<input checked="" type="checkbox"/> Roll rate	<input checked="" type="checkbox"/> Pitch rate	<input checked="" type="checkbox"/> Yaw rate		
Multi-Channel Weights -Inertia Method-	X Channel – 0.296345 Y Channel – 0.227346 Z Channel – 0.079612 Yaw Channel – 0.242396 Roll Channel – 0.030312 Pitch Channel – 0.123988			
O	Sprague-Geer Metrics Values less or equal to 40 are acceptable.	M	P	Pass?
		23.6	30.4	Y
P	ANOVA Metrics Both of the following criteria must be met: <ul style="list-style-type: none"> The mean residual error must be less than five percent of the peak acceleration ($\bar{e} \leq 0.05 \cdot a_{Peak}$) The standard deviation of the residuals must be less than 35 percent of the peak acceleration ($\sigma \leq 0.35 \cdot a_{Peak}$) 	Mean Residual	Standard Deviation of Residuals	Pass?
		0.04	0.27	Y

The Analysis Solution (check one) passes does NOT pass all the criteria in Table C1-3.

PART IV: PHENOMENA IMPORTANCE RANKING TABLE

Table C1-4. Evaluation Criteria Test Applicability Table.

Evaluation Factors	Evaluation Criteria			Applicable Tests	
Structural Adequacy	A	Test article should contain and redirect the vehicle; the vehicle should not penetrate, under-ride, or override the installation although controlled lateral deflection of the test article is acceptable.		10, 11, 12, 20, 21, 22, 35, 36, 37, 38	
	B	The test article should readily activate in a predictable manner by breaking away, fracturing or yielding.		60, 61, 70, 71, 80, 81	
	C	Acceptable test article performance may be by redirection, controlled penetration or controlled stopping of the vehicle.		30, 31,, 32, 33, 34, 39, 40, 41, 42, 43, 44, 50, 51, 52, 53	
Occupant Risk	D	Detached elements, fragments or other debris from the test article should not penetrate or show potential for penetrating the occupant compartment, or present an undue hazard to other traffic, pedestrians or personnel in a work zone.		All	
	E	Detached elements, fragments or other debris from the test article, or vehicular damage should not block the driver’s vision or otherwise cause the driver to lose control of the vehicle. (Answer Yes or No)		70, 71	
	F	The vehicle should remain upright during and after the collision although moderate roll, pitching and yawing are acceptable.		All except those listed in criterion G	
	G	It is preferable, although not essential, that the vehicle remain upright during and after collision.		12, 22 (for test level 1 – 30, 31, 32, 33, 34, 35, 36, 37, 38, 39, 40, 41, 42, 43, 44)	
	H	Occupant impact velocities should satisfy the following:			10, 20, 30,31, 32, 33, 34, 36, 40, 41, 42, 43, 50, 51, 52, 53, 80, 81
		Occupant Impact Velocity Limits (m/s)			
		Component	Preferred	Maximum	
Longitudinal and Lateral	9	12			
Longitudinal	3	5	60, 61, 70, 71		
I	Occupant ridedown accelerations should satisfy the following:			10, 20, 30,31, 32, 33, 34, 36, 40, 41, 42, 43, 50, 51, 52, 53, 60, 61, 70, 71, 80, 81	
	Occupant Ridedown Acceleration Limits (g’s)				
	Component	Preferred	Maximum		
Longitudinal and Lateral	15	20			
Vehicle Trajectory	L	The occupant impact velocity in the longitudinal direction should not exceed 40 ft/sec and the occupant ride-down acceleration in the longitudinal direction should not exceed 20 G’s.		11,21, 35, 37, 38, 39	
	M	The exit angle from the test article preferable should be less than 60 percent of test impact angle, measured at the time of vehicle loss of contact with test device.		10, 11, 12, 20, 21, 22, 35, 36, 37, 38, 39	
	N	Vehicle trajectory behind the test article is acceptable.		30, 31, 32, 33, 34, 39, 42, 43, 44, 60, 61, 70, 71, 80, 81	

Table C1-5. Roadside Safety Phenomena Importance Ranking Table.

		Evaluation Criteria	Known Result	Analysis Result	Difference Relative/ Absolute	Agree?
Structural Adequacy		A1 Test article should contain and redirect the vehicle; the vehicle should not penetrate, under-ride, or override the installation although controlled lateral deflection of the test article is acceptable. (Answer Yes or No)	Yes	Yes	X	YES
		A2 Maximum dynamic deflection: - Relative difference is less than 20 percent or - Absolute difference is less than 0.15 m	1.0 m	0.985m	1.5% 0.02 m	YES
		A3 Length of vehicle-barrier contact: - Relative difference is less than 20 percent or - Absolute difference is less than 2 m	0.691 s	0.690 s	0.1%	YES
	A	A4 Number of broken or significantly bent posts is less than 20 percent.	3	3	0	YES
		A5 Did the rail element rupture or tear (Answer Yes or No)	No	No	X	YES
		A6 Were there failures of connector elements (Answer Yes or No).	Yes	Yes	X	YES
		A7 Was there significant snagging between the vehicle wheels and barrier elements (Answer Yes or No).	Yes	Yes	X	YES
		A8 Was there significant snagging between vehicle body components and barrier elements (Answer Yes or No).	No	No	X	YES

Table C1-5. Roadside Safety Phenomena Importance Ranking Table (continued).

Evaluation Criteria		Known Result	Analysis Result	Difference Relative/ Absolute	Agree?		
Occupant Risk	D	Detached elements, fragments or other debris from the test article should not penetrate or show potential for penetrating the occupant compartment, or present an undue hazard to other traffic, pedestrians or personnel in a work zone. (Answer Yes or No)	Pass	Pass	X	YES	
		F1	The vehicle should remain upright during and after the collision although moderate roll, pitching and yawing are acceptable. (Answer Yes or No)	Pass	Pass	X	YES
	F	F2	Maximum roll of the vehicle: - Relative difference is less than 20 percent or - Absolute difference is less than 5 degrees.	-8.7	-10.1	16% 1.4 deg	YES
		F3	Maximum pitch of the vehicle is: - Relative difference is less than 20 percent or - Absolute difference is less than 5 degrees.	-3.3	-4.3	30% 1.0 deg	YES
		F4	Maximum yaw of the vehicle is: - Relative difference is less than 20 percent or - Absolute difference is less than 5 degrees.	41	42.8	4% 1.8 deg	YES
	L	L1	Occupant impact velocities: - Relative difference is less than 20 percent or - Absolute difference is less than 2 m/s.				
			• Longitudinal OIV (m/s)	5.4	4.7	13% 0.7m/s	YES
			• Lateral OIV (m/s)	4.4	5.0	13.6% 0.6 m/s	YES
			• THIV (m/s)	6.3	6.4	1.6% 0.1 m/s	YES
		L2	Occupant accelerations: - Relative difference is less than 20 percent or - Absolute difference is less than 4 g's.				
			• Longitudinal ORA	7.9	8.9	12.7% 1.0 G	YES
			• Lateral ORA	8.4	10.0	19.0% 1.6 G	YES
			• PHD	12.1	13.2	9.1% 1.2 G	YES
			• ASI	0.68	0.72	5.9% 0.04	YES

Table C1-5. Roadside Safety Phenomena Importance Ranking Table (continued).

Evaluation Criteria			Known Result	Analysis Result	Difference Relative/Absolute	Agree?	
Vehicle Trajectory		M1	The exit angle from the test article preferable should be less than 60 percent of test impact angle, measured at the time of vehicle loss of contact with test device.	15.5° 61%	17.3° 68%	X	YES
	M	M2	Exit angle at loss of contact: - Relative difference is less than 20 percent or - Absolute difference is less than 5 degrees.	15.5°	17.3°	11.6% 1.8 deg	YES
		M3	Exit velocity at loss of contact: - Relative difference is less than 20 percent or - Absolute difference is less than 5 degrees.	55 km/h	62 km/h	12.7% 7.0 km/hr	YES
		M4	One or more vehicle tires failed or de-beaded during the collision event (Answer Yes or No).	Yes	N.M.*	X	

*N.M. – Not Modeled

The Analysis Solution (check one) passes does NOT pass all the criteria in Tables C1-5
 with exceptions as noted without exceptions .

Plots of the time histories used to evaluate the comparison metrics

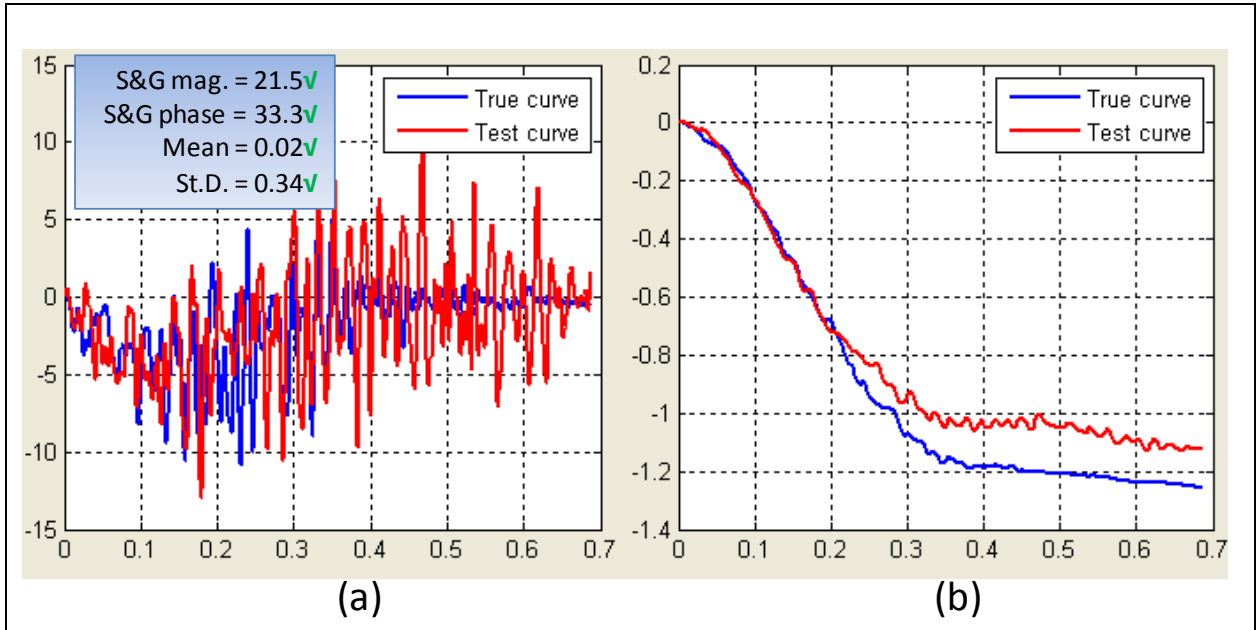


Figure C1-1. X-channel (a) acceleration-time history data used to compute metrics and (b) integration of acceleration-time history data.

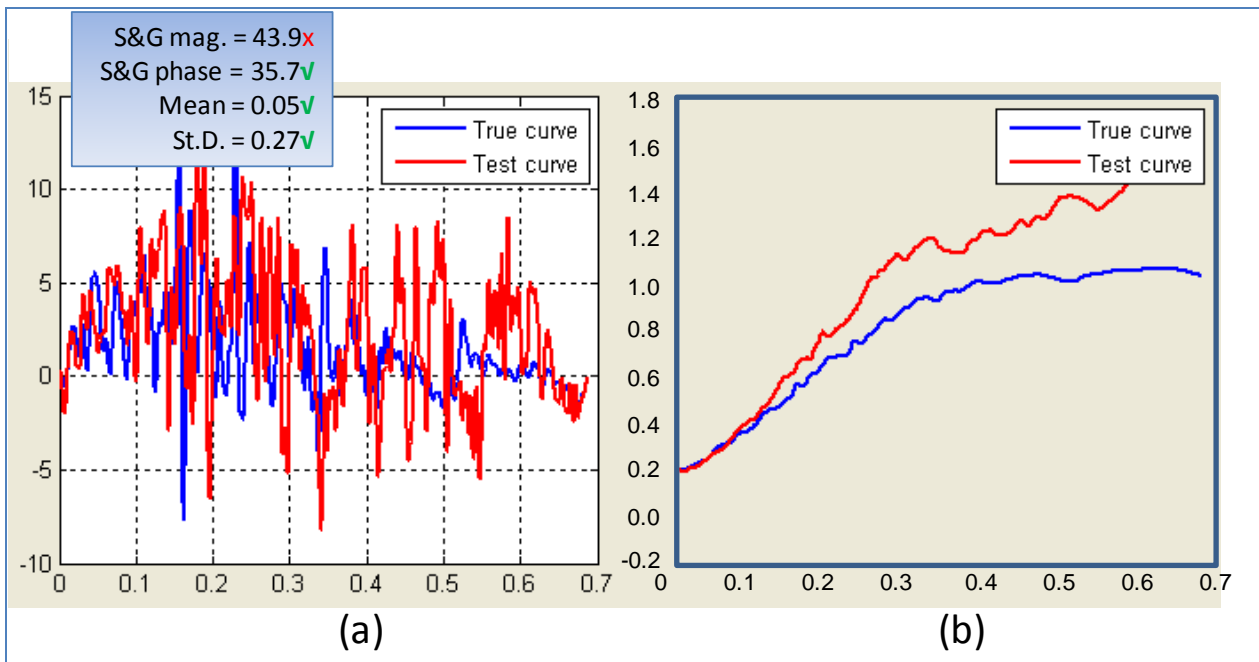


Figure C1-2. Y-channel (a) acceleration-time history data used to compute metrics and (b) integration of acceleration-time history data

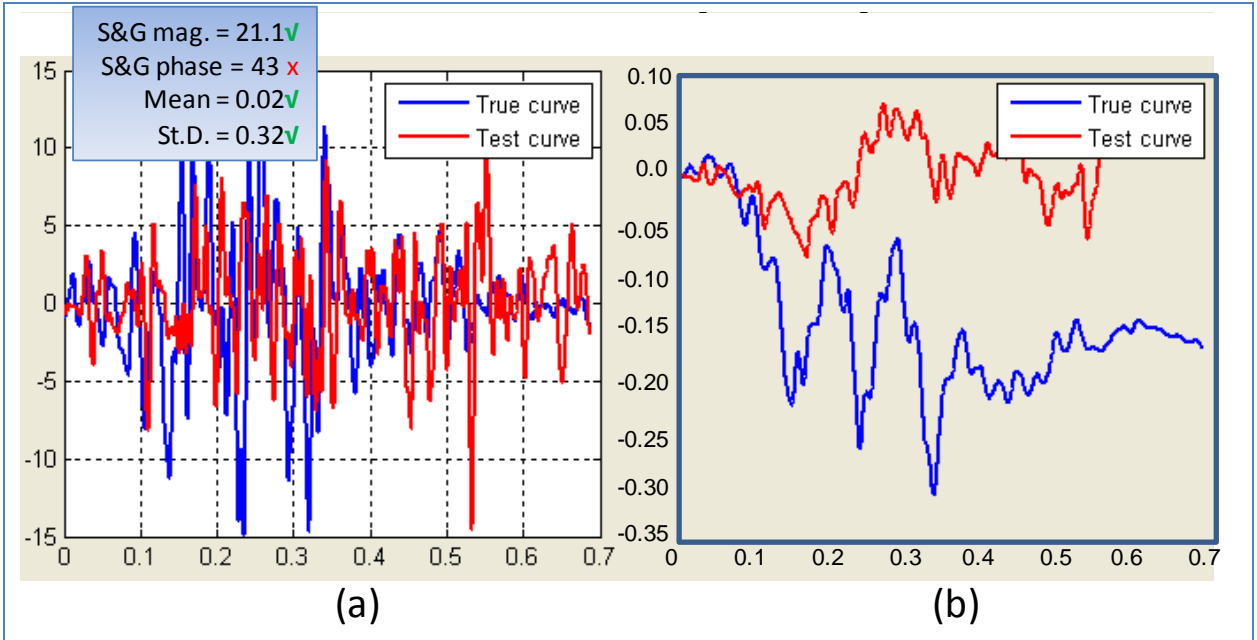


Figure C1-3. Z-Channel (a) acceleration-time history data used to compute metrics and (b) integration of acceleration-time history data.

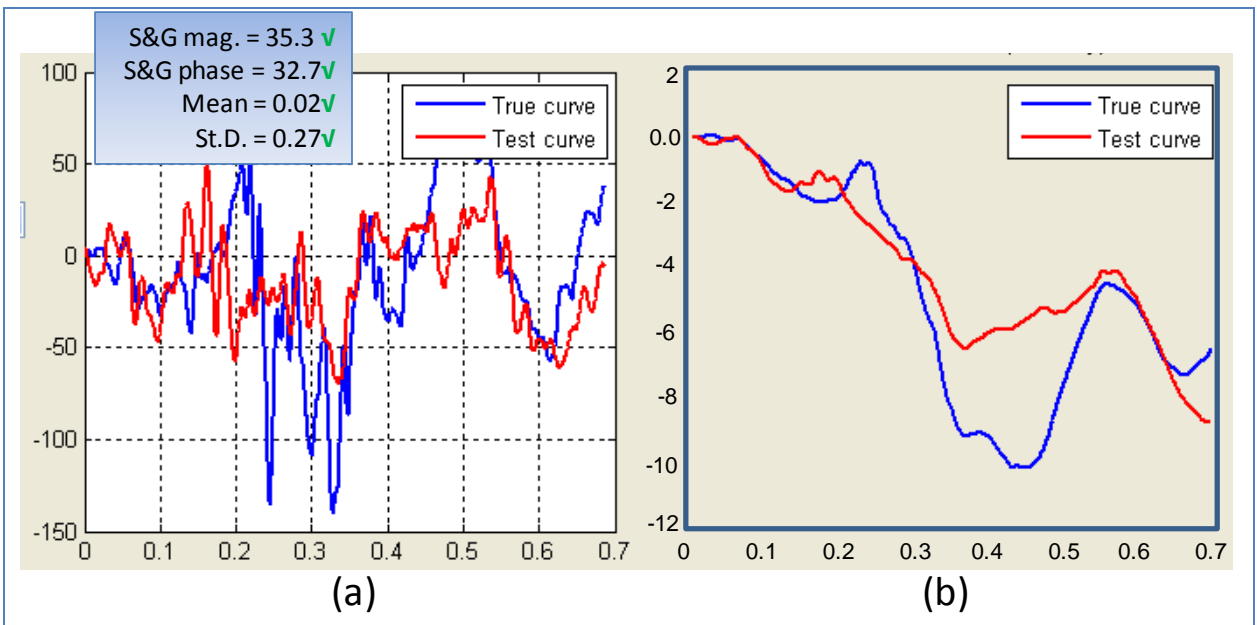


Figure C1-4. Roll-Channel (a) angular rate-time history data used to compute metrics and (b) integration of angular rate-time history data.

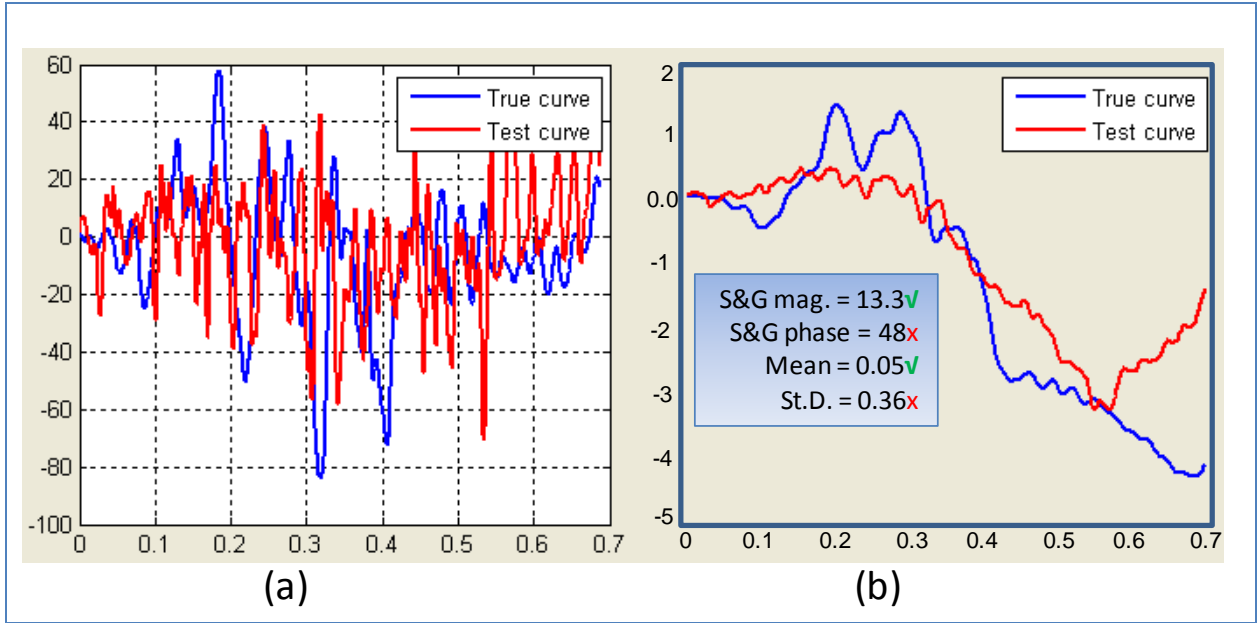


Figure C1-5. Pitch-Channel (a) angular rate-time history data used to compute metrics and (b) integration of angular rate-time history data.

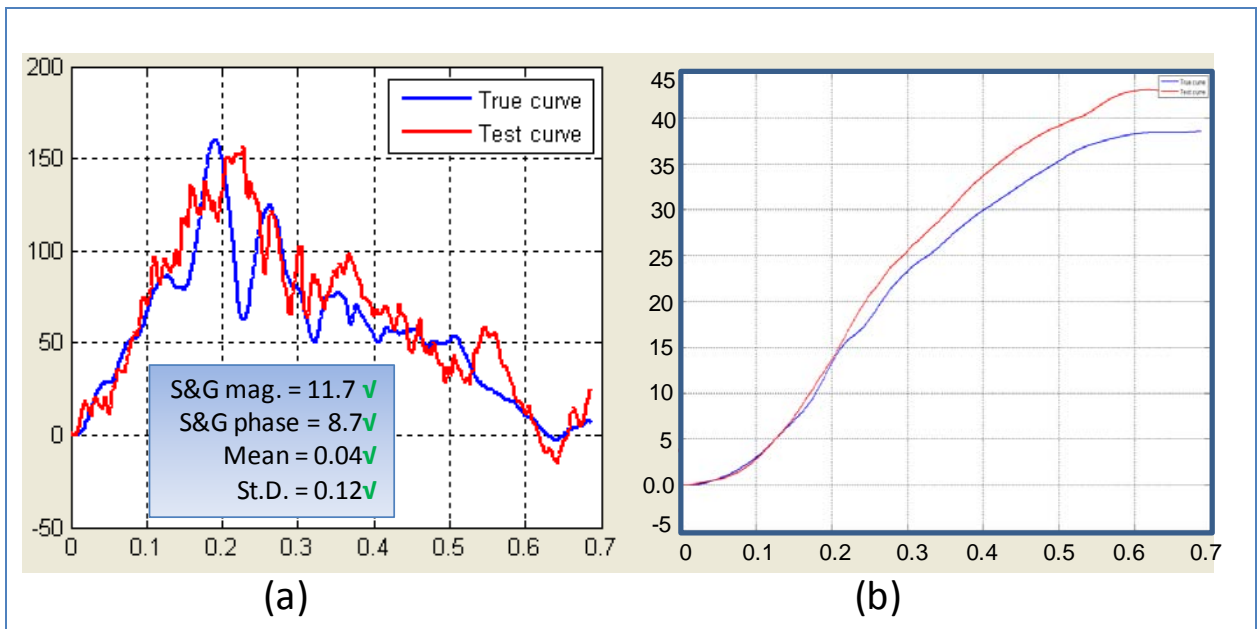
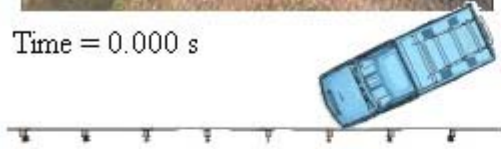


Figure C1-6. Yaw-Channel (a) angular rate-time history data used to compute metrics and (b) integration of angular rate-time history data.



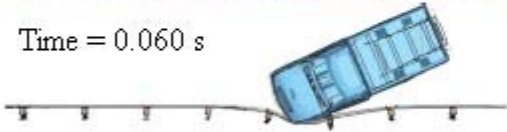
Time = 0.000 s



Time = 0.181 s



Time = 0.060 s



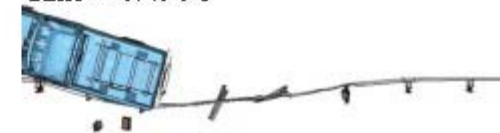
Time = 0.360 s



Time = 0.120 s

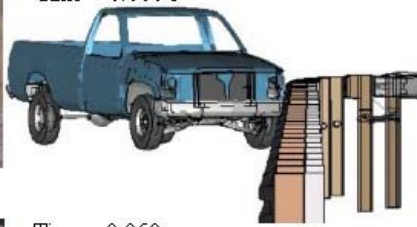


Time = 0.490 s

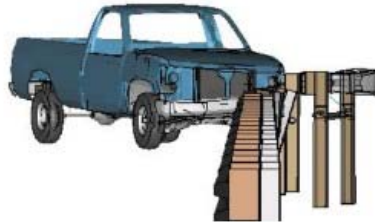




Time = 0.000 s



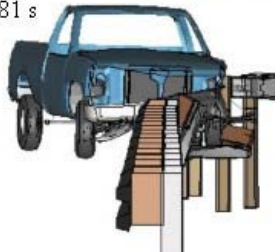
Time = 0.060 s



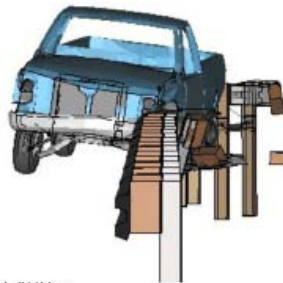
Time = 0.120 s



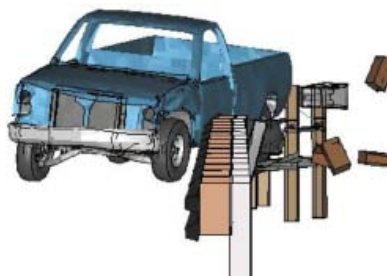
Time = 0.181 s



Time = 0.360 s



Time = 0.490 s



**APPENDIX C2: PICKUP TRUCK STRIKING A STRONG-POST W-BEAM GUARDRAIL
IN COMBINATION WITH AN AASHTO TYPE B CURB**

VALIDATION/VERIFICATION REPORT

FOR

A Report 350 2000P Pickup Truck

(Report 350 or MASH or EN1317 Vehicle Type)

Striking a Steel deformable barrier G4(1S) with Wood Blockouts and with an AASHTO Type B curb positioned underneath the barrier “flush” with the w-beam face

(roadside hardware type and name)

Report Date: 11-30-2009

Type of Report (check one)

- Verification (known numerical solution compared to new numerical solution) or
 Validation (full-scale crash test compared to a numerical solution).

General Information	Known Solution	Analysis Solution
Performing Organization	ETECH	WPI
Test/Run Number:	52-2556-001 (6/5/2003)	B-0m-85-FEA (7/8/2002)
Vehicle:	1998 GMC 3/4-ton	WPI modified (NCAC C2500R)
Impact Conditions		
Vehicle Mass:	1,993 kg	2,000 kg
Speed:	85.6 km/hr	85.0 km/hr
Angle:	25 degrees	25 degrees
Impact Point:	0.6 m upstream of post 14	0.49 m upstream of post 14

Composite Validation/Verification Score

List the Report 350/MASH or EN1317 Test Number		
Step I	Did all solution verification criteria in Table C2-1 pass?	Yes
Step II	Do all the time history evaluation scores from Table C2-2 result in a satisfactory comparison (i.e., the comparison passes the criterion)? If all the values in Table C2-2 did not pass, did the weighted procedure shown in Table C2-3 result in an acceptable comparison. If all the criteria in Table C2-2 pass, enter “yes.” If all the criteria in Table C2-2 did not pass but Table C2-3 resulted in a passing score, enter “yes.”	Yes
Step III	All the criteria in Table 2-5 passed	No
	Are the results of Steps I through III all affirmative (i.e., YES)? If all three steps result in a “YES” answer, the comparison can be considered validated or verified. If one of the steps results in a negative response, the result cannot be considered validated or verified.	No

The analysis solution (check one) is is NOT verified/validated against the known solution.

PART I: BASIC INFORMATION

- 1. What type of roadside hardware is being evaluated (check one)?
 - Longitudinal barrier or transition
 - Terminal or crash cushion
 - Breakaway support or work zone traffic control device
 - Truck-mounted attenuator
 - Other hardware: AASHTO Type B curb underneath and flush with guardrail face

- 2. What test guidelines were used to perform the full-scale crash test (check one)?
 - NCHRP Report 350
 - MASH
 - EN1317
 - Other: _____

- 3. Indicate the test level and number being evaluated (fill in the blank). 3-11

- 4. Indicate the vehicle type appropriate for the test level and number indicated in item 3 according to the testing guidelines indicated in item 2.

NCHRP Report 350/MASH

- 700C
- 2000P
- 8000S
- 36000V
- 36000T
- 820C
- 2270P
- 10000S
- 1100C

EN1317

- Car (900 kg)
- Rigid HGV (10 ton)
- Bus (13 ton)
- Articulated HGV (38 ton)
- Car (1300 kg)
- Rigid HGV (16 ton)
- Car (1500 kg)
- Rigid HGV (30 ton)

PART II: ANALYSIS SOLUTION VERIFICATION

Table C2-1. Analysis Solution Verification Table.

Verification Evaluation Criteria	Change (%)	Pass?
Total energy of the analysis solution (i.e., kinetic, potential, contact, etc.) must not vary more than 10 percent from the beginning of the run to the end of the run.	0.3	Yes
Hourglass Energy of the analysis solution at the end of the run is less than <i>five percent</i> of the total <i>initial energy</i> at the <i>beginning</i> of the run.	2.1	Yes
Hourglass Energy of the analysis solution at the end of the run is less than <i>ten percent</i> of the total <i>internal energy</i> at the <i>end</i> of the run.	5.5	Yes
The part/material with the highest amount of hourglass energy at any time during the run is less than five percent of the total initial energy at the beginning of the run.	0.8	Yes
Mass added to the total model is less than five percent of the total model mass at the beginning of the run.	3.4e-4	Yes
The part/material with the most mass added had less than 10 percent of its initial mass added.	0.3	Yes
The moving parts/materials in the model have less than five percent of mass added to the initial moving mass of the model.	0.006	Yes
There are no shooting nodes in the solution?	Yes	Yes
There are no solid elements with negative volumes?	Yes	Yes

The Analysis Solution (check one) passes does NOT pass all the criteria in Table C2-1
 with without exceptions as noted.

PART III: TIME HISTORY EVALUATION TABLE

Table C2-2. Roadside Safety Validation Metrics Rating Table – Time History Comparisons (single channel option).

Evaluation Criteria							Time interval [0 sec; 1.22 sec]						
O	Sprague-Geer Metrics List all the data channels being compared. Calculate the M and P metrics using RSVVP and enter the results. Values less than or equal to 40 are acceptable.												
		Filter Option	Sync. Option	Shift		Drift		M	P	Pass?			
				True Curve	Test Curve	True Curve	Test Curve						
	X acceleration	CFC 180	Min. area of Residuals	Y	N	Y	N	1.2	41.6	N			
	Y acceleration	CFC 180	Min. area of Residuals	Y	N	Y	N	5.7	43.1	N			
	Z acceleration	CFC 180	Min. area of Residuals	Y	N	Y	N	0.5	48.6	N			
	Roll rate	CFC 180	Min. area of Residuals	N	N	N	N	1.5	44.5	N			
	Pitch rate	CFC 180	Min. area of Residuals	N	N	N	N	9.7	25.2	Y			
Yaw rate	CFC 180	Min. area of Residuals	N	N	N	N	9.6	10.4	Y				
P	ANOVA Metrics List all the data channels being compared. Calculate the ANOVA metrics using RSVVP and enter the results. Both of the following criteria must be met: <ul style="list-style-type: none"> The mean residual error must be less than five percent of the peak acceleration ($\bar{e} \leq 0.05 \cdot a_{peak}$) and The standard deviation of the residuals must be less than 35 percent of the peak acceleration ($\sigma \leq 0.35 \cdot a_{peak}$) 							Mean Residual	Standard Deviation of Residuals	Pass?			
	X acceleration/Peak										0.00	0.17	Y
	Y acceleration/Peak										0.02	0.17	Y
	Z acceleration/Peak										0.01	0.23	Y
	Roll rate										0.02	0.51	N
	Pitch rate										0.07	0.36	N
	Yaw rate										0.06	0.14	Y

The Analysis Solution (check one) passes does NOT pass all the criteria in Table C2-2.

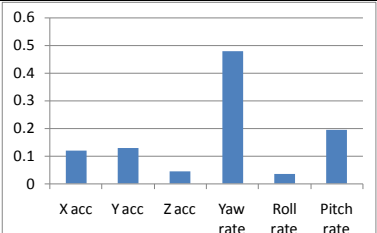
Table C2-3(a).

Roadside Safety Validation Metrics Rating Table for the G4(1S) with curb model– (multi-channel option using Area II method).

Evaluation Criteria (time interval [0 sec; 1.22 sec])			
Channels (Select which was used)			
<input checked="" type="checkbox"/> X Acceleration	<input checked="" type="checkbox"/> Y Acceleration	<input checked="" type="checkbox"/> Z Acceleration	
<input checked="" type="checkbox"/> Roll rate	<input checked="" type="checkbox"/> Pitch rate	<input checked="" type="checkbox"/> Yaw rate	
Multi-Channel Weights - Area II Method -	X Channel – 0.268011 Y Channel – 0.145893 Z Channel – 0.086096 Yaw Channel – 0.446323 Roll Channel – 0.028886 Pitch Channel – 0.02479		
	Sprague-Geer Metrics Values less or equal to 40 are acceptable.		M
		5.7	28.2
ANOVA Metrics Both of the following criteria must be met: <ul style="list-style-type: none"> The mean residual error must be less than five percent of the peak acceleration ($\bar{e} \leq 0.05 \cdot a_{peak}$) The standard deviation of the residuals must be less than 35 percent of the peak acceleration ($\sigma \leq 0.35 \cdot a_{peak}$) 		Mean Residual	Standard Deviation of Residuals
		0.03	0.18
			Pass?
			Y

The Analysis Solution (check one) passes does NOT pass all the criteria in Table C2-3.

Table C2-3(b). Roadside Safety Validation Metrics Rating Table for the G4(1S) with curb model– (multi-channel option using Inertia method).

Evaluation Criteria (time interval [0 sec; 1.22 sec])				
Channels (Select which was used)				
<input checked="" type="checkbox"/> X Acceleration	<input checked="" type="checkbox"/> Y Acceleration	<input checked="" type="checkbox"/> Z Acceleration		
<input checked="" type="checkbox"/> Roll rate	<input checked="" type="checkbox"/> Pitch rate	<input checked="" type="checkbox"/> Yaw rate		
Multi-Channel Weights - Inertia Method -	X Channel – 0.119486			
	Y Channel – 0.129217			
Z Channel – 0.04426				
Yaw Channel – 0.477606				
Roll Channel – 0.034208				
Pitch Channel – 0.195224				
O	Sprague-Geer Metrics Values less or equal to 40 are acceptable.	M	P	Pass?
		7.3	24.2	Y
P	ANOVA Metrics Both of the following criteria must be met: <ul style="list-style-type: none"> The mean residual error must be less than five percent of the peak acceleration ($\bar{e} \leq 0.05 \cdot a_{Peak}$) The standard deviation of the residuals must be less than 35 percent of the peak acceleration ($\sigma \leq 0.35 \cdot a_{Peak}$) 	Mean Residual	Standard Deviation of Residuals	Pass?
		0.02	0.21	Y

The Analysis Solution (check one) passes does NOT pass all the criteria in Table C2-3.

PART IV: PHENOMENA IMPORTANCE RANKING TABLE

Table C2-4. Evaluation Criteria Test Applicability Table.

Evaluation Factors	Evaluation Criteria			Applicable Tests											
Structural Adequacy	A	Test article should contain and redirect the vehicle; the vehicle should not penetrate, under-ride, or override the installation although controlled lateral deflection of the test article is acceptable.		10, 11, 12, 20, 21, 22, 35, 36, 37, 38											
	B	The test article should readily activate in a predictable manner by breaking away, fracturing or yielding.		60, 61, 70, 71, 80, 81											
	C	Acceptable test article performance may be by redirection, controlled penetration or controlled stopping of the vehicle.		30, 31,, 32, 33, 34, 39, 40, 41, 42, 43, 44, 50, 51, 52, 53											
Occupant Risk	D	Detached elements, fragments or other debris from the test article should not penetrate or show potential for penetrating the occupant compartment, or present an undue hazard to other traffic, pedestrians or personnel in a work zone.		All											
	E	Detached elements, fragments or other debris from the test article, or vehicular damage should not block the driver’s vision or otherwise cause the driver to lose control of the vehicle. (Answer Yes or No)		70, 71											
	F	The vehicle should remain upright during and after the collision although moderate roll, pitching and yawing are acceptable.		All except those listed in criterion G											
	G	It is preferable, although not essential, that the vehicle remain upright during and after collision.		12, 22 (for test level 1 – 30, 31, 32, 33, 34, 35, 36, 37, 38, 39, 40, 41, 42, 43, 44)											
	H	Occupant impact velocities should satisfy the following: <table border="1" data-bbox="396 1108 1045 1283"> <thead> <tr> <th colspan="3" data-bbox="396 1108 1045 1140">Occupant Impact Velocity Limits (m/s)</th> </tr> <tr> <th data-bbox="396 1140 613 1178">Component</th> <th data-bbox="613 1140 824 1178">Preferred</th> <th data-bbox="824 1140 1045 1178">Maximum</th> </tr> </thead> <tbody> <tr> <td data-bbox="396 1178 613 1245">Longitudinal and Lateral</td> <td data-bbox="613 1178 824 1245">9</td> <td data-bbox="824 1178 1045 1245">12</td> </tr> <tr> <td data-bbox="396 1245 613 1283">Longitudinal</td> <td data-bbox="613 1245 824 1283">3</td> <td data-bbox="824 1245 1045 1283">5</td> </tr> </tbody> </table>		Occupant Impact Velocity Limits (m/s)			Component	Preferred	Maximum	Longitudinal and Lateral	9	12	Longitudinal	3	5
Occupant Impact Velocity Limits (m/s)															
Component	Preferred	Maximum													
Longitudinal and Lateral	9	12													
Longitudinal	3	5													
I	Occupant ridedown accelerations should satisfy the following: <table border="1" data-bbox="396 1314 1045 1451"> <thead> <tr> <th colspan="3" data-bbox="396 1314 1045 1346">Occupant Ridedown Acceleration Limits (g’s)</th> </tr> <tr> <th data-bbox="396 1346 613 1383">Component</th> <th data-bbox="613 1346 824 1383">Preferred</th> <th data-bbox="824 1346 1045 1383">Maximum</th> </tr> </thead> <tbody> <tr> <td data-bbox="396 1383 613 1451">Longitudinal and Lateral</td> <td data-bbox="613 1383 824 1451">15</td> <td data-bbox="824 1383 1045 1451">20</td> </tr> </tbody> </table>		Occupant Ridedown Acceleration Limits (g’s)			Component	Preferred	Maximum	Longitudinal and Lateral	15	20	10, 20, 30,31, 32, 33, 34, 36, 40, 41, 42, 43, 50, 51, 52, 53, 60, 61, 70, 71, 80, 81			
Occupant Ridedown Acceleration Limits (g’s)															
Component	Preferred	Maximum													
Longitudinal and Lateral	15	20													
Vehicle Trajectory	L	The occupant impact velocity in the longitudinal direction should not exceed 40 ft/sec and the occupant ride-down acceleration in the longitudinal direction should not exceed 20 G’s.		11,21, 35, 37, 38, 39											
	M	The exit angle from the test article preferable should be less than 60 percent of test impact angle, measured at the time of vehicle loss of contact with test device.		10, 11, 12, 20, 21, 22, 35, 36, 37, 38, 39											
	N	Vehicle trajectory behind the test article is acceptable.		30, 31, 32, 33, 34, 39, 42, 43, 44, 60, 61, 70, 71, 80, 81											

Table C2-5(a). Roadside Safety Phenomena Importance Ranking Table (Structural Adequacy).

		Evaluation Criteria	Known Result	Analysis Result	Difference Relative/Absolute	Agree?
Structural Adequacy		A1 Test article should contain and redirect the vehicle; the vehicle should not penetrate, under-ride, or override the installation although controlled lateral deflection of the test article is acceptable. (Answer Yes or No)	Yes	Yes	X	YES
		A2 Maximum dynamic deflection: - Relative difference is less than 20 percent or - Absolute difference is less than 0.15 m	0.5 m	0.6 m	20% 0.1 m	YES
	A	A3 Length of vehicle-barrier contact: - Relative difference is less than 20 percent or - Absolute difference is less than 2 m	~6.32 m	~6.19 m	2.1% 0.13 m	YES
		A4 The relative difference in the number of broken or significantly bent posts is less than 20 percent.	2	2		YES
		A5 The rail element did not rupture or fail (Answer Yes or No)	Yes	Yes	X	YES
		A6 There were no failures of connector elements (Answer Yes or No).	No	No	X	YES
		A6a Number of detached posts from rail	2	2	X	YES
		A6b Number of detached blockouts from posts	1	1	X	YES

Table C2-5(b). Roadside Safety Phenomena Importance Ranking Table (Occupant Risk).

Evaluation Criteria		Known Result	Analysis Result	Difference Relative/ Absolute	Agree?		
Occupant Risk	D	Detached elements, fragments or other debris from the test article should not penetrate or show potential for penetrating the occupant compartment, or present an undue hazard to other traffic, pedestrians or personnel in a work zone. (Answer Yes or No)	Pass	Pass	X	YES	
		F1	The vehicle should remain upright during and after the collision although moderate roll, pitching and yawing are acceptable. (Answer Yes or No)	Pass	Pass	X	YES
	F	F2	Maximum roll of the vehicle: - Relative difference is less than 20 percent or - Absolute difference is less than 5 degrees.	6.5	4.9	24.6% 1.6 deg.	YES
		F3	Maximum pitch of the vehicle is: - Relative difference is less than 20 percent or - Absolute difference is less than 5 degrees.	10.2	12.8	25.5% 2.6 deg	YES
		F4	Maximum yaw of the vehicle is: - Relative difference is less than 20 percent or - Absolute difference is less than 5 degrees.	42.0	43.2	2.9% 1.2 deg	YES
	L	L1	Occupant impact velocities: - Relative difference is less than 20 percent or - Absolute difference is less than 2 m/s.				
			• Longitudinal OIV (m/s)	4.9	4.2	14.3% 0.7 m/s	YES
			• Lateral OIV (m/s)	4.7	4.1	12.8% 0.6 m/s	YES
			• THIV (m/s)	24.1	26.8	11.2% 2.7 m/s	YES
		L2	Occupant accelerations: - Relative difference is less than 20 percent or - Absolute difference is less than 4 g's.				
			• Longitudinal ORA	8.1	8.1	0.0	YES
			• Lateral ORA	6.3	10.6	68.3% 4.3 G	NO
	• ASI		0.7	0.67	4.3% 0.03	YES	

Table C2-5(c). Roadside Safety Phenomena Importance Ranking Table (Vehicle Trajectory).

Evaluation Criteria			Known Result	Analysis Result	Difference Relative/Absolute	Agree?	
Vehicle Trajectory	<input checked="" type="checkbox"/> M	M1	The exit angle from the test article preferable should be less than 60 percent of test impact angle, measured at the time of vehicle loss of contact with test device.	Yes 14 deg	No 16 deg		NO***
		M2	Exit angle at loss of contact: - Relative difference is less than 20 percent or - Absolute difference is less than 5 degrees.	14 deg	16 deg	14 % 2 deg	YES
		M3	Exit velocity at loss of contact: - Relative difference is less than 20 percent or - Absolute difference is less than 10 m/s.	41.3*	56.7 km/hr	37.3% 15.4 km/hr	YES
			53.1** km/hr	6.8% 3.6 km/hr		YES	
		M4	One or more vehicle tires failed or de-beaded during the collision event (Answer Yes or No).	Yes	N.M.		-
		M5	One or more tires separated from the vehicle (Answer Yes or No).	No	N.M.		-

* Velocity reported in the test report computed by integrating the raw x-acceleration channel

** Velocity computed by integrating the x-channel data processed by RSVVP (e.g., with drift and shift)

*** The exit angle was one degree below the 15 degree limit for the test and one degree over for the simulation.

Both the test and simulation, therefore, were essentially at the limit so this should be considered an agreeing result.

The Analysis Solution (check one) passes does NOT pass all the criteria in Tables C2-5 with exceptions as noted without exceptions .

Plots of the time histories used to evaluate the comparison metrics

A. Accelerations

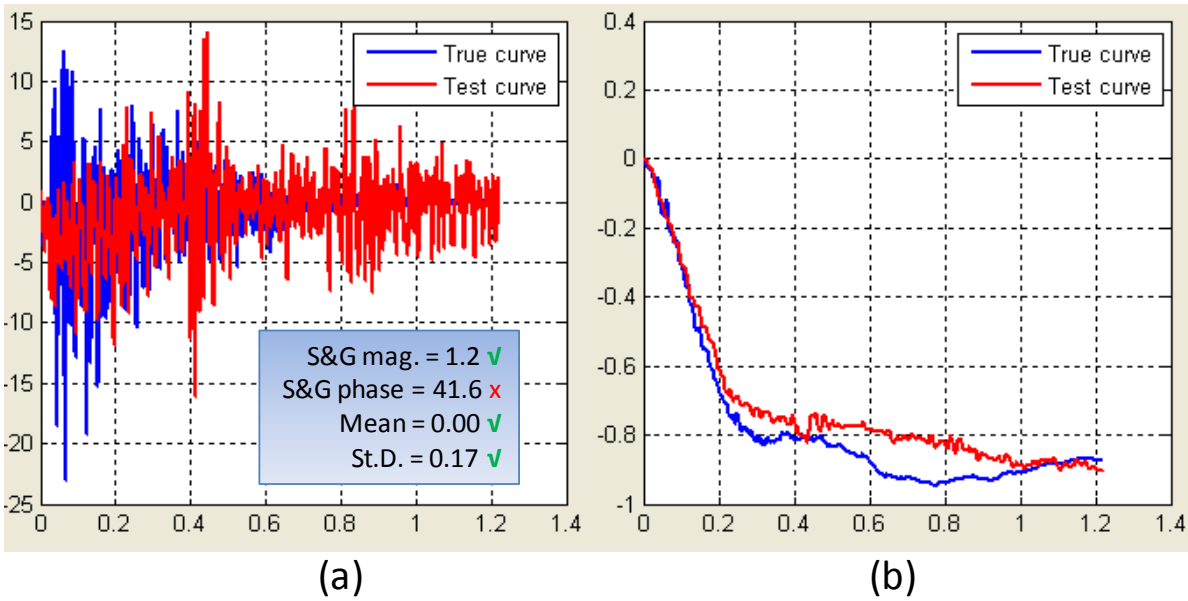


Figure C2-1. X-channel (a) acceleration-time history data used to compute metrics and (b) integration of acceleration-time history data.

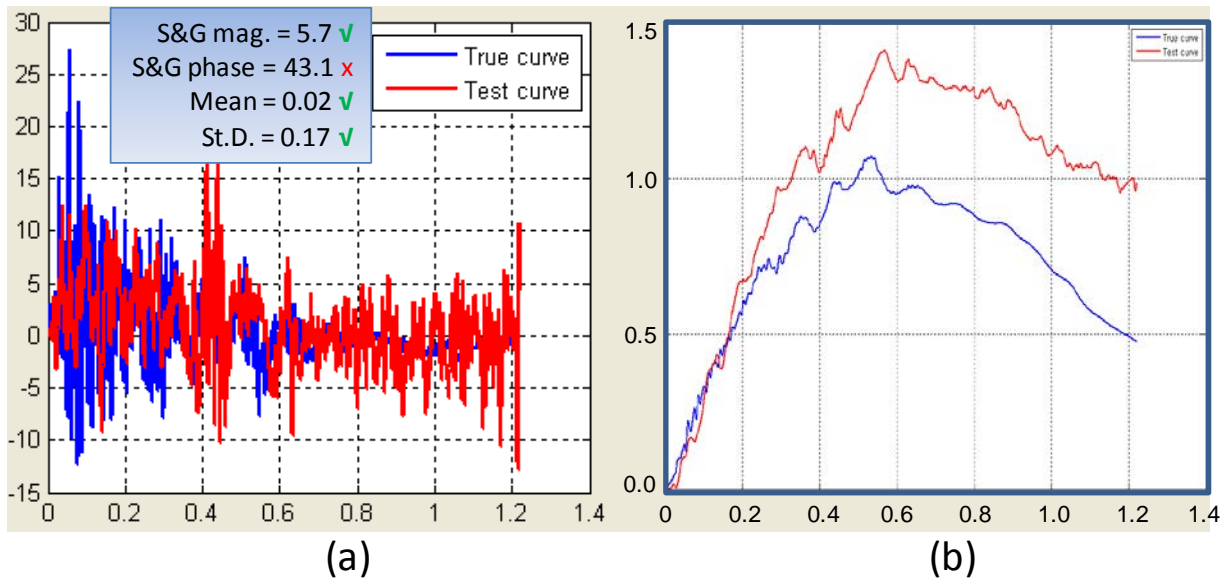


Figure C2-2. Y-channel (a) acceleration-time history data used to compute metrics and (b) integration of acceleration-time history data.

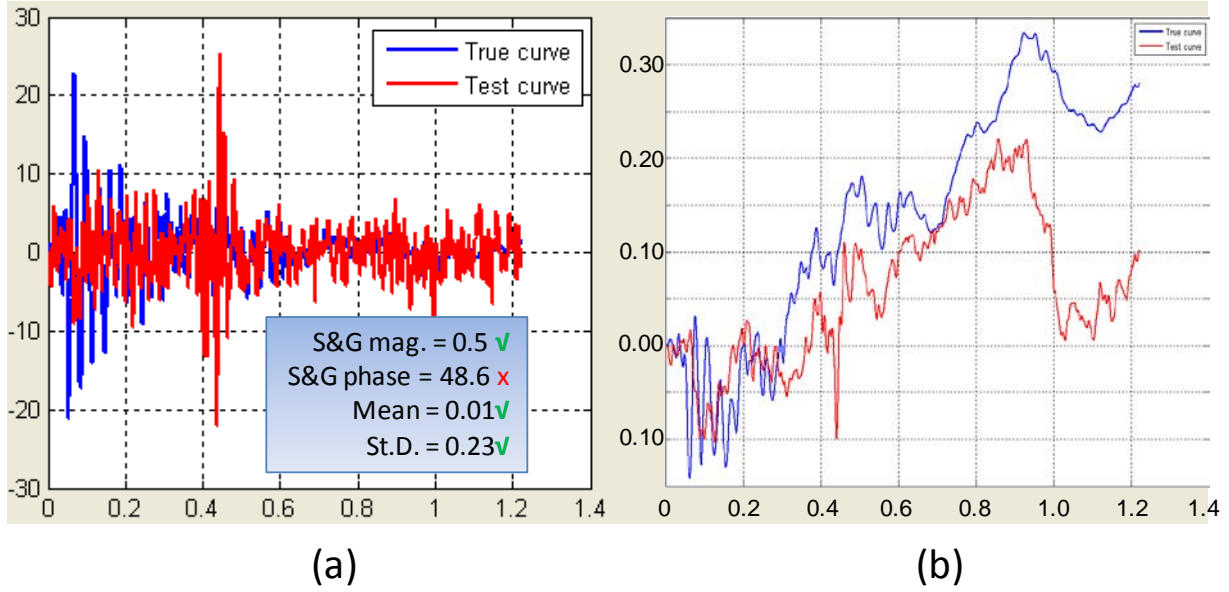


Figure C2-3. Z-Channel (a) acceleration-time history data used to compute metrics and (b) integration of acceleration-time history data.

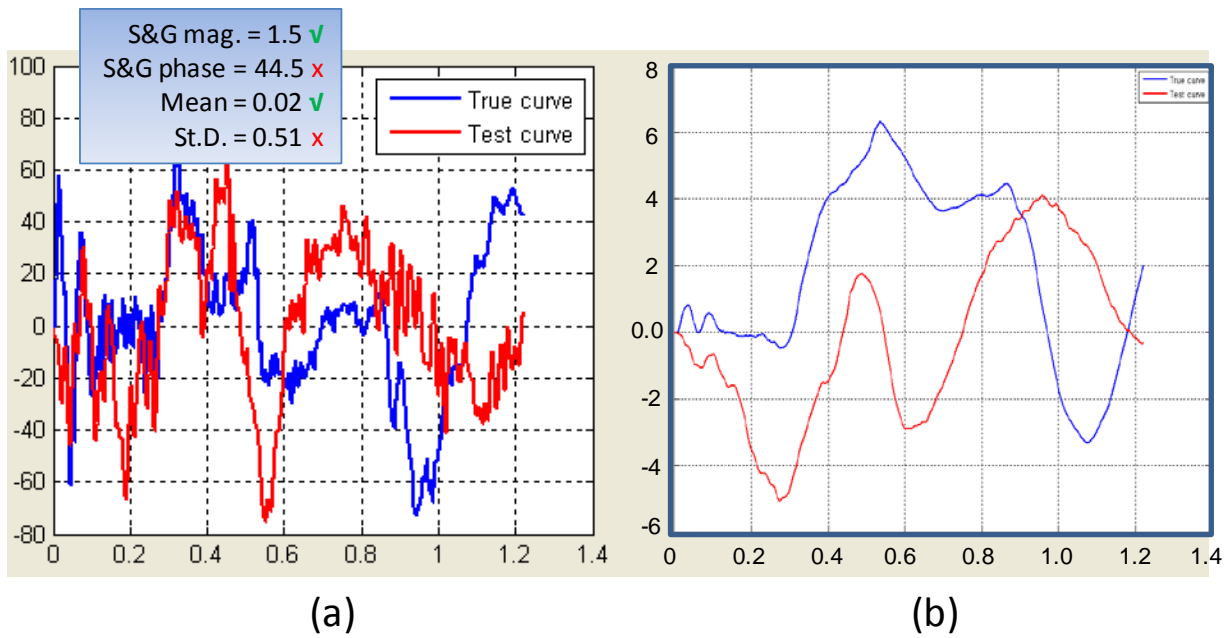


Figure C2-4. Roll-Channel (a) angular rate-time history data used to compute metrics and (b) integration of angular rate-time history data.

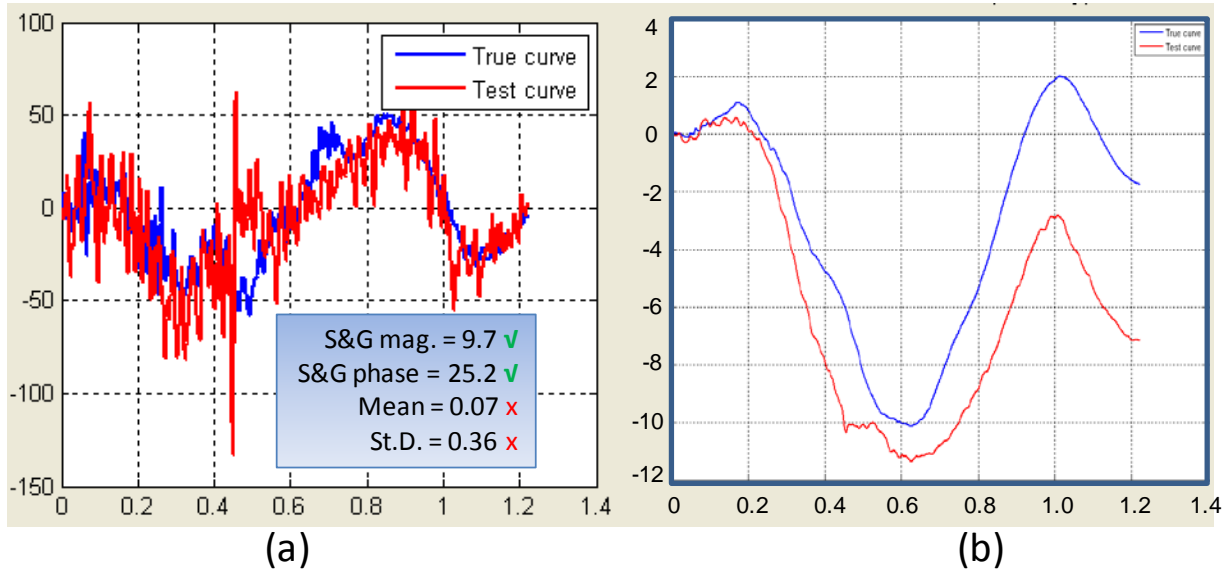


Figure C2-5. Pitch-Channel (a) angular rate-time history data used to compute metrics and (b) integration of angular rate-time history data.

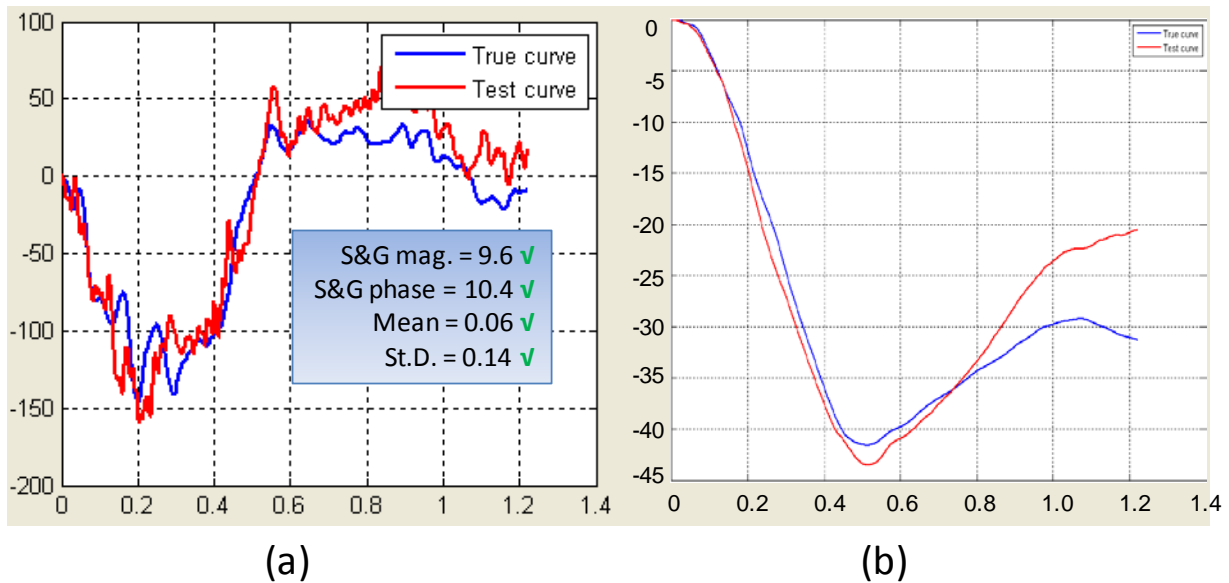


Figure C2-6. Yaw-Channel (a) angular rate-time history data used to compute metrics and (b) integration of angular rate-time history data.

APPENDIX C3: SMALL CAR STRIKING A VERTICAL RIGID WALL

**VALIDATION/VERIFICATION REPORT
FOR**

A EN 1317 Vehicle
(Report 350 or MASH or EN1317 Vehicle Type)

Striking a Concrete barrier
(roadside hardware type and name)

Report Date: 12/30/09

Type of Report (check one)

- Verification (known numerical solution compared to new numerical solution) or
 Validation (full-scale crash test compared to a numerical solution).

General Information	Known Solution	Analysis Solution
Performing Organization	Test agency 1	Politecnico di Milano
Test/Run Number:	S 70	GM_R5 Round Robin
Vehicle:	F i a t U N O	Geo Metro (GM_R5)
Impact Conditions		
Vehicle Mass:	922 kg	860 kg
Speed:	100.33 km/h	100 km/h
Angle:	20deg	20 deg.
Impact Point:	10 m from beginning	4.5 m from the beginning

Composite Validation/Verification Score

List the Report 350/MASH or EN1317 Test Number		
Step I	Did all solution verification criteria in Table C3-1 pass?	YES
Step II	Do all the time history evaluation scores from Table C3-2 result in a satisfactory comparison (i.e., the comparison passes the criterion)? If all the values in Table C3-2 did not pass, did the weighted procedure shown in Table C3-3 result in an acceptable comparison. If all the criteria in Table C3-2 pass, enter “yes.” If all the criteria in Table C3-2 did not pass but Table C3-3 resulted in a passing score, enter “yes.”	YES
Step III	All the criteria in Table C3-5 passed	NO
	Are the results of Steps I through III all affirmative (i.e., YES)? If all three steps result in a “YES” answer, the comparison can be considered validated or verified. If one of the steps results in a negative response, the result cannot be considered validated or verified.	NO

The analysis solution (check one) is is NOT verified/validated against the known solution.

PART I: BASIC INFORMATION

- 1. What type of roadside hardware is being evaluated (check one)?
 - Longitudinal barrier or transition
 - Terminal or crash cushion
 - Breakaway support or work zone traffic control device
 - Truck-mounted attenuator
 - Other hardware: _____

- 2. What test guidelines were used to perform the full-scale crash test (check one)?
 - NCHRP Report 350
 - MASH
 - EN1317
 - Other: _____

- 3. Indicate the test level and number being evaluated (fill in the blank). TB-11

- 4. Indicate the vehicle type appropriate for the test level and number indicated in item 3 according to the testing guidelines indicated in item 2.

NCHRP Report 350/MASH

- 700C 820C 1100C
- 2000P 2270P
- 8000S 10000S
- 36000V
- 36000T

EN1317

- Car (900 kg) Car (1300 kg) Car (1500 kg)
- Rigid HGV (10 ton) Rigid HGV (16 ton) Rigid HGV (30 ton)
- Bus (13 ton)
- Articulated HGV (38 ton)

PART II: ANALYSIS SOLUTION VERIFICATION

Table C3-1. Analysis Solution Verification Table.

Verification Evaluation Criteria	Change (%)	Pass?
Total energy of the analysis solution (i.e., kinetic, potential, contact, etc.) must not vary more than 10 percent from the beginning of the run to the end of the run.	-1	YES
Hourglass Energy of the analysis solution at the end of the run is less than five percent of the total initial energy at the beginning of the run.	0.5	YES
The part/material with the highest amount of hourglass energy at any time during the run is less than five percent of the total initial energy at the beginning of the run.	0.5	YES
Mass added to the total model is less than five percent of the total model mass at the beginning of the run.	0	YES
The part/material with the most mass added had less than 10 percent of its initial mass added.	0	YES
The moving parts/materials in the model have less than five percent of mass added to the initial moving mass of the model.	0	YES
There are no shooting nodes in the solution?	No	YES
There are no solid elements with negative volumes?	No	YES

The Analysis Solution (check one) passes does NOT pass all the criteria in Table C3-1.

PART III: TIME HISTORY EVALUATION TABLE

Table C3-2. Roadside Safety Validation Metrics Rating Table – Time History Comparisons (single channel option).

Evaluation Criteria							Time interval [0 sec; 0.4 sec]			
O	Sprague-Geer Metrics List all the data channels being compared. Calculate the M and P metrics using RSVVP and enter the results. Values less than or equal to 40 are acceptable.						M [%]	P [%]	Pass?	
	RSVVP Curve Preprocessing Options									
		Filter Option	Sync. Option	Shift		Drift				
				True Curve	Test Curve	True Curve	Test Curve			
	X acceleration	CFC 180	Min. area of Residuals	N	N	N	N	7.7	36.8	Y
	Y acceleration	CFC 180	Min. area of Residuals	N	N	N	N	24.5	38.5	Y
	Z acceleration	CFC 180	Min. area of Residuals	N	N	N	N	218.4	41.5	N
	Yaw rate	N/A	N/A	N/A	N/A	N/A	N/A	0.7	11.1	Y
Roll rate	N/A	N/A	N/A	N/A	N/A	N/A	N/A	N/A	N/A	
Pitch rate	N/A	N/A	N/A	N/A	N/A	N/A	N/A	N/A	N/A	
P	ANOVA Metrics List all the data channels being compared. Calculate the ANOVA metrics using RSVVP and enter the results. Both of the following criteria must be met: <ul style="list-style-type: none"> The mean residual error must be less than five percent of the peak acceleration ($\bar{e} \leq 0.05 \cdot a_{peak}$) and The standard deviation of the residuals must be less than 35 percent of the peak acceleration ($\sigma \leq 0.35 \cdot a_{peak}$) 						Mean Residual [%]	Standard Deviation of Residuals [%]	Pass?	
	X acceleration/Peak						0.82	17.4	Y	
	Y acceleration/Peak						-2.32	30.5	Y	
	Z acceleration/Peak						-2.84	54.2	N	
	Yaw rate						3.3	9.5	Y	
	Roll rate						N/A	N/A	N/A	
Pitch rate						N/A	N/A	N/A		

The Analysis Solution (check one) passes does NOT pass all the criteria in Table C3-2.

Table C3-3. Roadside Safety Validation Metrics Rating Table – Time History Comparisons (Multiple channels).

Evaluation Criteria (time interval [0 sec; 0.4 sec])														
Channels (Select which was used)														
<input checked="" type="checkbox"/> X Acceleration	<input checked="" type="checkbox"/> Y Acceleration	<input checked="" type="checkbox"/> Z Acceleration												
<input checked="" type="checkbox"/> Roll rate	<input type="checkbox"/> Pitch rate	<input type="checkbox"/> Yaw rate												
Multi-Channel Weights -Area (II) Method-	X Channel – 0.16 Y Channel – 0.30 Z Channel – 0.04 Yaw rate Channel – 0.5		<table border="1"> <caption>Multi-Channel Weights Data</caption> <thead> <tr> <th>Channel</th> <th>Weight</th> </tr> </thead> <tbody> <tr> <td>X acc</td> <td>0.16</td> </tr> <tr> <td>Y acc</td> <td>0.30</td> </tr> <tr> <td>Z acc</td> <td>0.04</td> </tr> <tr> <td>Yaw rate</td> <td>0.50</td> </tr> </tbody> </table>		Channel	Weight	X acc	0.16	Y acc	0.30	Z acc	0.04	Yaw rate	0.50
	Channel	Weight												
X acc	0.16													
Y acc	0.30													
Z acc	0.04													
Yaw rate	0.50													
O Sprague-Geer Metrics Values less or equal to 40 are acceptable.			M [%]	P [%]	Pass?									
			17.6	24.7	Y									
P ANOVA Metrics Both of the following criteria must be met: <ul style="list-style-type: none"> The mean residual error must be less than five percent of the peak acceleration ($\bar{e} \leq 0.05 \cdot a_{Peak}$) The standard deviation of the residuals must be less than 35 percent of the peak acceleration ($\sigma \leq 0.35 \cdot a_{Peak}$) 			Mean Residual	Standard Deviation of Residuals	Pass?									
			1%	18.8%	Y									

The Analysis Solution (check one) passes does NOT pass all the criteria in Table C3-3.

PART IV: PHENOMENA IMPORTANCE RANKING TABLE

Table C3-4. Evaluation Criteria Test Applicability Table.

Evaluation Factors	Evaluation Criteria	Applicable Tests													
Structural Adequacy	A Test article should contain and redirect the vehicle; the vehicle should not penetrate, under-ride, or override the installation although controlled lateral deflection of the test article is acceptable.	10, 11, 12, 20, 21, 22, 35, 36, 37, 38													
	B The test article should readily activate in a predictable manner by breaking away, fracturing or yielding.	60, 61, 70, 71, 80, 81													
	C Acceptable test article performance may be by redirection, controlled penetration or controlled stopping of the vehicle.	30, 31,, 32, 33, 34, 39, 40, 41, 42, 43, 44, 50, 51, 52, 53													
Occupant Risk	D Detached elements, fragments or other debris from the test article should not penetrate or show potential for penetrating the occupant compartment, or present an undue hazard to other traffic, pedestrians or personnel in a work zone.	All													
	E Detached elements, fragments or other debris from the test article, or vehicular damage should not block the driver’s vision or otherwise cause the driver to lose control of the vehicle. (Answer Yes or No)	70, 71													
	F The vehicle should remain upright during and after the collision although moderate roll, pitching and yawing are acceptable.	All except those listed in criterion G													
	G It is preferable, although not essential, that the vehicle remain upright during and after collision.	12, 22 (for test level 1 – 30, 31, 32, 33, 34, 35, 36, 37, 38, 39, 40, 41, 42, 43, 44)													
	H	Occupant impact velocities should satisfy the following:													
		<table border="1" data-bbox="396 1115 1040 1148"> <thead> <tr> <th colspan="3" data-bbox="396 1115 613 1148">Occupant Impact Velocity Limits (m/s)</th> </tr> <tr> <th data-bbox="396 1148 613 1182">Component</th> <th data-bbox="613 1148 824 1182">Preferred</th> <th data-bbox="824 1148 1040 1182">Maximum</th> </tr> </thead> <tbody> <tr> <td data-bbox="396 1182 613 1245">Longitudinal and Lateral</td> <td data-bbox="613 1182 824 1245">9</td> <td data-bbox="824 1182 1040 1245">12</td> </tr> <tr> <td data-bbox="396 1245 613 1283">Longitudinal</td> <td data-bbox="613 1245 824 1283">3</td> <td data-bbox="824 1245 1040 1283">5</td> </tr> </tbody> </table>	Occupant Impact Velocity Limits (m/s)			Component	Preferred	Maximum	Longitudinal and Lateral	9	12	Longitudinal	3	5	10, 20, 30,31, 32, 33, 34, 36, 40, 41, 42, 43, 50, 51, 52, 53, 80, 81
		Occupant Impact Velocity Limits (m/s)													
Component	Preferred	Maximum													
Longitudinal and Lateral	9	12													
Longitudinal	3	5													
Longitudinal	3	5	60, 61, 70, 71												
I	Occupant ridedown accelerations should satisfy the following:														
	<table border="1" data-bbox="396 1316 1040 1350"> <thead> <tr> <th colspan="3" data-bbox="396 1316 613 1350">Occupant Ridedown Acceleration Limits (g’s)</th> </tr> <tr> <th data-bbox="396 1350 613 1383">Component</th> <th data-bbox="613 1350 824 1383">Preferred</th> <th data-bbox="824 1350 1040 1383">Maximum</th> </tr> </thead> <tbody> <tr> <td data-bbox="396 1383 613 1451">Longitudinal and Lateral</td> <td data-bbox="613 1383 824 1451">15</td> <td data-bbox="824 1383 1040 1451">20</td> </tr> </tbody> </table>	Occupant Ridedown Acceleration Limits (g’s)			Component	Preferred	Maximum	Longitudinal and Lateral	15	20	10, 20, 30,31, 32, 33, 34, 36, 40, 41, 42, 43, 50, 51, 52, 53, 60, 61, 70, 71, 80, 81				
	Occupant Ridedown Acceleration Limits (g’s)														
Component	Preferred	Maximum													
Longitudinal and Lateral	15	20													
Longitudinal and Lateral	15	20													
Vehicle Trajectory	L The occupant impact velocity in the longitudinal direction should not exceed 40 ft/sec and the occupant ride-down acceleration in the longitudinal direction should not exceed 20 G’s.	11,21, 35, 37, 38, 39													
	M The exit angle from the test article preferable should be less than 60 percent of test impact angle, measured at the time of vehicle loss of contact with test device.	10, 11, 12, 20, 21, 22, 35, 36, 37, 38, 39													
	N Vehicle trajectory behind the test article is acceptable.	30, 31, 32, 33, 34, 39, 42, 43, 44, 60, 61, 70, 71, 80, 81													

Table C3-5. Roadside Safety Phenomena Importance Ranking Table.

		Evaluation Criteria	Known Result	Analysis Result	Difference Relative/Absolute	Agree?		
Structural Adequacy	A	A1	Test article should contain and redirect the vehicle; the vehicle should not penetrate, under-ride, or override the installation although controlled lateral deflection of the test article is acceptable. (Answer Yes or No)	Yes	Yes	X	YES	
		A2	Maximum dynamic deflection: - Relative difference is less than 20 percent or - Absolute difference is less than 0.15 m	0	0	0 % 0 m	YES	
		A3	Length of vehicle-barrier contact: - Relative difference is less than 20 percent or - Absolute difference is less than 2 m	7 m	10 m ⁽¹⁾	30% 3 m	NO	
		A4	The relative difference in the number of broken or significantly bent posts is less than 20 percent.	0	0	0	YES	
		A5	The rail element did not rupture or fail (Answer Yes or No)	Yes	Yes	X	YES	
		A6	There were no failures of connector elements (Answer Yes or No).	Yes	Yes	X	YES	
		A7	There was no significant snagging between the vehicle wheels and barrier elements (Answer Yes or No).	Yes	Yes	X	YES	
		A8	There was no significant snagging between vehicle body components and barrier elements (Answer Yes or No).	Yes	Yes	X	YES	
	B	B1	The test article should readily activate in a predictable manner by breaking away, fracturing or yielding. (Answer Yes or No)			X		
		C	C1	Acceptable test article performance may be by redirection, controlled penetration or controlled stopping of the vehicle. (Answer Yes or No)			X	
			C2	The relative difference in maximum system stroke is less than 20 percent.				
			C3	The relative difference in the number of broken or significantly bent posts is less than 20 percent.				
			C4	The rail element did not rupture or tear (Answer Yes or No).			X	
			C5	There were no failures of connector elements (Answer Yes or No).			X	

⁽¹⁾ The vehicle slid along the barrier due to collapse of the steering system (front right wheel turned towards the barrier).

Table C3-5. Roadside Safety Phenomena Importance Ranking Table (continued).

Evaluation Criteria		Known Result	Analysis Result	Relative Diff. (%)	Agree?		
Occupant Risk	D	Detached elements, fragments or other debris from the test article should not penetrate or show potential for penetrating the occupant compartment, or present an undue hazard to other traffic, pedestrians or personnel in a work zone. (Answer Yes or No)	Pass	Pass		YES	
	E	Detached elements, fragments or other debris from the test article, or vehicular damage should not block the driver's vision or otherwise cause the driver to lose control of the vehicle. (Answer Yes or No)					
	F1	The vehicle should remain upright during and after the collision although moderate roll, pitching and yawing are acceptable. (Answer Pass or Not pass)	Pass	Pass		YES	
	F	F2	Maximum roll of the vehicle: - Relative difference is less than 20 percent or - Absolute difference is less than 5 degrees.	≈3° ⁽¹⁾	2.5°	16 % 0.5°	YES
		F3	Maximum pitch of the vehicle is: - Relative difference is less than 20 percent or - Absolute difference is less than 5 degrees.	N/A	N/A	N/A	N/A
		F4	Maximum yaw of the vehicle is: - Relative difference is less than 20 percent or - Absolute difference is less than 5 degrees.	16.8°	17.5°	4 % 0.7°	YES
		H	H1	Occupant impact velocities: - Relative difference is less than 20 percent or - Absolute difference is less than 2 m/s. ⁽²⁾ : • Longitudinal OIV (m/s) • Lateral OIV (m/s)	4.5	3.3	-27% 1.2 m/s
	-7.2				-7.2	0 % 0 m/s	YES
	H2		• Longitudinal OIV	4.5	3.3	-27% 1.2 m/s	YES
	H3		• THIV (m/s)	7.9	7.6	-3.8 % 0.3 m/s	YES
	I	Occupant accelerations: - Relative difference is less than 20 percent or - Absolute difference is less than 4 g's. ⁽²⁾ : • Longitudinal ORA (g) • Lateral ORA (g) • PHD (g) • ASI					
			-5	-3.5	30 % 1.5 g's	YES	
			19.8	10	-49.5 % 9.8 g's	NO	
			20.4	11.2	-45 % 9.2 g's	NO	
		1.59	1.78	11% 0.2	YES		

⁽¹⁾ The value was visually assessed from the image sequence of the test.

⁽²⁾ The severity indexes were computed considering the curves preprocessed by RSVVP on the time interval [0 sec, 0.2 sec].

Table C3-5. Roadside Safety Phenomena Importance Ranking Table (continued).

Evaluation Criteria			Known Result	Analysis Result	Relative Diff. (%)	Agree?
Vehicle Trajectory	L	The occupant impact velocity in the longitudinal direction should not exceed 40 ft/sec and the occupant ridedown acceleration in the longitudinal direction should not exceed 20 G's.				
	M1	The exit angle from the test article preferable should be less than 60 percent of test impact angle, measured at the time of vehicle loss of contact with test device.	≈10 ⁽¹⁾ Yes	0° ⁽²⁾ Yes		YES
	M2	The relative difference in the exit angle at loss of contact is less than 20 percent or 5 degrees	10	0° ⁽²⁾	-100% 10°	NO
	M3	The relative difference in the exit velocity at loss of contact is less than 20 percent or 10 km/hr	78.8 km/h	82 ^(2,3) km/h	4% 3.2 km/hr	YES
	M4	One or more vehicle tires failed or de-beaded during the collision event (Answer Yes or No).	Yes	Yes	X	YES
	M5	One or more tires separated from the vehicle (Answer Yes or No).	No	No	X	YES
	N	Vehicle trajectory went behind the test article (Answer Yes or No)			X	

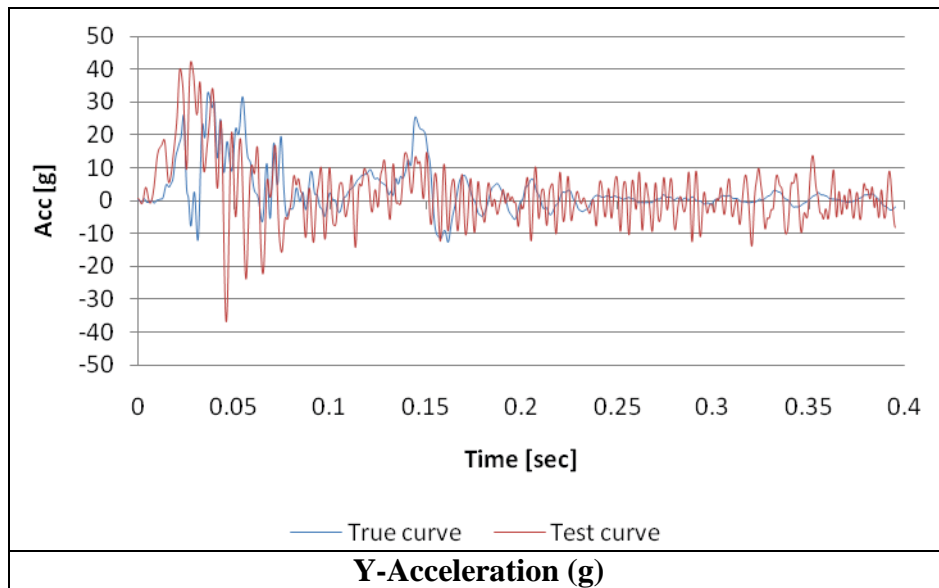
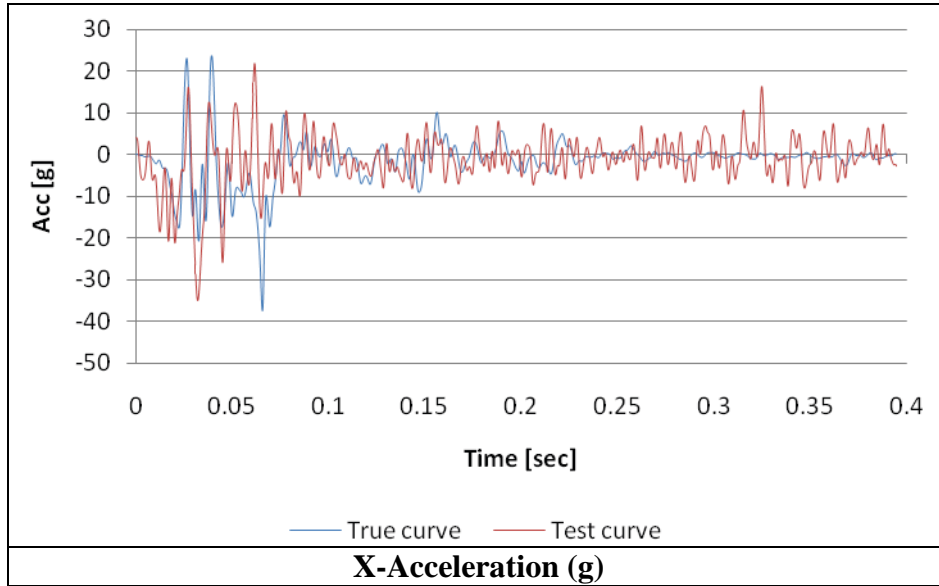
⁽¹⁾ The value was visually assessed from the image sequence of the test.

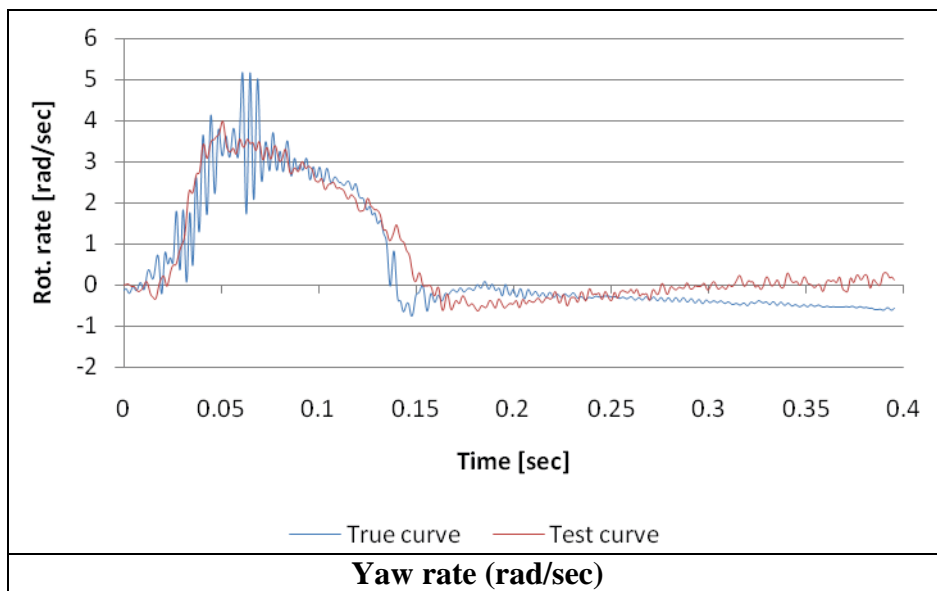
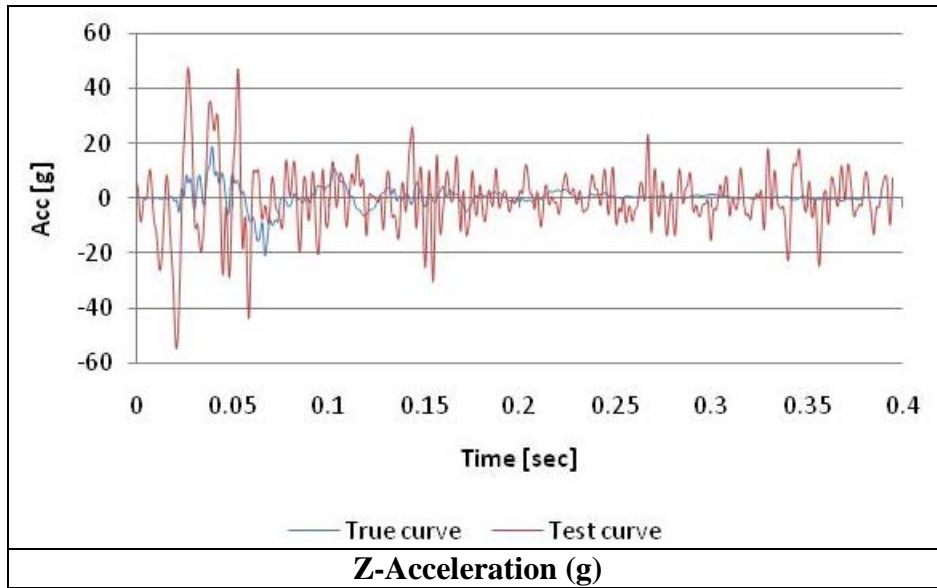
⁽²⁾ The vehicle slid along the whole length of the barrier and never lost contact.

⁽³⁾ The exit velocity was considered at the same time the vehicle lost contact w/ barrier in the experimental test (t = 0.35 sec).

The Analysis Solution (check one) passes does NOT pass all the criteria in Tables C3-5
 with exceptions as noted without exceptions .

Plot of the time histories used to evaluate the comparison metrics





APPENDIX C4: SMALL CAR STRIKING A VERTICAL RIGID WALL

VALIDATION/VERIFICATION REPORT

FOR

A EN 1317 Vehicle
(Report 350 or MASH or EN1317 Vehicle Type)

Striking a Concrete barrier
(roadside hardware type and name)

Report Date: 01/07/09

Type of Report (check one)

- Verification (known numerical solution compared to new numerical solution) or
 Validation (full-scale crash test compared to a numerical solution).

General Information	Known Solution	Analysis Solution
Performing Organization	Test agency 2	Politecnico di Milano
Test/Run Number:	ROU/ROB-02/664	GM_R5 Round Robin
Vehicle:	Peugeot 205	Geo Metro (GM_R5)
Impact Conditions		
Vehicle Mass:	862 kg	860 kg
Speed:	100.4 km/h	100 km/h
Angle:	20deg	20 deg.
Impact Point:	10.7 m from beginning	4.5 m from the beginning

Composite Validation/Verification Score

List the Report 350/MASH or EN1317 Test Number		
Step I	Did all solution verification criteria in Table C4-1 pass?	YES
Step II	Do all the time history evaluation scores from Table C4-2 result in a satisfactory comparison (i.e., the comparison passes the criterion)? If all the values in Table C4-2 did not pass, did the weighted procedure shown in Table C4-3 result in an acceptable comparison. If all the criteria in Table C4-2 pass, enter “yes.” If all the criteria in Table C4-2 did not pass but Table C4-3 resulted in a passing score, enter “yes.”	YES
Step III	All the criteria in Table C4-5 passed	NO
	Are the results of Steps I through III all affirmative (i.e., YES)? If all three steps result in a “YES” answer, the comparison can be considered validated or verified. If one of the steps results in a negative response, the result cannot be considered validated or verified.	NO

The analysis solution (check one) is is NOT verified/validated against the known solution.

PART I: BASIC INFORMATION

- 1. What type of roadside hardware is being evaluated (check one)?
 - Longitudinal barrier or transition
 - Terminal or crash cushion
 - Breakaway support or work zone traffic control device
 - Truck-mounted attenuator
 - Other hardware: _____

- 2. What test guidelines were used to perform the full-scale crash test (check one)?
 - NCHRP Report 350
 - MASH
 - EN1317
 - Other: _____

- 3. Indicate the test level and number being evaluated (fill in the blank). TB-11

- 4. Indicate the vehicle type appropriate for the test level and number indicated in item 3 according to the testing guidelines indicated in item 2.

NCHRP Report 350/MASH

- 700C 820C 1100C
- 2000P 2270P
- 8000S 10000S
- 36000V
- 36000T

EN1317

- Car (900 kg) Car (1300 kg) Car (1500 kg)
- Rigid HGV (10 ton) Rigid HGV (16 ton) Rigid HGV (30 ton)
- Bus (13 ton)
- Articulated HGV (38 ton)

PART II: ANALYSIS SOLUTION VERIFICATION

Table C4-1. Analysis Solution Verification Table.

Verification Evaluation Criteria	Change (%)	Pass?
Total energy of the analysis solution (i.e., kinetic, potential, contact, etc.) must not vary more than 10 percent from the beginning of the run to the end of the run.	-1	YES
Hourglass Energy of the analysis solution at the end of the run is less than five percent of the total initial energy at the beginning of the run.	0.5	YES
The part/material with the highest amount of hourglass energy at any time during the run is less than five percent of the total initial energy at the beginning of the run.	0.5	YES
Mass added to the total model is less than five percent of the total model mass at the beginning of the run.	0	YES
The part/material with the most mass added had less than 10 percent of its initial mass added.	0	YES
The moving parts/materials in the model have less than five percent of mass added to the initial moving mass of the model.	0	YES
There are no shooting nodes in the solution?	No	YES
There are no solid elements with negative volumes?	No	YES

The Analysis Solution (check one) passes does NOT pass all the criteria in Table C4-1
 with without exceptions as noted.

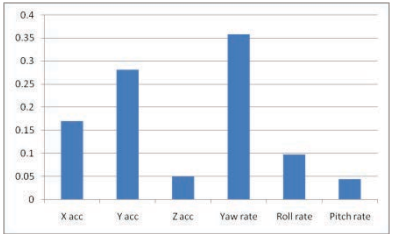
PART III: TIME HISTORY EVALUATION TABLE

Table C4-2. Roadside Safety Validation Metrics Rating Table – Time History Comparisons (single channel option).

Evaluation Criteria							Time interval [0 sec; 0.4 sec]			
O	Sprague-Geer Metrics List all the data channels being compared. Calculate the M and P metrics using RSVVP and enter the results. Values less than or equal to 40 are acceptable.						M [%]	P [%]	Pass?	
	RSVVP Curve Preprocessing Options									
		Filter Option	Sync. Option	Shift		Drift				
				True Curve	Test Curve	True Curve	Test Curve			
	X acceleration	CFC 180	Min. area of Residuals	N	N	N	N	6.8	41.3	N
	Y acceleration	CFC 180	Min. area of Residuals	N	N	N	N	12.3	39.7	Y
	Z acceleration	CFC 180	Min. area of Residuals	N	N	N	N	181.3	47.8	N
Yaw rate	CFC 180	Min. area of Residuals	N	N	N	N	16.4	12	Y	
Roll rate	CFC 180	Min. area of Residuals	N	N	N	N	46.2	50.1	N	
Pitch rate	CFC 180	Min. area of Residuals	N	N	N	N	38.7	40.2	N	
P	ANOVA Metrics List all the data channels being compared. Calculate the ANOVA metrics using RSVVP and enter the results. Both of the following criteria must be met: <ul style="list-style-type: none"> The mean residual error must be less than five percent of the peak acceleration ($\bar{e} \leq 0.05 \cdot a_{Peak}$) and The standard deviation of the residuals must be less than 35 percent of the peak acceleration ($\sigma \leq 0.35 \cdot a_{Peak}$) 						Mean Residual [%]	Standard Deviation of Residuals [%]	Pass?	
	X acceleration/Peak						0.9	16.7	Y	
	Y acceleration/Peak						-1	20	Y	
	Z acceleration/Peak						-3	53	N	
	Yaw rate						-11	11.8	N	
	Roll rate						6.2	36.7	N	
Pitch rate						-0.11	16.1	Y		

The Analysis Solution (check one) passes does NOT pass all the criteria in Table C4-2.

Table C4-3. Roadside Safety Validation Metrics Rating Table – Time History Comparisons (Multiple channels).

Evaluation Criteria (time interval [0 sec; 0.4 sec])					
Channels (Select which was used)					
<input checked="" type="checkbox"/> X Acceleration	<input checked="" type="checkbox"/> Y Acceleration	<input checked="" type="checkbox"/> Z Acceleration			
<input checked="" type="checkbox"/> Roll rate	<input checked="" type="checkbox"/> Pitch rate	<input checked="" type="checkbox"/> Yaw rate			
Multi-Channel Weights -Area (II) Method-	X Channel – 0.17 Y Channel – 0.28 Z Channel – 0.05 Yaw rate Channel – 0.36 Roll rate Channel – 0.10 Pitch rate Channel – 0.04				
	ANOVA Metrics Both of the following criteria must be met: <ul style="list-style-type: none"> The mean residual error must be less than five percent of the peak acceleration ($\bar{e} \leq 0.05 \cdot a_{Peak}$) The standard deviation of the residuals must be less than 35 percent of the peak acceleration ($\sigma \leq 0.35 \cdot a_{Peak}$) 		Mean Residual [%] -3.7	Standard Deviation of Residuals [%] 19.6	
O	Sprague-Geer Metrics Values less or equal to 40 are acceptable.		M [%] 25.7	P [%] 31.5	Pass? Y
P	ANOVA Metrics Both of the following criteria must be met: <ul style="list-style-type: none"> The mean residual error must be less than five percent of the peak acceleration ($\bar{e} \leq 0.05 \cdot a_{Peak}$) The standard deviation of the residuals must be less than 35 percent of the peak acceleration ($\sigma \leq 0.35 \cdot a_{Peak}$) 		Mean Residual [%] -3.7	Standard Deviation of Residuals [%] 19.6	Pass? Y

The Analysis Solution (check one) passes does NOT pass all the criteria in Table C4-3.

PART IV: PHENOMENA IMPORTANCE RANKING TABLE

Table C4-4. Evaluation Criteria Test Applicability Table.

Evaluation Factors	Evaluation Criteria	Applicable Tests										
Structural Adequacy	A Test article should contain and redirect the vehicle; the vehicle should not penetrate, under-ride, or override the installation although controlled lateral deflection of the test article is acceptable.	10, 11, 12, 20, 21, 22, 35, 36, 37, 38										
	B The test article should readily activate in a predictable manner by breaking away, fracturing or yielding.	60, 61, 70, 71, 80, 81										
	C Acceptable test article performance may be by redirection, controlled penetration or controlled stopping of the vehicle.	30, 31,, 32, 33, 34, 39, 40, 41, 42, 43, 44, 50, 51, 52, 53										
Occupant Risk	D Detached elements, fragments or other debris from the test article should not penetrate or show potential for penetrating the occupant compartment, or present an undue hazard to other traffic, pedestrians or personnel in a work zone.	All										
	E Detached elements, fragments or other debris from the test article, or vehicular damage should not block the driver’s vision or otherwise cause the driver to lose control of the vehicle. (Answer Yes or No)	70, 71										
	F The vehicle should remain upright during and after the collision although moderate roll, pitching and yawing are acceptable.	All except those listed in criterion G										
	G It is preferable, although not essential, that the vehicle remain upright during and after collision.	12, 22 (for test level 1 – 30, 31, 32, 33, 34, 35, 36, 37, 38, 39, 40, 41, 42, 43, 44)										
	H	Occupant impact velocities should satisfy the following:	10, 20, 30,31, 32, 33, 34, 36, 40, 41, 42, 43, 50, 51, 52, 53, 80, 81									
		<table border="1" style="width: 100%; border-collapse: collapse;"> <thead> <tr> <th colspan="3" style="text-align: center;">Occupant Impact Velocity Limits (m/s)</th> </tr> <tr> <th style="width: 33%;">Component</th> <th style="width: 33%;">Preferred</th> <th style="width: 33%;">Maximum</th> </tr> </thead> <tbody> <tr> <td>Longitudinal and Lateral</td> <td style="text-align: center;">9</td> <td style="text-align: center;">12</td> </tr> <tr> <td>Longitudinal</td> <td style="text-align: center;">3</td> <td style="text-align: center;">5</td> </tr> </tbody> </table>		Occupant Impact Velocity Limits (m/s)			Component	Preferred	Maximum	Longitudinal and Lateral	9	12
Occupant Impact Velocity Limits (m/s)												
Component	Preferred	Maximum										
Longitudinal and Lateral	9	12										
Longitudinal	3	5										
I	Occupant ridedown accelerations should satisfy the following:	10, 20, 30,31, 32, 33, 34, 36, 40, 41, 42, 43, 50, 51, 52, 53, 60, 61, 70, 71, 80, 81										
	<table border="1" style="width: 100%; border-collapse: collapse;"> <thead> <tr> <th colspan="3" style="text-align: center;">Occupant Ridedown Acceleration Limits (g’s)</th> </tr> <tr> <th style="width: 33%;">Component</th> <th style="width: 33%;">Preferred</th> <th style="width: 33%;">Maximum</th> </tr> </thead> <tbody> <tr> <td>Longitudinal and Lateral</td> <td style="text-align: center;">15</td> <td style="text-align: center;">20</td> </tr> </tbody> </table>		Occupant Ridedown Acceleration Limits (g’s)			Component	Preferred	Maximum	Longitudinal and Lateral	15	20	
Occupant Ridedown Acceleration Limits (g’s)												
Component	Preferred	Maximum										
Longitudinal and Lateral	15	20										
Vehicle Trajectory	L The occupant impact velocity in the longitudinal direction should not exceed 40 ft/sec and the occupant ride-down acceleration in the longitudinal direction should not exceed 20 G’s.	11,21, 35, 37, 38, 39										
	M The exit angle from the test article preferable should be less than 60 percent of test impact angle, measured at the time of vehicle loss of contact with test device.	10, 11, 12, 20, 21, 22, 35, 36, 37, 38, 39										
	N Vehicle trajectory behind the test article is acceptable.	30, 31, 32, 33, 34, 39, 42, 43, 44, 60, 61, 70, 71, 80, 81										

Table C4-5. Roadside Safety Phenomena Importance Ranking Table.

Evaluation Criteria			Known Result	Analysis Result	Difference Relative/ Absolute	Agree?	
Structural Adequacy	A	A1	Test article should contain and redirect the vehicle; the vehicle should not penetrate, under-ride, or override the installation although controlled lateral deflection of the test article is acceptable. (Answer Yes or No)	Yes	Yes		YES
		A2	Maximum dynamic deflection: - Relative difference is less than 20 percent or - Absolute difference is less than 0.15 m	0	0	0	YES
		A3	Length of vehicle-barrier contact: - Relative difference is less than 20 percent or - Absolute difference is less than 2 m	3 m	10 m ⁽¹⁾	233% 7 m	NO
		A4	The relative difference in the number of broken or significantly bent posts is less than 20 percent.	0	0	0 % 0	YES
		A5	The rail element did not rupture or fail (Answer Yes or No)	Yes	Yes		YES
		A6	There were no failures of connector elements (Answer Yes or No).	Yes	Yes		YES
		A7	There was no significant snagging between the vehicle wheels and barrier elements (Answer Yes or No).	Yes	Yes		YES
		A8	There was no significant snagging between vehicle body components and barrier elements (Answer Yes or No).	Yes	Yes		YES
	B	B1	The test article should readily activate in a predictable manner by breaking away, fracturing or yielding. (Answer Yes or No)				
		C1	Acceptable test article performance may be by redirection, controlled penetration or controlled stopping of the vehicle. (Answer Yes or No)				
	C	C2	The relative difference in maximum system stroke is less than 20 percent.				
		C3	The relative difference in the number of broken or significantly bent posts is less than 20 percent.				
		C4	The rail element did not rupture or tear (Answer Yes or No).				
		C5	There were no failures of connector elements (Answer Yes or No).				

⁽¹⁾ The vehicle slid along the barrier due to collapse of the steering system (front right wheel turned towards the barrier).

Table C4-5. Roadside Safety Phenomena Importance Ranking Table (continued).

Evaluation Criteria		Known Result	Analysis Result	Difference Relative/Absolute	Agree?			
Occupant Risk	D	Detached elements, fragments or other debris from the test article should not penetrate or show potential for penetrating the occupant compartment, or present an undue hazard to other traffic, pedestrians or personnel in a work zone. (Answer Yes or No)	Pass	Pass		YES		
	E	Detached elements, fragments or other debris from the test article, or vehicular damage should not block the driver's vision or otherwise cause the driver to lose control of the vehicle. (Answer Yes or No)						
	F1	The vehicle should remain upright during and after the collision although moderate roll, pitching and yawing are acceptable. (Answer Pass or Not pass)	Pass	Pass		YES		
	F	F2	Maximum roll of the vehicle: - Relative difference is less than 20 percent or - Absolute difference is less than 5 degrees.	3° ⁽¹⁾	2.5°	20% 0.5°	YES	
		F3	Maximum pitch of the vehicle is: - Relative difference is less than 20 percent or - Absolute difference is less than 5 degrees.	4.5°	3°	-33% 1.5°	YES	
		F4	Maximum yaw of the vehicle is: - Relative difference is less than 20 percent or - Absolute difference is less than 5 degrees.	25°	17.5°	-30% 7.5°	NO	
		H	H1	Occupant impact velocities: - Relative difference is less than 20 percent or - Absolute difference is less than 2 m/s. ⁽²⁾ :	4.8	3.3	31.2% 1.5 m/s	YES
	<ul style="list-style-type: none"> Longitudinal OIV (m/s) Lateral OIV (m/s) 			-8	-7.2	-10% 0.8 m/s	YES	
	H2		<ul style="list-style-type: none"> Longitudinal OIV 	4.8	3.3	31.2% 1.5 m/s	NO	
	H3		<ul style="list-style-type: none"> THIV (m/s) 	8.1	7.6	-6.1% 0.5 m/s	YES	
	I		Occupant accelerations: - Relative difference is less than 20 percent or - Absolute difference is less than 4 g's. ⁽²⁾ :					
				<ul style="list-style-type: none"> Longitudinal ORA (g) 	-3.7	-3.5	-5.4% 0.2 g's	YES
				<ul style="list-style-type: none"> Lateral ORA (g) 	14.3	10	-30% 4.3 g's	NO
				<ul style="list-style-type: none"> PHD (g) 	15.2	11.2	-26% 4 g's	NO
<ul style="list-style-type: none"> ASI 				1.93	1.78	-7% 0.15 g's	YES	

⁽¹⁾ The value was visually assessed from the image sequence of the test.

⁽²⁾ The severity indexes were computed considering the curves preprocessed by RSVVP on the time interval [0 sec, 0.2 sec].

Table C4-5. Roadside Safety Phenomena Importance Ranking Table (continued).

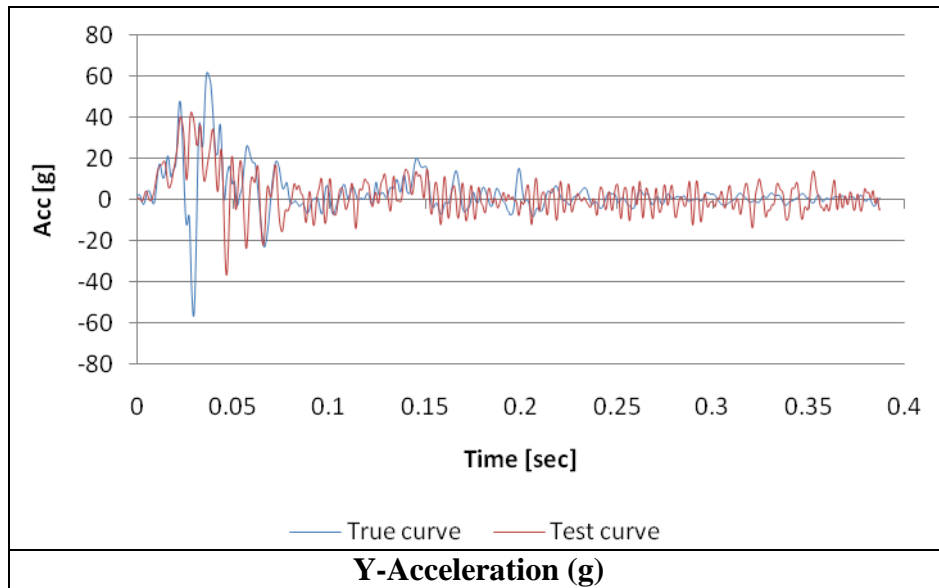
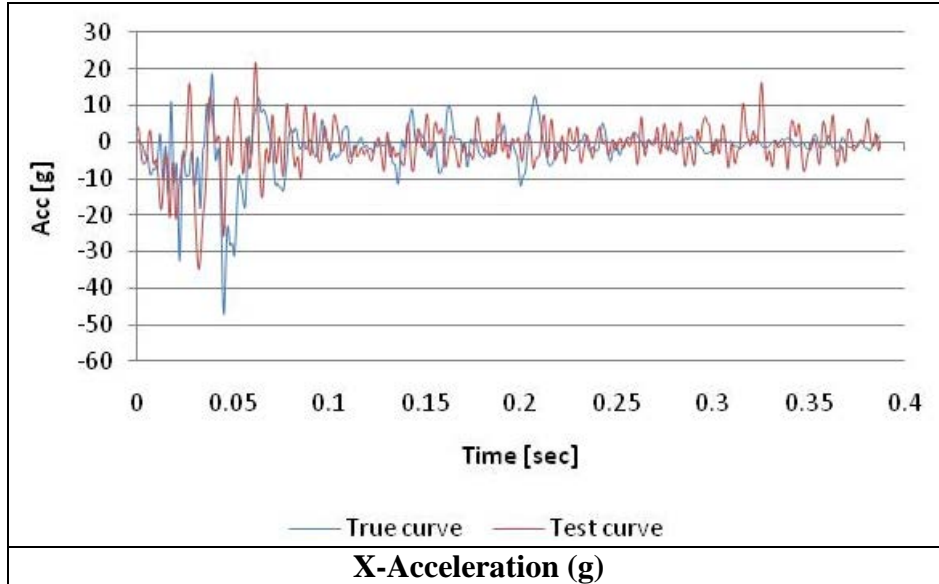
Evaluation Criteria		Known Result	Analysis Result	Difference Relative/ Absolute	Agree?	
Vehicle Trajectory	L	The occupant impact velocity in the longitudinal direction should not exceed 40 ft/sec and the occupant ridedown acceleration in the longitudinal direction should not exceed 20 G's.				
	M1	The exit angle from the test article preferable should be less than 60 percent of test impact angle, measured at the time of vehicle loss of contact with test device.	≈5.5° (27.5%) Yes	0° ⁽¹⁾ (0%) Yes		YES
	M2	Exit angle at loss of contact: - Relative difference is less than 20 percent or - Absolute difference is less than 5 degrees.	5.5°	0° ⁽¹⁾	-100% 5.5	NO
	M3	Exit velocity at loss of contact: - Relative difference is less than 20 percent or - Absolute difference is less than 10 m/s.	78.4 km/h	82 ^(1,2) km/h	4.6% 3.6 m/s	YES
	M4	One or more vehicle tires failed or de-beaded during the collision event (Answer Yes or No).	Yes	Yes	X	YES
	M5	One or more tires separated from the vehicle (Answer Yes or No).	No	No	X	YES
	N	Vehicle trajectory went behind the test article (Answer Yes or No)			X	

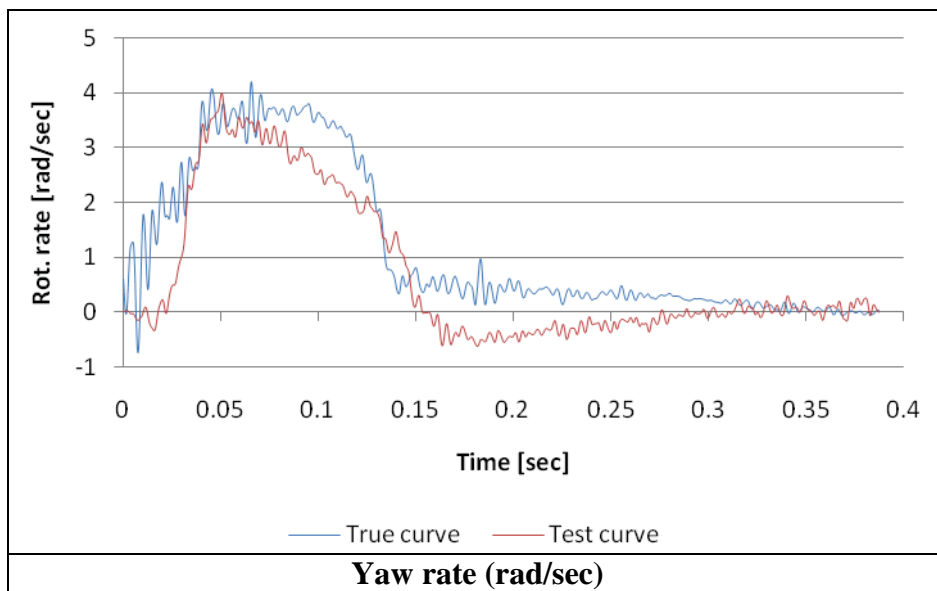
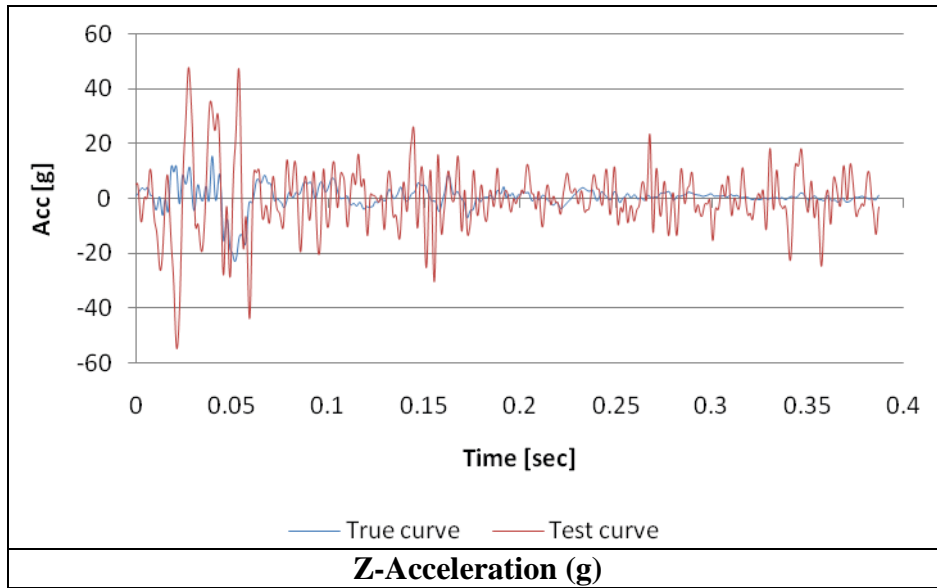
⁽¹⁾ The vehicle slid along the whole length of the barrier and never lost contact.

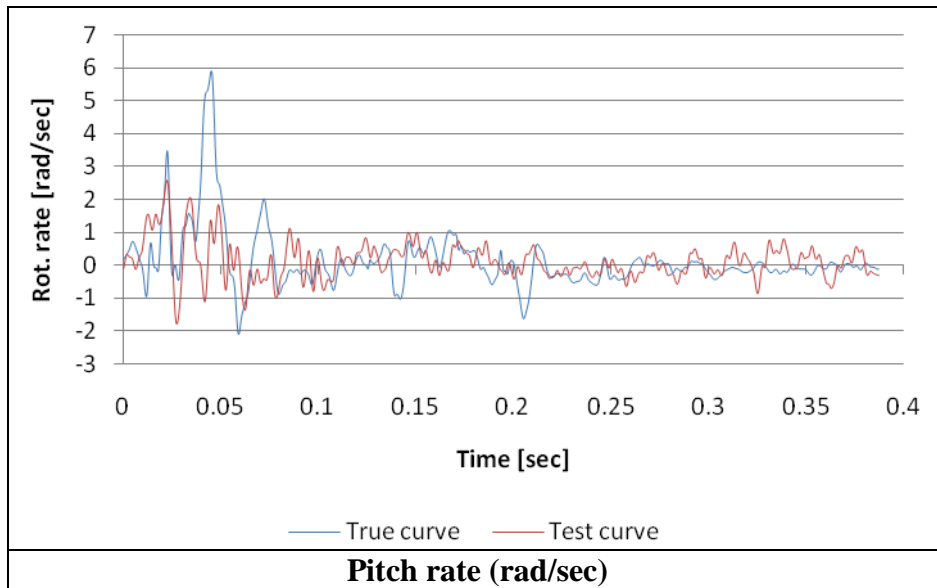
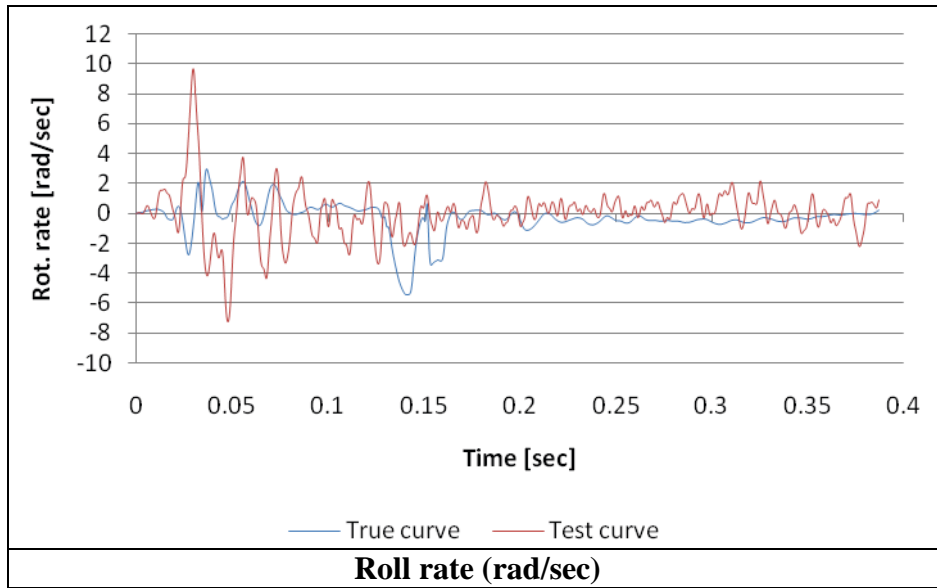
⁽²⁾ The exit velocity was considered at the same time the vehicle lost contact w/ barrier in the experimental test (t = 0.35 sec).

The Analysis Solution (check one) passes does NOT pass all the criteria in Tables C4-5
 with exceptions as noted without exceptions .

Plots of the time histories used to evaluate the comparison metrics







APPENDIX C5: TRACTOR TRAILER TRUCK STRIKING A 42" TALL RIGID CONCRETE MEDIAN BARRIER

VALIDATION/VERIFICATION REPORT

FOR

A Tractor-Semitrailer Model (36000V)

(Report 350 Vehicle Type)

Striking a 42-inch tall "rigid" concrete median barrier

(roadside hardware type and name)

Report Date: 11-30-2009

Type of Report (check one)

Verification (known numerical solution compared to new numerical solution) or

Validation (full-scale crash test compared to a numerical solution).

General Information	Known Solution	Analysis Solution
Performing Organization	MwRSF	WPI/Battelle
Test/Run Number:	TL5CMB-2	TT090518_RUN1_200ms-approach-SP
Vehicle:	1991 White/GMC Tractor 1988 Pines 48-ft Trailer	01aTrac_Day_v1a_090506.k 02aSemiTrailer48_090520.k
Impact Conditions		
Vehicle Mass:	36,154 kg	36,200 kg
Speed:	84.9 km/hr	84.9 km/hr
Angle:	15.5 degrees	15.5 degrees
Impact Point:		

Composite Validation/Verification Score

List the Report 350/MASH or EN1317 Test Number		
Step I	Did all solution verification criteria in Table C5-1 pass?	Y?
Step II	Do all the time history evaluation scores from Table C5-2 result in a satisfactory comparison (i.e., the comparison passes the criterion)? If all the values in Table C5-2 did not pass, did the weighted procedure shown in Table C5-3 result in an acceptable comparison. If all the criteria in Table C5-2 pass, enter "yes." If all the criteria in Table C5-2 did not pass but Table C5-3 resulted in a passing score, enter "yes."	Y
Step III	All the criteria in Table C5-5 passed	Y
	Are the results of Steps I through III all affirmative (i.e., YES)? If all three steps result in a "YES" answer, the comparison can be considered validated or verified. If one of the steps results in a negative response, the result cannot be considered validated or verified.	Y?

The analysis solution (check one) is is NOT verified/validated against the known solution.

PART I: BASIC INFORMATION

- 1. What type of roadside hardware is being evaluated (check one)?
 - Longitudinal barrier or transition
 - Terminal or crash cushion
 - Breakaway support or work zone traffic control device
 - Truck-mounted attenuator
 - Other hardware: _____

- 2. What test guidelines were used to perform the full-scale crash test (check one)?
 - NCHRP Report 350
 - MASH
 - EN1317
 - Other: _____

- 3. Indicate the test level and number being evaluated (fill in the blank). 5-12

- 4. Indicate the vehicle type appropriate for the test level and number indicated in item 3 according to the testing guidelines indicated in item 2.

NCHRP Report 350/MASH

- 700C 820C 1100C
- 2000P 2270P
- 8000S 10000S
- 36000V
- 36000T

EN1317

- Car (900 kg) Car (1300 kg) Car (1500 kg)
- Rigid HGV (10 ton) Rigid HGV (16 ton) Rigid HGV (30 ton)
- Bus (13 ton)
- Articulated HGV (38 ton)

PART II: ANALYSIS SOLUTION VERIFICATION

Table C5-1. Analysis Solution Verification Table.

Verification Evaluation Criteria	Change (%)	Pass?
Total Energy of the analysis solution (i.e., kinetic, potential, contact, etc.) must not vary more than 10 percent from the beginning of the run to the end of the run. <ul style="list-style-type: none"> Sliding Interface Energy was the source of the increase in total energy 	10	YES
Hourglass Energy of the analysis solution at the end of the run is less than 5 percent of the total initial energy at the beginning of the run.	0.1	YES
Hourglass Energy of the analysis solution at the end of the run is less than <i>ten percent</i> of the total <i>internal energy</i> at the <i>end</i> of the run.	0.6	Yes
The part/material with the highest amount of hourglass energy at any time during the run is less than five percent of the total initial energy at the beginning of the run.	0.02	Yes
Mass added to the total model is less than five percent of the total model mass at the beginning of the run.	0.0	Yes
The part/material with the most mass added had less than 10 percent of its initial mass added. <ul style="list-style-type: none"> - Weld element connecting trailer side panels to vertical posts - 200 kg (added) /50 kg (initial) 	400	NO*
The moving parts/materials in the model have less than five percent of mass added to the initial moving mass of the model.	0.0	Yes
There are no shooting nodes in the solution?	Yes	Yes
There are no solid elements with negative volumes?	Yes	Yes

* Part 7803 are weld elements used to connect the trailer’s outer side panels to the vertical support posts. These connector elements are relatively “rigid” and the mass added is considered insignificant to the overall mass of the parts to which they connect.

The Analysis Solution (check one) passes does NOT pass all the criteria in Table C5-1
 with without exceptions noted.

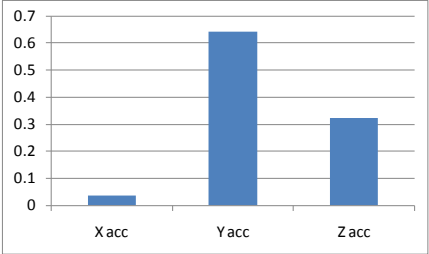
PART III: TIME HISTORY EVALUATION TABLE

Table C5-2. Roadside Safety Validation Metrics Rating Table – Time History Comparisons (single channel option).

Evaluation Criteria							Time interval [0 sec; 1.54 sec]					
O	Sprague-Geer Metrics List all the data channels being compared. Calculate the M and P metrics using RSVVP and enter the results. Values less than or equal to 40 are acceptable.						M	P	Pass?			
	RSVVP Curve Preprocessing Options											
		Filter Option	Sync. Option	Shift		Drift						
				True Curve	Test Curve	True Curve				Test Curve		
	X acceleration	CFC 180	Min. area of Residuals	N	N	N				N	12.4	48.5
Y acceleration	CFC 180	Min. area of Residuals	N	N	N	N	13.5	31.4	Y			
Z acceleration	CFC 180	Min. area of Residuals	N	N	N	N	12.8	47.1	N			
P	ANOVA Metrics List all the data channels being compared. Calculate the ANOVA metrics using RSVVP and enter the results. Both of the following criteria must be met: <ul style="list-style-type: none"> The mean residual error must be less than five percent of the peak acceleration ($\bar{e} \leq 0.05 \cdot a_{Peak}$) and The standard deviation of the residuals must be less than 35 percent of the peak acceleration ($\sigma \leq 0.35 \cdot a_{Peak}$) 						Mean Residual	Standard Deviation of Residuals	Pass?			
	X acceleration/Peak									0.02	0.10	Y
	Y acceleration/Peak									0.0	0.08	Y
	Z acceleration/Peak									0.0	0.14	Y

The Analysis Solution (check one) passes does NOT pass all the criteria in Table C5-2.

Table C5-3. Roadside Safety Validation Metrics Rating Table – Time History Comparisons (multi-channel option using Area II method).

Evaluation Criteria (time interval [0 sec; 1.54 sec])						
Channels (Select which was used)						
<input checked="" type="checkbox"/> X Acceleration	<input checked="" type="checkbox"/> Y Acceleration	<input checked="" type="checkbox"/> Z Acceleration				
<input type="checkbox"/> Roll rate	<input type="checkbox"/> Pitch rate	<input type="checkbox"/> Yaw rate				
Multi-Channel Weights -Area (II) Method-	X Channel – 0.038 Y Channel – 0.640 Z Channel – 0.322					
	O <i>Sprague-Geer Metrics</i> Values less or equal to 40 are acceptable.			M	P	Pass?
			13.2	37.1	Y	
P <i>ANOVA Metrics</i> Both of the following criteria must be met:	<ul style="list-style-type: none"> The mean residual error must be less than five percent of the peak acceleration ($\bar{e} \leq 0.05 \cdot a_{peak}$) The standard deviation of the residuals must be less than 35 percent of the peak acceleration ($\sigma \leq 0.35 \cdot a_{peak}$) 			Mean Residual	Standard Deviation of Residuals	Pass?
				0.00	0.10	Y

The Analysis Solution (check one) passes does NOT pass all the criteria in Table C5-3.

PART IV: PHENOMENA IMPORTANCE RANKING TABLE

Table C5-4. Evaluation Criteria Test Applicability Table.

Evaluation Factors	Evaluation Criteria	Applicable Tests															
Structural Adequacy	A Test article should contain and redirect the vehicle; the vehicle should not penetrate, under-ride, or override the installation although controlled lateral deflection of the test article is acceptable.	10, 11, 12 , 20, 21, 22, 35, 36, 37, 38															
	B The test article should readily activate in a predictable manner by breaking away, fracturing or yielding.	60, 61, 70, 71, 80, 81															
	C Acceptable test article performance may be by redirection, controlled penetration or controlled stopping of the vehicle.	30, 31,, 32, 33, 34, 39, 40, 41, 42, 43, 44, 50, 51, 52, 53															
Occupant Risk	D Detached elements, fragments or other debris from the test article should not penetrate or show potential for penetrating the occupant compartment, or present an undue hazard to other traffic, pedestrians or personnel in a work zone.	All															
	E Detached elements, fragments or other debris from the test article, or vehicular damage should not block the driver’s vision or otherwise cause the driver to lose control of the vehicle. (Answer Yes or No)	70, 71															
	F The vehicle should remain upright during and after the collision although moderate roll, pitching and yawing are acceptable.	All except those listed in criterion G															
	G It is preferable, although not essential, that the vehicle remain upright during and after collision.	12 , 22 (for test level 1 – 30, 31, 32, 33, 34, 35, 36, 37, 38, 39, 40, 41, 42, 43, 44)															
	H <table border="1" data-bbox="396 1094 1040 1297"> <tr> <td colspan="3" style="text-align: center;">Occupant impact velocities should satisfy the following:</td> </tr> <tr> <td colspan="3" style="text-align: center;">Occupant Impact Velocity Limits (ft/s)</td> </tr> <tr> <td style="text-align: center;">Component</td> <td style="text-align: center;">Preferred</td> <td style="text-align: center;">Maximum</td> </tr> <tr> <td style="text-align: center;">Longitudinal and Lateral</td> <td style="text-align: center;">30</td> <td style="text-align: center;">40</td> </tr> <tr> <td style="text-align: center;">Longitudinal</td> <td style="text-align: center;">10</td> <td style="text-align: center;">15</td> </tr> </table>	Occupant impact velocities should satisfy the following:			Occupant Impact Velocity Limits (ft/s)			Component	Preferred	Maximum	Longitudinal and Lateral	30	40	Longitudinal	10	15	10, 20, 30,31, 32, 33, 34, 36, 40, 41, 42, 43, 50, 51, 52, 53, 80, 81
		Occupant impact velocities should satisfy the following:															
		Occupant Impact Velocity Limits (ft/s)															
Component	Preferred	Maximum															
Longitudinal and Lateral	30	40															
Longitudinal	10	15															
I <table border="1" data-bbox="396 1297 1040 1465"> <tr> <td colspan="3" style="text-align: center;">Occupant ridedown accelerations should satisfy the following:</td> </tr> <tr> <td colspan="3" style="text-align: center;">Occupant Ridedown Acceleration Limits (g’s)</td> </tr> <tr> <td style="text-align: center;">Component</td> <td style="text-align: center;">Preferred</td> <td style="text-align: center;">Maximum</td> </tr> <tr> <td style="text-align: center;">Longitudinal and Lateral</td> <td style="text-align: center;">15</td> <td style="text-align: center;">20</td> </tr> </table>	Occupant ridedown accelerations should satisfy the following:			Occupant Ridedown Acceleration Limits (g’s)			Component	Preferred	Maximum	Longitudinal and Lateral	15	20	10, 20, 30,31, 32, 33, 34, 36, 40, 41, 42, 43, 50, 51, 52, 53, 60, 61, 70, 71, 80, 81				
	Occupant ridedown accelerations should satisfy the following:																
Occupant Ridedown Acceleration Limits (g’s)																	
Component	Preferred	Maximum															
Longitudinal and Lateral	15	20															
Vehicle Trajectory	J The occupant impact velocity in the longitudinal direction should not exceed 40 ft/sec and the occupant ride-down acceleration in the longitudinal direction should not exceed 20 G’s.	11,21, 35, 37, 38, 39															
	M The exit angle from the test article preferable should be less than 60 percent of test impact angle, measured at the time of vehicle loss of contact with test device.	10, 11, 12 , 20, 21, 22, 35, 36, 37, 38, 39															
	N Vehicle trajectory behind the test article is acceptable.	30, 31, 32, 33, 34, 39, 42, 43, 44, 60, 61, 70, 71, 80, 81															

Table C5-5. Structural Adequacy Phenomena for the Tractor-Semitrailer Test Case.

Evaluation Criteria		Known Result	Analysis Result	Difference Relative/Absolute	Agree?
Structural Adequacy	A Test article should contain and redirect the vehicle; the vehicle should not penetrate, under-ride, or override the installation although controlled lateral deflection of the test article is acceptable. (Answer Yes or No)	Yes	Yes		YES
Occupant Risk	D Detached elements, fragments or other debris from the test article should not penetrate or show potential for penetrating the occupant compartment, or present an undue hazard to other traffic, pedestrians or personnel in a work zone. (Answer Yes or No)	Pass	Pass		N.M.*
	G1 It is preferable, although not essential, that the vehicle remain upright during and after collision. (Answer Yes or No)	Pass	Pass		YES
	G G2 The relative difference between the maximum roll of the vehicle is less than 20 percent.	42 deg.	42.8 deg.	2% 0.8 deg	YES
	G3 The relative difference between the maximum pitch of the vehicle is less than 20 percent.	Not measured			
	G4 The relative difference between the maximum yaw of the vehicle is less than 20 percent.	15.5	15.5	0	YES
Vehicle Trajectory	M1 The exit angle from the test article preferable should be less than 60 percent of test impact angle, measured at the time of vehicle loss of contact with test device.	Yes	Yes		YES
	M2 The relative difference in the yaw angle at loss of contact is less than 20 percent.	15.5 deg	15.5 deg	0	YES
	M M3 The relative difference in the exit velocity at loss of contact is less than 20 percent.				
	M4 One or more vehicle tires failed or de-beaded during the collision event (Answer Yes or No).	Yes	N/A		-
	M5 One or more tires separated from the vehicle (Answer Yes or No).	No	N/A		-

*In this analysis structural adequacy was not of interest. The barrier was modeled as rigid; therefore criterion D could not be assessed.

The Analysis Solution (check one) passes does NOT pass all the criteria in Tables C5-5 with exceptions as noted without exceptions .

Plots of the time histories used to evaluate the comparison metrics

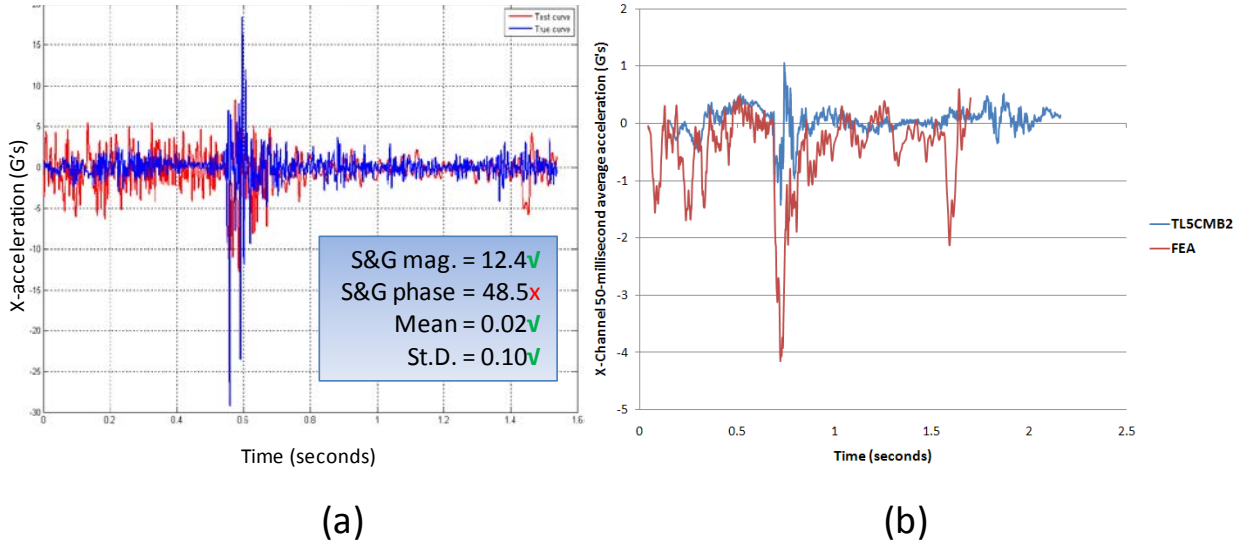


Figure C5-1. X-channel (a) acceleration-time history data used to compute metrics and (b) 50-millisecond average acceleration -time history data.

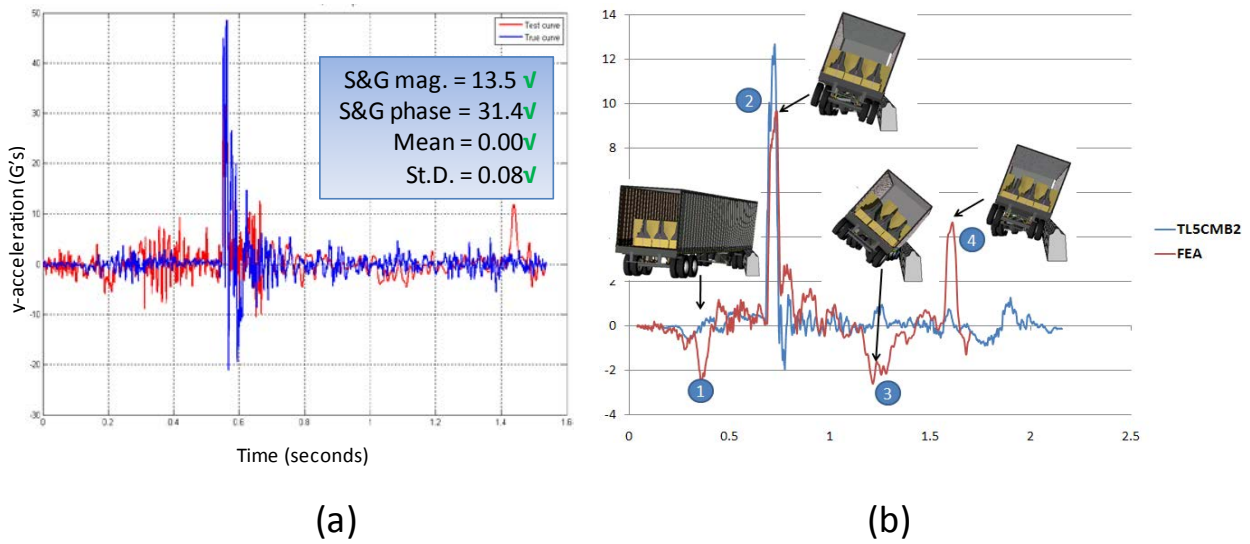


Figure C5-2. Y-channel (a) acceleration-time history data used to compute metrics and (b) 50-millisecond average acceleration -time history data.

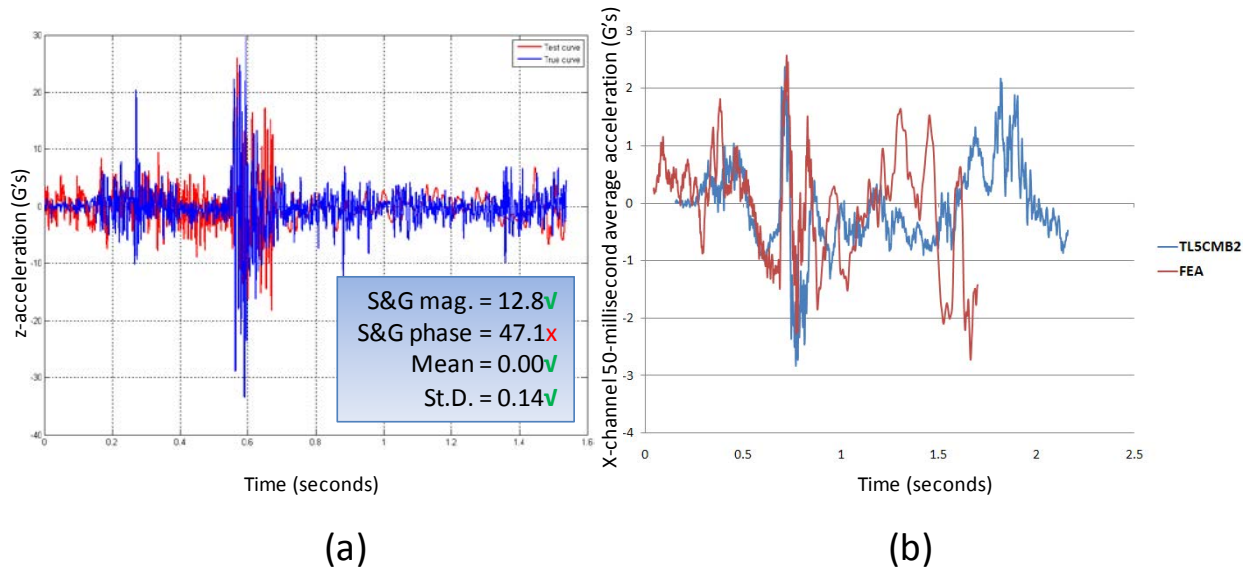


Figure C5-3. Z-channel (a) acceleration-time history data used to compute metrics and (b) 50-millisecond average acceleration -time history data.

APPENDIX C6: **ROADSIDE HARDWARE PIRT FOR A STRONG-POST W-BEAM GUARDRAIL WITH WOOD BLOCKOUTS**

Developer: Worcester Polytechnic Institute
 Worcester, MA

Model Date: January 2002

Report Date: November 30, 2009

Barrier: The modified G4(1S) guardrail with wood blockouts is composed of 12-gauge w-beam rails supported by W150x13.5 steel posts with 150x200 mm wood blockouts (*i.e.*, the type of blockout used in the G4(2W) guardrail system), as shown in Figure C6-1. The posts are spaced at 1.905 m center-to-center. The w-beam rails are spliced together using eight 16-mm diameter bolts at each splice connection, and the rails are connected to the posts and blockouts using a single bolt at each post location.



Figure C6-1: Modified G4(1S) guardrail with routed wood blockouts

Model: The guardrail model is shown in Figure C6-2. The model consists of 34.6 m of the guardrail system with thirteen 3.81-m sections of w-beam rail, twenty-six W150x13.5 steel posts spaced at 1.905 m, and twenty-six 150 x 200-mm wood blockouts. The up-stream end included the MELT guardrail terminal (validated in a previous study). The downstream anchor was modeled using nonlinear springs representative of a MELT guardrail terminal.

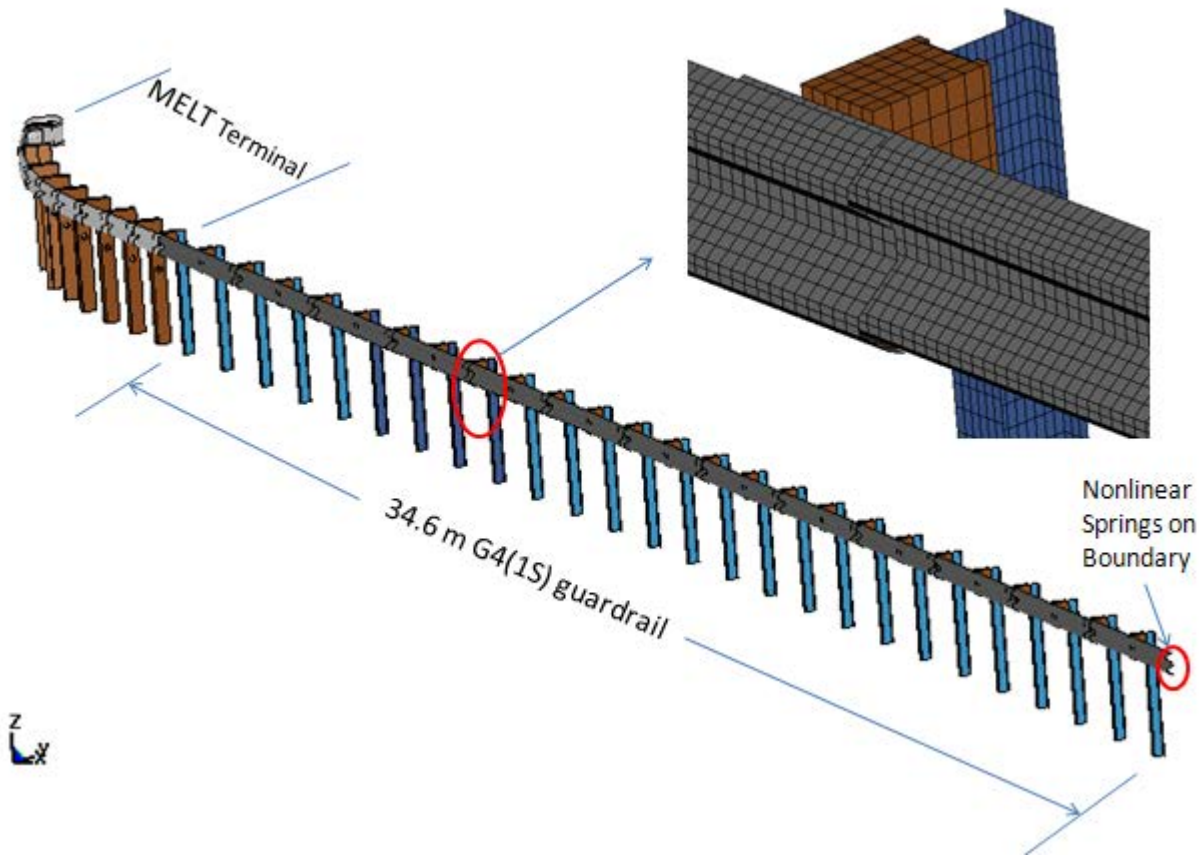


Figure C6-2. Model of the G4(1S0 Strong-Post W-Beam Guardrail Model.

Table C6-1. List of Experiments used in the PIRT Development

1. Three-point bend test of a W150x13.5 steel post about its weak axis.
2. Load-to-rupture of splice connection under quasi-static loading.
3. Pull-through of post-bolt head connection to w-beam using axial load machine.
4. Full-scale bogie impact tests of W150x13.5 posts embedded in soil with density of 1,980 kg/m³.
5. Full-scale bogie impact tests of W150x13.5 posts embedded in soil with density of 2,110 kg/m³.
6. Full-scale bogie impact tests of W150x13.5 posts embedded in soil with density of 2,240 kg/m³.

Table C6-2. Comparison Metric Evaluation Table for Phenomena #1.

PHENOMENA # 1: Plastic deformation of guardrail posts due to bending about weak axis			
<p>Sprague-Geers Metrics List all the data channels to be compared below. Using RSVVP calculate the M and P metrics comparing the experiment and the simulation. Values less than or equal to 20 are acceptable.</p>	M	P	Pass?
<ul style="list-style-type: none"> <i>Force-Displacement</i> 	3.6	1.1	Yes
<p>ANOVA Metrics List all the data channels to compare in the rows below. Use RSVVP to calculate the ANOVA metrics and enter the values below. The following criteria must be met:</p> <ul style="list-style-type: none"> The mean residual error must be less than or equal to five percent of the peak acceleration ($\bar{e} \leq 0.05 \cdot a_{Peak}$) The standard deviation of the residuals must be less than or equal to 25 percent of the peak acceleration ($\sigma \leq 0.25 \cdot a_{Peak}$) 	Mean Residual	Standard Deviation of Residuals	Pass?
<ul style="list-style-type: none"> <i>Force-Displacement</i> 	0.03	0.03	Yes
PHENOMENA			
<i>Three-Point Bend Test of W150x13.5 Post About Weak Axis</i>			

Table C6-3. Comparison Metric Evaluation Table for Phenomena #2.

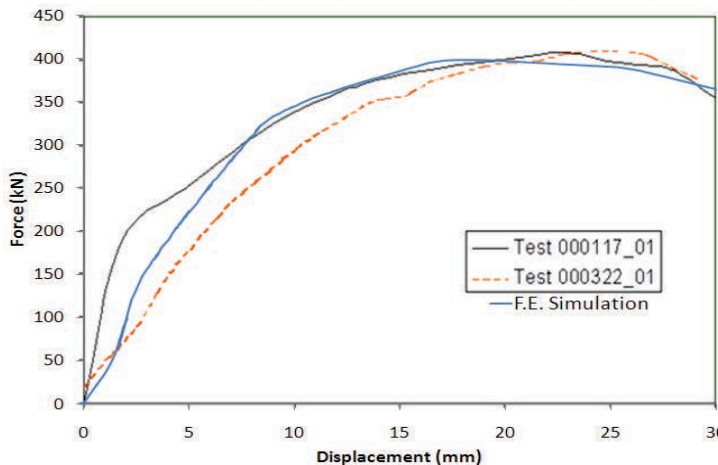
PHENOMENA # 2: Splice Rupture due to Tensile Load in W-Beam				
<p>Sprague-Geers Metrics List all the data channels to be compared below. Using RSVVP calculate the M and P metrics comparing the experiment and the simulation. Values less than or equal to 20 are acceptable.</p>		M	P	Pass?
<ul style="list-style-type: none"> • <i>Force-Displacement</i> 				
<p>ANOVA Metrics List all the data channels to compare in the rows below. Use RSVVP to calculate the ANOVA metrics and enter the values below. The following criteria must be met:</p> <ul style="list-style-type: none"> • The mean residual error must be less than or equal to five percent of the peak acceleration ($\bar{e} \leq 0.05 \cdot a_{Peak}$) • The standard deviation of the residuals must be less than or equal to 25 percent of the peak acceleration ($\sigma \leq 0.25 \cdot a_{Peak}$) 		Mean Residual	Standard Deviation of Residuals	Pass?
<ul style="list-style-type: none"> • <i>Force-Displacement</i> 				
<p>PHENOMENA <i>Load-to-rupture of splice connection under quasi-static axial loading</i></p>				
 <p>The graph plots Force (kN) on the y-axis (0 to 450) against Displacement (mm) on the x-axis (0 to 30). Three curves are shown: a solid black line for Test 000117_01, a dashed orange line for Test 000322_01, and a solid blue line for F.E. Simulation. All curves show a non-linear increase in force with displacement, peaking between 20 and 25 mm displacement at approximately 400 kN.</p>		 <p>The photograph shows a vertical test rig with a central splice connection between two W-beams. The rig is supported by large vertical columns and is used for applying axial loads to the splice.</p>		

Table C6-4. Comparison Metric Evaluation Table for Phenomena #3.

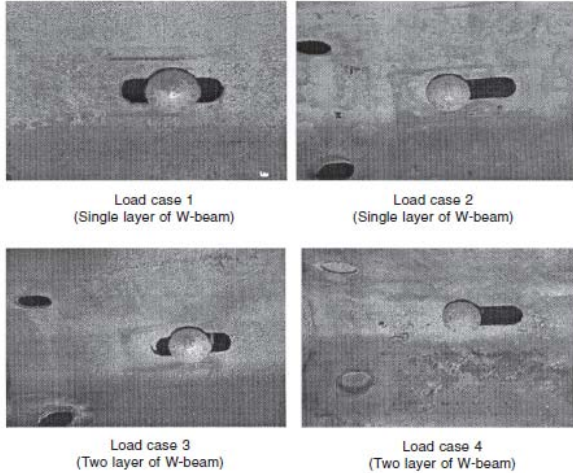
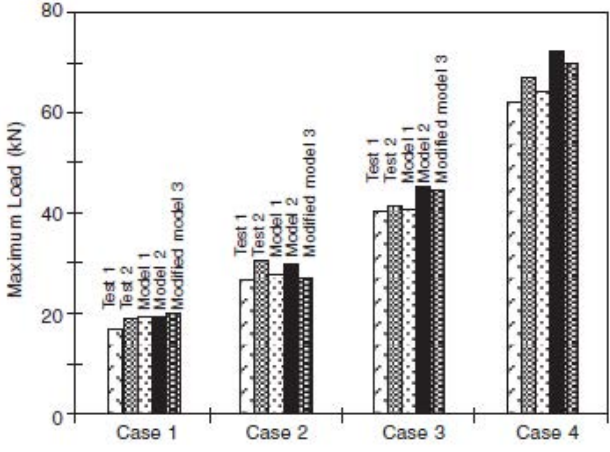
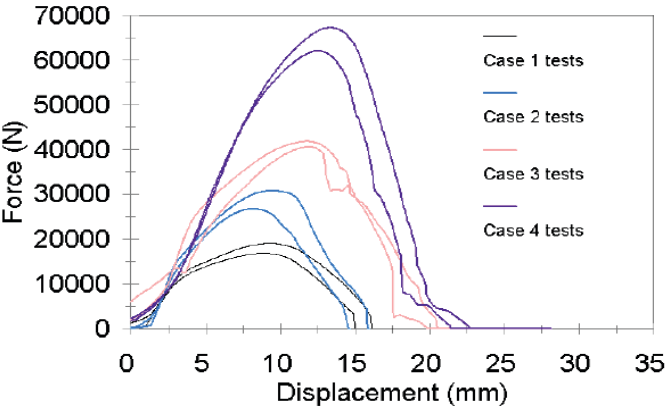
PHENOMENA # 3: Post-Bolt-Head Pull-Through and Release from W-Beam																																	
<i>Sprauge-Geers Metrics</i>																																	
List all the data channels to be compared below. Using RSVVP calculate the M and P metrics comparing the experiment and the simulation. Values less than or equal to 20 are acceptable.																																	
	M	P	Pass?																														
• Case 1																																	
• Case 2																																	
• Case 3																																	
PHENOMENA TEST CASE																																	
<i>Pull-through of post-bolt-head connection to w-beam using axial load machine</i>																																	
 <p>Load case 1 (Single layer of W-beam)</p> <p>Load case 2 (Single layer of W-beam)</p> <p>Load case 3 (Two layer of W-beam)</p> <p>Load case 4 (Two layer of W-beam)</p>		 <table border="1"> <caption>Maximum Load (kN) Data</caption> <thead> <tr> <th>Case</th> <th>Test 1</th> <th>Test 2</th> <th>Model 1</th> <th>Model 2</th> <th>Modified model 3</th> </tr> </thead> <tbody> <tr> <td>Case 1</td> <td>~18</td> <td>~18</td> <td>~18</td> <td>~18</td> <td>~18</td> </tr> <tr> <td>Case 2</td> <td>~28</td> <td>~32</td> <td>~30</td> <td>~30</td> <td>~28</td> </tr> <tr> <td>Case 3</td> <td>~42</td> <td>~40</td> <td>~40</td> <td>~40</td> <td>~40</td> </tr> <tr> <td>Case 4</td> <td>~62</td> <td>~68</td> <td>~65</td> <td>~65</td> <td>~70</td> </tr> </tbody> </table>		Case	Test 1	Test 2	Model 1	Model 2	Modified model 3	Case 1	~18	~18	~18	~18	~18	Case 2	~28	~32	~30	~30	~28	Case 3	~42	~40	~40	~40	~40	Case 4	~62	~68	~65	~65	~70
Case	Test 1	Test 2	Model 1	Model 2	Modified model 3																												
Case 1	~18	~18	~18	~18	~18																												
Case 2	~28	~32	~30	~30	~28																												
Case 3	~42	~40	~40	~40	~40																												
Case 4	~62	~68	~65	~65	~70																												
		 <table border="1"> <caption>Force (N) vs Displacement (mm) Data</caption> <thead> <tr> <th>Case</th> <th>Peak Force (N)</th> <th>Peak Displacement (mm)</th> </tr> </thead> <tbody> <tr> <td>Case 1 tests</td> <td>~18000</td> <td>~10</td> </tr> <tr> <td>Case 2 tests</td> <td>~30000</td> <td>~12</td> </tr> <tr> <td>Case 3 tests</td> <td>~40000</td> <td>~14</td> </tr> <tr> <td>Case 4 tests</td> <td>~65000</td> <td>~15</td> </tr> </tbody> </table>		Case	Peak Force (N)	Peak Displacement (mm)	Case 1 tests	~18000	~10	Case 2 tests	~30000	~12	Case 3 tests	~40000	~14	Case 4 tests	~65000	~15															
Case	Peak Force (N)	Peak Displacement (mm)																															
Case 1 tests	~18000	~10																															
Case 2 tests	~30000	~12																															
Case 3 tests	~40000	~14																															
Case 4 tests	~65000	~15																															

Table C6-5. Comparison Metric Evaluation Table for Phenomena #4.

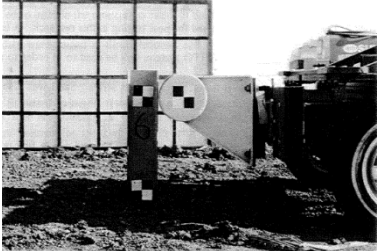
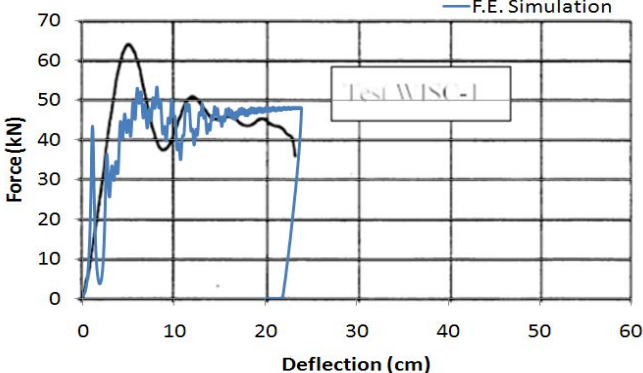
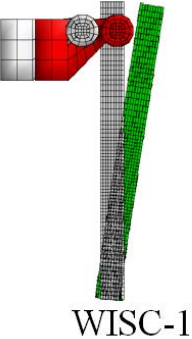
PHENOMENA # 4: Post-Soil Interaction/Response (soil density = 1,980 kg/m³)			
<p>Sprauge-Geers Metrics List all the data channels to be compared below. Using RSVVP calculate the M and P metrics comparing the experiment and the simulation. Values less than or equal to 20 are acceptable.</p> <ul style="list-style-type: none"> • <i>Force-Displacement History</i> 	M	P	Pass?
<p>ANOVA Metrics List all the data channels to compare in the rows below. Use RSVVP to calculate the ANOVA metrics and enter the values below. The following criteria must be met:</p> <ul style="list-style-type: none"> • The mean residual error must be less than or equal to five percent of the peak acceleration ($\bar{e} \leq 0.05 \cdot a_{Peak}$) • The standard deviation of the residuals must be less than or equal to 25 percent of the peak acceleration ($\sigma \leq 0.25 \cdot a_{Peak}$) <ul style="list-style-type: none"> • <i>Force-Displacement History</i> 	Mean Residual	Standard Deviation of Residuals	Pass?
General Comparisons	Test	FEA	Error
• Peak Force (kN)	63	50	21%
• Average Force (kN)	42.8	40.2	6.1%
• Maximum Deflection (mm)	234	249	6.4%
<p>PHENOMENA The post-soil model was validated with full-scale bogie impact tests of the W150x13.5 post embedded in soil. Test WISC-1 was conducted at the Midwest Roadside Safety Facility. The impact point on the posts was at 550-mm above grade and the impact direction was perpendicular to the flange of the post (<i>i.e.</i>, strong direction of post).</p> <ul style="list-style-type: none"> • Impactor – 946-kg MwRSF rigid nose bogie vehicle • Impact speed = 4.6 m/s • Soil type – AASHTO M 147-65 Gradation B • Soil density – 1,980 kg/m³ <p>Reference: Coon, B.A., J.D. Reid, and J.R. Rhode, .Dynamic Impact Testing of Guardrail Posts Embedded in Soil., Research Report No. TRP-03-77-98, Midwest Roadside Safety Facility, University of Nebraska-Lincoln, Lincoln, Nebraska (July 21, 1999).</p>			
		 <p>WISC-1</p>	

Table C6-6. Comparison Metric Evaluation Table for Phenomena #5.

PHENOMENA # 5: Post-Soil Interaction/Response (soil density = 2,110 kg/m³)			
<p>Sprauge-Geers Metrics List all the data channels to be compared below. Using RSVVP calculate the M and P metrics comparing the experiment and the simulation. Values less than or equal to 20 are acceptable.</p> <ul style="list-style-type: none"> • <i>Acceration-Time History</i> 	M	P	Pass?
<p>ANOVA Metrics List all the data channels to compare in the rows below. Use RSVVP to calculate the ANOVA metrics and enter the values below. The following criteria must be met:</p> <ul style="list-style-type: none"> • The mean residual error must be less than or equal to five percent of the peak acceleration ($\bar{e} \leq 0.05 \cdot a_{Peak}$) • The standard deviation of the residuals must be less than or equal to 25 percent of the peak acceleration ($\sigma \leq 0.25 \cdot a_{Peak}$) <ul style="list-style-type: none"> • <i>Force-Displacement History</i> 	Mean Residual	Standard Deviation of Residuals	Pass?
General Comparisons	Test	FEA	Error
• Peak Force (kN)	66	50	24%
• Average Force (kN)	43.9	45.1	2.7%
• Maximum Deflection (mm)	314	306	2.5%
<p>PHENOMENA The post-soil model was validated with full-scale bogie impact tests of the W150x13.5 post embedded in soil. Test WISC-3 was conducted at the Midwest Roadside Safety Facility. The impact point on the posts was at 550-mm above grade and the impact direction was perpendicular to the flange of the post (<i>i.e.</i>, strong direction of post).</p> <ul style="list-style-type: none"> • Impactor – 946-kg MwRSF rigid nose bogie vehicle • Impact speed = 5.4 m/s • Soil type – AASHTO M 147-65 Gradation B • Soil density – 2,110 kg/m³ <p>Reference: Coon, B.A., J.D. Reid, and J.R. Rhode, .Dynamic Impact Testing of Guardrail Posts Embedded in Soil., Research Report No. TRP-03-77-98, Midwest Roadside Safety Facility, University of Nebraska-Lincoln, Lincoln, Nebraska (July 21, 1999).</p>			

Table C6-7. Comparison Metric Evaluation Table for Phenomena #6.

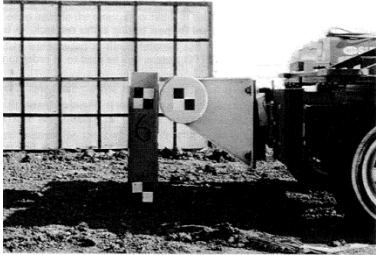
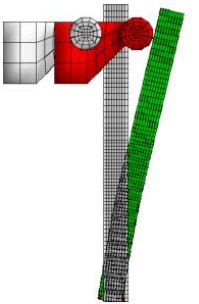
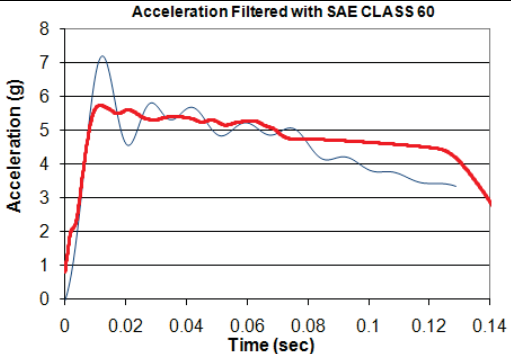
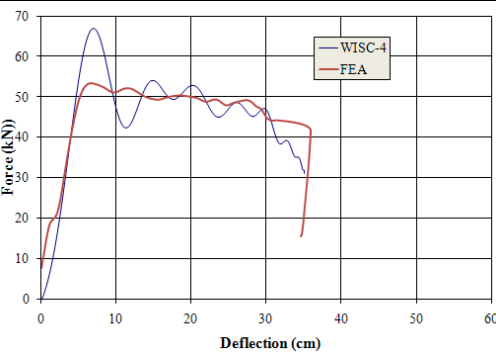
PHENOMENA # 6: Post-Soil Interaction/Response (soil density = 2,240 kg/m³)			
<i>Sprauge-Geers Metrics</i> List all the data channels to be compared below. Using RSVVP calculate the M and P metrics comparing the experiment and the simulation. Values less than or equal to 20 are acceptable.	M	P	Pass?
<ul style="list-style-type: none"> • <i>Acceleration-Time History</i> 	4	4	Y
<i>ANOVA Metrics</i> List all the data channels to compare in the rows below. Use RSVVP to calculate the ANOVA metrics and enter the values below. The following criteria must be met: <ul style="list-style-type: none"> • The mean residual error must be less than or equal to five percent of the peak acceleration ($\bar{e} \leq 0.05 \cdot a_{Peak}$) • The standard deviation of the residuals must be less than or equal to 25 percent of the peak acceleration ($\sigma \leq 0.25 \cdot a_{Peak}$) 	Mean Residual	Standard Deviation of Residuals	Pass?
<ul style="list-style-type: none"> • <i>Acceleration-Time History</i> 	0.04	0.08	Y
General Comparisons	Test	FEA	Error
<ul style="list-style-type: none"> • <i>Peak Force (kN)</i> 	66	52	21%
<ul style="list-style-type: none"> • <i>Average Force (kN)</i> 	47.3	48.1	1.7%
<ul style="list-style-type: none"> • <i>Maximum Deflection (mm)</i> 	348	342	1.7%
<p>PHENOMENA</p> <p>The post-soil model was validated with full-scale bogie impact tests of the W150x13.5 post embedded in soil. Test WISC-4 was conducted at the Midwest Roadside Safety Facility. The impact point on the posts was at 550-mm above grade and the impact direction was perpendicular to the flange of the post (<i>i.e.</i>, strong direction of post).</p> <ul style="list-style-type: none"> • Impactor – 946-kg MwRSF rigid nose bogie vehicle • Impact speed = 5.9 m/s • Soil type – AASHTO M 147-65 Gradation B • Soil density – 2,240 kg/m³ <p>Reference: Coon, B.A., J.D. Reid, and J.R. Rhode, .<i>Dynamic Impact Testing of Guardrail Posts Embedded in Soil.</i>, Research Report No. TRP-03-77-98, Midwest Roadside Safety Facility, University of Nebraska-Lincoln, Lincoln, Nebraska (July 21, 1999).</p>			
		 <p>WISC-4</p>	
			

Table C6-8. Phenomenon Importance Ranking Table for the Modified G4(1S) Guardrail with Wood Blockouts

	Validated Phenomenon	Validated? Verified? Calibrated?
1.	Three-Point Bend Test of W150x13.5 Post About Weak Axis	Validated
2.	Load-to-rupture of splice connection under quasi-static axial loading	Qualitatively Validated
3.	Pull-through of post-bolt-head connection to w-beam using axial load machine	Qualitatively Validated
4.	Full-scale bogie impact tests of the W150x13.5post embedded in soil (soil density = 1,980 kg/m ³)	Qualitatively Validated
5.	Full-scale bogie impact tests of the W150x13.5post embedded in soil (soil density = 1,980 kg/m ³)	Qualitatively Validated
6.	Full-scale bogie impact tests of the W150x13.5post embedded in soil (soil density = 1,980 kg/m ³)	Validated

* Qualitative assessment only

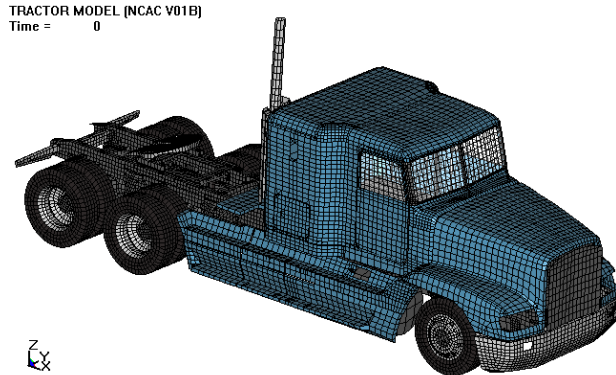
APPENDIX C7: VEHICLE PIRT FOR A 1992 FREIGHTLINER FLD120 TRACTOR

PHENOMENA IMPORTANCE RANKING TABLE FOR A 1992 FREIGHTLINER FLD120 TRACTOR

Developer: NCAC/Battelle/ORNL/University of Tennessee at Knoxville

Date: 11/30/2009

Model: Reduced Element (i.e., bullet model) model of a 1992 Freightliner FLD120 Tractor with integral sleeper-cabin. Wheel-base length measured from center of front axle to the center of the rear tandem assembly is 6.1 m (240 in).



NTRCI has funded the research team of Battelle, Oak Ridge National Laboratory (ORNL) and the University of Tennessee at Knoxville (UTK) to conduct a three-phase investigation to enhance and refine an FE model for simulating tractor-trailer crash events involving barriers and roadside safety hardware such as bridge rails and median barriers. This model was originally developed by the National Crash Analysis Center (NCAC) of George Washington University (GWU) and requires refinement and testing before it can be used by the engineering community for infrastructure design.

Table C7-1. List of Experiments to be used in the PIRT Development

1. Front leaf-spring compression load-displacement test.
2. Compression load/unload displacement test of suspension displacement load limiter.
3. Uniaxial sinusoidal displacement test to measure load-velocity time history of the rear shock absorber at various displacement rates.
4. Uniaxial sinusoidal displacement tests to measure load-velocity time history of the front shock absorbers at various displacement rates.
5. Compression/extension tests of the rear “air bag” suspension at various load rates and bag pressures.
6. Failure tests of front suspension u-bolts.

Table C7-2. Comparison Metric Evaluation Table. For Phenomena #1

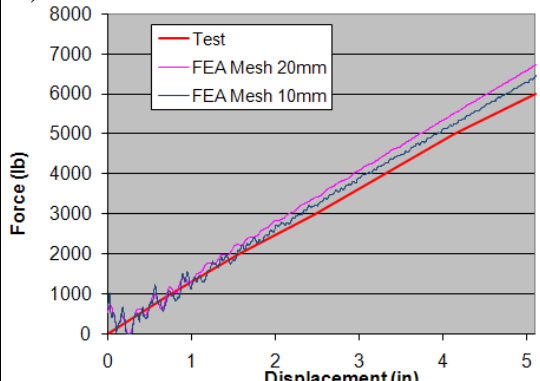
PHENOMENA #1: Front Leaf Suspension			
<i>Sprague-Geers Metrics</i> List all the data channels to be compared below. Using RSVVP calculate the M and P metrics comparing the experiment and the simulation. Values less than or equal to 20 are acceptable.	M	P	Pass?
<ul style="list-style-type: none"> Force-Displacement History (Element Size 20 mm) * Mesh size used in Model 	11.3	0.9	Y
<ul style="list-style-type: none"> Force-Displacement History (Element Size 10 mm) 	5.9	1.1	Y
<i>ANOVA Metrics</i> List all the data channels to compare in the rows below. Use RSVVP to calculate the ANOVA metrics and enter the values below. The following criteria must be met: <ul style="list-style-type: none"> The mean residual error must be less than or equal to five percent of the peak acceleration ($\bar{e} \leq 0.05 \cdot a_{Peak}$) The standard deviation of the residuals must be less than or equal to 25 percent of the peak acceleration ($\sigma \leq 0.25 \cdot a_{Peak}$) 	Mean Residual	Standard Deviation of Residuals	Pass?
<ul style="list-style-type: none"> Force-Displacement History (Element Size 20 mm) * Mesh size used in Model 	0.06	0.04	N
<ul style="list-style-type: none"> Force-Displacement History (Element Size 10 mm) 	0.03	0.03	Y
General Comparisons	Test	FEA	Error
<ul style="list-style-type: none"> Stiffness (lb/in) – Element Size 20 mm * Mesh size used in Model 	1176	1317	12%
<ul style="list-style-type: none"> Stiffness (lb/in) – Element Size 10 mm 	1176	1262	7.3%
<i>Front leaf-spring suspension compression test</i> A leaf spring assembly for a 1992 Freightliner FLD120 tractor was purchased from a local Freightliner dealer. A laboratory test was conducted to measure the force/velocity response of the leaf spring assembly using a MTS uniaxial machine. The FE model of the leaf-spring was modeled with two different mesh densities for comparison: 1) nominal element size =20 mm and 2) nominal element size = 10mm.			
			

Table C7-3. Comparison Metric Evaluation Table for Phenomena #2.

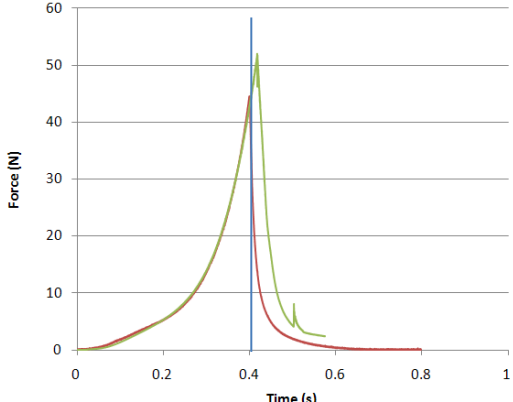
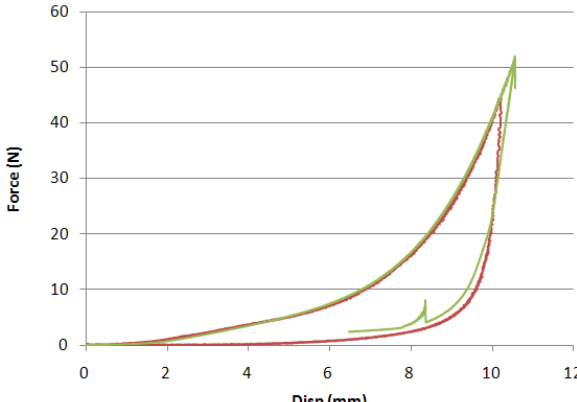
PHENOMENA #2: Suspension Displacement Limiter			
<p>Sprague-Geers Metrics List all the data channels to be compared below. Using RSVVP calculate the M and P metrics comparing the experiment and the simulation. Values less than or equal to 20 are acceptable.</p>	M	P	Pass?
<ul style="list-style-type: none"> <i>Uniaxial Force-Time History</i> 	0	0.8	Y
<p>ANOVA Metrics List all the data channels to compare in the rows below. Use RSVVP to calculate the ANOVA metrics and enter the values below. The following criteria must be met:</p> <ul style="list-style-type: none"> The mean residual error must be less than or equal to five percent of the peak acceleration ($\bar{e} \leq 0.05 \cdot a_{Peak}$) The standard deviation of the residuals must be less than or equal to 25 percent of the peak acceleration ($\sigma \leq 0.25 \cdot a_{Peak}$) 	Mean Residual	Standard Deviation of Residuals	Pass?
<ul style="list-style-type: none"> <i>Uniaxial Force-Time History</i> 	0	0.01	Y
<p>Suspension Displacement Limiter Load/Unload-Displacement Test The load-deflection response of the rubber tip was measured in the laboratory using displacement control on a uniaxial load machine. The displacement was ramped at a constant velocity from 0 to 0.417 inches in 447 seconds and immediately unloaded at the same rate. <i>Note: Comparison is made based on the first 0.4 seconds of loading, since the simulation “overshot” the displacement by 1 mm.</i></p>			
			
			

Table C7-4. Comparison Metric Evaluation Table for Phenomena #3.

PHENOMENA #3: Rear Shock Absorbers (*Calibration Tests*)

Uniaxial sinusoidal displacement calibration tests

The shock absorbers (Monroe Gas-Magnum) were tested in a uniaxial loading machine using sinusoidal displacement input with ± 0.5 inch maximum displacement. Load-velocity data were collected for loading rates of 0.5, 1, 2, 4, and 8 Hz. The shock absorbers are modeled in the as discrete elements with response characterized using *mat_damper_nonlinear in LS-Dyna. The force-velocity characterization curve for the shock absorber is represented by the bold-red curve in the plot below.

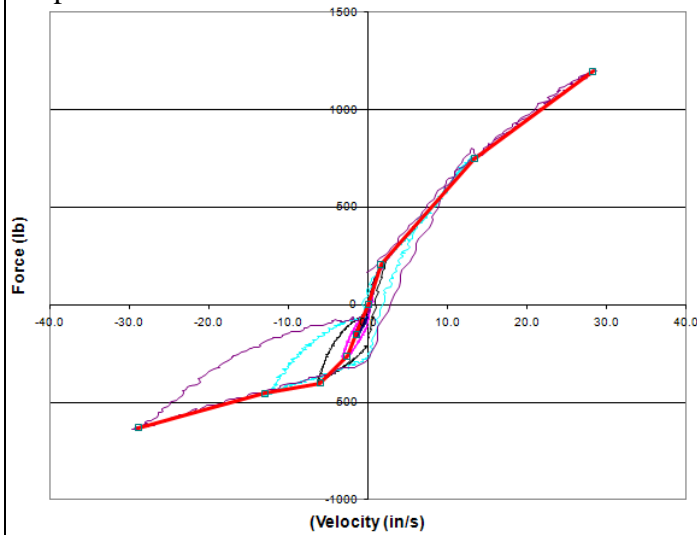


Table C7-5. Comparison Metric Evaluation Table for Phenomena #4.

PHENOMENA #4: Front Shock Absorbers (*Calibration Tests*)

Uniaxial sinusoidal displacement calibration tests

The shock absorbers (Monroe Gas-Magnum) were tested in a uniaxial loading machine using sinusoidal displacement input with ± 0.5 inch maximum displacement. Load-velocity data were collected for loading rates of 0.5, 1, 2, 4, and 8 Hz. The shock absorbers are modeled in the as discrete elements with response characterized using `*mat_damper_nonlinear` in LS-Dyna. The force-velocity characterization curve for the shock absorber is represented by the bold-red curve in the plot below.

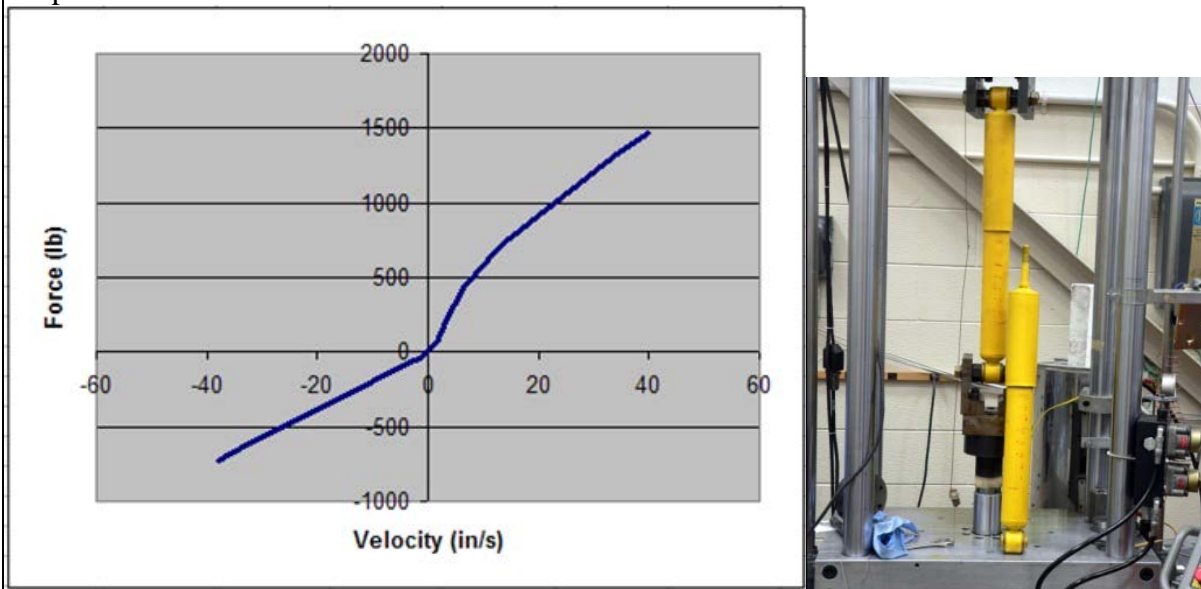


Table C7-6. Comparison Metric Evaluation Table for Phenomena #5.

PHENOMENA #5: Rear “Air-Bag” Suspension (20 psig bag pressure, 1.2 in/sec)			
<p>Sprague-Geers Metrics List all the data channels to be compared below. Using RSVVP calculate the M and P metrics comparing the experiment and the simulation. Values less than or equal to 20 are acceptable.</p> <ul style="list-style-type: none"> • <i>Uniaxial Force-Time History</i> 	M	P	Pass?
	1.1	1.6	Y
<p>ANOVA Metrics List all the data channels to compare in the rows below. Use RSVVP to calculate the ANOVA metrics and enter the values below. The following criteria must be met:</p> <ul style="list-style-type: none"> • The mean residual error must be less than or equal to five percent of the peak acceleration ($\bar{e} \leq 0.05 \cdot a_{Peak}$) • The standard deviation of the residuals must be less than or equal to 25 percent of the peak acceleration ($\sigma \leq 0.25 \cdot a_{Peak}$) 	Mean Residual	Standard Deviation of Residuals	Pass?
<ul style="list-style-type: none"> • <i>Uniaxial Force-Time History</i> 	0.01	0.02	Y
<p>Rear “Air-Bag” Suspension: Compression/extension tests at various load rates and bag pressures</p> <p>Firestone Airide suspension, Part No. 1T15ZR6. The airbag was modeled via discrete spring and damper elements. Tests were conducted at various bag pressures and deflection rates. For each test, the “zero position” of the Airide component was set to mid-stroke, corresponding to a spring height of 12.5 inches, and held at this position while the internal air pressure in the component was set to the desired value. The tests were conducted under displacement control. Starting from the zero position, the displacement was ramped up 3 inches to a spring height of 15.5 inches, and the displacement was held at this position for a period of time (typically 10 seconds) to allow for relaxation/recovery of the load. The displacement was then ramped down 6 inches to a spring height of 9.5 inches, and again held for a period of time. The displacement was then ramped back up 6 inches to a spring height of 15.5 inches and again held.</p>			

Table C7-7. Comparison Metric Evaluation Table for Phenomena #5.

PHENOMENA #5: Rear “Air-Bag” Suspension (20 psig bag pressure, 6 in/sec)			
<p>Sprague-Geers Metrics List all the data channels to be compared below. Using RSVVP calculate the M and P metrics comparing the experiment and the simulation. Values less than or equal to 20 are acceptable.</p>	M	P	Pass?
<ul style="list-style-type: none"> <i>Uniaxial Force-Time History</i> 	1.5	1.7	Y
<p>ANOVA Metrics List all the data channels to compare in the rows below. Use RSVVP to calculate the ANOVA metrics and enter the values below. The following criteria must be met:</p> <ul style="list-style-type: none"> The mean residual error must be less than or equal to five percent of the peak acceleration ($\bar{e} \leq 0.05 \cdot a_{Peak}$) The standard deviation of the residuals must be less than or equal to 25 percent of the peak acceleration ($\sigma \leq 0.25 \cdot a_{Peak}$) 	Mean Residual	Standard Deviation of Residuals	Pass?
<ul style="list-style-type: none"> <i>Uniaxial Force-Time History</i> 	0.02	0.02	Y
<p>Rear “Air-Bag” Suspension: Compression/extension tests at various load rates and bag pressures</p> <p>Firestone Airide suspension, Part No. 1T15ZR6. The airbag was modeled via discrete spring and damper elements. Tests were conducted at various bag pressures and deflection rates. For each test, the “zero position” of the Airide component was set to mid-stroke, corresponding to a spring height of 12.5 inches, and held at this position while the internal air pressure in the component was set to the desired value. The tests were conducted under displacement control. Starting from the zero position, the displacement was ramped up 3 inches to a spring height of 15.5 inches, and the displacement was held at this position for a period of time (typically 10 seconds) to allow for relaxation/recovery of the load. The displacement was then ramped down 6 inches to a spring height of 9.5 inches, and again held for a period of time. The displacement was then ramped back up 6 inches to a spring height of 15.5 inches and again held.</p>			

Table C7-8 Comparison Metric Evaluation Table for Phenomena #5.

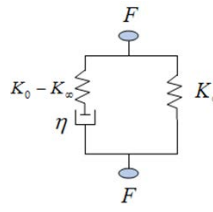
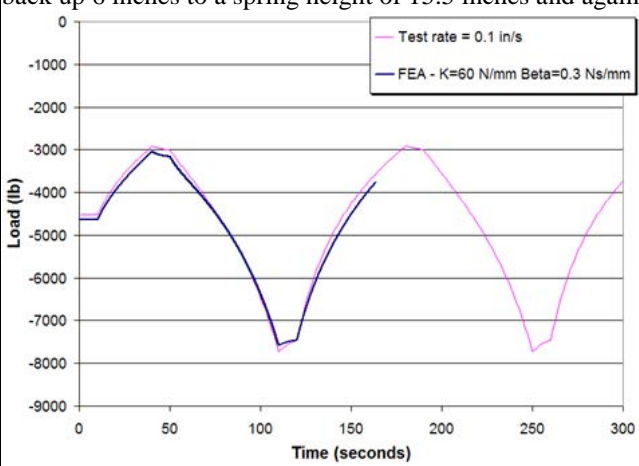
PHENOMENA #5: Rear “Air-Bag” Suspension (60 psig bag pressure, 0.1 in/sec)			
<i>Sprague-Geers Metrics</i> List all the data channels to be compared below. Using RSVVP calculate the M and P metrics comparing the experiment and the simulation. Values less than or equal to 20 are acceptable.	M	P	Pass?
<ul style="list-style-type: none"> <i>Uniaxial Force-Time History</i> 	4.7	1.9	Y
<i>ANOVA Metrics</i> List all the data channels to compare in the rows below. Use RSVVP to calculate the ANOVA metrics and enter the values below. The following criteria must be met: <ul style="list-style-type: none"> The mean residual error must be less than or equal to five percent of the peak acceleration $(\bar{e} \leq 0.05 \cdot a_{Peak})$ The standard deviation of the residuals must be less than or equal to 25 percent of the peak acceleration $(\sigma \leq 0.25 \cdot a_{Peak})$ 	Mean Residual	Standard Deviation of Residuals	Pass?
<ul style="list-style-type: none"> <i>Uniaxial Force-Time History</i> 	0	0.03	Y
Rear “Air-Bag” Suspension: Compression/extension tests at various load rates and bag pressures			
Firestone Airide suspension, Part No. 1T15ZR6. The airbag was modeled via discrete spring and damper elements. Tests were conducted at various bag pressures and deflection rates. For each test, the “zero position” of the Airide component was set to mid-stroke, corresponding to a spring height of 12.5 inches, and held at this position while the internal air pressure in the component was set to the desired value. The tests were conducted under displacement control. Starting from the zero position, the displacement was ramped up 3 inches to a spring height of 15.5 inches, and the displacement was held at this position for a period of time (typically 10 seconds) to allow for relaxation/recovery of the load. The displacement was then ramped down 6 inches to a spring height of 9.5 inches, and again held for a period of time. The displacement was then ramped back up 6 inches to a spring height of 15.5 inches and again held.			
			

Table C7-9 . Comparison Metric Evaluation Table for Phenomena #5.

PHENOMENA #5: Rear “Air-Bag” Suspension (60 psig bag pressure, 6 in/sec)			
<p>Sprague-Geers Metrics List all the data channels to be compared below. Using RSVVP calculate the M and P metrics comparing the experiment and the simulation. Values less than or equal to 20 are acceptable.</p>	M	P	Pass?
<ul style="list-style-type: none"> • <i>Uniaxial Force-Time History</i> 	2.5	2.9	Y
<p>ANOVA Metrics List all the data channels to compare in the rows below. Use RSVVP to calculate the ANOVA metrics and enter the values below. The following criteria must be met:</p> <ul style="list-style-type: none"> • The mean residual error must be less than or equal to five percent of the peak acceleration ($\bar{e} \leq 0.05 \cdot a_{Peak}$) • The standard deviation of the residuals must be less than or equal to 25 percent of the peak acceleration ($\sigma \leq 0.25 \cdot a_{Peak}$) 	Mean Residual	Standard Deviation of Residuals	Pass?
<ul style="list-style-type: none"> • <i>Uniaxial Force-Time History</i> 	0.02	0.04	Y
<p>Rear “Air-Bag” Suspension: Compression/extension tests at various load rates and bag pressures</p> <p>Firestone Airide suspension, Part No. 1T15ZR6. The airbag was modeled via discrete spring and damper elements. Tests were conducted at various bag pressures and deflection rates. For each test, the “zero position” of the Airide component was set to mid-stroke, corresponding to a spring height of 12.5 inches, and held at this position while the internal air pressure in the component was set to the desired value. The tests were conducted under displacement control. Starting from the zero position, the displacement was ramped up 3 inches to a spring height of 15.5 inches, and the displacement was held at this position for a period of time (typically 10 seconds) to allow for relaxation/recovery of the load. The displacement was then ramped down 6 inches to a spring height of 9.5 inches, and again held for a period of time. The displacement was then ramped back up 6 inches to a spring height of 15.5 inches and again held.</p>			

Table C7-10. Comparison Metric Evaluation Table for Phenomena #6.

PHENOMENA #6: Front Suspension U-Bolt Calibration Tests

Uniaxial Load-to-Failure Calibration Tests

A front suspension u-bolt was cut into a tensile test specimen and a uniaxial tensile test was carried out up to failure of the bolt. The data from the test was processed in order to generate true stress versus true plastic strain data for input into *MAT_24 in LS-DYNA.

Additional Information:

- Yield Strength = 152,009 psi
- Ultimate Strength = 162,933 psi
- $A_0 = 0.19737 \text{ in}^2$
- $A_f = 0.12285 \text{ in}^2$
- R.A. = 62%
- Elongation = 11%
- Load Rate = 0.01/minute
- Gauge length = 2 in

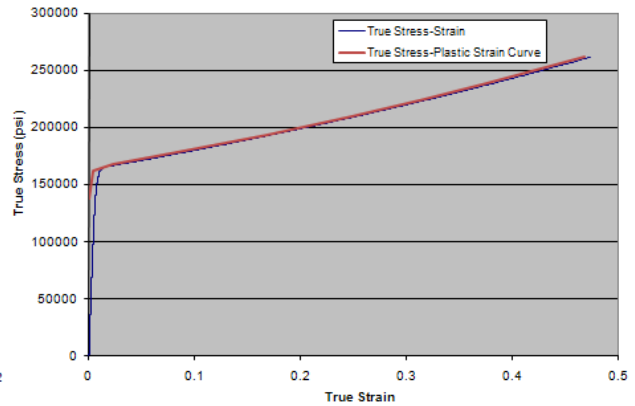
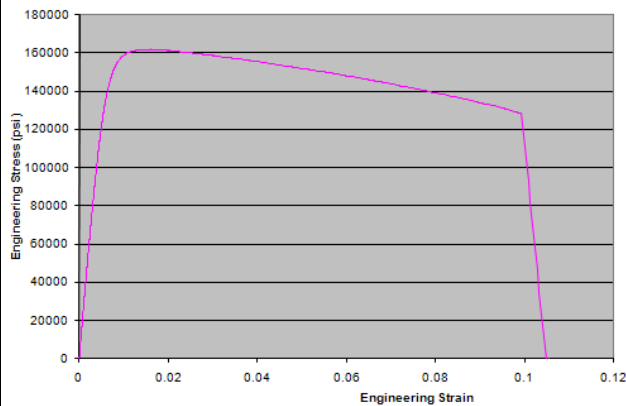


Table C7-11. Phenomenon Importance Ranking Table for Tractor-Semitrailer Model.

No.	Phenomenon	Validated? Verified? Calibrated?
1.	Front Leaf-Spring Suspension	Validated
2.	Suspension Displacement Limiter	Validated
3.	Rear Shock Absorbers (<i>Calibration Tests</i>)	Calibrated
4.	Front Shock Absorbers (<i>Calibration Tests</i>)	Calibrated
5.	Rear “Air-Bag” Suspension	Validated
6.	Front Suspension U-Bolts (Calibration Test)	Calibrated

APPENDIX C8: VEHICLE PIRT FOR THE MODIFIED C2500R VEHICLE MODEL

Developer: National Crash Analysis Center
George Washington University

Modified by: Worcester Polytechnic Institute
Worcester, MA

Model Date: January 2002

Model:

The NCAC C2500R finite element model is a reduced element model of a 1995 Chevrolet 2500 pickup truck. The C2500R model, shown in Figure C8-1, has been used by several research organizations over the years and each organization has made changes and improvements to the model based on their particular analysis needs. As a result, the model has become very efficient and robust for use in crash analyses.

The research team at WPI made several modifications to the model in order to improve its accuracy in simulating vehicle interaction with curbs, with particular emphasis on the suspension system. A list of the modifications and the extent of verification, calibration, and validation of each component model is provided in the following tables and described in a paper by Tiso. (83, 145) The development of a comprehensive PIRT for the vehicle model was not possible since the electronic data was no longer available for quantitative assessment. All validation assessments reported herein were based on qualitative comparison of test and simulation data, as reported in the literature but had a PIRT been developed for this model when it was first created, the electronic data should have been used.



Figure C8-1. View of a 1995 C2500 pickup truck (a) actual vehicle and (b) finite element model of the vehicle.

Table C8-1. List of Experiments used in the PIRT Development

1.	Uniaxial tests of front suspension coil springs
2.	Uniaxial leaf spring test
3.	Front suspension dampers
4.	Front suspension displacement limiter
5.	Dynamic tests on front suspension
6.	Dynamic tests on rear suspension
7.	90-degree curb traversal tests – 6-inch AASHTO type B curb
8.	25-degree curb traversal tests – 6-inch AASHTO type B curb

Table C8-2. Comparison Metric Evaluation Table. For Phenomena #1

PHENOMENA # 1: Front Coil Springs (Calibration Tests)

The front coil spring was tested with the Sintech axial test machine. The spring was tested to a maximum load of 22.27 kN, the maximum force that could be measured with the load cell installed on the tester. The maximum compression was approximately 120 mm. The behavior of the spring was found to be linear throughout the displacement range explored. According to the test, the stiffness coefficient of the coil spring was approximately 185 N/mm.

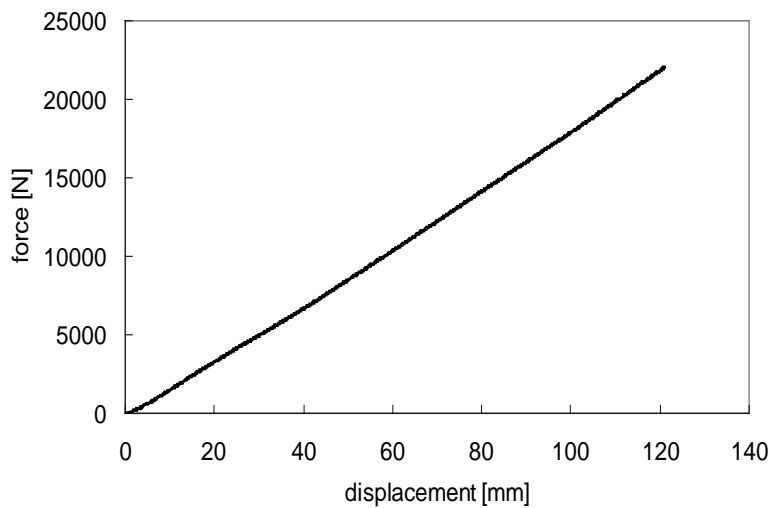
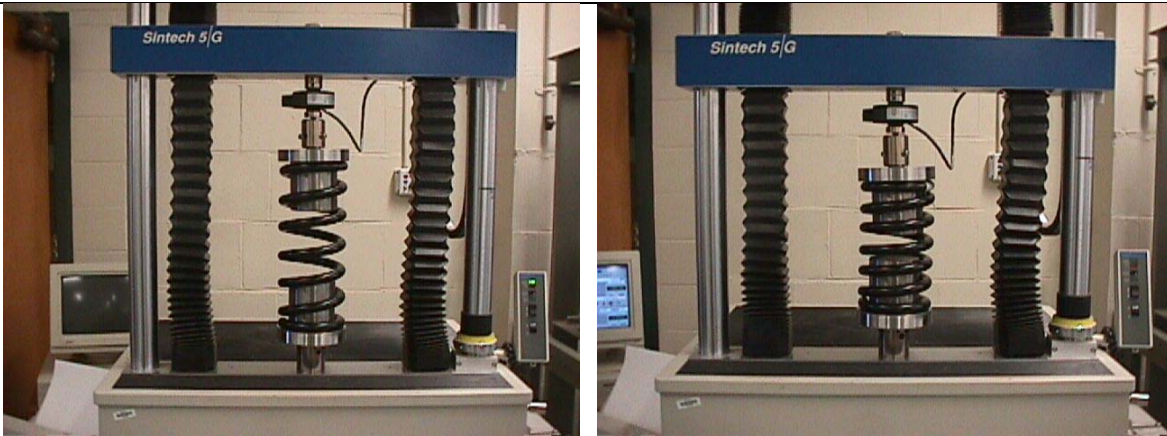


Table C8-3. Comparison Metric Evaluation Table. For Phenomena #2

PHENOMENA # 2: Rear Leaf Springs (*Calibration Tests*)

The leaf spring was tested with the Sintech axial test machine. Because of the complex geometry of the system, the fixture that applies the force on the leaf spring had to be designed carefully, in order not to introduce additional bending moment into the leaf spring. The maximum compressive load applied in the test was 8900 N followed by a 2220 N load applied in the rebound direction.

In the compression phase, the load-deflection response of the leaf spring is linear until the overload leaf contacts the other leaves. The behavior in the compression phase is adequately represented by a bi-linear curve, with the knee of the curve at a displacement value of approximately 145 millimeters. The overload leaf was found to roughly double the value of the stiffness coefficient. The slopes of the two lines are about 34 N/mm and 68 N/mm. The shackle pivoted about its hinge to a maximum angle of approximately 27 degrees.

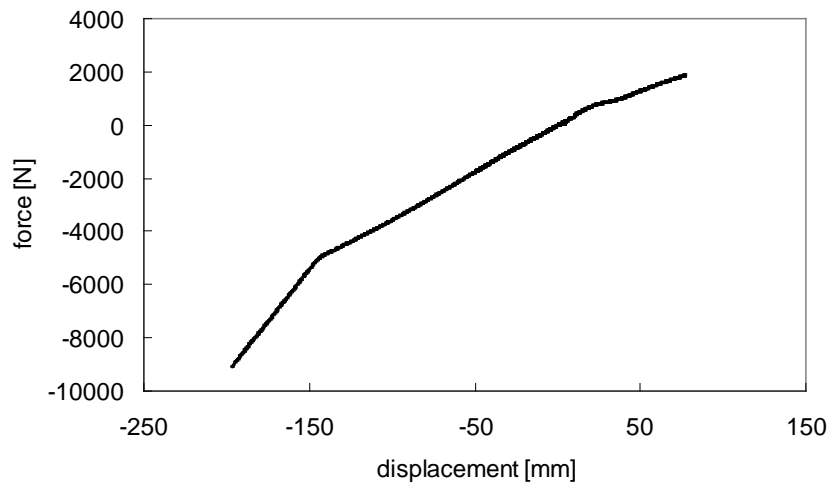


Table C8-4. Comparison Metric Evaluation Table. For Phenomena #3

PHENOMENA # 3: Shock Absorbers (*Calibration Data from Literature*)

The shock absorber should be tested by imposing a known position waveform to the moving ram of the testing machine and measuring the force at the other end with a load cell. Since high velocities (e.g., up at least to 2 m/s) need to be explored for typical vehicle impact scenarios, the high amount of hydraulic power and the strict requirements on the feedback control of the axial machine makes this a demanding test requiring specialized testing facilities.

Some data, however, were obtained from a shock absorber manufacturer concerning the front and rear struts of the C2500 pickup truck. They do not cover the whole range of velocities expected in a vehicle to curb impact scenario but they do consider component non-linearity and non-symmetrical behavior in compression and extension. The curves are shown below.

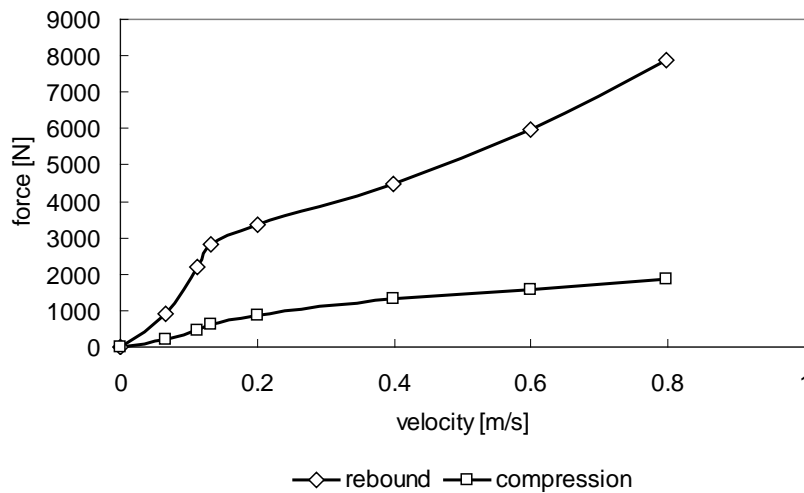
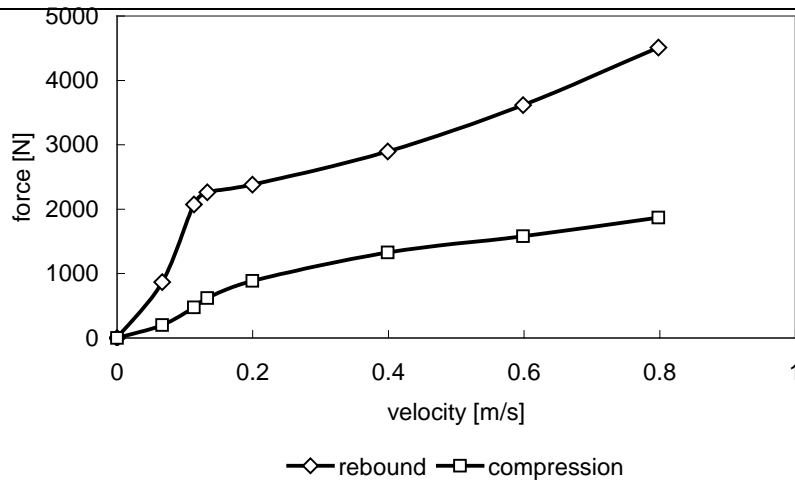


Table C8-5. Comparison Metric Evaluation Table. For Phenomena #6

PHENOMENA # 4: Front suspension displacement limiter (*Calibration tests*)

The front displacement limiter (i.e., bump stop) of the C2500 pickup truck consists of a wedge-shaped piece of hard rubber. Two lateral, shorter edges provide extra stiffness when large relative displacements (e.g., greater than 25 mm) between the frame and the lower A-arm occur.

The front bump stop was tested in compression with the Sintech axial test machine. The bump stop was simply laid on a flat piece of steel and compressed with the moving head of the machine. The test setup and results are shown below.

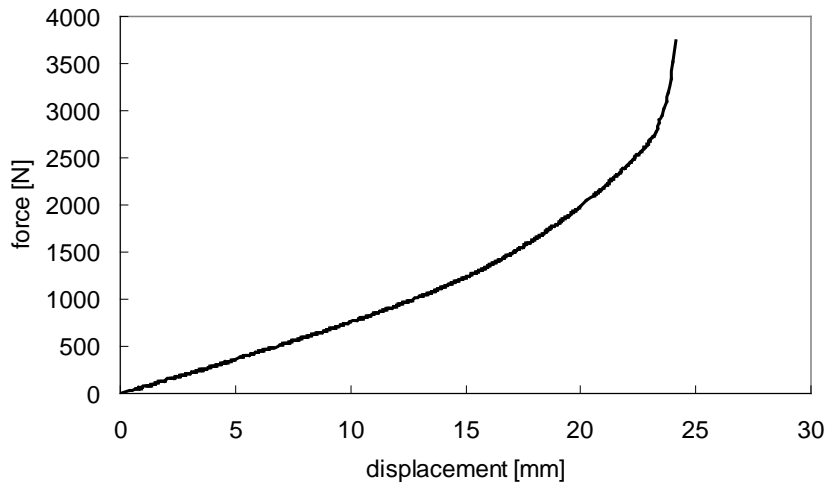
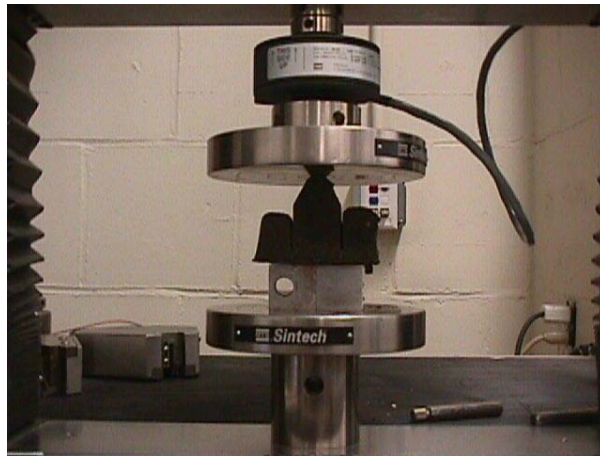


Table C8-6. Comparison Metric Evaluation Table. For Phenomena #6

PHENOMENA # 5: Dynamic tests of Front Suspension (Validation)

The test vehicle was driven up onto 220-mm high wooden ramps and stopped. The instrumentation system was then initialized and the vehicle slowly rolled off the ramps. The relative displacement between the wheels and the frame where acquired during the test. High-speed video cameras were used for a visual comparison with the simulation. The simulations were similar but instead of driving the vehicle off ramps the vehicle was simply dropped from the same height. This accounts for the time discrepancy in the plot below. The magnitude of the initial displacement in the test compared favorably to the simulation. The response tends to compare less favorably as the event progresses. This may be partly due to the age of the actual shock absorbers in the actual vehicle

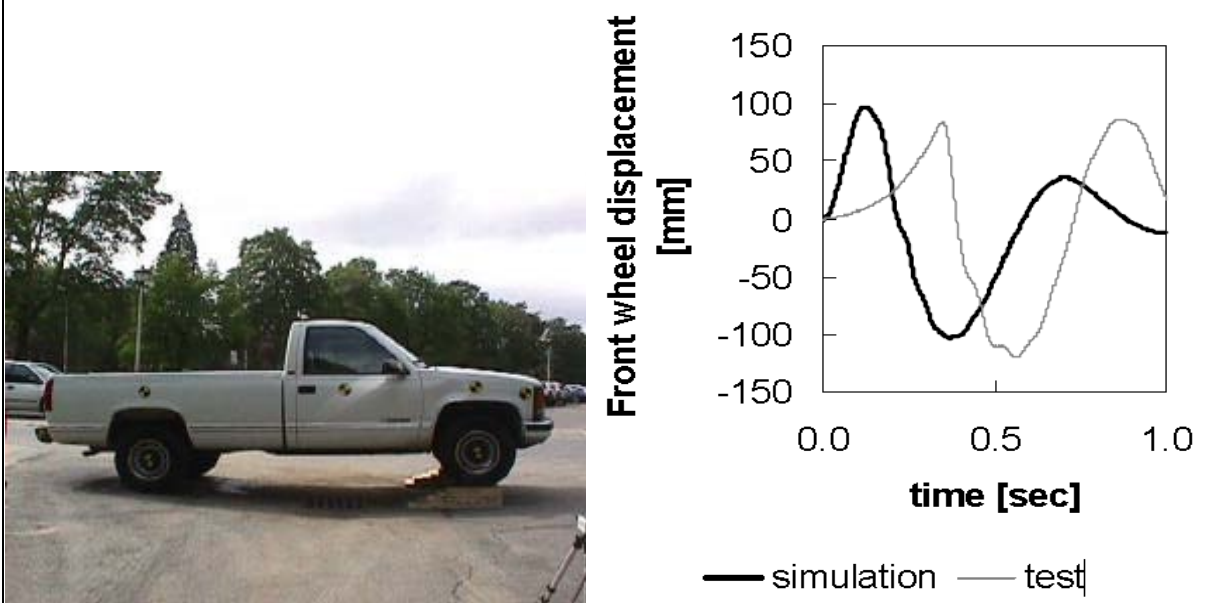
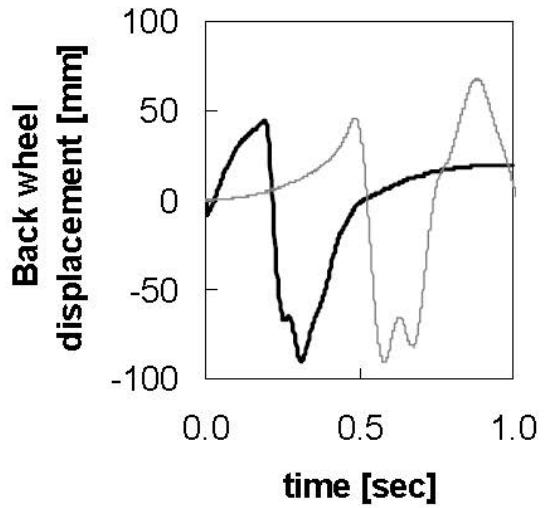


Table C8-7. Comparison Metric Evaluation Table. For Phenomena #6

PHENOMENA # 6: Dynamic tests of Rear Suspension (Validation)

The test vehicle was driven up onto 220-mm high wooden ramps and stopped. The instrumentation system was then initialized and the vehicle slowly rolled off the ramps. The relative displacement between the wheels and the frame where acquired during the test. High-speed video cameras were used for a visual comparison with the simulation. The simulations were similar but instead of driving the vehicle off ramps the vehicle was simply dropped from the same height. This accounts for the time discrepancy in the plot below. The magnitude of the initial displacement in the test compared favorably to the simulation. The response tends to compare less favorably as the event progresses. This may be partly due to the age of the actual shock absorbers in the actual vehicle.



— simulation — test

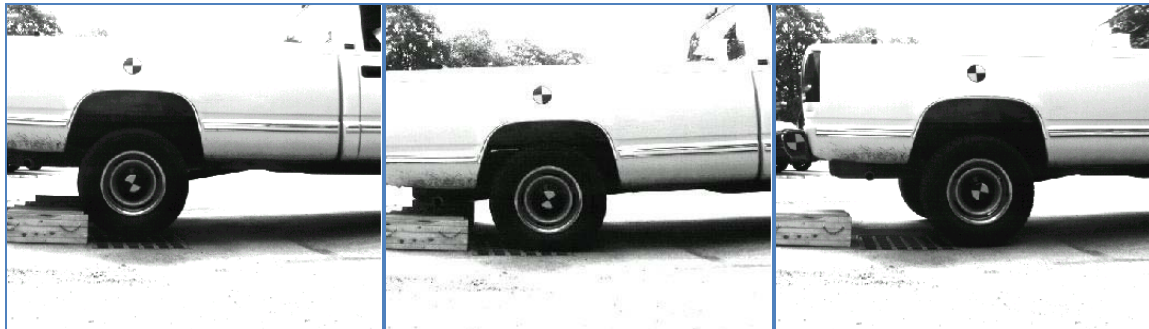
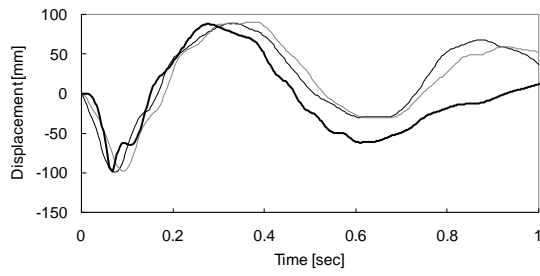


Table C8-8. Comparison Metric Evaluation Table. For Phenomena #7

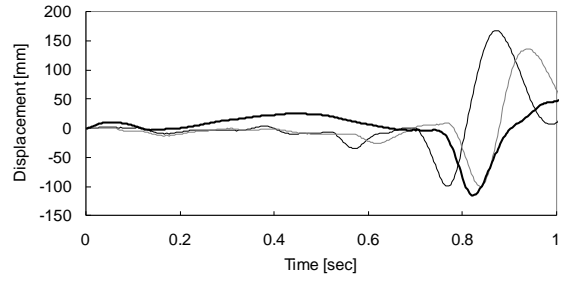
PHENOMENA # 7: 90-degree curb traversal tests (Validation)

The validation test series used 150-mm tall AASHTO Type B curbs. The curbs were made using reinforced concrete cast in 1.2-m long sections. Each set of curbs was attached to the ground with steel rods driven through holes in the curbs into the gravel. The area behind the curb was backfilled with gravel up to the top of the curb.

The tests were performed at a nominal speed of 25 and 18 km/hr and at an approach angle of 25 and 90 degrees, respectively. The driver left the steering wheel free just before the impact. Two high-speed digital video cameras and a real-time video camera were used to record the impact event. High-contrast targets were mounted on the vehicle body and wheel hubs to aid in post processing the data from the high-speed video cameras and determining the actual impacting speed.



Comparison of the front wheel relative displacement for the 90 degrees test



Comparison of the back wheel relative displacement for the 90 degrees test



Table C8-9. Comparison Metric Evaluation Table. For Phenomena #8

PHENOMENA # 8: 25-degree curb traversal tests (Validation)

The validation test series used 150-mm tall AASHTO Type B curbs. The curbs were made using reinforced concrete cast in 1.2-m long sections. Each set of curbs was attached to the ground with steel rods driven through holes in the curbs into the gravel. The area behind the curb was backfilled with gravel up to the top of the curb.

The tests were performed at a nominal speed of 25 and 18 km/hr and at an approach angle of 25 and 90 degrees, respectively. The driver left the steering wheel free just before the impact. Two high-speed digital video cameras and a real-time video camera were used to record the impact event. High-contrast targets were mounted on the vehicle body and wheel hubs to aid in post processing the data from the high-speed video cameras and determining the actual impacting speed.

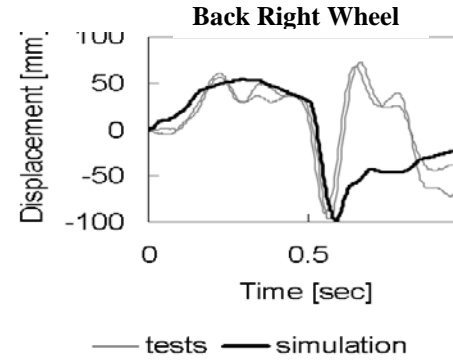
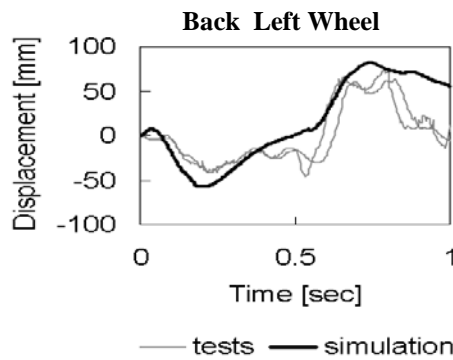
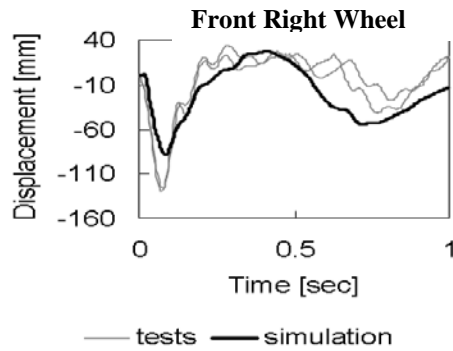
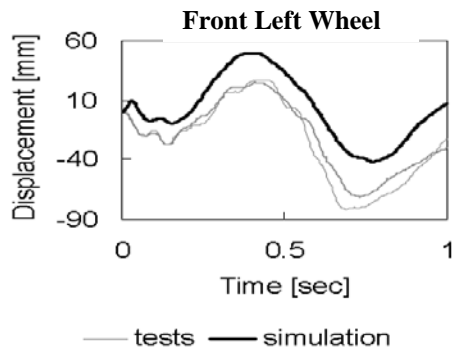


Table C8-10. Phenomenon Importance Ranking Table for the *Modified C2500 Vehicle Model*

	Validated Phenomenon	Validated? Verified? Calibrated?
1.	Uniaxial tests of front suspension coil springs	Calibrated
2.	Uniaxial leaf spring test	Calibrated
3.	Front suspension dampers	Calibrated
4.	Front suspension displacement limiter	Calibrated
5.	Dynamic tests on front suspension	Qualitative Validation
6.	Dynamic tests on rear suspension	Qualitative Validation
7.	90-degree curb traversal tests – 6-inch AASHTO type B curb	Qualitative Validation
8.	25-degree curb traversal tests – 6-inch AASHTO type B curb	Qualitative Validation

* Qualitative assessments were made because the original experimental data was no longer available.

Table C8-5. Comparison Metric Evaluation Table. For Phenomena #6

PHENOMENA # 4: Front suspension displacement limiter (*Calibration tests*)

The front displacement limiter (i.e., bump stop) of the C2500 pickup truck consists of a wedge-shaped piece of hard rubber. Two lateral, shorter edges provide extra stiffness when large relative displacements (e.g., greater than 25 mm) between the frame and the lower A-arm occur.

The front bump stop was tested in compression with the Sintech axial test machine. The bump stop was simply laid on a flat piece of steel and compressed with the moving head of the machine. The test setup and results are shown below.

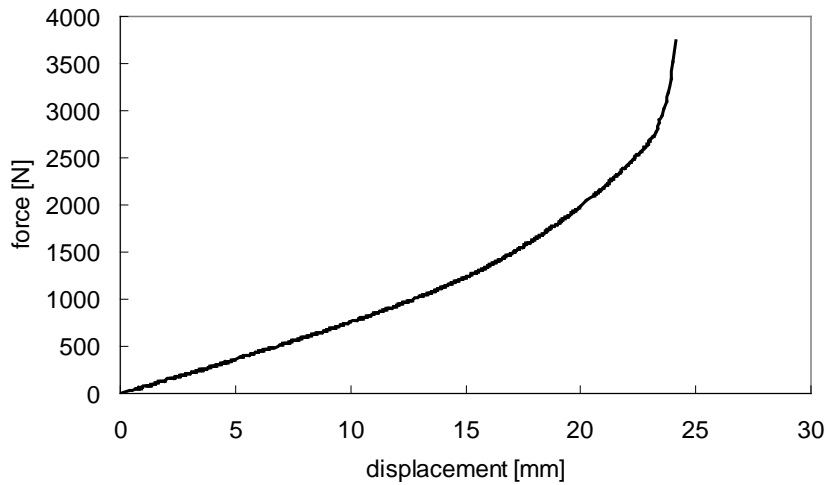
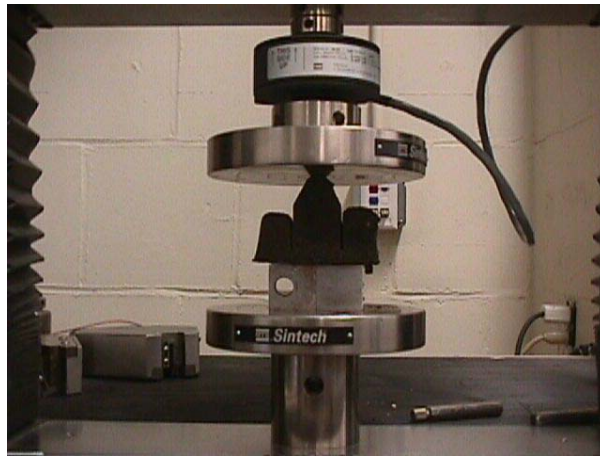


Table C8-6. Comparison Metric Evaluation Table. For Phenomena #6

PHENOMENA # 5: Dynamic tests of Front Suspension (Validation)

The test vehicle was driven up onto 220-mm high wooden ramps and stopped. The instrumentation system was then initialized and the vehicle slowly rolled off the ramps. The relative displacement between the wheels and the frame where acquired during the test. High-speed video cameras were used for a visual comparison with the simulation. The simulations were similar but instead of driving the vehicle off ramps the vehicle was simply dropped from the same height. This accounts for the time discrepancy in the plot below. The magnitude of the initial displacement in the test compared favorably to the simulation. The response tends to compare less favorably as the event progresses. This may be partly due to the age of the actual shock absorbers in the actual vehicle

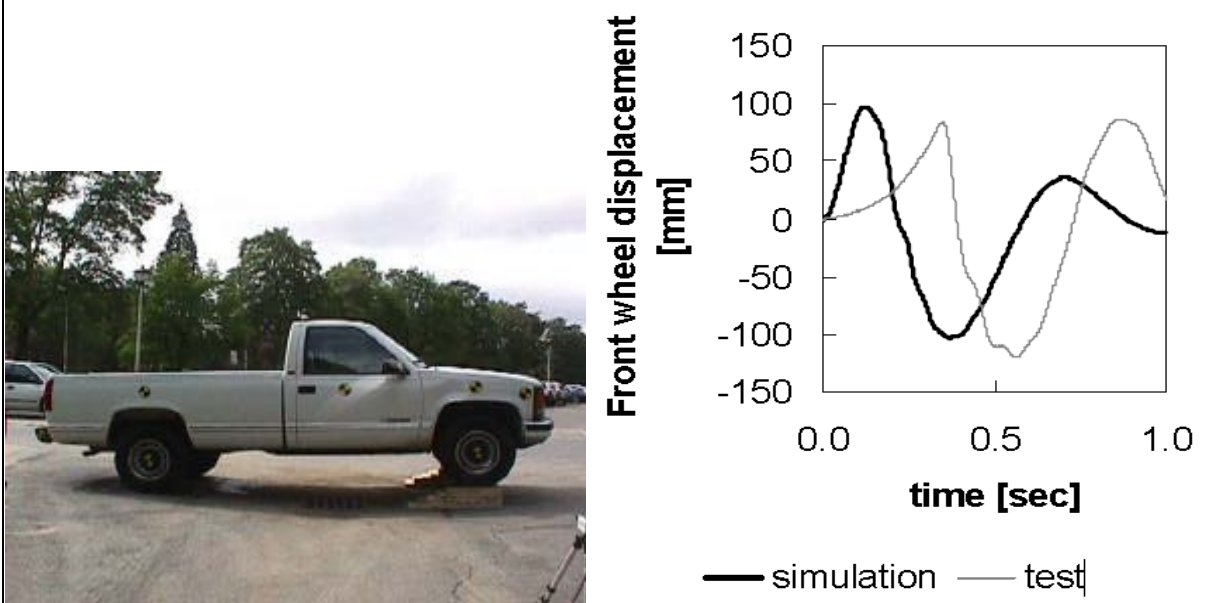
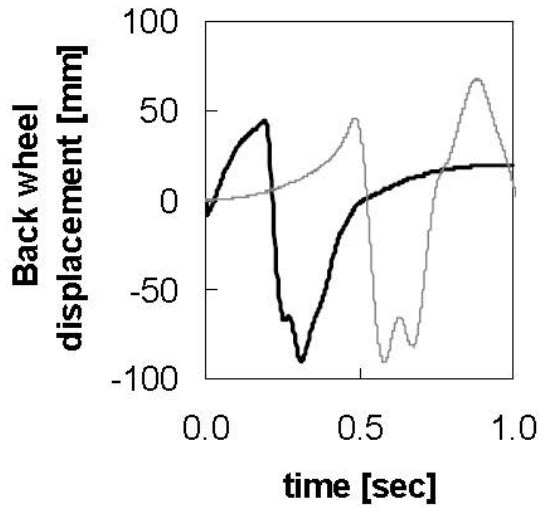


Table C8-7. Comparison Metric Evaluation Table. For Phenomena #6

PHENOMENA # 6: Dynamic tests of Rear Suspension (Validation)

The test vehicle was driven up onto 220-mm high wooden ramps and stopped. The instrumentation system was then initialized and the vehicle slowly rolled off the ramps. The relative displacement between the wheels and the frame where acquired during the test. High-speed video cameras were used for a visual comparison with the simulation. The simulations were similar but instead of driving the vehicle off ramps the vehicle was simply dropped from the same height. This accounts for the time discrepancy in the plot below. The magnitude of the initial displacement in the test compared favorably to the simulation. The response tends to compare less favorably as the event progresses. This may be partly due to the age of the actual shock absorbers in the actual vehicle.



— simulation — test

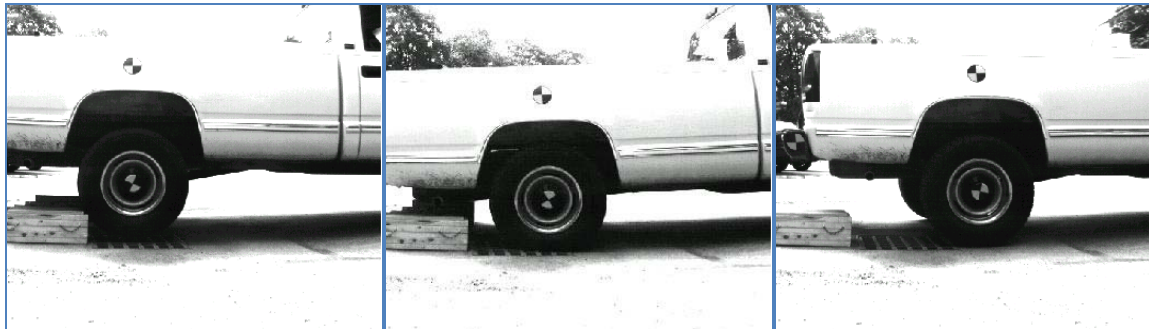
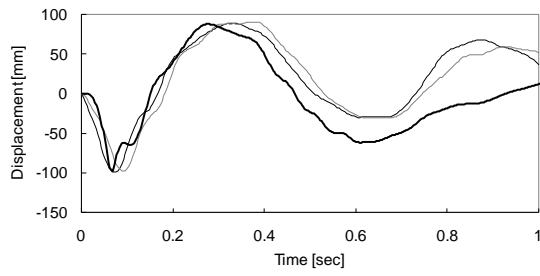


Table C8-8. Comparison Metric Evaluation Table. For Phenomena #7

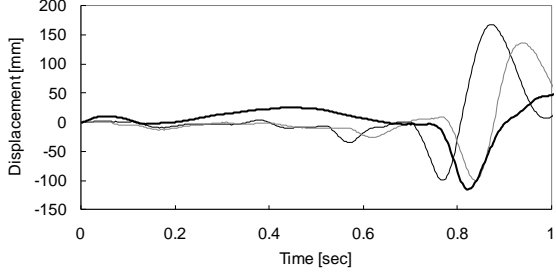
PHENOMENA # 7: 90-degree curb traversal tests (Validation)

The validation test series used 150-mm tall AASHTO Type B curbs. The curbs were made using reinforced concrete cast in 1.2-m long sections. Each set of curbs was attached to the ground with steel rods driven through holes in the curbs into the gravel. The area behind the curb was backfilled with gravel up to the top of the curb.

The tests were performed at a nominal speed of 25 and 18 km/hr and at an approach angle of 25 and 90 degrees, respectively. The driver left the steering wheel free just before the impact. Two high-speed digital video cameras and a real-time video camera were used to record the impact event. High-contrast targets were mounted on the vehicle body and wheel hubs to aid in post processing the data from the high-speed video cameras and determining the actual impacting speed.



Comparison of the front wheel relative displacement for the 90 degrees test



Comparison of the back wheel relative displacement for the 90 degrees test



Table C8-9. Comparison Metric Evaluation Table. For Phenomena #8

PHENOMENA # 8: 25-degree curb traversal tests (Validation)

The validation test series used 150-mm tall AASHTO Type B curbs. The curbs were made using reinforced concrete cast in 1.2-m long sections. Each set of curbs was attached to the ground with steel rods driven through holes in the curbs into the gravel. The area behind the curb was backfilled with gravel up to the top of the curb.

The tests were performed at a nominal speed of 25 and 18 km/hr and at an approach angle of 25 and 90 degrees, respectively. The driver left the steering wheel free just before the impact. Two high-speed digital video cameras and a real-time video camera were used to record the impact event. High-contrast targets were mounted on the vehicle body and wheel hubs to aid in post processing the data from the high-speed video cameras and determining the actual impacting speed.

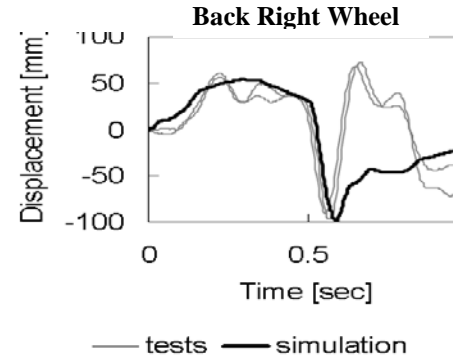
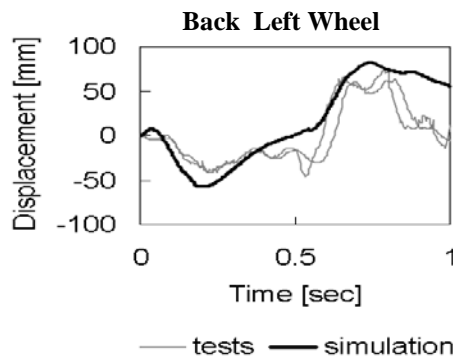
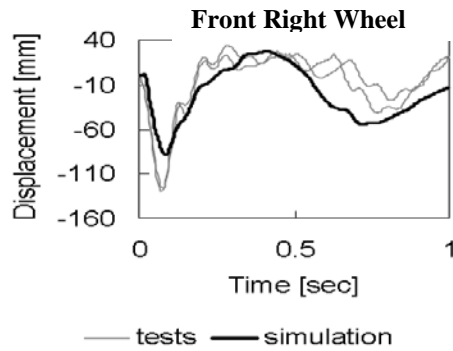
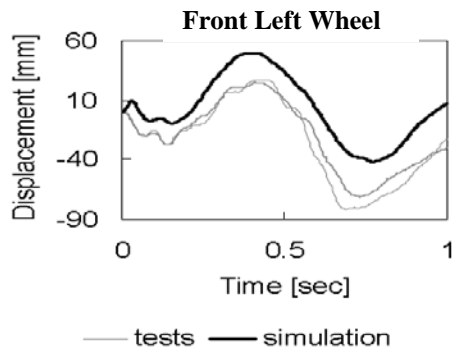


Table C8-10. Phenomenon Importance Ranking Table for the *Modified C2500 Vehicle Model*

	Validated Phenomenon	Validated? Verified? Calibrated?
1.	Uniaxial tests of front suspension coil springs	Calibrated
2.	Uniaxial leaf spring test	Calibrated
3.	Front suspension dampers	Calibrated
4.	Front suspension displacement limiter	Calibrated
5.	Dynamic tests on front suspension	Qualitative Validation
6.	Dynamic tests on rear suspension	Qualitative Validation
7.	90-degree curb traversal tests – 6-inch AASHTO type B curb	Qualitative Validation
8.	25-degree curb traversal tests – 6-inch AASHTO type B curb	Qualitative Validation

* Qualitative assessments were made because the original experimental data was no longer available.

APPENDIX D SURVEY OF PRACTITIONERS

The survey of practitioners is included in the following pages. The actual survey form itself is provided first and a tabulation of the survey responses is provided second.

SURVEY FORMS

The following pages contain copies of the survey forms that were distributed to participants using the web service [surveymonkey.com](https://www.surveymonkey.com).

PRACTITIONER INFORMATION

Development of Verification and Validation Procedures for Computer simulation Used in Roadside Safety Applications (NCHRP Project 22-24)

The following survey is being performed by the project team of NCHRP Project 22-24 in order to gain the perspectives of practitioners who use LSDYNA in roadside safety applications. Your assistance will provide valuable insight into how practitioners verify and validate their finite element models and will help the project team develop useful and practical guidance.

1. Personal information

Name

E-mail address

2. LSDYNA experience

Years of experience using LSDYNA

Years of experience in roadside safety

Approximate numbers of projects you have used LSDYNA to evaluate roadside hardware

3. Would you like a project team member to contact you by phone to discuss your Verification and Validation procedures?

- No
- Yes

Model Building

The following questions address how you typically develop models for roadside safety applications .

4. I generally obtain geometry for my roadside hardware models from (check all that apply):

- Drawings
- Solid geometry created in Solid Works, ProEnginner, etc.
- Digitized surfaces (i.e., reverse engineering)
- Based new models on previously developed models
- Other (please specify)

5. I generally obtain my vehicle models from (check all that apply):

	Always	Mostly	Sometimes	Rarely	Never
The NCAC library	<input type="radio"/>				
Other public domain source of vehicle models	<input type="radio"/>				
I purchase proprietary models	<input type="radio"/>				
I obtain models from the automotive industry	<input type="radio"/>				
I build my own vehicle models	<input type="radio"/>				
I obtain public domain models and modify them for my particular needs	<input type="radio"/>				

6. If you develop your own models or modify models of others, rate the importance of the following features for roadside safety application:

	High	Medium	Low
Detailed geometry	<input type="radio"/>	<input type="radio"/>	<input type="radio"/>
Fast run time	<input type="radio"/>	<input type="radio"/>	<input type="radio"/>
Rolling tires	<input type="radio"/>	<input type="radio"/>	<input type="radio"/>
Failing Tires	<input type="radio"/>	<input type="radio"/>	<input type="radio"/>

NCHRP_22-24 Verification & Validation Procedures for Computer Simulations

Articulated suspensions	<input type="radio"/>	<input type="radio"/>	<input type="radio"/>
Vehicle component failure	<input type="radio"/>	<input type="radio"/>	<input type="radio"/>

7. I have used the following NCAC models (check all that apply):

	Without changes	With my own modifications	Never used
Reduced Single unit truck	<input type="radio"/>	<input type="radio"/>	<input type="radio"/>
Reduced C2500 pickup truck	<input type="radio"/>	<input type="radio"/>	<input type="radio"/>
Reduced Geo Metro	<input type="radio"/>	<input type="radio"/>	<input type="radio"/>
Detailed F250 pickup	<input type="radio"/>	<input type="radio"/>	<input type="radio"/>
Detailed Ford Taurus	<input type="radio"/>	<input type="radio"/>	<input type="radio"/>
Detailed Ford Explorer	<input type="radio"/>	<input type="radio"/>	<input type="radio"/>
Detailed S10 pickup	<input type="radio"/>	<input type="radio"/>	<input type="radio"/>
Detailed C2500 pickup model	<input type="radio"/>	<input type="radio"/>	<input type="radio"/>
Detailed Dodge Neon	<input type="radio"/>	<input type="radio"/>	<input type="radio"/>
Detailed Dodge Caravan	<input type="radio"/>	<input type="radio"/>	<input type="radio"/>
Detailed Geo Metro	<input type="radio"/>	<input type="radio"/>	<input type="radio"/>
Detailed Econoline van	<input type="radio"/>	<input type="radio"/>	<input type="radio"/>
Detailed C1500 pickup truck	<input type="radio"/>	<input type="radio"/>	<input type="radio"/>
60 mi/hr bogie vehicle	<input type="radio"/>	<input type="radio"/>	<input type="radio"/>
20 mi/hr bogie vehicle	<input type="radio"/>	<input type="radio"/>	<input type="radio"/>
FOIL pendulum	<input type="radio"/>	<input type="radio"/>	<input type="radio"/>

8. Are you using any of the following updated vehicle models (check all that apply)?

- C2500 model updated by Worcester Polytechnic Institute
- F800 model updated by Battelle
- GeoMetro updated by Politecnico di Milano
- Other (please specify)

9. How do you model complex articulated systems like suspensions, steering system, roll bars, etc.?

	Always	Mostly	Sometimes	Rarely	Never
In detail (i.e., model each of the components and joints explicitly)	<input type="radio"/>				
Using kinematic equivalent systems (e.g., rigid/deformable elements connected by kinematic joints)	<input type="radio"/>				
Other (please specify)	<input type="text"/>				

10. What do you usually model in detail and what do you usually approximate using techniques like tiednodes, tied-surfaces, springs, etc. (check all that apply)?

	Detailed	Approximated
Bolts	<input type="checkbox"/>	<input type="checkbox"/>
Rivets	<input type="checkbox"/>	<input type="checkbox"/>
Welds	<input type="checkbox"/>	<input type="checkbox"/>
Soil	<input type="checkbox"/>	<input type="checkbox"/>
Road surface	<input type="checkbox"/>	<input type="checkbox"/>
Other (please specify)	<input type="text"/>	

11. Where do you generally obtain material properties for your models (check all that apply)?

	Always	Mostly	Sometimes	Rarely	Never
ASTM/AASHTO/ANSI material specifications	<input type="checkbox"/>				
Laboratory experiments	<input type="checkbox"/>				
Other FE	<input type="checkbox"/>				

simulations

Other source of material data (explain)

12. List the Material Constitutive Laws you most often use (LSDYNA material number)?

13. How do you model possible material failure (check all that apply)?

- Maximum effective plastic strain
- Element erosion
- No failure
- Other (please specify)

14. How do you determine failure parameters (check all that apply)?

- From experimental data
- From data in literature
- Using theoretical formulas
- Using empirical formulas
- Other (please specify)

15. When modeling materials, do you usually take into consideration Strain Rate Sensitivity?

- No
- Yes

16. How do you model welded connection (check all that apply)?

	Always	Mostly	Sometimes	Rarely	Never
Merged nodes	<input type="radio"/>				
Spot welds with failure	<input type="radio"/>				
Tied contact	<input type="radio"/>				
Tied contact with failure	<input type="radio"/>				

Other (please specify)

17. How do you model bolted connection (check all that apply)?

	Always	Mostly	Sometimes	Rarely	Never
Merged nodes	<input type="radio"/>				
Spot welds with failure	<input type="radio"/>				
Tied contact	<input type="radio"/>				
Tied contact with failure	<input type="radio"/>				
Springs	<input type="radio"/>				

Other (please specify)

18. How do you model post-soil interaction (check all that apply)?

	Always	Mostly	Sometimes	Rarely	Never
Non-linear springs	<input type="radio"/>				
Eulerian solid meshing	<input type="radio"/>				
Fixed nodes (SPC)	<input type="radio"/>				
Explicit model of the post and soil volumes	<input type="radio"/>				

Other (please specify)

Model Verification

In the questions below, Model Verification refers to the way you develop your model and ensure that there will not be any numerical or computational problems. Verification should guarantee successful completion of the simulation but it usually is not sufficient to assess the physical correctness of the solution (i.e., validation).

19. The DoD/AIAA define Verification as:

“The process of determining that a model implementation represents the developer’s conceptual description of the model and the solution to the model.”

For the purposes of this project, Verification is defined as:

“Verification in roadside safety simulations involves using parameters and techniques based on the collective experience of the roadside safety simulation community that should maximize the likelihood of developing models that do not experience numerical instabilities or other run-time problems.”

Do you agree with this statement?

Yes

No. Please enter your alternate definition below

20. What is the largest shell element dimension (in millimeters) you would be likely to use in modeling steel components that (fill in the blank):

Contact other components?

Do not contact other components but are expected to deform significantly?

Are not in a contact or high deformation region of the model?

21. What is the largest solid element dimension (in millimeters) you would be likely to use in modeling a wood post if (fill in the blank):

The post was expected for fracture?

The post was expected not to fracture but displace in the soil?

The post was not expected to deform or displace significantly?

22. For typical roadside hardware simulations, I generally try to keep my initial time step at about (check one):

- Less than 1e-6 sec
- [1e-6 sec - 5e-6 sec]
- [5e-6 sec - 10e-6 sec]
- Greater than 10e-6 sec

Other (please specify)

23. I control my time step by (select one):

	True	False
Controlling the element dimensions	<input type="radio"/>	<input type="radio"/>
Using the minimum time step option (i.e., mass scaling)	<input type="radio"/>	<input type="radio"/>
Both element dimensions and time step	<input type="radio"/>	<input type="radio"/>
Neither	<input type="radio"/>	<input type="radio"/>

24. Which one of the following statements best applies about the use of Mass-Scaling (check one):

- I never use mass scaling to achieve a minimum time step.
- I often use mass scaling to develop and de-bug my model but then turn it off when I use it for my final simulations.
- I generally use some mass scaling in my models to achieve a minimum time step.
- Other (please specify)

25. When you use the mass-scaling option, which is your main objective (check all that apply)?

NCHRP_22-24 Verification & Validation Procedures for Computer Simulations

- I determine the geometry that is required first and then use mass scaling to make sure the time step does not get too small
- I make sure the overall mesh is adequate for the contacts and deformations that I expect and use mass scaling to prevent the time step getting too small.
- I usually define a very fine mesh to ensure good contact and deformation results and use mass scaling to increase the time step to an acceptable run time.
- Other (please specify)

26. When I experience contact instabilities like shooting nodes or tangling meshes, I usually attempt to solve the problem by doing the following (put in rank order):

Refine my mesh in the contact area	▼
Modify the contact parameters like the penalty factors	▼
Change the contact type	▼
Other	▼

27. Check the range such that you agree with the statement

	< 5%	[5% - 10%]	[10% - 15%]	> 15%	N/A
I am generally not concerned about Total energy balance in my simulation as long as, during the run, the total energy varies by less than:	<input type="radio"/>				
I am generally not concerned with hourglass energy as long as the percentage compared to the total internal energy is less than:	<input type="radio"/>				
I am comfortable using mass scaling in my final model as long as the percentage of added mass compared to the total physical mass is less than.	<input type="radio"/>				
If mass is added to a part of the model that is stationary at the beginning of the simulation, I would feel comfortable adding the following percentage of the total physical mass.	<input type="radio"/>				

28. Maximum warpage angle (check one):

	1°	3°	5°	10°	N/A
I generally try to keep the maximum warpage angle of the elements in the model smaller	<input type="radio"/>				

than

29. Elements with biggest warpage angle (check one):

	0%-5%	5%-10%	10%-15%	15%-20%	N/A
I generally try to keep the percentage of elements with the biggest warpage angle in the model smaller than	<input type="radio"/>				

30. Mesh aspect ratio(check one):

	2 to 1	3 to 1	5 to 1	8 to 1	N/A
I generally try to keep the aspect ratio of my mesh smaller than	<input type="radio"/>				

Model Validation

Validation in the questions below refers to comparing the results of a finite element simulation to a physical fullscale crash test. Validation may involve a material model, component, subassembly or full model, but Validation always involves comparison to a physical experiment of some type.

31. The DoD/AIAA define Validation as :

“The process of determining the degree to which a model is an accurate representation of the real world from the perspective of its intended use.”

Do agree with this definition?

- Yes
- No. Please enter your alternate definition below

32. Rank the following statement in order of importance in validating a finite element simulation with a physical test (1 = least important, 5 = most important).

Qualitative comparison of barrier damage	<input type="text" value="1"/>
Qualitative comparison of vehicle damage	<input type="text" value="1"/>
Qualitative comparison of trajectories	<input type="text" value="1"/>
Qualitative comparison of crash sequence (i.e., what happens)	<input type="text" value="1"/>

Quantitative comparison of acceleration time histories	<input type="checkbox"/>				
Quantitative comparison of velocity time histories	<input type="checkbox"/>				
Quantitative comparison of displacement/rotation time histories	<input type="checkbox"/>				

33. Which qualitative comparisons do you use to compare your simulation results to the physical tests (Check all that apply)?

	Always	Mostly	Sometimes	Rarely	Never
Hardware deformations	<input type="radio"/>				
Location/number of failed components	<input type="radio"/>				
Visual methods (i.e., pictures / movies)	<input type="radio"/>				
Phenomenological (i.e., the same general response)	<input type="radio"/>				
Other (please specify)	<input type="text"/>				

34. Which quantitative time history comparisons do you use for comparing the simulation to the physical test (Check all that apply)?

	Always	Mostly	Sometimes	Rarely	Never
Accelerations	<input type="radio"/>				
Velocity	<input type="radio"/>				
Displacements and rotations	<input type="radio"/>				
Energy	<input type="radio"/>				
Stress/Strain	<input type="radio"/>				
Other (please specify)	<input type="text"/>				

35. Which of the following parameters or metrics do you use to compare your simulation results with experimental results (check all that apply)?

	Always	Mostly	Sometimes	Rarely	Never
TRAP parameters	<input type="radio"/>				

NCHRP_22-24 Verification & Validation Procedures for Computer Simulations

(i.e., OIV, ORA, THIV, ASI, etc)

GEER's parameters	<input type="radio"/>				
NARD Validation Manual parameters	<input type="radio"/>				
Ray's T-statistic method	<input type="radio"/>				

Other metrics (please specify)

36. Do you have a standard procedure for model verification and validation?

- No
 Yes

If yes, please explain

37. Do you use different validation methods according to the specific roadside hardware you are using (check one)?

- No
 Yes

If yes, please explain

38. How do you filter time history data before using it to compare to physical tests (check all that apply)?

- I use the SAE J211 filter specifications
 I use TRAP to filter my simulation data
 I use LSPREPOST to filter my simulation data
 I use a running average in LSPREPOST to effectively filter my data

I do not filter my simulation data

Other filters (please specify)

39. Do you use any other finite element programs other than LS-DYNA for validation purposes (check one)?

Yes

No

40. When building a large model, do you validate components or subassemblies of that model and compare the results with physical tests?

Yes

No

41. Are there any validation or verification issues that you think were not addressed by this survey? If so, please list them in the space below.

Done!

If you have written any papers or reports that you feel provide a good example of the way you verify and validate simulations with physical experiments, please send them to:

Malcolm Ray
Department of Civil Engineering
Worcester Polytechnic Institute
Worcester MA 01609
email: mhray@wpi.edu

Thank you for your help in completing this survey. Your effort will provide valuable insight and allow the project team to develop practical and useful guidelines.

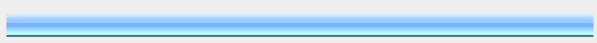
Sincerely,



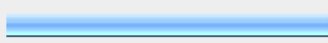
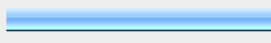
Malcolm H. Ray, P.E., Ph.D.
Professor of Civil Engineering
Professor Mechanical Engineering

Summary of the survey responses

NCHRP_22-24 Verification & Validation Procedures for Computer Simulations PRACTITIONER SURVEY

1. Personal information			
		Response Percent	Response Count
Name		100.0%	
E-mail address		100.0%	
		<i>answered question</i>	
		<i>skipped question</i>	

2. LSDYNA experience				
		Response Average	Response Total	Response Count
Years of experience using LSDYNA		8.58	283	
Years of experience in roadside safety		8.48	280	
Approximate numbers of projects you have used LSDYNA to evaluate roadside hardware		22.94	757	
		<i>answered question</i>		
		<i>skipped question</i>		

3. Would you like a project team member to contact you by phone to discuss your Verification and Validation procedures?			
		Response Percent	Response Count
No		54.8%	
Yes		45.2%	
		<i>answered question</i>	
		<i>skipped question</i>	

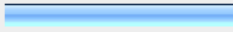
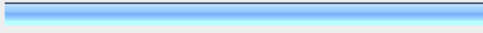
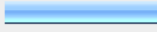
4. I generally obtain geometry for my roadside hardware models from(check all that apply):			Response Percent	Response Count
Drawings			84.8%	
Solid geometry created in Solid Works, ProEnginner, etc.			48.5%	
Digitized surfaces (i.e., reverse engineering)			21.2%	
Based new models on previously developed models			63.6%	
Other (please specify)			18.2%	
			<i>answered question</i>	
			<i>skipped question</i>	

5. I generally obtain my vehicle models from (check all that apply):							
	Always	Mostly	Sometimes	Rarely	Never	Rating Average	Response Count
The NCAC library	6.3% (2)	46.9% (15)	25.0% (8)	15.6% (5)	6.3% (2)	1.00	
Other public domain source of vehicle models	0.0% (0)	13.3% (4)	40.0% (12)	26.7% (8)	20.0% (6)	1.00	
I purchase proprietary models	0.0% (0)	0.0% (0)	7.1% (2)	7.1% (2)	85.7% (24)	1.00	
I obtain models from the automotive industry	0.0% (0)	3.7% (1)	18.5% (5)	7.4% (2)	70.4% (19)	1.00	
I build my own vehicle models	3.2% (1)	22.6% (7)	32.3% (10)	19.4% (6)	22.6% (7)	1.00	
I obtain public domain models and modify them for my particular needs	28.1% (9)	43.8% (14)	21.9% (7)	0.0% (0)	6.3% (2)	1.00	
							<i>answered question</i>
							<i>skipped question</i>

6. If you develop your own models or modify models of others, rate the importance of the following features for roadside safety application:					
	High	Medium	Low	Rating Average	Response Count
Detailed geometry	46.9% (15)	50.0% (16)	3.1% (1)	1.00	33
Fast run time	45.2% (14)	41.9% (13)	12.9% (4)	1.00	33
Rolling tires	67.7% (21)	32.3% (10)	0.0% (0)	1.00	33
Failing Tires	16.1% (5)	64.5% (20)	19.4% (6)	1.00	33
Articulated suspensions	74.2% (23)	22.6% (7)	3.2% (1)	1.00	33
Vehicle component failure	32.3% (10)	51.6% (16)	16.1% (5)	1.00	33
	<i>answered question</i>				33
	<i>skipped question</i>				0

7. I have used the following NCAC models (check all that apply):					
	Without changes	With my own modifications	Never used	Rating Average	Response Count
Reduced Single unit truck	6.9% (2)	51.7% (15)	41.4% (12)	1.00	29
Reduced C2500 pickup truck	10.3% (3)	62.1% (18)	27.6% (8)	1.00	29
Reduced Geo Metro	3.2% (1)	87.1% (27)	9.7% (3)	1.00	33
Detailed F250 pickup	7.1% (2)	7.1% (2)	85.7% (24)	1.00	29
Detailed Ford Taurus	22.2% (6)	22.2% (6)	55.6% (15)	1.00	27
Detailed Ford Explorer	7.4% (2)	3.7% (1)	88.9% (24)	1.00	27
Detailed S10 pickup	7.4% (2)	11.1% (3)	81.5% (22)	1.00	27
Detailed C2500 pickup model	14.8% (4)	33.3% (9)	51.9% (14)	1.00	27
Detailed Dodge Neon	11.1% (3)	25.9% (7)	63.0% (17)	1.00	27
Detailed Dodge Caravan	11.1% (3)	7.4% (2)	81.5% (22)	1.00	27
Detailed Geo Metro	13.8% (4)	51.7% (15)	34.5% (10)	1.00	29
Detailed Econoline van	3.6% (1)	7.1% (2)	89.3% (25)	1.00	29
Detailed C1500 pickup truck	3.7% (1)	22.2% (6)	74.1% (20)	1.00	27

60 mi/hr bogie vehicle	11.1% (3)	7.4% (2)	81.5% (22)	1.00	
20 mi/hr bogie vehicle	11.1% (3)	14.8% (4)	74.1% (20)	1.00	
FOIL pendulum	11.1% (3)	22.2% (6)	66.7% (18)	1.00	
<i>answered question</i>					
<i>skipped question</i>					

8. Are you using any of the following updated vehicle models (check all that apply)?					
				Response Percent	Response Count
C2500 model updated by Worcester Polytechnic Institute				30.4%	
F800 model updated by Battelle				39.1%	
GeoMetro updated by Politecnico di Milano				82.6%	
Other (please specify)				26.1%	
<i>answered question</i>					
<i>skipped question</i>					

9. How do you model complex articulated systems like suspensions, steering system, roll bars, etc.?							
	Always	Mostly	Sometimes	Rarely	Never	Rating Average	Response Count
In detail (i.e., model each of the components and joints explicitly)	0.0% (0)	32.1% (9)	28.6% (8)	28.6% (8)	10.7% (3)	2.29	
Using kinematic equivalent systems (e.g., rigid/deformable elements connected by kinematic joints)	13.3% (4)	40.0% (12)	36.7% (11)	6.7% (2)	3.3% (1)	1.33	
Other (please specify)							
<i>answered question</i>							
<i>skipped question</i>							

10. What do you usually model in detail and what do you usually approximate using techniques like tiednodes, tied-surfaces, springs, etc. (check all that apply)?				
	Detailed	Approximated	Rating Average	Response Count
Bolts	37.9% (11)	62.1% (18)	1.00	29
Rivets	6.9% (2)	93.1% (27)	1.00	29
Welds	13.3% (4)	86.7% (26)	1.00	30
Soil	37.9% (11)	62.1% (18)	1.00	29
Road surface	10.3% (3)	89.7% (26)	1.00	29
		Other (please specify)		5
		<i>answered question</i>		31
		<i>skipped question</i>		2

11. Where do you generally obtain material properties for your models (check all that apply)?							
	Always	Mostly	Sometimes	Rarely	Never	Rating Average	Response Count
ASTM/AASHTO/ANSI material specifications	3.3% (1)	16.7% (5)	40.0% (12)	26.7% (8)	13.3% (4)	1.00	30
Laboratory experiments	6.1% (2)	57.6% (19)	33.3% (11)	3.0% (1)	0.0% (0)	1.00	33
Other FE simulations	0.0% (0)	27.3% (9)	57.6% (19)	6.1% (2)	9.1% (3)	1.00	33
					Other source of material data (explain)		11
					<i>answered question</i>		33
					<i>skipped question</i>		0

12. List the Material Constitutive Laws you most often use (LSDYNA material number)?	
	Response Count
	30
	<i>answered question</i> 30
	<i>skipped question</i> 3

13. How do you model possible material failure (check all that apply)?

		Response Percent	Response Count
Maximum effective plastic strain		87.9%	29
Element erosion		72.7%	24
No failure		39.4%	13
Other (please specify)		18.2%	6
<i>answered question</i>			33
<i>skipped question</i>			0

14. How do you determine failure parameters (check all that apply)?

		Response Percent	Response Count
From experimental data		90.9%	30
From data in literature		93.9%	31
Using theoretical formulas		33.3%	11
Using empirical formulas		27.3%	9
Other (please specify)		6.1%	2
<i>answered question</i>			33
<i>skipped question</i>			0

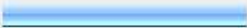
15. When modeling materials, do you usually take into consideration Strain Rate Sensitivity?

		Response Percent	Response Count
No		39.4%	13
Yes		60.6%	20
<i>answered question</i>			33
<i>skipped question</i>			0

16. How do you model welded connection (check all that apply)?							
	Always	Mostly	Sometimes	Rarely	Never	Rating Average	Response Count
Merged nodes	0.0% (0)	30.0% (9)	46.7% (14)	13.3% (4)	10.0% (3)	1.00	30
Spot welds with failure	0.0% (0)	51.6% (16)	32.3% (10)	6.5% (2)	9.7% (3)	1.00	31
Tied contact	0.0% (0)	14.3% (4)	46.4% (13)	14.3% (4)	25.0% (7)	1.00	28
Tied contact with failure	0.0% (0)	20.0% (6)	33.3% (10)	10.0% (3)	36.7% (11)	1.00	30
					Other (please specify)		7
					answered question		32
					skipped question		1

17. How do you model bolted connection (check all that apply)?							
	Always	Mostly	Sometimes	Rarely	Never	Rating Average	Response Count
Merged nodes	0.0% (0)	6.9% (2)	41.4% (12)	13.8% (4)	37.9% (11)	1.00	29
Spot welds with failure	0.0% (0)	46.7% (14)	26.7% (8)	10.0% (3)	16.7% (5)	1.00	30
Tied contact	0.0% (0)	3.8% (1)	26.9% (7)	23.1% (6)	46.2% (12)	1.00	26
Tied contact with failure	0.0% (0)	11.5% (3)	19.2% (5)	19.2% (5)	50.0% (13)	1.00	26
Springs	3.7% (1)	11.1% (3)	33.3% (9)	37.0% (10)	14.8% (4)	1.00	27
					Other (please specify)		14
					answered question		31
					skipped question		2

18. How do you model post-soil interaction (check all that apply)?							
	Always	Mostly	Sometimes	Rarely	Never	Rating Average	Response Count
Non-linear springs	3.3% (1)	30.0% (9)	13.3% (4)	16.7% (5)	36.7% (11)	1.00	30
Eulerian solid meshing	3.4% (1)	0.0% (0)	20.7% (6)	24.1% (7)	51.7% (15)	1.00	29
Fixed nodes (SPC)	3.4% (1)	6.9% (2)	27.6% (8)	17.2% (5)	44.8% (13)	1.00	29
Explicit model of the post and soil volumes	6.9% (2)	31.0% (9)	17.2% (5)	13.8% (4)	31.0% (9)	1.00	29
					Other (please specify)		7
					<i>answered question</i>		33
					<i>skipped question</i>		7

19. The DoD/AIAA define Verification as: "The process of determining that a model implementation represents the developer's conceptual description of the model and the solution to the model." For the purposes of this project, Verification is defined as: "Verification in roadside safety simulations involves using parameters and techniques based on the collective experience of the roadside safety simulation community that should maximize the likelihood of developing models that do not experience numerical instabilities or other run-time problems." Do you agree with this statement?			
		Response Percent	Response Count
Yes		57.6%	19
No. Please enter your alternate definition below		42.4%	14
		<i>answered question</i>	33
		<i>skipped question</i>	0

20. What is the largest shell element dimension (in millimeters) you would be likely to use in modeling steel components that (fill in the blank):			
	Response Average	Response Total	Response Count
Contact other components?	22.82	639	28
Do not contact other components but are expected to deform significantly?	44.22	1194	27
Are not in a contact or high deformation region of the model?	92.85	2414	26
	<i>answered question</i>		28
	<i>skipped question</i>		5

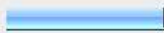
21. What is the largest solid element dimension (in millimeters) you would be likely to use in modeling a wood post if (fill in the blank):			
	Response Average	Response Total	Response Count
The post was expected for fracture?	45495.95	1000911	22
The post was expected not to fracture but displace in the soil?	45507.36	1001162	22
The post was not expected to deform or displace significantly?	45528.45	1001626	22
	<i>answered question</i>		22
	<i>skipped question</i>		11

22. For typical roadside hardware simulations, I generally try to keep my initial time step at about (check one):

		Response Percent	Response Count
Less than 1e-6 sec	<input type="checkbox"/>	20.0%	
[1e-6 sec - 5e-6 sec]	<input checked="" type="checkbox"/>	76.7%	2
[5e-6 sec - 10e-6 sec]	<input type="checkbox"/>	0.0%	
Greater than 10e-6 sec	<input type="checkbox"/>	3.3%	
Other (please specify)			
<i>answered question</i>			3
<i>skipped question</i>			

23. I control my time step by (select one):

	True	False	Rating Average	Response Count
Controlling the element dimensions	66.7% (2)	33.3% (1)	1.00	
Using the minimum time step option (i.e., mass scaling)	75.0% (3)	25.0% (1)	1.00	
Both element dimensions and time step	100.0% (24)	0.0% (0)	1.00	2
Neither	16.7% (1)	83.3% (5)	1.00	
<i>answered question</i>				3
<i>skipped question</i>				

24. Which one of the following statements best applies about the use of Mass-Scaling (check one):		Response Percent	Response Count
I never use mass scaling to achieve a minimum time step.		6.7%	
I often use mass scaling to develop and de-bug my model but then turn it off when I use it for my final simulations.		6.7%	
I generally use some mass scaling in my models to achieve a minimum time step.		60.0%	
Other (please specify)		26.7%	
		<i>answered question</i>	
		<i>skipped question</i>	

25. When you use the mass-scaling option, which is your main objective (check all that apply)?		Response Percent	Response Count
I determine the geometry that is required first and then use mass scaling to make sure the time step does not get too small		7.1%	
I make sure the overall mesh is adequate for the contacts and deformations that I expect and use mass scaling to prevent the time step getting too small.		75.0%	
I usually define a very fine mesh to ensure good contact and deformation results and use mass scaling to increase the time step to an acceptable run time.		10.7%	
Other (please specify)		7.1%	
		<i>answered question</i>	
		<i>skipped question</i>	

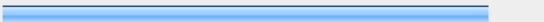
26. When I experience contact instabilities like shooting nodes or tangling meshes, I usually attempt to solve the problem by doing the following (put in rank order):				
	1	2	3	Response Count
Refine my mesh in the contact area	35.5% (11)	38.7% (12)	25.8% (8)	3
Modify the contact parameters like the penalty factors	51.6% (16)	22.6% (7)	25.8% (8)	3
Change the contact type	27.6% (8)	37.9% (11)	34.5% (10)	2
Other	40.0% (2)	20.0% (1)	40.0% (2)	
<i>answered question</i>				3
<i>skipped question</i>				

27. Check the range such that you agree with the statement							
	< 5%	[5% - 10%]	[10% - 15%]	> 15%	N/A	Rating Average	Response Count
I am generally not concerned about Total energy balance in my simulation as long as, during the run, the total energy varies by less than:	51.6% (16)	41.9% (13)	3.2% (1)	0.0% (0)	3.2% (1)	1.00	3
I am generally not concerned with hourglass energy as long as the percentage compared to the total internal energy is less than:	41.9% (13)	41.9% (13)	3.2% (1)	0.0% (0)	12.9% (4)	1.00	3
I am comfortable using mass scaling in my final model as long as the percentage of added mass compared to the total physical mass is less than:	64.5% (20)	3.2% (1)	6.5% (2)	3.2% (1)	22.6% (7)	1.00	3
If mass is added to a part of the model that is stationary at the beginning of the simulation, I would feel comfortable adding the following percentage of the total physical mass.	30.0% (9)	20.0% (6)	16.7% (5)	3.3% (1)	30.0% (9)	1.00	3
<i>answered question</i>							3
<i>skipped question</i>							

28. Maximum warpage angle (check one):							
	1°	3°	5°	10°	N/A	Rating Average	Response Count
I generally try to keep the maximum warpage angle of the elements in the model smaller than	0.0% (0)	10.3% (3)	37.9% (11)	27.6% (8)	24.1% (7)	1.00	29
	<i>answered question</i>						29
	<i>skipped question</i>						4

29. Elements with biggest warpage angle (check one):							
	0%-5%	5%-10%	10%-15%	15%-20%	N/A	Rating Average	Response Count
I generally try to keep the percentage of elements with the biggest warpage angle in the model smaller than	48.3% (14)	13.8% (4)	13.8% (4)	3.4% (1)	20.7% (6)	1.00	29
	<i>answered question</i>						29
	<i>skipped question</i>						4

30. Mesh aspect ratio(check one):							
	2 to 1	3 to 1	5 to 1	8 to 1	N/A	Rating Average	Response Count
I generally try to keep the aspect ratio of my mesh smaller than	19.4% (6)	45.2% (14)	22.6% (7)	0.0% (0)	12.9% (4)	1.00	31
	<i>answered question</i>						31
	<i>skipped question</i>						2

31. The DoD/AIAA define Validation as : "The process of determining the degree to which a model is an accurate representation of the real world from the perspective of its intended use." Do agree with this definition?			
		Response Percent	Response Count
Yes		90.6%	29
No. Please enter your alternate definition below		9.4%	3
<i>answered question</i>			32
<i>skipped question</i>			1

32. Rank the following statement in order of importance in validating a finite element simulation with a physical test (1 = least important, 5 = most important).					
	1	2	3	4	5
Qualitative comparison of barrier damage	6.5% (2)	3.2% (1)	12.9% (4)	48.4% (15)	29.0% (9)
Qualitative comparison of vehicle damage	3.4% (1)	17.2% (5)	51.7% (15)	20.7% (6)	6.9% (2)
Qualitative comparison of trajectories	6.7% (2)	20.0% (6)	23.3% (7)	30.0% (9)	20.0% (6)
Qualitative comparison of crash sequence (i.e., what happens)	12.9% (4)	3.2% (1)	22.6% (7)	35.5% (11)	25.8% (8)
Quantitative comparison of acceleration time histories	11.1% (3)	18.5% (5)	22.2% (6)	25.9% (7)	22.2% (6)
Quantitative comparison of velocity time histories	16.1% (5)	12.9% (4)	19.4% (6)	32.3% (10)	19.4% (6)
Quantitative comparison of displacement/rotation time histories	10.7% (3)	10.7% (3)	21.4% (6)	39.3% (11)	17.9% (5)
<i>answered question</i>					
<i>skipped question</i>					

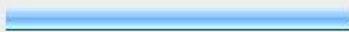
33. Which qualitative comparisons do you use to compare your simulation results to the physical tests (Check all that apply)?							
	Always	Mostly	Sometimes	Rarely	Never	Rating Average	Response Count
Hardware deformations	67.7% (21)	25.8% (8)	6.5% (2)	0.0% (0)	0.0% (0)	1.00	31
Location/number of failed components	51.6% (16)	29.0% (9)	16.1% (5)	3.2% (1)	0.0% (0)	1.00	31
Visual methods (i.e., pictures / movies)	64.5% (20)	25.8% (8)	9.7% (3)	0.0% (0)	0.0% (0)	1.00	31
Phenomological (i.e., the same general response)	65.5% (19)	31.0% (9)	3.4% (1)	0.0% (0)	0.0% (0)	1.00	29
					Other (please specify)		2
					<i>answered question</i>		31
					<i>skipped question</i>		2

34. Which quantitative time history comparisons do you use for comparing the simulation to the physical test (Check all that apply)?							
	Always	Mostly	Sometimes	Rarely	Never	Rating Average	Response Count
Accelerations	32.3% (10)	29.0% (9)	22.6% (7)	16.1% (5)	0.0% (0)	1.00	31
Velocity	29.0% (9)	41.9% (13)	19.4% (6)	9.7% (3)	0.0% (0)	1.00	31
Displacements and rotations	45.2% (14)	32.3% (10)	16.1% (5)	6.5% (2)	0.0% (0)	1.00	31
Energy	19.4% (6)	16.1% (5)	22.6% (7)	29.0% (9)	12.9% (4)	1.00	31
Stess/Strain	9.7% (3)	3.2% (1)	48.4% (15)	22.6% (7)	16.1% (5)	1.00	31
					Other (please specify)		5
					<i>answered question</i>		31
					<i>skipped question</i>		2

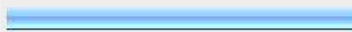
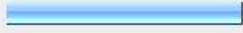
35. Which of the following parameters or metrics do you use to compare your simulation results with experimental results (check all that apply)?

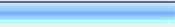
	Always	Mostly	Sometimes	Rarely	Never	Rating Average	Response Count
TRAP parameters (i.e., OIV, ORA, THIV, ASI, etc)	64.3% (18)	17.9% (5)	10.7% (3)	3.6% (1)	3.6% (1)	1.00	
GEER's parameters	0.0% (0)	3.8% (1)	7.7% (2)	15.4% (4)	73.1% (19)	1.00	
NARD Validation Manual parameters	0.0% (0)	3.8% (1)	7.7% (2)	11.5% (3)	76.9% (20)	1.00	
Ray's T-statistic method	3.8% (1)	0.0% (0)	11.5% (3)	15.4% (4)	69.2% (18)	1.00	
Other metrics (please specify)							
<i>answered question</i>							
<i>skipped question</i>							

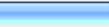
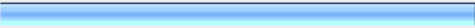
36. Do you have a standard procedure for model verification and validation?

		Response Percent	Response Count
No		59.4%	
Yes		40.6%	
If yes, please explain			
<i>answered question</i>			
<i>skipped question</i>			

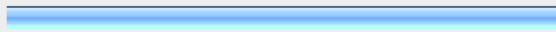
37. Do you use different validation methods according to the specific roadside hardware you are using (check one)?

		Response Percent	Response Count
No		60.0%	
Yes		40.0%	
If yes, please explain			
<i>answered question</i>			
<i>skipped question</i>			

38. How do you filter time history data before using it to compare to physical tests (check all that apply)?			Response Percent	Respon Count
I use the SAE J211 filter specifications			46.7%	
I use TRAP to filter my simulation data			30.0%	
I use LSPREPOST to filter my simulation data			66.7%	
I use a running average in LSPREPOST to effectively filter my data			6.7%	
I do not filter my simulation data			13.3%	
Other filters (please specify)			30.0%	
			<i>answered question</i>	
			<i>skipped question</i>	

39. Do you use any other finite element programs other than LS-DYNA for validation purposes (check one)?			Response Percent	Respon Count
Yes			18.8%	
No			81.3%	
			<i>answered question</i>	
			<i>skipped question</i>	

40. When building a large model, do you validate components or subassemblies of that model and compare the results with physical tests?

		Response Percent	Response Count
Yes		93.5%	
No		6.5%	
		<i>answered question</i>	
		<i>skipped question</i>	

41. Are there any validation or verification issues that you think were not addressed by this survey? If so, please list them in space below.

		Response Count
		<i>answered question</i>
		<i>skipped question</i>

APPENDIX E VALIDATION/VERIFICATION REPORT FORMS

A _____
 (Report 350 or MASH or EN1317 Vehicle Type)

Striking a _____
 (roadside hardware type and name)

Report Date: _____

Type of Report (check one)

- Verification (known numerical solution compared to new numerical solution) or
 Validation (full-scale crash test compared to a numerical solution).

General Information	Known Solution	Analysis Solution
Performing Organization		
Test/Run Number:		
Vehicle:		
Reference:		
Impact Conditions		
Vehicle Mass:		
Speed:		
Angle:		
Impact Point:		

Composite Validation/Verification Score

List the Report 350/MASH or EN1317 Test Number	
Part I	Did all solution verification criteria in Table E-1 pass?
Part II	Do all the time history evaluation scores from Table E-2 result in a satisfactory comparison (i.e., the comparison passes the criterion)? If all the values in Table E-2 did not pass, did the weighted procedure shown in Table E-3 result in an acceptable comparison. If all the criteria in Table E-2 pass, enter "yes." If all the criteria in Table E-2 did not pass but Table E-3 resulted in a passing score, enter "yes."
Part III	All the criteria in Table E-4 (Test-PIRT) passed?
	Are the results of Steps I through III all affirmative (i.e., YES)? If all three steps result in a "YES" answer, the comparison can be considered validated or verified. If one of the steps results in a negative response, the result cannot be considered validated or verified.

The analysis solution (check one) is is NOT verified/validated against the known solution.

PART I: BASIC INFORMATION

These forms may be used for validation or verification of roadside hardware crash tests. If the known solution is a full-scale crash test (i.e., physical experiment) which is being compared to a numerical solution (e.g., LSDYNA analysis) then the procedure is a validation exercise. If the known solution is a numerical solution (e.g., a prior finite element model using a different program or earlier version of the software) then the procedure is a verification exercise. This form can also be used to verify the repeatability of crash tests by comparing two full-scale crash test experiments. Provide the following basic information for the validation/verification comparison:

- 1. What type of roadside hardware is being evaluated (check one)?
 - Longitudinal barrier or transition
 - Terminal or crash cushion
 - Breakaway support or work zone traffic control device
 - Truck-mounted attenuator
 - Other hardware: _____

- 2. What test guidelines were used to perform the full-scale crash test (check one)?
 - NCHRP Report 350
 - MASH
 - EN1317
 - Other: _____

- 3. Indicate the test level and number being evaluated (fill in the blank). _____

- 4. Indicate the vehicle type appropriate for the test level and number indicated in item 3 according to the testing guidelines indicated in item 2.

NCHRP Report 350/MASH

- | | | |
|---------------------------------|---------------------------------|---------------------------------------|
| <input type="checkbox"/> 700C | <input type="checkbox"/> 820C | <input type="checkbox"/> 1100C |
| <input type="checkbox"/> 2000P | <input type="checkbox"/> 2270P | <input type="checkbox"/> Other: _____ |
| <input type="checkbox"/> 8000S | <input type="checkbox"/> 10000S | |
| <input type="checkbox"/> 36000V | | |
| <input type="checkbox"/> 36000T | | |

EN1317

- | | | |
|---|---|---|
| <input type="checkbox"/> Car (900 kg) | <input type="checkbox"/> Car (1300 kg) | <input type="checkbox"/> Car (1500 kg) |
| <input type="checkbox"/> Rigid HGV (10 ton) | <input type="checkbox"/> Rigid HGV (16 ton) | <input type="checkbox"/> Rigid HGV (30 ton) |
| <input type="checkbox"/> Bus (13 ton) | <input type="checkbox"/> Articulated HGV (38 ton) | <input type="checkbox"/> Other: _____ |

PART II: ANALYSIS SOLUTION VERIFICATION

Using the results of the analysis solution, fill in the values for Table E-1. These values are indications of whether the analysis solution produced a numerically stable result and do not necessarily mean that the result is a good comparison to the known solution. The purpose of this table is to ensure that the numerical solution produces results that are numerically stable and conform to the conservation laws (e.g., energy, mass and momentum).

Table E-1. Analysis Solution Verification Table.

Verification Evaluation Criteria	Change (%)	Pass?
Total energy of the analysis solution (i.e., kinetic, potential, contact, etc.) must not vary more than 10 percent from the beginning of the run to the end of the run.		
Hourglass Energy of the analysis solution at the end of the run is less than five percent of the total initial energy at the beginning of the run.		
Hourglass Energy of the analysis solution at the end of the run is less than ten percent of the total internal energy at the end of the run.		
The part/material with the highest amount of hourglass energy at the end of the run is less than ten percent of the total internal energy of the part/material at the end of the run.		
Mass added to the total model is less than five percent of the total model mass at the beginning of the run.		
The part/material with the most mass added had less than 10 percent of its initial mass added.		
The moving parts/materials in the model have less than five percent of mass added to the initial moving mass of the model.		
There are no shooting nodes in the solution?		
There are no solid elements with negative volumes?		

If all the analysis solution verification criteria are scored as passing, the analysis solution can be verified or validated against the known solution. If any criterion in Table E-1 does not pass one of the verification criterion listed in Table E-1, the analysis solution cannot be used to verify or validate the known solution. If there are exceptions that the analyst thinks are relevant these should be footnoted in the table and explained below the table.

The Analysis Solution (check one) passes does NOT pass all the criteria in Table E1-1
with without exceptions as noted.

PART III: TIME HISTORY EVALUATION TABLE

Using the RSVVP computer program ('Single channel' option), compute the Sprague & Geers MPC metrics and ANOVA metrics using time-history data from the known and analysis solutions for a time period starting at the beginning of the contact and ending at the loss of contact. Both the Sprague & Geers and ANOVA metrics must be calculated based on the original units the data was collected in (e.g., if accelerations were measured in the experiment with accelerometers then the comparison should be between accelerations. If rate gyros were used in the experiment, the comparison should be between rotation rates). If all six data channels are not available for both the known and analysis solutions, enter "N/A" in the column corresponding to the missing data. Enter the values obtained from the RSVVP program in Table E-2 and indicate if the comparison was acceptable or not by entering a "yes" or "no" in the "Agree?" column. Attach a graph of each channel for which the metrics have been compared at the end of the report.

Enter the filter, synchronization method and shift/drift options used in RSVVP to perform the comparison so that it is clear to the reviewer what options were used. Normally, SAE J211 filter class 180 is used to compare vehicle kinematics in full-scale crash tests. Either synchronization option in RSVVP is acceptable and both should result in a similar start point. The shift and drift options should generally only be used for the experimental curve since shift and drift are characteristics of sensors. For example, the zero point for an accelerometer sometimes "drifts" as the accelerometer sits out in the open environment of the crash test pad whereas there is no sensor to "drift" or "shift" in a numerical solution.

In order for the analysis solution to be considered in agreement with the known solution (i.e., verified or validated), all the criteria scored in Table E-2 must pass. If all the channels in Table E-2 do not pass, fill out Table E-3, the multi-channel weighted procedure.

If one or more channels do not satisfy the criteria in Table E-2, the multi-channel weighting option may be used. Using the RSVVP computer program ('Multiple channel' option), compute the Sprague-Geers MPC metrics and ANOVA metrics using all the time histories data from the known and analysis solutions for a time period starting at the beginning of the contact and ending at the loss of contact. If all six data channels are not available for both the known and analysis solutions, enter "N/A" in the column corresponding to the missing data.

For some types of roadside hardware impacts, some of the channels are not as important as others. An example might be a breakaway sign support test where the lateral (i.e., Y) and vertical (i.e., Z) accelerations are insignificant to the dynamics of the crash event. The weighting procedure provides a way to weight the most important channels more highly than less important channels. The procedure used is based on the area under the curve, therefore, the weighing scheme will weight channels with large areas more highly than those with smaller areas. In general, using the "Area (II)" method is acceptable although if the complete inertial properties of the vehicle are available the "inertial" method may be used. Enter the values obtained from the RSVVP program in Table E-3 and indicate if the comparison was acceptable or not by entering a "yes" or "no" in the "Agree?" column.

In order for the analysis solution to be considered in agreement with the known solution (i.e., verified or validated), all the criteria scored in Table E-3 must pass.

Table E-2. Roadside Safety Validation Metrics Rating Table – Time History Comparisons (single channel option).

Evaluation Criteria							Time interval []					
O	Sprague-Geers Metrics List all the data channels being compared. Calculate the M and P metrics using RSVVP and enter the results. Values less than or equal to 40 are acceptable.						M	P	Pass?			
	RSVVP Curve Preprocessing Options											
		Filter Option	Sync. Option	Shift		Drift						
				True Curve	Test Curve	True Curve				Test Curve		
	X acceleration											
	Y acceleration											
	Z acceleration											
	Roll rate											
Pitch rate												
Yaw rate												
P	ANOVA Metrics List all the data channels being compared. Calculate the ANOVA metrics using RSVVP and enter the results. Both of the following criteria must be met: <ul style="list-style-type: none"> The mean residual error must be less than five percent of the peak acceleration ($\bar{e} \leq 0.05 \cdot a_{Peak}$) and The standard deviation of the residuals must be less than 35 percent of the peak acceleration ($\sigma \leq 0.35 \cdot a_{Peak}$) 						Mean Residual	Standard Deviation of Residuals	Pass?			
	X acceleration/Peak											
	Y acceleration/Peak											
	Z acceleration/Peak											
	Roll rate											
	Pitch rate											
	Yaw rate											

The Analysis Solution (check one) passes does NOT pass all the criteria in Table E-2 (single-channel time history comparison). If the Analysis Solution does NOT pass, perform the analysis in Table E-3 (multi-channel time history comparison).

Table E-3. Roadside Safety Validation Metrics Rating Table – Time History Comparisons (multi-channel option).

Evaluation Criteria (time interval [_____])			
Channels (Select which were used)			
<input type="checkbox"/> X Acceleration	<input type="checkbox"/> Y Acceleration	<input type="checkbox"/> Z Acceleration	
<input type="checkbox"/> Roll rate	<input type="checkbox"/> Pitch rate	<input type="checkbox"/> Yaw rate	
Multi-Channel Weights <input type="checkbox"/> Area II method <input type="checkbox"/> Inertial method	X Channel: Y Channel: Z Channel: Yaw Channel: Roll Channel: ____ Pitch Channel:		
O	Sprague-Geer Metrics Values less or equal to 40 are acceptable.		M P Pass?
P	ANOVA Metrics Both of the following criteria must be met: <ul style="list-style-type: none"> The mean residual error must be less than five percent of the peak acceleration $(\bar{e} \leq 0.05 \cdot a_{Peak})$ The standard deviation of the residuals must be less than 35 percent of the peak acceleration $(\sigma \leq 0.35 \cdot a_{Peak})$ 		Mean Residual Standard Deviation of Residuals Pass?

The Analysis Solution (check one) passes does NOT pass all the criteria in Table E-3.

PART IV: PHENOMENA IMPORTANCE RANKING TABLE

Table E-4 is similar to the evaluation tables in Report 350 and MASH. For the Report 350 or MASH test number identified in Part I (e.g., test 3-10, 5-12, etc.), circle all the evaluation criteria applicable to that test in Table E-4. The tests that apply to each criterion are listed in the far right column without the test level designator. For example, if a Report 350 test 3-11 is being compared (i.e., a pickup truck striking a barrier at 25 degrees and 100 km/hr), circle all the criteria in the second column where the number “11” appears in the far right column. Some of the Report 350 evaluation criteria have been removed (i.e., J and K) since they are not generally useful in assessing the comparison between the known and analysis solutions.

Table E-4. Evaluation Criteria Test Applicability Table.

Evaluation Factors	Evaluation Criteria			Applicable Tests	
Structural Adequacy	A	Test article should contain and redirect the vehicle; the vehicle should not penetrate, under-ride, or override the installation although controlled lateral deflection of the test article is acceptable.		10, 11, 12, 20, 21, 22, 35, 36, 37, 38	
	B	The test article should readily activate in a predictable manner by breaking away, fracturing or yielding.		60, 61, 70, 71, 80, 81	
	C	Acceptable test article performance may be by redirection, controlled penetration or controlled stopping of the vehicle.		30, 31,, 32, 33, 34, 39, 40, 41, 42, 43, 44, 50, 51, 52, 53	
Occupant Risk	D	Detached elements, fragments or other debris from the test article should not penetrate or show potential for penetrating the occupant compartment, or present an undue hazard to other traffic, pedestrians or personnel in a work zone.		All	
	E	Detached elements, fragments or other debris from the test article, or vehicular damage should not block the driver's vision or otherwise cause the driver to lose control of the vehicle. (Answer Yes or No)		70, 71	
	F	The vehicle should remain upright during and after the collision although moderate roll, pitching and yawing are acceptable.		All except those listed in criterion G	
	G	It is preferable, although not essential, that the vehicle remain upright during and after collision.		12, 22 (for test level 1 – 30, 31, 32, 33, 34, 35, 36, 37, 38, 39, 40, 41, 42, 43, 44)	
	H	Occupant impact velocities should satisfy the following:			10, 20, 30,31, 32, 33, 34, 36, 40, 41, 42, 43, 50, 51, 52, 53, 80, 81
		Occupant Impact Velocity Limits (m/s)			
		Component	Preferred	Maximum	
Longitudinal and Lateral	9	12			
Longitudinal	3	5	60, 61, 70, 71		
I	Occupant ridedown accelerations should satisfy the following:			10, 20, 30,31, 32, 33, 34, 36, 40, 41, 42, 43, 50, 51, 52, 53, 60, 61, 70, 71, 80, 81	
	Occupant Ridedown Acceleration Limits (g's)				
	Component	Preferred	Maximum		
Longitudinal and Lateral	15	20			
Vehicle Trajectory	L	The occupant impact velocity in the longitudinal direction should not exceed 40 ft/sec and the occupant ride-down acceleration in the longitudinal direction should not exceed 20 G's.		11,21, 35, 37, 38, 39	
	M	The exit angle from the test article preferable should be less than 60 percent of test impact angle, measured at the time of vehicle loss of contact with test device.		10, 11, 12, 20, 21, 22, 35, 36, 37, 38, 39	
	N	Vehicle trajectory behind the test article is acceptable.		30, 31, 32, 33, 34, 39, 42, 43, 44, 60, 61, 70, 71, 80, 81	

Complete Table E-5 according to the results of the known solution (e.g., crash test) and the numerical solution (e.g., simulation). Consistent with Report 350 and MASH, Task E-5 has three parts: the structural adequacy phenomena listed in Table E-5a, the occupant risk phenomena listed in Table E-5b and the vehicle trajectory criteria listed in Table E-5c. If the result of the analysis solution agrees with the known solution, mark the “agree” column “yes.” For example, if the vehicle in both the known and analysis solutions rolls over and, therefore, fails criterion F1, the known and the analysis columns for criterion F1 would be evaluated as “no.” Even though both failed the criteria, they agree with each other so the “agree” column is marked as “yes.” Any criterion that is not applicable to the test being evaluated (i.e., not circled in Table E-4) should be indicated by entering “NA” in the “agree?” column for that row.

Many of the Report 350 evaluation criteria have been subdivided into more specific phenomenon. For example, criterion A is divided into eight sub-criteria, A1 through A8, that provide more specific and quantifiable phenomena for evaluation. Some of the values are simple yes or no questions while other request numerical values. For the numerical phenomena, the analyst should enter the value for the known and analysis result and then calculate the relative difference. Relative difference is always the absolute value of the difference of the known and analysis solutions divided by the known solution. Enter the value in the “relative difference” column. If the relative difference is less than 20 percent, enter “yes” in the “agree?” column.

Sometimes, when the values are very small, the relative difference might be large while the absolute difference is very small. For example, the longitudinal occupant ride down acceleration (i.e., criterion L2) in a test might be 3 g’s and in the corresponding analysis might be 4 g’s. The relative difference is 33 percent but the absolute difference is only 1 g and the result for both is well below the 20 g limit. Clearly, the analysis solution in this case is a good match to the experiment and the relative difference is large only because the values are small. The absolute difference, therefore, should also be entered into the “Difference” column in Table E-5.

The experimental and analysis result can be considered to agree as long as either the relative difference or the absolute difference is less than the acceptance limit listed in the criterion. Generally, relative differences of less than 20 percent are acceptable and the absolute difference limits were generally chosen to represent 20 percent of the acceptance limit in Report 350 or MASH. For example, Report 350 limits occupant ride-down accelerations to those less than 20 g’s so 20 percent of 20 g’s is 4 g’s. As shown for criterion L2 in Table E-5, the relative acceptance limit is 20 percent and the absolute acceptance limit is 4 g’s.

If a numerical model was not created to represent the phenomenon, a value of “NM” (i.e., not modeled) should be entered in the appropriate column of Table E-5. If the known solution for that phenomenon number is “no” then a “NM” value in the “test result” column can be considered to agree. For example, if the material model for the rail element did not include the possibility of failure, “NM” should be entered for phenomenon number T in Table E-5. If the known solution does not indicate rail rupture or failure (i.e., phenomenon T = “no”), then the known and analysis solutions agree and a “yes” can be entered in the “agree?” column. On the other hand, if the known solution shows that a rail

rupture did occur resulting in a phenomenon T entry of “yes” for the known solution, the known and analysis solutions do not agree and “no” should be entered in the “agree?” column. Analysts should seriously consider refining their model to incorporate any phenomena that appears in the known solution and is shown in Table E-5.

All the criteria identified in Table E-4 are expected to agree but if one does not and, in the opinion of the analyst, is not considered important to the overall evaluation for this particular comparison, then a footnote should be provided with a justification for why this particular criterion can be ignored for this particular comparison.

Table E-5(a). Roadside Safety Phenomena Importance Ranking Table (Structural Adequacy).

Evaluation Criteria			Known Result	Analysis Result	Difference Relative/ Absolute	Agree?	
Structural Adequacy	A	A1	Test article should contain and redirect the vehicle; the vehicle should not penetrate, under-ride, or override the installation although controlled lateral deflection of the test article is acceptable. (Answer Yes or No)			X	
		A2	Maximum dynamic deflection: - Relative difference is less than 20 percent or - Absolute difference is less than 0.15 m				
		A3	Length of vehicle-barrier contact: - Relative difference is less than 20 percent or - Absolute difference is less than 2 m				
		A4	Number of broken or significantly bent posts is less than 20 percent.				
		A5	Did the rail element rupture or tear (Answer Yes or No)			X	
		A6	Were there failures of connector elements (Answer Yes or No).			X	
		A7	Was there significant snagging between the vehicle wheels and barrier elements (Answer Yes or No).			X	
		A8	Was there significant snagging between vehicle body components and barrier elements (Answer Yes or No).			X	

Table E-5(b). Roadside Safety Phenomena Importance Ranking Table (Occupant Risk).

Evaluation Criteria		Known Result	Analysis Result	Difference Relative/Absolute	Agree?	
Occupant Risk	D	Detached elements, fragments or other debris from the test article should not penetrate or show potential for penetrating the occupant compartment, or present an undue hazard to other traffic, pedestrians or personnel in a work zone. (Answer Yes or No)		X		
	F1	The vehicle should remain upright during and after the collision although moderate roll, pitching and yawing are acceptable. (Answer Yes or No)		X		
	F	F2	Maximum roll of the vehicle: - Relative difference is less than 20 percent or - Absolute difference is less than 5 degrees.			
		F3	Maximum pitch of the vehicle is: - Relative difference is less than 20 percent or - Absolute difference is less than 5 degrees.			
		F4	Maximum yaw of the vehicle is: - Relative difference is less than 20 percent or - Absolute difference is less than 5 degrees.			
		L	L1	Occupant impact velocities: - Relative difference is less than 20 percent or - Absolute difference is less than 2 m/s.		
	• Longitudinal OIV (m/s)					
	• Lateral OIV (m/s)					
	• THIV (m/s)					
	L2		Occupant accelerations: - Relative difference is less than 20 percent or - Absolute difference is less than 4 g's.			
			• Longitudinal ORA			
			• Lateral ORA			
			• PHD			
	• ASI					

Table E-5(c). Roadside Safety Phenomena Importance Ranking Table (Vehicle Trajectory).

Evaluation Criteria			Known Result	Analysis Result	Difference Relative/Absolute	Agree?	
Vehicle Trajectory	M	M1	The exit angle from the test article preferable should be less than 60 percent of test impact angle, measured at the time of vehicle loss of contact with test device.			X	
		M2	Exit angle at loss of contact: - Relative difference is less than 20 percent or - Absolute difference is less than 5 degrees.				
		M3	Exit velocity at loss of contact: - Relative difference is less than 20 percent or - Absolute difference is less than 5 degrees.				
		M4	One or more vehicle tires failed or de-beaded during the collision event (Answer Yes or No).			X	

The Analysis Solution (check one) passes does NOT pass all the criteria in Tables E-5a through E-5c with exceptions as noted without exceptions .